VOLUME 64
NUMBER 3 / NUMÉRO 3
MARCH / MARS
2007

An NRC Research Press
JOURNAL
Une REVUE des
Presses scientifiques du CNRC

Canadian Journal of
FISHERIES AND AQUATIC SCIENCES
cjfas.nrc.ca

Journal canadien des
SCIENCES HALIEUTIQUES ET AQUATIQUES
jcsha.cnrc.ca

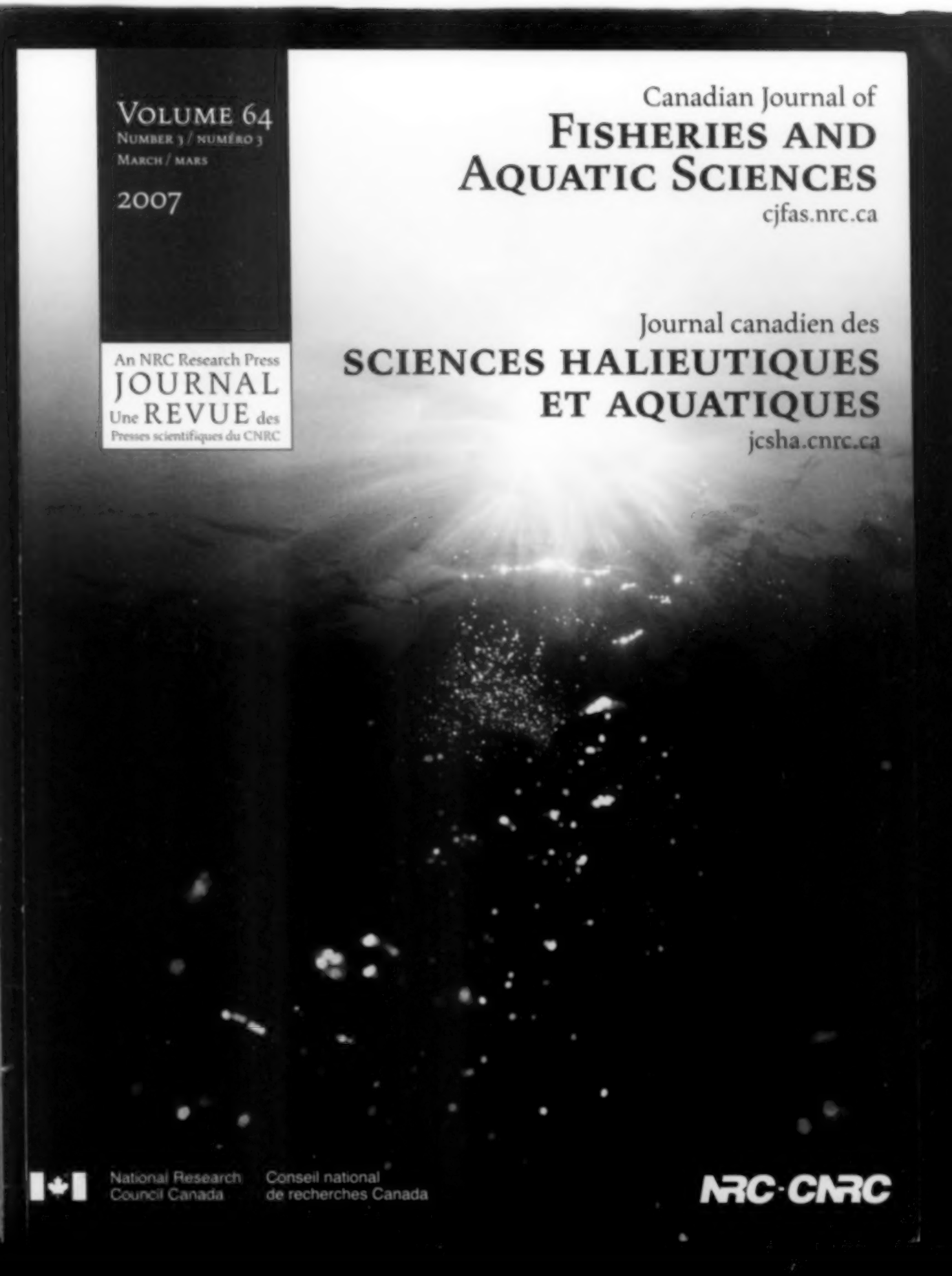

National Research Council Canada
Conseil national de recherches Canada
NRC·CNRC

ISSN 0706-652X / CJFSDX 64(3) 387–585 (2007)

The *Canadian Journal of Fisheries and Aquatic Sciences*, previously published as *Contributions to Canadian Biology* 1901–1925, *Contributions to Canadian Biology and Fisheries* 1926–1934, *Journal of the Biological Board of Canada* 1934–1937, and *Journal of the Fisheries Research Board of Canada* 1938–1979, is issued monthly to form annual volumes of 12 numbers plus supplements.

Editorial policy. The Journal publishes original research articles, perspectives (syntheses, critiques, reevaluations), discussions (comment and reply), and rapid communications. Manuscripts may concern cells, organisms, populations, communities, ecosystems, or processes that affect aquatic systems. They may cover a range of disciplines including biology and ecology of marine and freshwater organisms, limnology, oceanography, physiology, toxicology, genetics, economics, disease, and management. Preference will be given to manuscripts that emphasize understanding of observed phenomena and interpretation of experimental results. The Journal encourages papers that lead from clearly stated purpose or rationale and from testable hypotheses, concepts, or questions to identifiable conclusions or syntheses. Such papers may amplify, modify, question, or redirect accumulated knowledge embodied in contemporary perceptions of a particular state of aquatic sciences. The Journal discourages papers that are essentially descriptive, except in emerging disciplines; have only site-specific or local applications (a certain year, place, taxon, chemical compound, etc.); only confirm previously established principles; or apply standard techniques without breaking new methodological ground.

Manuscripts for publication should be submitted to the Editorial Office via NRC Research Press' online submission and peer review system (**OSPREY**) at http://pubs.nrc-cnrc.gc.ca/cjfas/osprey. Alternatively, manuscripts may be submitted to the Senior Editor, *Canadian Journal of Fisheries and Aquatic Sciences*, Department of Integrative Biology, Building #006, Room 118, University of Guelph, Guelph, ON N1G 2W1, Canada (519-824-4120 ext. 52646; fax: 519-767-9798; e-mail: cjfas@uoguelph.ca).

Submissions in either English or French are acceptable. The information must be original, that is, not copyrighted, published, or submitted elsewhere except in abstract form or unless by written consent of the Editor.

Correspondence concerning accepted manuscripts and corrected proofs should be sent to NRC Research Press, National Research Council of Canada, Ottawa, ON K1A 0R6, Canada (fax: 613-952-7656; e-mail: pubs@nrc-cnrc.gc.ca).

Instructions to Authors are published once a year in the first issue of each volume. Copies are available from NRC Research Press or at cjfas.nrc.ca. The **Publication Policy** of NRC Research Press is available at pubs.nrc-cnrc.gc.ca.

Microfilm. Issues from 1934 through the current volume can be purchased on 16- or 35-mm microfilm. Photocopies of individual articles or issues can be purchased from University Microfilms International, 330 North Zeeb Road, Ann Arbor, MI 48106, USA.

The *Canadian Journal of Fisheries and Aquatic Sciences*, ISSN 0706-652X, is published monthly, 12 times per year, by NRC Research Press, c/o USACAN Media Dist. Srv. Corp. at 26 Power Dam Way, Suite S1-S3, Plattsburgh, NY 12901, USA. Periodicals postage paid at Plattsburgh, NY. POSTMASTER: Send address changes to *Canadian Journal of Fisheries and Aquatic Sciences*, c/o NRC, P.O. Box 2888, Plattsburgh, NY 12901, USA.

Publié sans interruption depuis 1901, le *Journal canadien des sciences halieutiques et aquatiques* a paru sous plusieurs titres : *Contributions to Canadian Biology* 1901–1925, *Contributions to Canadian Biology and Fisheries* 1926–1934, *Journal of the Biological Board of Canada* 1934–1937, et *Journal of the Fisheries Research Board of Canada* 1938–1979. Le Journal paraît tous les mois, formant ainsi un volume de 12 numéros, et offre en plus jusqu'à deux suppléments par année.

Politique éditoriale. On publie, dans le Journal, des articles rendant compte de recherche originale, des perspectives (synthèses, critiques et réévaluations), des discussions (commentaires et réponses) et des communications rapides. Les documents peuvent porter sur les cellules, organismes, populations, communautés, écosystèmes ou processus qui affectent les systèmes aquatiques. Ils peuvent relever de divers domaines y compris la biologie et l'écologie des organismes marins et d'eau douce, la limnologie, l'océanographie, la physiologie, la toxicologie, la génétique, l'économie, la pathologie et la gestion. On accorde la préséance aux articles qui contribuent à la compréhension de phénomènes observés et à l'interprétation de résultats expérimentaux. On invite les auteurs à soumettre des articles ayant des objectifs précis ou relevant d'hypothèses, de concepts ou de questions vérifiables et se terminant par de solides conclusions ou d'utiles synthèses. Ces articles enrichissent, changent, mettent en question ou réorientent les connaissances acquises sur divers aspects des sciences aquatiques. On décourage toutefois la soumission d'articles simplement descriptifs (à moins qu'il ne s'agisse de nouvelles disciplines), d'application très limitée (applicables à une seule année, une seule région ou un seul taxon, portant sur un unique composé chimique, etc.); d'articles qui ne font que reprendre les principes énoncés dans des articles précédents; et d'articles rendant compte de l'application de normes sans gain de méthodologie.

Les auteurs sont invités à soumettre leur **manuscrit** au Bureau de la rédaction par le truchement du Système de soumission et d'examen en direct des articles (**OSPREY**) des Presses scientifique du CNRC à http://pubs.nrc-cnrc.gc.ca/jcsha/osprey. Sinon, ils peuvent transmettre leur manuscrit par la poste à la directrice scientifique principale, *Journal canadien des sciences halieutiques et aquatiques*, Département de biologie intégrative, édifice 006, bureau 118, University of Guelph, Guelph, ON N1G 2W1, Canada (519-824-4120 poste 52646; télécopieur : 519-767-9798; courriel : cjfas@uoguelph.ca).

Les contributions peuvent être en anglais ou en français. Elles doivent être originales, c.-à.-d. qu'elles ne doivent pas avoir fait l'objet d'un copyright, avoir été publiées ou soumises ailleurs, sauf sous forme abrégée ou avec le consentement du rédacteur. Le CNRC ne se tient en aucune façon responsable des opinions exprimées par un collaborateur ou des déclarations qui pourrait faire ce dernier.

La correspondance ayant trait aux manuscrits acceptés et les **épreuves corrigés** doivent être envoyées aux Presses scientifiques du CNRC, Conseil national de recherches du Canada, Ottawa, ON K1A 0R6, Canada (télécopieur : 613-952-7656; courriel : pubs@nrc-cnrc.gc.ca).

Les Recommandations aux auteurs sont publiées une fois par année dans le premier numéro de chaque volume. Des copies sont disponibles auprès du Bureau de la rédaction aux Presses scientifiques du CNRC ou au jcsha.cnrc.ca. **La Politique de publication** est disponible auprès des Presses scientifiques du CNRC ou au pubs.nrc-cnrc.gc.ca.

Microfilms. On peut acheter sur microfilms de 16 ou 35 mm tous les numéros depuis 1934. Des photocopies d'articles ou de numéros individuels sont aussi en vente auprès de University Microfilms International, 330 North Zeeb Road, Ann Arbor, MI 48106, É.-U.

This Journal is indexed or abstracted in / Cette revue est signalée ou résumée dans

ABSEARCH; Applied Science and Technology Index and Abstracts; Aquatic Sciences and Fisheries Abstracts; Biological Abstracts; Biological and Agricultural Abstracts; CAB Abstracts; Chemical Abstracts; Current Contents; Elsevier BIOBASE; Environmental Abstracts; ETDE Energy Database; General Science Index and Abstracts; GEOBASE; GeoRef; Life Sciences Collection; Meteorological and Geoastrophysical Abstracts; Oceanic Abstracts; PASCAL Database; Science Citation Index.

Volume 64, Number 3, March 2007

Canadian Journal of Fisheries and Aquatic Sciences

Published by the National Research Council of Canada

Volume 64, numéro 3, mars 2007

Journal canadien des sciences halieutiques et aquatiques

Publié par le Conseil national de recherches du Canada

Senior Editor / Directrice scientifique principale **Moira M. Ferguson**

Editors / Directeurs

Jeffrey A. Hutchings, *Dalhousie University, Halifax*
Pierre Pepin, *Northwest Atlantic Fisheries Centre, DFO/MPO, St. John's, Newfoundland*
W. Gary Sprules, *University of Toronto at Mississauga*
Assistant to the Editors / Adjointe aux directeurs scientifiques **Holly Foster**

Associate Editors / Directeurs scientifiques associés

D. Boisclair, *Université de Montréal*
U. Borgmann, *Environment Canada, Burlington*
M.J. Bradford, *DFO/MPO and Simon Fraser University*
S.E. Campana, *DFO/MPO, Dartmouth*
R. Carignan, *Université de Montréal*
K.T. Frank, *DFO/MPO, Dartmouth*
J.W.A. Grant, *Concordia University*
M.M. Hansen, *Danish Institute for Fisheries Research, Silkeborg, Denmark*
R. Hilborn, *University of Washington*
D.F. Houlihan, *University of Aberdeen*
F.A. Huntingford, *University of Glasgow*
J.M. Jech, *NFSC/NOAA, Woods Hole, Mass.*
B. Jonsson, *Norwegian Institute for Nature Research, Oslo, Norway*
K.A. Kidd, *University of New Brunswick*
D.L. MacLatchy, *University of New Brunswick, Saint John*
P. Magnan, *Université du Québec à Trois Rivières*
C.T. Marshall, *University of Aberdeen*
R.B. Millar, *University of Auckland, New Zealand*
W.P. Patterson, *University of Saskatchewan*
Y.T. Prairie, *Université du Québec à Montréal*
T.J. Quinn II, *University of Alaska–Fairbanks, Juneau, Alaska*
T.P. Quinn, *University of Washington*
C.W. Ramcharan, *Laurentian University*
J.S. Richardson, *The University of British Columbia*
B. Sainte-Marie, *DFO/MPO, Mont-Joli*
R.E.H. Smith, *University of Waterloo*
S.J. Smith, *DFO/MPO, Dartmouth*
E.B. Taylor, *The University of British Columbia*
W.F. Vincent, *Université Laval*
R.D. Vinebrooke, *University of Alberta*
C.J. Walters, *The University of British Columbia*
B. de Young, *Memorial University of Newfoundland*

NRC Research Press / Presses scientifiques du CNRC

Fax / Télécopieur : 613-952-7656; e-mail / courriel : pubs@nrc-cnrc.gc.ca; URL / URL : pubs.nrc-cnrc.gc.ca
Editor-in-Chief / Directeur scientifique en chef **Bruce P. Dancik**
Assistant Editor-in-Chief / Adjoint au directeur scientifique en chef **Donald S. Mavinic**
Director / Directeur **Cameron D. Macdonald**

Acting Business Manager / Gestionnaire des affaires commerciales par intérim **Mike Boroczki**
Advertising and reprints / Annonces publicitaires et tirés à part **Roxanne Landriault** (613-990-2254)
Subscriptions / Abonnements **Eileen Evans-Nantais** (613-990-7873), **André Séguin** (613-993-9084)

Manager, Journals Program / Gestionnaire du Programme des revues **Carolyn Brown**
Managing Editor / Rédactrice administrative **Cecily M. Pearson** (613-993-9099)
Publication Officers / Agents de publication **Jennifer McColl, Thad Costigan**
Editorial Publication Assistant / Adjointe à la publication **Diana Leck**

Production Manager / Gestionnaire de la production **Brad Stoppa**
Production Application Support Technician / Technicienne au soutien de la production **Judy Hum**
Desktop Publishing Technician / Technicienne en éditique **Lisette Séguin**
Graphics Technician / Technicien en graphisme **Jeff Wisking**
Web Technician / Technicien Web **Dennis Cafferty**

The National Research Council of Canada accepts no responsibility for statements or opinions expressed by a contributor. Acceptance of an advertisement, announcement, or other material does not imply endorsement by either the Journal's Senior Editor or the National Research Council.

© National Research Council of Canada 2007. All rights reserved.

No part of this publication may be reproduced, stored, or transmitted in any form or by any means, without the written permission of the publisher, except as stated below.

The National Research Council of Canada grants **permission*** to individuals to make single copies of articles for personal use. Any person may reproduce short excerpts from articles in the journal for any purpose that respects the moral rights of authors, provided that the source is fully acknowledged. As a courtesy, the consent of authors of such material should be obtained directly from the author.

Authorization to reproduce items for other than personal use, as stated above, is granted by the National Research Council of Canada provided that the copyright fee of $7.00 per copy is paid directly to Access Copyright, The Canadian Copyright Licensing Agency, One Yonge Street, Suite 800, Toronto, ON M5E 1E5, Canada.

*The above permission does not extend to other kinds of copying, such as copying for general distribution, for advertising, or promotional purposes, for creating new collective works, or for resale. For such copying, arrangements must be made with the publisher, National Research Council of Canada, Ottawa, ON K1A 0R6, Canada.

Subscription information

The *Canadian Journal of Fisheries and Aquatic Sciences* (ISSN 0706-652X) is published monthly by the National Research Council of Canada. The 2007 annual subscription rates (second class postage) for Canada are $1051CAN institutional and $325CAN personal, for US & foreign $1051US institutional and $325US personal. For air mail add $150US to foreign rate. Canadian customers please include 6% GST (business no. 12149 1807 RT 0275). Subscriptions are entered for the calendar year. Remittances should be made payable to the Receiver General for Canada, credit NRC. Price for regular single issues: institutional, $110.00; personal, $35.00. Supplements will be priced separately. Special rates apply to members of Canadian scientific and engineering societies if they subscribe through their respective societies.

There are no refunds on cancelled subscriptions once delivery has begun. Claims for missing issues should be made within four months (North America) or six months (outside North America) following the date of publication. The publisher expects to supply missing issues only when losses have occurred in transit and when the reserve stock will permit. For change of address and subscription enquiries: Subscription Office, NRC Research Press, National Research Council of Canada, Ottawa, ON K1A 0R6, Canada; tel.: 613-993-9084; fax: 613-952-7656; e-mail: pubs@nrc-cnrc.gc.ca.

Microform backfiles are available from UMI, P.O. Box 1346, Ann Arbor, MI 48106-1346, USA, and Micromedia Ltd., 20 Victoria St., Toronto, ON M5C 2N8, Canada.

All issues of the *Canadian Journal of Fisheries and Aquatic Sciences* since 1996 are available on the Web. Pricing information can be found at pubs.nrc-cnrc.gc.ca.

Le Conseil national de recherches du Canada ne se tient en aucune façon responsable des opinions exprimées par un collaborateur ou des déclarations que pourrait faire ce dernier. La publication d'annonces publicitaires, d'avis et autres n'implique pas l'endossement de leur contenu par la directrice principale de la Revue ou le CNRC.

© Conseil national de recherches du Canada 2007. Tous droits réservés.

Il est interdit de reproduire, de sauvegarder ou de transmettre quelque partie de la présente publication dans quelque format ou de quelque façon sans le consentement écrit de l'éditeur, à l'exception des conditions suivantes.

Le Conseil national de recherches du Canada accorde aux particuliers le droit de faire des copies individuelles pour leur usage personnel. Toute personne peut reproduire de courts extraits des articles de la Revue pour autant que les droits moraux de l'auteur soient respectés et que la mention de provenance soit clairement indiquée. Il est de convenance de demander le consentement de l'auteur avant de faire mention de son travail.

On obtiendra l'autorisation de reproduire des articles à d'autres fins que l'usage personnel (tel qu'on l'a décrit ci-dessus) auprès du Conseil national de recherches du Canada pour autant que des redevances de droits d'auteurs de 7,00 $/copie soient versées au Access Copyright, The Canadian Copyright Licensing Agency, 1, rue Yonge, bureau 800, Toronto, ON M5E 1E5, Canada.

*La permission ci-dessus ne s'applique pas à la reproduction à grande échelle, telle que la reproduction aux fins de distribution générale, publicitaire ou promotionnelle, de compilation de nouveaux ouvrages collectifs ou de revente. Dans de tels cas, il faudra ratifier une entente particulière avec l'éditeur, le Conseil national de recherches du Canada, Ottawa, ON K1A 0R6, Canada.

Renseignements sur l'abonnement

Journal canadien des sciences halieutiques et aquatiques (ISSN 0706-652X) est une publication mensuelle du Conseil national de recherches du Canada. Le prix de l'abonnement annuel en 2007 au Canada (courrier de deuxième classe) est de 1051 $CAN pour les organismes et de 325 $CAN pour les particuliers. À l'étranger (y compris les É.-U.), le prix de l'abonnement est de 1051 $US pour les organismes et de 325 $US pour les particuliers. L'expédition par avion exige des frais de 150 $US en sus du prix d'abonnement à l'étranger. Les clients du Canada doivent ajouter la TPS de 6 % (numéro d'entreprise 12149 1807 RT 0275). Les abonnements sont pour l'année civile. Tout paiement doit être adressé au Receveur général du Canada, crédit du CNRC. Le prix par numéro est de 110 $ pour les organismes et de 35 $ pour les particuliers. Le prix des hors-série varie. Les membres des sociétés canadiennes de sciences et de génie bénéficient de taux préférentiels en s'abonnant via leurs sociétés respectives.

Aucun remboursement ne sera accordé ni aucune annulation acceptée une fois que les livraisons auront commencé. Les réclamations de numéros manquants devront être soumises dans les quatre mois (Amérique du Nord) ou dans les six mois (à l'extérieur de l'Amérique du Nord) suivant la date de publication. L'éditeur ne fournira de numéros manquants que si le document a été perdu pendant l'expédition et que si le stock le permet. Adressez tout changement d'adresse ou toute question quant à l'abonnement au : Bureau des abonnements, Presses scientifiques du CNRC, Conseil national de recherches Canada, Ottawa, ON K1A 0R6, Canada; téléphone : 613-993-9084; télécopieur : 613-952-7656; courriel : pubs@nrc-cnrc.gc.ca.

On peut obtenir les fichiers rétrospectifs sur **microforme** auprès de UMI, P.O. Box 1346, Ann Arbor, MI 48106-1346, É.-U., et auprès de Micromedia Ltée, 20, rue Victoria, Toronto, ON M5C 2N8, Canada.

À partir de 1996, tous les numéros de *Journal canadien des sciences halieutiques et aquatiques* sont accessibles sur le Web. On trouvera des renseignements sur les tarifs à pubs.nrc-cnrc.gc.ca.

RAPID COMMUNICATION / COMMUNICATION RAPIDE

Remote sensing of particle depletion by coastal suspension-feeders

Jon Grant, Gary Bugden, Edward Horne, Marie-Claude Archambault, and Michel Carreau

Abstract: Marine bivalves have been designated ecosystem engineers owing to their capacity to control estuarine water quality, particle dynamics, and primary production. Globally, bivalves have higher production than any other cultured animal. Large populations of natural, invasive, and cultured bivalves are suggested to cause changes in coastal ecosystem function through suspension-feeding of particles and biodeposition of waste materials. Association of bivalves with particle depletion is a trophic tenet of coastal ecosystems, but there are no previous observations of this process except at small scales. Using airborne hyperspectral remote sensing, we show direct evidence of aquaculture impacts at the ecosystem scale (kilometres), documenting significant depletion of phytoplankton through a blue mussel (*Mytilus edulis*) farm in eastern Canada, compared with dispersion in circulation model results without mussels. Understanding of factors controlling primary production and ecosystem processes in the coastal zone is critical in light of growing reliance on this region for development and resource extraction worldwide.

Résumé : Dans les estuaires, les bivalves marins sont considérés comme des ingénieurs de l'écosystème, car ils sont capables de contrôler la qualité de l'eau, la dynamique des particules et la production primaire. À l'échelle globale, les bivalves ont une production plus importante que tout autre animal élevé en culture. On croit que les fortes populations de bivalves naturels, envahissants et cultivés dans les écosystèmes côtiers causent des changements dans le fonctionnement de l'écosystème par l'intermédiaire de leur alimentation à partir des particules en suspension et de la biodéposition de leurs déchets. L'association des bivalves avec la réduction des particules est l'un des principes trophiques fondamentaux de l'étude des écosystèmes côtiers, mais il n'existe pas d'observations antérieures de ce processus, excepté à de petites échelles. À l'aide de la télédétection aérienne hyperspectrale, nous démontrons de façon directe les impacts de l'aquaculture à l'échelle de l'écosystème (kilomètres), en illustrant une réduction significative du phytoplancton à travers un élevage de moules bleues (*Mytilus edulis*) dans l'est du Canada par comparaison à la dispersion prédite par l'utilisation d'un modèle de circulation en l'absence de moules. La compréhension des facteurs qui contrôlent la production primaire et les processus de l'écosystème dans la zone côtière est indispensable, compte tenu de la dépendance de plus en plus grande dans laquelle nous nous trouvons de cette région marine pour le développement et l'extraction des ressources à l'échelle de la planète.

[Traduit par la Rédaction]

Through suspension-feeding and release of fecal material and nutrients, bivalves often play a dominant role in elemental cycling in coastal waters. Ecosystems such as Chesapeake Bay have undergone drastic changes in water clarity, nutrient levels, aquatic plant growth, and zooplankton community structure as oyster stocks were overharvested (Newell 2004). In areas of San Francisco Bay, the spring bloom has been eliminated via suspension-feeding by introduced clam populations (Cloern 1982). In eastern Canada, the native blue mussel *Mytilus edulis* is cultured off-bottom extensively in shallow bays and estuaries. Owing to the pervasive nature of culture operations, we hypothesised that "seston

Received 4 October 2006. Accepted 30 January 2007. Published on the NRC Research Press Web site at http://cjfas.nrc.ca on 6 March 2007.
J19576

J. Grant[1] **and M.-C. Archambault.** Department of Oceanography, Dalhousie University, Halifax, NS B3H 4J1, Canada.
G. Bugden. Ocean Sciences Division, Fisheries and Oceans Canada, Bedford Institute of Oceanography, P.O. Box 1006, Dartmouth, NS B2Y 4A2, Canada.
E. Horne. Ecosystem Research Division, Fisheries and Oceans Canada, Bedford Institute of Oceanography, P.O. Box 1006, Dartmouth, NS B2Y 4A2, Canada.
M. Carreau. Synexus Global Inc., 1801 McGill College, Suite 1060, Montreal, QC H3A 2N4, Canada.

[1]Corresponding author (e-mail: jon.grant@dal.ca).

 doi:10.1139/F07-021 © 2007 NRC Canada

Fig. 1. Inset: Tracadie Bay, Prince Edward Island, eastern Canada. Extent of blue mussel culture farms (boxes) in Tracadie Bay, Prince Edward Island. The region near the tidal inlet is occupied by a large tidal flat and is too shallow for culture. The Winter River mouth is used for collection and nursery culture of juvenile mussels. The thick box outline is the extent of CASI flight data shown and analysed. The area of the farm completely within the box outline is 0.21 km^2 with an average depth of 3 m. The density of mussels is variable within culture, but an average over the farm would be 3–10 individuals·m^{-3}, or approximately 2–6 million mussels.

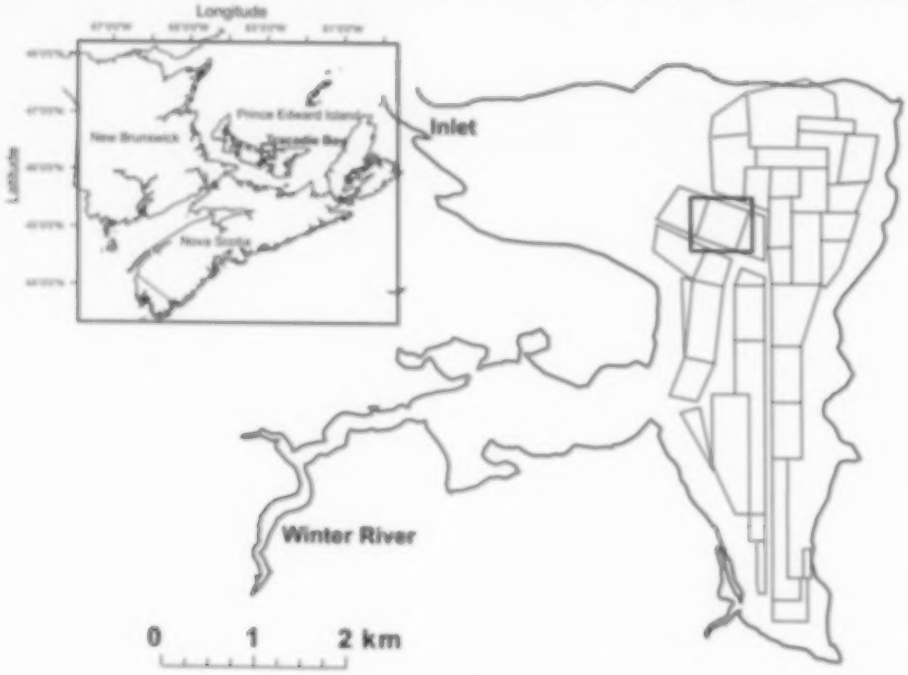

depletion" (clarification of the water by grazers) was likely. Particle fields in estuarine systems are especially dynamic owing to water movement controlled by winds and tides. Although the means of observing potentially ephemeral phenomenon at the ecosystem scale are limited, aircraft remote sensing provides the right combination of spectral properties, altitude, and resolution to optimize observation of aquaculture-influenced ecosystems. We undertook remote sensing to elucidate large-scale patterns of chlorophyll distribution and their regulation by cultured suspension-feeders in Prince Edward Island, Canada, site of the largest blue mussel culture operations in North America.

Although suspension-feeding bivalves are cultured by a variety of methods, hanging culture on ropes (longlines) is a common technique, creating "curtains" of filtering elements and three-dimensional structure in the estuarine water column. Tracadie Bay on the north shore of Prince Edward Island is an extensively cultured shallow estuary (<6 m depth) where mussel farming occupies >50% of the bay's surface area (see Fig. 1 for details of the farms). Remote sensing images of Tracadie Bay were obtained in August 2000 using a compact airborne spectrographic imager (CASI), which recorded 19 spectral bands from 400–1000 nm at 1 m resolution. Bands 4, 5, and 8 centred on wavelengths 522.1, 547.4, and 607.7 nm, respectively, were used to generate an algorithm for chlorophyll *a* as an indicator of phytoplankton biomass, similar to that used previously for coastal chlorophyll (Sathyendranath et al. 2004). Simultaneous collection of water samples for ground-truthing was used to fit a power function to these bands. Although the entire bay was imaged from multiple overflights, only a subsection of the image and a specific farm are analysed here (Fig. 1) to test the hypothesis that chlorophyll reduction within the farm was a consequence of bivalve feeding.

The calibrated image showed a V-shaped patch of high chlorophyll entering the farm region, with values up to 54 $\mu g \cdot L^{-1}$ (Fig. 2*a*), similar to Tracadie Bay maxima in Grant et al. (2005). Rows of mussel longlines were clearly visible. Ebb tidal currents directed this patch through the farm in a northwestern direction (mean speed = 1 $cm \cdot s^{-1}$). Even in the raw form of the image, there was strong indication of reduced chlorophyll load through the farm. To reduce small-scale spatial variation, we analysed neighbourhood means at a 10 m resolution within a geographic information system (GIS; ArcInfo v.9.1 ESRI Redlands, California) and contoured the resulting data. This smoothing integrated the extreme values and indicated peak contours of 7 $\mu g \cdot L^{-1}$, declining to <1 $\mu g \cdot L^{-1}$ as water flowed through the farm. Application of spatial clustering via BoundarySeer (www.terraseer.com) delineated seven significant boundaries between chlorophyll regions ($p < 0.05$), corresponding to successive depletion of chlorophyll in the predominant flow direction (Fig. 2*b*). This analysis confirms significant particle reduction through the farm.

Although compelling, these data require verification that bivalve filtration was responsible for particle reduction rather than dilution, sinking, or other loss processes. We refined the mesh of an existing two-dimensional hydrody-

© 2007 NRC Canada

Fig. 2. (*a*) CASI image of the analysed area showing the gradient of phytoplankton biomass calibrated as chlorophyll *a* through the blue mussel farm. Central arrows are ~1 cm·s^{-1}. (*b*) Image of neighbourhood mean statistics of CASI chlorophyll (10 m resolution). Significant boundary regions of chlorophyll from neighbourhood mean CASI values delineated with spatial clustering indicate a progressive decline in chlorophyll through the studied farm. Mean chlorophyll concentrations are indicated within the clusters. The chlorophyll scale has a different range compared with Fig. 2*a*. Transect lines were used to obtain chlorophyll value cross sections. (*c*) Finite element model output of chlorophyll dispersion as a conservative tracer (mussels absent) for the tidal conditions at the time of the CASI overflight. A pulse of chlorophyll was modelled entering the farm area as in Fig. 2*a*. Although the entire bay was included in the hydrodynamic model, only the studied farm area is shown. (*d*) Transects sampled through the CASI image and the finite element model to illustrate chlorophyll gradients from the phytoplankton patch through the mussel farm. The solid line is from the CASI image and the broken line is from the model prediction. Each line is the mean ± SE of the three transect locations shown in Fig. 2*b*, starting at the bottom of the panel and moving to the northwest.

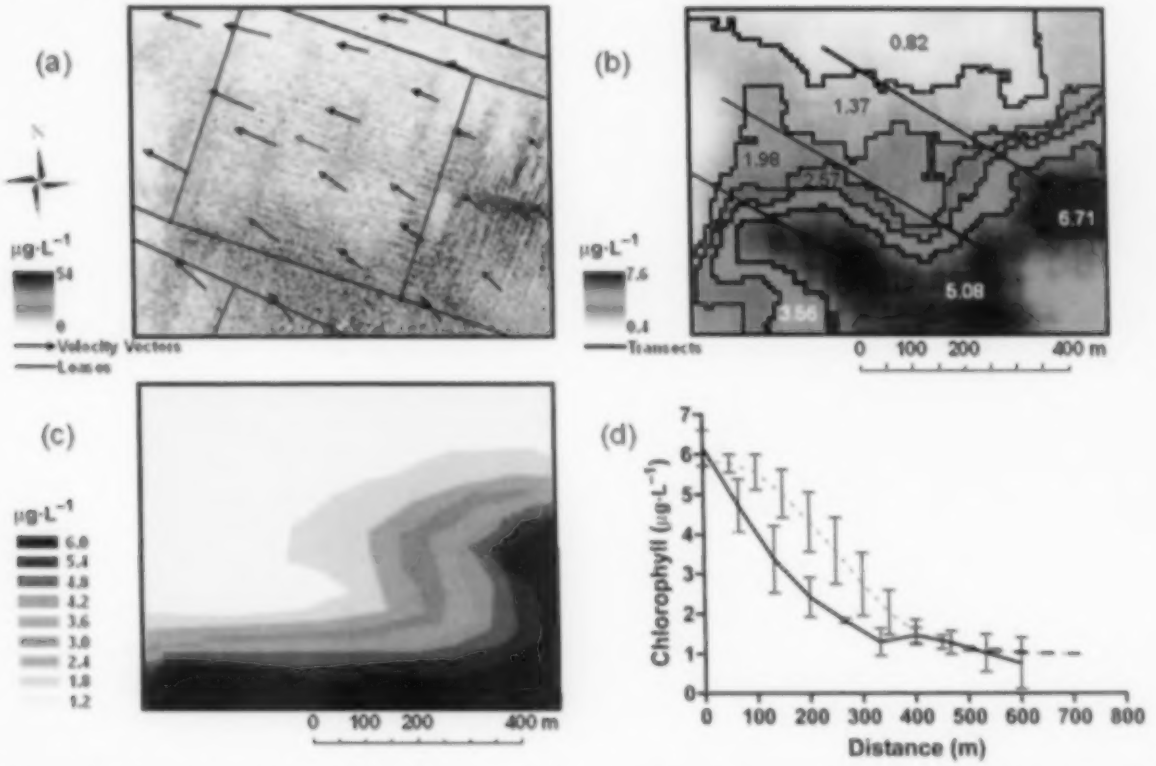

namic model of Tracadie Bay (Grant et al. 2005) to simulate phytoplankton concentration in the absence of mussels, hypothesizing that dispersion could not account for the observed degree of seston loss. In the farm area, the finite element mesh was modified to 100 m node spacing. A conservative tracer was introduced to simulate the V-shape shown in Fig. 2*a* for 1000 s during the middle of the ebb tide. Tidal forcing (range = 60 cm) of the model was specific to the date and time of the CASI flight. The model scenario without mussels indicated that 1 h after the tracer was introduced, there was some dispersion of chlorophyll from the high patch, reflecting advection along the current vectors (Fig. 2*c*). Representative cross sections sampled through the model (Fig. 2*b*) showed that chlorophyll was diluted to half of its starting level at a distance of 300 m from the source (Fig. 2*d*). In contrast, CASI observations plotted along similar transects demonstrated that chlorophyll was reduced to 50% in 150 m from the source, indicating a much more rapid loss through the farm than can be explained by simple dilution (Fig. 2*d*). Analysis of covariance indicated a significant difference between the mean loss curves ($p = 0.00023$), with greater chlorophyll reduction observed in CASI images than in the model scenario without mussels. Based on the modelled loss curve in Fig. 2, a change in chlorophyll concentration from 6 to 1 µg·L^{-1} over a period of 1 h corresponds to a horizontal flux of 20 mg·m^{-2}. Our sediment trap studies near the farm site (Grant et al. 2005) demonstrated a vertical chlorophyll flux <1 mg·m^{-2}·h^{-1}, indicating that sinking would make a minimum contribution to short-term particle depletion. Losses because of other suspension-feeders such as fouling tunicates are unlikely, since they were not well established in the bay at the time of the study.

Although remote sensing was able to capture an image of seston depletion, modelling was required to characterize the rate of seston removal in relation to tidal hydrodynamics. Our extensive field and modelling work in Tracadie Bay indicates that pulses of high chlorophyll may be common features emanating from Winter River (Fig. 1), where primary production is stimulated by agricultural inputs (J. Grant et al., unpublished data). The larger-scale CASI image (not

© 2007 NRC Canada

shown) indicates that the observed patch of high chlorophyll was the only elevated phytoplankton biomass in the bay at this time. The scale of seston depletion is regulated by patch size of chlorophyll entering a farm area, in this case on the order of 1 km. High chlorophyll patches leaving the Winter River will be maintained under calm conditions but dispersed in the shallow waters of the bay during wind events. The integrity of the patches and their detection through remote sensing will be a function of mixing in the bay. We therefore do not expect to observe seston depletion in every image, since the patchiness of phytoplankton and their control by grazers are a function of culture location, tidal stage, weather, season, and proximity to the well-flushed tidal inlet.

Beyond documenting seston depletion, our results demonstrate an ecosystem-wide example of top-down regulation of nutrient flux. Phytoplankton blooms produced from agricultural eutrophication in Winter River are grazed by cultured mussels, resulting in rapid amelioration of nutrient loading. A proportion of these nutrients are removed from Tracadie Bay when mussels are harvested. The ability of bivalves to clean coastal waters via filtration has previously been proposed as a mitigation technique for eutrophication (Officer et al. 1982; Wilkinson et al. 1996).

Previous application of remote sensing to aquaculture has been used only to catalog land use changes (e.g., shrimp ponds) (Giap et al. 2004). Although remote sensing has been employed to infer water quality features of coastal locations (Ruhl et al. 2001), our study is the first application of remote sensing to investigate ecosystem processes involving aquaculture. Given the potential impact of bivalves on particle fields, remote sensing should provide an effective tool for its quantification. Our image represents the first time that particle depletion by suspension-feeders has been directly observed over large spatial scales. Spatial statistics allow definition of distinct depletion zones as phytoplankton are grazed while being advected through the farm.

Phytoplankton are an obviously important component of the bay system, providing the basis of the food chain not only for mussels but also for zooplankton, juvenile fish, and benthic communities. The addition of herbivores such as cultured suspension-feeders has been suggested to cause significant changes in trophodynamics of coastal ecosystems (Newell 2004). The worldwide growth in coastal aquaculture will impose even greater suspension-feeder biomass into coastal waters as aquaculture overtakes harvest fisheries in seafood production over the next 20 years (Josupeit 2006). Most of these effects are implemented via "seston depletion", a term that has been enshrined in coastal marine ecology. The effects of suspension-feeders on coastal ecosystems have been the topic of several books and numerous papers (Dame and Olenin 2005). Despite system-level controls attributed to suspension-feeding, these influences have previously been undocumented except at small scales and (or) using point measurements. For example, moored instruments or short-term sampling has been used to examine reduction of chlorophyll (25%–80%) through bivalve culture at scales of $10–10^2$ m (Strohmeier et al. 2005; Grizzle et al. 2006); ecosystem effects have only been inferred. Temporal and spatial variation in hydrodynamics, phytoplankton biomass, and suspension-feeder distribution makes it difficult to observe seston depletion, but it is demonstrated herein to be substantial at 10^2 m (50%) and extending to the entire length and breadth of a farm (10^3 km scale). Although remote sensing is a powerful tool to detect seston depletion, its broader application will be dependent on further studies that link local particle removal with system-level food limitation. Even in Tracadie Bay where cultured shellfish biomass is extensive, seston depletion must be interpreted against a background of hydrodynamics, nutrient input, and primary production, which regulate the spatial mosaic of coastal phytoplankton distribution.

Acknowledgements

We thank Peter Cranford for providing assistance in the field and Cedric Bacher for comments on the manuscript. Don Forbes oversaw the CASI logistics. This study was funded by the Natural Sciences and Engineering Research Council of Canada and by Fisheries and Oceans Canada.

References

Cloern, J.E. 1982. Does the benthos control phytoplankton biomass in South San Francisco Bay? Mar. Ecol. Prog. Ser. **9**: 191–202.

Dame R.F., and Olenin, S. 2005. Comparative roles of suspension-feeders in ecosystems. Kluwer Academic Publishers, New York.

Giap, D., Yi, Y., and Yakupitiyage, A. 2004. Remote sensing to assess shrimp farming development in Haiphong of Vietnam. J. Aquacult. Trop. **19**: 201–214.

Grant, J., Cranford, P., Hargrave, B., Carreau, M., Schofield, B., Armsworthy, S., Burdett-Coutts, V., and Iburra, D. 2005. A model of aquaculture biodeposition for multiple estuaries and field validation at blue mussel (*Mytilus edulis*) culture sites in eastern Canada. Can. J. Fish. Aquat. Sci. **62**: 1271–1285.

Grizzle, R.E., Greene, J.K., Luckenbach, M.W., and Coen, L.D. 2006. A new in situ method for measuring seston uptake by suspension-feeding bivalve mollusks. J. Shellfish Res. **25**: 643–650.

Josupeit, H. 2006. FAO Globefish reports. Available from http://www.globefish.org/ [accessed June 2006].

Newell, R.I.E. 2004. Ecosystem influences of natural and cultivated populations of suspension-feeding bivalve molluscs: a review. J. Shellfish Res. **23**: 51–62.

Officer, C.B., Smayda, T.J., and Mann, R. 1982. Benthic filter feeding: a natural eutrophication control. Mar. Ecol. Prog. Ser. **9**: 203–210.

Ruhl, C.A., Schoellhamer, D.H., Stumpf, R.P., and Lindsay, C.L. 2001. Combined use of remote sensing and continuous monitoring to analyse the variability of suspended-sediment concentrations in San Francisco Bay, California. Estuar. Coast. Shelf Sci. **53**: 801–812.

Sathyendranath, S., Platt, T., Irwin, B., Horne, E., Borstad, G., Stuart, V., Payzant, L., Mauss, H., Kepkay, P., Li, W.K.W., Spry, J., and Gower, J. 2004. A multispectral remote sensing study of coastal waters off Vancouver Island. Int. J. Remote Sens. **25**: 893–919.

Strohmeier, T., Aure, J., Duinker, A., Castberg, G., Svardal, A., and Strand, O. 2005. Flow reduction, seston depletion, meat content and distribution of diarrhetic shellfish toxins in a long-line blue mussel (*Mytilus edulis*) farm. J. Shellfish Res. **24**: 15–24.

Wilkinson, S.B., Zheng, W.Z., Allen, J.R., Fielding, N.J., Wanstall, V.C., Russell, G., and Hawkins, S.J. 1996. Water quality improvements in Liverpool docks: the role of filter feeders in algal and nutrient dynamics. Mar. Ecol. **17**: 197–211.

© 2007 NRC Canada

Toxicity of copper to larval *Pimephales promelas* in the presence of photodegraded natural dissolved organic matter

Marjorie L. Brooks, Joseph S. Meyer, and Connie J. Boese

Abstract: Copper (Cu) complexation with natural dissolved organic matter (DOM) mitigates Cu bioavailability to aquatic biota by decreasing the activity of the cupric ion ($[Cu^{2+}]$). However, DOM is photochemically unstable. In a previous study, we demonstrated that irradiation (~13 days sunlight) of DOM collected from a river decreased its binding-site density for Cu by 45%, but increased binding-site density in wetland DOM by 147%. Binding-site densities correlated positively with ketones and aldehydes (C-II groups). Herein, we determined the mortality of larval fathead minnows (FHM; *Pimephales promelas*) as a function of $[Cu^{2+}]$ in 96 h static-renewal toxicity tests without DOM. Next, we calculated $[Cu^{2+}]$ in control and photooxidized DOM and then predicted mortality of larval FHM in toxicity tests. Observed mortalities agreed with predictions ($r^2 \approx 0.96$) in treatments with lowest binding-site densities and proportions of C-II groups (highest $[Cu^{2+}]$). However, treatments with ~50% lower $[Cu^{2+}]$, containing higher proportions of C-II groups, had equally high mortalities and poorer fits with predictions ($r^2 \approx 0.75$), possibly indicating that Cu bound to C-II groups are bioavailable. To our knowledge, this study is the first to predict and then directly test the effects of DOM photooxidation on Cu toxicity.

Résumé : La formation de complexes entre le cuivre (Cu) et la matière organique dissoute (DOM) naturelle atténue la biodisponibilité du Cu aux organismes aquatiques en réduisant l'activité de l'ion cuprique ($[Cu^{2+}]$). Cependant, la DOM est photochimiquement instable. Dans une étude antérieure, nous avons démontré qu'une irradiation (~13 jours d'ensoleillement) de la DOM récoltée dans une rivière réduit la densité de ses sites de liaison avec le Cu de 45 %, alors que l'irradiation augmente la densité des sites de liaison de la DOM de terres humides de 147 %. Il y a une corrélation positive entre la densité des sites de liaison et les cétones et les aldéhydes (groupes C-II). Dans la présente étude, nous déterminons la mortalité de larves de têtes-de-boule (FHM; *Pimephales promelas*) en fonction de $[Cu^{2+}]$ après 96 h dans des tests de toxicité à renouvellement statique en l'absence de DOM. Nous avons ensuite calculé $[Cu^{2+}]$ dans des conditions témoins et en présence de DOM photooxydée et prédit la mortalité des larves de FHM dans les tests de toxicité. Les mortalités observées s'accordent aux prédictions ($r^2 \approx 0,96$) dans les situations expérimentales correspondant aux densités les plus faibles de sites de liaison et de proportions de groupes C-II ($[Cu^{2+}]$ les plus fortes). Cependant, dans les conditions expérimentales avec $[Cu^{2+}]$ ~50 % inférieures et de plus fortes proportions de groupes C-II, les mortalités sont également élevées et correspondent moins bien aux prédictions ($r^2 \approx 0,75$), ce qui indique peut-être que Cu lié aux groupes C-II demeure biodisponible. À notre connaissance, notre étude est la première à prédire les effets de la photooxydation de la DOM sur la toxicité du Cu et à les vérifier directement.

[Traduit par la Rédaction]

Introduction

Complexation with dissolved organic matter (DOM) in aquatic ecosystems can greatly decrease the toxicity of metals. For copper (Cu), such binding decreases the chemical activity of the cupric ion ($[Cu^{2+}]$), which is the most toxic Cu species (Playle et al. 1993; Erickson et al. 1996; MacRae et al. 1999). DOM originates from autochthonous (aquatic algae, bacteria, and macrophytes) and allochthonous (vascular, terrestrial plants) sources. With concentrations of 2–10 $mg \cdot L^{-1}$ dissolved organic carbon (DOC, which comprises about half of DOM; Thurman 1985), DOM typically comprises the largest pool of organic or inorganic ligands for Cu in natural waters (McKnight and Aiken 1998). However, the binding affinity of DOM for Cu varies by orders of magnitude depending on the DOM source (McKnight et al. 1983;

Received 23 February 2006. Accepted 11 January 2007. Published on the NRC Research Press Web site at http://cjfas.nrc.ca on 16 March 2007.
J19194

M.L. Brooks.[1] Department of Zoology and Physiology, University of Wyoming, Laramie, WY 82071, USA; National Center for Ecological Analysis and Synthesis, 735 State Street, Suite 300, Santa Barbara, CA 93101, USA.[2]
J.S. Meyer and C.J. Boese. Department of Zoology and Physiology, University of Wyoming, Laramie, WY 82071, USA.

[1]Corresponding author (e-mail: brooks@nceas.ucsb.edu).
[2]Present address.

 doi:10.1139/F07-012 © 2007 NRC Canada

Cabaniss and Shuman 1988; Breault et al. 1996). Consequently, at the same concentration of DOC, mortality of aquatic biota exposed to Cu can vary by a factor of two among DOM sources (Richards et al. 2001; De Schamphelaere et al. 2003; Ryan et al. 2004).

In addition to apparent source-related differences, DOM is photochemically unstable. Photooxidation by sunlight can alter DOM in several important ways, such as photomineralization, photobleaching, and production of low molecular weight (LMW) organics. Photomineralization converts organic carbon to CO and dissolved inorganic carbon (defined as $CO_2 + H_2CO_3 + HCO_3^- + CO_3^{2-}$; Miller and Zepp 1995; Xie et al. 2004). Sunlight can remove 15%–50% of DOC from natural waters in the span of 2–11 days (Molot and Dillon 1997; Moran et al. 2000; Brooks et al. 2007). Photobleaching (loss of absorbance of ultraviolet and visible radiation) is an indirect measure of chemical transformation in the DOM remaining after photomineralization. For example, photobleaching of DOM across the ultraviolet spectrum (UV, 280–400 nm) normalized by DOC concentration can indicate loss of sp^2 hybridized bonds, (i.e., double bonds in aromatics and olefins; Weishaar et al. 2003).

The photochemistry of DOM can differ considerably between DOM leached from algal cultures and allochthonous DOM, particularly with regard to production of LMW organics. Irradiation of allochthonous DOM cleaves its large macromolecules into LMW organics, such as carboxylic acids that are microbially labile (biologically available carbon sources; Moran and Zepp 1997; Bertilsson and Tranvik 2000; Miller et al. 2002). DOM from algal cultures is photobleached, indicating chemical transformation (Obernosterer and Benner 2004). However, irradiation of algal DOM does not produce labile compounds (Tranvik and Kokalj 1998) nor is it photomineralized (Obernosterer and Benner 2004). Differences in photoreactivity due to algal input are attenuated in natural waters because lakes and streams receive a mixture of allochthonous DOM from surface runoff in addition to autochthonous inputs. Thus, is variation in Cu–DOM complexation due to source-related differences in precursor organics or to DOM photodegradation, or both?

Little is known about effects of photooxidation of natural DOM on its complexation of Cu. In a previous study, irradiation of the same wetland and riverine DOM used in our current study had unexpectedly opposite effects on Cu–DOM complexation (Brooks et al. 2007). Irradiation of DOM collected from a wetland increased its binding-site density for Cu by 147%, but decreased binding-site density in DOM from a river by 45%. Binding affinities of the two DOM types were virtually identical after photooxidation. The net outcome of photochemical changes was that the wetland DOM bound 148% more Cu per milligram DOC than the riverine DOM. Because photooxidation of DOM profoundly altered Cu complexation and the $[Cu^{2+}]$ in solution, we predicted that irradiation of riverine and wetland DOM would also alter Cu toxicity. The specific objectives of this study were to (*i*) quantify how photooxidation and source of DOM alter Cu toxicity to larval fathead minnows (FHM, *Pimephales promelas*) and (*ii*) examine the relationship between $[Cu^{2+}]$ and Cu toxicity in the presence of DOM.

Materials and methods

Study sites, DOM collection, and irradiation of DOM

We collected DOM during spring runoff (16 and 17 June 1999) from two surface waters with contrasting hydrology: Chimney Park wetland (41.05°N, 106.37°W, 2715 m altitude; designated CPWDOM) and the Laramie River (41.10°N, 106.19°W, 2280 m; designated LRDOM) in the Rocky Mountains of Wyoming, USA. Chimney Park, a palustrine wetland, receives a mixture of organic input from the adjacent lodgepole pine (*Pinus contorta*) forest, willows (*Salix* spp.), emergent sedges (*Carex* sp.), and submersed vascular macrophytes (*Myriophylum* sp.) colonized by epiphytic microbial communities. The Laramie River is a third-order, cobble-bottom river that drains a mixed *Poaceae* grassland – lodgepole pine watershed.

After filtration through prerinsed 10, 5 (Hytrex II, Osmonics Incorporated), 1 (Corning Costar Corporation), and 0.2 µm filters (Corning Costar Corporation), natural waters were passed through a H^+ cation-exchange resin that removed ≥95% of all metals (Ca, K, Mg, Na, Cd, Cu, Fe, Ni, Pb, and Zn). Processing for ~8 h through a portable reverse osmosis system (PROS/2S, RealSoft; Serkiz and Perdue 1990) increased initial DOC concentrations ([DOC]) from 14.8 to 606 mg DOC·L^{-1} (CPWDOM) and from 7.5 to 353 mg DOC·L^{-1} (LRDOM). Mass balance calculations showed that 95% of DOC was recovered by reverse osmosis. Maurice et al. (2002) demonstrated that reverse osmosis does not alter DOM structure or elemental composition from that of raw water. Concentrates were stored in the dark at 4 °C in acid-washed, ashed (500 °C for 2 h) borosilicate bottles at pH 6. Storage pH is extremely important because natural organics rapidly undergo spontaneous hydrolysis if stored at pH near or below 2 (Schwarzenbach et al. 1993). Monitoring of storage effects over the span of several months indicated no change in [DOC] or the rate of DOC loss during irradiation.

We photodegraded DOM for toxicity tests at radiation intensities approximating natural sunlight. Prior to irradiation, we normalized photoreactivity by diluting DOM concentrates to a standard absorbance of 0.33 ± 0.02 absorbance units (a.u.) (mean ± standard deviation (SD)) at 350 nm in a 1 cm cell, resulting in [DOC] of ~40 mg C·L^{-1} (CPWDOM) and ~30 mg C·L^{-1} (LRDOM). We irradiated DOM solutions in tightly capped, quartz Hungate tubes (14.6 cm × 1.9 cm) in a solar simulator (Atlas Suntest CPS+) under a full-spectrum 1.0 kW xenon lamp for 72 h in a continuous-circulation cooling bath (25.4 ± 1.3 °C; mean ± SD). To obtain adequate volumes of irradiated DOM, solutions were irradiated during several separate sessions in the solar simulator, then pooled to standardize any potential variation among irradiation sessions. Radiation intensities were measured with an International Light radiometer (model 1400). Compared with noontime cloudless conditions recorded at the field sites on 21 June 2003, intensities within the solar simulator were 1.4 times greater for UV-B (detector: 265–332 nm), 1.8 times for UV-A (subtraction of UV-B from total UV detector: 250–400 nm), or equal to photosynthetically active radiation (detector: 400–1000 nm). In 1 day, surface water theoretically receives the equivalent of 7.6 h of noon sun (= 12 h × 2 × π^{-1}) (Miller and Zepp 1995). Therefore, 72 h of irradiation in the solar simulator at 1.4 times field in-

© 2007 NRC Canada

tensities of ambient UV-B radiation theoretically equaled 13.2 days of UV-B at our field sites. Thus, 13.2 days of full spectrum exposure is an environmentally reasonable period of ambient solar exposure in a region that receives 75% of cloudless summer sunlight (Curtis and Grimes 2004).

Water chemistry

Unless otherwise designated, all reagents were analytical grade, except HCl (trace-metal grade, Spectrum) and HNO_3 (OPTIMA, Seastar Chemicals). We used the higher-grade acids for pH adjustment during titrations and geochemical analyses. All glassware and labware were soaked in 18% analytical-grade HNO_3 (*v/v*) for at least 2 h and rinsed five times with 18 MOhm water (Milli-Q, Millipore Corporation). The 18 MOhm water was used for analytical dilutions and analytical blanks. Dionized water was used to dilute well water for toxicity tests.

Chemistries of DOM solutions for toxicity tests were directly measured by a variety of analytical methods. Anions (F^-, Cl^-, NO_3^-, PO_4^{3-}, SO_4^{2-}) were analyzed by ion chromatography (Dionex, model DX-100). Cations (Ca^{2+}, Mg^{2+}, Na^+, K^+), Ni, and Zn were analyzed by flame atomic absorption spectrophotometry (Perkin-Elmer, model 372). Concentrations of other trace metals were determined by graphite furnace atomic absorption spectrophotometry with Zeeman background correction (Varian, model SpectrAA-600). [DOC] were analyzed by catalytic combustion on a total organic carbon analyzer (Shimadzu, model 5000A) in samples acidified to pH < 3 and sparged for 8 min with hydrocarbon-free air using regular-sensitivity catalyst. pH was measured with a meter (Corning model 340) and a Corning flat-surface combination pH electrode. Alkalinity of water samples was determined by titration to pH 4.5 with H_2SO_4 according to standard methods (APHA 1995).

Toxicity tests

Larval FHM for all bioaccumulation experiments came from a resident brood population of FHM at the University of Wyoming. When fully "eyed-up" and nearing hatch (~5 days after spawn), tiles containing FHM eggs were placed in laboratory incubators containing test matrix water that was free of added Cu or DOM (Table 1). After hatching, we collected larval fish for each test within 24 h and immediately started a test. Larvae were not fed during the tests.

Carboys and 150 mL test chambers were acid-washed by soaking in 18% HNO_3 (*v/v*) for at least 2 h, then rinsed five times before use with 18 MOhm water. Carboys and test chambers were preconditioned for each test by filling with the appropriate test solution, allowing potential adsorption to occur for >24 h, and refilling with fresh test solution. We were unable to detect any loss of Cu in preconditioned carboys and test chambers. Test solutions were mixed >24 h prior to the start of each test to allow sufficient time for maximal Cu–DOM complexation (Ma et al. 1999). Copper was added as $CuCl_2$. Any solutions containing DOM were stored at 4 °C in the dark until ~3 h before introducing fish, during which time the solutions warmed to the test temperature of 25 °C. We measured pH, alkalinity, and hardness in each exposure chamber at the onset and the end of each toxicity test.

Table 1. Chemistry of matrix water solutions used in toxicity tests without added dissolved organic carbon (DOC; tests NODOC 1 and NODOC 2) and in toxicity tests (TOX 1 and TOX 2) using dissolved organic matter (DOM) collected from Chimney Park wetland (CPW) and Laramie River (LR) in southeast Wyoming, USA.

					Concentration (μmol·L^{-1})								
DOC source	Experiment	DOC (mg·L^{-1})	pH	Alkalinity (mequiv.·L^{-1})	Ca^{2+}	Mg^{2+}	Na^+	K^+	Cl^-	NO_3^-	SO_4^{2-}	Cu	Fe
	NODOC 1, NODOC 2	<0.10	7.1	0.64	109	150	52	5.7	22	15	29	Varied[a]	<0.02
CPW	TOX 1	Varied[b]	7.0	0.60	116	122	122	2.7	68	108	42	1.5±0.07	0.17
	TOX 2	Varied[b]	6.8	0.61	216	164	146	6.7	138	34	68	1.4±0.06	0.13
LR	TOX 1	Varied[b]	6.8	0.48	137	126	175	6.9	44	124	55	1.3±0.07	0.65
	TOX 2	Varied[b]	6.9	0.60	184	163	155	7.1	3.9	51	46	1.8±0.01	0.56

Note: The matrix water of all tests was a mixture of deionized and well waters. pH, alkalinity, hardness, and Cu encompass values from all treatments of varying DOC concentration (n = 10). Values for anions, cations, and Fe were taken from analyses of the exposure solutions irradiated for 72 h and diluted to ~2.5 mg DOC·L^{-1} in each toxicity test. Cu values are mean ± standard deviation (SD). The following analytes were below detection limits (detection limits in μmol·L^{-1} in parentheses): Cd (0.002), F^- (0.74), Fe (0.02), Ni (0.54), Pb (0.002), PO_4^{3-} (2.48), and Zn (0.092).

[a]Cu concentrations ranged 0.01–2.9 μmol·L^{-1} (for specific values see Brooks 2003).

[b]For DOC concentrations see Table 2.

© 2007 NRC Canada

Table 2. Measured dissolved organic carbon (DOC) concentrations (mean ± standard deviation (SD)) and cupric ion activity ($[Cu^{2+}]$) determined by MINTEQA2 calculations in unirradiated (0 h) and irradiated (72 h) dissolved organic matter (DOM) from Chimney Park wetland (CPWDOM) and the Laramie River (LRDOM) using average DOC concentrations and other chemistries in Table 1 for toxicity tests TOX 1 and TOX 2.

	DOC ($mg \cdot L^{-1}$)				$[Cu^{2+}]$ ($\mu mol \cdot L^{-1}$)			
	CPWDOM		LRDOM		CPWDOM		LRDOM	
Experiment	0 h	72 h	0 h	72 h	0 h	72 h	0 h	72 h
TOX 1	0.8	1.1	0.7	0.7	0.23	0.13	0.21	0.26
	1.5	1.3	1.0	1.1	0.14	0.10	0.16	0.19
	1.7	1.7	1.6	1.3	0.12	0.07	0.08	0.17
	2.3	2.0	1.8	1.7	0.08	0.06	0.06	0.13
	3.0	2.6	2.2	2.0	0.05	0.04	0.05	0.10
TOX 2	0.7±0.67	0.7±0.62	0.6±0.01	0.4±0.03	0.32	0.19	0.36	0.47
	1.4±0.42	1.5±0.08	1.2±0.02	1.2±0.05	0.16	0.08	0.22	0.31
	2.4±0.78	2.5±0.20	2.3±0.07	2.5±0.03	0.09	0.04	0.08	0.17
	3.6±0.41	3.4±0.35	3.3±0.03	3.6±0.16	0.05	0.03	0.05	0.09
	4.7±0.48	4.7±0.38	4.5±0.06	4.8±0.04	0.03	0.01	0.03	0.06

Note: For toxicity test TOX 1, $n = 1$ analytical replicates; for toxicity test TOX 2, $n = 2$ analytical replicates.

We performed two different types of 96 h static-renewal toxicity tests. In one type (TOX 1 and TOX 2), we evaluated the protective effect of DOM before and after photodegradation in treatments standardized to the same series of DOC concentrations. In the other type of test, which lacked added DOC (NODOC A and NODOC B), we determined the concentration–response relationship between $[Cu^{2+}]$ and mortality of larval FHM.

In TOX 1 and TOX 2 tests, larval FHM were exposed to five DOC concentrations from each of the two sources of irradiated and unirradiated DOM with [Cu] held constant (Table 1). TOX 1 was a preliminary test of [DOC] ranging from 0 to 3 $mg \cdot L^{-1}$. In TOX 2, we increased the range of [DOC] to ~0–5 $mg \cdot L^{-1}$ (Table 2). Irradiation of DOM generally photomineralizes 10%–20% of organic carbon to inorganic carbon as CO_2 and CO (Miller and Zepp 1995; Brooks et al. 2007; see also Results). Thus, in the tests with irradiated DOM, we added higher percentages of DOM to test solutions to compensate for loss of DOC due to photomineralization. This protocol standardized irradiated solutions to the same [DOC] as contained in solutions of unirradiated DOM. At each [DOC], three replicate chambers contained 10 fish in 100 mL of toxicity test solution. Before daily replacement, we warmed fresh solutions of test waters to 25 °C to avoid thermal shock to the fish.

No DOM was added to NODOC A and NODOC B tests, which contained a low background [DOC] of 0.1 $mg \cdot L^{-1}$ in the same matrix water used in TOX 1 and TOX 2 tests (Table 1). We exposed fish to a series of five [Cu] ranging from 0.01 to 1.6 $\mu mol\ Cu \cdot L^{-1}$ in NODOC A and from 0.01 to 2.9 $\mu mol\ Cu \cdot L^{-1}$ in NODOC B (see Brooks 2003 for measured [Cu]). Each exposure level had three replicate chambers containing 10 fish per 100 mL solution. From the combined concentration–response relationships of NODOC A and NODOC B, we calculated the expected mortality as a function of $[Cu^{2+}]$.

For all toxicity tests, we calculated $[Cu^{2+}]$ with the geochemical speciation program MINTEQA2 (Version 3.1; Allison et al. 1991). In these MINTEQA2 calculations, we entered measured water chemistries (Table 1) and the conditional stability constants (K_1 and K_2) and binding-site densities ($[L_1]$ and $[L_2]$) for 2-ligand models of Cu–DOM complexation in control and irradiated solutions of the same CPWDOM and LRDOM (Table 3), which were determined in a previous study (Brooks et al. 2007). We did not directly measure $[Cu^{2+}]$ in toxicity solutions because reliable readings with a cupric ion selective electrode required the addition of 0.01 $mol \cdot L^{-1}$ $NaNO_3$ for ionic strength adjustment to stabilize the electrode (Saar and Weber 1982; Christl et al. 2005). Such measures taken at a higher ionic strength would not constitute direct measures.

Because those Cu–DOM binding parameters were determined at pH 6.0 but the toxicity tests were conducted at pH ~6.9, we increased the conditional stability constants by 0.9 $\log_{10}$ units in MINTEQA2 calculations, consistent with a one $\log_{10}$ unit increase in conditional stability constants of Cu–DOM complexes per pH unit from pH 4 to 8.5 (Cabaniss and Shuman 1986; Lu and Allen 2002). The 1:1 ratio of the log$K$ and pH of metal–organic complexation is consistent for many metals and a variety of natural organic compounds: Cu–fulvic acid (Cabaniss and Shuman 1988; Christl et al. 2005); Cu – natural DOM (Lu and Allen 2002); Cu –, Cd –, Al – natural DOM complexes (Kinniburgh et al. 1996); and Al – fulvic acid (Brown and Driscoll 1993; see review in Tipping 2002).

Some variation exists in this 1:1 ratio at high Cu concentrations (total [Cu] > 0.1 $mmol \cdot L^{-1}$) because Cu–DOM complexation changes the electrostatic properties of unoccupied DOM sites. High pH values (pH > 8.4) also alter the ratio (Cabaniss and Shuman 1988; Lu and Allen 2002) by dissociation of protons from phenolic binding sites on DOM (Lu and Allen 2002) or increases in monovalent metal

© 2007 NRC Canada

Table 3. Photochemical effects for controls (0 h) and irradiated (72 h) dissolved organic matter (DOM) collected from Chimney Park wetland (CPWDOM) and Laramie River (LRDOM) (all data from Brooks et al. 2007).

DOM source	Irradiation time (h)	Ligand densities (μmol·mg DOC^{-1})						
		$[L_1]$	$[L_2]$	$\log_{10} K_1$	$\log_{10} K_2$	[LMWOA] (mmol·L^{-1})	C-II (%)	AR/AL-I
CPWDOM	0	0.13±0.01	0.70±0.08	8.0±0.1	6.3±0.1	1.3±0.01	2.11	0.13
	72	0.22±0.03	1.83±0.36	7.6±0.2	5.9±0.1	1.4±0.02	5.60	0.08
LRDOM	0	0.17±0.02	1.60±0.42	7.6±0.1	5.8±0.1	0.94±0.06	4.0	0.53
	72	0.10±0.01	0.88±0.16	7.6±0.1	5.9±0.1	1.60±0.02	2.88	0.23

Note: Parameter descriptions are as follows: copper-binding site concentrations ($[L_1]$, $[L_2]$) and conditional stability constants (K_1, K_2) in a two-ligand model of Cu–DOM complexation; summed concentrations of six low molecular weight organic acids ([LMWOA]: acetic, citric, lactic, malic, oxalic, and succinic); the percentage of carbon in carbonyl groups of ketone and aldehyde substituents (C-II region of ^{13}C NMR spectra); and the ratio of aromatic rings and olefins (AR region) to aliphatic carbohydrate carbons, ester carbons, and amines (AL-I region). Parameters are conditional for pH 6.0, 25 °C, and 0.01 mol·L^{-1} $NaNO_3$. Values for Cu–DOM complexation parameters and [LMWOA] were determined from three separate irradiation replicates of a single dilution of DOM concentrate from each field site. DOM solutions from several irradiation sessions were pooled to collect an adequate mass for ^{13}C NMR spectral analysis.

hydroxyl species able to complex with monodentate DOM ligands (Browne and Driscoll 1993). These caveats do not apply to the conditions of our study.

In addition, we input the conditional stability constants ($\log_{10} K_{Cu\text{-}FHM} = 6.6$) and binding-site densities ($[L_{Cu\text{-}FHM}] = 4.9 \times 10^{-11}$ mol·fish^{-1}) of larval FHM from bioaccumulation experiments (Brooks et al. 2006). In MINTEQA2 calculations, we did not include acid dissociation constants for the DOM or competition by Ca^{2+}, Mg^{2+}, and K^+. The Cu–DOM conditional stability constants and their pH-dependent adjustments implicitly included Cu^{2+} competition with H^+ for binding to DOM, thus obviating the need to incorporate H^+ competition into the MINTEQA2 calculations. Any potential competition by Ca^{2+}, Mg^{2+}, and K^+ with Cu for DOM ligands was implicitly included in the toxicity tests because concentrations in test matrices (Table 1) were similar or virtually identical to those present in the DOM solutions used to develop Cu–DOM binding parameters (Brooks et al. 2007). Moreover, we excluded Ca^{2+}, Mg^{2+}, and K^+ from speciation calculations because several studies have demonstrated their minimal competition with Cu for binding sites on DOM (Hering and Morel 1988; Alberts et al. 1992; Breault et al. 1996). Including such competition would have underestimated Cu complexation by DOM.

After calculating the $\{Cu^{2+}\}$ for each [Cu] in NODOC A and NODOC B tests, the logit transform of mortality was calculated as $\ln[M/(1 - M)]$, where M is the average proportion of mortality (number of dead fish per number of total fish at each $\{Cu^{2+}\}$). We then regressed the logit of mortality versus $\ln\{Cu^{2+}\}$:

$$(1) \qquad \ln[M/(1-M)] = a \ln\{Cu^{2+}\} + b$$

Rearranging eq. 1 to solve for mortality, we used the regression slope (a) and the ordinate intercept (b) to predict the percent mortality (m) in TOX 1 and TOX 2 tests as

$$(2) \qquad m = [\exp(a \ln\{Cu^{2+}\} + b)] \times \{1 + [\exp(a \ln\{Cu^{2+}\} + b)]\}^{-1} \times 100$$

where $\{Cu^{2+}\}$ was calculated at each [DOC] using MINTEQA2. Finally, we compared the expected mortality with the observed mortality at each [DOC] in TOX 1 and TOX 2.

Statistical analyses

The $\{Cu^{2+}\}$ associated with 50% lethality (i.e., $\{Cu^{2+}\}_{LC50}$) for all toxicity tests (TOX 1 and TOX 2; NODOC A and NODOC B) were calculated using the Trimmed Spearman–Karber LC50 procedure in TOXSTAT (Version 3.5; WEST, Inc. and Gulley 1996). For TOX 1 and TOX 2 tests, which contained DOM, we first calculated the $[DOC]_{LC50}$ using the same procedure in TOXSTAT, then calculated the $\{Cu^{2+}\}_{LC50}$ at that [DOC] in MINTEQA2. In all hypothesis testing, we set $\alpha = 0.05$. t tests were used to evaluate miscellaneous differences as noted in the text.

Results

Photochemical changes in DOM

In photooxidation experiments of DOM, photomineralization removed 15%–20% of DOC from CPWDOM and LRDOM after 72 h of irradiation The extent of photomineralization for the current study did not differ significantly from earlier irradiation of DOM in the solar simulator (Brooks et al. 2007). After exposure, we diluted the irradiated DOM for toxicity tests to the [DOC] listed in Table 2.

MINTEQA2 calculations of $\{Cu^{2+}\}$ in our toxicity test solutions TOX 1 and TOX 2 indicated that photochemical changes in Cu–DOM complexation produced an average of 31%–85% greater calculated $\{Cu^{2+}\}$ per unit DOC in the DOM solutions with lower Cu binding-site densities (i.e., irradiated LRDOM and unirradiated CPWDOM) than in the corresponding treatments with higher Cu-ligand density (i.e., unirradiated LRDOM and irradiated CPWDOM; Table 2). The inclusion of $K_{Cu\text{-}FHM}$ and $[L_{Cu\text{-}FHM}]$ for biotic ligands (the larval fish) in MINTEQA2 calculations (parameters from Brooks et al. 2006) had little influence on aqueous Cu speciation in the test solutions because the small mass of fish in the exposure chambers bound ≤0.2% of total Cu (0.000 12 g dry weight·fish^{-1} with 10 fish·chamber^{-1}).

© 2007 NRC Canada

Table 4. Photochemical changes in the concentration of dissolved organic carbon ([DOC]) in unirradiated and irradiated solutions of dissolved organic matter (DOM) from Chimney Park wetland (CPWDOM) and Laramie River (LRDOM).

		[DOC] (μmol·L^{-1})	
DOM source	Irradiation time (h)	TOX 1	TOX 2
CPWDOM	0	41±0.9	41±1.1
	72	35±0.9*	33±0.6*
Decrease (%)		15	20
LRDOM	0	30±0.1	32±0.6
	72	25±0.8*	25±0.4*
Decrease (%)		19	20

Note: Data from three separate irradiation replicates of a single dilution of DOM concentrate from each field site. Neither the extent nor rate of photomineralization differed significantly between this study and an earlier study (Brooks et al. 2007). These DOM solutions were subsequently used in toxicity tests TOX 1 and TOX 2.

*$p \leq 0.05$.

Toxicity tests

Using combined data from NODOC A and NODOC B tests (Fig. 1), the regression relationship between logit mortality and ln[Cu^{2+}] in the absence of DOC had a slope of 1.326 with an intercept of –3.017 (eq. 1). Observed mortalities varied by 1%–34% from the composite concentration–response curve. Based on that regression relationship, we predicted mortality as a function of MINTEQA2-calculated [Cu^{2+}] for each [DOC] in TOX 1 and TOX 2 tests using eq. 2 (Fig. 2). The observed mortalities at a given [DOM] did not differ considerably between the irradiated and unirradiated DOM treatments (Fig. 2). Measuring mortality as a function of [Cu^{2+}], with the exception of TOX 1 conducted in CPWDOM, the $[Cu^{2+}]_{LC50}$ differed significantly between irradiated and unirradiated treatments in all TOX 1 and TOX 2 tests (Table 5) based on lack of overlap in confidence intervals and t test results (CPWDOM t test = 2.56 and $p = 0.047$; LRDOM TOX 1 t test = 5.72 and $p = 0.004$; LRDOM TOX 2 t test = 3.36 and $p = 0.021$). Measuring mortality as a function of DOC, the $[DOC]_{LC50}$ in the presence of the same total [Cu] were virtually identical between irradiated and control treatments regardless of source.

We compared expected with observed results (relative difference = (predicted – observed)/observed × 100%) for TOX 2 because of its greater range of DOC. In DOM treatments with low binding-site density (i.e., higher [Cu^{2+}]; expected to follow topmost curves in Figs. 2*c*, 2*d*), the observed mortalities were within an average of 9% ± 7% (mean ± SD; irradiated LRDOM, $r^2 = 0.95$) to 22% ± 6% (control CPWDOM, $r^2 = 0.97$) of our predictions based on [Cu^{2+}]. These residuals fall within the 1%–34% range of relative residuals in DOM-free NODOC A and NODOC B tests (Fig. 1). In contrast, treatments with higher binding-site densities for which we estimated lower mortality because of their 30%–50% lower [Cu^{2+}], our predictions (lower curves in Figs. 2*c*, 2*d*) underestimated observed mortality by 43% ± 11% (mean ± SD; control LRDOM, $r^2 = 0.66$) to 51% ± 9% (irradiated CPWDOM, $r^2 = 0.83$). Moreover, the $[Cu^{2+}]_{LC50}$ of these two treatments are significantly lower than that calculated for the average $[Cu^{2+}]_{LC50}$ determined for larval FHM in toxicity tests without DOC (NODOC A and NODOC B; Table 5), as demonstrated by the lack of overlap in the 95% confidence intervals and results of t tests (irradiated CPWDOM t test = 3.36 and $p = 0.021$; control LRDOM t test = 3.01 and $p = 0.032$).

Fig. 1. Composite concentration–response curve for fathead minnow (*Pimephales promelas*) larvae exposed to Cu in toxicity tests NODOC A (■) and NODOC B (○), which were conducted in matrix waters to which dissolved organic matter was not added. The solid line is the modeled concentration–response curve predicted from logit transformations of the mortality data regressed on the natural logarithm of the cupric ion activity ([Cu^{2+}]) (eq. 2: $m = [\exp(a \ln[Cu^{2+}] + b)][1 + [\exp(a \ln[Cu^{2+}] + b)]]^{-1} \times 100$), where $a = 1.520\,34$, and $b = 2.949\,85$.

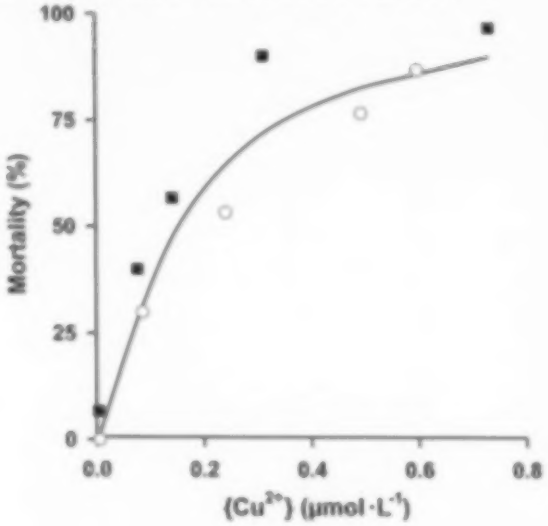

Discussion

Photochemical effects on Cu bioavailability

Because Cu toxicity is dominated by Cu^{2+} (e.g., Chakoumakos et al. 1979; Laurén and McDonald 1986; Erickson et al. 1996), we expected mortality of larval FHM would increase as [Cu^{2+}] increased in the otherwise constant water quality of the toxicity tests containing DOM (TOX 1 and TOX 2). Toxicity tests conducted in DOM treatments with low binding-site density and higher [Cu^{2+}] coincided with predictions. However, our predictions were an average of ~45% below observed mortality in treatments with higher binding-site densities and 30%–50% lower [Cu^{2+}].

These results present an interesting quandary. Regardless of source, the DOM treatments that bound the most Cu (i.e., having the lowest [Cu^{2+}]) were no more protective against Cu toxicity than the DOM treatments with lower binding-site densities that had higher [Cu^{2+}]. This quandary is illustrated by virtually identical $[DOC]_{LC50}$ values among treatments within the same test despite significant differences in their corresponding $[Cu^{2+}]_{LC50}$ values. Possible explanations

© 2007 NRC Canada

Fig. 2. Concentration–response curves from toxicity test TOX 1 for (*a*) dissolved organic matter (DOM) from Chimney Park wetland (CPWDOM) and (*b*) DOM from Laramie River (LRDOM), and from toxicity test TOX 2 for (*c*) CPWDOM and (*d*) LRDOM, comparing the lethality of a constant [Cu] in the presence of unirradiated DOM (■) or in the presence of DOM that was irradiated for 72 h in a solar simulator (○). Water chemistry for these toxicity tests are listed in Tables 1 and 4. Calculated LC50s are shown in Table 5. The curves are estimated mortalities using eq. 2 with $\{Cu^{2+}\}$ calculated in MINTEQA2 for each concentration of dissolved organic carbon (DOC) in irradiated DOM (broken line) and unirradiated DOM (solid line). Error bars are ±SE.

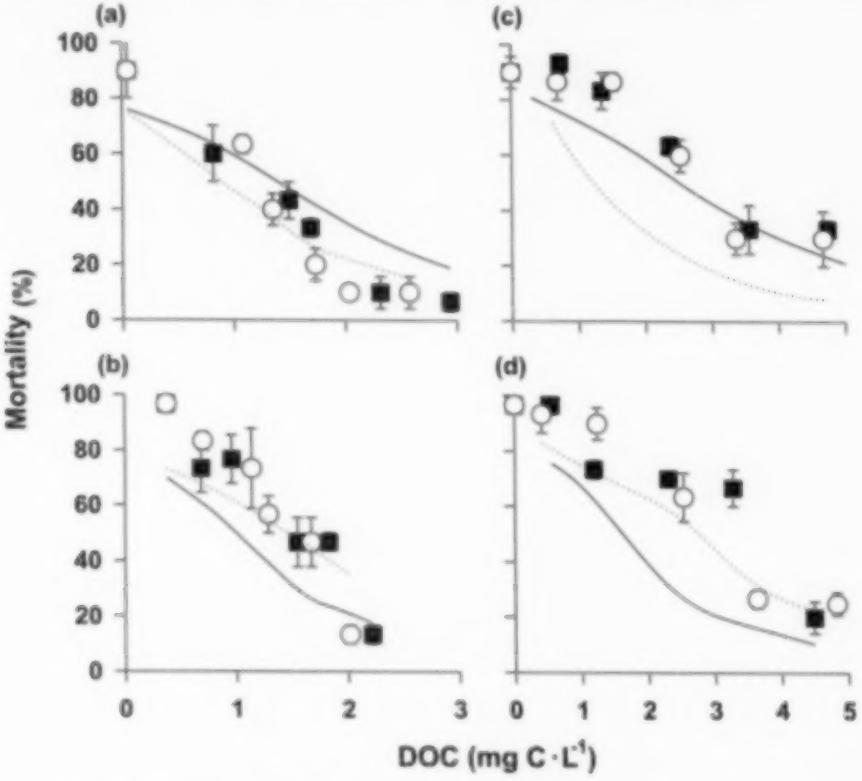

for this inconsistency are (*i*) lack of a good fit between actual $\{Cu^{2+}\}$ and those predicted by MINTEQA2 modeling, (*ii*) random variability within or among toxicity tests, and (*iii*) Cu species other than $\{Cu^{2+}\}$ that contributed to toxicity. The first explanation is unlikely, because in both irradiated and unirradiated treatments of CPWDOM and LRDOM, MINTEQA2-estimated $\{Cu^{2+}\}$ were within 9% ± 1% (mean ± SE; range 0.2%–17%) of actual $\{Cu^{2+}\}$ measured with an ion-selective electrode across a Cu titration range of 1.6×10^{-7} to 1.7×10^{-5} µmol·L^{-1} into 5 mg DOC·L^{-1} (Brooks et al. 2007). Regarding random variability in toxicity tests, toxicity data commonly differ by twofold between predicted and observed values (e.g., fig. 5 in Santore et al. 2001). However, our calculations consistently underpredicted observed mortality in treatments with low $\{Cu^{2+}\}$ (i.e., irradiated CPWDOM and unirradiated LRDOM), suggesting a systematic rather than random difference.

In addition to Cu^{2+}, Cu–inorganic complexes might have contributed to Cu toxicity. A number of researchers have reported that $CuCO_3^0$ (Shaw and Brown 1974) and $Cu(OH)_x$ species appear to contribute to toxicity (e.g., Chakoumakos et al. 1979; Laurén and McDonald 1986; Meador 1991). However, it is unlikely that $Cu(CO_3)_x$ or $Cu(OH)_x$ species contributed substantially to toxicity in our study for several reasons. First, in the presence of high [DOM] and circumneutral pH, dissolved inorganic ligands bound relatively little of the Cu. For example, MINTEQA2 calculations showed that inorganics complexed less than 2% of Cu (~0.03 µmol·L^{-1}) at the highest [DOC] having the greatest binding-site density and the lowest $\{Cu^{2+}\}$ in each toxicity test (i.e., the irradiated CPWDOM and unirradiated LRDOM). In the two highest [DOC] exposure solutions, mortality tended to remain constant at ~10% (TOX 1) and ~15% (TOX 2). Thus, constant mortality in the presence of increasing concentrations of organics and decreasing concentrations of $Cu(CO_3)_x$ and $Cu(OH)_x$ species, which lowered $\{Cu^{2+}\}$, indicates that some fraction of Cu complexed by DOM was either directly toxic or enhanced the uptake of Cu^{2+}.

This conclusion is consistent with findings that $\{Cu^{2+}\}$ alone is not a precise indicator of toxicity in the presence of Aldrich humic acid (a commercially available organic matter of terrestrial origin, Erickson et al. 1996). In that study, the $[Cu^{2+}]_{LC50}$ decreased linearly as [DOC] increased, indicating that a constant percentage of Cu bound to Aldrich humic acid was bioavailable.

Copper–organic complexes might enhance Cu bioavailability via several mechanisms: (*i*) alleviation of diffusion limitation of Cu^{2+} from the exposure water to the biotic

© 2007 NRC Canada

Table 5. Concentrations of dissolved organic carbon ($[DOC]_{LC50}$) and cupric ion activity ($[Cu^{2+}]_{LC50}$) at 50% mortality (means with 95% confidence intervals) for 96 h static-renewal toxicity tests (TOX 1 and TOX 2), containing unirradiated or irradiated dissolved organic matter (DOM) from Chimney Park wetland (CPWDOM) or Laramie River (LRDOM).

DOM source	Experiment	Irradiation time (h)	$[DOC]_{LC50}$ (mg·L^{-1})	$[Cu^{2+}]_{LC50}$ (μmol·L^{-1})
CPWDOM	TOX 1	0	1.45 (1.26–1.63)	0.22 (0.17–0.27)
		72	1.44 (1.29–1.58)	0.13 (0.10–0.17)
	TOX 2	0	2.42 (1.92–2.92)	0.12 (0.09–0.18)
		72	2.98 (2.38–3.58)	0.05 (0.04–0.07)*†
LRDOM	TOX 1	0	1.10 (0.78–1.41)	0.10 (0.09–0.12)
		72	1.12 (0.88–1.36)	0.17 (0.16–0.19)*
	TOX 2	0	3.08 (2.61–3.55)	0.06 (0.04–0.08)†
		72	2.79 (2.39–3.22)	0.13 (0.10–0.16)*
Matrix water	NODOC A	NA	NA	0.13 (0.10–0.18)
	NODOC B	NA	NA	0.26 (0.18–0.34)
	Mean NODOC	NA	NA	0.17 (0.10–0.24)

Note: Total [Cu] was constant in TOX 1 and TOX 2 (Table 1), whereas [Cu] varied in NODOC A and NODOC B (range: 0.01–2.9 μmol·L^{-1}; Brooks 2003). $[DOC]_{LC50}$ was calculated with TOXSTAT. From the resulting average [DOC] and confidence intervals, we calculated corresponding $[Cu^{2+}]$ in MINTEQA2. For toxicity tests without DOC (NODOC A and NODOC B and the average of both), $[DOC]_{LC50}$ was not applicable (NA). In those tests, we calculated $[Cu^{2+}]$ at each total [Cu] (Table 2) in MINTEQA2 and then determined the $[Cu^{2+}]_{LC50}$ with TOXSTAT.

*$p < 0.05$; compares control (0 h) with irradiated treatments (72 h).

†$p < 0.05$; compares the absolute difference between $[Cu^{2+}]_{LC50}$ in TOX 1 or TOX 2 ($[Cu^{2+}]_{LC50\,TOX\,1\,or\,2}$) versus the mean $[Cu^{2+}]_{LC50}$ for mean NODOC in bottom row.

membrane via direct exchange of Cu between the Cu–organic complexes and binding sites on the membrane, (*ii*) alteration of permeability of the biotic membrane, and (*iii*) passage of intact Cu–organic moieties across cell membranes. Regarding the first mechanism, most bioaccumulation studies indicate that diffusion delivers aqueous Cu^{2+} and other Cu species to the surface of the biotic ligands more quickly than the maximal potential rate of biologic uptake (Campbell 1995; Grosell and Wood 2002). A disjunctive pathway could overcome this bottleneck. By this pathway, Cu–organic complexes diffuse rapidly into the boundary layer, then Cu dissociates from the Cu–DOM complex to equalize the chemical gradient in $[Cu^{2+}]$ induced by rapid biological internalization of Cu^{2+} at the biotic surface. Thus, the direct movement of exchangeable Cu from a Cu–organic complex to a binding site on the membrane surface could enhance the rate of Cu supply. In a supply-limited transport system, any increase in the rate of Cu supply could greatly increase the rate of Cu uptake. If this mechanism applied to all Cu–organic complexes, then metal uptake would be insensitive to Cu speciation. Our results indicate that few, if any, Cu–organic complexes contributed to Cu toxicity in experiments with high $[Cu^{2+}]$ and low carbonyl concentrations (i.e., unirradiated CPWDOM and irradiated LRDOM). However, in experiments with low $[Cu^{2+}]$, the diffusion limitation was potentially alleviated by Cu dissociation from a limited fraction of Cu–organics. Given that acidification of the gill boundary layer has been shown to alter ion exchange (Wilson et al. 1994), it is possible that acidic moieties on DOM alter the boundary layer and allow direct Cu passage.

Another possible explanation for greater bioavailability of Cu in some treatments is alteration of the biotic ligands via interaction between organic matter and the biological receptor. For example, increased metal uptake occurs in the presence of natural organics that alter the negative surface charge of algae (*Chlorella pyrenoidosa*, *Synechoccus leopolienis*) and isolated fish gill cells (*Salmo salar*; Campbell et al. 1997) or increases membrane permeability of an alga *C. pyrenoidosa* (Parent et al. 1996). Although our data do not preclude them, these mechanisms have not been demonstrated with in vivo studies in fish.

Finally, passage through membranes of metals bound to commercial organics as metal–lipophilic complexes occurs in rainbow trout (*Oncorhynchus mykiss*; Block et al. 1991) and several algal, invertebrate, and fish species (reviewed in Campbell 1995). We did not test this possibility with our natural DOM, and thus cannot reject it.

Although other researchers report enhanced uptake of Cu bound to LMW organics such as amino acids, nitrilotriacetic acid, citrate, or ethylenediamine (Campbell 1995; Errecalde et al. 1998), this study did not correlate mortality with photoproduction of the LMW organic acids (acetic, citric, lactic, malic, oxalic, and succinic). In CPWDOM, constant concentrations of LMW organic acids during irradiation indicated that they did not contribute to increased Cu bioavailability in toxicity tests with irradiated CPWDOM. In LRDOM, irradiation increased the concentration of LMW organic acids by 70%. However, the unirradiated LRDOM treatments with low concentrations of these LMW organic acids apparently had the highest concentrations of bioavailable Cu–organic complexes. Thus, it appears that at radiation intensities approximating those of ambient sunlight, photoproduction of the LMW organic acids neither correlated with nor contributed to Cu bioavailability. Our findings are consistent with those of Playle et al. (1993), who showed no apparent transport of Cu by LMW organics in adult FHM

© 2007 NRC Canada

Table 6. Ratio of dissolved organic carbon concentration in all binding sites ([DOC] of $[L_{TOT}]$) to [DOC] concentration in C-II region of ^{13}C NMR spectra ([DOC] of C-II) in unirradiated (0 h) and irradiated (72 h) solutions of dissolved organic matter (DOM) from Chimney Park wetland (CPWDOM) and Laramie River (LRDOM) (data from Brooks et al. 2007).

DOM source	Irradiation time (h)	[DOC] of $[L_{TOT}]$ (μmol C·L^{-1})	[DOC] of C-II (μmol C·L^{-1})	C-II/$[L_{TOT}]$
CPWDOM	0	36	76	2.1
	72	72	165	2.3
LRDOM	0	57	107	1.9
	72	25	60	2.4

at environmentally relevant concentrations of ethylenediaminetetraacetic acid, nitrilotriacetic acid, ethylenediamine, citrate, or oxalic acid.

Possible photochemical mechanism for bioavailable Cu–organic complexes

Based on ^{13}C nuclear magnetic resonance (^{13}C NMR) spectra collected during an earlier study of photochemical effects on CPWDOM and LRDOM (Brooks et al. 2007), the proportions of carbonyls on ketone and aldehyde carbons (C-II groups) in both DOM types were positively correlated with both L_1 ($r^2 = 0.83$, $p = 0.10$, $n = 4$) and L_2 ($r^2 = 0.92$, $p = 0.02$, $n = 4$). In CPWDOM, photooxidation apparently increased Cu complexation by producing new binding sites on C-II groups, whereas photolysis apparently removed this class of ligands in LRDOM. Although absolute changes in the fraction of C associated with ketones and aldehydes were small, twice as many C atoms occurred in C-II groups as the density of Cu-binding sites. Assuming a conservative average of ≤6 C atoms per binding site (Leenheer et al. 1998), they were adequate to account for at least one-third of the change in density of Cu-binding sites, (Table 6). This class of oxy-functional ligands is located in the most downfield, unshielded region of ^{13}C NMR spectra, representing moieties that are highly electronegative, probably because of their association with aromatic groups. Therefore, it is logical that small changes in the relative proportions of these ligands would impact the Cu binding-site densities of DOM. Because mortality did not differ between irradiated and unirradiated DOM in TOX 1 and TOX 2 tests despite significant differences in $\{Cu^{2+}\}$, we conclude that Cu–ketone or Cu–aldehyde complexes might act as Cu transporters by altering the microenvironment of biologic receptors, directly exchanging Cu with binding sites on membranes, or by passing through membranes as intact Cu–organic complexes. For example, Campbell et al. (1997) showed that binding of Al–DOM complexes to algal cells affected membrane permeability and postulated that direct exchange could occur. In addition, Errécalde et al. (1998) demonstrated active uptake of Cd– and Zn–citrate complexes by citrate transporters. Although plausible, this conclusion is tenuous because we base it on Cu toxicity in the presence of DOM from only two sources before and after irradiation.

Metal-binding sites are oxygen-rich groups on substituents of aromatics, such as ethers, esters, ketones, and aldehydes (Leenheer et al. 1995, 1998; Brooks et al. 2007). Different photochemical mechanisms related to the initial chemical composition of DOM from allochthonous versus autochthonous sources might explain the production (wetland DOM) and loss (riverine DOM) of DOM ligands that could act as Cu transporters. Compared with allochthonous DOM, autochthonous DOM derived from algae, macrophytes, and bacteria contains more proteins and lipids, resulting in lower ratios of aromatic to aliphatic components (McKnight and Aiken 1998). Consistent with higher lipid fractions, Brooks et al. (2007) report that CPWDOM had a much lower aromatic to aliphatic ratio than that of LRDOM (Table 3, 0.13 versus 0.53 prior to irradiation). In CPWDOM, we propose that irradiation might have created bioavailable Cu–DOM complexes by polymerization and photooxidation of polyunsaturated lipids that produces aldehydes and is the proposed mechanism for production of humic substances in marine environments (Harvey et al. 1983; Kieber et al. 1997).

Allochthonous DOM contains lignin, which is only produced by vascular plants and is not found in algae or bacteria. Degradation of allochthonous plants releases low amounts of proteins and lipids compared with relatively high carbohydrate concentrations. Dissolved lignin in allochthonous DOM contains a variety of oxygen functional substituents (McKnight and Aiken 1998) on an array of phenolic compounds such as syringyl and vanillyl phenols with oxygen-rich links (Castellan et al. 1987; Opsahl and Benner 1995). Photodegradation of allochthonous DOM cleaves ester and ether linkages, removes ketones and aldehydes, and photomineralizes the majority of the lignin (Castellan et al. 1987; Opsahl and Benner 1993, 1998), thus decreasing aromaticity and removing oxy-functional substituents (Brooks et al. 2007). We propose that photodegradation destroyed the apparently bioavailable Cu–DOM complexes in LRDOM, possibly by cleaving ketones and aldehydes (C-II groups) from the lignin-rich, allochthonous DOM. Photochemical cleavage of oxy-functional groups coincided with, and might explain, the 70% increase in LMW organic acids in the riverine DOM.

In conclusion, whether sunlight interacts with DOM to create or deplete metal-binding sites varies among sources of DOM. In addition, the apparent photochemical production or loss of DOM fractions that act as Cu–organic transporters is source dependent. At coarse resolution, $\{Cu^{2+}\}$ alone is a general predictor of Cu bioavailability. However, at a finer level of resolution, it appears that some Cu–organic complexes — possibly carbonyls in ketones and aldehydes in DOM — appear to facilitate transport of Cu across cell membranes, which explains why some Cu–DOM complexes apparently contribute to toxicity. Additional research is

© 2007 NRC Canada

needed to (*i*) clarify the mechanisms by which Cu bioavailability increases, particularly to larval life stages, (*ii*) improve predictions of Cu toxicity in the presence of DOM from different sources with varying histories of photooxidation, and (*iii*) to examine the long-term effects of intensifying photooxidation of DOM due to global increases in ultraviolet radiation.

Acknowledgements

This work was funded by the University of Wyoming National Science Foundation's Experimental Program to Stimulate Competitive Research (EPSCoR) program and a United States Environmental Protection Agency's (USEPA) Science to Acieve Results (STAR) Fellowship No. U915640 awarded to MLB. JSM was funded through a USEPA subcontract from the University of Delaware's Center for the Study of Metals in the Environment. We thank Megin Rux for laboratory assistance. We thank two anonymous reviewers for helpful comments that greatly improved this manuscript.

References

Alberts, J.J., Filip, Z., and Herrkorn, N. 1992. Fulvic and humic acids isolated from groundwater: compositional characteristics and cation binding. J. Contam. Hydrol. **11**: 317–330.

Allison, J.D., Brown, D.S., and Novo-Gradac, K.J. 1991. MINTEQA2 / PRODEFA2. A geochemical assessment model for environmental systems. Version 3.1 Users' manual. EPA/600/3-91/021. US Environmental Protection Agency, Athens, Ga.

APHA (American Public Health Association, American Water Works Association, and Water Environment Federation). 1995. Standard methods for the examination of water and wastewater. 19th ed. Washington, D.C.

Bertilsson, S., and Tranvik, L.J. 2000. Photochemical transformation of dissolved organic matter in lakes. Limnol. Oceanogr. **45**: 753–762.

Block, M., Wicklund Glynn, A., and Pärt, P. 1991. Xanthate effects on cadmium uptake and intracellular distribution in rainbow trout (*Oncorhynchus mykiss*) gills. Aquat. Toxicol. **20**: 267–283.

Breault, R.F., Colman, J.A., Aiken, G.R., and McKnight, D. 1996. Copper speciation and binding by organic matter in copper-contaminated streamwater. Environ. Sci. Technol. **30**: 3477–3486.

Brooks, M.L. 2003. Photochemical effects on wetland and riverine dissolved organic matter, copper speciation, and copper toxicity to larval fathead minnows (*Pimephales promelas*). Ph.D thesis, University of Wyoming, Laramie, Wyo.

Brooks, M.L., Boese, C.J., and Meyer, J.S. 2006. Complexation and time-dependent accumulation of copper by larval fathead minnows (*Pimephales promelas*): implications for modeling toxicity. Aquat. Toxicol. **78**: 42–49.

Brooks, M.L., McKnight, D.M., and Meyer, J.S. 2007. Changes in copper-organic complexation druing photooxidation of wetland and riverine dissolved organic matter. Hydrobiologia, **579**: 95–113.

Browne, B.A., and Driscoll, C.T. 1993. pH-dependent binding of aluminum by a fulvic acid. Environ. Sci. Technol. **27**: 915–922.

Cabaniss, S., and Shuman, M.S. 1986. Combined ion selective electrode and fluorescence quenching detection for copper-dissolved organic matter titrations. Anal. Chem. **58**: 398–401.

Cabaniss, S.E., and Shuman, M.S. 1988. Copper binding by dissolved organic matter. II. Variation in type and source of organic matter. Geochim. Cosmochim. Acta, **52**: 195–200.

Campbell, P.G.C. 1995. Interactions between trace metals and aquatic organisms: a critique of the free-ion model. *In* Metal speciation and bioavailability. *Edited by* A. Tessier and D.R. Turner. John Wiley and Sons, New York. pp. 45–102.

Campbell, P.G.C., Twiss, M.R., and Wilkinson, K.J. 1997. Accumulation of natural organic matter on the surfaces of living cells: implications for the interaction of toxic solutes with aquatic biota. Can. J. Fish. Aquat. Sci. **54**: 2543–2554.

Castellan, A., Vanucci, C., and Bouas-Laurent, H. 1987. Photochemical degradation of lignin through α C—O bond cleavage of non phenolic benzyl aryl ether units. A study of the photochemistry of α (2′,4′,6′-trimethyl-phenoxy)-3,4 dimethoxy toluene. Holsforschung, **41**: 231–238.

Chakoumakos, C., Russo, R.C., and Thurston, R.V. 1979. Toxicity of copper to cutthroat trout (*Salmo clarki*) under different conditions of alkalinity, pH, and hardness. Environ. Sci. Technol. **13**: 213–219.

Christl, I., Metzger, A., Heidmann, I., and Kretzschmar, R. 2005. Effect of humic and fulvic acid concentrations and ionic strength on copper and lead binding. Environ. Sci. Technol. **39**: 5319–5326.

Curtis, J., and Grimes, K. 2004. Wyoming climate atlas. State Climatologist, Laramie, Wyo.

De Schamphelaere, K.A.C., Vasconcelos, V.M., Heijerick, D.G., Tack, F.M.G., Delbeke, K., Allen, H.E., and Janssen, C.R. 2003. Development and field validation of a predictive copper toxicity model for the green alga *Pseudokirchneriella subcapitata*. Environ. Toxicol. Chem. **22**: 2454–2465.

Erickson, R.J., Benoit, D.A., Mattson, V.R., Nelson, H.P., Jr., and Leonard, E.N. 1996. The effects of water chemistry on the toxicity of copper to fathead minnows. Environ. Toxicol. Chem. **15**: 181–193.

Errécalde, O., Seidl, M., and Campbell, P.G.C. 1998. Influence of a low molecular weight metabolite (citrate) on the toxicity of cadmium and zinc to the unicellular green alga *Selenastrum capricornutum*: an exception to the free-ion model. Water Res. **32**: 419–429.

Grosell, M., and Wood, C.M. 2002. Copper uptake across rainbow trout gills: mechanisms of apical entry. J. Exp. Biol. **205**: 1179–1188.

Harvey, G.R., Boran, D.A., Chesal, L.A., and Tokar, J.M. 1983. The structure of marine fulvic and humic acids. Mar. Chem. **12**: 119–132.

Hering, J.G., and Morel, F.M.M. 1988. Humic acid complexation of calcium and copper. Environ. Sci. Technol. **22**: 1234–1237.

Kieber, R.J., Hydro, L.H., and Seaton, P.J. 1997. Photooxidation of triglycerides and fatty acids in seawater: implication toward the formation of marine humic substances. Limnol. Oceanogr. **42**: 1454–1462.

Kinniburgh, D.G., Milne, C.J., Benedetti, M.F., Pinheiro, J.P., Filius, J., Koopal, L.K., and Van Reimsdijk, W.H. 1996. Metal ion binding by humic acid: application of the NICA–Donnan model. Environ. Sci. Technol. **30**: 1687–1698.

Laurén, D.J., and McDonald, D.G. 1986. Influence of water hardness, pH, and alkalinity on the mechanisms of copper toxicity in juvenile rainbow trout, *Salmo gairdneri*. Can. J. Fish. Aquat. Sci. **43**: 1488–1496.

Leenheer, J.A., Wershaw, R.L., and Reddy, M.M. 1995. Strong-acid, carboxyl-group structures in fulvic acid from the Suwannee River, Georgia. 2. Major structures. Environ. Sci. Technol. **29**: 399–405.

Leenheer, J.A., Brown, G.K., MacCarthy, P., and Cabaniss, S.E. 1998. Models of metal binding structures in fulvic acid from the Suwannee River, Georgia. Environ. Sci. Technol. **32**: 2410–2416.

© 2007 NRC Canada

Lu, Y., and Allen, H.E. 2002. Characterization of copper complexation with natural dissolved organic matter (DOM) — link to acidic moieties of DOM and competition by Ca and Mg. Water Res. **36**: 5083–5101.

Ma, H., Kim, S.D., Cha, D.K., and Allen, H.E. 1999. Effect of kinetics of complexation by humic acid on toxicity of copper to *Ceriodaphnia dubia*. Environ. Toxicol. Chem. **18**: 828–837.

MacRae, R.K., Smith, D.E., Swoboda-Colberg, N., Meyer, J.S., and Bergman, H.L. 1999. Copper binding affinity of rainbow trout (*Oncorhynchus mykiss*) and brook trout (*Salvelinus fontinalis*) gills: implications for assessing bioavailable metal. Environ. Toxicol. Chem. **18**: 1180–1189.

Maurice, P.A., Pullin, M.J., Cabaniss, S.E., Zhou, Q., Namjesnik-Dejanovic, K., and Aiken, G. 2002. A comparison of surface water natural organic matter in raw filtered water samples, XAD, and reverse osmosis isolates. Water Res. **36**: 2357–2371.

McKnight, D.M., and Aiken, G.R. 1998. Sources and age of aquatic humus. *In* Aquatic humic substances. *Edited by* D.O. Hessen and L.J. Tranvik. Springer-Verlag, Berlin. pp. 9–39.

McKnight, D.M., Thurman, E.M., and Wershaw, R.L. 1983. Complexation of copper by aquatic humic substances from different environments. Sci. Tot. Environ. **28**: 65–76.

McKnight, D.M., Harnish, R., Wershaw, R.L., Baron, J.S., and Schiff, S. 1997. Chemical characteristics of particulate, colloidal, and dissolved organic material in Loch Vale Watershed, Rocky Mountain National Park. Biogeochemistry, **36**: 99–124.

Meador, J.P. 1991. The interaction of pH, dissolved organic carbon, and total copper in the determination of ionic copper and toxicity. Aquat. Toxicol. **19**: 13–32.

Miller, W.L., and Zepp, R.G. 1995. Photochemical production of dissolved inorganic carbon from terrestrial organic matter: significance to the oceanic organic carbon cycle. Geophys. Res. Lett. **22**: 417–420.

Miller, W.L., Moran, M.A., Sheldon, W.M., Zepp, R.G., and Opsahl, S. 2002. Determination of apparent quantum yield spectra for the formation of biologically labile photoproducts. Limnol. Oceanogr. **47**: 343–352.

Molot, L.A., and Dillon, P.J. 1997. Photolytic regulation of dissolved organic carbon in northern lakes. Global Biogeochem. Cycles, **11**: 357–365.

Moran, M.A., and Zepp, R.G. 1997. Role of photoreactions in the formation of biologically labile compounds from dissolved organic matter. Limnol. Oceanogr. **42**: 1307–1316.

Moran, M.A., Sheldon, W.M., Jr., and Zepp, R.G. 2000. Carbon loss and optical property changes during long-term photochemical and biological degradation of estuarine dissolved organic matter. Limnol. Oceanogr. **45**: 1254–1264.

Obernosterer, I., and Benner, R. 2004. Competition between biological and photochemical processes in the mineralization of dissolved organic carbon. Limnol. Oceanogr. **49**: 117–124.

Opsahl, S., and Benner, R. 1993. Decomposition of senescent blades of the seagrass *Halodule wrightii* in a subtropical lagoon. Mar. Ecol. Prog. Ser. **94**: 191–205.

Opsahl, S., and Benner, R. 1995. Early diagenesis of vascular plant tissues: lignin and cutin decomposition and biogeochemical implications. Geochim. Cosmochim. Acta, **59**: 4889–4904.

Opsahl, S., and Benner, R. 1998. Photochemical reactivity of dissolved lignin in river and ocean waters. Limnol. Oceanogr. **43**: 1297–1304.

Parent, L., Twiss, M.R., and Campbell, P.G.C. 1996. Influences of natural dissolved organic matter on the interaction of aluminum with the microalga *Chlorella*: a test of the free-ion model of trace metal toxicity. Environ. Sci. Technol. **30**: 1713–1720.

Playle, R.C., Dixon, D.G., and Burnison, K. 1993. Copper and cadmium binding to fish gills: modification by dissolved organic carbon and synthetic ligands. Can. J. Fish. Aquat. Sci. **50**: 2667–2677.

Richards, J.G., Curtis, P.J., Burnison, B.K., and Playle, R.C. 2001. Effects of natural organic matter source on reducing metal toxicity to rainbow trout (*Oncorhynchus mykiss*) and on metal binding to their gills. Environ. Toxicol. Chem. **20**: 1159–1166.

Ryan, A.C., Van Genderen, E.J., Tomasso, J.R., and Klaine, S.J. 2004. Influence of natural organic matter source on copper toxicity to the larval fathead minnow (*Pimephales promelas*): implications for the biotic ligand model. Environ. Toxicol. Chem. **23**: 1567–1574.

Saar, R.A., and Weber, J.H. 1982. Fulvic acid: modifier of metal-ion chemistry. Environ. Sci. Technol. **16**: 510A–517A.

Santore, R.C., Di Toro, D.M., Paquin, P.R., Allen, H.E., and Meyer, J.S. 2001. Biotic ligand model of the acute toxicity of metals. 2. Application to acute copper toxicity in freshwater fish and *Daphnia*. Environ. Toxicol. Chem. **20**: 2397–2402.

Schwarzenbach, R.P., Gschwend, P., and Imboden, D.M. 1993. Environmental organic chemistry. John Wiley and Sons, Inc., New York.

Serkiz, S.M., and Perdue, E.M. 1990. Isolation of dissolved organic matter from the Suwannee River using reverse osmosis. Water Res. **24**: 911–916.

Shaw, T.L., and Brown, V.M. 1974. The toxicity of some forms of copper to rainbow trout. Water Res. **8**: 377–382.

Thurman, E.M. 1985. Organic geochemistry of natural waters. Nijhoff/Junk, Boston, Mass.

Tipping, E. 2002. Cation binding by humic substances. Cambridge University Press, Cambridge, UK.

Tranvik, L.J., and Kokalj, S. 1998. Decreased biodegradability of algal DOC due to interactive effects of UV radiation and humic matter. Aquat. Microb. Ecol. **14**: 301–307.

Weishaar, J.L., Aiken, G.R., Bergamaschi, B.A., Fram, M.S., Fujii, R., and Mopper, K. 2003. Evaluation of specific ultraviolet absorbance as an indicator of the chemical composition and reactivity of dissolved organic carbon. Environ. Sci. Technol. **37**: 4702–4708.

WEST, Inc., and Gulley, D. 1996. TOXSTAT. Version 3.5 user's manual. Western EcoSystems Technology (WEST), Inc. Cheyenne, Wyo.

Wilson, R., Wright, P., Munger, S., and Wood, C. 1994. Ammonia excretion in freshwater rainbow trout (*Oncorhynchus mykiss*) and the importance of gill boundary layer acidification: lack of evidence for Na^+/NH_4^+ exchange. J. Exp. Biol. **191**: 37–58.

Xie, H., Zafiriou, O.C., Cai, W.-J., Zepp, R.G., and Wang, Y. 2004. Photooxidation and its effects on the carboxyl content of dissolved organic matter in two coastal rivers in the southeastern United States. Environ. Sci. Technol. **38**: 4113–4119.

© 2007 NRC Canada

The influence of eutrophication and population biomass on common whitefish (*Coregonus lavaretus*) growth — the Lake Constance example revisited

Gregor Thomas and Reiner Eckmann

Abstract: Accelerated growth of freshwater fish during anthropogenic eutrophication has been attributed almost exclusively to the increased nutrient content, while density-dependent effects have been largely neglected. We evaluated the relative importance of these factors by studying the growth of 43 consecutive year classes of common whitefish (*Coregonus lavaretus*) from Upper Lake Constance. This prealpine lake underwent eutrophication from the 1950s to 1970s, followed by reoligotrophication. Because whitefish are harvested with gill nets in a strongly size-selective way, we used back-calculated lengths of average fast-growing fish to compare growth among cohorts. Standing stock biomass was estimated based upon virtual year-class strengths. Multiple linear regression analysis revealed that growth of whitefish during their second year was most strongly related to standing stock biomass followed by PO_4-P content during spring turnover and by calendar year, which was incorporated as a third independent variable (adjusted $R^2 = 0.84$). The negative correlation between whitefish growth rate and calendar year is interpreted as evidence of an evolutionary response to the highly size-selective fishery during at least four decades. We conclude that density-dependent effects on whitefish growth are more important than had been realized previously and that the impact of eutrophication on growth of whitefish needs to be reconsidered.

Résumé : La croissance accélérée des poissons d'eau douce dans les conditions d'eutrophisation anthropique a été attribuée presque exclusivement à l'augmentation du contenu en nutriments; en revanche, les effets reliés à la densité ont été en grande partie négligés. Nous évaluons l'importance relative de ces facteurs dans une étude de la croissance de 43 classes d'âge consécutives de corégones lavarets (*Coregonus lavaretus*) du lac supérieur de Constance. Ce lac préalpin a subi une eutrophisation des années 1950 aux années 1970, suivie d'une ré-oligotrophisation. Parce que les corégones sont récoltés dans des filets maillants qui font une forte sélection en fonction de la taille, nous avons utilisé les longueurs obtenues par rétro-calcul de poissons moyens à croissance rapide pour comparer la croissance entre les cohortes. Nous avons estimé la biomasse du stock d'après les forces des classes d'âge virtuelles. Une analyse de régression multiple linéaire montre que la croissance des corégones durant leur seconde année est surtout reliée à la biomasse du stock, puis au contenu de P-PO_4 durant le brassage du printemps et à l'année du calendrier qui a été incorporée à l'analyse comme troisième variable indépendante (R^2 ajusté = 0,84). Nous interprétons la corrélation négative qui existe entre la croissance des corégones et l'année du calendrier comme une indication de la réponse évolutive à la pêche très sélective au cours d'au moins de quatre décennies. Nous concluons que les effets reliés à la densité sur la croissance des corégones sont plus importants qu'on ne le croyait antérieurement et qu'il est nécessaire d'évaluer de nouveau l'impact de l'eutrophisation sur la croissance du corégone.

[Traduit par la Rédaction]

Introduction

Understanding the effects of abiotic and biotic factors on fish growth is of both scientific and commercial interest. Among the abiotic factors, water temperature and a water body's trophic state are generally considered to be most important, while competition for food, either inter- or intraspecific, is probably the most relevant biotic factor. The trophic state of a water body and the intensity of competition for food can be modified intentionally or unintentionally by human activities over short time scales. A better understanding of human impacts on fish growth, through changes to a water body's trophic state or in competitor density, is therefore a prerequisite for the successful management of exploited fish populations.

The common whitefish (*Coregonus lavaretus*) is a species of great commercial importance in many prealpine lakes in central Europe (Nümann 1972; Gerdeaux 2004), as are other

Received 12 May 2006. Accepted 14 December 2006. Published on the NRC Research Press Web site at http://cjfas.nrc.ca on 16 March 2007.
J19320

G. Thomas[1] and R. Eckmann. Limnological Institute, University of Konstanz, D-78457 Konstanz, Germany.

[1]Corresponding author (e-mail: gregor.thomas@uni-konstanz.de).

 doi:10.1139/F07-019 © 2007 NRC Canada

species of the genus *Coregonus* in lakes, rivers, and estuaries of northern Eurasia and North America (Price et al. 2003; Hoff and Todd 2004; Salonen and Mutenia 2004). Any major changes in coregonid yields, therefore, attract the immediate attention of fishermen and managers and challenge fishery scientists to explore the likely reasons and eventually to recommend appropriate measures to stabilize yields.

The most dramatic changes in coregonid growth in central European lakes occurred during the 1960s and 1970s, when fish of consecutively younger ages were caught (Nümann 1972). Most of the studies of coregonid population dynamics claimed that anthropogenic eutrophication was the main cause of the acceleration in whitefish growth (Grimås et al. 1972; Nümann 1972). The decrease in whitefish growth from many European lakes towards the end of the 20th century was generally attributed to reoligotrophication (Kirchhofer 1995; Müller and Mbwenembo Bia 1998). Thus, it was an accepted hypothesis that changes of a lake's trophic state, through changes of primary and secondary production, was the main, if not the only, mechanism that controlled fish growth (Downing et al. 1990).

In addition to lake trophic state, however, density dependence is another key factor influencing fish growth (Walters and Post 1993; Post et al. 1999; Lorenzen and Enberg 2002). With higher population density, intraspecific competition for food can become more intense, resulting in slower individual growth. Several studies on density-dependent growth in coregonid populations have confirmed this general concept. These studies have compared whitefish growth rates among lakes with different whitefish densities (Bidgood 1973; Lehtonen and Niemelä 1998; Mayr 2001), compared growth rates before and after stock size reduction through intensive fishing (Amundsen 1988; Valkeajärvi 1992; Mills et al. 1995), or monitored whitefish stock oscillations over longer time periods (Helminen et al. 1993; Salonen et al. 1998; Viljanen et al. 2004). Most of the published studies on whitefish growth have, however, focussed either on lake trophic state or on population density.

The earlier studies on whitefish growth in European prealpine lakes were all done during the time of rapid anthropogenic eutrophication, whereby the obvious parallelism between nutrient content and whitefish growth was considered to be evidence for a monocausal relationship. As a much more extensive set of data on whitefish population dynamics, covering 43 year classes, is now available for Upper Lake Constance, we took advantage of this unique opportunity to reanalyse the earlier concepts about the influence of eutrophication on whitefish growth. The first aim of our study was to disentangle the effects of density dependence and lake trophic state on the growth of whitefish using multiple linear regression analysis.

Size-selective harvesting by a commercial fishery can change life-history traits such as size-at-age or age-at-maturity of the fish (Rijnsdorp 1993; Sinclair et al. 2002). If some of the phenotypic variation in these traits is genetic, then fishing may cause evolutionary changes in the life history (Law 2000; Conover et al. 2005). In an experimental study with *Menidia menidia*, size-dependent mortality did indeed select for the evolution of genotypes with growth rates that were in directions counter to the size-selective harvest within only four generations (Conover and Munch 2002). Additionally, a gillnet fishery for lake whitefish (*Coregonus clupeaformis*) in Lesser Slave Lake evoked changes in growth rate, condition, and mean age, and it was suggested that the highly selective harvest of large, fast-growing fish might provoke an evolutionary response in this stock (Handford et al. 1977). As the fishery for common whitefish in Lake Constance has been highly size-selective, at least since the mid-1960s, when monofilament gill nets of a fixed mesh size replaced all formerly used fishing gears, evolutionary changes in the common whitefish stock may have occurred during the past four decades. It was, therefore, the second aim of our study to screen the available data for indications of evolutionary responses to this size-selective harvesting.

Materials and methods

Study site

Upper Lake Constance (ULC) is a large (472 km^2), deep (z_{max} = 254 m, z_{mean} = 101 m), warm–monomictic, prealpine lake situated at the northern fringe of the European Alps (47°39′N, 9°18′E), shared by Austria, Germany, and Switzerland. The lake underwent pronounced eutrophication during the 20th century, whereby total phosphorus (P) concentrations during winter mixing in February–March (TP_{mix}) increased from 7 $\mu g \cdot L^{-1}$ in 1951 to >80 $\mu g \cdot L^{-1}$ around 1980 (IGKB 2004). As a result of drastically reduced P inputs, including the banning of phosphate-containing detergents, sewage collection, and the inclusion of P stripping in sewage treatment, the lake had returned to oligotrophy by the beginning of the 21st century (TP_{mix} in 2004 = 9 $\mu g \cdot L^{-1}$) (cf. Fig. 1).

Twenty-nine fish species presently occur in the lake (Eckmann and Rösch 1998), among which common whitefish is commercially the most important. An uninterrupted record of commercial catches from ULC is available since 1910. Regular surveys of the whitefish stock have been carried out monthly since the beginning of the 1960s, while less regular surveys were conducted in the 1930s, the late 1940s, and during the 1950s. These surveys showed that whitefish growth had accelerated to such a degree by the beginning of the 1960s that whitefish reached the legal minimum size (30 cm, legal gill net mesh size 38–40 mm) about 2 years earlier than during the 1930s (Nümann 1972). As a consequence, an increasing fraction of the commercial yields consisted of age-1 fish that had not yet reproduced. The obvious risk of recruitment overfishing was counteracted in 1965 by increasing the minimum mesh size to 44 mm and the legal minimum size to 35 cm (Nümann 1972).

The whitefish fishery at Upper Lake Constance

At the beginning of the 20th century, about 460 professional fishermen were licensed to fish at Lake Constance using drifting cotton gill nets and Klusgarn, a seine operated in the pelagic zone. By the mid-1960s, both gears had been replaced almost completely by more efficient monofilament nylon gill nets. During the following decades, the number of nets per licence was successively reduced from 10 to 3, only 4 fishing days per week were allowed instead of 5, and the number of commercial fishing licences was cut by 30%.

© 2007 NRC Canada

Fig. 1. Phosphorus concentration during spring turnover (triangles) and total whitefish (*Coregonus lavaretus*) yield (bars) in Upper Lake Constance.

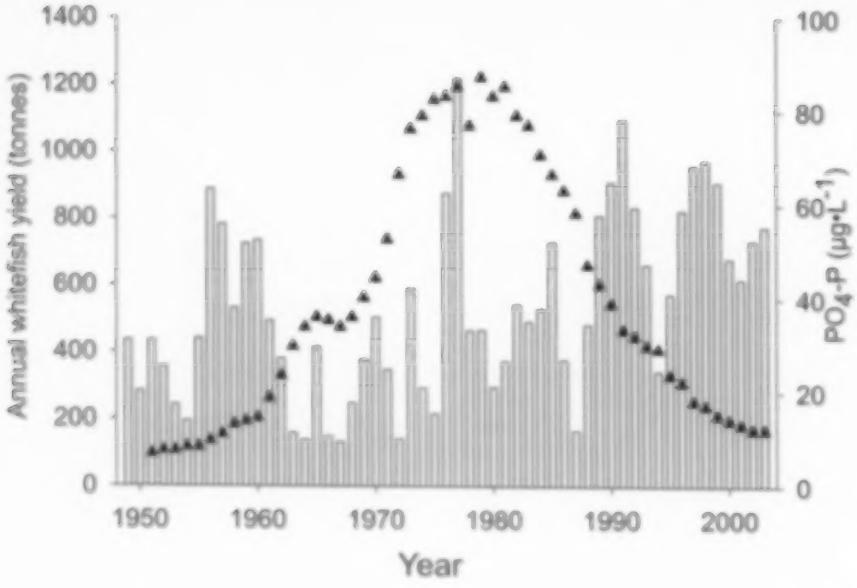

These measures were taken firstly to allow for a reasonable income to the commercial fishermen and secondly to avoid overharvesting the stock as in the 1960s and early 1970s. Altogether, fishing intensity in 2005 had dropped to 17% of what it was in 1961 (R. Rösch, Fischereiforschungsstelle, Langenargen, Germany, personal communication).

Virtual year-class strength

Virtual year-class strength (YCS) was calculated for the annual cohorts of 1947 to 1997. These estimates are based upon biweekly to monthly test catches using gill nets of legal mesh size. Samples are analyzed with regard to age and body weight, which provides an estimate of catch composition by age classes. Using the monthly fishermen's catch data, the number of individuals of a certain year class harvested from the lake can then be calculated month by month. Integrating all monthly harvests from year class *i* across time yields an estimate of the virtual size of this year class (cf. Eckmann et al. 1988). To account for natural mortality, an instantaneous mortality rate of 0.2 per year was incorporated (Eckmann et al. 2002). The estimates of whitefish YCS at Lake Constance, thus, are not based on estimates of fishing mortality but on the well-documented monthly catch reports of all fishermen. These reports are made anonymous during compilation, and they are not supplied to revenue authorities to avoid bias towards low yields. Subtracting the monthly harvests from year class *i* successively from the initial size of this cohort provides an estimate of the number of fish of year class *i* that were present in the population in each month, from its recruitment into the fishery until the cohort was fished out. By adding up these numbers across year classes for each month, the numerical age composition of the whitefish standing stock was obtained.

Size-selective harvest

Nümann (1959) was the first to point out that whitefish are harvested in a size-selective fashion from ULC using gill nets of a legally fixed mesh size, the faster-growing fish being harvested earlier than the slower-growing members of the same cohort. In this situation, growth of fish from different year classes cannot be compared by determining size-at-age, because this measure depends on the time of harvest of the fish, from which size-at-age is determined. We assessed this potential bias by back-calculating length at the end of the second year for all whitefish from the cohorts of 1991 and 1992, which had been collected with legal size (44 mm) gill nets in the regular monthly test fishery. For both year classes, size-at-age was significantly related to the year of harvest (analysis of variance, ANOVA, $F_{[2,157]} = 22.09$, $P < 0.0001$; $F_{[3,210]} = 35.22$, $P < 0.0001$, for the year classes 1991 and 1992, respectively). The mean length after 2 years of whitefish sampled in their third, fourth, and fifth years of life decreased from 25.4 cm through 23.2 to 20.7 cm, respectively, for the 1991 cohort and from 25.3 cm through 23.2 to 22.1 cm, respectively, for the 1992 cohort. Thus, considerable bias may arise when length-at-age is determined without taking into account the age at which the fish are harvested. We therefore decided to compare growth of whitefish from different cohorts by using those fish that were harvested around the time when 50% of the total harvest from a cohort was being obtained (termed average fast-growing fish hereafter).

Back-calculation of growth

Scales were generally sampled from the left body side between the dorsal fin and the lateral line. Three scales from each of about 50 average fast-growing fish per year class were used for growth analysis. The widths of annual growth

© 2007 NRC Canada

increments and total scale radius were measured on each scale. Length-at-age was back-calculated according to Lee (Ricker 1968) using a y intercept of 2 cm, which had been established in a previous regression analysis of fish length on scale radius. The results from three scales were averaged, and the mean back-calculated lengths-at-age were calculated for each cohort. In total, 2347 fish were used in this growth analysis.

Biomass

The standing stock biomass of whitefish was estimated based upon the monthly numerical age-class compositions. For fish in their first and second years of life, growth in length was linearly interpolated between the initial and final lengths. The initial length for age-0 fish was set at 12 mm, i.e., their length at hatching, while lengths after 1 and 2 years were those that had been back-calculated from the scales. The growing season of whitefish in ULC lasts from April to October. Therefore, growth was interpolated only for these months, while it was assumed to be zero in the other months. For the year classes 1947–1954, 1982–1984, and 1986–1997, length at the end of the third year could be back-calculated from scales, and the same procedure was applied for these cohorts. For fish older than 2 or 3 years, whose length-at-age could not be back-calculated from scales, von Bertalanffy growth curves were constructed. We used the available back-calculated lengths, including length at hatching (12 mm) and a generalized asymptotic length of 73 cm (www.fishbase.com) to construct Ford–Walford plots, from which the growth parameter k was estimated for each cohort. From the von Bertalanffy growth model, the lengths-at-ages for fish older than 2 or 3 years were calculated. As for the younger fish, growth was linearly interpolated for the months April to October.

Length was converted into weight using separate length–weight regressions for each decade. These were constructed from the length–weight data of around 100 fish sampled during the growing seasons in each decade. As these data covered a size range of 25–40 cm only, we also incorporated length–weight data for fish from 2 to 8 cm length, which were obtained during a standardized beach seine fishery from 1997 to 2004 (Reyjol et al. 2005). All decadal length–weight regressions had R^2 values of 0.995 and above. For each month, the average length per age class was converted into weight, multiplied by the number of fish per age class, and then summed across age classes. Finally, to obtain an estimate of standing stock biomass for each year, we averaged monthly biomass values per year.

Statistical analysis

Multiple linear regression analysis was performed using JMP Version 4.0.4 (SAS Institute Inc., Cary, North Carolina). The length increment of the whitefish during their second year was used as the dependent variable. We considered two independent variables, PO_4-P concentration during spring turnover and the natural logarithm of standing stock biomass and also incorporated the calendar year as an independent variable at a later stage in the analysis. As the standing stock biomass could be reconstructed only from 1954 onwards, i.e., when the 1947 cohort was fished out, we based our analysis on 43 years of data.

Results

YCS of the whitefish for the years 1947 to 1997 ranged between 94 000 (year classes 1964 and 1965) and 4 460 000 (year class 1974), with a median value of 950 000 individuals. In the 1950s and from the late 1980s until present, the standing stock comprised five to six age classes, and biomass ranged from 500 tonnes (9.3 kg·ha^{-1}) to 2000 tonnes (37.3 kg·ha^{-1}) (Fig. 2). During the 1960s and early 1970s, biomass never exceeded 500 tonnes and even fell below 30 tonnes in the spring of 1967. This stock comprised only young fish up to 3 years of age. Exceptionally strong year classes dominated the standing stock biomass during 2–3 years, most notably the year classes of 1974 and 1982. Biomass increased steadily from the early 1980s, except for the years 1986–1987 and 1992–1994. During the 1990s, standing stock biomass reached the highest values on record, being about twice as high as in the 1950s. Age classes 3 and 4 dominated the stock during the most recent years.

Length of whitefish after their first year did not vary much, i.e., by a factor of 1.5, during the study period (Fig. 3), but by contrast, length increment during the second year differed by a factor of 1.9. The fish grew nearly 10 cm more during their second year in the 1970s when compared with the 1950s and 1990s. Although the length after 3 years could not be back-calculated from scales for the entire study period, it showed a similar trend.

Linear regression analysis revealed that length after the first year was only weakly correlated with standing stock biomass ($R^2 = 0.24$, $P = 0.0008$, $n = 43$), and no correlation existed with PO_4-P concentration ($R^2 = 0.06$, $P = 0.103$) or calendar year ($R^2 = 0.005$, $P = 0.609$). The length increments of the whitefish during their second year, however, were significantly correlated with the natural logarithm of standing stock biomass (tonnes) ($P < 0.0001$) and with the PO_4-P concentration (μg·L^{-1}) during spring mixing ($P < 0.0001$), with an adjusted R^2 value of 0.78 (Table 1). The year 1954, the first year in our analysis, was excluded because it was considered to be an outlier. When the calendar year was included as the third independent variable, the model fit improved (adjusted $R^2 = 0.84$). The first two independent variables were still significant at $P < 0.0001$, and the variable calendar year was significant at $P < 0.0004$ with a negative influence on length increment during the second year (Table 1). In both models, the residuals were normally distributed and not autocorrelated.

To assess the relative importance of the three independent variables, scaled estimates centred by their means were used. These estimates indicate how much the length increment during the second year changes when one variable ranges from its lowest to its highest value while the other two variables are set to their mean value. Length increment changes due to standing stock biomass (range: 52.9–1976 tonnes) are 6.0 cm; they are 3.5 cm due to PO_4-P concentration (range: 8.3–87.2 μg·L^{-1}) and 2.6 cm due to the variable calendar year (range 1955–1997). This analysis indicates that standing stock biomass had the strongest influence on the growth

© 2007 NRC Canada

Fig. 2. Standing stock biomass by age classes of whitefish (*Coregonus lavaretus*) in Upper Lake Constance based upon virtual year-class strengths.

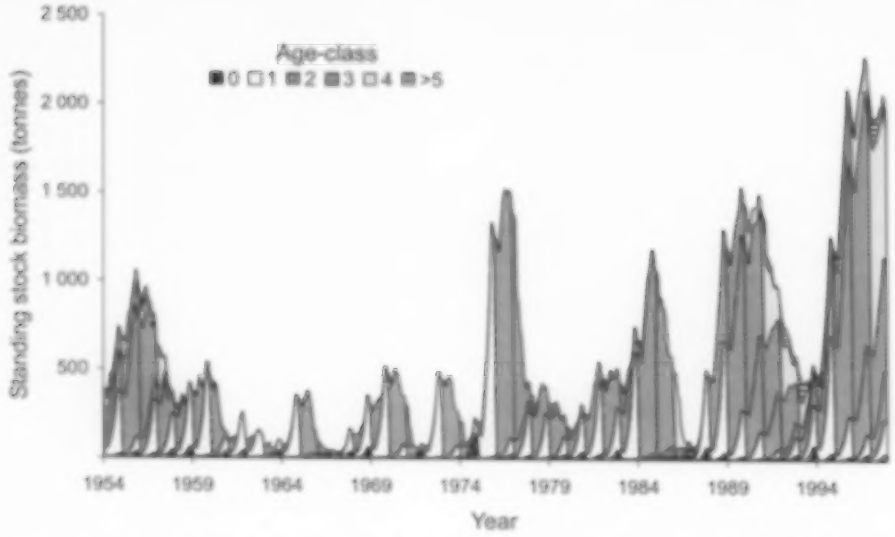

Fig. 3. Back-calculated lengths for the 1947–1997 cohorts of whitefish (*Coregonus lavaretus*) from Upper Lake Constance at the end of their first (solid triangles), second (shaded triangles), and third (open triangles) year of life. Second-degree polynomials were fit to the data to show trends.

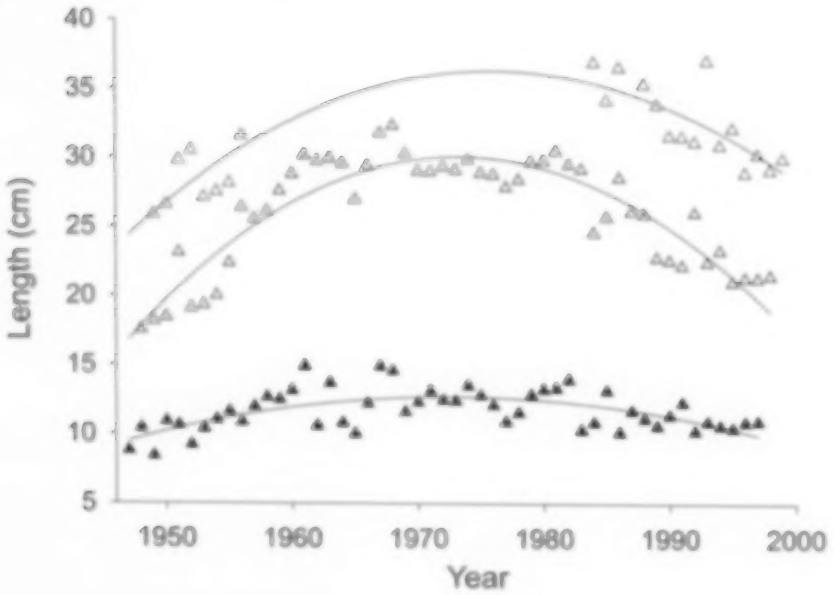

of whitefish during their second year, followed by PO_4-P concentration and the variable calendar year.

Discussion

Our results support and at the same time extend the earlier concept about the influence of eutrophication on the growth of whitefish. The earlier studies focussed exclusively on lake nutrient content and considered increasing lake P loads and their bottom-up effects on the pelagic food chain to be the ultimate and only cause of faster fish growth (Downing et al. 1990). Growth deceleration towards the end of the 20th century was attributed exclusively to lake reoligotrophication (Kirchhofer 1995; Eckmann and Rösch 1998; Müller and Mbwenembo Bia 1998). The similar time course of P concentration and whitefish growth, e.g., in ULC (Fig. 4), lends

© 2007 NRC Canada

Table 1. Results of two- and three-factor multiple regression analyses of whitefish (*Coregonus lavaretus*) growth in Upper Lake Constance from 1955 to 1997.

	Model 1		Model 2	
Term	Estimate	*P*	Estimate	*P*
Intercept	26.596	<0.0001	143.223	<0.0001
ln biomass	−2.150	<0.0001	−1.668	<0.0001
PO_4-P	0.034	<0.0001	0.044	<0.0001
Calendar year	—	—	−0.061	<0.0004
Adjusted R^2	0.78		0.84	

Note: Length increment in the second year is the dependent variable. The natural logarithm of standing stock biomass (ln biomass), PO_4-P concentration during spring mixing, and calendar year were used as independent variables.

Fig. 4. Length increment of whitefish (*Coregonus lavaretus*) in their second year (open triangles), phosphorus concentration (open squares), and yearly averages of standing stock biomass of lake whitefish (solid diamonds) in Upper Lake Constance.

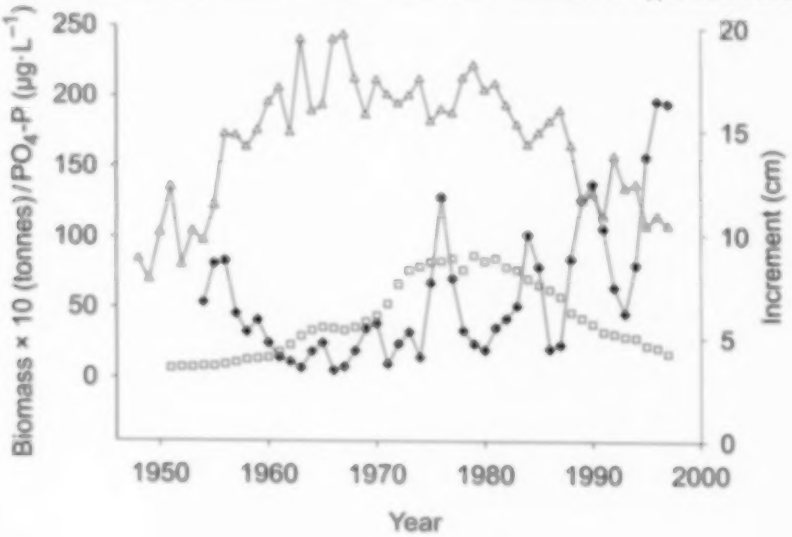

supports to this general concept. Our analysis, by contrast, demonstrates that standing stock biomass has an even stronger effect on whitefish growth.

Standing stock biomass of whitefish showed an opposite trend as compared with P concentration during the study period, decreasing to consistently low levels in the 1960s and early 1970s and increasing towards the 1990s, suggesting an influence of stock biomass on whitefish growth in parallel to that of eutrophication. The evolution of standing stock biomass over time was, however, more irregular than the regular increase and then decrease of P concentration. Particularly weak or strong year classes resulted in low or high levels of whitefish biomass, respectively, which were observed at similar levels of P concentration. This allowed disentangling the effects of both factors on whitefish growth using data from 43 consecutive years. The decrease in the standing stock biomass of whitefish during the late 1950s to early 1960s was most likely caused by greater fishing intensity because of the increased use of efficient nylon gill nets. The subsequent increase in the standing stock biomass of whitefish can be attributed in part to the global reduction of fishing intensity down to 17% from 1961 to 2005 and to the slower growth of whitefish, which results in higher age-at-capture.

Lake trophic state is supposed to influence whitefish growth because of bottom-up enhancement of secondary production. The yearly average crustacean zooplankton density in ULC, integrated over the entire water column, increased from 4×10^5 individuals·m^{-2} to above 10^6 during the 1960s and 1970s and has dropped back in recent years to values between 4 and 6×10^5 individuals·m^{-2} (IGKB 2004). Whitefish stock biomass, on the other hand, most probably affects growth because of intraspecific competition for food, because lake whitefish are by far the dominant consumers of zooplankton in ULC. Potential heterospecific competitors are either not very abundant (brown trout (*Salmo trutta*)) or they use the pelagic zone only sporadically (Eurasian perch (*Perca fluviatilis*)). Intraspecific competition for food is, therefore, much more crucial than interspecific competition.

Density-dependent growth of fish, mediated through intraspecific resource competition, can be an important controlling factor of fish population dynamics (Wanzenböck et al.

© 2007 NRC Canada

2002). Food limitation is of course a prerequisite for density-dependent effects on growth. A comparison between whitefish and zooplankton biomasses in ULC during the past decades highlights the potential for intraspecific competition for food in this lake. During the year 1989, an average whitefish standing stock of 1270 tonnes consumed roughly 13 000 tons of zooplankton during the growing season (Eckmann et al. 2002). When we assume a similar consumption of zooplankton for the entire study period, the demand for zooplankton would range from 730 to 20 200 tonnes, i.e., more than a 27-fold difference. The yearly average crustacean zooplankton density in ULC, however, ranged from 4×10^5 to 1.4×10^6 individuals·m^{-2} (IGKB 2004), i.e., only a 3.5-fold difference.

The influence of both P concentration and standing stock biomass on whitefish growth is much less pronounced in the first year than in the second year of their life. This can be attributed to the different temperatures experienced and to the different food sources utilized by young-of-the-year and older whitefish. During their first months of life, whitefish live in the epilimnion, where their growth is mainly controlled by temperature rather than zooplankton concentration (Eckmann and Pusch 1989). Only later in summer do young whitefish avoid the warm epilimnion and move to deeper layers, where they eventually join their older conspecifics. Nevertheless, they utilize different food resources, preying mainly on daphnids, whereas larger whitefish select large carnivorous crustaceans, such as *Bythotrephes longimanus* and *Leptodora kindtii* in addition to daphnids (Eckmann et al. 2002). Juvenile and adult whitefish stay within or slightly below the thermocline during the growing season (Ptak and Appenzeller 1998) at temperatures below 14 °C. Their growth, therefore, depends much less on temperature when compared with the very young whitefish, and the influence of food concentration, which depends on lake trophic state and competitor biomass, on their growth is more pronounced.

Including the calendar year as the third independent variable in the regression model improved the model fit, suggesting that whitefish growth rate declined with time, independent of lake trophic state and intensity of competition. The scaled estimate for the variable calendar year suggests that growth of 2-year-old fish declined by almost 0.6 cm every 10 years. We consider this result to be circumstantial evidence that the highly size-selective fishery during at least four decades provoked an evolutionary response in the stock by selecting for genotypes with lower growth potential. A similar conclusion was reached by (Handford et al. 1977), who studied growth rates, condition, and mean ages of a lake whitefish stock over 34 years.

The potential for an evolutionary change in the growth rate of ULC whitefish is supported by the differences in growth rates of fish from the 1991 and 1992 cohorts, which were harvested from the lake in consecutive years. The selection differential, in this case the difference in length after two growing seasons between the fish harvested at the end of their second year and the population mean, was 1.7 cm for the 1991 cohort and 1.6 cm for the 1992 cohort. Assuming a heritability of 0.2, which is typical for life-history traits (Conover and Munch 2002), these data demonstrate the potential for an evolutionary response to size-selective harvest. This estimate of the selection differential is, however, conservative, because it is based upon cohorts that were fished out during 68 and 71 months, respectively. During the 1960s and early 1970s, whitefish grew so fast that cohorts were fished out over 17–44 months. Up to 60% of these cohorts were even fished at age 1+, i.e., before the fish had reproduced, whereby the fastest-growing fish were effectively excluded from contributing genes to the next generation.

We decided to compare growth between cohorts by using the length after 2 years of the average fast-growing fish, because we have shown that whitefish are harvested in a highly size-selective way from ULC. The definition of the point in time when 50% of a cohort was fished out was possible with high accuracy, based upon monthly catch records and on the monthly age composition of catches derived from the test fishery. As whitefish yields are not evenly distributed across months within a fishing year, this approach is more accurate compared with traditional virtual population analysis using a constant instantaneous rate of fishing mortality. In the case of natural mortality, however, we have incorporated a constant instantaneous rate of 0.2 per year. Without considering natural mortality, the biomass of those cohorts that were fished out over a longer time (in some cases more than 5 years) would have been systematically underestimated as compared with cohorts fished out more quickly (during less than 2 years).

The highly significant influence of stock biomass on whitefish growth needs to be carefully considered in the future management of the whitefish fishery in ULC and elsewhere. An earlier analysis of the factors that influence whitefish year-class strength in ULC has demonstrated that stronger year classes are produced when lake surface temperature increases earlier in spring (Eckmann et al. 1988). This hypothesis has recently been supported by a reanalysis of an extended data set covering 52 years (Straile et al. 2007). Based upon the earlier analysis, Trippel et al. (1991) have predicted that whitefish year-class strength will likely increase as a result of global climate change. This would probably result in larger stock size, which might translate into enhanced intraspecific competition for food and ultimately into a further reduction of growth rate. Under this scenario, the present stocking practice will need reconsideration. The high standing stock biomass of whitefish in Lake Geneva, for example, is attributed among other factors to an intensive stocking program (Gerdeaux 2004). Even if the precise contribution of stocking to the whitefish population size in ULC were unknown so far, any reduction of stock biomass would contribute to alleviating intraspecific competition for food. This might be even more necessary in the future, as P concentrations in ULC are continuing to decrease and a further reduction of zooplankton biomass can be expected.

The present results apply not only to ULC but probably to many other coregonid lakes in Europe and elsewhere. Anthropogenic eutrophication was a worldwide problem during the second half of the 20th century, and it affected many lakes dominated by coregonids (Christie 1972; Colby et al. 1972; Grimås et al. 1972). In many of these lakes, eutrophication has been successfully abated in the meantime, and the lakes have returned or are returning to pre-eutrophication levels (Eckmann et al. 2007). Additionally,

© 2007 NRC Canada

fishing intensity has probably changed in many of these lakes in a way similar to that in ULC, as monofilament gill nets became widely used during the 1950s and early 1960s. It can therefore be speculated that stock size might have decreased in parallel to eutrophication in several other lakes as well, so that the former concepts about the sole dependence of whitefish growth on nutrient concentration deserve to be reconsidered.

Acknowledgements

We sincerely thank M. Kugler (Amt für Jagd und Fischerei, St. Gallen, Switzerland) for providing catch statistics, H. Loeffler and B. Engesser (Institute for Lake Research, Langenargen) and R. Roesch and H.P. Billmann (Fischereiforschungsstelle, Langenargen) for providing catch statistics, data from the regular test fishery, and whitefish scales for analysis. We are grateful to Nina Ebert, Felix Heindl, Barbara Schlick, and Daniel Sievers for their assistance in data input and scale analyses. M. Morris corrected the English. This project was supported within the priority program AQUASHIFT by the Deutsche Forschungsgemeinschaft (EC 146/3-1).

References

Amundsen, P.-A. 1988. Effects of an intensive fishing programme on age structure, growth and parasite infection of stunted whitefish (*Coregonus lavaretus* L. *s.l.*) in Lake Stuorajarvi, northern Norway. Finn. Fish. Res. **9**: 425–434.

Bidgood, B.F. 1973. Divergent growth in two lake whitefish (*Coregonus clupeaformis*) populations. J. Fish. Res. Board Can. **30**: 1683–1696.

Christie, W.J. 1972. Lake Ontario: effects of exploitation, introductions and eutrophication on the salmonid community. J. Fish. Res. Board Can. **29**(6): 913–929.

Colby, P.J., Spangler, G.R., Hurley, D.A., and McCombie, A.M. 1972. Effects of eutrophication on salmonid communities in oligotrophic lakes. J. Fish. Res. Board Can. **29**(6): 975–983.

Conover, D.O., and Munch, S.B. 2002. Sustaining fisheries yields over evolutionary time scales. Science (Washington, D.C.), **297**: 94–96.

Conover, D.O., Arnott, S.A., Walsh, M.R., and Munch, S.B. 2005. Darwinian fishery science: lessons from the Atlantic silverside (*Menidia menidia*). Can. J. Fish. Aquat. Sci. **62**: 730–737.

Downing, J.A., Plante, C., and Lalonde, S. 1990. Fish production correlated with primary productivity, not the morphoedaphic index. Can. J. Fish. Aquat. Sci. **47**: 1929–1936.

Eckmann, R., and Pusch, M. 1989. The influence of temperature on growth of young coregonids (*Coregonus lavaretus* L.) in a large prealpine lake. Rapp. P.-V. Réun. Cons. Int. Explor. Mer, **191**: 201–208.

Eckmann, R., and Rösch, R. 1998. Lake Constance fisheries and fish ecology. Arch. Hydrobiol. Spec. Issues Adv. Limnol. **53**: 285–301.

Eckmann, R., Gaedke, U., and Wetzlar, J. 1988. Effects of climatic and density-dependent factors on year-class strength of *Coregonus lavaretus* in Lake Constance. Can. J. Fish. Aquat. Sci. **45**(6): 1088–1093.

Eckmann, R., Becker, M., and Schmid, M. 2002. Estimating food consumption by a heavily fished stock of zooplanktivorous *Coregonus lavaretus*. Trans. Am. Fish. Soc. **131**: 946–955.

Eckmann, R., Gerdeaux, D., Müller, R., and Rösch, R. 2007. Re-oligotrophication and whitefish fisheries management — a workshop summary. Arch. Hydrobiol. Spec. Issues Adv. Limnol. **60**: 351–358.

Gerdeaux, D. 2004. The recent restoration of whitefish fisheries in Lake Geneva: the role of stocking, reoligotrophication, and climate change. Ann. Zool. Fenn. **41**: 181–189.

Grimås, U., Milsson, N.-A., and Wendt, C. 1972. Lake Vättern: effects of expoitation, eutrophication, and introduction on the salmonid community. J. Fish. Res. Board Can. **29**(6): 807–817.

Handford, P., Bell, G., and Reimchen, T. 1977. A gillnet fishery considered as an experiment in artificial selection. J. Fish. Res. Board Can. **34**: 954–961.

Helminen, H., Auvinen, H., Hirvonen, A., Sarvala, J., and Toivonen, J. 1993. Year-class fluctuations of vendace (*Coregonus albula*) in Lake Pyhäjärvi, southwest Finland, during 1971–90. Can. J. Fish. Aquat. Sci. **50**: 925–931.

Hoff, M.H., and Todd, T.N. 2004. Status of the shortjaw cisco (*Coregonus zenithicus*) in Lake Superior. Ann. Zool. Fenn. **41**(1): 147–154.

IGKB. 2004. Limnologischer Zustand des Bodensees **31**. Available from the Internationale Gewässerschutzkommission für den Bodensee (IGKB). 2. Auflage. Bregenz, Austria. ISBN 3-902290-04-8. pp. 31–39.

Kirchhofer, A. 1995. Growth characteristics of coregonid populations in three lakes with different trophic states and decreasing nutrient concentrations. Arch. Hydrobiol. Spec. Issues Adv. Limnol. **46**: 61–70.

Law, R. 2000. Fishing, selection, and phenotypic evolution. ICES J. Mar. Sci. **57**: 659–668.

Lehtonen, H., and Niemelä, E. 1998. Growth and population structure of whitefish (*Coregonus lavaretus* (L.)) in mountain lakes of northern Finland. Arch. Hydrobiol. Spec. Issues Adv. Limnol. **50**: 81–95.

Lorenzen, K., and Enberg, K. 2002. Density-dependent growth as a key mechanism in the regulation of fish populations: evidence from among-population comparisons. Proc. R. Soc. Lond. B Biol. Sci. **269**: 49–54.

Mayr, C. 2001. The influence of population density on growth of whitefish (*Coregonus lavaretus* L.) in four prealpine lakes. Limologica, **31**: 53–60.

Mills, K.H., Chalanchuk, S.M., Allan, D.J., and Mohr, L.C. 1995. Responses of lake whitefish (*Coregonus clupeaformis*) to exploitation at the Experimental Lakes Area, northwestern Ontario. Arch. Hydrobiol. Spec. Issues Adv. Limnol. **46**: 361–368.

Müller, R., and Mbwenembo Bia, M. 1998. Adaptive management of whitefish stocks in lakes undergoing re-oligotrophication: the Lake Lucern example. Arch. Hydrobiol. Spec. Issues Adv. Limnol. **50**: 391–399.

Nümann, W. 1959. Das Wachstum der Blaufelchen und seine Berechnung bei Erfassung aller Individuen der einzelnen Jahrgänge in Abhängigkeit von der Stärke des Jahrgangs, den jährlich variierenden Aussenfaktoren, der Eutrophierung und den regionalen Unterschieden des Sees. Archiv. Fischwiss. **10**: 5–20.

Nümann, W. 1972. The Bodensee: effects of expoitation and eutrophication on the salmonid community. J. Fish. Res. Board Can. **29**(6): 833–847.

Post, J.R., Parkinson, E.A., and Johnston, N.T. 1999. Density-dependent processes in structured fish populations: interaction strengths in whole-lake experiments. Ecol. Monogr. **69**: 155–175.

Price, H., Pothoven, S.A., McCormick, M.J., Jensen, P.C., and Fahnenstiel, G.L. 2003. Temperature influence on commercial

© 2007 NRC Canada

lake whitefish harvest in Eastern Lake Michigan. J. Gt. Lakes. Res. **29**(2): 296–300.

Ptak, J.K., and Appenzeller, A.R. 1998. Size, depth, and frequency of pelagic Lake Constance whitefish (*Coregonus lavaretus* L.) shoals during the seasons: a hydroacoustic study. Arch. Hydrobiol. Spec. Issues Adv. Limnol. **50**: 237–248.

Reyjol, Y., Fischer, P., Lek, S., Rösch, R., and Eckmann, R. 2005. Studying the spatiotemporal variation of the littoral fish community in a large prealpine lake, using self-organizing mapping. Can. J. Fish. Aquat. Sci. **62**: 2294–2302.

Ricker, W.E. 1968. Methods for assessment of fish production in fresh-waters. Blackwell Scientific Publications, Oxford and Edinburgh.

Rijnsdorp, A.D. 1993. Fisheries as a large-scale experiment on life-history evolution: disentangling phenotypic and genetic effects in changes in maturation and reproduction of North Sea plaice, *Pleuronectes platessa* L. Oecologia, **96**(3): 391–401.

Salonen, E., and Mutenia, A. 2004. The commercial coregonid fishery in northernmost Finland — a review. Ann. Zool. Fenn. **41**(1): 351–355.

Salonen, E., Ahonen, M., and Mutenia, A. 1998. Development of whitefish (*Coregonus lavaretus*) population and effects of large-scale compensation stocking in Lake Inari northern Finland. Arch. Hydrobiol. Spec. Issues Adv. Limnol. **50**: 439–448.

Sinclair, A.F., Swain, D.P., and Hanson, J.M. 2002. Measuring changes in the direction and magnitude of size-selective mortality in a commercial fish population. Can. J. Fish. Aquat. Sci. **59**: 361–371.

Straile, D., Eckmann, R., Jüngling, T., Thomas, G., and Löffler, H. 2007. Influence of climate variability on whitefish (*Coregonus lavaretus*) year-class strength in a deep, warm monomictic lake. Oecologia, **151**: 521–529.

Trippel, E.A., Eckmann, R., and Hartmann, J. 1991. Potential effects of global warming on whitefish in Lake Constance, Germany. Ambio, **20**(6): 226–231.

Valkeajärvi, P. 1992. Effects of increased fishing effort on the european whitefish (*Coregonus wartmanni*) stock in Lake Päijänne. Pols. Arch. Hydrobiol. **39**: 817–825.

Viljanen, M., Turunen, T., and Väisänen, P. 2004. Fluctuations in year-class strength of the vendace (*Coregonus albula* (L.)) in the small, mesohumic, oligotrophic Suomunjärvi, a lake in eastern Finland. Ann. Zool. Fenn. **41**: 241–248.

Walters, C.J., and Post, J.R. 1993. Density-dependent growth and competitive asymmetries in size-structured fish populations: a theoretical model and recommendations for field experiments. Trans. Am. Fish. Soc. **122**: 34–45.

Wanzenböck, J., Gassner, H., Hassan, Y., Lahnsteiner, B., and Hauseder, G. 2002. Ecology of European whitefish, *Coregonus lavaretus*, in two Austrian lakes in relation to fisheries management and lake productivity. *In* Management and ecology of lake and reservoir fisheries. *Edited by* I.G. Cowx. Blackwell Science, Oxford. pp. 58–69.

© 2007 NRC Canada

Relating otolith chemistry to surface water chemistry in a coastal plain estuary

Emmanis Dorval, Cynthia M. Jones, Robyn Hannigan, and Jacques van Montfrans

Abstract: Although laboratory studies confirm that otoliths incorporate trace elements and stable isotopes from surrounding waters, few studies explore the relationship of otolith chemistry to water chemistry in the field and none include a larger suite of environmental tracers, such as rare earth elements. Using spotted seatrout (*Cynoscion nebulosus*) as model species, we tested the hypothesis that otoliths record the water chemistry of seagrass habitats in Chesapeake Bay. In summer 2001, we sampled water and juvenile fish in seagrass beds of the bay. Weighted linear regressions showed that $[Ba/Ca]_{otolith}$ and $[La/Ca]_{otolith}$ were best predicted by salinity and were modeled as $[Ba/Ca]_{otolith}$ ($\mu mol \cdot mol^{-1}$) = –2.25 ± 0.35 × salinity + 59.47 ± 7.01) and $[La/Ca]_{otolith}$ ($pmol \cdot mol^{-1}$) = –8.71 ± 0.65 × salinity + 243.87 ± 12.52. $[Ba/Ca]_{otolith}$ increased with $[Ba/Ca]_{water}$, but the relationship was nonlinear. Salinity did not influence $[Mn/Ca]_{otolith}$, but this ratio was positively correlated with $[Mn/Ca]_{water}$. Although the partition coefficient of Sr (D_{Sr} = 0.23 ± 0.019) was similar to that in laboratory experiments, [Sr/Ca] in waters and otoliths was decoupled despite equal temperature exposure, suggesting that $[Sr/Ca]_{otolith}$ concentration may not be a simple function of water composition. However, there was a predictive relationship between $[\delta^{18}O]_{otolith}$ and $[Sr/Ca]_{water}$ ($[\delta^{18}O]_{otolith}$ = 1.18 ± 0.09 × $[Sr/Ca]_{water}$ ($mmol \cdot mol^{-1}$) – 14.286 ± 0.78) resulting from mixing between fluvial and oceanic waters. Water chemistry showed mixed values as a proxy for otolith chemistry and may not be a surrogate for otolith chemistry in wide estuaries.

Résumé : Bien que les études en laboratoire confirment que les otolithes accumulent les éléments en trace et les isotopes stables à partir du milieu aquatique environnant, peu d'études examinent la relation entre la chimie des otolithes et la chimie de l'eau en nature; aucune n'inclut un éventail élargi de traceurs environnementaux, tels que les éléments de terres rares. Utilisant l'acoupa royal (*Cynoscion nebulosus*) comme espèce modèle, nous vérifions l'hypothèse selon laquelle les otolithes reflètent la chimie des habitats d'herbes marines dans la baie de Chesapeake. À l'été 2001, nous avons échantillonné l'eau et les jeunes poissons dans les herbiers à herbes marines dans la baie. Des régressions linéaires pondérées montrent que $[Ba/Ca]_{otolithe}$ et $[La/Ca]_{otolithe}$ sont le mieux prédites par la salinité, selon les modèles $[Ba/Ca]_{otolithe}$ ($\mu mol \cdot mol^{-1}$) = –2,25 ± 0,35 × salinité + 59,47 ± 7,01 et $[La/Ca]_{otolithe}$ ($pmol \cdot mol^{-1}$) = –8,71 ± 0,65 × salinité + 243,87 ± 12,52. $[Ba/Ca]_{otolithe}$ augmente en fonction de $[Ba/Ca]_{eau}$, mais la relation n'est pas linéaire. La salinité n'influence pas $[Mn/Ca]_{otolithe}$, mais ce rapport est en corrélation positive avec $[Mn/Ca]_{eau}$. Bien que le coefficient de partition de Sr (D_{Sr} = 0,23 ± 0,019) soit semblable à celui observé dans les expériences de laboratoire, les [Sr/Ca] des eaux et des otolithes sont dissociées malgré une exposition semblable à la température, ce qui laisse croire que $[Sr/Ca]_{otolithe}$ puisse ne pas être une fonction simple de la composition de l'eau. Il existe cependant une relation prédictive entre $[\delta^{18}O]_{otolithe}$ et $[Sr/Ca]_{eau}$ selon la formule $[\delta^{18}O]_{otolithe}$ = 1,18 ± 0,09 × $[Sr/Ca]_{eau}$ ($mmol \cdot mol^{-1}$) – 14,286 ± 0,78, relation qui résulte du mélange des eaux fluviales et océaniques. La chimie de l'eau sert de façon inégale comme variable de rechange de la chimie des otolithes et peut ne pas être un remplacement valable pour la chimie des otolithes dans les estuaires de grande largeur.

[Traduit par la Rédaction]

Introduction

The use of trace elements in otoliths, as tracers of water mass chemistry (and by corollary, habitat residency), relies on the premise that otolith chemistry accurately records the water chemistry experienced by fish throughout their lives (Begg et al. 1998; Thorrold et al. 2001; Dorval et al. 2005*b*). The validity of this assumption has been tested using laboratory-controlled experiments, which have generated a growing body of evidence demonstrating a direct and pre-

Received 5 April 2006. Accepted 4 November 2006. Published on the NRC Research Press Web site at http://cjfas.nrc.ca on 17 March 2007.
J19260

E. Dorval[1,2] and C.M. Jones. Center for Quantitative Fisheries Ecology, Department of Ocean, Earth and Atmospheric Sciences, Old Dominion University, Norfolk VA 23529, USA.
R. Hannigan. Environmental Sciences, Arkansas State University, State University, AR 72467, USA.
J. van Montfrans. Virginia Institute of Marine Science, College of William and Mary, Gloucester Point, VA 23062, USA.

[1]Corresponding author (e-mail: emmanis.dorval@noaa.gov).
[2]Present address: Southwest Fisheries Science Center, 8604 La Jolla Shores Drive, La Jolla, CA 92037, USA.

 doi:10.1139/F07-015 © 2007 NRC Canada

dictable relationship between water chemistry and otolith chemistry (Bath et al. 2000; Milton and Chenery 2001; Zimmerman 2005). For example, Secor et al. (1995) showed that the ratio [Sr/Ca] in otoliths of juvenile striped bass (*Morone saxatilis*) was positively correlated with salinity. In a subsequent study, Kraus and Secor (2004) demonstrated that [Sr/Ca] values in otoliths of a congener (white perch (*Morone americana*)) were significantly related to salinity, albeit nonlinearly. Likewise, Gallahar and Kingsford (1996) observed that [Sr/Ca] in otoliths of *Girella elevata* increased with increasing Sr in water. Bath et al. (2000) and Milton and Chenery (2001) found predictable fractionation between water and otolith [Sr/Ca] and [Ba/Ca] and quantified these relationships by calculating D_{Me}, the partition coefficient, which measures the molar proportion of uptake in the otolith to the concentration in water. Specifically, Bath et al. (2000) demonstrated that [Sr/Ca] exhibited linear relationships that were dependent on temperature (D_{Sr} at 20 °C = 0.18, D_{Sr} at 25 °C = 0.21), whereas [Ba/Ca] showed a linear relationship independent of temperature (D_{Ba} = 0.06).

Although laboratory experiments allow the testing of specific hypotheses in a controlled environment, they also create artificial conditions that may depart from conditions occurring in nature. For example, Bath et al. (2000) set the water [Sr/Ca] significantly higher in test water (15.21–22.80 mmol·mol^{-1} on average) than that of natural seawater (8–9 mmol·mol^{-1}). Further, these experiments do not reproduce the scale at which physical and chemical factors interact to control the environmental variability that individual fish experience in the wild. In estuaries, diurnal and fortnightly tidal cycles, river discharges, Coriolis acceleration, convergence flow, etc., interact to determine spatial and temporal distribution of trace elements (e.g., Shumilin et al. 1993; Paucot and Wollast 1997; Dorval et al. 2005*a*). In such dynamic systems, water masses are more heterogeneous within a large estuary owing to the interaction of these physical processes. Moreover, trace elements interact with one another during their incorporation in biogenic mineral phases, such as in otolith aragonite, and the effect of this interaction may vary with a given environment (De Vries et al. 2005). All of these factors, chemical, biological, and physical, have the potential to cause major discrepancies between field and laboratory experiments.

Despite the acknowledged limitations of laboratory-based experiments, only three studies have directly tested the validity of the assumptions underlying the use of otolith chemistry in the field. Kraus and Secor (2004) found a direct relationship between [Sr/Ca] measured in the otolith of *M. americana* with salinity and [Sr/Ca] in waters of the Patuxent River estuary. Wells et al. (2003) determined that there was a linear dependence between [Ba/Ca] and [Sr/Ca] in ambient waters and in otoliths of Westslope cutthroat trout (*Oncorhynchus clarkii lewisi*) caught in the Coeur d'Alene river (Idaho). Similarly, Elsdon and Gillanders (2005) measured [Mn/Ca], [Sr/Ca], and [Ba/Ca] in waters and in otoliths of black bream (*Acanthopagrus butcheri*). However, to our knowledge, no previous studies have looked at the response of multiple trace elements in otoliths to water chemistry in a large estuary, and none have evaluated the rare earth elements, widely used as water mass tracers. The incorporation of rare earth elements in coral has been previously explored (e.g., Sholkovitz and Shen 1995) but has had little application in otolith chemistry. In a laboratory experiment, Ennevor and Beames (1993) demonstrated that La could be absorbed from water and deposited in otoliths, but this element has only been used in Dorval et al. (2005*b*) to discriminate habitat residency for fish.

Further, several elements that are commonly incorporated in otolith aragonite are often correlated because their concentrations are mediated by similar physical processes. For example, Thorrold et al. (1997) observed that patterns in Sr measured in otoliths of Atlantic croaker (*Micropogonias undulatus*) are consistent with movement from offshore to estuarine nurseries in the Mid- and South Atlantic Bight and were likely to be correlated with [δ^{18}O] in seawater. Hence, these authors argued that it was necessary to develop trace elements, such as Sr, in otoliths as tracers of variation in temperature exposure by fish to corroborate the assumption that [δ^{18}O] values of otolith aragonite unequivocally reflect changes in temperature as observed in several studies (e.g., Kalish 1991*a*; Radtke et al. 1996). We believe that the reverse process is also necessary when trying to elucidate which environmental factors control patterns of trace elements in otolith aragonite.

Indeed, various studies have established that [δ^{18}O] composition in calcite and aragonite of marine species is controlled by physical factors such as temperature and salinity. Polyak et al. (2003) found that the distribution of [δ^{18}O] in foraminiferal calcite is primarily controlled by the mixing of runoff and seawater in near-estuarine environments. Further, Khim et al. (2003) showed that [δ^{18}O] profiles of bivalve mollusks recorded seasonal changes in estuarine water discharges in the Bering Strait region, whereas Lécuyer et al. (2004) observed that [δ^{18}O] in both aragonite and calcite shells of marine tropical mollusks was determined by temperature and seawater composition. Similarly, the interaction effect between temperature and salinity was also found to be significant on otolith [δ^{18}O] of laboratory-reared black bream (Elsdon and Gillanders 2002). Accordingly, Elsdon and Gillanders (2002) argued for a multifactorial approach to testing hypotheses that otoliths record environmental conditions. Because trace elements interact with one another and because this interaction may vary with species as well, independent validation procedures documenting the effect of temperature on trace elements, such as Sr, would be valuable before extrapolation and application of results originating from both laboratory and field experiments. In either case, such an approach would also be valuable because it is often too difficult and too costly to sample fish and to collect information on all environmental parameters (e.g., water trace element concentration and stable isotopic composition) synoptically from the same experiment or sampling event.

In this study, we sought to determine (*i*) how the concentration of trace elements in otoliths reflects small-scale temporal and spatial changes in water chemistry within a large estuary, specifically salinity and elemental concentrations, and (*ii*) if there is a predictive relationship between water chemistry and otolith chemistry and, if so, at what spatial scale. Although we did not measure [δ^{18}O] in water, to be thorough in addressing these questions, we performed an ad-

© 2007 NRC Canada

ditional test using otolith [$\delta^{18}O$] as tracer for temperature to validate observed patterns in otolith [Sr/Ca]. To use otolith chemistry as a proxy for changes in water masses in the field and to reconstruct the environmental life histories of fishes, it is critical to answer these questions. Further, it is of practical value to determine whether there is a predictive relationship between water and otolith chemistry. A predictive relationship is causative, meaning if we know water chemistry in the field, then we can estimate otolith chemistry without the necessity of establishing an otolith chemistry baseline by sampling a cohort of fish directly. When a predictive relationship does not exist, then we must establish a cohort-specific otolith library to adequately study life history and population dynamics (Wells et al. 2003). Acquisition of otolith chemistry libraries is expensive and time-consuming compared with estimating water chemistry parameters.

In addressing the in situ relationship between otolith and water chemistry, we chose a species that is closely associated with its habitat, spotted seatrout (*Cynoscion nebulosus*). Spotted seatrout are estuarine-dependent fish that have developed a strong adaptation to seagrass habitats in most estuaries (McMichael and Peters 1989; Chester and Thayer 1990; Rooker et al. 1998). Thus, spotted seatrout can display strong spatial structure within estuaries (e.g., Baker and Matlock 1993). In most estuaries, mature spotted seatrout spawn in surface waters, and their yolk sac larvae spend approximately 1 week in the pelagic environment (N. Smith and C.M. Jones, personal communication (2006)) before settling in seagrass beds at 5–6.1 mm (Rutherford et al. 1989; Poling and Fuiman 2000). Larvae transform into juveniles at 10 mm (Ditty et al. 2006), and the juveniles remain in the seagrass habitats from late spring through summer (Chester and Thayer 1990; Rooker et al. 1998). As a direct result, Dorval et al. (2005*b*) found that otolith chemistry for those juveniles differed significantly between seagrass habitats along and across the lower Chesapeake Bay within and between years. As most seagrass beds in Chesapeake Bay possess their own distinct surface water chemical signatures (Dorval et al. 2005*a*), we could appropriately assume that otoliths of juvenile spotted seatrout caught in a seagrass bed carry geochemical signatures of the surface waters of that specific bed.

Using juvenile spotted seatrout, we tested the assumption that otoliths accurately record the chemistry of the habitats for salinity, [Mg/Ca], [Mn/Ca], [Sr/Ca], [Ba/Ca], and [La/Ca]. We predict the relationship between water and otolith chemistry for these trace elements in the context of the physical and chemical processes that may regulate such relationships in Chesapeake Bay. In addition, observed patterns in otolith [Sr/Ca] were validated using otolith [$\delta^{18}O$]. This study is the first report of a field-based test of the relationship between otolith and water chemistry in a large estuary and the first to quantify this relationship for otolith rare earth element chemistry.

Materials and methods

Collection: location, fish, and water

Juvenile spotted seatrout were collected in five seagrass habitats in the lower Chesapeake Bay: Potomac, Rappahannock, York, Island, and Pocomoke (Fig. 1). Juvenile spotted seatrout are residents of these seagrass habitats from the early juvenile stage (11–40 mm standard length) to the late juvenile stage (140 mm) (Orth and Heck 1980; Brown 1981; Rooker et al. 1998). In this study, we included fish that had standard lengths between 15 and 70 mm. This size restriction insured that we sampled fish that had not migrated and had been exposed only to the water chemistry of the seagrass habitats where they were resident before capture.

We sampled water and juvenile fish fortnightly in the five seagrass habitats of Chesapeake Bay from July through September 2001 using a nested design with individual seagrass beds (stations) nested within habitat (Fig. 1). At each station, salinity was measured and water collected and filtered using trace element clean procedures as described in Dorval et al. (2005*a*). We also monitored long-term temperature (Fig. 2) and salinity variation in the bay using HOBO sensors (Onset U.S. Patent 5373346) and microcat-seabird thermosalinographs (SBE 37). We collected a total of 120 water samples in the five seagrass habitats over the 3-month period. Juvenile spotted seatrout were collected randomly at each station using an otter trawl (0.64 cm stretched mesh, 7.9 m length; see Dorval et al. 2005*b*). In the laboratory, we recorded weight and standard and total length of individual fish and all fish were subsequently frozen. All fish caught in the Island, York, and Rappahannock habitats were used for analysis, but fish from the Potomac and Pocomoke Sound habitats were more numerous and were randomly subsampled.

Trace element analysis in waters

Dissolved trace and minor elements in water were quantified using a double-focusing sector field inductively coupled plasma mass spectrometer (Finningan MAT Element 2 ICP–MS) based on the method of external calibration with internal standardization (Taylor 2001). Indium was used as the internal standard and samples (n = 19–21) collected in a given week were analyzed as a batch following Dorval et al. (2005*a*). We measured the concentration of Mg, Ca, Mn, Sr, Ba, and La in each aliquot (see Table 1 for the isotopes that were measured). Mg, Ca, Mn, Sr, and Ba were selected because they are commonly used in otolith chemistry. La has had little application in otolith chemistry research but shows great potential for discriminating habitat use by fish, particularly in estuarine ecosystems (e.g., Dorval et al. 2005*b*). The method resolution and precision (percent relative standard deviation) of measurement for these six elements are reported in Table 1. Concentration of each element was determined from calibration curves based on known concentration of analytes in calibration standard solutions (Table 1).

Trace element analysis in otoliths

We extracted the sagittal otoliths from individual fish in a class-100 clean room using acid-washed glass probes. The right sagittal otolith was selected for solution-based ICP–MS analysis, while the left otolith was used to determine [$\delta^{18}O$].

Each sagittal otolith was cleaned with ultrapure water and all tissue was physically removed with acid-washed glass probes and the otolith then soaked for 5 min in ultrapure H_2O_2 (30% H_2O_2) to remove all possible remnant tissues. Otoliths were rinsed three times with ultrapure water and

© 2007 NRC Canada

Fig. 1. Map of lower Chesapeake Bay (modified from Dorval et al. 2005*a*) showing the locations of collection of water samples and juvenile fish used in this study. Water and juvenile fish were collected from July to September 2001 in five seagrass habitats: Potomac (□), Rappahannock (◇), York (▽), Island (○), and Pocomoke (△).

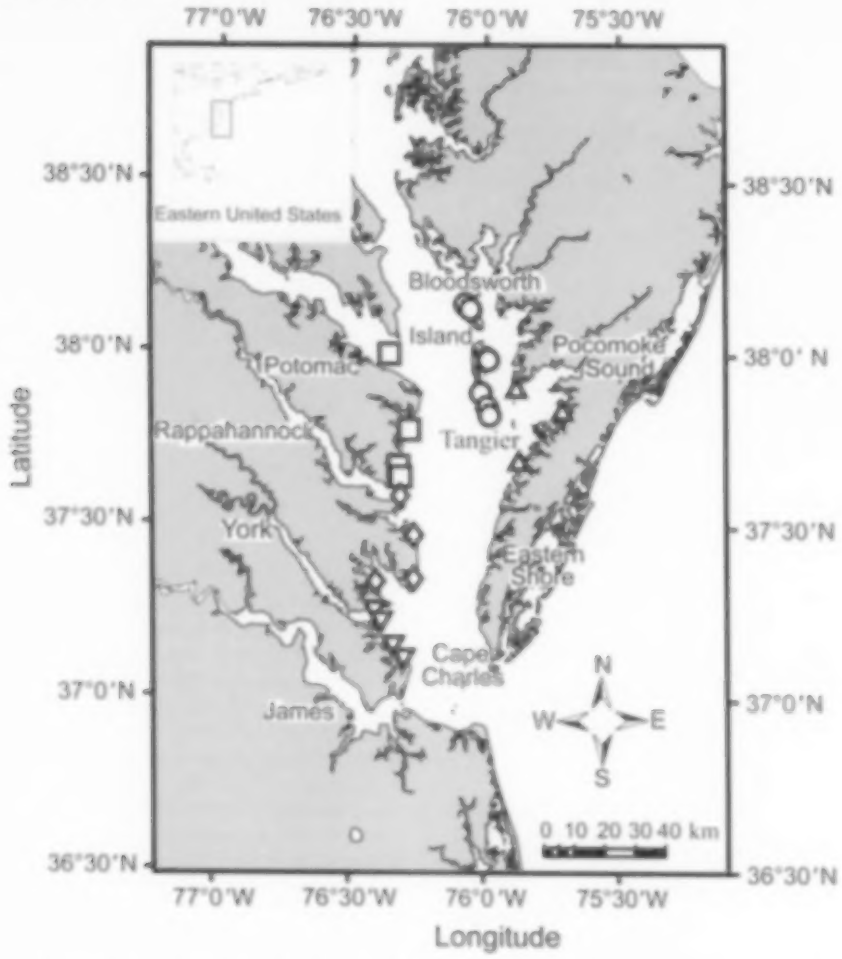

dried under a positive-flow hood, transferred to 5 mL of ultrapure water in acid-washed centrifuge-vials, sonicated for 5 min, and allowed to dry under a positive-flow hood. Subsequently, all otoliths were weighed to the nearest 10 μg and dissolved in 100 μL of ultrapure concentrated HNO_3 and then made up to 1 mL with 900 μL of 1% ultrapure HNO_3.

Otolith solutions were analyzed based on the same analytical procedures as for water using ICP–MS and indium as the internal standard. Otolith solutions were subsampled and spiked with indium, preparing aliquots of 1 mL and 2 ppb indium concentration. The aliquots were randomized within trays. The six elements Mg, Ca, Mn, Sr, Ba, and La were also measured in otoliths. We report the precision (percent relative standard deviation) of measurement of these elements in Table 1. Relative standard deviation was estimated for each element based on repeated measurement of a quality control check standard ($n = 30$) whose concentration was between the concentrations of the two lowest standards. Calibration procedures and correction for instrument drift and matrix effects were performed similarly as for water analysis. Further, all elements in both water and otoliths were normalized to Ca to allow comparison with other previously published studies.

Stable isotope analysis of otoliths

Left sagittal otoliths were analyzed to determine oxygen isotopic composition using an IsoPrime mass spectrometer (GV instrument, Manchester, UK) at the Stable Isotope Laboratory of the University of Maryland (College Park, Maryland). Each otolith was ground into a fine powder and 60–100 μg was analyzed for [δ^{18}O] (see Dorval et al. 2005*b*). After analysis, the raw data were corrected and reported in ‰PDB (Peedee Belemnite) using the standard δ notation. Precision of the measurements was 0.004‰ for δ^{13}C and 0.006‰ for [δ^{18}O] (average standard deviation of repeated measurements of the standards).

Data analysis

We calculated partition coefficients (D_{Me}) for each seagrass habitat using the method of Morse and Bender (1990,

© 2007 NRC Canada

Fig. 2. Mean daily temperature measured in three seagrass habitats (Potomac (□), Eastern Shore including Pocomoke Sound (△), and Island (○)) from July to September 2001. Note that because of a loss of probes, temperature was not recorded in Island from August to September and in the Eastern Shore from July to August. Nevertheless, the overall trend showed that there was no difference in temperature between habitats across the bay. This graph was reproduced from Dorval et al. (2005*a*).

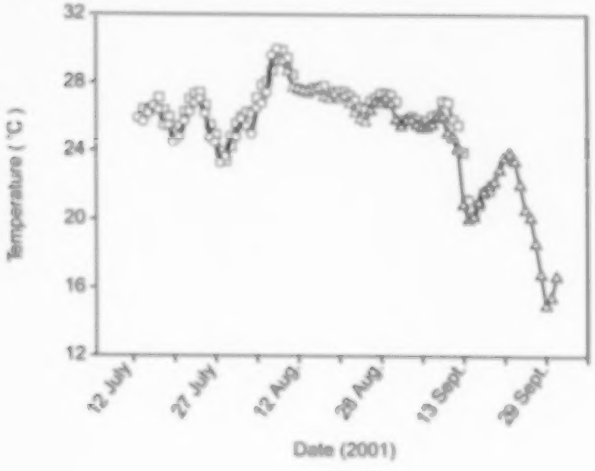

eq. 1). This method assumes a zero intercept but allows for comparisons between habitats when the overall relationship between [Me/Ca] in otoliths and [Me/Ca] in water is nonlinear. From these habitat-specific D_{Me}, we calculated the mean, SE, and proportional SEs (PSEs) of the estimate.

We used regression analyses to determine whether the ratios of metal to Ca (Me/Ca) and $[\overline{\delta}^{18}O]$ measured in otoliths were related to otolith weight. Otolith weight may confound the effect of water chemistry on otolith chemistry. Thus, regressions were performed for each element and for the pooled data independently of seagrass habitats. When linear relationships were significant, we adjusted the concentrations as follows:

$$(1) \qquad y_{i,adj} = y_i - b \times w_i$$

where $y_{i,adj}$ is the adjusted concentration for the ith otolith, y_i is the original concentration of the ith otolith in trace element or stable isotope, b is the slope estimated from the regression, and w_i is the weight of the ith otolith.

Least squares methods were used to quantify the relationship of trace element chemistry in otoliths with either salinity or $[Me/Ca]_{water}$ within habitats as independent, fixed factors and with the mean $[Me/Ca]_{otolith}$ as dependent variables. Observations used to compute the $[Me/Ca]_{otolith}$ were tested for lack of linear fit with both independent variables. Subsequently, we performed a weighted-regression analysis on the mean of $[Me/Ca]_{otolith}$ against mean salinity or mean $[Me/Ca]_{water}$ within habitats for variables showing no significant lack of linear fit. Weights were sample size divided by variance of $[Me/Ca]_{otolith}$ in a given habitat. A model was reported when the regression coefficient was different from zero along with SE for the regression coefficient and the intercept. Also, we used Spearman's correlation to quantify monotonic behavior between the mean of $[Me/Ca]_{otolith}$ and salinity or $[Me/Ca]_{water}$.

Because $[Sr/Ca]_{otolith}$ is influenced by temperature, we addressed the potential for differences in degree-day exposures by addressing the time series of hatch dates and corollary evidence. Importantly, temperature was similar among seagrass habitats at any given time, fluctuating seasonally from an overall mean of 25.66 °C in July to 27.4 °C in August and 23.1 °C in September (Fig. 2). Thus, we need only establish similar hatch dates to dismiss differences in fish temperature exposures as an underlying influence on otolith Sr chemistry. However, in 2001, both saggital otoliths were used for chemical analyses and it was not possible to age the juveniles from lapilli. To dispel concerns that different mean habitat birthdates could lead to degree-day temperature effects on otolith [Sr/Ca], we compared hatch dates of juvenile spotted seatrout collected from 1997 through 1999 and 2002 in Chesapeake Bay (Fig. 3). These plots showed that hatch date distribution of these juveniles was not significantly different among the major seagrass habitats within a given year in 4 years of a 6-year period. Thus, we could reasonably assume that juvenile spotted seatrout collected in 2001 in seagrasses would also have similar hatch date distribution and experience the same degree-day exposure. We also tested the hypothesis that if the cumulative change in temperature did alter the $[Sr/Ca]_{otolith}$, then either $[Sr/Ca]_{otolith}$ or its partition coefficient (D_{Sr}) in each habitat would be highly correlated with any variables that represented the influence of temperature over time. We compared $[Sr/Ca]_{otolith}$ with $[\overline{\delta}^{18}O]_{otolith}$, which was previously assumed by many authors to represent the integrated temperature effect (otolith $\overline{\delta}^{18}O$ was found to be highly and negatively correlated with temperature, e.g., Kalish 1991*a*, 1991*b*; Radtke et al. 1996). Further, in this study, we adjusted otolith $[\overline{\delta}^{18}O]$ so that it was neither age nor weight dependent assuming that older fish had larger otoliths.

In this context, we estimated D_{Sr} in each habitat along with the relationship between $[Sr/Ca]_{water}$ and $[\overline{\delta}^{18}O]$ in otoliths. Regressions of otolith $[\overline{\delta}^{18}O]$ on water chemistry were based on the same statistical procedure as for the trace elements. All regression analyses were done using NCSS (2001).

Results

Somatic characteristics of sampled juveniles

A total of 83 fish were used in the study, with the smallest measuring 15.7 mm standard length and the largest 64.29 mm standard length (Fig. 3). About 90% of the juveniles had an otolith weight below 3 g (Figs. 4 and 5), thus allowing comparison with results from laboratory experiments (e.g., Fowler et al. 1995; Bath et al. 2000; Milton and Chenery 2001).

Otolith weight was not significantly different among habitats ($p = 0.12$, power = 0.53). Regression and correlation of otolith chemistry and otolith weight (w) were significant only for [Mg/Ca] and $[\overline{\delta}^{18}O]$ following the equations below:

$$(2) \qquad [Mg/Ca]_{otolith}\,(\mu mol \cdot mol^{-1}) = -0.026 \times w + 0.34 \ (r^2 = 0.83,\ n = 81)$$

© 2007 NRC Canada

Table 1. Method resolution, concentration of standards, and mean estimate of precision (%RSD, relative standard deviation) from inductively coupled plasma mass spectrometry analysis of water samples and otoliths of juvenile spotted seatrout (*Cynoscion nebulosus*) collected in seagrass habitats of Chesapeake Bay from July to September 2001.

	Isotope						
	^{25}Mg	^{43}Ca	^{55}Mn	^{88}Sr	^{115}In	^{137}Ba	^{139}La
Water							
Concentration units	ppm	ppm	ppt	ppb	ppb	ppb	ppt
Resolution	Medium	Medium	Medium	Medium	Low/medium	Low	Low
Standard (low)	20.07	20.48	50.79	39.95	4.01	1.02	2.08
Standard (medium)	106.01	102.99	250.69	196.61	4.01	10.02	10.25
Standard (high)	212.49	206.28	503.18	397.67	4.02	15.06	20.55
%RSD	3.90	1.90	1.80	1.85		1.13	1.45
Otoliths							
Concentration units	ppb	ppm	ppb	ppb	ppb	ppb	ppt
Resolution	Low	Medium	Low	Medium	Low/medium	Low	Low
Standard (low)	10.03	50.01	4.05	103.88	2.03	2.05	10.35
Standard (medium)	50.15	249.68	20.32	504.18	2.03	10.17	51.46
Standard (high)	100.19	499.12	40.57	1016.32	2.03	20.4	102.41
%RSD	0.70	6.60	0.60	1.80		1.40	1.40

Fig. 3. Mean hatch date (±2 SD) of juvenile spotted seatrout (*Cynoscion nebulosus*) collected in seagrass habitats of the Eastern Shore, the Western Shore, and the Island (Tangier-Bloodsworth) of Chesapeake Bay in the summer of (*a*) 1997, (*b*) 1998, (*c*) 1999, and (*d*) 2002.

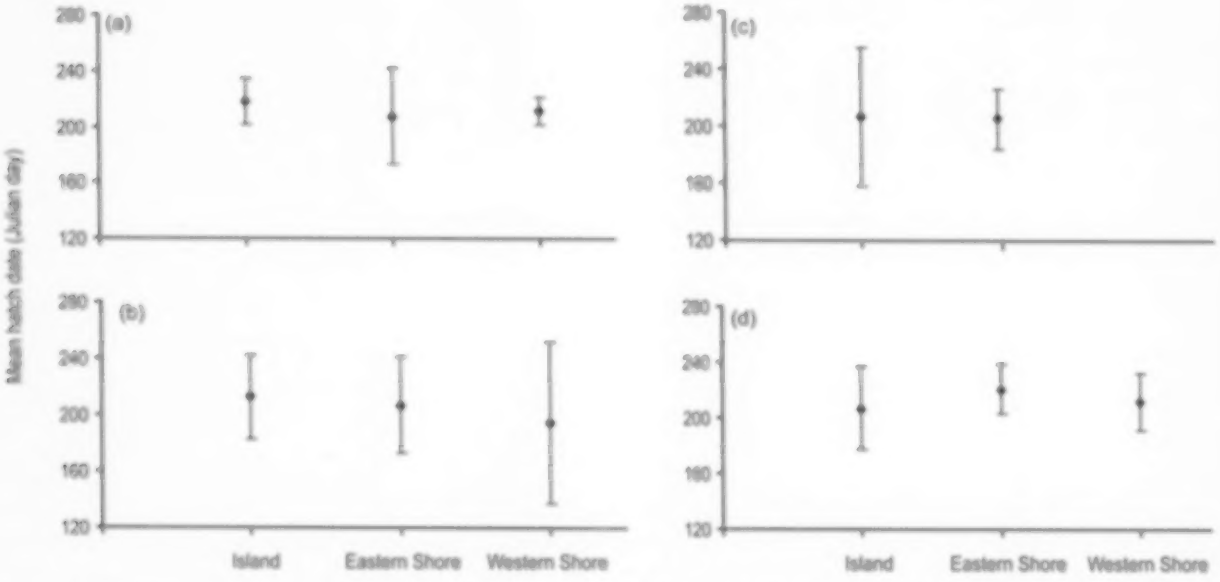

$$(3)\quad [\delta^{18}O]_{otolith} = 0.186 \times w - 4.53[\delta^{18}O]_{otolith}$$

$$(r^2 = 0.20,\ n = 83)$$

Note parenthetically that the equivalence of otolith weight also provides proxy evidence of similar age and growth across habitats.

[Me/Ca]$_{otolith}$ versus salinity

Salinity within each habitat varied little during the sampling period (Dorval et al. 2005*a*) but was significantly different among habitats (Table 2). However, there was no significant difference between (*i*) the Island and the Potomac habitats and (*ii*) the Pocomoke and the Rappahannock habitats. This pattern of variability in salinity provided an ideal test to determine whether fish that have experienced similar levels of salinity would have similar levels of [Me/Ca]$_{otolith}$ while contrasting the effect of salinity on [Me/Ca]$_{otolith}$ among habitats along the estuary.

The regression and correlation coefficients of [Mg/Ca]$_{otolith}$ and salinity were not significantly different from zero (Table 3). These results show that [Mg/Ca]$_{otolith}$ was not a good indicator of salinity of the seagrass beds in the bay (Fig. 6*a*).

Both [Mn/Ca]$_{otolith}$ and [Sr/Ca]$_{otolith}$ relationships with salinity deviated from linearity (Figs. 6*b* and 6*c*). These patterns indicated that concentrations of these ratios in otoliths

© 2007 NRC Canada

Fig. 4. Frequency distribution and standard length of juvenile spotted seatrout collected in five seagrass habitats of Chesapeake Bay from July to September in 2001 (total sample size $n = 83$).

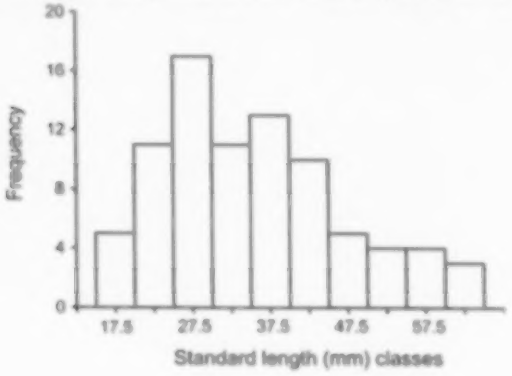

of juveniles did not trace the spatial variation in salinity along and across the bay.

Otolith [Ba/Ca] and [La/Ca] were not significantly different in habitats that had similar salinity concentration across the Bay (Fig. 6). However, $[Ba/Ca]_{otolith}$ and $[La/Ca]_{otolith}$ showed significant differences among habitats along the longitudinal gradient from north to south. The mean of $[Ba/Ca]_{otolith}$ estimated in seagrass habitats decreased with increasing salinity (Fig. 6*d*). This relationship was linear and the weighted regression explained 92% of the variation (Table 3). The model can be described as follows:

$$(4)\quad [Ba/Ca]_{otolith}\,(\mu mol{\cdot}mol^{-1}) = -2.25 \pm 0.35 \times \text{salinity} + 59.47 \pm 7.01$$

Similarly, $[La/Ca]_{otolith}$ was highly and negatively correlated with salinity (Fig. 6*e*). The relationship was strongly linear with a weighted regression that explained 98% of the variability.

$$(5)\quad [La/Ca]_{otolith}\,(pmol{\cdot}mol^{-1}) = -8.71 \pm 0.65 \times \text{salinity} + 243.87 \pm 12.52$$

$[Me/Ca]_{otolith}$ versus $[Me/Ca]_{water}$

The relationship between $[Mg/Ca]_{otolith}$ and $[Mg/Ca]_{water}$ was not linear, and regression and correlation coefficients were not significantly different from zero (Table 3; Fig. 7*a*). These results reflect the same patterns with salinity. Also note that the partition coefficient of Mg ($D_{Mg} = 0.073$) had the lowest variability (PSE = 2%) of any partition coefficients that we measured in the field.

$[Mn/Ca]_{otolith}$ increased with increasing $[Mn/Ca]_{water}$ (Fig. 7*b*) but not linearly (Table 3). Again, this was mostly due to the Pocomoke habitat where [Mn/Ca] in ambient water and otoliths was nearly double the average of the other habitats (Table 2). The other four habitats formed a well-defined cluster with little variability in their $[Mn/Ca]_{otolith}$ (Fig. 7*b*). Thus, the $[Mn/Ca]_{otolith}$ from the Pocomoke fish may be directly related to water concentration.

The relationship between $[Sr/Ca]_{otolith}$ and $[Sr/Ca]_{water}$ (Fig. 7*c*) departed strongly from the positive and linear relationship predicted in Bath et al. (2000) and Milton and Chenery (2001). Because there was no significant variation

Fig. 5. Relationship between otolith weight and standard length of juvenile spotted seatrout collected in five seagrass habitats (Potomac (□), Rappahannock (◇), York (▲), Island (○), and Pocomoke Sound (△)) of Chesapeake Bay from July to September 2001 (total sample size $n = 83$).

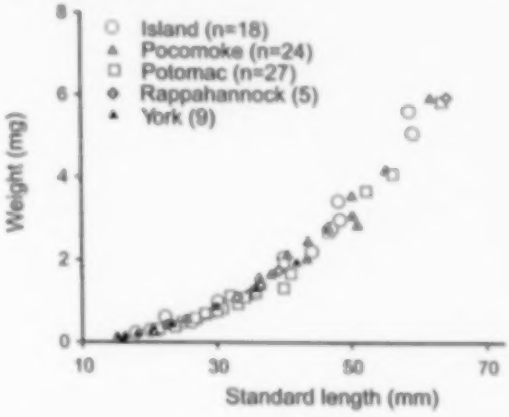

in temperature among habitats (Fig. 2) and hatch date distribution of juvenile spotted seatrout was similar historically (Fig. 3), we could not explain these differences as direct temperature effects. Further, $[\delta^{18}O]_{otolith}$ did not show a linear relationship with either $[Sr/Ca]_{otolith}$ or D_{Sr} (Table 3; Figs. 8*b* and 8*d*), again discounting a temperature effect. However, the isotopic composition of oxygen generally increased with salinity and was correlated with $[Sr/Ca]_{water}$ (Figs. 8*a* and 8*c*). There was a linear and predictive relationship between $[\delta^{18}O]_{otolith}$ and $[Sr/Ca]_{water}$ (Table 3), which can be described based on a weighted regression as

$$(6)\quad [\delta^{18}O]_{otolith} = 1.18 \pm 0.09 \times [Sr/Ca]_{water}\,(mmol{\cdot}mol^{-1}) - 14.14 \pm 0.78$$

$[Ba/Ca]_{otolith}$ generally increased with increasing $[Ba/Ca]_{water}$ but this relationship was not linear (Fig. 7*d*; Table 4). Although the monotonic behavior agreed with that of laboratory studies (i.e., Bath et al. 2000; Milton and Chenery 2001), a linear model was not suitable to fit the data as was determined experimentally by those authors. The lack of linearity resulted mostly from fish caught in the Pocomoke habitat (Table 2). The $[Ba/Ca]_{otolith}$ in these fish was different from that in fish in the Island and Potomac habitats, whereas the difference in[Ba/Ca] in surface waters of these three habitats was less pronounced. Except for the Pocomoke habitat, which is the only habitat that is not influenced by major freshwater input, linearity was preserved.

There was no linear relationship and no correlation between $[La/Ca]_{water}$ and $[La/Ca]_{otolith}$ (Table 3; Fig. 7*e*). These results suggest that $[La/Ca]_{otolith}$ may be best predicted by salinity rather than by the concentration of this ratio in water of the seagrass habitats. Because this is the first study to evaluate a rare earth element in the field, we have no point of comparison for the D_{La} ($D_{La} = 0.018$) (Tables 2 and 4).

Discussion

Our results show that otolith chemistry is influenced more strongly by salinity and mixing processes than by [Me/Ca]

© 2007 NRC Canada

Table 2. Summary of mean estimates of salinity, [Mg/Ca], [Mn/Ca], [Sr/Ca], [Ba/Ca], and [La/Ca] measured in water samples and otoliths, mean [$\delta^{18}O$] measured in otoliths, and trace element partition coefficients in the aragonite of juvenile spotted seatrout otoliths.

Habitat	Potomac	Rappahannock	York	Islands	Pocomoke	Bay-wide	PSE
Water							
Salinity (‰)	17.39±0.17	19.51±0.34	22.23±0.14	17.39±0.17	19.14±0.71	19.13±0.89	0.05
[Mg/Ca] (mol·mol^{-1})	4.54±0.06	4.57±0.06	4.55±0.06	4.50±0.04	4.63±0.07	4.56±0.02	0.00
[Mn/Ca] (μmol·mol^{-1})	0.77±0.08	2.31±0.37	2.83±0.46	1.89±0.20	4.95±0.62	2.55±0.69	0.27
[Sr/Ca] (mmol·mol^{-1})	8.01±0.25	8.64±0.34	8.75±0.83	8.28±0.22	8.62±0.35	8.46±0.14	0.02
[Ba/Ca] (μmol·mol^{-1})	53.37±2.16	46.60±1.80	37.35±3.18	61.29±2.06	55.09±2.47	50.74±4.08	0.08
[La/Ca] (nmol·mol^{-1})	3.06±0.22	3.33±0.15	4.45±0.55	4.57±0.28	7.65±0.78	4.61±0.82	0.18
Otoliths							
[Mg/Ca] (μmol·mol^{-1})	343.84±6.39	317.52±15.04	329.08±14.13	342.08±7.75	334.74±7.75	333.45±4.78	0.01
[Mn/Ca] (μmol·mol^{-1})	25.28±1.18	27.53±2.38	21.70±1.37	25.35±1.43	40.51±2.86	28.07±3.25	0.12
[Sr/Ca] (mmol·mol^{-1})	2.07±0.03	1.78±0.12	2.03±0.04	1.96±0.03	2.01±0.04	1.97±0.05	0.03
[Ba/Ca] (μmol·mol^{-1})	22.09±1.09	12.94±3.15	10.00±0.71	20.83±1.18	14.77±0.83	16.13±2.32	0.14
[La/Ca] (pmol·mol^{-1})	94.04±5.25	65.42±14.09	51.81±5.29	93.11±4.82	75.39±4.17	75.95±8.11	0.11
[$\delta^{18}O$] (‰)	–4.68±0.06	–4.28±0.31	–3.78±0.09	–4.42±0.11	–3.97±0.007	–4.23±0.14	0.03
D_{Me}							
D_{Mg}	0.08	0.07	0.07	0.08	0.07	0.07±0.00	0.02
D_{Mn}	32.83	11.92	7.67	13.41	8.18	14.80±4.64	0.31
D_{Sr}	0.26	0.21	0.23	0.24	0.23	0.23±0.01	0.04
D_{Ba}	0.41	0.28	0.27	0.34	0.27	0.31±0.03	0.09
D_{La}	0.03	0.02	0.01	0.02	0.01	0.018±0.00	0.20

Note: ±SE of the mean of each trace element is provided for each habitat. Also presented are the bay-wide estimate of the mean, SE, and proportional SE (PSE) for each trace element, each D_{Me}, and salinity.

Table 3. Results of the quantification of the relationships between juvenile spotted seatrout otoliths and surface water chemistry of Chesapeake Bay.

	Linear fit		Weighted regression		Spearman correlation	
Relationship	Total df	Statistical significance	r^2	Statistical significance	r	Statistcal significance
$[Mg/Ca]_{otolith}$ vs. salinity	80	0.7046	0.582	0.133	–0.732	0.160
$[Mn/Ca]_{otolith}$ vs. salinity	82	0.0000				
$[Sr/Ca]_{otolith}$ vs. salinity	82	0.0028				
$[Ba/Ca]_{otolith}$ vs. salinity	79	0.0650	0.923	0.009	–0.9314	0.021
$[La/Ca]_{otolith}$ vs. salinity	74	0.7429	0.980	0.001	–0.8806	0.000
$[Mg/Ca]_{otolith}$ vs. $[Mg/Ca]_{water}$	80	0.2520	0.442	0.442	–0.6146	0.270
$[Mn/Ca]_{otolith}$ vs. $[Mn/Ca]_{water}$	82	0.0083				
$[Sr/Ca]_{otolith}$ vs. $[Sr/Ca]_{water}$	82	0.008				
$[Ba/Ca]_{otolith}$ vs. $[Ba/Ca]_{water}$	79	0.0000				
$[La/Ca]_{otolith}$ vs. $[La/Ca]_{water}$	74	0.0003				
$[\delta^{18}O]_{otolith}$ vs. salinity	73	0.0002				
$[\delta^{18}O]_{otolith}$ vs. $[Sr/Ca]_{otolith}$	73	0.0000				
$[\delta^{18}O]_{otolith}$ vs. $[Sr/Ca]_{water}$	73	0.3066	0.983	0.001	0.9554	0.011
$[\delta^{18}O]_{otolith}$ vs. D_{Sr}	73	0.0001				

Note: Lack of linear fit tests were performed using [Me/Ca] of otolith samples collected in a given habitat against mean salinity or mean $[Me/Ca]_{water}$. Weighted regressions were based on mean $[Me/Ca]_{otolith}$ against mean salinity or mean $[Me/Ca]_{water}$. Weights were sample size divided by variance. Similar statistical procedures were used for regressing [$\delta^{18}O$] against water chemistry. Also note that [Mg/Ca] and [$\delta^{18}O$] in otoliths were adjusted for otolith weight based on a linear equation.

in surface waters in a broad coastal estuary. The influence of salinity was most dramatic for Ba and La. $[Mg/Ca]_{otolith}$ and $[Mn/Ca]_{otolith}$ variation relative to salinity was in the range of expectation, but the effect of salinity on $[Sr/Ca]_{otolith}$ contrasted with previous results from laboratory experiments.

The relationship of $[Mg/Ca]_{otolith}$ to salinity and to $[Mg/Ca]_{water}$ chemistry was as expected. Mg is conservative in surface waters of Chesapeake Bay and exhibits increased concentration with increasing salinity; thus, it is likely that juvenile spotted seatrout strongly regulate the concentration of Mg in their blood plasma. However, Fowler et al. (1995) observed a negative correlation between $[Mg/Ca]_{otolith}$ and salinity, whereas in foraminiferal calcite, Nurnberg et al. (1996) observed a positive correlation. In this study, al-

© 2007 NRC Canada

Fig. 6. Effect of salinity on the ratios (*a*) $[Mg/Ca]_{otolith}$, (*b*) $[Mn/Ca]_{otolith}$, (*c*) $[Sr/Ca]_{otolith}$, (*d*) $[Ba/Ca]_{otolith}$, and (*e*) $[La/Ca]_{otolith}$ measured in otoliths of juvenile spotted seatrout. Salinity was measured and juvenile fish were collected in five seagrass habitats (Potomac (□), Rappahannock (◇), York (▲), Island (○), and Pocomoke Sound (△)) of Chesapeake Bay from July to September 2001.

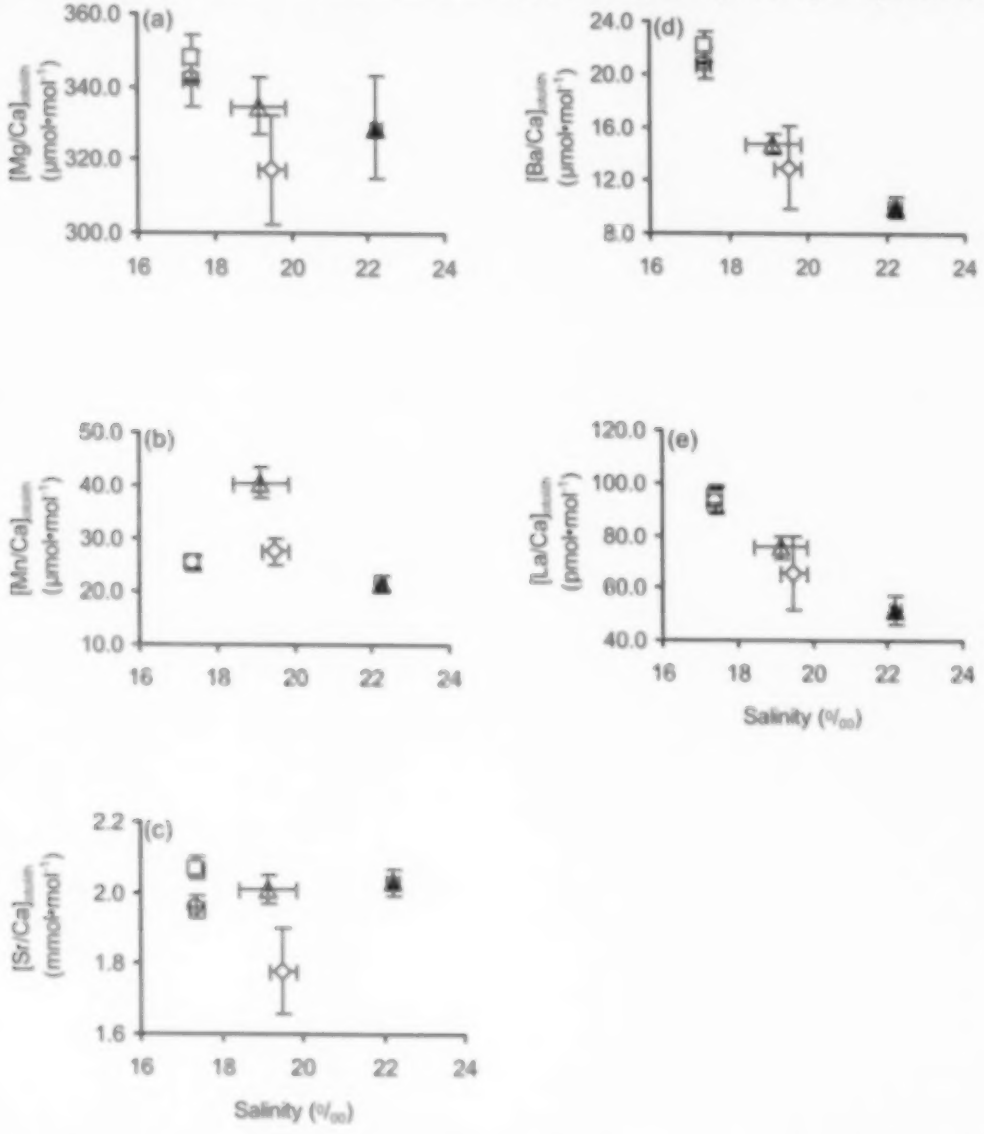

though $[Mg/Ca]_{otolith}$ often decreased with increased salinity, it did not do so predictably. The decoupling of $[Mg/Ca]_{otolith}$ with $[Mg/Ca]_{water}$, along with a low PSE for D_{Mg}, suggests that as in biogenic calcite (Morse and Bender 1990), the partition coefficient in juvenile spotted seatrout otoliths may be strongly influenced by biochemical processes (Evans 1993; Campana 1999). However, an alternative explanation would be that [Mg/Ca] in otoliths are not stable as previously assumed and therefore may not be an accurate record of water chemistry. Indeed, Mitsugushi et al. (1996) pointed out that the location of Mg^{2+} in coral aragonite crystal is not well understood, and it may be weakly bound to the lattice owing to its small ionic radius. Similarly, Amiel et al. (1973) observed that in coral aragonite, Mg was preferentially released from the lattice to distilled water. This suggests that Mg may also leach out of otoliths, rendering its concentration less stable relative to other elements.

$[Mn/Ca]_{otolith}$ showed no linear relationship with either salinity or $[Mn/Ca]_{water}$, although it was positively correlated with $[Mn/Ca]_{water}$. These patterns were tied to the nonconservative behavior of Mn (Eaton 1979; Sholkovitz et al. 1992; Dorval et al. 2005*a*) in Chesapeake Bay waters. Concentration of Mn in the water column of Chesapeake Bay peaks during summer when anoxic conditions dominate in deep bottom water and in surface sediment (Eaton 1979; Sholkovitz et al. 1992). Consequently, variation of [Mn/Ca]

© 2007 NRC Canada

Fig. 7. Relationship between water chemistry and otolith chemistry of juvenile spotted seatrout for (*a*) [Mg/Ca], (*b*) [Mn/Ca], (*c*) [Sr/Ca], (*d*) [Ba/Ca], and (*e*) [La/Ca]. Water samples and juvenile fish were collected in five seagrass habitats (Potomac (□), Rappahannock (◇), York (▲), Island (○), and Pocomoke Sound (△)) of Chesapeake Bay in 2001. Bars are standard errors of the mean values estimated for each habitat. $[Mg/Ca]_{otolith}$ was adjusted for otolith weight.

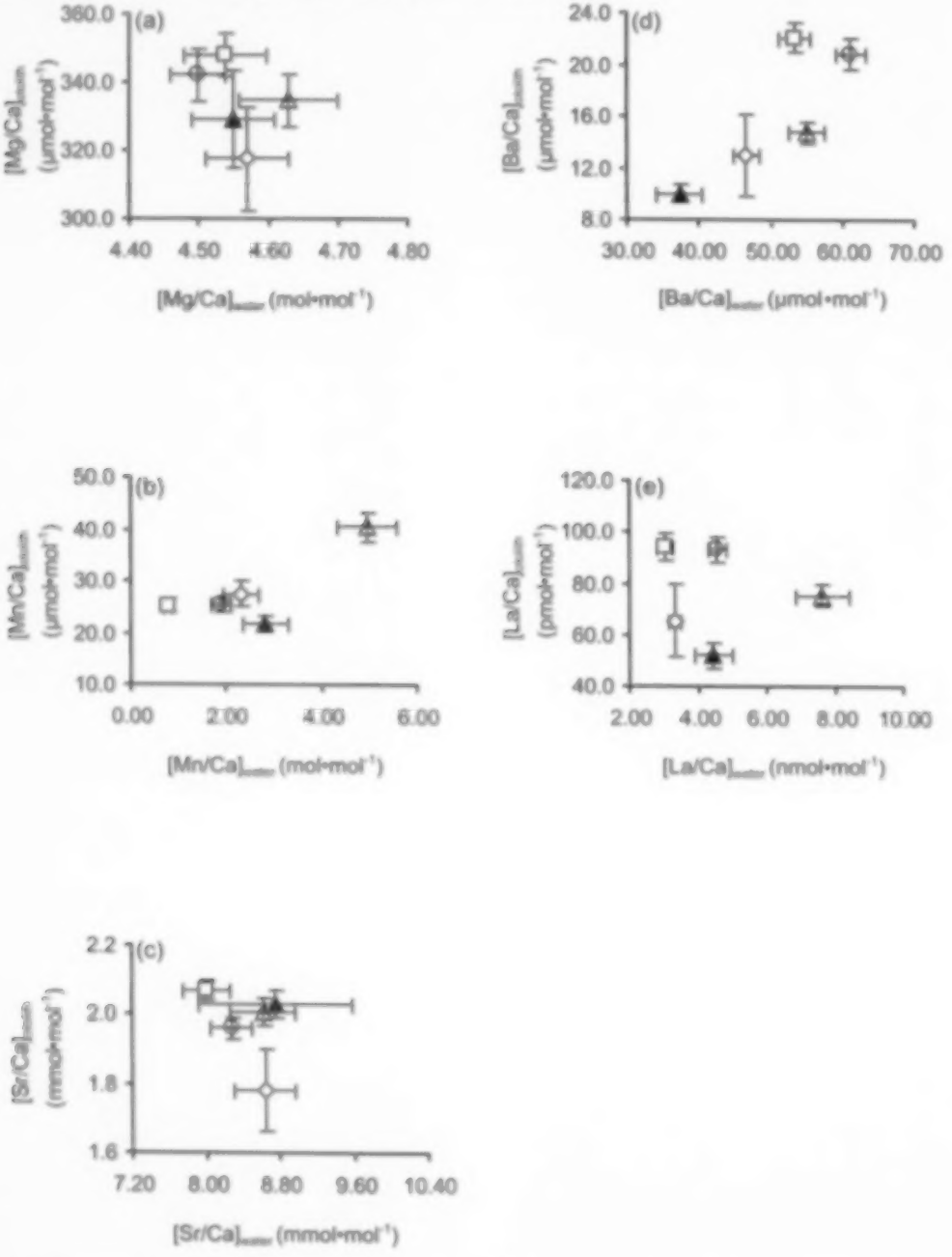

is not coupled to the magnitude of freshwater input from the major tributaries. Although, using limited data, Campana (1999) suggested that Mn is among the trace elements whose uptake in otoliths is not likely to be regulated to any significant extent, other studies argued that Mn is both toxic in high concentrations (Rainbow 1997) and actively used in metabolic processes (Lehman and Joyce 1993). Further, Martin and Thorrold (2005) showed that both temperature and salinity influenced otolith Mn, whereas Elsdon and Gillanders (2002, 2003) found no relationship between Mn

© 2007 NRC Canada

Fig. 8. Mean [$\delta^{18}O$] measured in otoliths of juvenile spotted seatrout plotted against (*a*) mean salinity, (*b*) mean $[Sr/Ca]_{otolith}$, (*c*) mean $[Sr/Ca]_{water}$, and (*d*) D_{Sr} for each habitat. Water samples and juvenile fish were collected in five seagrass habitats (Potomac (□), Rappahannock (◇), York (▲), Island (○), and Pocomoke Sound (△)) of Chesapeake Bay in 2001. Bars are standard errors of the mean values estimated for each habitat. $[\delta^{18}O]_{otolith}$ was adjusted for otolith weight.

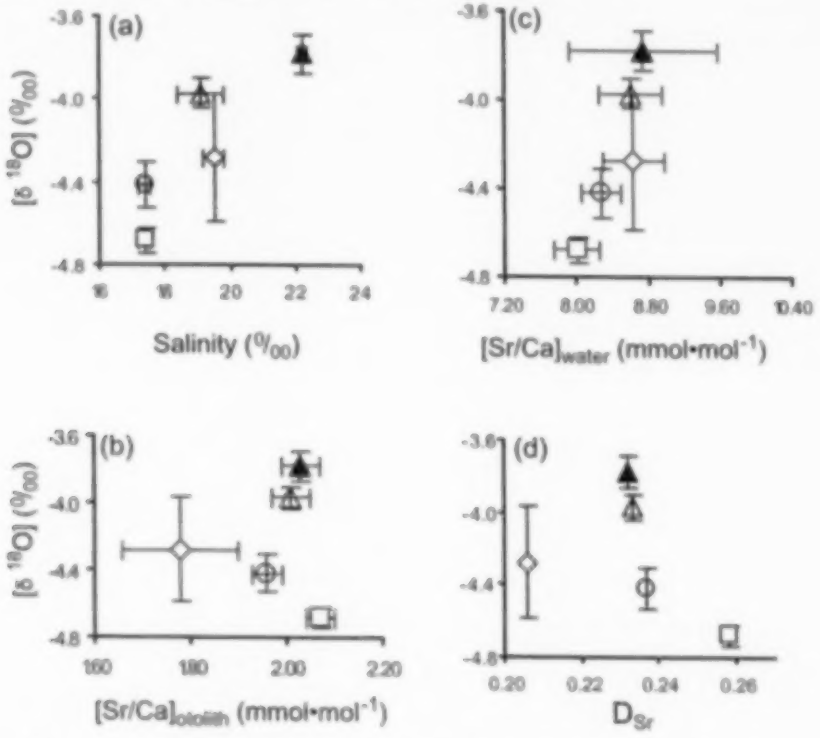

Table 4. Comparison of element partition coefficients (D_{Me}) estimated in this study with previously published results from field and laboratory experiments.

Study	D_{Mg}	D_{Mn}	D_{Sr}	D_{Ba}	D_{La}
Laboratory					
Milton and Chenrery 2001				0.03	
Bath et al. 2000			0.182 at 20 °C	0.06	
Elsdon and Gillanders 2003		0.683	0.131 at 20 °C	0.099	
Elsdon and Gillanders 2005			0.28	0.27	
Field					
Elsdon and Gillanders 2005			0.52	0.26	
This study	0.073	14.803	0.233	0.313	0.018

concentration in otolith and in water. In contrast, our study showed that $[Mn/Ca]_{otolith}$ was not related to either temperature or salinity but instead resulted from differences in the magnitude of redox reactions that regulate Mn in Chesapeake Bay during summer (Eaton 1979; Sholkovitz et al. 1992). Nevertheless, because no other study has measured D_{Mn} in the field, we have no basis for comparison beyond the Elsdon and Gillanders (2003) laboratory study. With so little work done on Mn, there is little that can be said about the apparent discrepancy between the laboratory and the field.

The heterogeneous spatial distribution of Mn in both water and otoliths, which is associated with the highest PSE for D_{Me} among elements, shows clearly that the chemical processes acting on very small spatial scales in the bay may confer to $[Mn/Ca]_{otolith}$ unique characteristics as a habitat-specific biogeochemical marker.

The uptake of $[Sr/Ca]_{otolith}$ by juvenile spotted seatrout contrasted with results from recent laboratory studies. In the lower bay, we found no obvious relationship of $[Sr/Ca]_{otolith}$ to either salinity or $[Sr/Ca]_{water}$. First, this is contrary to the positive correlation with salinity reported by Fowler et al. (1995), Secor et al. (1995), and Martin et al. (2004) in the laboratory. Second, the $[Sr/Ca]_{otolith}$ and $[Sr/Ca]_{water}$ relationship in this study deviated from the linear relationship predicted by Bath et al. (2000) and Milton and Chenery (2001). Temperature was similar among seagrass habitats during our

© 2007 NRC Canada

sampling period, and based on $[\delta^{18}O]_{otolith}$ and the distribution coefficients estimated for [Sr/Ca], we found no evidence that $[Sr/Ca]_{otolith}$ was directly affected by temperature. In that respect, these results were consistent with those of Kalish (1989), who did not show a linear relationship between $[Sr/Ca]_{otolith}$ and temperature for Australian salmon (*Arripis trutta*) raised in the laboratory. Further, hatch date distribution of juvenile spotted seatrout in Chesapeake Bay was similar among seagrass beds across years. Consequently, there was little likelihood that degree-day temperature exposure may have confounded the effect of salinity or $[Sr/Ca]_{water}$ on $[Sr/Ca]_{otolith}$. Nevertheless, as D_{Sr} estimated across seagrass beds fell well within the range measured in the laboratory (Martin et al. 2004) for its cofamiliar species (spot (*Leiostomus xanthurus*), family Sciaenidae), an unequivocal understanding of the factors controlling $[Sr/Ca]_{otolith}$ in juvenile spotted seatrout awaits the replication of this study with determination of age and lifetime temperature exposure for each individual fish.

The relationship of $[Ba/Ca]_{otolith}$ with salinity was inversely linear. This result showed that [Ba/Ca] in otoliths could be predicted when average salinity in a given habitat was known over the period of residence of juvenile spotted seatrout in seagrasses. Also, this result demonstrated that very small changes in salinity may result in significant differences in $[Ba/Ca]_{otolith}$ within the estuary. The model reflected the conservative behavior of Ba in the lower Chesapeake Bay, where Ba decreases with increasing salinity within and across months from July to September (Dorval et al. 2005*a*). This distribution of Ba is typical in estuaries when there is no significant input from biological activity in the water column (e.g., Zwolsman and van Eck 1999). However, the relationship of $[Ba/Ca]_{otolith}$ and $[Ba/Ca]_{water}$ was nonlinear and depended on the geographic location of the habitats. Thus, the linear relationship predicted by Bath et al. (2000) and Milton and Chenery (2001) did not hold in our field test and was mostly due to the behavior of [Ba/Ca] in the Pocomoke habitat. Among the five habitats studied, Pocomoke Sound is the only one that is not directly influenced by a major tributary. It is likely that other chemical processes might have interacted with Ba uptake in otoliths within the Pocomoke habitat. Even so, the D_{Ba} (D_{Ba} = 0.313) was greater than shown by laboratory studies of estuarine fish but of a magnitude similar to that of the only field study that previously measured this partition coefficient for an estuarine-dependent fish (Elsdon and Gillanders 2005). More replications of this study are needed to determine whether $[Ba/Ca]_{otolith}$ in the Pocomoke habitat results from physical and chemical processes that control the concentration of this ratio in water and otoliths. Nevertheless, in Chesapeake Bay, salinity appears to be the chief regulator of [Ba/Ca] in otoliths of fish caught in the seagrass habitats.

$[La/Ca]_{otolith}$ varied with salinity similarly to $[Ba/Ca]_{otolith}$, but $[La/Ca]_{otolith}$ patterns resulted from different physical and chemical processes. First, the decrease of dissolved La from low to high salinity is regulated by colloidal complexation reactions and adsorption onto particles (Sholkovitz and Elderfield 1988). At low pH, light rare earth elements such as La are preferentially removed from solution, relative to heavy rare earth elements, by dissolved particulate matter, with most of this fractionation occurring during early estuarine mixing. In addition, colloidal complexation of rare earth elements increases with salinity in the mixing zone, leading to further removal of these elements from the water column (e.g., Sholkovitz and Elderfield 1988; Elderfield et al. 1990). In seawater, $LaCO_3$ is the most abundant species of La and as much as 86% of La may be complexed in this form (e.g., Cantrell and Byrne 1987). Likewise, fish from higher salinity habitats had lower $[La/Ca]_{otolith}$ because of higher removal of La in surface waters (Millero 1992; Bertine et al. 1996) by carbonate at lower salinity.

Although the otolith chemistries of Ba and La do have some similarities, overall they differ greatly. Indeed, neither La nor Ba is biologically controlled and therefore, it is more likely that their composition in water would predict their concentration in the otoliths. However, the bulk of Ba^{2+} incorporation in otoliths is achieved through substitution to Ca^{2+} or coprecipitation in the crystalline matrix because these elements have the same valence and close ionic radii. In contrast, La is a trivalent element with a different ionic radius than Ca. Therefore, La^{3+} mostly occurs within the spaces of the aragonite lattice (Fritz et al. 1990; Geffen et al. 1998). This may also explain why D_{La} was much smaller but more variable (i.e., PSE) than D_{Ba}. The differences between the rare earth elements and other trace metals confer on them unique properties to be useful in identifying habitat at small spatial scales.

An important finding of this study was the significant correlation between otolith $[Sr/Ca]_{water}$ and $[\delta^{18}O]_{otolith}$, which also showed a positive increase with salinity. Previous studies have established a positive relationship between salinity and $[\delta^{18}O]$ measured in calcite and aragonite of marine species (e.g., Elsdon and Gillanders 2002; Polyak et al. 2003; Lécuyer et al. 2004), but direct correlation of otolith $[\delta^{18}O]$ with $[Sr/Ca]_{water}$ in an estuary had not been reported before. These patterns are indicators of different water provenance among the seagrass habitats and thus are a direct result of mixing processes between oceanic and freshwater discharges in Chesapeake Bay. Although we did not measure $[\delta^{18}O]$ in the water, our data suggest that temperature would have played little role in determining the magnitude of $[\delta^{18}O]$ measured in juvenile otoliths (at the spatial scale considered). Rather, the oxygen isotopic composition of the otolith may better reflect environmental conditions such as salinity and Sr concentration in surface waters.

In an estuary such as Chesapeake Bay, water chemistry will be predictive of otolith chemistry only for trace elements such as Ba and La that are not under strong biological control and that are not sensitive to temperature. Although water chemistry may be predictive of [Ba/Ca] and [La/Ca] in otoliths along the estuary, it may not be a good predictor to locate individual fish laterally across Chesapeake Bay. In small and narrow estuaries dominated by one river system (e.g., Hudson River), dissolved Ba and La may be used as a surrogate to predict otolith chemistry. However, in wide estuaries having different tributaries with varying freshwater input, analysis of water chemistry variations may not be powerful enough to predict otolith chemistry, especially in detecting lateral differences. In such environments, a library of juvenile otoliths is required to study population dynamics and life history of fish. The need for an otolith library is further emphasized because extrapolation of otolith trace ele-

© 2007 NRC Canada

ment composition from laboratory experiments might significantly depart from that observed in wild-caught fish.

Acknowledgements

We thank Z.J. Chen (Laboratory of Isotope and Trace Element Research) and A.J. Kaufman (Stable Isotope Laboratory of the University of Maryland) for their laboratory support. We also thank D. Combs (Virginia Institute of Marine Sciences) for field support and F. Crock and N.B. Smith (CQFE) for ageing of otoliths. Finally, we are grateful to two reviewers whose comments contributed significantly to the improvement of the paper. This work was funded by a grant to R.H. and C.M.J. from the Virginia Sea Grant (R/CF-37) and additional grants to R.J. Orth (RS00-45 and RF01-2) and C.M.J. (RF00-5) from the Virginia Salt Water Recreational Fishing Development Board administered by the Virginia Marine Resources Commission. This study is part of a Ph.D. dissertation in the Ecological Sciences Program at Old Dominion University (E.D.).

References

Amiel, A.J., Friedman, G.M., and Miller, D.S. 1973. Distribution and nature of incorporation of trace elements in modern aragonitic corals. Sedimentology, **20**: 47–64.

Baker, W.B., Jr., and Matlock, G.C. 1993. Movement of spotted seatrout tagged in Trinity Bay, Texas. Northeast Gulf Sci. **13**: 29–34.

Bath, G.E., Thorrold, S.R., Jones, C.M., Campana, S.E., McLaren, A.J.W., and Lam, J.W.H. 2000. Strontium and barium uptake in aragonitic otoliths of marine fish. Geochim. Cosmochim. Acta, **64**: 1705–1714.

Begg, G.A., Cappo, M., Cameron, D.S., Boyle, S., and Sellin, M.J. 1998. Stock discrimination of school mackerel, *Scomberomorus queenslandicus*, and spotted mackerel, *Scomberomorus munroi*, in coastal waters of eastern Australia by analysis of minor and trace elements in whole otoliths. Fish. Bull. **96**: 653–666.

Bertine, K.K., Koide, M., and Goldberg, E.D. 1996. Comparative marine chemistries of some trivalent metals — bismuth, rhodium and rare earth elements. Mar. Chem. **53**: 89–100.

Brown, N.J. 1981. Reproductive biology and recreational fishery for spotted seatrout, *Cynoscion nebulosus*, in the Chesapeake Bay area. M.A. thesis, College of William and Mary, Williamsburg, Va.

Campana, S.E. 1999. Chemistry and composition of fish otoliths: pathways, mechanisms and applications. Mar. Ecol. Prog. Ser. **188**: 263–297.

Cantrell, K.J., and Byrne, R.H. 1987. Rare earth element complexation with carbonate and oxalate ions. Geochim. Cosmochim. Acta, **51**: 597–605.

Chester, A., and Thayer, G.W. 1990. Distribution of spotted seatrout (*Cynoscion nebulosus*) and gray snapper (*Lutjanus griseus*) juveniles in seagrass habitats of western Florida Bay. Bull. Mar. Sci. **46**: 345–357.

De Vries, M.C., Gillanders, B.M., and Elsdon, T.S. 2005. Facilitation of barium uptake into otoliths: influence of strontium concentration and salinity. Geochim. Cosmochim. Acta, **69**: 4061–4072.

Ditty, J.C., Shaw, R.F., and Farooqi, T. 2006. Sciaenidae. *In* Early stages of Atlantic fishes: an identification guide for the western central North Atlantic. Vol. II. Chap. 143. *Edited by* W.J. Richards. Taylor & Francis, CRC Press, Boca Raton, Fla. pp. 1669–1723.

Dorval, E., Jones, C.M., and Hannigan, R. 2005*a*. Chemistry of sea grass habitats: distinguishing fine spatial scale differences in sea grass habitats of the Chesapeake Bay. Limnol. Oceanogr. **50**: 1073–1083.

Dorval, E., Jones, C.M., Hannigan, R., and van Montfrans, J. 2005*b*. Can otolith chemistry be used for identifying essential seagrass habitats for juvenile spotted seatrout, *Cynoscion nebulosus*, in Chesapeake Bay. Mar. Freshw. Res. **56**: 1–9.

Eaton, A. 1979. The impact of anoxia on Mn fluxes in the Chesapeake Bay. Geochim. Cosmochim. Acta, **43**: 429–432.

Elderfield, H., Upstill-Goddard, R., and Sholkovithz, E.R. 1990. The rare earth elements in rivers, estuaries, and coastal seas and their significance to the composition of ocean waters. Geochim. Cosmochim. Acta, **54**: 971–991.

Elsdon, T.S., and Gillanders, B.M. 2002. Interactive effects of temperature and salinity on otolith chemistry: challenges for determining environmental histories of fish. Can. J. Fish. Aquat. Sci. **59**: 1796–1808.

Elsdon, T.S., and Gillanders, B.M. 2003. Relationship between water and otolith elemental concentrations in juvenile black bream *Acanthopagrus butcheri*. Mar. Ecol. Prog. Ser. **260**: 263–272.

Elsdon, T.S., and Gillanders, B.M. 2005. Consistency of patterns between laboratory experiments and field collected fish in otolith chemistry: an example and applications for salinity reconstructions. Mar. Freshw. Res. **36**: 609–617.

Ennevor, B.C., and Beames, R.M. 1993. Use of lanthanide elements to mass mark juvenile salmonids. Can. J. Fish. Aquat. Sci. **50**: 1039–1044.

Evans, D.H. (*Editor*). 1993. Osmotic and ionic regulation. *In* The physiology of fishes. CRC Press, Boca Raton, Fla. pp. 315–341.

Fowler, A.J., Campana, S.E., Jones, C.M., and Thorrold, S.R. 1995. Experimental assessment of the effect of temperature and salinity on elemental composition of otoliths using solution-based ICP–MS. Can. J. Fish. Aquat. Sci. **52**: 1421–1430.

Fritz, L.W., Ragone, L.M., and Lutz, R.A. 1990. Biomineralization of barite in the shell of the freshwater Asiatic clam *Corbicula fluminea* (Mollusca: Bivalvia). Limnol. Oceanogr. **35**: 758–762.

Gallahar, N.K., and Kingsford, M.J. 1996. Factors influencing Sr/Ca ratios in otoliths of *Girella elevata*: an experimental investigation. J. Fish Biol. **48**: 174–186.

Geffen, A.J., Pearce, N.J.G., and Perkins, W.T. 1998. Metal concentration in fish otoliths in relation to body composition after laboratory exposure to mercury and lead. Mar. Ecol. Prog. Ser. **141**: 13–20.

Kalish, J.M. 1989. Otolith chemistry: validation of the effects of physiology, age and environment on otolith composition. J. Exp. Mar. Biol. Ecol. **132**: 161–178.

Kalish, J.M. 1991*a*. ^{13}C and ^{18}O isotopic composition disequlibria in fish otoliths: metabolic and kinetic effects. Mar. Ecol. Prog. Ser. **75**: 191–203.

Kalish, J.M. 1991*b*. Oxygen and carbon stable isotopes in the otoliths of wild and laboratory maintained Australian salmon (*Arripis trutta*). Mar. Biol. **110**: 37–47.

Khim, B.K., Krantz, D.E., Cooper, L.W., and Gredbmeier, J.M. 2003. Seasonal discharge of estuarine freshwater to the western Chuckchi Sea shelf identified in stable isotope profiles of mollusk shells. J. Geophys. Res. **108**(C9): 16-1–16-10.

Kraus, R.T., and Secor, D.H. 2004. Incorporation of strontium into otoliths of an estuarine fish. J. Exp. Mar. Biol. Ecol. **302**: 85–106.

Lécuyer, C., Reynard, B., and Martineau, F. 2004. Stable isotope fractionation between mollusk shells and marine waters from Martinique Island. Chem. Geol. **213**: 293–305.

© 2007 NRC Canada

Lehman, N., and Joyce, G.F. 1993. Evolution in vitro of an RNA enzyme with altered metal dependence. Nature (London), **361**: 182–185.

Martin, G.B., and Thorrold, S.R. 2005. Temperature and salinity effects on magnesium, manganese incorporation in otoliths of larval and early juvenile spot, *Leiostomus xanthurus*. Mar. Ecol. Prog. Ser. **293**: 223–232.

Martin, G.B., Thorrold, S.R., and Jones, C.M. 2004. Temperature and salinity effects on strontium incorporation in otoliths of larval spot (*Leiostomus xanthurus*). Can. J. Fish. Aquat. Sci. **61**: 34–42.

McMichael, R.H., and Peters, K.M. 1989. Early life history of spotted seatrout, *Cynoscion nebulosus* (Pisce: Sciaenidae), in Tampa Bay, Florida. Estuaries, **12**: 98–110.

Millero, F.J. 1992. Stability constants for the formation of rare earth inorganic complexes as a function of ionic strength. Geochim. Cosmochim. Acta, **56**: 3123–3132.

Milton, D.A., and Chenery, S.R. 2001. Sources and uptake of trace metals in juvenile barramundi (*Lates calcacifer*). J. Exp. Mar. Biol. Ecol. **264**: 47–65.

Mitsugushi, T., Matsumoto, E., Abe, O., Uchida, T., and Isdale, P.J. 1996. Mg/Ca termometry in coral skeletons. Science (Washington, D.C.), **274**(5289): 961–963.

Morse, J.W., and Bender, M.L. 1990. Partition coefficients in calcite: examination of factors influencing the validity of experimental results and their application to natural systems. Chem. Geol. **82**: 265–277.

NCSS. 2001. Number Cruncher Statistical System. Released by Dr Jerry L. Hintze, 329 North 1000 East, Kaysville, UT 84037, USA.

Nurnberg, D., Bijma, J., and Hemleben, C. 1996. Assessing the reliability of magnesium in foraminiferal calcite as a proxy for water mass temperatures. Geochim. Cosmochim. Acta, **60**: 803–814.

Orth, R.J., and Heck, K.L., Jr. 1980. Structural components of eelgrass (*Zostera marina*) meadows in the lower Chesapeake Bay — fishes. Estuaries, **3**: 278–288.

Pascot, H., and Wollast, R. 1997. Transport and transformation of trace metals in the Scheldt estuary. Mar. Chem. **58**: 229–244.

Poling, K.R., and Fuiman, L.A. 2000. Behavioral specialization in developing sciaenids and its relationship to morphology and habitat. Environ. Biol. Fishes, **54**: 119–133.

Polyak, L., Stanovoy, V., and Lubinski, D.J. 2003. Stable isotopes in benthic foraminiferal calcite from a river-influenced Arctic marine environment. Paleoceanography, **18**: 3-1–3-17.

Rashke, R., Showers, W., Moksness, E., and Lenz, P. 1996. Environmental information stored in otoliths: insights from stable isotopes. Mar. Biol. **127**: 161–170.

Rainbow, P.S. 1997. Trace metal accumulation in marine invertebrates: marine chemistry? Mar. Biol. Assoc. U.K. **77**: 195–210.

Rooker, J.R., Holt, S.A., Soto, M.A., and Holt, G.J. 1998. Post-settlement patterns of habitats use by sciaenid fishes in subtropical seagrass meadows. Estuaries, **21**: 318–327.

Rutherford, E.S., Schmidt, T.W., and Tilmant, J.T. 1989. Early life history of spotted seatrout (*Cynoscion nebulosus*) and gray snapper (*Lutjanus griseus*) in Florida Bay, Everglades National Park, Florida. Bull. Mar. Sci. **44**: 49–64.

Secor, D.H., Henderson-Arzapalo, A., and Piccoli, P.M. 1995. Can otolith microchemistry chart patterns of migration and habitat utilization in anadromous fishes? J. Exp. Mar. Biol. Ecol. **192**: 15–53.

Sholkovitz, E.R., and Elderfield, H. 1988. Cycling of dissolved rare earth elements in Chesapeake Bay. Global Biogeochem. Cycles, **2**: 157–176.

Sholkovitz, E., and Shen, G.T. 1995. The incorporation of rare earth elements in modern coral. Geochim. Cosmochim. Acta, **59**: 2749–2756.

Sholkovitz, E., Shaw, T.J., and Schneider, D.L. 1992. The geochemistry of rare earth elements in the seasonally anoxic water column and porewaters of the Chesapeake Bay. Geochim. Cosmochim. Acta, **56**: 3389–3402.

Shumilin, E.N., Anikiev, V.V., Goryachev, N.A., Kassatkina, A.P., and Fazlullin, S.M. 1993. Estimation of the role of biogeochemical barriers in trace metal migration in the river–sea system. Mar. Chem. **43**: 217–224.

Taylor, H.E. 2001. Inductively coupled plama-mass spectrometry, practices and techniques. Academic Press, San Diego, Calif.

Thorrold, S.R., Jones, C.M., Campana, S.E., and Swart, P.K. 1997. Factors determining $\delta^{13}C$ and $[\delta^{18}O]$ fractionation in aragonitic otoliths of marine fish. Geochim. Cosmochim. Acta, **61**: 2909–2919.

Thorrold, S.R., Latkoczy, C., Swart, P.K., and Jones, C.M. 2001. Natal homing in a marine fish population. Science (Washington, D.C.), **291**(5502): 297–299.

Wells, B.K., Rieman, B., Clayton, J.L., Horan, D.L., and Jones, C.M. 2003. Relationship between water, otolith, and scale chemistry of Westslope cutthroat trout from the Coeur d'Arlene River, Idaho: the potentials for hard scale chemistries to describe movement in freshwater. Trans. Am. Fish. Soc. **132**: 409–424.

Zimmerman, C. 2005. Relationship of otolith strontium-to-calcium ratios and salinity: experimental validation for juvenile salmonids. Can. J. Fish. Aquat. Sci. **62**: 88–97.

Zwolsman, J.J.G., and van Eck, G.T.M. 1999. Geochemistry of major elements and trace metals in suspended matter of the Scheldt estuary, southwest Netherlands. Mar. Chem. **66**: 91–111.

© 2007 NRC Canada

Interactions between food quantity and quality (long-chain polyunsaturated fatty acid concentrations) effects on growth and development of *Chironomus riparius*

Willem Goedkoop, Marnie Demandt, and Gunnel Ahlgren

Abstract: We quantified somatic growth, development, and emergence of the midge *Chironomus riparius* on experimental diets (oats, *Spirulina*, and Tetraphyll®) covering gradients in food quality (differing polyunsaturated fatty acids) and quantity (0.1–5.4 mg C·day^{-1}). Additionally, similar incubations without food additions were made using a food-poor sediment containing peat and the green alga *Scenedesmus obliquus*. Larval and adult size was affected by both food quantity and quality and increased some three to four times across the food concentration gradients. Adult emergence, however, was affected only by food quantity. A type 3 response model showed that a saturation level was reached for the oats treatment at 2.7 mg C·day^{-1} (or 3.9 µg ω3 and 120 µg ω6 polyunsaturated fatty acids·day^{-1}), indicating that the quality of oats constrained further stimulation of larval growth. In the peat treatment, larval growth was very low, no adults emerged, and no larvae even made it to the pupa stage. Fatty acid analyses showed that larvae were capable of synthesizing arachidonic acid via γ-linolenic acid by Δ6- and Δ5-desaturase activity using linoleic acid available in food sources. This strongly suggests that *C. riparius* is not dependent on dietary sources of eicosapentaenoic acid and arachidonic acid and can sustain viable populations even under a low-quality food regimen.

Résumé : Nous avons mesuré quantitativement la croissance somatique, le développement et l'émergence chez des moucherons *Chironomus riparius* nourris de régimes expérimentaux (avoine, *Spirulina* et Tetraphyll®) qui représentent des gradients de qualité (différences d'acides gras polyinsaturés) et de quantité (0,1–5,4 mg C·jour^{-1}) de nourriture. Nous avons, de plus, fait des incubations semblables sans ajout de nourriture sur un sédiment pauvre en nourriture et contenant de la tourbe et l'algue verte *Scenedesmus obliquus*. La taille des larves et des adultes est affectée tant par la quantité que la qualité de la nourriture et elle augmente par un facteur d'environ 3–4 sur les gradients de concentration de nourriture. L'émergence des adultes, cependant, n'est affectée que par la quantité de nourriture. Un modèle de réponse de type 3 montre que le niveau de saturation dans le cas du régime d'avoine est atteint à 2,7 mg C·jour^{-1} (ou 3,9 µg ω3 et 120 µg ω6 acides gras polyinsaturés·jour^{-1}), ce qui indique que la qualité de l'avoine restreint toute stimulation subséquente de la croissance larvaire. Dans les conditions expérimentales avec de la tourbe, la croissance larvaire est très basse, aucun adulte n'émerge et même aucune larve n'atteint le stade nymphal. Des analyses des acides gras montrent que les larves sont capables de synthétiser l'acide arachidonique en passant par l'acide γ-linoléique par l'activité des désaturases Δ6 et Δ5 en utilisant l'acide linoléique présent dans les sources alimentaires. Ces résultats indiquent nettement que *C. riparius* ne dépend pas de sources alimentaires d'acide eicosapentaénoïque et d'acide arachidonique et qu'il peut maintenir des populations viables même avec un régime alimentaire de faible qualité.

[Traduit par la Rédaction]

Introduction

Understanding the processes and mechanisms of population regulation, food web dynamics, and ecosystem function is a major challenge in ecology. The conversion of food resources to primary consumer biomass is of particular importance, since it may imply substantial trophic upgrading and improve food quality for consumers at higher trophic levels. Studies of the effects of food quality in aquatic food webs have traditionally addressed the role of nitrogen and phos-

Received 5 May 2006. Accepted 7 December 2006. Published on the NRC Research Press Web site at http://cjfas.nrc.ca on 22 March 2007.
J19305

W. Goedkoop.[1] Department of Environmental Assessment, Swedish University of Agricultural Sciences, Box 7050, SE-750 07, Uppsala, Sweden.
M. Demandt. Department of Animal Ecology, Evolutionary Biology Centre, Uppsala University, Norbyvägen 18D, SE-752 36, Uppsala, Sweden.
G. Ahlgren. Department of Limnology, Evolutionary Biology Centre, Uppsala University, Norbyvägen 20, SE-752 36, Uppsala, Sweden.

[1]Corresponding author (e-mail: willem.goedkoop@ma.slu.se).

 doi:10.1139/F07-016 © 2007 NRC Canada

phorus and have had a strong focus on the trophic transfer of energy and nutrients from phytoplankton to zooplankton (e.g., Sterner and Hessen 1994; Sterner and Schulz 1998). In recent years, there has been a growing awareness that also essential polyunsaturated fatty acids (PUFA), in particular eicosapentaenoic acid (EPA) (20:5ω3) and docosahexaenoic acid (DHA) (22:6ω3), are good descriptors of high food quality for pelagic grazers (Brett and Müller-Navarra 1997; Müller-Navarra et al. 2003) and of the efficiency of trophic transfer in aquatic food webs (Müller-Navarra et al. 2000; Kainz et al. 2004). The most well-studied pelagic grazer, *Daphnia* species, is capable of synthesizing EPA and arachidonic acid (ARA) (20:4ω6) from the shorter homologues α-linolenic acid (ALA) (18:3ω3) and linoleic acid (LA) (18:2ω6), respectively (Elendt 1990; von Elert 2002). Also, other aquatic invertebrates like calanoid copepods (Moreno et al. 1979) and sea urchins (Bell et al. 2001) have the capacity to synthesize EPA and DHA from ALA and LA, respectively, but synthesis rates are very low. However, the several elongation and desaturation steps involved in the synthesis of ARA, EPA, and DHA are metabolically costly and likely limit optimal growth rates in zooplankters (Brett and Müller-Navarra 1997; Arts et al. 2001).

Three 20-C PUFA, dihomo-γ-linolenic acid (20:3ω6), EPA, and ARA, are precursor molecules of prostaglandins, a group of hormones involved in a number of regulatory functions in invertebrates, such as reproduction (oviposition) and ion transport (see reviews by Stanley-Samuelson and Pedibhotla 1996; Rowley et al. 2005). Specific examples of the importance of eicosanoid action in invertebrate biology and physiology involve sexual maturation and mating behavior in insects (e.g., Howard and Stanley-Samuelson 1996), development and viability of newly emerged adult mosquitoes (e.g., Dadd and Kleinjan 1984), hatching in barnacles (e.g., Hill et al. 1992), spawning in gastropods and mussels (e.g., Morse et al. 1977), and tissue regeneration in *Hydra* (e.g., Stanley-Samuelson 1994). ARA, or structurally-related 20-C PUFA, is an essential dietary requirement for several species of mosquitoes (Dadd et al. 1987). DHA is strongly associated with neural tissue, including the retina, and plays an important role in neural development and vision (Sargent et al. 1995). For example, juvenile Atlantic herring (*Clupea harengus*) deprived of DHA showed decreased predation efficiency, resulting in reduced fitness (Bell et al. 1995). Relatively high levels of DHA have been reported for predatory species and scavengers and interpreted as being associated with their high motility and dependence on vision. However, little is known of the capacity of freshwater invertebrates to synthesize ARA, EPA, and DHA from shorter homologues and whether synthesis rates can meet the physiological demands during periods of active growth and (or) reproduction.

The role of long-chain PUFA for growth and reproduction in benthic invertebrates has thus far been poorly studied. Several studies have reported on concentrations of fatty acids (FA) in benthic invertebrate species in lotic (e.g., Hanson et al. 1985; Bell et al. 1994) and lentic habitats (Goedkoop et al. 2000; Makhutova et al. 2003), but evidence of the effects of PUFA on benthic invertebrate growth and survival comes primarily from aquaculture of economically important species (e.g., D'Abramo and Sheen 1993; Xu et al. 1993). Evidence for the importance of PUFA for benthic invertebrate reproduction was provided by Ederington and coworkers (1995) who showed a severalfold increase in the fecundity of the copepod *Acartia tonsa* when fed diatoms compared with those fed a diet of bacteria-fed ciliates or starved individuals. Also, for zebra mussels (*Dreissena polymorpha*), dietary concentrations of EPA and DHA are strong descriptors of growth (VanderPloeg et al. 1996; Wacker et al. 2002) and egg quality (Wacker and von Elert 2004). Similar to *Daphnia*, *Dreissena* feeds on pelagic seston and has good access to fresh algal cells during a large part of the year. For profundal deposit-feeders, sedimentation events following diatom blooms provide a seasonally reoccurring supply of long-chain PUFA (e.g., Ahlgren et al. 1997) that is rapidly assimilated by sediment-dwelling invertebrates (Goedkoop et al. 2000). Studies that experimentally test the role of long-chain PUFA for the growth, development, and fecundity of deposit-feeding macroinvertebrates have not been published thus far. Considering the relative importance of benthic pathways in lake food webs (Vadeboncoeur et al. 2002), information on the mechanisms that govern the efficiency of trophic transfer in benthic habitats contributes to a better understanding of these trophic pathways. Furthermore, data on the trophodynamics of FA between food particles and deposit-feeding macroinvertebrate allow for comparisons of different functional groups, i.e., relatively long-lived taxa of benthic invertebrates that live on food of relatively poor quality compared with highly opportunistic (r-selecting) pelagic microcrustaceans.

In this study, we quantified larval growth and development of the midge *Chironomus riparius* on experimental diets covering gradients in food quality (differing PUFA composition) and food quantity. This experimental setup also allowed for the evaluation of the effects of food quality at different food quantity levels. We hypothesized that (*i*) *Chironomus* larvae would grow less well on diets low in 20-C PUFA and (*ii*) larvae would be able to convert shorter PUFA homologues to EPA and ARA, since they are relatively well adapted to a food-poor environment. Higher food quality (i.e., higher concentrations of 20-C PUFA) was expected to result in a more rapid development and to have positive effects on adult size. We used three particulate food sources that differed with respect to their concentrations of 20-C PUFA (EPA and ARA) and their 18-C precursors (ALA, LA, and γ-linolenic acid (GLA) (18:3ω6)) but that were relatively rich in carbon, nitrogen, and phosphorus. Additionally, we used a food-poor, formulated sediment where peat was the only source of organic matter. Besides providing insight into the above questions, the controlled feeding experiments provided knowledge of the transfer of FA across the food–invertebrate interface in benthic food webs.

Materials and methods

Chironomus riparius is a deposit-feeding species that is common in the shallow sediments of lakes but that can also be found in streams. The ecology of the species is well known and it is commonly used as a model organism in ecotoxicology (Organisation for Economic Cooperation and Development 2004). Following oviposition, *C. riparius* eggs hatch within a few days and first-instar larvae invade the

© 2007 NRC Canada

sediment. Development then involves another three tube-inhabiting larval stages and a pupal stage. The relatively short pupal stage involves major changes in morphology that leads to the emergence of adult midges. In the laboratory, when food is supplied ad libitum, some 3–4 weeks are needed for the development from egg to adult. Feeding studies were performed with food types of different quality, determined as FA composition (in particular, levels of EPA, ARA, and DHA and their precursors ALA, LA, and GLA, respectively), supplied at different food quantity levels.

Ten newly hatched first-instar larvae from at least five egg ropes (obtained from cultures) were incubated in 1 L glass beakers (surface area 80 cm^2) containing 100 g of acid-purified sea sand (Merck, Germany) as a bottom substrate (approximately 1 cm) and 200 mL of artificial fresh water (Organisation for Economic Cooperation and Development 2004). The size fraction of sand particles was >0.2 mm to avoid the ingestion by *Chironomus* larvae (Davies et al. 1999). Experimental units were aerated (approximately one bubble per second) using aquarium pumps, tubing, and Pasteur pipettes. A full factorial design was set up with three different food treatments and five food concentrations corresponding to 0.1, 0.3, 0.9, 2.7, and 5.4 mg C·day^{-1} (determined in pilot studies). The food types used were the aquarium fish food Tetraphyll® (Tetrawerke, Germany), the cyanobacterium *Spirulina* species (Lindroos, Örebro, Sweden), and oat cereals (AXA Foods, Järna, Sweden). These food types were chosen because they differ markedly in their FA composition while being similar in their energy contents (see below). Food types were finely ground and added to the experimental units twice weekly (at the start and on day 5). The experiment was performed at 20 °C with a 16 h light – 8 h dark cycle. Light intensity was 5 µmol photons·m^{-2}·s^{-1}, which is far below the light compensation level of *Spirulina* (17 µmol photons·m^{-2}·s^{-1}), thus avoiding carbon fixation through photosynthesis (Kebede and Ahlgren 1996). Oxygen concentrations in the experimental units were measured just prior to the additions of larvae using an oxygen probe (model 51B YSI oxygen meter equipped with a 5739 electrode; YSI Scientific, Yellow Springs, Ohio) and ranged from 4.8 to 7.2 mg O_2·L^{-1}.

After 10 days, three experimental units of each treatment were sacrificed. Larvae were collected from the sand by sieving (0.35 mm), anaesthetized in carbonated water, and length determined at 20× magnification using a measuring ocular (precision 0.03 mm). Length measurements allowed for a rapid processing of the large number of larvae at the termination of the experiment. For calculating specific growth rates, length data were converted to wet weight using a length (l, mm) – wet weight (ww, mg) relationship: $\ln(ww) = 2.736 \times \ln(l) - 5.1255$ ($R^2 = 0.94$). Larval specific growth rate was calculated as $(\ln(ww_t) - \ln(ww_0))/t$, where ww_0 is initial larval wet weight (first instars) and ww_t is larval wet weight after $t = 10$ days of incubation. Larvae from the highest food concentration (5.4 mg C·day^{-1}) were stored under N_2 in a fridge at –20 °C for later quantitative analysis of FA concentrations. Briefly, samples were lyophilized, finely ground, and 0.1 g dry weight transferred to small tin capsules.

Methyl esters of FA were analyzed using gas chromatography techniques (Hewlett-Packard 5890 GC equipped with a 25 m silica capillary column (80730F, inner diameter 0.32 mm, film thickness 0.24 µm; Quadrex, New Haven, Connecticut)) following the procedure described in detail in Zenebe et al. (2003). Briefly, extraction of preweighed samples was done by homogenization in methanol–chloroform containing the antioxidant butylated hydoxytoluene and Na_2PO_4 as a buffer and subsequent storage for 1–2 days at 4 °C. The chloroform phase was removed and the sample was evaporated to dryness under a flow of N_2. The lipid esters were transmethylated at 60 °C in 5% H_2SO_4 overnight. The methyl esters were extracted in petroleum ether containing some water and butylated hydoxytoluene; the solvent was evaporated again and redissolved in 1 mL of Uvasol, grade hexane. FA were identified by comparing their retention time with those of a known standard mixture (GCL-68A; NU CHEK Prep, Elysian, Minn.) mixed in fish oil 30 (Larodan Fine Chemicals, Malmö, Sweden). Individual FA were quantified (mg·g dry $weight^{-1}$, used throughout) by comparing the area of their peaks with that of an internal standard, i.e., tricosanoic acid (23:0) (a single concentration ranging from 12.5 to 62.5 µg per sample). This internal standard was recommended by Einig and Ackman (1987) and gives a similar response as the PUFA that were the focus of this study. Peaks registering less than 0.02 mg·g dry $weight^{-1}$ were considered as "undetected". Total FA content was calculated from the total area under the curve in the chromatogram minus the peaks for the added butylated hydroxytoluene and internal standard. FA are named by standard nomenclature, i.e., the total number of carbon atoms followed by the number of double bonds and the position of the first double bond, which is indicated by "ω" followed by the number of carbon atoms counted from the methyl end. Nitrogen and carbon concentrations of the different food resources were analyzed using an elemental analyzer (NA1500, CE Elantech, Inc., Lakewood, N.J.). Total phosphorus concentrations of food types were oxidized with persulphate and analyzed according to Murphy and Riley (1962).

For the additional two experimental units of each treatment, the emergence of adult midges was scored over a period of 61 days (total incubation time). Food additions and feeding frequency were similar to those made during the initial 10 days. Daily checks for adult midges were made from day 15. Adults were removed from the experimental units, sex was scored, and midges were preserved in 70% ethanol. Mean larval development rate, i.e., the mean time span between the introduction of larvae and the emergence of the experimental cohort, was calculated as

$$\bar{x} = \sum_{i=1}^{m} \frac{f_i x_i}{n_e}$$

where $\bar{x}$ is mean development rate, i is the index of the inspection intervals, m is the maximum number of inspection intervals, f_i is the number of midges emerged in the inspection interval, n_e is the total number of midges emerged until the end of the experiment, and x_i is the development rate of midges emerged in interval i calculated as

$$x_i = \frac{1}{\text{day}_i - \frac{l_i}{2}}$$

© 2007 NRC Canada

where day_i is the inspection day and l_i is the length of the inspection interval (days, usually 1 day). Adult wing length, from the cleft where the alula turns into the anal lobe to the tip of the wing, was measured (20× magnification) as a proxi of adult size following the method described in Armitage (1995).

In an additional experiment (n = 2), performed under identical experimental conditions as described above, we measured the growth and development of newly hatched first-instar *C. riparius* larvae in a formulated sediment (Organisation for Economic Cooperation and Development 2004). The organic fraction of this sediment (5% of dry weight) is made up of finely ground peat (Hasselfors Garden AB, Örebro, Sweden). Slight modifications compared with the experimental setup described above were the addition of 25 larvae instead of 10 larvae to experimental units and incubations of 28 days instead of 10 days. This longer incubation time was chosen because a pilot study had shown that larvae showed slow growth and development in this sediment when no food was added. No food additions were made in this experiment, thereby forcing the larvae to feed on the peat fraction. In this experiment, larval dry weight was measured on a microbalance (C-30, Cahn Instruments, Cerritos, Calif.). Oxygen concentrations in these experimental units ranged from 7.7 to 8.2 mg $O_2 \cdot L^{-1}$, while water pH ranged from 7.9 to 8.1. The peat fraction of the formulated sediment was analyzed (as described above) for nitrogen, phosphorus, carbon, and FA (Table 1).

Lastly, in a separate 10-day feeding experiment (n = 2) that followed the methods described above for pulverized food sources (i.e., same food concentrations and experimental conditions), we fed *Chironomus* larvae with the green alga *Scenedesmus obliquus* cultured in a turbidostat (Kebede and Ahlgren 1996) at 20 °C and 60–70 µmol photons·m^{-2}·s^{-1} and harvested at steady state. This green alga entirely lacks ≥20-C FA but is relatively rich in LA (1.9 ± 0.03 mg·g^{-1}) and ALA (12.4 ± 0.2 mg·g^{-1}) (Table 1). Fresh algae were retained on filters (Millipore polycarbonate, 3 µm) and fed to *Chironomus* larvae at concentrations equivalent to those used. Analyses on algal food and larvae were done as described above. However, larval samples were pooled in FA analyses to obtain sufficient biomass, resulting in single analysis of FA.

The food sources used in our experiments differed largely in their FA composition and concentrations of PUFA (Table 1). *Spirulina* contained only traces of both ALA and EPA but was relatively high in LA and GLA, while Tetraphyll was rich in LA but also contained low concentrations of ALA, EPA, and DHA. Furthermore, Tetraphyll was almost twice as high in PUFA than was *Spirulina*, which instead had a higher relative dominance of saturated FA. Oats lacked ARA, EPA, and DHA but were strongly dominated by LA, which made up 97% of the PUFA and 40% of its total FA concentration. The only source of ω3 PUFA in oats was ALA (0.63 mg·g^{-1}). It should be noted that these three food sources have low ω3:ω6 FA ratios compared with the algal diets (e.g., *Scenedesmus*) commonly used in feeding studies with zooplankters. Peat was generally poor in FA and lacked all PUFA except traces of LA.

Statistical analyses

All data were log-transformed prior to statistical analysis, except for emergence data, which were arcsine square root transformed. Analysis of covariance (ANCOVA) and Tukey–Kramer honestly significant difference (HSD) tests were used to evaluate effects of food type (quality) and food quantity (covariate) on larval and adult size. ANCOVA models with separate slopes, specifying the main effect, the covariate, and the interactions between both were run. Tukey–Kramer HSD tests were run to test for differences between food types within each of the food concentrations. Statistical analyses were run using the JMP IN software package (version 5.1) for MacIntosh (SAS Institute Inc., Cary, North Carolina) with α set at 0.05. Principal components analysis (PCA) of FA concentrations of larvae and their diets was run using the CANOCO 4.5 software package (ter Braak and Smilauer 2002). Food types were run passively, i.e., were positioned in the biplot without affecting the PCA of larval FA composition. Monte Carlo permutations (999) were run to test if separation of samples was significant along the PC axes.

Results

Larval size was affected both by food type and food concentration ($p < 0.001$ for both) (Table 2), with the ANCOVA model explaining 94.1% of the variation in larval size. As expected, *Chironomus* larvae generally grew faster as more food was added to the experimental units (Fig. 1*a*). Interestingly, the increase in larval size across the food gradient was larger in the Tetraphyll treatment than for the other two food types (Tukey–Kramer HSD, $p < 0.05$). Larvae increased in size from 4.43 ± 0.16 to 12.93 ± 0.84 mm (mean ± SD, used throughout, or almost three times, along the Tetraphyll concentration gradient and from 2.88 ± 0.15 to 12.55 ± 0.21 mm (or 4.3 times) along the *Spirulina* concentration gradient. In the oats treatment, larval size increased from 3.63 ± 0.29 to 10.28 ± 1.91 mm across the food concentration gradient and showed higher variation. At the lower end of the food concentration gradient, i.e., at 0.1 and 0.3 mg C·day^{-1}, larvae fed Tetraphyll were larger than those fed oats and *Spirulina* (Tukey–Kramer HSD, $p < 0.05$). At food concentrations exceeding 0.3 mg C·day^{-1}, no differences among food types were found. Survival generally exceeded 83% ± 6%, except for one replicate of the 5.4 mg C·day^{-1} *Spirulina* treatment where only five of 10 larvae were recovered (data not shown).

Adult emergence was affected by food concentration but not by food type (Table 2). Emergence gradually increased across the food concentration gradient and peaked at 2.7 mg C·day^{-1} for the oats and Tetraphyll treatments when 100% emergence was recorded (Fig. 1*b*). Surprisingly, emergence for these two treatments was less than 100% at the highest food concentration tested, 5.4 mg C·day^{-1}. In the *Spirulina* treatment, however, emergence was lower at 2.7 mg C·day^{-1} than that for the other treatments (Tukey–Kramer HSD) and never reached 100%. Even for emergence, significant differences between treatments were found at the lower end of the food concentration gradient. At 0.3 mg C·day^{-1}, emergence was higher in the *Spirulina* and Tetraphyll treatments than in

© 2007 NRC Canada

Table 1. Mean (±SD) FA ($n = 2$ or $n = 1$) and elemental concentrations (mg·g dry weight^{-1}, $n = 5$ for carbon and nitrogen, $n = 2$ for phosphorus) of the four pulverized food types and *Scenedesmus obliquus*.

Acid code	Acid name (abbreviation)	Oats	*Spirulina*	Tetraphyll	Peat	*S. obliquus*
14:0	Myristic	0.10±0.01	0.58±0.01	1.20	0.10	1.32±0.0
16:0	Palmitic	7.52±1.17	10.90±0.43	6.82	0.44	2.36±0.03
16:1ω7	Palmitoleic	0.12±0.02	1.29±0.02	1.56	0.10	1.10±0.02
18:0	Stearic	0.75±0.06	9.23±1.21	2.67	0.18	0.07±0.01
18:1ω9	Oleic	17.06±2.81	1.13±0.00	6.51	0.19	1.30±0.03
18:1ω7	Vaccenic	—	0.36±0.01	0.67	—	0.81±0.01
18:2ω6	Linoleic (LA)	19.49±3.66	2.15±0.04	8.97	0.12	1.90±0.03
18:3ω6	γ-Linolenic (GLA)	—	4.29±0.013	0.06	—	0.61±0.01
18:3ω3	α-Linolenic (ALA)	0.63±0.16	0.04±0.03	0.98	—	12.37±0.19
20:0	Arachidic	0.06±0.00	0.08±0.00	1.08	0.11	—
20:4ω6	Arachidonic (ARA)	—	0.10±0.00	0.17	—	—
20:5ω3	Eicosapentaenoic (EPA)	—	0.10±0.02	0.96	—	—
22:6ω3	Docosahexaenoic (DHA)	—	—	1.43	—	—
ΣSAFA		8.61±1.45	20.98±1.66	12.11	1.86	11.63±0.55
ΣMUFA		17.44±2.54	1.49±0.01	9.86	0.43	4.08±0.06
ΣPUFA		20.12±3.82	6.85±0.07	12.67	0.12	18.08±0.14
ΣFA		46.27±7.94	29.32±1.74	34.61	5.72	38.37±1.61
Σω3		0.63±0.16	0.21±0.01	1.94	0.00	15.56±0.10
Σω6		19.49±3.66	6.72±0.09	9.31	0.06	2.52±0.04
Σω3:Σω6		0.03±0.00	0.03±0.00	0.36	0.00	6.19±0.05
Total FA		48.54±7.05	36.18±2.05	39.82	5.72	43.66±0.14
C		438±16.5	430±5.5	437±9.3	549±6.4	48.6±1.2
N		20.7±5.2	96.0±1.2	79.3±2.7	9.4±0.3	7.8±1.8
P		5.0±0.14	11.5±0.04	13.0±0.0	0.25±0.01	1.2±0.7
Mean C:N		21.9	4.5	5.5	61	6.5
Mean C:P		87.6	37.4	33.6	2196	41.2
Mean N:P		4.1	8.3	6.1	37.6	6.6

Note: SAFA, saturated FA; MUFA, monounsaturated FA. ΣFA refers to the sum of FA, while total FA is calculated from the total area of peaks in the chromatograms. Note that elemental ratios are calculated from dry weight estimates. Dashes indicate that these FA were not detected (≤0.02 mg·g^{-1}).

Table 2. ANCOVA statistics showing model R^2 and F ratios and p values for effects tests for food type (treatment: Tetraphyll, oats, peat) and food concentration (covariate) for several response variables (sources).

		Food type		Food concentration		Food type × food concentration		
Response variable	R^2	F	p	F	p	F	p	HSD
Larval length	0.94	11.64	0.0001	8.22	<0.0001	9.20	0.0005	T > O T > S
Emergence*	0.46	1.15	ns	7.69	0.0125	2.59	ns	ns
Mean development rate*	0.63	0.39	ns	23.01	0.0002	1.83	ns	ns
Wing length*	0.87	8.01	0.0039	84.81	<0.0001	2.98	ns	T > O T > S

Note: The last column gives the results of the Tukey–Kramer HSD test used to compare treatments (T, Tetraphyll; O, oats; S, *Spirulina*). ns, nonsignificant results.

*Data for 0.1 mg C·day^{-1} excluded because of zero or low emergence.

those receiving oats (Tukey–Kramer HSD, $p < 0.05$). In the lowest food concentration tested, only a single adult emerged during the 61 days in the *Spirulina* treatment, while at 0.3 mg C·day^{-1}, on average, 1.5 and 4 adults emerged from the *Spirulina* and Tetraphyll treatments, respectively (Fig. 1*b*). The day of first emergence was always earlier in the Tetraphyll treatment and lowest in the oats treatment and showed particularly large differences between the 0.9 and 2.7 mg C·day^{-1} food concentrations (Fig. 2). In the experimental units fed 0.9 and 2.7 mg C·day^{-1}, Tetraphyll adult midges started emerging after 21 ± 0.71 and 15 ± 0.71 days, respectively. In the corresponding units fed oats, first emergence occurred after 26 ± 0.0 and 20 ± 0.71 days and in those fed *Spirulina* after 37.5 ± 2.1 and 19 ± 1.4 days. In all treatments, males emerged earlier than females.

Mean development rate showed significant effects of food concentration but not of food type (Table 2; Fig. 3*a*). Among the Tetraphyll concentrations, a feeding rate of 0.9 mg

© 2007 NRC Canada

Fig. 1. Mean *Chironomus riparius* (*a*) larval size and (*b*) emergence across food concentration gradients of oats (open bars), *Spirulina* (shaded bars), and Tetraphyll (solid bars). Error bars denote 1 SD and letter codes denote significant differences between treatments (Tukey–Kramer HSD).

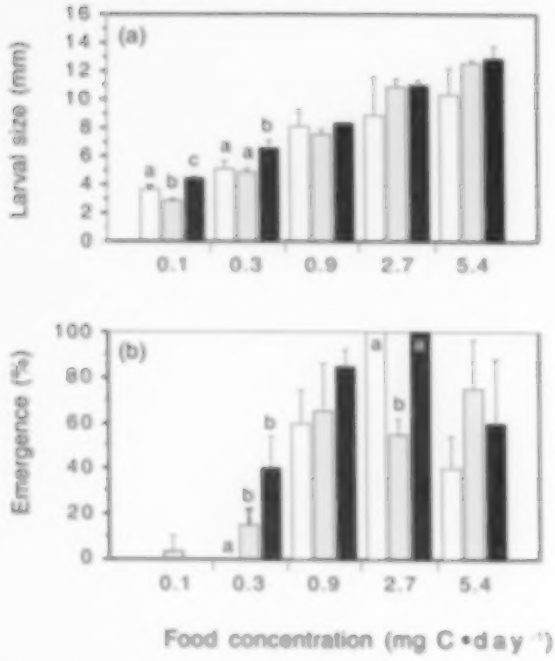

C·day^{-1} resulted in a twofold higher mean development rate than did 0.3 mg C·day^{-1}, 0.039 ± 0.001 and 0.0208 ± 0.001·day^{-1}, respectively (Tukey–Kramer HSD, $p < 0.05$), while even higher mean development rates were found for the two highest food additions, 0.056 ± 0.005 and 0.061 ± 0.001·day^{-1}. Within a single concentration, food type effects on development rates were found at 0.9 mg C·day^{-1}, where the Tetraphyll treatment showed a higher development rate (0.039 ± 0.001·day^{-1}) than did the oats treatment (0.028 ± 0.002·day^{-1}) and *Spirulina* treatment (0.023 ± 0.001·day^{-1}) (Tukey–Kramer HSD, $p < 0.05$). At 0.1 mg C·day^{-1} in all treatments and at 0.3 mg C·day^{-1} in the oats treatment, no adults emerged and mean development rates could not be calculated. Similarly, the high mean development rate in the oats treatment with 5.4 mg C·day^{-1} is due to low emergence in this treatment

Also, adult size (wing length) showed significant effects of both food type and concentration (Table 2). These effects originated from larger adults in the Tetraphyll treatment than in the other two treatments (Tukey–Kramer HSD, $p < 0.05$). Across the Tetraphyll and *Spirulina* concentration gradients, mean wing length increased from 3.25 ± 0.07 to 4.13 ± 0.25 mm and from 3.24 ± 0.25 to 3.73 ± 0.07 mm, respectively (Fig. 3*b*). In the oats treatment, mean wing length increased from 3.17 ± 0.27 mm at 0.9 mg C·day^{-1} to 4.10 ± 0.37 mm at 5.4 mg C·day^{-1}. Males tended to be slightly smaller than females in all treatments, but sex-specific differences in wing length were only found for the oats treatment at 5.4 mg C·day^{-1} (*t* test, $p = 0.0199$).

Fig. 2. Cumulative emergence of adult *Chironomus riparius* in duplicate treatments with (*a*) oats, (*b*) *Spirulina*, and (*c*) Tetraphyll during 60 days. The different symbols refer to food concentrations of 5.4 mg C·day^{-1} (x), 2.7 mg C·day^{-1} (y), 0.9 mg C·day^{-1} (*z*), and 0.3 mg C·day^{-1} (+).

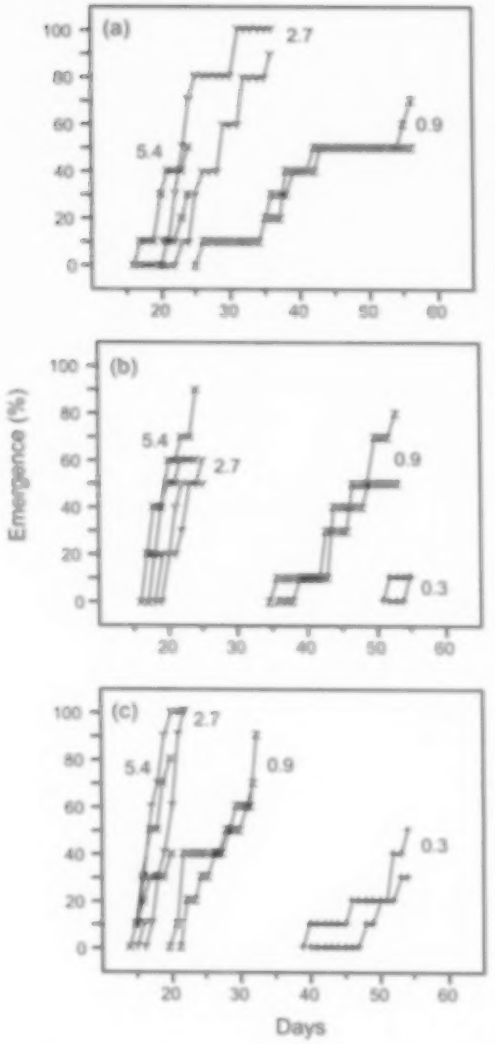

Larval growth in the peat treatment, incubated for 28 days, was on average only 1.3 ± 0.2 mg wet weight. For comparison, calculated larval wet weight (using the power relationship between larval length and wet weight given above) after 10 days of incubation in treatments with pulverized food types was 6.7 ± 1.2 mg for larvae fed Tetraphyll, 6.2 ± 0.60 for those fed *Spirulina*, and 3.8 ± 1.8 mg for those fed oats. In the peat treatment, no adults emerged and no larvae even made it to the pupa stage. Hence, development rate could not be calculated and wing length could not be measured in this treatment. Larval survival in the peat treatment was 80% ± 10%.

FA concentrations in *Chironomus* larvae showed marked differences among treatments, visualized by the PCA

© 2007 NRC Canada

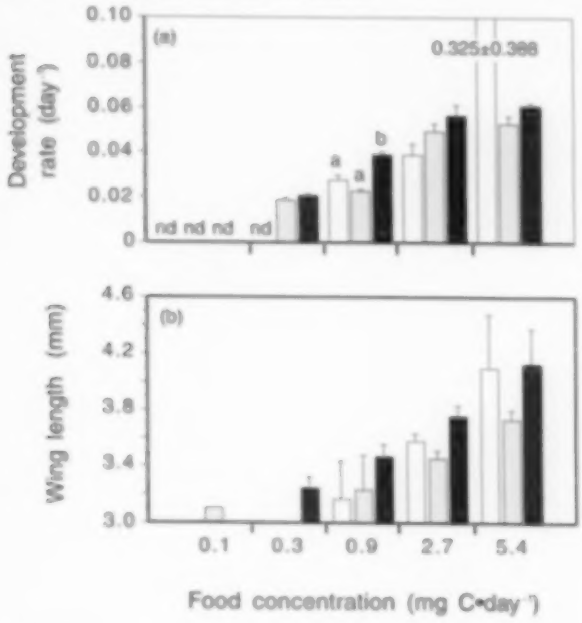

Fig. 3. Mean (*a*) development rate and (*b*) adult size (wing length) of *Chironomus* across food concentration gradients of oats (open bars) *Spirulina* (shaded bars), and Tetraphyll (solid bars) during 61 days of incubations. Error bars denote 1 SD and letter codes denote significant differences among treatments from pairwise comparisons (Tukey–Kramer HSD). nd (not determined) denotes that development rates could not be calculated owing to the lack of emergence in these treatments.

(Fig. 4). The first PC axis explained 44.0% of the variation in larval FA contents and represented a gradient between 18:1ω7 and ARA (to the right) and all other FA (to the left). Also, samples of larvae fed peat were placed to the right in the PCA plot and well separated from those of the other treatments. The FA 20:0 and 16:1ω7 as well as the ω3 PUFA ALA and EPA were positively correlated and 16:0, 18:0, and ω6 PUFA negatively correlated with the second PC axis, which explained 25.9% of the variation in larval FA. Also, the third PC axis explained a substantial amount of the variation (10.6%) in larval FA composition. Monte Carlo permutations showed that larval samples were significantly separated along both the first axis ($p = 0.022$) and other axes ($p = 0.003$). The PCA plot further showed that larval FA contents largely resembled those of their food source. For example, larvae fed Tetraphyll were closely associated with ω3 FA and clearly separated from those fed *Spirulina* and oats, which were more closely associated with the ω6 FA. However, a number of interesting exceptions to this pattern were found. Larvae fed oats contained GLA, ARA, and EPA (Table 3), despite the fact that these FA were not detected in their food (cf. Table 1). Similarly in the Tetraphyll treatment, GLA, although absent in the food, was abundant in larvae at low concentrations. Conversely, DHA, available in Tetraphyll at concentrations of 1.43 mg·g^{-1} (dry weight, used throughout for FA data), was not detected in larvae reared on this food source. Surprisingly, larvae grown on the peat diet, lacking basically all PUFA except LA, contained ARA at concentrations of 1.0 ± 0.35 mg·g^{-1} and had LA levels of 2.7 ± 0.65 mg·g^{-1}, implying a high degree of accumulation of LA and subsequent elongation to ARA in larvae.

Concentrations of single FA and total FA in larvae also varied largely among treatments (Table 3). Larvae fed oat cereals showed the highest total FA concentrations, 83.2 ± 16.9 mg·g^{-1}, which were markedly higher than those for the other food types. Larvae fed oats were particularly rich in LA, which also was the single most dominant FA in their food with concentrations of 17.7 ± 3.6 mg·g^{-1} followed by palmitic acid (16:0) at concentrations of 14.2 ± 2.3 mg·g^{-1}. Larvae fed *Spirulina* and Tetraphyll, both of algal origin, were fairly similar in their concentrations of FA, except for EPA, which was markedly higher in larvae fed Tetraphyll, and GLA, which was much higher in those fed *Spirulina*. Larvae grown on peat were generally lower in most FA than those from the other treatments, except for 18:1ω7 (3.6 ± 0.05 mg·g^{-1}) and ARA (1.0 ± 0.35 mg·g^{-1}). Combining the data in Tables 1 and 3 gives insight into the degree to which FA were accumulated in *C. riparius* larvae relative to their food. In all treatments, palmitoleic acid (16:1ω7) was strongly concentrated in *Chironomus* larvae, with concentrations being 9 times higher (Tetraphyll) and 43 times higher (oats) in larvae than in food. Only in the peat treatment were LA concentrations in larvae manifold (22 times) higher than in the food, while also, 18:1ω7, not detectable in the peat, was strongly accumulated in larvae. Furthermore, larval concentrations of LA, ALA, ARA, and EPA were approximately 3–4 times higher than in *Spirulina*, whereas larvae fed Tetraphyll only accumulated ARA and EPA (2–3 times higher).

In the experiment with *S. obliquus*, both larval size and survival were consistently lower across the food quantity gradient than in the treatments with pulverized food sources (data not shown). Larval size ranged from 1.9 ± 0.1 to 2.9 ± 0.1 mm at the three lowest food concentrations but increased markedly to 6.9 ± 0.4 and 6.7 ± 0.3 mm at the 2.7 and 5.4 mg C ·day^{-1} food concentrations, respectively. Survival ranged from 45% to 80% across the food quantity gradient. Larvae fed *S. obliquus* contained 1.12 mg ARA·g^{-1} and 0.84 mg EPA·g^{-1} (Table 3).

Discussion

Our results from the oats treatment show that *C. riparius* larvae can grow and develop well without dietary sources of EPA and ARA and with only very low levels of their precursors ALA and LA, respectively. These results strongly suggest that this species is not dependent on dietary sources of EPA and ARA but apparently has the physiological capacity of synthesizing these FA from shorter homologues. The observed relatively high growth and development rates and the lack of differences among food types at food additions exceeding 0.9 mg C·day^{-1} further suggest that *C. riparius* larvae can do so at rates that can support normal larval growth and development. These findings are further confirmed by the *S. obliquus* experiment that revealed that *C. riparius* larvae synthesized and accumulated 1.12 mg ARA·g^{-1} and 0.84 mg EPA·g^{-1} in their body tissue. This accumulation of ARA and EPA also implies a marked trophic upgrading by *Chironomus*.

© 2007 NRC Canada

Fig. 4. PCA biplot showing *Chironomus riparius* larvae fed Tetraphyll (TL), *Spirulina* (SL), oats (OL), and peat (PL) and gradients in FA. Numbers refer to triplicate samples. Food sources (circles) were run passively in the PCA.

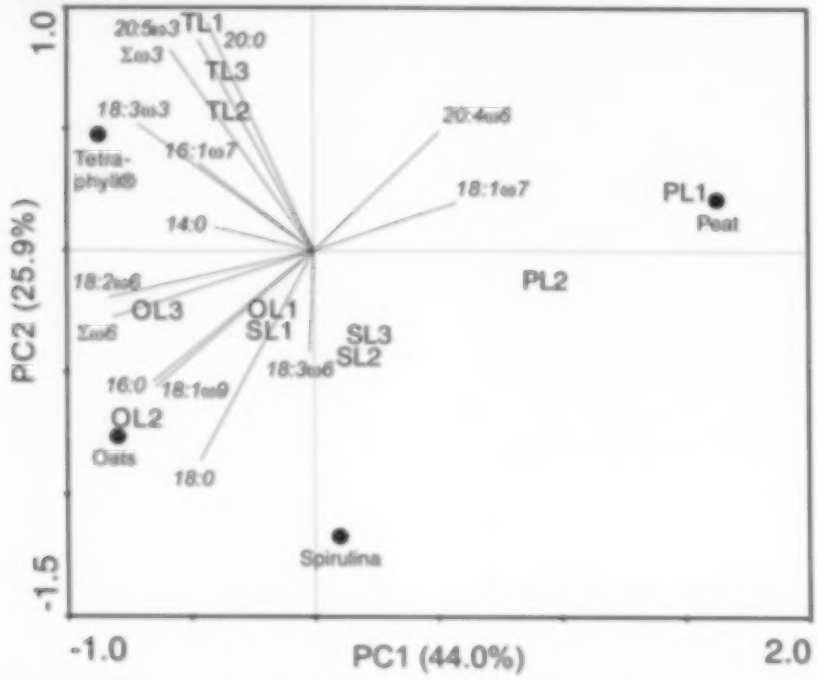

The conclusion that *C. riparius* larvae can grow and develop well on a diet low in ALA and lacking EPA may, however, be inflated by several processes and (or) mechanisms. Firstly, larvae could have been supported by EPA resulting from trophic upgrading (e.g., by ciliates and protozoans). This is not likely, however, since the peat-based formulated sediment is very low in microbial biomass and activity (Goedkoop et al. 2005). Moreover, Ederington et al. (1995) showed that trophic upgrading of FA from heterotrophic bacteria by ciliates did not produce 20-C PUFA owing to the fact that bacteria are known to lack PUFA (Pinkart et al. 2002). Secondly, subsidies of EPA from the egg stage may have been a source for larvae. Indeed, analysis of a pooled sample of *C. riparius* eggs from our culture (fed Tetraphyll) showed concentrations of 1.5 mg EPA·g^{-1} and 0.11 mg DHA·g^{-1} (unpublished data). Considering that the wet weight of a single egg is 1.5 ± 0.2 µg (determined by volume determination at 150× magnification) and assuming dry weight to be 10% of wet weight would mean that the absolute amount of EPA increased approximately 350-fold (from 0.22 ng·egg^{-1} to 77 ng·larva^{-1}) in the oats treatment. This large increase in the amount of EPA per individual implies considerable synthesis of EPA (likely by elongation of dietary ALA) during growth and development. Considering this, we feel confident about our conclusion that the major share of EPA in *Chironomus* larvae originates from the elongation of dietary ALA.

Results from the oats and peat treatments further show that *C. riparius* larvae were capable of synthesizing ARA (via GLA) by Δ6- and Δ5-desaturase activity using LA available in both food sources. Surprisingly, ARA concentrations in larvae from the peat treatment were 1.0 ± 0.35 mg/g, i.e., 2–4 times higher than those in the other treatments, despite the fact that ARA was not detectable in peat. Considering the very high C:N and C:P ratios of 61 and 2196, respectively, however, it is likely to assume that the larvae in the peat treatment experienced elemental rather than biochemical limitation. Peat is residual plant material, resulting in extremely low levels of lipids and likely also proteins. The oats treatment further showed that larvae apparently were able to grow on a diet strongly dominated by ω6 FA and very poor in ω3 FA. At the two lowest feeding levels (0.1 and 0.3 mg C·day^{-1}), however, larvae in the oats treatment were smaller than those reared on the other two pulverized food sources, suggesting that food quality (possibly ω3 FA) was limiting growth and development at low food quantity. A type 3 response model (Begon et al. 1996) fitted to the growth rate data showed that a saturation level was reached for the oats treatment at 2.7 mg C·day^{-1} (or 3.9 µg ω3 and 120 µg ω6 PUFA·day^{-1}), whereas both algal-based food sources still promoted higher growth beyond the highest food concentration tested (Fig. 5). This suggests that although more food was available (at 5.4 mg C·day^{-1}), the food quality in the oats treatment constrained further stimulation of larval growth. The differences in specific growth at food saturation levels have in earlier studies been attributed to a difference in food quality (cf. Lampert 1977; Sterner and Schulz 1998). These results and the finding that larvae grew faster on the high-quality diet (Tetraphyll) at the two lowest food concentrations provide evidence of food quality effects at both ends of our food quantity gradients.

The dependence on dietary sources of 20-C PUFA likely varies among primary consumers owing to differences in the synthesis capacities (and rates). Synthesis capacities (and

© 2007 NRC Canada

Table 3. Mean (±1 SD) concentrations (mg·g dry weight^{-1}) of FA and lipid classes in *Chironomus riparius* larvae from treatments with oats, *Spirulina*, Tetraphyll, and peat (n = 3) and the experiment with *Scenedesmus obliquus* (n = 1).

FA	Oats	Spirulina	Tetraphyll	Peat	*S. obliquus*
14:0	1.70±0.03	1.44±0.56	1.89±0.18	1.68±1.62	0.99
16:0	14.23±2.28	11.90±2.88	9.49±0.99	7.33±5.52	6.24
16:1ω7	5.18±0.74	12.38±2.63	13.22±2.27	2.64±0.09	6.52
18:0	7.49±2.14	6.78±0.93	4.19±0.06	4.00±2.07	3.75
18:1ω9	9.79±3.23	4.21±1.37	3.91±0.44	2.72±1.26	4.64
18:1ω7	2.78±0.26	2.87±0.23	2.87±0.45	3.57±0.05	5.34
18:2ω6	17.65±3.58	9.08±2.99	10.59±0.49	2.68±0.65	6.41
18:3ω6	0.06±0.10	2.38±0.93	0.15±0.01	—	0.30
18:3ω3	0.43±0.10	0.11±0.02	0.55±0.08	—	2.41
20:0	0.57±0.09	0.40±0.02	0.91±0.09	0.45±0.04	0.60
20:4ω6	0.24±0.25	0.41±0.14	0.54±0.11	1.01±0.35	1.12
20:5ω3	0.21±0.20	0.31±0.18	1.66±0.55	—	0.84
22:6ω3	—	—	—	—	—
ΣSAFA	23.99±4.53	20.53±2.66	16.48±1.17	13.46±9.25	11.57
ΣMUFA	17.75±2.57	19.46±4.16	20.00±3.11	8.93±1.22	16.49
ΣPUFA	18.58±3.73	12.29±4.22	13.50±1.17	3.69±1.01	11.08
ΣFA	60.32±9.47	52.28±10.89	49.98±4.62	26.08±11.48	39.14
Σω3	0.64±0.28	0.43±0.19	2.21±0.61	0.00±0.00	3.25
Σω6	17.95±3.59	11.87±4.04	11.29±0.56	3.69±1.01	7.83
Total FA	83.16±16.86	65.23±16.04	63.59±6.19	46.20±0.51	63.24

Note: Σω3 and Σω6 give the sum of all ω3 FA and ω6 FA, respectively. ΣFA refers to the sum of identified FA, while total FA is calculated from the total area of peaks in the chromatograms. Dashes indicate that these FA were not detected (≤0.02 mg·g^{-1}).

Fig. 5. Nonlinear response model for *Chironomus riparius* specific growth rate as a function of food concentrations for Tetraphyll (solid circles), *Spirulina* (shaded circles), and oats (open circles).

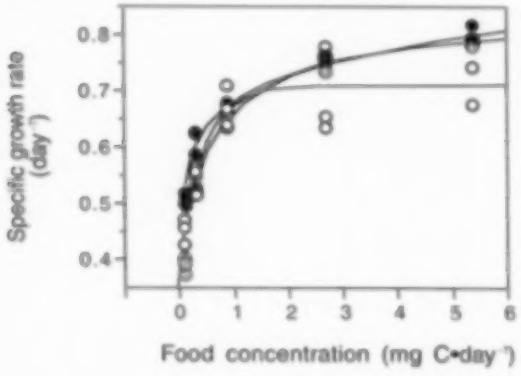

rates) will, in turn, be dependent on life cycle strategies and the FA composition of available food in the habitat where the animal has evolved. Several *Daphnia* species showed higher growth resulting from dietary supplements of EPA (Weers and Gulati 1997; Boersma 2000), whereas our data showed that *C. riparius* larvae grew equally well if supplied with shorter homologues. The interspecific differences in the dietary dependence of 20-C PUFA between *Daphnia* and *Chironomus* may be related to differences in their feeding and life cycle strategies. *Daphnia* is a highly opportunistic (*r*-selecting) species that grows rapidly and reproduces asexually when appropriate food sources are available in high quantities. Conversely, when food availability and (or) quality ceases, sexual reproduction in *Daphnia* is triggered and resting eggs are produced. In other words, the species is constrained by a lack of adaptation to poor food conditions. *Chironomus*, and many other taxa of benthic macroinvertebrates, are rather K-selectors that lack distinct resting stages but survive periods of low (and poor) food availability by feeding at lower rates on the poor-quality food, resulting in slow (or negative) growth and development. The elongated gut of *Chironomus* larvae and many other deposit-feeders can be seen as an adaptation to a diet of poor quality (Strayer 1991). Deposit-feeders, like many chironomid larvae and oligochaetes, are therefore able to compensate for low-quality food by ingesting large quantities of poor-quality food (i.e., sediment) to get to the high-quality food particles embedded in this sediment matrix. Similarly, among microcrustaceans, the curled gut in *Chydorus* species can be regarded as an adaptation to a diet of lower food quality. Schulz and Sterner (1999) showed also that *Bosmina* (*Bosmina leideri*, formerly *Bosmina longirostris*) is less dependent on high food quality than is *Daphnia*. The issue of dependence on dietary sources of 20-C PUFA has been poorly addressed but may vary largely among primary consumer species (and possibly among ecotypes). For example, the calanoid copepod *Acartia tonsa* shows very low fecundity (Ederington et al. 1995; Kleppel et al. 1998) is due to incomplete oogenesis (Støttrup and Jensen 1990) on a diet deprived of EPA and DHA. Conversely, the harpacticoid copepod *Thisbe holothyriae*, living and feeding more explicitly in the sediment, can complete ontogenesis on a diet deficient in 20-C PUFA owing to sufficiently high synthesis rates of EPA and DHA from ALA (Norsker and Støttrup

© 2007 NRC Canada

1994). The evolution of the harpacticoid species in a lower-quality food environment (i.e., sediments) has likely preserved a sufficiently high capacity of elongation and desaturation reactions to sustain growth rates that balance food availability. Harpacticoids are known to have relatively small clutches (few eggs), suggesting more pronounced K-selecting strategies than calanoids.

The observed poor larval growth on the *Scenedesmus* diet may seem surprising considering that this green alga is a model organism in zooplankton feeding studies. Two processes have likely contributed to this result. In our experimental vessels, we observed the burial of *Scenedesmus* cells in the interstitials of the sandy substrate that was used, thereby likely decreasing the availability of these cells. More important, however, is the observed poor digestion of *Scenedesmus* cells by *C. riparius* as revealed by a very large share of intact algal cells in the hindgut of larvae (microscopic examination). This is likely due to the lack of carbohydrase activity in *C. riparius*, as also reported for other *Chironomus* species (Bjarnov 1972). The marked growth stimulation at 2.7 and 5.4 mg C·day^{-1} is likely a consequence of a higher degree of microbial conditioning and subsequent increased availability of algal nutrients and energy. These findings show that not only elemental and (or) biochemical composition but also digestibility are important descriptors of food quality, in line with the results for *Daphnia* by van Donk and Hessen (1993) and van Donk et al. (1997).

Our result that deposit-feeding *C. riparius* larvae can perform well on a diet deprived of 20-C PUFA and with very low ω3:ω6 ratios suggests that this species, and perhaps even other *Chironomus* species, can sustain viable populations with a low-quality food diet. However, our results also showed that the generation time of this species was shorter and adults larger when food quality improved, suggesting higher reproductive output, providing a potential for higher populations densities. Earlier studies have shown that dietary EPA concentrations can have strong repercussions on consumer fecundity (e.g., Sundbom and Vrede 1997; Kleppel et al. 1998; Wacker and von Elert 2004). Considering the physiological importance of the eicosanoid precursors EPA, ARA, and 20:3ω6 in sexual maturation and reproduction, however, future studies on benthic invertebrates should include fecundity (or rather viable offspring) as an experimental end point. Furthermore, future work should also address the implications of trophic (biochemical) upgrading by benthic invertebrates to higher trophic levels.

Wallis et al. (2002) mentions for animals unique pathways of PUFA synthesis in the free-living nematode *Caenorhabditis elegans*. *Caenorhabditis elegans* possesses all of the desaturase enzymes required for the synthesis of EPA and ARA from oleic acid (18:0), including the Δ9- and Δ12-desaturases that are common in plants and the FAT1-n3 desaturase that converts ω6 FA to ω3 FA. This nematode species cannot, however, further elongate EPA to DHA, likely because it has no need for DHA. The capacity to synthesize EPA and ARA from saturated FA seems an excellent adaptation to the highly heterotrophic environment that is the natural habitat of *C. elegans*. Indeed, this highly opportunistic nematode species is able to grow and reproduce at very high rates on an *Escherichia coli* diet deprived of PUFA. This capacity may have a wider distribution in aquatic animals that live on poor-quality food resources (e.g., deposit-feeders and detritivores). Likely, we are only just beginning to understand the role of these FA in the physiology and ecology of aquatic invertebrates and in food webs.

Acknowledgements

The authors acknowledge Tobias Vrede and Richard K. Johnson and two anonymous reviewers for their input on an earlier draft of the manuscript and Siv Tengblad for analyzing fatty acids.

References

Ahlgren, G., Goedkoop, W., Markensten H., Sonesten, L., and Boberg, M. 1997. Seasonal variations in food quality for pelagic and benthic invertebrates in Lake Erken — the role of fatty acids. Freshw. Biol. **38**: 555–570.

Armitage, P.D. 1995. Behaviour and ecology of adults. *In* The chironomidae. The biology and ecology of non-biting midges. *Edited by* P. Armitage, P.S. Cranston, and L.V.C. Pinder. Chapman and Hall, London, U.K. pp. 194–224.

Arts, M.T., Ackman, R.G., and Holub, B.J. 2001. "Essential fatty acids" in aquatic ecosystems: a crucial link between diet and human health and evolution. Can. J. Fish. Aquat. Sci. **58**: 122–137.

Begon, M., Harper, J.L., and Townsend, C.R. 1996. Ecology — individuals, populations, communities. Blackwell Science, London, U.K.

Bell, J.G., Ghioni, C., and Sargent, J.R. 1994. Fatty acid compositions of 10 freshwater invertebrates which are natural food organisms of Atlantic parr (*Salmo salar*): a comparison with commercial diets. Aquaculture, **128**: 301–313.

Bell, M.V., Batty, R.S., Dick, J.R., Fretwell, K., Navarro, J.C., and Sargent, J.R. 1995. Dietary deficiency of docosahexaenoic acid impairs vision at low light intensities in juvenile herring (*Clupea harengus* L.). Lipids, **30**: 443–449.

Bell, M.V., Dick, J.R., and Kelly, M.S. 2001. Biosynthesis of eicosapentaenoic acid in the sea urchin *Psammechinus miliaris*. Lipids, **36**: 79–82.

Bjarnov, N. 1972. Carbohydrases in *Chironomus*, *Gammarus* and some trichopteran larvae. Oikos, **23**: 261–263.

Boersma, M. 2000. The nutritional quality of P-limited algae for *Daphnia*. Limnol. Oceanogr. **45**: 189–199.

Brett, M.T., and Müller-Navarra, D.C. 1997. The role of highly unsaturated fatty acids in aquatic foodweb processes. Freshw. Biol. **38**: 483–499.

D'Abramo, L.R., and Sheen, S.-S. 1993. Polyunsaturated fatty acid nutrition in juvenile freshwater prawn *Macrobrachium rosenbergii*. Aquaculture, **115**: 63–86.

Dadd, R.H., and Kleinjan, J.E. 1984. Prostaglandin synthetase inhibitors modulate the effect of essential dietary arachidonic acid in the mosquito *Culex pipiens*. J. Insect Physiol. **30**: 721–728.

Dadd, R.H., Kleinjan, J.E., and Stanley-Samuelson, D.W. 1987. Polyunsaturated fatty acids of mosquitoes reared with single dietary polyunsaturates. Insect Biochem. **17**: 7–16.

Davies, N.A., Edwards, P.A., Lawrence, M.A.M., Simkiss, K., and Taylor, M.G. 1999. Biocide testing using particles with controlled surface properties (artificial sediments). Environ. Toxicol. Chem. **18**: 2337–2342.

Ederington, M.C., McManus, G.B., and Harvey, H.R. 1995. Trophic transfer of fatty acids, sterols, and a triterpenoid alcohol

© 2007 NRC Canada

between bacteria, a ciliate, and the copepod *Acartia tonsa*. Limnol. Oceanogr. **40**: 860–867.

Einig, R.G., and Ackman, R.G. 1987. Omega-3 PUFA in marine oil products. J. Am. Oil Chem. Soc. **64**: 499–502.

Elendt, B.-P. 1990. Nutrional quality of a microencapsulated diet for *Daphnia magna*. Effects on reproduction, fatty acid composition, and midgut ultrastructure. Arch. Hydrobiol. **118**: 461–475.

Goedkoop, W., Sonesten, L., Ahlgren, G., and Boberg, M. 2000. Fatty acids in profundal benthic invertebrates and their major food resources in Lake Erken, Sweden: seasonal variation and trophic indications. Can. J. Fish. Aquat. Sci. **57**: 2267–2279.

Goedkoop, W., Widenfalk, A., Haglund, A.-L., Steger, K., and Bertilsson, S. 2005. Microbial characterization of artificial sediment and comparisons with natural sediment — implications for toxicity testing. Environ. Toxicol. Chem. **24**: 2725–2733.

Hanson, B.J., Cummins, K.W., Cargill, A.S., and Lowry, R.R. 1985. Lipid content, fatty acid composition and the effect of diet on fats of aquatic insects. Comp. Biochem. Physiol. B Comp. Biochem. **80**: 257–276.

Hill, C., Quigley, M.A., Cavaletto, J.F., and Gordon, W. 1992. Seasonal changes in lipid content and composition in the benthic amphipods *Monoporeia affinis* and *Pontoporeia femorata*. Limnol. Oceanogr. **37**: 1280–1289.

Howard, R.W., and Stanley-Samuelson, D.W. 1996. Fatty acid composition of fat body and malpighian tubules of the tenebrionid beetle, *Zophobas atratus*: significance in the eicosanoid-mediated physiology. Comp. Biochem. Physiol. B Comp. Biochem. **115**: 429–437.

Kainz, M., Arts, M.T., and Mazumder, A. 2004. Essential fatty acids in the planktonic food web and their ecological role for higher trophic levels. Limnol. Oceanogr. **49**: 1784–1793.

Kebede, E., and Ahlgren, G. 1996. Optimum growth conditions and light utilization efficiency of *Spirulina platensis* (= *Arthrospira fusiformis*) (Cyanophyta) from Lake Chitu, Ethiopia. Hydrobiologia, **332**: 99–109.

Kleppel, G.S., Burchart, C.A., and Houchin, L. 1998. Nutrition and the regulation of egg production in the calanoid copepod *Acartia tonsa*. Limnol. Oceanogr. **43**: 1000–1007.

Lampert, W. 1977. Studies on the carbon balance of *Daphnia pulex* as related to environmental conditions. Arch. Hydrobiol. Beihefte, **48**: 336–360.

Makhutova, O.N., Kalachova, G.S., and Gladyshev, M.I. 2003. A comparison of the fatty acid composition of *Gammarus lacustris* and its food sources from a freshwater reservoir, Bugach, and the saline Lake Shira in Siberia, Russia. Aquat. Ecol. **37**: 159–167.

Moreno, V.J., De Moreno, J.E.A., and Brenner, R.R. 1979. Fatty acid metabolism in the calanoid copepod *Paracalanus parvus*: I. Polyunsaturated fatty acids. Lipids, **14**: 313–317.

Morse, D.E., Dunkan, H., Hooker, N., and Morse, A. 1977. Hydrogen peroxide induces spawning in mollusks with activiation of prostaglandin endoperoxide synthetase. Science (Washington, D.C.), **196**: 298–300.

Murphy, J., and Riley, J.P. 1962. A modified single-solution method for the determination of phosphate in natural waters. Anal. Chim. Acta, **27**: 31–36.

Müller-Navarra, D.C., Brett, M.T., Liston, A.M., and Goldman, C.R. 2000. A highly unsaturated fatty acid predicts carbon transfer between primary producers and consumers. Nature (Lond.), **403**: 74–77.

Müller-Navarra, D.C., Brett, M.T, Park, S., Chandra, S., Ballantyne, A.P., Zorita, E., and Goldman, C.R. 2003. Unsaturated fatty acid content in seston and trophodynamic coupling in lakes. Nature (Lond.), **427**: 69–72.

Norsker, N.-H., and Støttrup, J.G. 1994. The importance of dietary HUFAs for fecundity and HUFA content in the harpacticoid *Thisbe holothuriae*. Aquaculture, **125**: 155–166.

Organisation for Economic Cooperation and Development. 2004. OECD guidelines for the testing of chemicals 219: sediment-water chironomid toxicity test using spiked water. Organisation for Economic Cooperation and Development, Paris, France.

Pinkart, H.C., Ringelberg, D.B., Piceno, Y.M., MacNaughton, S.J., and White, S.J. 2002. Biochemical approaches to biomass measurements and community structure analysis. *In* Manual of environmental microbiology. *Edited by* C.J. Hurst and V.A. Hendon. ASM Press, Washington, D.C. pp. 101–113.

Rowley, A.F., Vogan, C.L., Taylor, G.W., and Clare, A.S. 2005. Prostaglandins in non-insectan invertebrates: recent insight and unresolved problems. J. Exp. Biol. **208**: 3–14.

Sargent, J.R., Bell, J.G., Bell, M.V., Hendersen, R.J., and Tocher, D.R. 1995. Requirement criteria for essential fatty acids. J. Appl. Ichthyol. **11**: 183–198.

Schulz, K.L., and Sterner, R.W. 1999. Phytoplankton phosphorus limitation and food quality for *Bosmina*. Limnol. Oceanogr. **44**: 1549–1556.

Stanley-Samuelson, D.W. 1994. The biological significance of prostaglandines and related eicosanoids in invertebrates. Am. Zool. **34**: 589–598.

Stanley-Samuelson, D.W., and Pedibhotla, V.K. 1996. What can we learn from prostaglandins and related eicosanoids in insects? Minireview. Insect Biochem. Mol. Biol. **26**: 223–234.

Sterner, R.W., and Hessen, D. 1994. Algal nutrient limitation and the nutrition of aquatic herbivores. Annu. Rev. Ecol. Syst. **25**: 1–29.

Sterner, R.W., and Schulz, K.L. 1998. Zooplankton nutrition: recent progress and reality check. Aquat. Ecol. **32**: 261–279.

Støttrup, J.G., and Jensen, J. 1990. Influence of algal diet on feeding and egg production of the calanoid copepod, *Acartia tonsa* Dana. J. Exp. Mar. Biol. Ecol. **141**: 87–105.

Strayer, D. 1991. Perspectives on the size structure of lacustrine zoobenthos, its causes, and its consequences. J. North Am. Benthol. Soc. **10**: 210–221.

Sundbom, M., and Vrede, T. 1997. Effects of fatty acid and phosphorus content of food on the growth, survival and reproduction of *Daphnia*. Freshw. Biol. **38**: 665–674.

ter Braak, C.J.F., and Šmilauer, P. 2002. Canoco for Windows. Biometris, Wageningen, the Netherlands.

Vadeboncoeur, Y., Vander Zanden, M.J., and Lodge, D.M. 2002. Putting the lake back together: reintegrating benthic pathways into lake food web models. Bioscience, **52**: 44–54.

VanderPloeg, H.A., Liebig, J.R., and Gluck, A.A. 1996. Evaluation of different phytoplankton for supporting development of zebra mussel larvae (*Dreissena polymorpha*): the importance of size and polyunsaturated fatty acid content. J. Gt. Lakes Res. **22**: 36–45.

van Donk, E., and Hessen, D.O. 1993. Grazing resistance in nutrient stressed phytoplankton. Oecologia (Berl.), **93**: 508–511.

van Donk, E., Lürling, M, Hessen, D.O., and Lokhorst, G.M. 1997. Altered cell wall morphology in nutrient deficient phytoplankton and its impact on grazers. Limnol. Oceanogr. **42**: 357–364.

von Elert, E. 2002. Determination of limiting polyunsaturated fatty acids in *Daphnia galeata* using a new method to enrich food algae with single fatty acids. Limnol. Oceanogr. **47**: 1764–1773.

Wacker, A., and von Elert, E. 2004. Food quality controls egg quality of the zebra mussel *Dreissena polymorpha*: the role of fatty acids. Limnol. Oceanogr. **49**: 1794–1801.

© 2007 NRC Canada

Wacker, A., Becher, P., and von Elert, E. 2002. Food quality effects of unsaturated fatty acids on larvae of the zebra mussel *Dreissena polymorpha*. Limnol. Oceanogr. **47**: 1242–1248.

Wallis, J.G., Watts, J.L., and Brown, J. 2002. Polyunsaturated fatty acid synthesis: what will they think of next? Trends Biochem. Sci. **27**: 467–473.

Weers, P.M.M., and Gulati, R.D. 1997. Effect of addition of polyunsaturated fatty acids to the diet on the growth and fecundity of *Daphnia galeata*. Freshw. Biol. **38**: 721–729.

Xu, X., Ji, W., Castell, J.D., and O'Dor, R. 1993. The nutritional value of dietary *n*–3 and *n*–6 fatty acids for the Chinese prawn (*Panaeus chinensis*). Aquaculture, **118**: 277–285.

Zenebe, T., Ahlgren, G., and Boberg, M. 2003. Effects of algal diets and temperature on the growth and fatty acid content of the cichlid fish *Oreochromis niloticus* L. — a laboratory study. Aquat. Ecol. **37**: 169–182.

© 2007 NRC Canada

Genetic divergence and connectivity among river and reef spawning groups of walleye (*Sander vitreus vitreus*) in Lake Erie

Rex Meade Strange and Carol A. Stepien

Abstract: Discerning population genetic structure is challenging for highly vagile open water animals, as contemporary gene flow may obscure historic phylogeographic patterns. We examined genetic variation among all 10 major river and reef spawning groups of walleye (*Sander vitreus vitreus*) in Lake Erie for evidence of isolation by distance, segregation by physiographic partitions, and natal site fidelity using 10 nuclear DNA microsatellite loci. Results revealed that although most spawning groups were distinguishable, relationships did not correspond with physiographic basins or distances among localities. Bayesian analyses showed connectivity among some southern shore spawning groups, which included the largest-sized groups. Significant genetic divergence was discerned among walleye spawning in the river systems of eastern Lake Erie, as well as in two sites in western Lake Erie, along with marked isolation from Lake St. Clair. Population structure of Lake Erie walleye thus appears to reflect the interaction of two different intrinsic factors: isolation due to natal site fidelity that maintains patterns of divergence, and connectivity due to individuals that stray from their natal sites to spawn.

Résumé : Il n'est pas facile de déterminer la structure génétique de la population chez les animaux très mobiles dans la masse d'eau, car le flux génique actuel peut obscurcir les patrons phylogéographiques du passé. Par l'analyse de 10 locus microsatellites d'ADN nucléaire, nous avons étudiéla variation génétique dans l'ensemble des dix principaux groupes de dorés jaunes (*Sander vitreus vitreus*) qui fraient dans les rivières et sur les récifs au lac Érié, à la recherche d'indices d'isolement par la distance, de ségrégation par partitions physiographiques et de fidélité au site de naissance. Nos résultats montrent que, bien qu'on puisse reconnaître la plupart des groupes de fraie, leurs relations ne correspondent pas aux bassins hydrographiques, ni aux distances entre les localités. Des analyses bayésiennes révèlent l'existence de connectivité entre certains groupes de fraie de la rive sud, qui incluent les groupes de plus grande taille. Nos données indiquent aussi une divergence génétique significative chez les dorés qui fraient dans les bassins versants de l'est du lac Érié, de même qu'à deux sites dans l'ouest du lac Érié; elles montrent aussi un isolement vis-à-vis le lac St-Clair. La structure de population des dorés du lac Érié semble donc refléter l'interaction de deux facteurs intrinsèques distincts, l'isolement due à la fidélité au site de naissance qui maintient les patrons de divergence et la connectivité due aux individus qui s'éloignent de leur site de naissance pour se reproduire.

[Traduit par la Rédaction]

Introduction

The walleye (*Sander* (= *Stizostedion*) *vitreus vitreus*; Percidae) is one of the most economically important fish species in the Great Lakes. The species is a large and highly vagile piscivore endemic to the riverine and lacustrine systems of eastern North America and attains greatest abundance in western Lake Erie (Hubbs and Lagler 2004). Only 10 primary spawning groups are recognized by Lake Erie fishery managers (Fig. 1), making the lake a geographically simple and relatively isolated system in which to assess mechanisms defining contemporary patterns of population connectivity and isolation. Understanding the ecological mechanisms regulating genetic divergences among spawning groups is important for successful resource management.

Adult walleye forage in open water habitats and separate into discrete spawning groups in the spring. Walleye mature at age 2–3 in Lake Erie (Wolfert 1963) and spawn at night in small groups shortly after the ice breaks up in spring, with females depositing their eggs in a single night and males staying on the spawning grounds for up to several weeks (Scott and Crossman 1973). Some walleye groups spawn in specific tributary rivers, while other groups spawn on shallow shoals or reefs of Lake Erie (Olson and Scidmore 1962; Todd and Haas 1993). Tagging studies indicate that individuals tend to return to their natal spawning locations (Regier et

Received 31 July 2006. Accepted 14 December 2006. Published on the NRC Research Press Web site at http://cjfas.nrc.ca on 27 March 2007.
J19455

R.M. Strange[1] and C.A. Stepien.[2] Great Lakes Genetics Laboratory, Lake Erie Center and Department of Environmental Sciences, The University of Toledo, 6200 Bayshore Road, Toledo, OH 43618, USA.

[1]Present address: Department of Biology, University of Southern Indiana, Evansville, IN 47712, USA.
[2]Corresponding author (e-mail: carol.stepien@utoledo.edu)

 doi:10.1139/F07-022 © 2007 NRC Canada

Fig. 1. Locations of the 11 primary walleye spawning sites in Lakes Erie and St. Clair and depiction of their genetic relationships. Solid circles denote sites with interconnectivity (i.e., the track), and open circles designate sites that significantly differ from all other groups. Heavy straight lines denote primary discontinuities in gene flow determined using BARRIER (Manni et al. 2004) and are sequentially numbered (I–III) in order of decreasing relative support. Grey regions (basins) and lines (rivers) inside modern-day Lake Erie depict its early development about 10 000 years before present (after Bolsenga and Herdendorf 1993).

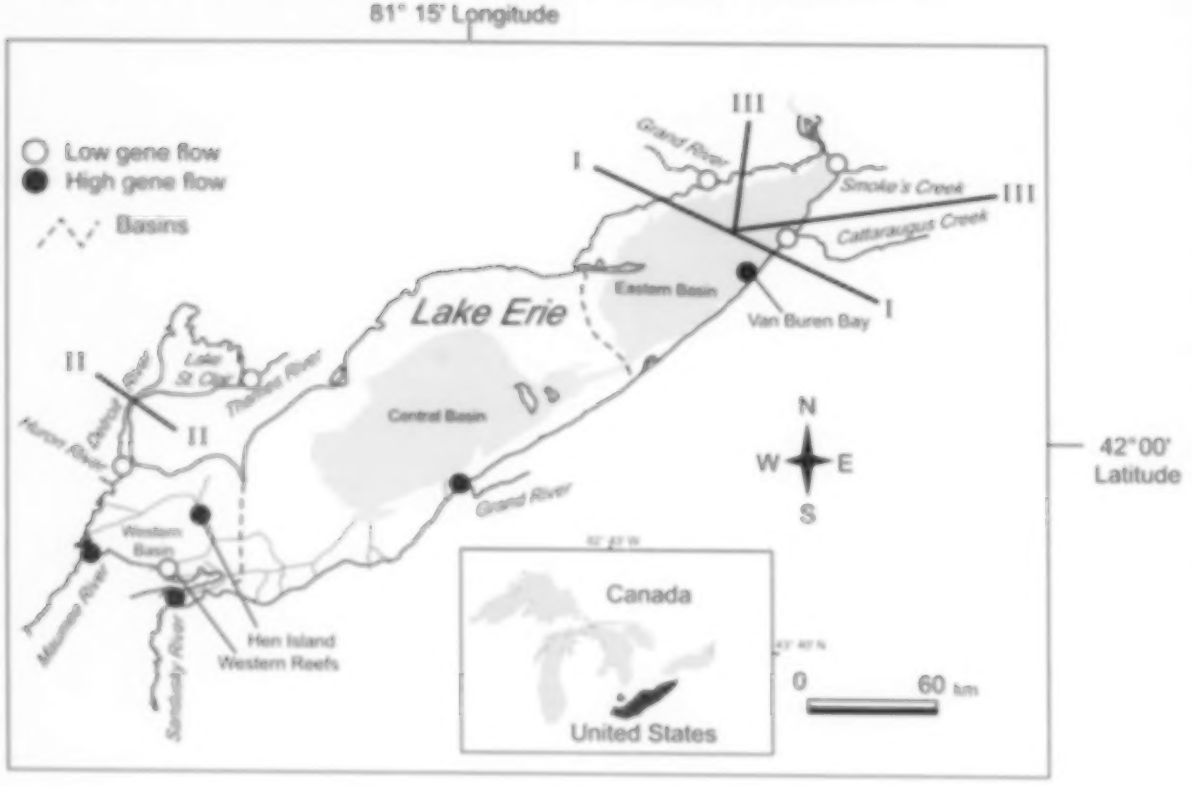

al. 1969; Goodyear et al. 1982), which appears to have a genetic basis (Jennings et al. 1996). Thus, natal site fidelity is a likely mechanism for maintaining population structure in walleye.

Demographic mechanisms may further regulate genetic structure in Lake Erie walleye. The largest spawning runs occur in the west, and smaller groups spawn in rivers and reefs of the central and eastern basins (Wolfert 1963; Schneider and Leach 1977). Although tagging studies have revealed relatively little overall migration, some walleye move seasonally from the west to the east (Thomas et al. 2005) or west into Lake St. Clair (Ferguson and Derksen 1971; Todd and Haas 1993). Walleye in the western basin outnumber those in the east by an order of magnitude (Thomas et al. 2005); thus, connectivity may be driven by different intrinsic growth rates among spawning groups. In other words, patterns of gene flow may be dominated by the largest spawning groups, which have greater reproductive success (i.e., increased recruitment) and from which more migratory individuals may stray (e.g., owing to overcrowding) to spawn with other groups. Great year-class variation, faster growth, and earlier maturity characterize walleye in western Lake Erie from those in the east (Colby and Nepszy 1981). Moreover, genetic structure within Lake Erie may be complicated by the population crash of walleye (as measured by annual catches) from the late 1950s through 1970s because of exploitation and habitat loss and their later recovery (Colby and Nepszy 1981; Hatch et al. 1987; Knight 1997), which likely altered patterns of gene flow and divergence.

The objective of this study was to test whether population genetic structure exists within Lake Erie walleye and to infer its defining mechanisms. Although geographically isolated populations of walleye are known to be genetically distinct (Billington and Strange 1995; Stepien and Faber 1998), few studies have investigated isolation and connectivity in a single system with a comprehensive sampling design (but see Stepien 1995 and Stepien and Faber 1998 for an mtDNA sequence analysis of Lake Erie walleye). Here we employed a landscape genetics analytical approach (Manel et al. 2003) to test the spatial distribution of genetic diversity in relation to extrinsic environmental features and intrinsic behavior. This study examined genetic variation at 10 microsatellite loci among walleye from all primary river and lake spawning groups in Lake Erie for evidence of (*i*) isolation by geographic distance, (*ii*) physiographic differences, and

© 2007 NRC Canada

Table 1. Summary statistics for walleye spawning groups from Lakes Erie and St. Clair based on 10 microsatellite loci.

Spawning group	N	H_O	H_E	F_{IS}	N_A	N_{PA}	P_{PA}
Lake St. Clair							
Thames River, Ont. 2004	38	0.745	0.766	0.028	79	1	0.013
Western basin, Lake Erie							
Huron River, Mich. 2003	20	0.745	0.761	0.021	84	1	0.012
Maumee River, Ohio 2003	76	0.698	0.758	0.073*	107	3	0.028
Western Reefs, Ohio 2004	20	0.675	0.675	0.001	72	1	0.014
Hen Island Reef, Ont. 2003	82	0.671	0.735	0.087*	108	2	0.019
Sandusky River, Ohio 2003	20	0.775	0.780	0.007	82	2	0.024
Central basin, Lake Erie							
Grand River, Ohio 2003	30	0.660	0.793	0.168*	88	1	0.011
Eastern basin, Lake Erie							
Van Buren Bay, N.Y. 2003	77	0.716	0.779	0.082*	104	7	0.067
Cattaraugus Creek, N.Y. 2003	30	0.700	0.764	0.084*	92	3	0.033
Smoke's Creek, N.Y. 2003	20	0.780	0.787	0.009	84	2	0.024
Grand River, Ont. 2003–2004	35	0.674	0.779	0.134*	91	2	0.022
Total for Lake Erie	410	0.704	0.778	0.095*			
Total for all sites	448	0.707	0.779	0.093*			

Note: N, sample size; H_O, observed and H_E, expected heterozygosity; F_{IS}, deviation from Hardy–Weinberg (HW) proportions; N_A, number of alleles; N_{PA}, number of private alleles; P_{PA}, proportion of private alleles. Divergences from HW proportions prior to Bonferroni correction ($P < 0.05$) are denoted by asterisks (*), although all spawning groups conformed to equilibrium expectations following Bonferroni correction and exclusion of the *SviL8* locus ($P < 0.0056$).

(*iii*) natal site fidelity. Finally, we asked whether genetic structure is associated with or driven by demographic processes, and if so, to what extent.

Materials and methods

Study area

The Great Lakes are geologically young (<13 000 years) and formed during the retreat of the last of the Pleistocene glaciations (Bolsenga and Herdendorf 1993). Most fishes now present in the lower Great Lakes colonized the newly formed habitats from lotic systems located south of the glacial maximum. In particular, fishes are believed to have entered Lake Erie from the west through a connection between the Wabash River and Maumee River valleys, whereas others are hypothesized to have entered from an eastern glacial refugium (Bailey and Smith 1981; see also Billington et al. 1992). Such physical isolation of different glacial refugium groups within the Lake Erie system may have existed as recently as 7 000 – 10 000 years before present, when the central and eastern basins of Lake Erie were relatively isolated from one another and aquatic habitats in the western basin consisted of a river system draining a low lying plain (see shaded interior of Fig. 1; Holcombe et al. 2003).

Present-day Lake Erie is a relatively isolated system, and its drainage is separated by divides from adjacent river systems (e.g., the Ohio River system to the south, from Lake Ontario to the east by Niagara Falls, and from the upper Great Lakes to the west by the Detroit River that drains from Lake St. Clair) (see Fig. 1). The Detroit River presumably constrains gene flow between Lake Erie and the upper Great Lakes through a narrow connection and thus may represent a potential bottleneck relative to the open water connections of Lake Erie.

Lake Erie is the shallowest of the five Great Lakes, and its natural division into three physiographic basins is of considerable ecological importance. The western basin is the most biologically productive region of the Lake and houses many islands and associated shoals (Bolsenga and Herdendorf 1993). The western region of the Lake constitutes the most important walleye spawning and nursery area in Lake Erie (Nepszy 1977). Each year, river spawning groups of walleye enter the Huron (Michigan), Maumee (Ohio), and Sandusky (Ohio) rivers of the western basin, with the largest spawning run occurring in the Maumee River (Nepszy 1977). Walleye also spawn over an extensive reef system consisting of numerous shoals in the western basin (Jeffrey Tyson, Ohio Division of Wildlife, 305 E. Shoreline Drive, Sandusky, OH 44870, personal communication).

In contrast, the central basin is deeper, has few islands, and contains a single primary spawning location for walleye in the south (e.g., Grand River (Ohio)). Habitats along the northern coast of the Lake are unsuitable for walleye spawning. The eastern basin contains the deepest regions of the Lake, has few shoal areas, and is not as biologically productive as the western basin (Bolsenga and Herdendorf 1993). Resident populations of walleye are known to spawn at a single shoal area (Van Buren Bay, New York) and in three rivers of the eastern basin: Cattaraugus Creek (New York), Smoke's Creek (New York), and Grand River (Ontario). The shoal area at Van Buren Bay once housed the "blue pike" walleye subspecies *Sander vitreus glaucus*, which became extinct by the late 1950s because of exploitation (see Stone 1948; Scott and Crossman 1973; Stepien and Faber 1998). The physiographic differences in Lake Erie represent a heterogeneous suite of foraging habitats, which combined with the small number of spawning sites for walleye may result in the segregation of spawning groups situated in either the western or eastern basins.

Sample collection

A sound sampling strategy is necessary to avoid erroneous conclusions regarding population structure in highly migra-

© 2007 NRC Canada

tory fishes. Therefore, samples of fin clips in tag and release programs were taken from spawning walleye either entering or leaving or over their spawning locations, as recommended by the International Great Lakes Fishery Commission's Lake Erie Walleye Task Group (Roger Knight, Ohio Division of Wildlife, 305 E. Shoreline Drive, Sandusky, OH 44870, USA, personal communication). Most of the samples were taken by state, federal, and provincial agencies during their monitoring programs and included the 10 primary spawning groups in Lake Erie and a single spawning area in neighboring Lake St. Clair (Table 1; Fig. 1). The sampling sites did not have a known history of stocking, except Cattaraugus Creek and Smoke's Creek, New York, which are no longer being stocked (Donald Einhouse, New York Department of Environmental Conservation, Dunkirk, NY 14048, USA, personal communication) and whose brief stocking history was not successful and did not genetically affect the native genotypes (see Stepien et al. 2004).

To reduce possible complications in comparing spawning groups taken from different years, we restricted our Lake Erie samples to the 2003 spawning season, except for the Thames River (Lake St. Clair) and the Western Reefs, which were collected during the 2004 spawning season. The 2003 year class produced by walleye spawning in Lake Erie was the strongest for over 20 years (Roger Knight, Ohio Division of Wildlife, 305 E. Shoreline Drive, Sandusky, OH 44870, USA, personal communication), rendering the present study an important baseline. Sex information was recorded for seven of the spawning groups (e.g., Huron River, Sandusky River, Grand River (Ohio), Van Buren Bay, Cattaraugus Creek, Smoke's Creek, and Grand River (Ontario)), enabling us to test for differences in allelic distributions between males and females. Each sample consisted of a small (1–2 cm^2) piece of pectoral or caudal fin fixed in 95% ethanol (EtOH) and then stored at room temperature in the laboratory. Most specimens were subsequently released by agency personnel.

DNA extraction, amplification, and allelic determination

Genomic DNA was extracted from the EtOH-fixed tissues either following traditional phenol–chloroform procedures or with the Qiagen DNeasy kit, following the manufacturer's directions (Qiagen, Inc., Valencia, California). DNA extractions were frozen and archived in the Great Lakes Genetics Laboratory for future studies. The polymerase chain reaction (PCR) was used to amplify allelic length variants from 10 microsatellite loci developed by other investigators for walleye, including Borer et al. (1999: *Svi*4, *Svi*6, *Svi*17, *Svi*18, *Svi*33), Wirth et al. (1999: *Svi*L6, *Svi*L7, *Svi*L8), and Eldridge et al. (2002: *Svi*2 and *Svi*7). PCR reactions consisted of 50 mmol·L^{-1} KCl, 1.5 mmol·L^{-1} $MgCl_2$, 10 mmol·L^{-1} Tris–HCl, 50 µmol·L^{-1} of each deoxynucleotide, 0.5 µmol·L^{-1} of both forward and reverse primers, 5–30 ng DNA template, and 0.6–1.2 units of *Taq* polymerase per 10 microlitres of reaction volume. For each locus, the forward primer was synthesized with a 5′ fluorescent label to allow visualization on an ABI 3130 genetic analyzer (Applied Biosystems Inc., Fullerton, California), and four different dye labels were used to facilitate multi- and pool-plexing of loci. A sterile mineral oil overlay was added to ensure that the reaction volume remained constant throughout the PCR cycles. A thermal cycle of 2 min at 94 °C for initial denaturation was followed by 35 cycles of denaturation (94 °C, 30 s), primer annealing (1 min) at a primer-specific temperature, and polymerase extension (72 °C, 30 s). A final extension at 72 °C for 5 min was included to minimize the number of partial strands. Annealing temperatures were either 54 °C (*Svi*L6, *Svi*L7, *Svi*L8, *Svi*17) or 60 °C (*Svi*2, *Svi*3, *Svi*4, *Svi*6, *Svi*7, *Svi*18, *Svi*33). This procedure was found to be robust and allowed for multiplexing primer sets with similar annealing temperatures.

Amplification products were prepared prior to electrophoresis by diluting 1:50 with dH_2O; 1 µL of this dilution was then added to 13 µL of a solution containing formamide and Gene Scan 500 LIZ size standard (ABI) and loaded onto a 96-well plate. Finally, microsatellite products were denatured for 2 min at 95 °C prior to loading. Allelic variants were identified by size using GeneMapper 3.7 software (ABI).

Data analyses

The set of samples included in our data set was modeled as a spatial set of panmictic subpopulations within the total population of Lake Erie walleye. There is an ongoing debate as to which equivalents of F_{ST} (i.e., the degree of genetic divergence among putative subpopulations) are best suited for analyzing divergences based on microsatellite data (see Hedrick 1999; Balloux and Lugon-Moulin 2002). Since the relationships among recently diverged populations, such as those tested here for our fine-scale analyses of Lake Erie, have been shown to be better resolved in models with θ_{ST} (the F_{ST} estimate of Weir and Cockerham 1984; see Balloux and Lugon-Moulin 2002), that method was adopted here. Thus, F statistic analogs (Wright 1943; Weir and Cockerham 1984) and their associated levels of significance were used to quantify genetic heterogeneity using the programs FSTAT (Goudet 1995) and GENEPOP 3.3 (Raymond and Rousset 1995; also refer to http://genepop.curtin.edu.au/).

Genetic variability within subpopulations first was estimated as the number of alleles per locus (N_A), the number of private alleles (N_{PA}), the proportion of private alleles (P_{PA}), and estimates of the observed (H_O) and expected (H_E) heterozygosities (Table 1). Variation within each population was quantified as $F_{IS} = (1 - [H_O(H_E)^{-1}])$. Any departures from Hardy–Weinberg (HW) expectations were assessed by a Markov chain method analogous to Fisher's exact tests (Guo and Thompson 1992), as implemented by GENEPOP using 5000 dememorizations, 500 batches, and 5000 iterations per batch. In addition, the loci were tested for linkage disequilibrium. Possible occurrence of null (nonamplified) alleles was assessed using the procedure of van Oosterhout et al. (2004, 2006) in the program MICRO-CHECKER (also refer to http://www.microchecker.hull.ac.uk).

Comparative pairwise tests of allelic frequency heterogeneity also were conducted using Goudet et al.'s (1996) test for genetic differentiation based on an exact nonparametric procedure in GENEPOP, which was independent of F_{ST} and HW equilibrium expectations and employed the same parameters as above for the Markov chain. Critical values for all tests involving multiple comparisons were subjected to Bonferroni correction (Rice 1989). Similarly, we tested for

© 2007 NRC Canada

Table 2. Summary statistics for 10 microsatellite loci across the 11 spawning groups of walleye from Lakes Erie and St. Clair.

Locus	N_A	Size range (bp)	F_{IS}	F_{IT}	F_{ST}
*Svi*2	14	190–220	0.069	0.120***	0.016***
*Svi*4	11	104–122	0.072	0.079***	0.034***
*Svi*6	21	140–170	0.022	0.068***	0.017***
*Svi*7	13	156–172	0.055	0.116***	0.007*
*Svi*17	9	102–118	0.056	0.106***	0.019**
*Svi*18	10	116–130	0.199*	0.323***	0.154***
*Svi*33	12	82–104	0.046	–0.002	0.034***
*Svi*L6	19	108–136	0.044	0.043*	0.003***
*Svi*L7	22	192–226	0.045	0.054***	0.010***
*Svi*L8	18	120–144	0.266*	0.271***	0.008***
Total	149	—	0.093*	0.117***	0.029***

Note: N_A is the number of alleles, bp indicates base pairs, F_{IS} quantifies the average differentiation within a spawning group, F_{IT} quantifies deviation in the total sample (i.e., all walleye sampled in the two lakes), and F_{ST} represents the average genetic divergence between pairs of spawning groups. Significant contribution to population genetic structure is indicated by asterisks: *, $P < 0.05$; **, $P < 0.01$; ***, $P < 0.001$. The *Svi*L8 locus was not used in further analyses, since it did not conform to Hardy–Weinberg (HW) equilibrium expectations because of null alleles.

possible differences in allelic representation between males and females using Goudet et al.'s (1996) genetic differentiation test, within the seven spawning groups with available sex data.

The distribution of allelic combinations (genotypes) within the total population of Lake Erie walleye was analyzed by means of exact tests and quantified as F_{IT}. The degree of genetic divergence among putative subpopulations (either spawning groups or basins) was estimated as F_{ST}, which assumes that divergences represent equilibrium between gene flow and genetic drift (Wright 1978). Values of F_{ST} that differ significantly ($P < 0.05$) from zero falsify the null hypothesis of panmixia between the putative subpopulations (spawning groups; Wright 1978).

Although evidence suggests that adult walleye tend to return to their natal sites to spawn, it is reasonable to assume that some may stray and join other spawning groups. If this is true, it may be hypothesized that migrant walleye either spawn at localities close to their natal sites or randomly join other spawning groups in Lake Erie. Isolation by distance would be consistent with the elongate structure of the Lake (i.e., a stepping-stone model of gene flow). Therefore, we tested whether or not the stepping-stone model is an appropriate model for walleye in Lake Erie through the regression of $F_{ST}(1 - F_{ST})^{-1}$ against the natural logarithm of geographical distance (which is expected to be linear under isolation by distance in two dimensions; Rousset 1997). Geographical distance was measured as the shortest waterway distance (km) between pairs of spawning sites. The significance of the regression was tested using the procedure of Mantel (1967). Pairwise gene flow between spawning groups was estimated using Slatkin's (1985) private allele measure of Nm (migration rate m of N individuals exchanged between sites per generation) under the rationale that private alleles are likely to attain higher frequencies in sites when gene flow is low.

The relative magnitude of genetic structure among walleye spawning groups was further investigated by combining the philosophy of continuous track analysis developed by Alroy (1995) with an analytic approach based on computational geometry using algorithms implemented in the program BARRIER 2.2 (Manni et al. 2004; also refer to www.mnhn.fr/mnhn/ecoanthropologie/software/barrier.html). The locations of genetic discontinuities in these analyses were made without reference to a priori knowledge of landscape features that might define population structure (e.g., basins). A track is defined as a geographically continuous assemblage of sampling sites (i.e., spawning groups here) that are linked by appreciable gene flow (Wright 1978). Pairwise estimates of F_{ST} were mapped onto a matrix of their geographic coordinates (latitude and longitude), and a Monmonier maximum-difference algorithm identified which of the borders between neighboring populations exhibited the highest level of genetic divergence (Manni et al. 2004). Initial estimates of genetic discontinuities were made with a multilocus F_{ST} matrix, followed by a second analysis that incorporated single-locus F_{ST} values. This procedure ranked each identified barrier in relative magnitude, according to respective support from individual loci F_{ST} values.

To further distinguish populations, we used a Bayesian-based clustering algorithm, which is independent of assumptions about mutation process, as implemented in the program STRUCTURE (vers. 2.2; Pritchard et al. 2000; also refer to http://pritch.bsd.uchicago.edu). Briefly, this analysis assigns individual fish to putative groups on the basis of distinctive genotypic frequencies without prior knowledge of their true spawning population identity. We analyzed correspondence to spawning groups by specifying number of groups (K) in independent runs of the algorithm, ranging from $K = 1$ (thus testing the null hypothesis of panmixia) to $K = 10$ (the total N of spawning sites sampled in Lake Erie). The program assigned individuals to one or more groups, with their relative frequency of predicted membership in groups totaling 1.00. The burn-in period consisted of 100 000 replications, after which 700 000 Markov chain Monte Carlo (MCMC) simulations were run on pooled samples for $K = 1$–10 under a

© 2007 NRC Canada

Table 3. Pairwise estimates of migration (N_{em}; above diagonal) and F_{ST} values (below diagonal) among spawning populations of walleye from Lakes Erie and St. Clair based on nine microsatellite loci.

	Thames River, Ont.	Huron River, Mich.	Maumee River, Ohio	West Reefs, Ohio	Hen Island, Ont.	Sandusky River, Ohio	Grand River, Ohio	Van Buren Bay, N.Y.	Cattaraugus Creek, N.Y.	Smoke's Creek, N.Y.	Grand River, Ont.
Thames River	—	2.36	1.15	2.86	1.48	1.07	1.26	0.84	4.77	1.49	2.30
Huron River	0.046***	—	1.20	2.02	0.95	1.19	1.17	0.87	1.47	3.24	1.74
Maumee River	0.051***	0.038***	—	1.65	4.61	5.04	4.34	8.09	1.28	1.03	1.96
West Reefs	0.018***	0.061***	0.057***	—	1.58	1.96	1.52	1.09	2.41	2.06	2.43
Hen Island	0.049***	0.031***	0.004*	0.058***	—	4.61	3.70	3.70	1.27	1.20	2.43
Sandusky River	0.051***	0.045***	0.001	0.060***	0.003	—	2.75	3.52	1.54	1.10	1.58
Grand River, Ohio	0.043***	0.033***	0.001	0.051***	0.002	0.002	—	3.85	1.12	0.93	1.64
Van Buren Bay	0.059***	0.044***	0.002	0.063***	0.011*	0.001	0.008	—	0.90	0.83	1.70
Cattaraugus Creek	0.006	0.032***	0.048***	0.016***	0.047***	0.046***	0.037***	0.050***	—	1.71	2.50
Smoke's Creek	0.044***	0.001	0.033***	0.055***	0.027***	0.031***	0.033***	0.031***	0.034**	—	1.45
Grand River, Ont.	0.032***	0.051***	0.051***	0.055***	0.041***	0.045***	0.042***	0.052***	0.039***	0.029***	—

Notes: F_{ST} values represent Weir and Cockerham's (1984) correction of F_{ST}. Significance of divergence between spawning groups is indicated by asterisks after the F_{ST} value: *, $P < 0.05$; **, $P < 0.01$; ***, $P < 0.001$.

model assuming admixture. We then examined the consistency among 10 independent runs at each K, the comparative probabilities of individuals assigning to one or more groups, the log-likelihood and posterior probability values from each run, and their respective grouping patterns, following the program methodology. In addition, we calculated ΔK according to the procedure recommended by Evanno et al. (2005), which is based on the rate of change in the log probability of data between successive K values. The magnitude of ΔK over the 10 replicate runs was graphed against K for $K = 2$–10, and the height of the modal value of the distribution was used to additionally verify the correct K value. Results of the STRUCTURE analyses then were compared with spawning group relationships derived from the BARRIER and genetic divergence analyses.

Results

Variation within spawning groups

Genotypic data were collected for 448 walleye from 10 locations within Lake Erie and a single location in Lake St. Clair (Table 1; Fig. 1). Loci were unlinked and were highly polymorphic, ranging from 9 (*Svi*17) to 22 (*Svi*L7) alleles per locus (Table 2). Within each spawning group sample, each locus was represented by two to four common alleles and a larger number of alleles at lower frequencies. The average number of alleles per spawning group was 90.18 (range = 79–108); including one to three private alleles, except for Van Buren Bay where seven uniquely occurring alleles were present (Table 1). Walleye spawning at Van Buren Bay thus had the highest overall proportional representation of private alleles ($P_{PA} = 0.067$), whereas the sample from Grand River (Ohio) had the smallest proportion ($P_{PA} = 0.011$).

Observed heterozygosities for each spawning group were similar, ranging from 0.660 to 0.780 (Table 1). Out of the 11 spawning locations sampled, F_{IS} values for six (e.g., Hen Island, Maumee River, Grand River (Ohio), Van Buren Bay, Cattaraugus Creek, and Grand River, (Ontario)) showed significant deviations from HW equilibrium after Bonferroni correction (critical P for 10 loci = 0.005). All deviations from HW involved a single locus (*Svi*L8), which was due to the presence of null alleles for those spawning groups at that locus (based on analysis using MICRO-CHECKER (van Oosterhout et al. 2004)). After removal of the *Svi*L8 locus, all populations were in HW equilibrium using the remaining nine loci. Therefore, all subsequent genetic analyses were performed without the *Svi*L8 locus. We found no significant differences in allelic distributions between males and females collected from the same locality within the seven samples for which sex information was available.

Divergence patterns among spawning sites

Combining data from all 10 microsatellite loci for all sites combined revealed a significant departure from HW proportions ($F_{IT} = 0.117$, $P < 0.0001$), thus falsifying the null hypothesis of a single panmictic population. Similar significant results were obtained when data from the *Svi*L8 locus was then excluded from the analysis. Based on nine loci, significant allelic frequency differences were observed for 45 of the 55 pairwise comparisons among the 11 spawning sites

© 2007 NRC Canada

Fig. 2. Pairwise relationship between genetic divergence and geographic distance expressed as $F_{ST}(1 - F_{ST})^{-1}$ versus the natural logarithm of kilometres. Linear regression and correlation coefficients are $b = -0.003$ and $r = -0.12$, respectively (Mantel $P = 0.827$).

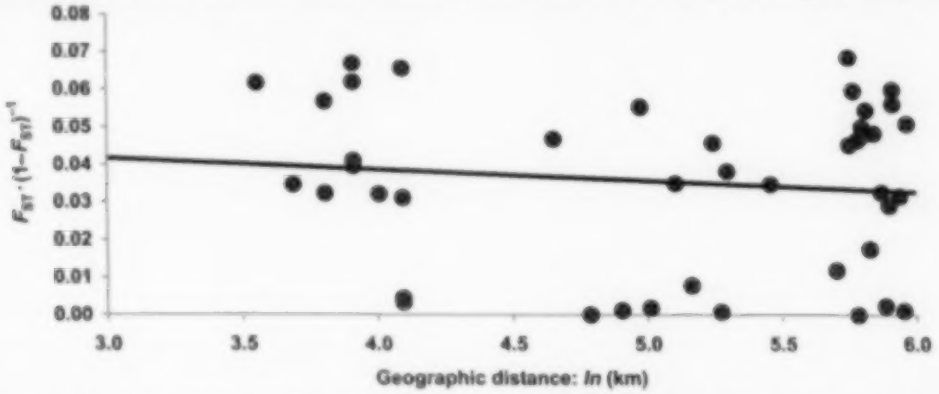

(Table 3). Using a critical $P = 0.05 \times 55^{-1}$ for Bonferroni correction, 42 pairwise F_{ST} values remained significant. Pooling genotypic data from each spawning group into respective physiographic regions (Table 1) revealed a statistically significant divergence between Lakes St. Clair and Erie ($F_{ST} = 0.026$, $P = 0.039$). Overall distinctions between the western and eastern basins of Lake Erie were not significant ($F_{ST} = 0.006$, $P = 0.341$) and suggest that walleye populations are not partitioned according to physiographic differences. Comparative pairwise tests of allelic frequency heterogeneity (Goudet et al. 1996) were congruent with the F_{ST} results shown in Table 3.

Genetic divergences were independent of spatial distances between pairs of spawning sites, as revealed by the regression of pairwise $F_{ST}(1 - F_{ST})^{-1}$ against the natural logarithm of geographical distance ($b = -0.003$, $r = -0.12$, $P = 0.827$; see Fig. 2). Likewise, pairwise estimates of the number of migrants per generation (N_m) varied unevenly across the Lake and did not correspond to physiographic regions (Table 3). Mean migration among all 11 samples after correction for sample size was $N_m = 6.94$, suggesting moderate levels of gene flow. However, pairwise estimates (Table 3) ranged from 0.83 to 8.09 between sites and most values were less than 2.00, thus indicating little gene flow among spawning groups from Lake St. Clair, two sites in western Lake Erie, and riverine locations in eastern Lake Erie. Interestingly, the highest pairwise rate of gene flow in Lake Erie ($N_m = 8.09$) occurred between the geographically distant spawning groups in the Maumee River (western basin) and Van Buren Bay (eastern basin).

Continuous track analysis of pairwise N_m estimates revealed a pattern of connectivity and isolation among walleye spawning groups uncorrelated with physiographic partitions in the Lake. In particular, a pathway of gene flow (= track) is suggested among some walleye spawning groups along the southern shore, including some western basin sites (Hen Island, Maumee River, and Sandusky River), the central basin location (Grand River (Ohio)), and Van Buren Bay in the eastern basin (designated by solid circles in Fig. 1). Spawning groups in the Huron River and Western Reefs (both in the western basin) fell outside the track and were genetically distinguishable from all other sites (shown with open circles in Fig. 1). BARRIER analysis of F_{ST} values (designated by straight lines in Fig. 1) confirmed the limits of the track; the first inferred barrier (i.e., the strongest, labeled I) separated the spawning groups from the western, central, and Van Buren Bay from the three rivers sampled in the eastern basin (Cattaraugus Creek, Smoke's Creek, and Grand River (Ontario)) and was supported by significant allelic divergences at eight separate loci. The second barrier (II) was supported by divergences at four of the loci and separated Lake Erie from the walleye spawning group in the Thames River (Lake St. Clair). The third barrier (III) separated walleye spawning in each of the three eastern rivers (Cattaraugus Creek, Smoke's Creek, and Grand River (Ontario)) from one another.

Bayesian analysis of genetic structure among all spawning groups included in this study was largely consistent with the results of the BARRIER analysis. The STRUCTURE analysis showed evidence for three population groups ($K = 3$ with posterior probability = 0.998 and maximum ΔK vs. K modal distribution peak height; see Fig. 3). The null hypothesis of panmixia across Lake Erie thus was rejected for $K = 1$, when all populations were considered in the overall analysis. Strongest assignments to single population groups were found for spawning groups from the Thames River, Lake St. Clair (0.848 for $K = 3$; Fig. 3), western Lake Erie reefs (0.813), and the eastern Lake Erie basin sites at Smoke's Creek (0.740), Cattaraugus Creek (0.724), and Grand River (Ontario) (0.672).

Moreover, the null hypothesis of panmixia was not rejected when a separate STRUCTURE analysis included only the five spawning groups comprising the track identified in the BARRIER analysis (posterior probability = 0.999 for $K = 1$). This restricted analysis thus indicated that spawning groups from the Maumee River, Sandusky River, Hen Island, Grand River (Ohio), and Van Buren Bay comprise a single interbreeding population of walleye.

Discussion

Patterns of microsatellite heterogeneity

Microsatellite DNA variation of Lake Erie walleye reveals greater diversity than that reported for the same loci in walleye populations from Minnesota (e.g., Borer et al. 1999; Eldridge et al. 2002) and Quebec (Wirth et al. 1999), likely

© 2007 NRC Canada

Fig. 3. Estimated population composition from Bayesian STRUCTURE analysis for $K = 3$ groups (posterior probability = 0.998). Each individual is represented by a thin vertical line, which is partitioned into three colored segments that represent the individual's estimated group membership fractions. Black lines separate individuals from different spawning sites. Ten STRUCTURE runs at each K produced nearly identical individual membership coefficients. Moreover, $K = 3$ was verified by calculation of the rate of change of the likelihood distribution and graphing ΔK vs. K, following Evanno et al. (2005).

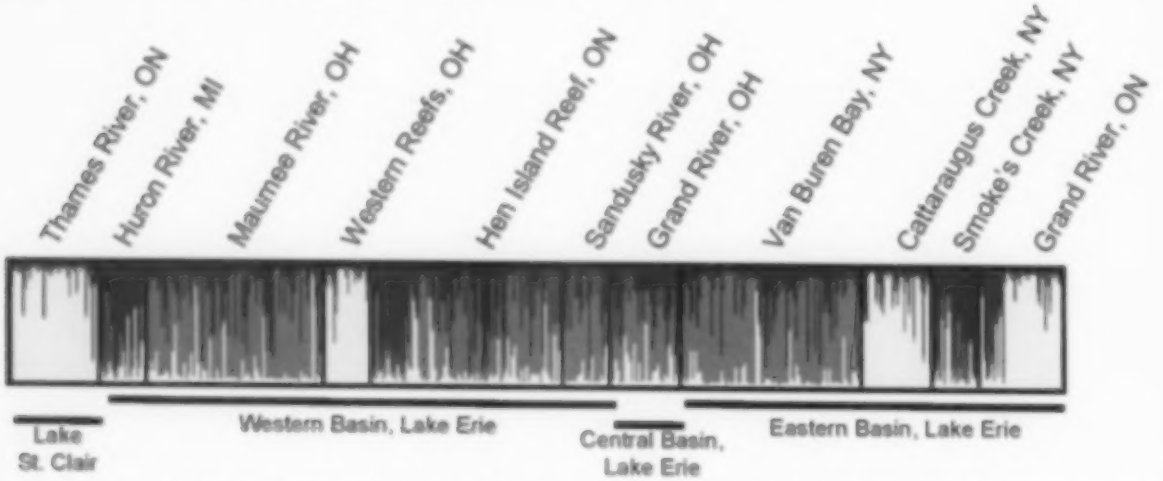

reflecting the greater number of spawning groups and larger spatial scale included in our data set. Cena et al. (2006) reported similar levels of microsatellite variation in their survey of 46 inland populations of walleye from Ontario, which may also represent such mixing. Cena et al. (2006) further noted that deviations from HW equilibrium in Ontario walleye involved a single (unspecified) locus per population. In the present study, all deviations from HW equilibrium within spawning groups from Lake Erie also involved a single locus (*Svi*L8), for which the presence of null alleles was indicated. Thus, we conclude that our microsatellite data (with the possible exception of *Svi*L8) appear to represent an unbiased estimator for genetic distinctions among spawning groups of Lake Erie walleye.

Combining the information from all Lake Erie spawning groups into a single population group showed significant heterozygote deficiencies (positive F_{IT} values) at most loci, indicating that allelic and genotypic distributions are incompatible with a single panmictic population. This conclusion is supported by both the number of significant F_{ST} values among spawning groups and an unequal distribution of N_m estimates. Further, the significant overall F_{IT} value is larger than the comparable F_{ST} value, suggesting that localized patterns of inbreeding are more important determinants of genetic structure in Lake Erie than are distinctions among random assemblages of spawning groups. In other words, some spawning groups are more closely related than others. Moreover, there were no significant differences in allelic distributions between males and females within spawning groups (similar to findings based on mtDNA for several of these sites; Stepien and Faber 1998; Stepien et al. 2004). Thus, both male and female walleye have similar migration and divergence patterns.

Patterns of divergence and connectivity

Metapopulation structure among a connected series of subpopulations can assume different forms, depending on the unique ecology of the species and contexts in which it occurs (Pulliam 1988; Hanski 1999; Strange 1999). In Lake Erie, walleye spawning groups could potentially be segregated by extrinsic factors such as habitat differences in the Lake (east versus west) or type of spawning site (lake versus river). The predominant feature of genetic structure in Lake Erie walleye is the divergence of spawning groups in the eastern basin. We found no evidence to suggest that population structure in walleye is constrained by contemporary physiographic partitions in Lake Erie (e.g., basins rather than individual spawning sites), nor did lake spawning groups form a unique assemblage exclusive of those spawning in rivers.

Another notable feature of population structure in Lake Erie is the presence of a track of gene flow (inferred from N_m estimates) connecting most of the walleye spawning sites along the southern shoreline (i.e., Hen Island, Maumee River, Sandusky River, Grand River (Ohio), and Van Buren Bay), punctuated by a genetic barrier (inferred from F_{ST} values) with walleye that spawn in the three eastern tributaries (i.e., Cattaraugus Creek, Smoke's Creek, and Grand River (Ontario)). This pattern of gene flow and divergence is largely congruent with relationships among many of the same walleye spawning populations inferred from mtDNA sequences (Stepien and Faber 1998; Stepien et al. 2004). Although sample sizes in the earlier studies may have precluded some detection of fine-scale divergences, microsatellite data lend credence to the hypothesis that some walleye spawning groups are connected by contemporary patterns of gene flow, whereas others likely maintain ancient (Pleistocene or earlier) patterns of differentiation.

The genetic discontinuity within the eastern basin is intriguing, as Van Buren Bay was formerly occupied by the blue pike (*S. vitreus glaucus*), an extinct subspecies endemic to the deeper habitats of eastern Lake Erie (Stone 1948). Stepien et al. (2004) reported a distinctive assemblage of mtDNA haplotypes in the Cattaraugus Creek population, and

© 2007 NRC Canada

our analyses further identified divergence between Cattaraugus Creek and each of the three eastern rivers. It is possible that the walleye populations in the eastern rivers are older, resident populations, whereas the spawning group in Van Buren Bay contains strays from the western basin that began to exploit this lake spawning habitat after the demise of the blue pike in the late 1950s. Prior hybridization between the two forms of walleye (*S. v. vitreus* and *S. v. glaucus*) may account for the higher number of private alleles documented from Van Buren Bay in our study.

Correspondence of patterns in walleye with other fishes

Many of these patterns are also evident in other Lake Erie fishes, indicating similar biogeographic history. Notably, several species of Lake Erie fishes show west–east patterns in allelic frequencies: walleye *S. vitreus* (Stepien and Faber 1998; Stepien et al. 2004; this study), brown bullhead *Ameiurus nebulosus* (Murdoch and Hebert 1997), yellow perch *Perca flavescens* (Ford and Stepien 2004), and smallmouth bass *Micropterus dolomieu* (Stepien et al. 2007). Each of these species represents a different suite of life history attributes, including reproductive strategies, vagility, and habitat affinities. Shared patterns among species as different as these have been used to postulate the role of Pleistocene–postPleistocene events responsible for the structure of freshwater fish faunal assemblages (e.g., Wiley and Mayden 1985; Strange and Burr 1997).

Unlike walleye, subpopulations of smallmouth bass across Lake Erie correspond to a broadscale isolation by geographic distance pattern (Stepien et al. 2007). Smallmouth bass spawning groups are linked by a smaller track along the southern Lake shore, which does not extend to Van Buren Bay. Also, additional population units were discerned among Lake Erie spawning populations of smallmouth bass using a similar STRUCTURE analysis of microsatellite data ($K = 4$, posterior probability = 0.997; Stepien et al. 2007). Differences between smallmouth bass and walleye likely reflect their respective life histories and vagilities, with smallmouth bass being largely confined to a limited home range throughout its life history (Scott and Crossman 1973).

As in walleye, natal site fidelity appears to maintain reproductive isolation in a number of species, including rainbow smelt (*Osmerus mordax*; Bernatchez 1997), Atlantic herring (*Clupea harengus*; Bekkevold et al. 2005; Jorgensen et al. 2005), walleye pollock (*Theragra chalcogramma*; O'Reilly et al. 2004), and mackerels (*Scomber* spp.; Zardoya et al. 2004). Other species within the genus *Sander* are known to migrate to specific rivers to spawn (Koed et al. 2000, 2002), and this behavior may be a general pattern in this genus. Although the mechanism for homing behavior is unknown in percids, a study by Gerlach et al. (2001) suggests that Eurasian perch *Perca fluviatilis* may recognize kin through olfactory cues. Thus, it is possible that walleye return to their natal locations guided by olfactory information imprinted during early stages of their life history, which may be a primary mechanism for maintaining divergence among the respective spawning groups.

Mechanisms: patterns of gene flow and divergence in walleye

Population genetic structure is the consequence of localized patterns of gene flow punctuated by isolation and divergence. Lake Erie walleye exhibit patterns of genetic variability consistent with both phenomena: a track running along the southern shore and across the Lake that ends abruptly at a border separating the three relatively isolated eastern rivers (e.g., Cattaraugus Creek, Smoke's Creek, and Grand River (Ontario)). Thus, there are two different attributes of population structure that must be considered to better understand the mechanisms responsible for genetic relationships in Lake Erie walleye: (*i*) genetic divergence in the rivers to the east and west and (*ii*) connectivity within the track.

Our results suggest that river spawning groups in the eastern basin of Lake Erie remain distinct because most adults return to their natal locations to reproduce. Similar to many anadromous fishes, walleye form seasonal mixed stocks in open water habitats, but then separate at spawning and return to their natal sites to spawn. This pattern of repeat homing to specific spawning locations is well documented in walleye (Olson et al. 1978), and it is widely accepted that most individuals display spawning-site philopatry (Regier et al. 1969; Colby and Nepszy 1981; Horrall 1981).

Whereas natal homing as a mechanism for divergence among walleye spawning groups from the eastern rivers is relatively easy to postulate, the dynamics of gene flow throughout the Lake is more challenging. Tagging studies indicate that walleye from the western basin tend to migrate eastward into the central and eastern basins, whereas those tagged in Van Buren Bay are nonmigratory (Thomas et al. 2005). The number of private alleles per spawning group within the track ranged from one (Grand River (Ohio)) to seven (Van Buren Bay), whereas the remaining three populations had two to three unique alleles each. A larger number of private alleles in the spawning group from Van Buren Bay may reflect an accumulation of private alleles from recipient migratory spawning groups (Kawecki and Holt 2002; Kennington et al. 2003). In other words, asymmetrical gene flow may result from a greater number of individuals in a sink subpopulation (here, Van Buren Bay), whose alleles trace to immigrants from source subpopulations (e.g., sites to the west along the track); this merits further testing in walleye. Alternatively, the additional private alleles in the Van Buren Bay spawning group may trace their ancestry to the now-extinct blue pike that is hypothesized to have introgressed with walleye (see Stone 1948 and Stepien and Faber 1998), which is being tested by the Great Lakes Genetics Laboratory.

The mechanism(s) responsible for the track may be demographic. For example, Fraser et al. (2004) reported evidence that asymmetric migration proceeds from sites with a larger effective population size in brook trout (*Salvelinus fontinalis*) from a postglacial lake in Quebec, and a similar situation may exist in Lake Erie walleye. Walleye population sizes and recruitment (as estimated by management agencies during spawning runs; Roger Knight, Ohio Division of Wildlife, 305 E. Shoreline Drive, Sandusky, OH 44870, USA, personal communication) are significantly higher in the western basin than in the eastern basin. The Lake Erie Walleye Task Group of the Great Lakes Fishery Commission estimates that western basin populations range from 30 to 40 million spawning individuals, whereas those in the eastern basin number about 0.5–2 million (Thomas et al. 2005). Thus, it is possible that the greater population size of

© 2007 NRC Canada

walleye in the western basin contributes more individuals to a migrant pool than does the spawning group from Van Buren Bay.

Origins of the pattern

Population structure in Lake Erie walleye appears to reflect contemporary differences in natal site fidelity and demographic processes (e.g., population sizes); however, the overall pattern (most notably the west–east distinction) may be attributable to postPleistocene colonization of the Lake. Tributaries of eastern Lake Erie were isolated from the rest of the Lake by ice sheets during the Pleistocene, and it is notable that the eastern and central basins remained isolated during the earliest stages of Lake Erie (about 7 000 to 10 000 years before present; Holcombe et al. 2003; see internal shading in Fig. 1). The spawning groups of the three eastern tributaries were separated from other walleye population groups until this barrier broke down, and this genetic discontinuity has been maintained by natal site fidelity as discussed above. On the other hand, the track consists of some spawning sites in the western basin and along the southern shore of the Lake. During the early stages of Lake Erie, the western basin was dominated by a large river system that included the present Maumee and Sandusky rivers as its headwaters. Kitchell et al. (1977) noted that the walleye is primarily a large river fish and occupies habitats similar to the pools of large rivers when it occurs in lakes. Western Lake Erie is such a habitat in terms of shallow depth, minimal flow, and appropriate spawning substrates (Kitchell et al. 1977, p. 1938), and it is likely that the spawning groups dominating the track are descendent from those occurring in the rivers of the western basin.

In conclusion, walleye in Lake Erie represent a classical subdivided population in which differences among spawning groups are likely the result of two contemporary intrinsic mechanisms: (*i*) demographic patterns in which the differential productivity and concomitant contributions to a common gene pool result in gene flow and (*ii*) natal site fidelity that maintains isolation of specific river spawning groups. These contemporary patterns have modified but not obscured historical patterns of divergence attributable to postglacial colonization by different source populations, which is being further investigated in a broader-scale study using both microsatellite and mtDNA (C.A. Stepien, R.L. Lohner, and D.J. Murphy, unpublished data). Although walleye do not segregate on the basis of physiographic differences in Lake Erie or on distinctions between subpopulations that spawn in rivers versus shoals, we found evidence that Lake Erie walleye appear to retain historic patterns of genetic diversity despite recent patterns of exploitation and habitat destruction.

Acknowledgements

This is publication No. 2007-006 from the Lake Erie Center. This project was developed by the Great Lakes Genetics Laboratory in conjunction with the Lake Erie Walleye Task Force of the Great Lakes Fishery Commission and Great Lakes fishery managers — especially the Ohio Division of Wildlife, the Michigan Department of Natural Resources, the Ontario Ministry of Natural Resources, the Pennsylvania Fish and Boat Commission, and the New York Department of Environmental Conservation. The study was supported by National Oceanic and Atmospheric Administration (NOAA) Ohio Sea Grants Nos. R/LR-4 and R/LR-8, an award from the US Fish and Wildlife Service Restoration Act through the Great Lakes Fishery Commission, and US Environmental Protection Agency (USEPA) grant No. CR-83281401-0 (all to CAS). Walleye were collected with the help of D. Einhouse, R. Haas, T. Johnson, K. Kayle, C. Knight, R. Knight, E. Roseman, M. Turner, M. Thomas, J. Tyson, C. Vandergoot, and C. Wilson. DNA technicians D. Murphy, C. Taylor, and R. Lohner provided valuable help with laboratory and data analysis. The manuscript additionally benefited from proofreading and suggestions by M. Neilson, R. Lohner, and D. Murphy.

References

Alroy, J. 1995. Continuous track analysis: a new phylogenetic and biogeographic method. Syst. Biol. **44**: 152–178.

Bailey, R.M., and Smith, G.R. 1981. Origin and geography of the fish fauna of the Laurentian Great Lakes basin. Can. J. Fish. Aquat. Sci. **38**: 1539–1561.

Balloux, F., and Lugon-Moulin, N. 2002. The estimation of population differentiation with microsatellite markers. Mol. Ecol. **11**: 155–165.

Bekkevold, D., Andre, C., Dahlgren, T.G., Clausen, L.A.W., Torstensen, E., Mosegaard, H., Carvalho, G.R., Christensen, T.B. Norlinder, E., and Ruzzante, D.E. 2005. Environmental correlates of population differentiation in Atlantic herring. Evolution, **59**: 2656–2668.

Bernatchez, L. 1997. Mitochondrial DNA analysis confirms the existence of two glacial races of rainbow smelt *Osmerus mordax* and their reproductive isolation in the St. Lawrence River estuary (Quebec, Canada). Mol. Ecol. **6**: 73–83.

Billington, N., and Strange, R.M. 1995. Mitochondrial DNA analysis confirms the existence of a genetically divergent walleye population in northeastern Mississippi. Trans. Am. Fish. Soc. **124**: 770–776.

Billington, N., Barrette, R.J., and Hebert, P.D.N. 1992. Management implications of mitochondrial DNA variation in walleye stocks. N. Am. J. Fish. Manag. **12**: 276–284.

Bolsenga, S.J., and Herdendorf, C.E. 1993. Lake Erie and Lake St. Clair handbook. Wayne State University Press, Detroit, Mich.

Borer, S.O., Miller, L.M., and Kapuscinski, A. 1999. Microsatellites in walleye *Stizostedion vitreum*. Mol. Ecol. **8**: 335–346.

Cena, C.J., Morgan, G.E., Malette, M.D., and Heath, D.D. 2006. Inbreeding, outbreeding, and environmental effects on genetic diversity in 46 walleye (*Sander vitreus*) populations. Mol. Ecol. **15**: 303–320.

Colby, P.J., and Nepszy, S.J. 1981. Variation among stocks of walleye (*Stizostedion vitreum*): management implications. Can. J. Fish. Aquat. Sci. **38**: 1814–1831.

Eldridge, W.H., Bacigalupi, M.D., Adelman, I.R., Miller, L.M., and Kapuscinski, A.R. 2002. Determination of relative survival of two stocked walleye populations and resident natural-origin fish by microsatellite DNA parentage assignment. Can. J. Fish. Aquat. Sci. **59**: 282–290.

Evanno, G., Regnaut, S., and Goudet, J. 2005. Detecting the number of clusters of individuals using the software STRUCTURE: a simulation study. Mol. Ecol. **14**: 2611–2620.

© 2007 NRC Canada

Ferguson, R.G., and Derksen, A.J. 1971. Migrations of adult and juvenile walleyes (*Stizostedion vitreum vitreum*) in southern Lake Huron, Lake St. Clair, Lake Erie, and connecting waters. J. Fish. Res. Board Can. **28**: 1133–1142.

Ford, A.M., and Stepien, C.A. 2004. Genetic variation and spawning population structure in Lake Erie yellow perch, *Perca flavescens*: a comparison with a Maine population. *In* Proceedings of Percis III, the 3rd International Symposium on Percid Fishes, 20–24 July 2003, University of Wisconsin, Madison, Wisc. *Edited by* T.P. Barry and J.A. Malison. University of Wisconsin Sea Grant Institute, Madison. pp. 131–132.

Fraser, D.J., Lippe, C., and Bernatchez, L. 2004. Consequences of unequal population size, asymmetric gene flow and sex-biased dispersal on population structure in brook charr (*Salvelinus fontinalis*). Mol. Ecol. **13**: 67–80.

Gerlach, G., Schardt, U., Eckmann, R., and Meyer, A. 2001. Kin structured subpopulations in Eurasian perch (*Perca fluviatilis*). Heredity, **86**: 213–221.

Goodyear, C.S., Edsall, T.A., Dempsey, D.M., Moss, G.D., and Polanski, P.E. 1982. Atlas of spawning and nursery areas of Great Lakes fishes. Vols. 1–14; Vol. 8: Detroit River. US Fish and Wildlife Service, Washington, D.C. FWS/OBS-82/52.

Goudet, J. 1995. FSTAT (Version 1.2): a computer program to calculate *F*-statistics. J. Hered. **86**: 485–486.

Goudet, J., Raymond, M., de Meeus, T., and Rousset, F. 1996. Testing differentiation in diploid populations. Genetics, **144**: 1933–1940.

Guo, S.W., and Thompson, E.A. 1992. Performing the exact test of Hardy–Weinberg proportions for multiple alleles. Biometrics, **48**: 361–372.

Hanski, I. 1999. Habitat connectivity, habitat continuity, and metapopulations in dynamic landscapes. Oikos, **87**: 209–219

Hatch, R.W., Nepszy, S.J., Muth, K.M., and Baker, C.T. 1987. Dynamics of the recovery of the western Lake Erie walleye (*Stizostedion vitreum vitreum*) stock. Can. J. Fish. Aquat. Sci. **44**: 15–22.

Hedrick, P.W. 1999. Perspective: Highly variable loci and their interpretation in evolution and conservation. Evolution, **53**: 313–318.

Holcombe, T.L., Taylor, L.A., Reid, D.F., Warren, J.S., Vincent, P.A., and Herdendorf, C.E. 2003. Revised Lake Erie postglacial lake level history based on new detailed bathymetry. J. Gt. Lakes Res. **29**: 681–704.

Horrall, R.M. 1981. Behavioral stock-isolating mechanisms in Great Lakes fishes with special reference to homing and site imprinting. Can. J. Fish. Aquat. Sci. **38**: 1481–1496.

Hubbs, C.L., and Lagler, K.F. 2004. Fishes of the Great Lakes region. *Revised by* G.R. Smith. The University of Michigan Press, Ann Arbor, Mich.

Jennings, M.J., Claussen, J.E., and Philipp, D.P. 1996. Evidence for heritable preferences for spawning habitat between two walleye groups. Trans. Am. Fish. Soc. **125**: 978–982.

Jorgensen, H.B.H., Hansen, M.M., Bekkevold, D., Ruzzante, D.E., and Loeschcke, V. 2005. Marine landscapes and population genetic structure of herring (*Clupea harengus* L.) in the Baltic Sea. Mol. Ecol. **14**: 3219–3234.

Kawecki, T.J., and Holt, R.D. 2002. Evolutionary consequences of asymmetric dispersal rates. Am. Nat. **160**: 333–347.

Kennington, W.J., Gockel, J., and Partridge, L. 2003. Testing for asymmetrical gene flow in a *Drosophila melanogaster* body-size cline. Genetics, **165**: 667–673.

Kitchell, J.F., Johnson, M.G., Minns, C.K., Loftus, K.H., Greig, L., and Oliver, C.H. 1977. Percid habitat: the river analogy. J. Fish. Res. Board Can. **34**: 1936–1940.

Knight, R.L. 1997. Successful interagency rehabilitation of Lake Erie walleye. Fisheries, **22**: 16–17.

Koed, A., Mejlhelde, P., Balleby, K., and Aarestrup, K. 2000. Annual movement of adult pikeperch in a lowland river. J. Fish Biol. **57**: 1266–1279.

Koed, A., Balleby, K., and Mejlhelde, P. 2002. Migratory behavior of adult pikeperch (*Stizostedion lucioperca*) in a lowland river. Hydrobiologia, **483**: 175–184.

Manel, S., Schwartz, M.K., Luikart, G., and Taberlet, P. 2003. Landscape genetics: combining landscape ecology and population genetics. Trend. Ecol. Evol. **18**: 189–197.

Manni, F., Guerard, E., and Heyer, E. 2004. Geographic patterns of (genetic, morphologic, linguistic) variation: how barriers can be detected by "Monmonier's algorithm". Hum. Biol. **76**: 173–190.

Mantel, N. 1967. The detection of disease clustering and a generalized regression approach. Cancer Res. **27**: 209–220.

Murdoch, M.H., and Hebert, P.D.N. 1997. Mitochondrial DNA evidence of distinct glacial refugia for brown bullhead (*Ameiurus nebulosus*) in the Great Lakes. Can. J. Fish. Aquat. Sci. **54**: 1450–1460.

Nepszy, S.J. 1977. Changes in percid populations and species interactions in Lake Erie. J. Fish. Res. Board Can. **34**: 1861–1868.

Olson, D.E., and Scidmore, W.J. 1962. Homing behavior in spawning walleyes. Trans. Am. Fish. Soc. **91**: 355–561.

Olson, D.E., Schupp, D.H., and Macins, V. 1978. An hypothesis of homing behavior of walleyes as related to observed patterns of passive and active movement. *In* Selected coldwater fishes of North America. *Edited by* R.L. Kendall. Am. Fish. Soc. Special Publ. 11. Bethesda, Md. pp. 52–57.

O'Reilly, P.T., Canino, M.F., Bailey, K.M., and Bentzen, P. 2004. Inverse relationship between F_{ST} and microsatellite polymorphism in the marine fish walleye pollock (*Theragra chalcogramma*): implications for resolving weak population structure. Mol. Ecol. **13**: 1799–1814.

Pritchard, J.K., Stephens, M., and Donelly, P. 2000. Inference of population structure using multilocus genotype data. Genetics, **155**: 945–959.

Pulliam, H.R. 1988. Sources, sinks and population regulation. Am. Nat. **132**: 652–661.

Raymond, M., and Rousset, F. 1995. GENEPOP. Version 1.2. Population genetics software for exact tests and ecumenicism. J. Hered. **86**: 248–249.

Regier, H.A., Applegate, V.C., and Ryder, R.A. 1969. The ecology and management of the walleye in western Lake Erie. Great Lakes Fish. Comm. Tech. Rep. **15**: 1–101.

Rice, W.R. 1989. Analyzing tables of statistical tests. Evolution, **43**: 223–225.

Rousset, F. 1997. Genetic differentiation and estimation of gene flow from *F*-statistics under isolation by distance. Genetics, **145**: 1219–1228.

Schneider, J.C., and Leach, J.H. 1977. Walleye (*Stizostedion vitreum vitreum*) fluctuations in the Great Lakes and possible causes, 1800–1975. J. Fish. Res. Board Can. **34**: 1878–1889.

Scott, W.B., and Crossman, E.J. 1973. Freshwater fishes of Canada. Bull. Fish. Res. Board Can. Bull. 184. pp. 767–774.

Slatkin, M. 1985. Rare alleles as indicators of gene flow. Evolution, **39**: 53–65.

Stepien, C.A. 1995. Population genetic divergence and geographic patterns from DNA sequences: examples from marine and freshwater fishes. *In* Symposium 17: Evolution and the Aquatic Ecosystem: Defining Unique Units in Group Conservation, Monterey, California, May 1994. *Edited by* J. Neilson. American Fisheries Society, Bethesda, Md. pp. 263–287.

© 2007 NRC Canada

Stepien, C.A., and Faber, J.E. 1998. Population genetic structure, phylogeography and spawning philopatry in walleye (*Stizostedion vitreum*) from mitochondrial DNA control region sequences. Mol. Ecol. **7**: 1757–1769.

Stepien, C.A., Taylor, C.D., and Einhouse, D.W. 2004. An analysis of genetic risk to a native spawning stock of walleye *Sander vitreus* (*Stizostedion vitreum*) due to stocking in Cattaraugus Creek. *In* Proceedings of Percis III, the 3rd International Symposium on Percid Fishes, 20–24 July 2003, University of Wisconsin, Madison, Wisc. *Edited by* T.P. Barry and J.A. Malison. University of Wisconsin Sea Grant Institute, Madison. pp. 93–94.

Stepien, C.A., Murphy, D., and Strange, R.M. 2007. Broad- to fine-scale genetic patterning in smallmouth bass *Micropterus dolomieu* across the Laurentian Great Lakes and beyond: an interplay of behavior and geography. Mol. Ecol. **16**. In press.

Stone, F.L. 1948. A study of the taxonomy of the blue and yellow pikeperches (*Stizostedion*) of Lake Erie and Lake Ontario. Ph.D. dissertation, University of Rochester, N.Y.

Strange, R.M. 1999. Historical biogeography, ecology, and fish distributions: conceptual issues for establishing IBI criteria. *In* Assessing the sustainability and biological integrity of water resources using fish communities. *Edited by* T.P. Simon. CRC Press, Boca Raton, Fla. pp. 65–78.

Strange, R.M., and Burr, B.M. 1997. Intraspecific phylogeography of North American highland fishes: a test of the Pleistocene vicariance hypothesis. Evolution, **51**: 885–897.

Thomas, M., Einhouse, D., Isermann, D., Kayle, K., Turner, M., Vandergoot, C., Belore, M., Cook, A., Johnson, T., Ryan, P., Wright, E., and Kenyon, R. 2005. Report for 2004 by the Lake Erie Walleye Task Group as presented to the Standing Technical Committee, Lake Erie Committee, Great Lakes Fishery Commission, Niagara Falls, Ont.

Todd, T.N., and Haas, R.C. 1993. Genetic and tagging evidence for movement of walleyes between Lake Erie and Lake St. Clair. J. Gt. Lakes Res. **19**: 445–452.

van Oosterhout, C., Hutchinson, W.F., Wills, D.P.M., and Shipley, P. 2004. MICRO-CHECKER: software for identifying and correcting genotyping errors in microsatellite data. Mol. Ecol. Notes, **4**: 535–538.

van Oosterhout, C., Weetman, D., and Hutchinson, W.F. 2006. Estimation and adjustment of microsatellite null alleles in nonequilibrium populations. Mol. Ecol. Notes, **6**: 255–256.

Weir, B.S., and Cockerham, C.C. 1984. Estimating *F*-statistics for the analysis of population structure. Evolution, **38**: 1358–1370.

Wiley, E.O., and Mayden, R.L. 1985. Species and speciation in phylogenetic systematics, with examples from the North American fish fauna. Ann. Missouri Bot. Gard. **72**: 596–635.

Wirth, T., Saint-Laurent, R., and Bernatchez, L. 1999. Isolation and characterization of microsatellite loci in the walleye (*Stizostedion vitreum*), and cross species amplification within the family Percidae. Mol. Ecol. **8**: 1957–1969.

Wolfert, D.R. 1963. The movements of walleyes tagged as yearlings from the eastern and western basins of Lake Erie. Trans. Am. Fish. Soc. **92**: 414–420.

Wright, S. 1943. Isolation by distance. Genetics, **28**: 139–156.

Wright, S. 1978. Evolution and the genetics of populations. Vol. 4. Variability within and among populations. University of Chicago Press, Chicago, Ill.

Zardoya, R., Castilho, R., Grande, C., Favre-Krey, L., Caetano, S., Marcato, S., Krey, G., and Patarnello, T. 2004. Differential population structuring of two closely related fish species, the mackerel (*Scomber scombrus*) and the cub mackerel (*Scomber japonicus*), in the Mediterranean Sea. Mol. Ecol. **13**: 1785–1798.

© 2007 NRC Canada

Thermal effects on behavior of juvenile walleye pollock (*Theragra chalcogramma*): implications for energetics and food web models

Thomas P. Hurst

Abstract: The behavioral responses of fishes to temperature variation have received little attention despite their direct implications to bioenergetics-based models of production and encounter-based models of food web dynamics. Behavioral characteristics of juvenile walleye pollock (*Theragra chalcogramma*), a pelagic marine zooplanktivore, were examined between 2 and 9 °C in large arenas. Routine swim speed, path sinuosity, and schooling cohesiveness of fish in small groups were described from overhead video observations. In a separate experiment, maximum swimming speeds were measured in a recirculating flume. Routine and maximum swimming speeds had contrasting responses to temperature demonstrating a behavioral rather than physiological regulation of activity level. Routine swim speed was 48% faster at 2 °C than at 9 °C. This result is inconsistent with the assumption of a constant activity multiplier for metabolism incorporated into most bioenergetics models of fish growth. Increased swim speed, along with the reduced path sinuosity observed at low temperatures, may reflect kinetic aspects of habitat selection. Group cohesion increased at low temperatures, with nearest neighbours averaging 32% closer at 2 °C than at 9 °C. These results demonstrate that representative models of energy flow through marine food webs depend on an improved understanding of the behavioral as well as physiological responses of fishes to thermal variation.

Résumé : On s'est peu intéressé aux réactions comportementales des poissons à la variation de température malgré leurs conséquences directes sur les modèles de production fondés sur la bioénergétique et sur les modèles de la dynamique des réseaux alimentaires basés sur les rencontres. Les caractéristiques du comportement de jeunes goberges de l'Alaska (*Theragra chalcogramma*), des poissons marins planctonophages pélagiques, ont pu être étudiées dans des grandes arènes entre 2 et 9 °C. Des observations vidéo en surplomb ont servi à décrire la vitesse de nage de routine, la sinuosité des trajets et la cohésion des bancs chez de petits groupes de poissons. Une expérience différente a permis de mesurer les vitesses maximales de nage dans un chenal à recirculation d'eau. La vitesse de nage de routine et la vitesse maximale réagissent différemment à la température, ce qui démontre qu'il existe une régulation comportementale du niveau d'activité plutôt qu'une régulation physiologique. La vitesse de nage de routine est de 48 % plus rapide à 2 °C qu'à 9 °C. Ce résultat ne s'accorde pas avec la présupposition de l'existence d'un multiplicateur constant d'activité pour le métabolisme que l'on incorpore dans la plupart des modèles bioénergétiques de croissance des poissons. La vitesse de nage accrue, de même que la sinuosité réduite des trajets, que l'on observe à températures basses, peuvent refléter les aspects cinétiques de la sélection de l'habitat. La cohésion des groupes augmente à basses températures et les voisins les plus proches sont en moyenne de 32 % plus près à 2 °C qu'à 9 °C. Ces résultats montrent que les modèles représentatifs du flux énergétique dans les réseaux alimentaires marins dépendent d'une compréhension améliorée des réactions comportementales en plus des réactions physiologiques des poissons à la variation thermique.

[Traduit par la Rédaction]

Introduction

All organisms respond to changes in the environment with changes in behavior. Well-understood examples include functional responses to changes in prey availability and reducing risky foraging behavior in the presence of predators (Milinski 1993). Temperature represents the most pervasive aspect of the environment affecting ectotherms and varies markedly on a variety of spatial and temporal scales. However, our understanding of the behavioral responses of marine fishes to temperature variation lags well behind our understanding of physiological responses. This has occurred despite the fact that behavior represents the link that allows (or prevents) physiological processes from scaling up to population- and ecosystem-level responses (Railsback 2001; Ovadia and Schmitz 2002).

While behavioral responses to thermal variation have not been thoroughly described for most fish species, routine (also called "volitional" or "voluntary") swimming speeds have been predicted to respond according to one of three general patterns. Swim speeds (and other measures of activity level) could parallel physiological processes, increasing

Received 23 May 2006. Accepted 9 November 2006. Published on the NRC Research Press Web site at http://cjfas.nrc.ca on 30 March 2007.
J19334

T.P. Hurst. Fisheries Behavioral Ecology Program, Alaska Fisheries Science Center, National Marine Fisheries Service, NOAA, Hatfield Marine Science Center, 2030 S. Marine Science Drive, Newport, OR 97365, USA (e-mail: thomas.hurst@noaa.gov).

 doi:10.1139/F07-025 © 2007 NRC Canada

with temperature within tolerance limits (Bennett 1990); as a component of behavioral thermoregulation, swim speed could increase with deviation from the preferred temperature (orthokenesis: Fraenkel and Gunn 1961); or fish could compensate for temperature variation, maintaining constant swim speeds across temperatures (Precht 1958). There is some support in the literature for each of these responses suggesting that such responses are specific to species or life history guild. Furthermore, largemouth bass (*Micropterus salmoides*) exhibit a combination of responses with activity levels remaining constant across a broad range of temperatures but declining at the lowest temperatures encountered (Lemons and Crawshaw 1985).

In addition to effects on swim speed, temperature may provide an ultimate or proximate cue for changes in other aspects of fish behavior. Effective behavioral thermoregulation in coastal or open oceans is thought to require responses in travel path (klinokenesis) as well as velocity (Fraenkel and Gunn 1961; Reynolds 1977; Neill 1979). Temperature-dependent shifts in the diel periodicity of activity in species using sheltering and crypsis as primary antipredator strategies appear to be linked to low foraging requirements at low temperatures (Fraser et al. 1993; Hurst and Duffy 2005). Little work has been done on the behavioral responses of continuously swimming pelagic fishes that use schooling as the primary antipredator tactic. Two studies examining thermal effects on schooling behavior (Griffith 1978; Weetman et al. 1998) found reduced group cohesion in threadfin shad (*Dorosoma petenense*) and guppy (*Poecilia reticulata*) schools at lower temperatures.

Walleye pollock (*Theragra chalcogramma*) are an integral component of North Pacific and Bering Sea food webs and support major regional fisheries (Livingston 1993). Juveniles inhabit the surface and subsurface waters of the Gulf of Alaska and Bering Sea where they encounter a broad range of temperatures. In addition to wintertime exposure to temperatures below 2 °C, the summertime persistence of a cold intermediate layer (~2 °C, surface waters up to 10 °C) over large portions of the eastern Bering Sea shelf creates significant spatial variation in temperature of juvenile walleye pollock habitat (Luchin et al. 1999). Walleye pollock can feed and maintain positive growth at temperatures as low as 2 °C (Smith et al. 1986), with maximum growth and consumption rates of juveniles estimated to occur near 10 °C (Ciannelli et al. 1998). Individuals can select preferred temperatures in experimental vertical gradients, with the preferred temperature varying with nutritional state (Sogard and Olla 1996). In addition, juveniles have considerably plastic patterns in schooling behavior, varying swim velocity and group cohesiveness in response to nutritional state, predator presence, and prey patchiness (Ryer and Olla 1995; Sogard and Olla 1996, 1997). Laboratory observations of the distributional and behavioral responses of walleye pollock to biotic and abiotic factors have been found to be robust when compared with field observations, even when operational scales differ (Olla et al. 1995, 1996). Hence, walleye pollock provide a useful model species for examination of thermal impacts on pelagic fishes and marine food webs.

In this paper, I explore the effects of temperature on both the capacity for and expression of swimming behavior of juvenile walleye pollock. Coordinated changes in swim speed, swim path, and schooling cohesiveness are described by observing free-swimming groups of temperature-acclimated fish in large circular arenas. The thermal dependence of maximum swimming speed is used to discriminate swimming changes due to behavioral regulation versus physiological constraints. I describe how these behavioral responses conflict with our current understanding of fish behavior as incorporated into encounter- and bioenergetics-based models of ecosystems.

Materials and methods

Capture and holding

Age-0 walleye pollock, 10–20 mm total length (TL), were captured from nearshore waters of Puget Sound at Port Townsend, Washington, with a lighted lift net suspended from a dock. Fish were held for at least 24 h in ambient seawater prior to shipment to the National Marine Fisheries Service laboratory in Newport, Oregon. Prior to use in the experiment, fish were reared in groups in 61 or 122 cm diameter round tanks. All tanks were maintained at 9–10 °C with a photoperiod of 12 h light : 12 h dark. Initially, fish were fed daily a combination of thawed *Artemia* sp. and commercially available food. Later, feeding was reduced to three times per week and food changed to a gelatinized combination of squid, krill, herring, commercial food, amino acid supplements, and vitamins.

Routine swimming characteristics

Routine swimming characteristics (speed, path sinuosity, and group cohesiveness) of juvenile walleye pollock in small groups (n = 6 fish per group) were examined at three temperatures, 2, 5, and 9 °C, representing most of the range encountered by juveniles of this species in the Bering Sea and Gulf of Alaska (Bailey et al. 1999). To minimize tank effects on fish behavior, fish were tested at the smallest body sizes (<100 mm) in the largest arenas (2.9 m diameter) that still permitted consistent discrimination in video observations.

Fish were transferred to acclimation tanks (1 m diameter) and temperatures adjusted at a rate of 1 °C·day^{-1} to achieve target treatment temperatures. Groups of >50 walleye pollock were acclimated to test temperatures for at least 2 months prior to testing. Sizes of fish used in trials averaged 82.4 mm TL, ranging from 63 to 103 mm, with fish in 2 °C trials averaging 7.2 mm shorter than fish in the 5 and 9 °C treatments owing to differential growth during the acclimation period (analysis of variance (ANOVA), $F_{[2,249]}$ = 22.22, $p < 0.05$). For each trial, groups of six similarly sized fish (within group average length CV = 5.0) were captured from acclimation tanks, measured, and introduced into the experimental arenas. Fish were acclimated to the experimental arena for approximately 40 h prior to making observations. Fish were fed thawed *Artemia* sp. once while in experimental arenas at 1600 on the day prior to experimental observations (14.5 h prior to making observations). Lights in the experimental arenas were off from 1800 to 0600. Experimental observations were made between 0630 and 0800 to eliminate any potential disturbance from routine laboratory activities.

Water depth in the 2.9 m diameter experimental arenas was restricted to 30 cm such that activity was largely con-

© 2007 NRC Canada

fined to the *X–Y* plane and could be described from a single overhead camera. Two arenas were maintained at each of the three test temperatures, and temperature treatments were run synchronously. Fourteen trials were conducted at each test temperature. Individual fish were reused within temperature treatments in the experiment, with at least 1 week between observations, and group membership was not maintained across trials. There were no temporal trends in any metric (i.e., replicate order not a significant factor in any analyses of swim speed, path, or group cohesiveness) indicative of biases associated with multiple observations of fish in the experiments.

The routine swimming speed of juvenile walleye pollock was described by digitizing the path of randomly chosen fish for 1 min at 5 min intervals throughout the observation period. The only criteria for selection of fish to be tracked was that the fish not be temporarily separated from the group such that the speed of the individual generally reflected that of the group. The average of 20 measurements of swimming speed during a trial was used as the level of observation in the analyses. Routine swimming speed ($mm \cdot s^{-1}$) was analyzed with analysis of covariance (ANCOVA) with temperature as the main effect and mean length of fish in the group as the covariate.

Path sinuosity was described by the area of the minimum convex polygon that contained an entire 1 min swim path. High path sinuosity (or high turning rate) is reflected in small polygon areas and straighter paths in larger polygon areas. Average swim path polygons during the 1 min observation periods occupied less than 25% of the total tank area, indicating that changes in path polygon areas reflected changes in path sinuosity, unconstrained by tank size. Owing to the inherent increase in area use with distance traveled in the 1 min sample, analysis of polygon area between temperature treatments was conducted with ANCOVA with path distance as the covariate. Path distance and polygon area were log-transformed prior to analysis. Trial replicate (n = 14) was treated as a random factor nested within temperature treatment.

The effect of temperature on schooling cohesiveness of walleye pollock was described through changes in nearest neighbor distances among fish in the group. Nearest neighbor distances were measured for each fish in the group from still frames at 5 min intervals between 0700 and 0800 (n = 13 per trial). Mean nearest neighbor values were averaged for each trial and compared between temperature treatments with ANCOVA. The potential for body size effects on nearest neighbor distances was evaluated by inclusion of mean fish length in each trial group as a covariate.

Maximum swimming speeds

Maximum swimming speeds (U_{crit}) of juvenile walleye pollock were tested at three temperatures, 2, 5, and 9 °C. Fish were transferred to temperature acclimation tanks (1 m diameter) and temperatures adjusted to test temperatures at a rate of 1 °C·day^{-1}. Fish were acclimated to test temperature for at least 2 months prior to testing. During acclimation, feeding was reduced to two times per week to reduce growth differences between temperatures. Fish were offered food 22–26 h prior to measurement of swimming capacity. At least 27 fish were tested at each temperature with individual fish used only once in swimming trials. Tested fish ranged from 67 to 143 mm TL and body size did not vary significantly among temperature treatments (ANOVA, $F_{[2,80]}$ = 0.249, p = 0.97).

The test flume consisted of a header tank (1000 L) that fed directly into the test chambers. Three 5-hp, 1750-rpm pumps returned water from the water bath to the header tank at a maximum rate of 95 $L \cdot s^{-1}$. A baffle in the header tank prevented pump turbulence from being introduced into test chambers. A 38 cm cylinder containing three 15 cm diameter test chambers was attached directly to the header tank. The test chambers were 115 cm long and had 6.4 mm mesh nylon netting at the upstream and downstream ends. Water temperature in the flume was maintained within 0.1 °C of test temperature by recirculating water through a glycol-supplied heat exchanger. Flow velocities were continuously measured 5 cm downstream of swimming chambers with an electromagnetic flowmeter (Marsh-McBirney Flo-Mate model 2000). Velocities in the three parallel swimming chambers were generally within 10 $mm \cdot s^{-1}$ and were never observed to differ by more than 20 $mm \cdot s^{-1}$.

For each trial, individual fish were captured from acclimation tanks, measured (TL), and introduced into the swimming chambers. Fish were acclimated to the swimming chambers for 15 min at a flow velocity of 50 $mm \cdot s^{-1}$. Flow velocities were then increased by 50 $mm \cdot s^{-1}$ at 10 min intervals until the fish became exhausted. When exhausted, the downstream barrier was removed and the fish captured from the swimming chamber.

Maximum swimming velocities were calculated according to the equation $U_{crit} = V + vT/t$, where V is the highest speed maintained for a full time interval, v is the velocity increment (50 $mm \cdot s^{-1}$), t is the time interval (10 min), and T is the amount of time spent at the fatigue velocity (Brett 1964). The U_{crit} velocites were not corrected for blocking effects, as the cross-sectional area of the fish was less than 2% of the swimming chamber. Differences in critical swimming velocities between temperature treatments were analyzed using ANCOVA with temperature as the main effect and body length as the covariate.

Results

Routine swimming speed

Routine swimming speed of juvenile walleye pollock in small groups was a function of both water temperature and body size (Fig. 1). Swimming speeds increased with mean body length of fish in the group (covariate effect, $F_{[1,38]}$ = 23.21, $p < 0.001$). Routine swimming speeds decreased with increasing temperature between 2 and 9 °C (ANCOVA, $F_{[2,38]}$ = 5.56, p = 0.008). For a common fish length of 80 mm TL, routine swimming speed decreased 32% from 82.4 $mm \cdot s^{-1}$ at 2 °C to 55.5 $mm \cdot s^{-1}$ at 9 °C. There was a nonsignificant interaction effect between fish length and temperature on swim speed (homogeneity of slopes, $F_{[2,36]}$ = 2.70, p = 0.08). There was also a trend for increased variation among trials at low temperatures (homogeneity of variances, $F_{[2,39]}$ = 2.91, p = 0.06).

© 2007 NRC Canada

Fig. 1. Routine swimming speeds of juvenile walleye pollock (*Theragra chalcogramma*) as a function of body size and temperature. Each point is the mean (±SE) of 20 measurements of swim speed over 1 min of individuals randomly selected from the group at 5 min intervals plotted against the mean length of fish in the group. Circles and dotted line, 2 °C; triangles and dashed line, 5 °C; squares and solid line, 9 °C. Regression lines shown are calculated separately for each temperature, but slopes did not differ significantly.

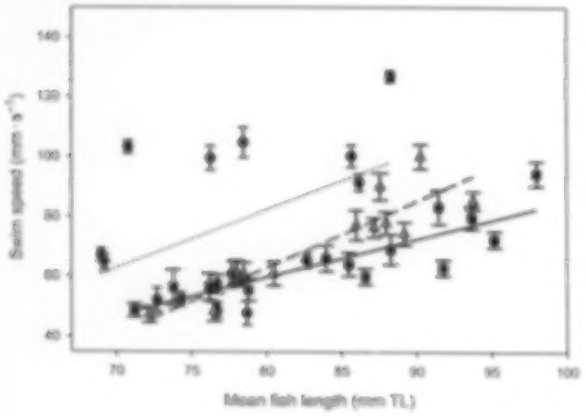

Fig. 2. Mean area of polygon occupied by juvenile walleye pollock (*Theragra chalcogramma*) during 1 min of routine swimming. Each point is the adjusted mean (±SE) polygon area measured during 14 trials corrected to a standard path length with ANCOVA across temperatures.

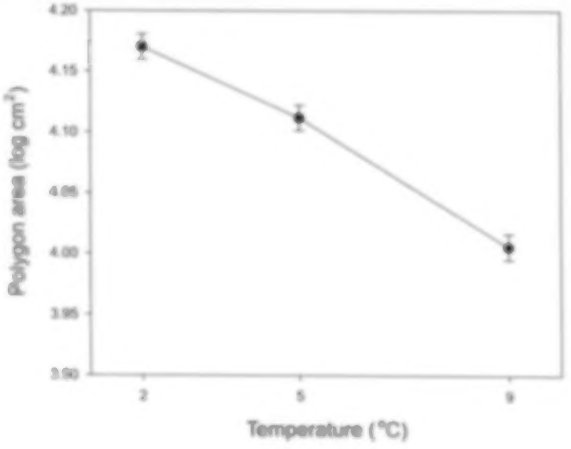

Fig. 3. Nearest neighbor distances of juvenile walleye pollock (*Theragra chalcogramma*) in six-member groups. Points represent the mean (±SE) of average measures within a trial. Twelve measurement points per trial, 14 trials per temperature.

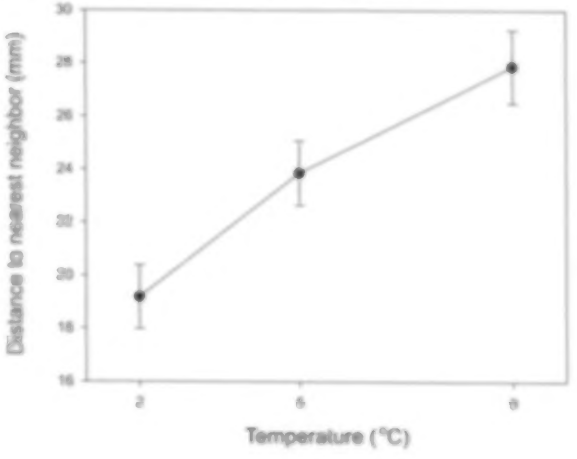

Path sinuosity

Swim path sinuosity of juvenile walleye pollock increased with water temperature. The area of the smallest polygon that contained a 1 min swim path decreased with increasing temperature (ANCOVA with distance traveled as covariate, $F_{[2,39]} = 7.69$, $p = 0.002$) (Fig. 2). Within temperature treatment, there was also a significant effect of replicate trial (ANCOVA, $F_{[39,797]} = 7.94$, $p < 0.001$). This variation among trials within temperature treatment was not correlated with the size of fish in the trial (ANCOVA, $F_{[1,38]} = 0.6468$, $p = 0.426$).

Schooling behavior

Group cohesiveness in the six-member walleye pollock groups was higher at the lower temperatures tested. Distances to nearest neighbors were on average 32% lower at 2 °C than at 9 °C (18.7 versus 27.3 mm; ANOVA $F_{[2,39]} = 36.08$, $p < 0.001$) (Fig. 3). In addition to the temperature effect, there was a significant effect of trial replicate within temperature (ANOVA, $F_{[39,504]} = 6.75$, $p < 0.001$). There was a nonsignificant trend toward groups with larger members maintaining closer neighbors (test of length as a covariate, $F_{[1,38]} = 2.99$, $p = 0.092$) and there was no interactive effect of fish size with temperature on nearest neighbor distances (homogeneity of slopes, $F_{[2,36]} = 0.90$, $p = 0.414$).

Maximum swimming speed

Water temperature had a significant positive effect ($p < 0.001$) on U_{crit} values of juvenile walleye pollock (Fig. 4). Maximum swimming speed increased with body length at all temperatures ($p < 0.001$). For a given size of 100 mm TL, maximum swim speed increased from 259 mm·s^{-1} at 2 °C to 349 mm·s^{-1} at 9 °C. There was no significant interaction effect between temperature and body size on swimming speed ($p = 0.390$).

Discussion

Juvenile walleye pollock responded to variation in water temperature with changes in characteristics of their routine swimming behavior. These responses reflect life history adaptation to a variable environment in which temperature directly affects physiological processes and serves as a proximate cue for changes in other environmental factors (Reynolds 1977; Komers 1997). Walleye pollock increased routine swim speed, reduced path sinuosity, and reduced the distance among fish in a group at lower temperatures. In ad-

© 2007 NRC Canada

Fig. 4. Maximum (critical) swimming speeds (U_{crit}) of juvenile walleye pollock (*Theragra chalcogramma*) measured in a recirculating swimming flume. Points are U_{crit} values of individual fish plotted against fish length. Circles and dotted line, 2 °C; triangles and dashed line, 5 °C; squares and solid line, 9 °C. Regression lines shown are calculated separately for each temperature, but slopes did not differ significantly.

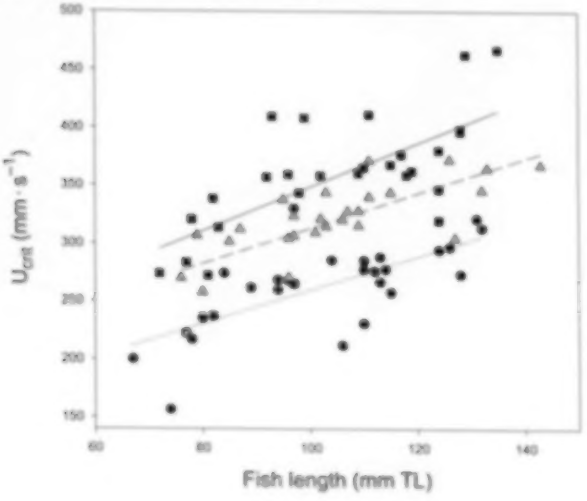

dition to reflecting mechanisms of habitat selection, behavioral characteristics play major roles in determining an organism's encounter rate with predators and prey and may affect the fate of an individual following a predator encounter. Hence, behavioral responses need be incorporated into models of fish energetics as well as food web dynamics.

The experiments presented here were conducted to isolate the effects of temperature on behavioral traits (routine speed, path, and group cohesion) known to also vary in response to factors such as hunger level and predator presence (Johansson and Leonardsson 1998). Several studies have documented such effects in walleye pollock (Sogard and Olla 1997; Ryer and Olla 1998). In this experiment, routine swimming characteristics were examined in fish that were not actively foraging. Fish had been fed 14.5 h prior to making observations at all temperatures to minimize the differences in hunger level across treatments. However, it remains possible that differences among treatments attributed to temperature variation could be due to slight differences in nutritional state. A set of preliminary observations made at 2 and 10 °C on the fourth day postfeeding produced results similar to those reported here (T.P. Hurst, unpublished data), suggesting a generality of the temperature response.

Scope for activity

Routine volitional swim speed and maximum swimming performance exhibited markedly contrasting patterns in thermal sensitivity in juvenile walleye pollock. The increase in maximum swimming speed with temperature in juvenile walleye pollock is similar to the pattern observed in other ectotherms (Bennett 1990; Hurst and Conover 2001; O'Steen and Bennett 2003). This increased performance at higher temperatures is also consistent with other physiological processes (growth, metabolism, and digestion) in walleye pollock (Smith et al. 1986, 1989; Sogard and Olla 2000). Such thermal dependencies of physiological processes demonstrate that the contrasting pattern observed in routine swim speeds of juvenile pollock is not due to a physiological constraint. Rather, the changes in volitional swimming speed reflect a behavioral regulation of activity levels in the face of changing physiological capacity (O'Steen and Bennett 2003).

Fig. 5. Scope for activity of an 80 mm juvenile walleye pollock (*Theragra chalcogramma*) as a function of temperature. Scope for activity is expressed as the difference between maximum swimming speed measured in a recirculating flume and routine swim speed measured in 2.9 m diameter arenas.

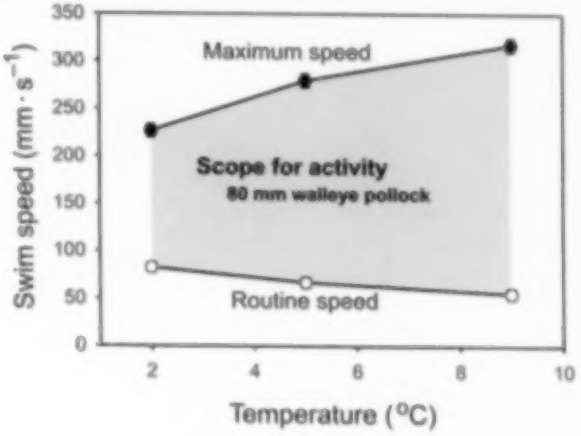

Scope for activity represents the degree to which an animal may increase activity levels beyond those routinely expressed or the difference between maximum physiological performance and routine activity (Irschick and Garland 2001). The scope for activity increased markedly with temperature in juvenile walleye pollock owing to the differences in thermal sensitivity of routine and maximum swimming speed (U_{crit}) (Fig. 5). Based on the laboratory experiments presented here, routine swimming activity (of an 80 mm TL walleye pollock) comprised 36% of maximum capacity at 2 °C but only 17% of maximum at 9 °C.

Swim speed and path

Observations of the effects of temperature on routine activity levels of fish vary markedly across species (Lemons and Crawshaw 1985; Hurst and Duffy 2005). Spontaneous activity of largemouth bass was constant across a wide range of temperatures but was reduced at the lowest temperatures encountered (Lemons and Crawshaw 1985). Hurst and Duffy (2005) observed a decrease in daytime, but not nighttime, activity of northern rock sole (*Lepidopsetta polyxystra*). The complexity and diversity of such responses demonstrate that activity does not routinely respond to thermal variation in parallel with physiological processes. Responses are species specific and need be evaluated and interpreted in a broader life history context (O'Steen and Bennett 2003).

In several species, marked increases in swimming speed were observed in response to declining temperatures and interpreted as an acute avoidance response (Sogard and Olla

© 2007 NRC Canada

1998). It does not appear that the higher swimming speeds of walleye pollock at 2 °C reflect such an acute avoidance response. Exposure to temperatures below 2 °C is a common aspect of the life history of walleye pollock and fish are able to maintain feeding and growth at these temperatures (Smith et al. 1986). In the present experiment, fish had been acclimated to test temperatures for at least 2 months with no ill effects. In fact, when exposed to rapid reductions in temperature (from 12 to 3 °C in 4 h), walleye pollock responded with a decrease in activity level (Sogard and Olla 1998).

Rather, the higher volitional swimming speed at lower temperatures may reflect an orthokinetic component (increased speed with departure from preferred conditions) of behavioral thermoregulation or a more general search strategy for thermally optimal habitats (Magnuson et al. 1979; Neill 1979). Reynolds and Casterlin (1979) referred to an "activity well" at the preferred temperature with activity levels increasing with increasing temperature deviation (Humston et al. 2000). Higher swimming speeds increase the probability of detecting thermal gradients in the environment. Correspondingly, the variability in swim paths observed in walleye pollock is consistent with a klinokinetic response (increased turning rates in preferred conditions) to temperature variation (Humston et al. 2000). Swim path sinuosity decreased significantly with temperature, further enhancing the probability of detection of positive thermal gradients (Bell 1991). In conjunction, the associated changes in speed and path may be representative of a gradient between an extensive searching pattern at low temperatures (for thermal cues) and an intensive searching pattern at warmer temperatures (for prey resources).

The interpretation of the swim path and speed changes in walleye pollock as components of behavioral thermoregulation assumes that the preferred temperature for this life stage is near or above 9 °C. Final preferendum experiments have not been performed, but laboratory experiments demonstrate ability for behavioral thermoregulation in walleye pollock. When placed in experimental gradients, age-0 walleye pollock selected warmer surface waters (8–9 °C) unless maintained on submaintenance rations (Sogard and Olla 1996) and age-2 walleye pollock selected temperatures above 10° independent of feeding history (Duffy-Anderson et al. 2003). In the wild, juvenile walleye pollock generally remain above the thermocline when foraging conditions are sufficient (Bailey 1989; Swartzman et al. 1994). Distribution relative to horizontal thermal gradients is less clear for juvenile walleye pollock because of their widespread distribution and the interactions with other physical and biological features but appears to be generally consistent with a preference for warmer waters. While age-0 walleye pollock have been observed at temperatures below 2 °C even in summer (Tang et al. 1996), they were most abundant in warmer waters of the western Gulf of Alaska (>8 °C at 50 m: Wilson et al. 1996) and the Aleutian Basin (7–9 °C surface and >4 °C at 100 m: Tang et al. 1996).

Schooling behavior

In both captivity and the wild, juvenile walleye pollock form dense, but not highly polarized, schools. The organization of fish into schools or shoals is considered the primary mechanism of predator defense in small pelagic fishes, potentially reducing both the rates of predator encounter and risk of capture following an encounter (Pitcher and Parrish 1993). Schooling may also allow fish to forage more efficiently on patchily distributed resources but resulting in increased competition when prey patches are encountered (Eggers 1976; Robinson 1995). School cohesiveness has been demonstrated to vary in response to the relative pressures imposed by predation risk and hunger level (Ryer and Olla 1995, 1998; Sogard and Olla 1997).

The use of small groups (six fish) in these experiments is consistent with previous experiments and is required by the need to locate and track individuals within the group. While nearest neighbor distances may also vary with group size, the experiments presented here successfully isolated the effect of temperature on group cohesiveness in walleye pollock. The marginal costs and benefits of changing interindividual distances within a school have not been explicitly measured but are generally assumed to reflect a trade-off between higher survival of predator encounters in tight schools and higher feeding rates in looser schools (Pitcher and Parrish 1993). The reduction in energetic requirements at low temperatures may allow walleye pollock to enhance antipredator strategies in an environment where the penalty in terms of foraging is minimal. Alternatively, or in addition, the reduction in nearest neighbor distances may also reflect the need to enhance the schooling aspect of predator evasion in a low-temperature environment where physiological constraints limit maximum escape velocities (Abrahams 2006) or predators are more abundant (Bailey 1989). In balancing the relative risks of starvation and predation, the schooling responses of pelagic walleye pollock to temperature variation may be functionally analogous to the change in diel rhythm of sheltering and cryptic species (Fraser et al. 1993; Hurst and Duffy 2005).

Implications for bioenergetics models

Applications of bioenergetics-based models have increased steadily in fisheries ecology. A long-recognized weakness of such models is the scarcity of detailed information on the behavior and activity levels of fish in situ (Boisclair and Leggett 1989; Rennie et al. 2005). In practice, the basal (or resting) metabolic rates of fish are measured in the laboratory and a multiplier is used to convert basal rates to rates of fish exhibiting "routine" activity levels in the wild. These "activity multipliers" are based on the investigator's intuition or determined through "solving" for the activity parameter to best fit the model to one set of laboratory or field data. The activity multiplier generally ranges from 1 to 3. Even in cases where metabolic rates have been measured across a range of swimming speeds, knowledge of swimming speeds exhibited in the wild, necessary for their application, is frequently lacking.

To date, most researchers have used a single activity multiplier across a the range of environmental conditions explored in a given application. However, several studies have demonstrated that behavioral responses to the environment conditions have important energetic consequences (Briggs and Post 1997; Hölker and Breckling 2002). A constant activity multiplier does not reflect a constant routine swim speed across temperatures. Rather, it implies that the energy expended on activity increases with temperature in parallel

© 2007 NRC Canada

with basal metabolic rate, implicitly assuming that routine swim speed increases with temperature (Briggs and Post 1997). For juvenile walleye pollock, Ciannelli et al. (1998, 2004) assumed an activity multiplier of 2.0, but the present experiments suggest the need for an activity multiplier that varies with water temperature.

A complete description of the bioenergetics of walleye pollock requires measurement of swimming metabolic rates as well as field validation of routine swim speeds. However, the available data are used to illustrate the significance of the observed patterns in routine swim speed on the activity multiplier (calculated for a 4.0 g, 80 mm TL walleye pollock). Temperature-dependent basal metabolic rates increase from 13.42 to 25.06 μg O_2·min^{-1} between 2 and 9 °C. To basal metabolic rates are added the costs of swimming to achieve routine metabolic rates. For this example, the cost of swimming is based on an assumption that the activity multiplier of 2.0 is accurate at 9 °C. Therefore, the isolated cost of routine swimming (i.e., excluding basal metabolism) at the observed speed of 93.1 mm·s^{-1} is 25.06 μg O_2·min^{-1}. Measurements of the cost of transport have indicated that the energy required to move a fish at a specific velocity is generally constant across temperatures (Rome 1986). Therefore, the cost of swimming at 93.1 mm·s^{-1} at 2 °C would similarly be 25.06 μg O_2·min^{-1}. However, routine swimming of this size walleye pollock was observed to be 48% faster at 2 °C than at 9 °C. Assuming that swimming costs increase linearly with velocity (likely to be true across speeds not requiring a gait change: Rome 1986), the isolated cost of activity for a walleye pollock at 2 °C would be 37.08 μg O_2·min^{-1}. When added to the basal metabolic rate, this results in a total metabolic rate of 50.51 μg O_2·min^{-1}, corresponding to an activity multiplier of 3.8. Hence, current models may be markedly underestimating the metabolic expenses and energetic requirements for growth of juvenile walleye pollock and species with similar thermal responses at low temperatures.

Implications for predator–prey encounter models

The behavioral responses of animals to environmental variation also have implications for food web models based on encounter rates between predators and their prey (Beauchamp et al. 1999). The increased routine swim velocity and straighter swim paths observed at low temperatures would be expected to increase encounter rates between walleye pollock and their predators. This effect would be most significant for encounters with slow-moving ambush predators (Petersen and DeAngelis 2000). Interestingly, while swim patterns would be expected to increase encounter rates at low temperatures, the observed schooling behaviors might serve to reduce encounters or increase survival following an encounter. Predator encounter rates reduce as the interfish distances and areal extent of the group decline. The reduction of distances between fish may also enhance the effectiveness of group responses when faced with an attack (Pitcher and Parrish 1993). The effect that environmental conditions, including temperature, have on the outcomes of predator–prey encounters is an area of study in need of clarification. Ultimately, a full understanding of the thermal effects on predator–prey encounter models requires incorporation of behavioral responses in both predator and prey and how they influence both encounters and outcomes.

Understanding individual and group behavior is a critical step in the approach of scaling up physiological factors to population- and community-level responses and one that has not received adequate attention. Juvenile walleye pollock responded to thermal variation by altering several aspects of routine behavior including swim speed, path, and school cohesiveness. These responses have major implications for our understanding of energy flows in the environment and do not conform to common assumptions based on physiological responses. It is unlikely that the thermal responses observed in juvenile walleye pollock, a semipelagic, subarctic zooplanktivore, will apply uniformly to species across a variety of thermal and foraging guilds. Future work should document species-specific behavioral responses that would allow the identification of broader patterns at work in structuring marine food webs.

Acknowledgments

I thank Mara Spencer, Scott Haines, and the Port Townsend Marine Science Center for assistance with capture and transport of walleye pollock. Michael Davis arranged collection and transportation permits and oversaw quarantine procedures. The swimming flume was designed and constructed by Michael Davis with assistance from Scott Haines. Michelle Ottmar, Sarah Hay, and Scott Haines assisted with video analyses. Lorenzo Ciannelli, Allan Stoner, Matt Wilson, and two anonymous reviewers provided helpful comments on earlier versions of this manuscript.

References

Abrahams, M. 2006. The physiology of antipredator behaviour: what you do with what you've got. *In* Behaviour and physiology of fish. *Edited by* K.A. Sloman, R.W. Wilson, and S. Balshine. Elsevier, San Diego, Calif. pp. 79–108.

Bailey, K.M. 1989. Interaction between the vertical distribution of juvenile walleye pollock *Theragra chalcogramma* in the eastern Bering Sea, and cannibalism. Mar. Ecol. Prog. Ser. **53**: 205–213.

Bailey, K.M., Powers, D.M., Quattro, J.M., Villa, G., Nishimura, A., Traynor, J.J., and Walters, G. 1999. Population ecology and structural dynamics of walleye pollock (*Theragra chalcogramma*). *In* Dynamics of the Bering Sea. *Edited by* T.R. Loughlin and K. Ohtani. University of Alaska Sea Grant, Fairbanks. pp. 581–650.

Beauchamp, D.A., Baldwin, C.M., Vogel, J.L., and Gubala, C.P. 1999. Estimating diel, depth-specific foraging opportunities with a visual encounter rate model for pelagic piscivores. Can. J. Fish. Aquat. Sci. **56**: 128–139.

Bell, W.J. 1991. Searching behaviour. Chapman and Hall, London, U.K.

Bennett, A.F. 1990. Thermal dependence of locomotor capacity. Am. J. Physiol. **259**: R253–R258.

Boisclair, D., and Leggett, W.C. 1989. The importance of activity in bioenergetics models applied to actively foraging fishes. Can. J. Fish. Aquat. Sci. **46**: 1859–1867.

Brett, J.R. 1964. The respiratory metabolism of and swimming performance of young sockeye salmon. J. Fish. Res. Board Can. **21**: 1183–1225.

© 2007 NRC Canada

Briggs, C.T., and Post, J.R. 1997. In situ activity metabolism of rainbow trout (*Oncorhynchus mykiss*): estimates obtained from telemetry of axial muscle electromyograms. Can. J. Fish. Aquat. Sci. **54**: 859–866.

Ciannelli, L., Brodeur, R.D., and Buckley, T.W. 1998. Development and application of a bioenergetics model for juvenile walleye pollock. J. Fish Biol. **52**: 879–898.

Ciannelli, L., Brodeur, R.D., and Napp, J.M. 2004. Foraging impact on zooplankton by age-0 walleye pollock (*Theragra chalcogramma*) around a front in the southeast Bering Sea. Mar. Biol. **144**: 515–526. doi: 10.1007/s00227-003-1215-4.

Duffy-Anderson, J.T., Ciannelli, L., Honkalehto, T., Bailey, K.M., Sogard, S.M., Springer, A.M., and Buckley, T.W. 2003. Distribution of age-1 and age-2 walleye pollock in the Gulf of Alaska and eastern Bering Sea: sources of variation and implications for higher trophic levels. *In* The Big Fish Bang: Proceedings of the 26th Annual Larval Fish Conference, 22–26 July 2002, Bergen, Norway. *Edited by* H.I. Browman and A.B. Skiftesvik. Institute of Marine Research, Bergen, Norway. pp. 381–394.

Eggers, D.M. 1976. Theoretical effect of schooling by planktivorous fish predators on rate of prey consumption. J. Theor. Biol. **33**: 1964–1971.

Fraenkel, G.S., and Gunn, D.L. 1961. The orientation of animals. Dover Publications, New York.

Fraser, N.H.C., Metcalfe, N.B., and Thorpe, J.E. 1993. Temperature-dependent switch between diurnal and nocturnal foraging in salmon. Proc. R. Soc. Lond. B Biol. Sci. **252**: 135–139.

Griffith, J.S. 1978. Effects of low temperature on the survival and behavior of threadfin shad, *Dorosoma petenese*. Trans. Am. Fish. Soc. **107**: 63–70.

Hölker, F., and Breckling, B. 2002. Influence of activity in a heterogeneous environment on the dynamics of fish growth: an individual-based model of roach. J. Fish Biol. **60**: 1170–1189. doi: 10.1006/jfbi.2002.1929.

Humston, R., Ault, J.S., Lutcavage, M., and Olson, D.B. 2000. Schooling and migration of large pelagic fishes relative to environmental cues. Fish. Oceanogr. **9**: 136–146.

Hurst, T.P., and Conover, D.O. 2001. Activity-related constraints on overwintering young-of-the-year striped bass (*Morone saxatilis*). Can. J. Zool. **79**: 129–136.

Hurst, T.P., and Duffy, T.A. 2005. Activity patterns in northern rock sole are mediated by temperature and feeding history. J. Exp. Mar. Biol. Ecol. **325**: 201–213. doi: 10.1016/j.jembe.2005.05.003.

Irschick, D.J., and Garland, T., Jr. 2001. Integrating function and ecology in studies of adaptation: investigations of locomotor capacity as a model system. Annu. Rev. Ecol. Syst. **32**: 367–396.

Johansson, F., and Leonardsson, K. 1998. Swimming speeds and activity levels of consumers at various resource and consumer densities under predation risk. Can. J. Zool. **76**: 76–82.

Komers, P.E. 1997. Behavioral plasticity in variable environments. Can. J. Zool. **75**: 161–169.

Lemons, D.E., and Crawshaw, L.I. 1985. Behavioral and metabolic adjustments to low temperatures in the largemouth bass (*Micropterus salmoides*). Physiol. Zool. **58**: 175–180.

Livingston, P.A. 1993. Importance of predation by groundfish, marine mammals and birds on walleye pollock *Theragra chalcogramma* and Pacific herring *Clupea pallasi* in the eastern Bering Sea. Mar. Ecol. Prog. Ser. **102**: 205–215.

Luchin, V.A., Menovshchikov, V.A., Lavrentiev, V.M., and Reed, R.K. 1999. Thermohaline structure and water masses in the Bering Sea. *In* Dynamics of the Bering Sea. *Edited by* T.R. Loughlin and K. Ohtani. University of Alaska Sea Grant, Fairbanks. pp. 61–91.

Magnuson, J.J., Crowder, L.B., and Medvick, P.A. 1979. Temperature as an ecological resource. Am. Zool. **19**: 331–343.

Milinski, M. 1993. Predation risk and feeding behaviour. *In* Behaviour of teleost fish. *Edited by* T.J. Pitcher. Chapman and Hall, London, UK. pp. 285–305.

Neill, W.H. 1979. Mechanisms of fish distribution in heterothermal environments. Am. Zool. **19**: 305–317.

Olla, B.L., Davis, M.W., Ryer, C.H., and Sogard, S.M. 1995. Behavioural responses of larval and juvenile walleye pollock (*Theragra chalcogramma*): possible mechanisms controlling distribution and recruitment. ICES Mar. Sci. Symp. **201**: 3–15.

Olla, B.L., Davis, M.W., Ryer, C.H., and Sogard, S.M. 1996. Behavioural determinants of distribution and survival in early stages of walleye pollock, *Theragra chalcogramma*: a synthesis of experimental studies. Fish. Oceanogr. **5**(Suppl. 1): 167–178.

O'Steen, S., and Bennett, A.F. 2003. Thermal acclimation effects differ between voluntary, maximum, and critical swimming velocities in two cyprinid fishes. Physiol. Biochem. Zool. **76**: 484–496.

Ovadia, O., and Schmitz, O.J. 2002. Linking individuals with ecosystems: experimentally identifying the relevant organizational scale for predicting trophic abundances. Proc. Natl. Acad. Sci. U.S.A. **99**: 12927–12931.

Petersen, J.H., and DeAngelis, D.L. 2000. Dynamics of prey moving through a predator field: a model of migrating juvenile salmon. Math. Biosci. **165**: 97–114.

Pitcher, T.J., and Parrish, J.K. 1993. Functions of shoaling behavior in teleosts. *In* Behaviour of teleost fish. *Edited by* T.J. Pitcher. Chapman and Hall, London, UK. pp. 363–439.

Precht, H. 1958. Concepts of the temperature adaptations of unchanging reaction systems of cold blooded animals. *In* Physiological adaptation. *Edited by* C.L. Prosser. American Physiological Society, Washington, D.C. pp. 50–78.

Railsback, S.F. 2001. Concepts from complex adaptive systems as a framework for individual based modelling. Ecol. Model. **139**: 47–62.

Rennie, M.D., Collins, N.C., Shuter, B.J., Rajotte, J.W., and Couture, P. 2005. A comparison of methods for estimating activity costs of wild fish populations: more active fish observed to grow slower. Can. J. Fish. Aquat. Sci. **62**: 767–780. doi: 10.1139/F05-052.

Reynolds, W.W. 1977. Temperature as a proximate factor in orientation behavior. J. Fish. Res. Board Can. **34**: 734–739.

Reynolds, W.W., and Casterlin, M.E. 1979. Effect of temperature on locomotor activity in the goldfish (*Carassius auratus*) and the bluegill (*Lepomis machrochirus*): presence of an 'activity well' in the region of the final preferendum. Hydrobiologia, **65**: 3–5.

Robinson, C.J. 1995. Food competition in a shoal of herring: the role of hunger. Mar. Behav. Physiol. **24**: 237–242.

Rome, L.C. 1986. The influence of temperature on muscle and locomotory performance. *In* Living in the cold: physiological and chemical adaptations. *Edited by* H.C. Heller, X.J. Mussachia, and L.C.H. Wang. Elsevier, New York. pp. 485–495.

Ryer, C.H., and Olla, B.L. 1995. Influences of food distribution on fish foraging behaviour. Anim. Behav. **49**: 411–418.

Ryer, C.H., and Olla, B.L. 1998. Shifting the balance between foraging and predator avoidance: the importance of food distribution for a schooling pelagic forager. Environ. Biol. Fishes, **52**: 467–475.

Smith, R.L., Paul, A.J., and Paul, J.M. 1986. Effect of food intake and temperature on growth and conversion efficiency of juvenile walleye pollock (*Theragra chalcogramma* (Pallas)): a laboratory study. J. Cons. Int. Explor. Mer, **42**: 241–253.

© 2007 NRC Canada

Smith, R.L., Paul, J.M., and Paul, A.J. 1989. Gastric evacuation in walleye pollock, *Theragra chalcogramma*. Can. J. Fish. Aquat. Sci. **46**: 489–493.

Sogard, S.M., and Olla, B.L. 1996. Food deprivation affects vertical distribution and activity of a marine fish in a thermal gradient: potential energy-conserving mechanisms. Mar. Ecol. Prog. Ser. **133**: 43–55.

Sogard, S.M., and Olla, B.L. 1997. The influence of hunger and predation risk on group cohesion in a pelagic fish, walleye pollock *Theragra chalcogramma*. Environ. Biol. Fishes, **50**: 405–413.

Sogard, S.M., and Olla, B.L. 1998. Contrasting behavioral responses to cold temperatures by two marine fish species during their pelagic juvenile interval. Environ. Biol. Fishes, **53**: 405–412.

Sogard, S.M., and Olla, B.L. 2000. Endurance of simulated winter conditions by age-0 walleye pollock: effects of body size, water temperature and energy stores. J. Fish Biol. **56**: 1–21.

Swartzman, G., Stuetzle, W., Kulman, K., and Powojowski, M. 1994. Relating the distribution of pollock schools in the Bering Sea to environmental factors. ICES J. Mar. Sci. **51**: 481–492.

Tang, Q., Jin, X., Li, F., Chen, J., Wang, W., Chen, Y., Zhao, X., and Dai, F. 1996. Summer distribution and abundance of age-0 walleye pollock, *Theragra chalcogramma*, in the Alutian Basin. *In* Ecology of juvenile walleye pollock, *Theragra chalcogramma*. NOAA Tech. Rep. NMFS 126. *Edited by* R.D. Brodeur, P.A. Livingston, T.R. Loughlin, and A.B. Hollowed. US Department of Commerce, Seattle, Wash. pp. 35–45.

Weetman, D., Atkinson, D., and Chubb, J.C. 1998. Effects of temperature on anti-predator behaviour in the guppy, *Poecilia reticulata*. Anim. Behav. **55**: 1361–1372.

Wilson, M.T., Brodeur, R.D., and Hinckley, S. 1996. Distribution and abundance of age-0 walleye pollock, *Theragra chalcogramma*, in the western Gulf of Alaska during September 1990. *In* Ecology of juvenile walleye pollock, *Theragra chalcogramma*. NOAA Tech. Rep. NMFS 126. *Edited by* R.D. Brodeur, P.A. Livingston, T.R. Loughlin, and A.B. Holloweed. US Department of Commerce, Seattle, Wash. pp. 11–24.

© 2007 NRC Canada

Bioaccumulation of mercury in pelagic fishes from the northern Gulf of Mexico

Yan Cai, Jay R. Rooker, Gary A. Gill, and Jason P. Turner

Abstract: Total mercury (Hg) concentration was determined in the tissues of 10 pelagic fishes in the northern Gulf of Mexico, and dietary tracers (stable isotopes and fatty acids) were used to evaluate the relationship between Hg and feeding history. Highest Hg levels were observed in blue marlin (*Makaira nigricans*), carcharhinid sharks (*Carcharhinus* spp.), and little tunny (*Euthynnus alletteratus*), ranging from 1.08 to 10.52 ppm. Moderate to low concentrations (<1.0 ppm) were observed in blackfin tuna (*Thunnus atlanticus*), cobia (*Rachycentron canadum*), dolphinfish (*Coryphaena hippurus*), greater amberjack (*Seriola dumerili*), king mackerel (*Scomberomorus cavalla*), wahoo (*Acanthocybium solandri*), and yellowfin tuna (*Thunnus albacares*). For the majority of species examined, Hg concentrations did not vary significantly between location (Texas vs. Louisiana) or collection period (2002 and 2003). Significant positive relationships between Hg concentration and body size and (or) weight were detected for 6 of the 10 taxa examined. Hg concentration was also positively associated with trophic position. Three natural associations were identified using stable isotope and fatty acid signatures. Still, no connection between these natural trophic associations and Hg concentration was observed, suggesting that Hg concentration in pelagic fishes was more closely linked to trophic position and size than feeding history.

Résumé : Nous avons déterminé les concentrations de mercure total (Hg) dans les tissus de 10 poissons pélagiques du nord du golfe du Mexique et utilisé des traceurs alimentaires (isotopes stables et acides gras) pour évaluer les relations entre Hg et l'histoire alimentaire. Les concentrations d'Hg les plus fortes s'observent chez le makaire bleu (*Makaira nigricans*), les requins carcharinidés (*Carcharhinus* spp.) et la thonine commune (*Euthynnus alletteratus*) et elles varient de 1,08 à 10,52 ppm. Les concentrations moyennes à faibles (<1,0 ppm) se retrouvent chez le thon à nageoires noires (*Thunnus atlanticus*), le cobia (*Rachycentron canadum*), la coryphène (*Coryphaena hippurus*), la sériole couronnée (*Seriola dumerili*), le tassard royal (*Scomberomorus cavalla*), le tassard bâtard (*Acanthocybium solandri*) et l'albacore à nageoires jaunes (*Thunnus albacares*). Chez la plupart des espèces examinées, les concentrations d'Hg ne varient pas significativement d'un endroit à une autre (Texas et Louisiane) ou d'une année à l'autre (2002 et 2003). Nous trouvons des relations positives significatives entre la concentration d'Hg et la taille et (ou) la masse du corps chez 6 des 10 taxons étudiés. Il y a aussi une corrélation positive entre la concentration d'Hg et le niveau trophique. Les signatures d'isotopes stables et d'acides gras révèlent trois associations naturelles. Néanmoins, nous ne trouvons aucun lien entre ces associations trophiques naturelles et les concentrations d'Hg, ce qui laisse croire que les concentrations d'Hg chez les poissons pélagiques sont plus intimement reliées à la position trophique et à la taille qu'à l'histoire alimentaire.

[Traduit par la Rédaction]

Introduction

Many biotic, ecological, and environmental factors contribute to the uptake of methylmercury (MeHg) in fishes (Wiener et al. 2003), with dietary uptake accounting for more than 90% of the total uptake of MeHg in wild fishes (Hall et al. 1997). When elimination rates of Hg are lower than the uptake rate, concentration of MeHg increases with increasing age or body size of the fish (Wiener and Spry 1996). The uptake of MeHg is also influenced by diet history and trophic position, with rates of Hg accumulation higher for fishes feeding at a higher trophic position (Cabana and Rasmussen 1994; Cabana et al. 1994; Wiener et al. 2003). Moreover, other studies have shown the spatial variation in fish Hg concentrations was attributed to environmental factors like pH, water temperature, lake size, and dissolved organic carbon (DOC) concentrations that control the biogeochemical processes and transformation of MeHg in the ecosystem (Håkanson et al. 1988; Bodaly et al. 1993).

Because most MeHg in fish is obtained through the food chain, information on the feeding ecology of marine consumers is needed to determine the source(s) of MeHg and

Received 18 February 2006. Accepted 25 November 2006. Published on the NRC Research Press Web site at http://cjfas.nrc.ca on 30 March 2007.
J19181

Y. Cai and J.R. Rooker.[1] Department of Marine Biology, Texas A&M University, 5007 Avenue U, Galveston, TX 77551, USA.
G.A. Gill. Department of Marine Science, Texas A&M University, 5007 Avenue U, Galveston, TX 77551, USA.
J.P. Turner. University of Hawaii at Hilo, Department of Marine Science, 200 W. Kawili Street, Hilo, HI 96720-4091, USA.

[1]Corresponding author (e-mail: rookerj@tamug.edu).

 doi:10.1139/F07-017 © 2007 NRC Canada

Fig. 1. Map of sampling locations: offshore area near Galveston–Freeport in Texas, USA, and Venice in Louisiana, USA, in the northern Gulf of Mexico.

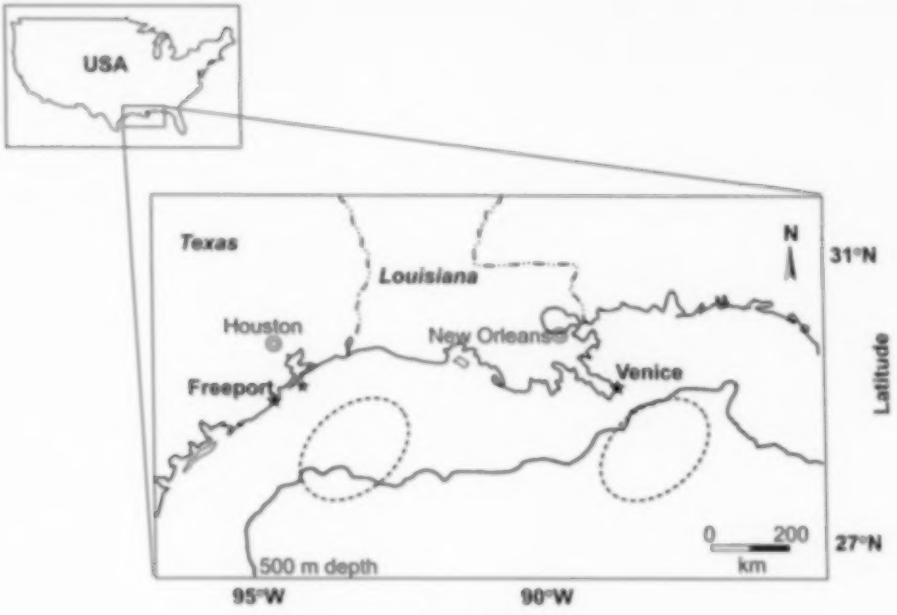

examine the bioaccumulation of this stressor in marine consumers. Because conventional gut analysis has a number of inherent constraints (e.g., reflects only short-term information on diet; provides limited information on source(s) of organic matter), stable isotope analysis and fatty acid analysis are increasingly used to reconstruct feeding histories and improve our understanding of trophic relationships within aquatic systems (e.g., Kharlamenko et al. 2001; Rooker et al. 2006; Turner and Rooker 2006). Recently, dietary tracer analysis has been coupled with contaminant analysis to determine the pattern and extent of biomagnification of Hg and other contaminants in aquatic food webs (Cook et al. 2004). However, most of these studies have been located in freshwater ecosystems. The purpose of the present study was to examine the trophic structure and contaminant bioaccumulation of Hg in pelagic fishes in the Gulf of Mexico. Efforts were focused on determining body burdens of Hg across several pelagic taxa targeted by recreational and commercial anglers in this region. In addition, stable isotopes and fatty acids were also used to relate feeding history and trophic position to the observed patterns of MeHg in the tissue of top-level predators.

Materials and methods

Sample collection

Pelagic fishes were sampled at docks from two regions of the northern Gulf of Mexico: Galveston–Freeport, Texas, and Venice, Louisiana (Fig. 1). In addition, samples were collected with hook-and-line to complement dock sampling efforts. To assess annual variation, samples were collected during the summer in 2002 and 2003. For each fish sample, ~20 g of muscle tissue were removed from the dorsal region behind the head. Samples were individually bagged and labeled with collection date, species name, and fish length (total length in cm). Samples were stored on ice in a cooler before being transported back to the laboratory and put into a freezer (–20 °C). Ten taxa–species were targeted: blackfin tuna (*Thunnus atlanticus*), blue marlin (*Makaira nigricans*), carcharhinid sharks (*Carcharhinus* spp.), cobia (*Rachycentron canadum*), dolphinfish (*Coryphaena hippurus*), greater amberjack (*Seriola dumerili*), king mackerel (*Scomberomorus cavalla*), little tunny (*Euthynnus alletteratus*), wahoo (*Acanthocybium solandri*), and yellowfin tuna (*Thunnus albacares*).

Determination of total Hg in fish tissues

Measurements of total Hg in fish tissue were conducted using a Milestone DMA-80 direct Hg analyzer (Cizdziel et al. 2002). Fish muscle samples were taken directly from the freezer, cut into 0.1–0.3 g pieces, weighed, and placed directly into sample boats for analysis. The instrument was calibrated each day using standard reference materials (SRM) prepared by the National Research Council of Canada (i.e., TORT-2 and DORM-2). Blanks and a separate standard reference material (DORM-1 or 1566*a*) were always analyzed at the beginning of every batch of 10 samples to assess accuracy. Blanks consisted of an empty boat. Three replicate analyses were conducted for the first three samples of each batch. If the relative percent difference was within 10%, the rest of the batch was analyzed once only. Otherwise, beginning samples of the batch were run again. Fish samples that did not fall within the concentration range of the standards were reanalyzed with a more appropriate amount of wet tissue.

© 2007 NRC Canada

To evaluate the effect of dehydration on samples with different storage times, a second piece of each sample was weighed when the first piece was introduced into the instrument for Hg analysis. After drying in the oven at 50 °C for 48 h, they were weighed again to determine the water concentration of the tissue at the time of analysis and then introduced into the instrument for Hg analysis. We observed no significant dehydration effect (y = mean dry Hg concentration, x = mean wet Hg concentration, $y = 3.80x + 0.04$, $R^2 = 1$); therefore, only wet-weight Hg concentrations are reported.

Calibration curves were linear (mean: $R^2 = 1.00$; range: $R^2 = 0.97–1.00$; $n = 68$), and regression equations were used to correct the wet-weight Hg concentration data directly measured by the DMA-80 Hg analyzer. Recovery of the SRM (DORM-2 or DOLT-1) ranged from 90.6% to 112.2% and averaged 97.8% (standard deviation, SD = 5.2%). Mean detection limit, based on three times the SD of blanks, was 0.2 ng Hg·g^{-1} of wet tissue. The coefficient of variation, based on triplicate measurements of the same samples, ranged from 0.3% to 7.1% and averaged 2.9%. Because MeHg comprises an average of more than 95% of the total Hg in fish tissue (Bloom 1998), total Hg was measured to represent the MeHg level in fish in the present study. To simplify the presentation, the term Hg concentration is used from this point on to represent total Hg wet-weight concentration in muscle tissue.

Stable isotope analysis

Tissue samples from randomly selected individuals (~five per species) of nine species (blackfin tuna, blue marlin, cobia, dolphinfish, greater amberjack, king mackerel, little tunny, wahoo, yellowfin tuna) were subject to stable isotope analysis. For each sample, ~0.6 mg of the fish muscle tissue was ground and used for isotopic determination. Isotope ratios ($^{13}C/^{12}C$ and $^{15}N/^{14}N$) and total carbon and nitrogen content were determined using a Finnigan MAT DeltaPlus continuous-flow stable isotope mass spectrometer attached to a Carlo Erba elemental analyzer at the University of Texas at Austin Marine Science Institute. Isotope ratios were reported in parts per thousand (relative to standards (PeeDee Belemnite for carbon and atmospheric N for nitrogen)) and defined in delta (δ) notation as

$$\delta^{15}N \text{ or } \delta^{13}C = (R_{sample}/R_{standard} - 1) \times 10^3$$

where $R = {}^{15}N/{}^{14}N$ or $^{13}C/^{12}C$. A secondary standard reference material (chitin of marine origin, Sigma Aldrich Co., No. C-8908) was used to verify the accuracy of isotopic measurements (Herzka and Holt 2000).

Fatty acid analysis

Tissue samples from randomly selected individuals of all 10 taxa were subject to fatty acid analysis. Lipid was extracted in duplicate aliquots using techniques from Folch et al. (1957) as modified by Iverson et al. (2001). The Hilditch procedure (Iverson et al. 1992) was used to prepare fatty acid methyl esters (FAME). Analysis of FAME was run in duplicate using temperature-programmed gas chromatography on a Perkin-Elmer Autosystem II Capillary FID gas chromatograph. Separation of FAME was performed on a 30 m × 0.25 mm internal diameter column coated with 50% cyanopropyl polysilohexane (0.25 µm film thickness; J&W DB-23, Folsom, California, USA). Helium was used as a carrier gas. Individual peaks of FAME were identified by comparing retention times with known composition and commercially available standards (Nu Check Prep., Elysian, Minnesota, USA). A computerized integration system (Turbochrome 4 software, PE Nelson) was used to calculate chromatographic data (Iverson et al. 1997*a*, 1997*b*). Individual fatty acids were converted to mass percentage of total fatty acids using conversion factors from Ackman (1972, 1991). The fatty acid nomenclature used here is of the form 18:2(n-3), where 8 designates the total number of carbon atoms, 2 is the number of double bonds, and (n-3) is the position of the first double bond from the methyl end of the fatty acid. Average data of the individual fatty acids are expressed as a mass percentage of total fatty acids.

Statistical analyses

To assess regional and interannual variability in Hg concentrations, analysis of covariance (ANCOVA) was performed for each species or taxon, setting location and year as main factors, with log Hg as the dependent variable. The covariate (size) was used to compensate for size-related differences between regions or years. To explore the relationship between Hg concentration and fish body size, linear regression analysis was conducted for each species, setting size as the independent variable and Hg concentration as the dependent variable. Linear regression analysis was also conducted to test for the effect of trophic position (expressed as $\delta^{15}N$) on Hg concentrations in the tissue of pelagic fishes. Hierarchical cluster analysis was used to identify natural associations or groupings with similar dietary histories using fatty acid signatures (based on percent composition). Euclidean distance and the average linkage-joining algorithm were used to produce hierarchical trees for fatty acid data. After observing that fishes from the same location, rather than fishes of the same species, were grouped together, one-way analysis of variance (ANOVA) tests were performed for each taxon to contrast fatty acid profiles of collections from Texas and Louisiana. Before all parametric testing, assumptions of normality (error terms) and homogeneity of variances were examined using Kolmogorov–Smirnov (K–S) test and Levene's test. Distributions of Hg were not always normal between years and locations for each taxon because of the lack of samples for those taxa in a certain year or location. To improve normality and homogeneity of variance, all Hg concentrations were $\log_{10}$-transformed. The α value was set as 0.05 for all statistical tests, and analyses were performed using SPSS software (version 12.0, SPSS Inc., Chicago, Illinois).

Results

Hg survey of pelagic fishes

Mean Hg concentrations across the 10 taxa ranged from 0.07 to 10.52 ppm ($n = 387$) (Table 1), and concentrations of three taxa were higher than the Food and Drug Administration (FDA) (2001) criterion value of 1.0 ppm wet weight: blue marlin, carcharhinid sharks, and little tunny (10.52, 1.61, and 1.08 ppm, respectively). In addition to these taxa, five others were above a reduced advisory level of 0.3 ppm

© 2007 NRC Canada

Table 1. Hg level of 10 taxa of pelagic fishes from the northern Gulf of Mexico.

		[Hg] (total ‰ wet weight)			Total length (cm)		
Species	*N*	Mean	SD	Range	Mean	SD	Range
AJ*	44	0.60	±0.23	0.24–1.07	84	±10	69–112
BM**	9	10.52	±5.03	4.95–18.72	285	±23	256–311
BX*	48	0.64	±0.31	0.00–1.41	73	±6	22–87
CO*	17	0.89	±0.52	0.20–2.40	97	±16	76–142
CS**	9	1.61	±0.45	0.46–4.08	69	±6	15–96
DF	57	0.07	±0.09	0.01–0.49	79	±30	38–135
KM*	39	0.96	±0.27	0.37–1.46	84	±9	64–104
LT**	9	1.08	±0.72	0.24–2.52	56	±4	52–66
WA*	52	0.78	±0.87	0.01–3.31	133	±16	103–175
YT	103	0.18	±0.15	0.07–0.87	112	±17	54–159

Note: Fish abbreviations are as follows: AJ, greater amberjack (*Seriola dumerili*); BM, blue marlin (*Makaira nigricans*); BX, blackfin tuna (*Thunnus atlanticus*); CO, cobia (*Rachycentron canadum*); CS, carcharhinid sharks; DF, dolphinfish (*Coryphaena hippurus*); KM, king mackerel (*Scomberomorus cavalla*); LT, little tunny (*Euthynnus alletteratus*); WA, wahoo (*Acanthocybium solandri*); YT, yellowfin tuna (*Thunnus albacares*). *N*, number of individuals; SD, standard deviation.

*Above US Environmental Protection Agency 2002 recommended criteria level (0.3 $\mu g \cdot g^{-1}$ wet weight).

**Above FDA 2001 recommended criteria level (1.0 $\mu g \cdot g^{-1}$ wet weight).

wet weight set by the US Environmental Protection Agency (EPA) (US Environmental Protection Agency 2002): king mackerel, mean = 0.96 ppm; cobia, mean = 0.89 ppm; wahoo, mean = 0.78 ppm; blackfin tuna, mean = 0.64 ppm; greater amberjack, mean = 0.60 ppm. Mean Hg concentrations in yellowfin tuna and dolphinfish were below all consumption advisory levels (0.18 ppm and 0.07 ppm, respectively).

Interannual and regional variation in Hg concentration was investigated, and the majority of taxa examined showed no effect for either factor. Hg levels of only one species, yellowfin tuna, varied significantly between years (P = 0.041), with lower levels in 2003 (0.10 ppm wet weight) compared with 2002 (0.25 ppm wet weight); no interannual effect was observed for blackfin tuna (P = 0.267), dolphinfish (P = 0.574), wahoo (P = 0.296), king mackerel (P = 0.506), or cobia (P = 0.230). Differences in Hg concentration between Texas and Louisiana were not statistically significant for blackfin tuna (P = 0.111), dolphinfish (P = 0.457), and wahoo (P = 0.234); however, Hg concentrations in yellowfin tuna were significantly higher (P = 0.009) in Texas (0.20 ppm) than in Louisiana (0.18 ppm). Sample size limitations did not warrant interannual and (or) regional comparisons for blue marlin, greater amberjack, little tunny, or carcharhinid sharks.

Relationships between length and Hg concentration, as well as between body weight and Hg concentration, were examined for six taxa, and all regressions were significant with positive slopes, indicating that Hg concentration increases with increasing length or weight (Table 2). Blackfin tuna, carcharhinid sharks, and yellowfin tuna showed highest coefficients of determination: blackfin tuna (R^2 = 0.73, n = 48, $P < 0.001$), carcharhinid sharks (R^2 = 0.69, n = 9, $P < 0.001$), yellowfin tuna (R^2 = 0.64, n = 103, $P < 0.001$). Linear regression analysis of Hg concentration by weight indicated that relationships were significant for the same six taxa. Highest R^2 values were observed in blackfin tuna (R^2 = 0.79, n = 48, $P < 0.001$), dolphinfish (R^2 = 0.56, n = 57, $P < 0.001$), and yellowfin tuna (R^2 = 0.55, n = 103, $P < 0.001$). For both length and weight regressions, slope values were significantly higher for blackfin tuna and wahoo than for other taxa examined (Fig 2).

Relationship between Hg tissue concentration and stable isotopes

Stable nitrogen and carbon isotopes ($\delta^{15}N$ and $\delta^{13}C$) were quantified for all species except carcharhinid sharks. $\delta^{15}N$ values ranged from 6.7‰ to 16.2‰, and the highest $\delta^{15}N$ values were observed for little tunny ($\delta^{15}N$ = 13.9‰–16.2‰) and king mackerel ($\delta^{15}N$ = 12.9‰–15.5‰) (Fig. 3). Although blue marlin had the highest Hg level (mean = 10.52 ppm), predicted trophic position of this consumer was intermediate ($\delta^{15}N$ = 10.0‰–11.2‰). The lowest $\delta^{15}N$ values were observed for dolphinfish (6.7‰–9.3‰). Excluding blue marlin, there was a significant positive relationship (R^2 = 0.63, P = 0.011) between Hg level and $\delta^{15}N$ (Hg = 0.004exp(0.38 ($\delta^{15}N$)) (Fig. 3). $\delta^{13}C$ values varied from −17.43‰ to −15.00‰ across species, and signatures of amberjack, yellowfin tuna, and blackfin tuna (range: −17.43‰ to −17.08‰) were depleted relative to other taxa (Fig. 4): cobia (−15.00‰), dolphinfish (−16.00‰), blue marlin (−16.12‰), little tunny (−16.41‰), and king mackerel (−16.59‰). No significant relationship was detected between total Hg and $\delta^{13}C$.

Relationship between Hg tissue concentration and fatty acids

The fatty acid composition of consumer pelagic fish tissue was analyzed, and ~70 fatty acids and their isomers were routinely identified. Only those found at levels ≥0.5% of the total fatty acids were presented here to simplify the presentation (Table 3). Fatty acid signatures of pelagic fishes were characterized by high levels of polyunsaturated fatty acids (PUFAs), which constituted between 41.99% (little tunny) and 57.87% (dolphinfish) of the total fatty acid content. Five major PUFAs (22:6(n-3) (docosahexaenoic acid), 22:5(n-3) (docosapentaenoic acid), 20:5(n-3) (eicosapentaenoic acid, EPA), 20:4(n-6) (arachidonic acid), and 18:2(n-6) (linoleic

© 2007 NRC Canada

Table 2. Regression analysis of Hg tissue concentrations as a function of size and body weight for apex predator species in northern Gulf of Mexico.

	[Hg] and size				[Hg] and weight			
Species	*a*	*b*	R^2	*P*	*a*	*b*	R^2	*P*
BX	−5.043	4.193	0.79	<0.001	−2.579	1.361	0.79	<0.001
CS	−1.478	2.463	0.35	<0.001	0.172	0.838	0.35	<0.001
DF	−1.821	1.857	0.56	<0.001	−0.497	0.720	0.56	<0.001
KM	−0.863	1.991	0.49	<0.001	0.389	0.688	0.49	<0.001
WA	−10.358	6.097	0.35	<0.001	−5.389	1.911	0.35	<0.001
YT[a]	−2.548	2.354	0.59	<0.001	−1.536	0.841	0.59	<0.001

Note: Significant linear functions ($Y = a + bX$) were fitted. Y (= $\log_{10}$[Hg]) is log-transformed Hg level (ng $^{-1}$); X is $\log_{10}$ total length (cm) or $\log_{10}$ total body weight (g). The estimated intercept (*a*), slope (*b*), R^2 value, and *P* value are listed by taxa–species: BX, blackfin tuna (*Thunnus atlanticus*); CS, carcharhinid sharks; DF, dolphinfish (*Coryphaena hippurus*); KM, king mackerel (*Scomberomorus cavalla*); WA, wahoo (*Acanthocybium solandri*); YT, yellowfin tuna (*Thunnus albacares*).

[a]Equation based on samples from Louisiana 2002 only.

Fig. 2. Comparison of regression of Hg tissue concentrations (wet weight) as a function of body weight for six pelagic taxa. BX, blackfin tuna (*Thunnus atlanticus*), $y = 1.36x - 2.6$, $R^2 = 0.79$; CS, carcharhinid sharks (*Carcharhinus* spp.), $y = 0.84x + 0.17$, $R^2 = 0.35$; DF, dolphinfish (*Coryphaena hippurus*), $y = 0.72x - 0.5$, $R^2 = 0.56$; KM, king mackerel (*Scomberomorus cavalla*), $y = 0.69x + 0.39$, $R^2 = 0.49$; WA, wahoo (*Acanthocybium solandri*), $y = 1.91x - 5.4$, $R^2 = 0.35$; YT, yellowfin tuna (*Thunnus albacares*), $y = 0.79x - 1.23$, $R^2 = 0.59$.

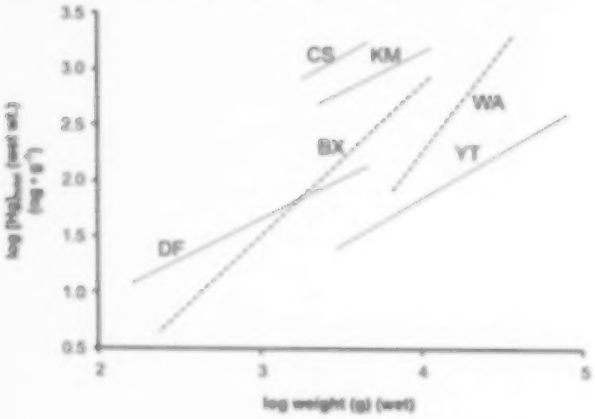

Fig. 3. Linear regression of Hg tissue concentrations (wet weight) as a function of trophic position for pelagic fishes collected in the northern Gulf of Mexico. An exponential equation was fitted to data from eight species. AJ, greater amberjack (*Seriola dumerili*); CO, cobia (*Rachycentron canadum*); DF, dolphinfish (*Coryphaena hippurus*); KM, king mackerel (*Scomberomorus cavalla*); LT, little tunny (*Euthynnus alletteratus*); WA, wahoo (*Acanthocybium solandri*); YT, yellowfin tuna (*Thunnus albacares*). BM blue marlin (*Makaira nigricans*) was not used in the regression.

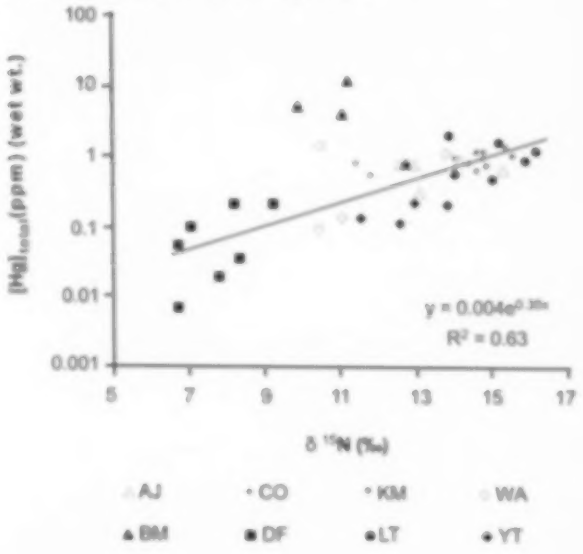

acid)) were present, and the relative quantities of each PUFA were relatively similar among the taxa examined (Fig. 5). 22:6(*n*-3) was the dominant PUFA, comprising more than 50% of the PUFA content of each taxon. Saturated fatty acids (SAT) were the second largest fatty acid group present in the muscle tissue of pelagic fishes, comprising an average of 32.55% of the total fatty acid content.

Hierarchical cluster analysis based on fatty acid profiles of 10 pelagic taxa showed that most species were grouped together by location first, then by species (Fig. 6). Year and size effect were not observed to have an impact on the natural associations, and measures of dissimilarity were highest between taxa from Texas and Louisiana (Fig. 6*a*). A classification tree based on fatty acid components was built for pelagic fishes from each region (Figs. 6*b*, 6*c*), and natural breaks in the fatty-acid-based trees were linked to natural breaks in stable carbon ($\delta^{13}C$) isotope values of these consumers. In Texas, three groups were detected basing on a rescaled squared Euclidean distance, and these groups could also be distinguished by their $\delta^{13}C$ value: cobia ($-15‰ < \delta^{13}C$); blue marlin, king mackerel, and dolphinfish ($-17‰ < \delta^{13}C < -15‰$); and greater amberjack, yellowfin tuna, and blackfin tuna ($\delta^{13}C < -17‰$). Similarly, the two groups based on fatty acid signatures in Louisiana could also be separated to a high degree by their $\delta^{13}C$ value: little tunny and wahoo ($-17‰ < \delta^{13}C < -15‰$); yellowfin tuna and

© 2007 NRC Canada

Table 3. Fatty acid composition (percent weight of total fatty acids) of pelagic fish from the northern Gulf of Mexico.

Fatty acid	AJ (n = 18)	BM (n = 4)	BX (n = 12)	CO (n = 6)	CS (n = 4)	DF (n = 17)	KM (n = 11)	LT (n = 3)	WA (n = 1)	YT (n = 7)
14:0	1.10	1.58	2.58	1.15	0.44	0.36	0.43	3.03	4.27	1.23
15:0	0.39	0.48	0.48	0.33	0.20	0.36	0.24	0.67	0.67	0.43
ISO16	0.70	1.88	1.16	3.54	3.22	4.62	0.85	0.34	0.19	1.59
16:0	21.14	18.30	19.31	15.25	18.89	15.76	19.74	22.75	21.45	18.36
16:1(n-9)	0.56	0.37	0.29	0.42	0.22	0.45	0.34	0.33	0.67	0.27
16:1(n-7)	2.22	2.26	4.55	2.14	1.54	0.89	1.09	5.07	6.76	2.30
16:2 (n-4)	0.96	1.03	0.87	0.53	0.18	1.25	0.67	0.72	0.63	0.96
16:4(n-1)	1.09	1.99	1.19	1.62	1.70	1.12	1.59	1.33	1.73	1.10
17:0	0.68	0.59	0.75	0.95	0.38	0.88	0.73	1.12	1.38	0.98
17:1	0.32	0.28	0.34	0.49	0.26	0.29	0.30	0.25	0.12	0.28
18:0	7.93	9.27	7.72	10.45	10.77	9.53	9.45	8.57	5.72	8.16
18:1(n-9)	8.41	9.51	10.11	10.96	4.99	7.74	7.68	7.44	10.13	8.31
18:1(n-7)	2.04	1.80	2.51	2.13	9.03	1.37	2.00	7.82	2.90	1.83
18:2(n-6)	0.53	0.87	0.97	0.83	0.51	0.43	0.58	0.88	0.96	0.89
20:1(n-7)	0.52	0.50	0.83	0.38	1.04	0.18	0.47	0.87	0.92	0.49
20:4(n-6)	3.49	4.70	2.71	9.49	5.16	7.09	5.50	2.19	2.41	3.44
20:5(n-3)	3.25	2.99	6.35	4.24	1.55	3.49	4.43	4.50	7.40	5.02
22:5(n-6)	2.92	3.51	2.00	3.33	7.23	3.76	3.69	1.93	1.55	2.95
22:5(n-3)	2.99	2.71	2.63	3.43	4.56	2.18	2.12	2.29	3.31	2.05
22:6(n-3)	33.57	29.36	23.63	22.70	22.80	34.26	32.27	20.02	20.38	33.45
SAT	31.94	32.10	32.00	31.67	33.89	31.50	31.44	36.48	33.68	30.76
MONO	13.76	14.43	18.28	16.02	16.82	10.62	11.58	21.53	21.38	13.19
PUFA	54.31	53.47	49.71	52.31	49.29	57.87	56.98	41.99	44.94	56.05

Note: AJ, greater amberjack (*Seriola dumerili*); BM, blue marlin (*Makaira nigricans*); BX, blackfin tuna (*Thunnus atlanticus*); CO, cobia (*Rachycentron canadum*); CS, carcharhinid sharks; DF, dolphinfish (*Coryphaena hippurus*); KM, king mackerel (*Scomberomorus cavalla*); LT, little tunny (*Euthynnus alletteratus*); WA, wahoo (*Acanthocybium solandri*); YT, yellowfin tuna (*Thunnus albacares*). SAT, saturated fatty acid; MONO, monounsaturated fatty acid; PUFA, polyunsaturated fatty acid.

blackfin tuna ($\delta^{13}C < -17‰$). Greater amberjack in Louisiana was an exception from the groupings.

Discussion

Hg tissue concentrations differed between species, and three general categories of Hg bioaccumulation were identified: high range (>1.0 ppm), middle range (between 0.3 and 1.0 ppm), and low range (<0.3 ppm). High range taxa included blue marlin, carcharhinid sharks, and little tunny; middle range included blackfin tuna, cobia, greater amberjack, king mackerel, and wahoo; low range included dolphinfish and yellowfin tuna. Hg tissue concentrations observed in this study for certain taxa were similar to results from other studies conducted in the Gulf of Mexico (Adams et al. 2003; FDA 2004; US Environmental Protection Agency 2004*a*). For example, blue marlin and little tunny were two of the three species observed in the high range category, and these two species had the highest Hg concentrations of pelagic fishes collected from a recent Hg survey completed in Florida (Adams et al. 2003). Moreover, carcharhinid sharks, the second highest Hg concentration taxa in this study, were also the second highest Hg fish on the EPA not-to-eat fish list (US Environmental Protection Agency 2004*b*). Even though taxa in the highest Hg category were similar to other studies, both blue marlin and carcharhinid sharks showed considerably higher Hg concentrations (up to two–three times higher) than previously reported (Adams et al. 2003; FDA 2004). Similarly, except for blackfin tuna, observed Hg levels of all taxa in the middle range (king mackerel, wahoo, greater amberjack, cobia) were 0.3–0.5 ppm higher than previous reports (Adams et al. 2003; Watanabe et al. 2003). Observed patterns suggest that regional variation in fish tissue Hg occurs within the Gulf of Mexico; however, differences in sample size and fish length–weight preclude further interpretation of these data.

MeHg accumulates from one trophic level to the next, and Hg concentrations in large, apex predators are often above advisory levels set by FDA and EPA (Andersen and Depledge 1997). Compared with most estuarine species, pelagic fishes attain larger body sizes and feed at higher trophic levels (Rooker et al. 2006), which likely increases the bioaccumulation process and may result in higher Hg concentrations. Sager (2004) measured the total Hg tissue concentrations of three estuarine fishes (southern flounder, *Paralichthys lethostigma*; spotted seatrout, *Cynoscion nebulosus*; and red drum, *Sciaenops ocellatus*) from the same area (NW Gulf of Mexico), and all three species showed lower Hg concentrations (range: 0.06–0.10 ppm) than the EPA 0.3 ppm threshold. Similarly, a study in Galveston Bay, Texas, examined the same species and indicated that Hg concentrations of these species were normally below 0.25 ppm, with an average near 0.10 ppm (GBNEP 1992). In contrast, 8 out of 10 pelagic taxa examined in the present study had higher Hg concentrations than the EPA 0.3 ppm threshold, with three species above the FDA 1.0 ppm level. Considering that all the pelagic fishes in this study were apex predators with either long life spans (>10 years) and

© 2007 NRC Canada

Fig. 4. Stable-carbon and stable-nitrogen isotope values (mean ± standard deviation) of nine pelagic fishes from northern Gulf of Mexico. AJ (n = 5), greater amberjack (*Seriola dumerili*); BX (n = 5), blackfin tuna (*Thunnus atlanticus*); BM (n = 4), blue marlin (*Makaira nigricans*); CO (n = 5), cobia (*Rachycentron canadum*); DF (n = 7), dolphinfish (*Coryphaena hippurus*); KM (n = 6), king mackerel (*Scomberomorus cavalla*); LT (n = 5), little tunny (*Euthynnus alletteratus*); WA (n = 5), wahoo (*Acanthocybium solandri*); YT (n = 5), yellowfin tuna (*Thunnus albacares*). Broken lines indicated groupings following fatty acid classification tree results.

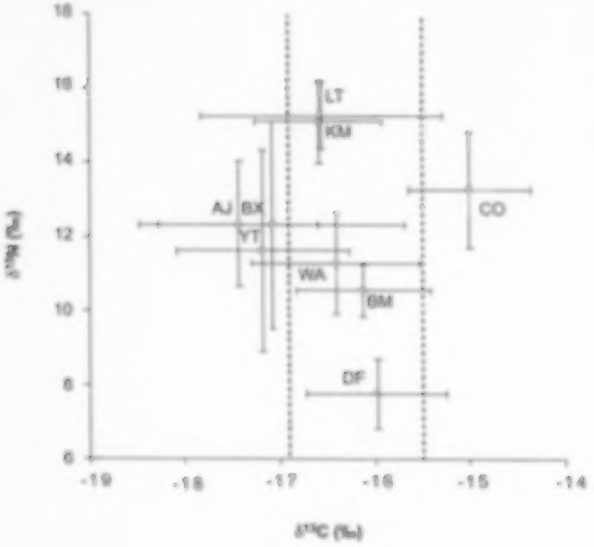

(or) large body size (>100 cm) or both (e.g., Collette and Nauen 1983; Bauchot 1987), elevated Hg concentrations detected in these fish were not surprising. Moreover, the species with the highest Hg concentration in this study, blue marlin, was the largest species examined (mean = 285 cm lower jaw fork length), and this species is very long-lived (>20 years) (Wilson et al. 1991). In contrast, several of the other species examined (e.g., dolphinfish, cobia, greater amberjack, yellowfin tuna) typically live 4–10 years (Manooch and Potts 1997; Franks et al. 1999; Massuti et al. 1999), and thus even with a relatively large body size, they may not live long enough to accumulate large amounts of Hg. The life span effect seems to apply particularly well to dolphinfish, since this species, which has the shortest lifespan of any of the taxa examined (3–5 years), also had the lowest Hg concentration in its tissue.

No regional or annual differences in Hg concentration were detected for the majority of taxa examined. The major reason for the lack of regional differences could be that many of the pelagic fishes surveyed here (e.g., yellowfin tuna, little tunny, blue marlin) are known to be highly migratory species and may travel hundreds to thousands of kilometres in short periods of time (e.g., Deriso et al. 1991; FAO Fisheries Department 1994; Kerstetter et al. 2003). As a result, individuals caught in Texas or Louisiana waters may have spent a portion of their life in the other region or other parts of the Gulf of Mexico. Electronic tagging studies are currently underway in the northern Gulf of Mexico, and migration between the two regions has been documented for billfishes (J. Rooker, unpublished data). With respect to temporal differences, the 2-year period was a relatively short time interval, and environmental changes or tissue turnover during this period may have been insufficient to produce notable changes in Hg tissue concentrations.

Significant positive relationships between Hg concentration and size (length and (or) weight) were detected for all species examined, and similar relationships have been documented previously (e.g., Monteiro and Lopes 1990; Wiener and Spry 1996; Sager 2002). Moreover, recent work by Adams (2004) on pelagic species (yellowfin tuna and little tunny) showed positive relationships between Hg concentration and fish length and (or) weight. In the present study, slope values from linear regressions of Hg concentration and size were similar (0.010–0.011) for several species (carcharhinid sharks, yellowfin tuna, dolphinfish, and king mackerel), suggesting that the rate of Hg accumulation may be closely tied to growth. To verify this theory, Hg was plotted against body weight. All six species not only showed significant positive relationships between their Hg concentration and body weight, but the same four species showed similar Hg accumulation rates (slope values). The positive relationship between Hg concentration and size is likely a function of a slow rate of elimination of MeHg relative to its rapid rate of uptake (Trudel and Rasmussen 1997). Given the fact that MeHg forms covalent bonds with proteins in muscle after it is transported through the blood (Carty and Malone 1979; Georgieva et al. 2004), and also that in carnivorous fish, protein assimilation is generally equal to 80% of total assimilation from food consumption (Brett and Groves 1979), the positive relationship between Hg concentration and body mass observed here is in accord with expected patterns of accumulation.

A positive exponential relationship between Hg concentration and trophic position (expressed as δ^{15}N) was observed here, and a positive relationship between these two parameters has been observed in other studies (Lyle 1984; Cabana et al. 1994). Besides Hg, concentrations of other contaminants in the tissue of fishes also increase with increasing trophic position. For example, Hobson et al. (2002) reported a linear relationship between PCB concentration and δ^{15}N values for organisms in the North Water food web. The positive relationships between Hg level (and other contaminants) and trophic position in fishes suggests that biomagnification of Hg takes place in marine ecosystems. This process occurs because consumers feeding at higher trophic positions consume larger prey with higher body burdens than smaller prey (Muir et al. 1988; Watras et al. 1998; Bowles et al. 2001). Although blue marlin did not occupy the highest trophic level, their Hg levels were well above the Hg–δ^{15}N regression line. This could be explained in part by the fact that blue marlin are relatively long-lived species (>20 years) (Wilson et al. 1991), which would allow them to accumulate more Hg relative to other shorter-lived taxa. Overlap of δ^{15}N values was observed for many pelagic fish species in this study because of the relatively large intraspecific variation of δ^{15}N values. The broad range of observed δ^{15}N values for

© 2007 NRC Canada

Fig. 5. Mean percent fatty acid composition of 10 pelagic fishes from (*a*) Texas and (*b*) Louisiana. AJ, greater amberjack (*Seriola dumerili*); BM, blue marlin (*Makaira nigricans*); BX, blackfin tuna (*Thunnus atlanticus*); CO, cobia (*Rachycentron canadum*); CS, carcharhinid sharks (*Carcharhinus* spp.); DF, dolphinfish (*Coryphaena hippurus*); KM, king mackerel (*Scomberomorus cavalla*); LT, little tunny (*Euthynnus alletteratus*); WA, wahoo (*Acanthocybium solandri*); YT, yellowfin tuna (*Thunnus albacares*). SAT, saturated fatty acid; MONO, monounsaturated fatty acid; PUFA, polyunsaturated fatty acid.

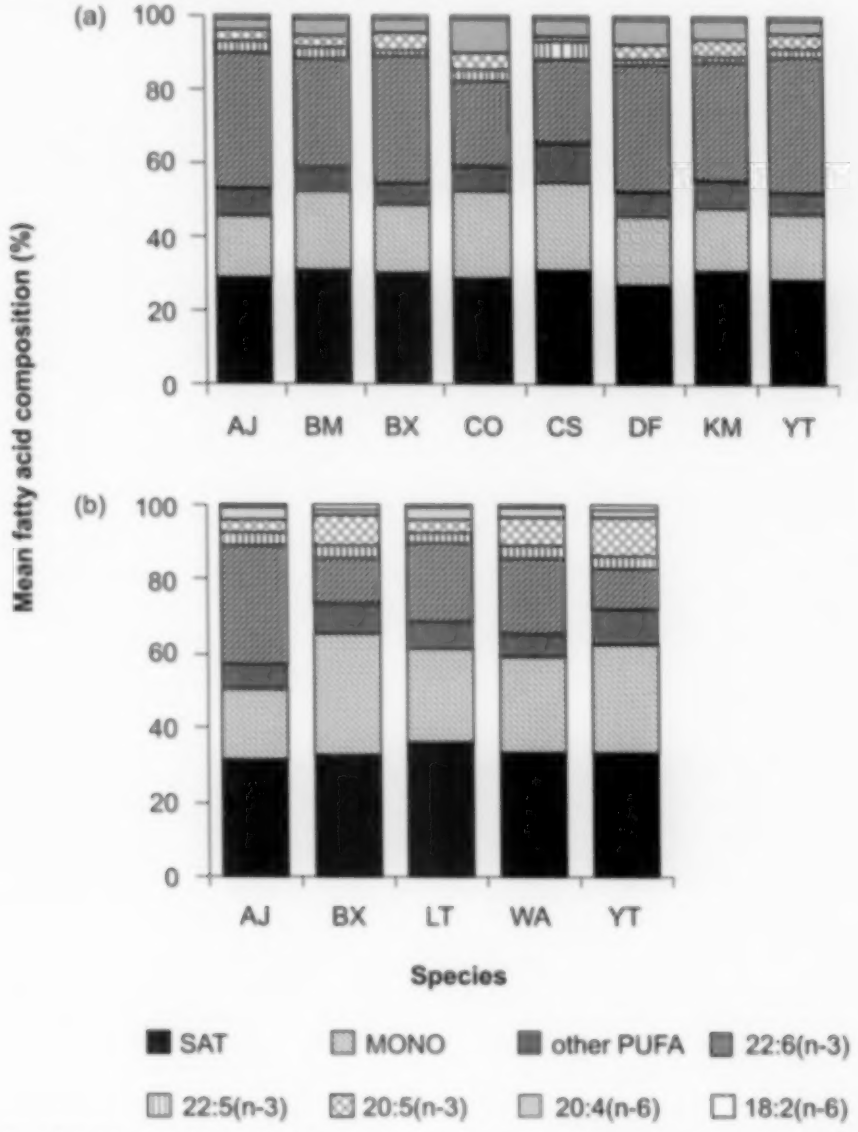

conspecifics may be related to individuals feeding on prey from different trophic levels (i.e., generalist feeding strategy) or ontogenetic shifts in diet (Kidd et al. 1995; Herzka and Holt 2000). Moreover, $\delta^{15}N$ values vary as a function of the isotopic composition of the inorganic nitrogen at the base of the food web. Thus, precaution must be exercised here because signatures of consumers will not be linked directly to trophic position when multiple producers (pathways) are present.

Three natural groupings of pelagic fishes were identified using either $\delta^{13}C$ values or fatty acid profiles, suggestive of common carbon sources or prey resources among members of each association. Rooker et al. (2006) examined the trophic ecology of pelagic fishes from the same region using stable isotopes and fatty acids. Findings from this study indicated that the largest fraction of organic matter used by pelagic consumers was derived from phytoplankton production; there did not appear to be multiple trophic pathways within this pelagic ecosystem. Stable isotope and fatty acid signatures of the majority of consumers in the present study also suggested a phytoplankton-based food web, and observed groupings may be linked to regional differences in phyto-

© 2007 NRC Canada

Fig. 6. Results of hierarchical cluster analysis on fatty acid profiles of pelagic fishes from Texas (TX) and Louisiana (LA). AJ, greater amberjack (*Seriola dumerili*); BX, blackfin tuna (*Thunnus atlanticus*); BM, blue marlin (*Makaira nigricans*); CO, cobia (*Rachycentron canadum*); CS, carcharhinid sharks (*Carcharhinus* spp.); DF, dolphinfish (*Coryphaena hippurus*); KM, king mackerel (*Scomberomorus cavalla*); LT, little tunny (*Euthynnus alletteratus*); WA, wahoo (*Acanthocybium solandri*); YT, yellowfin tuna (*Thunnus albacares*). (*a*) Fishes from the same location were grouped together according to a squared Euclidean distance value of 12. (*b*) Fishes from Texas were clustered into three groups according to a squared Euclidean distance value of 4. (*c*) Fishes from Louisiana were clustered into two groups according to a squared Euclidean distance value of 4. Stable isotope categories used in (*b*) and (*c*) are mean values; the range of observed values for each taxon may be outside the category containing the mean value.

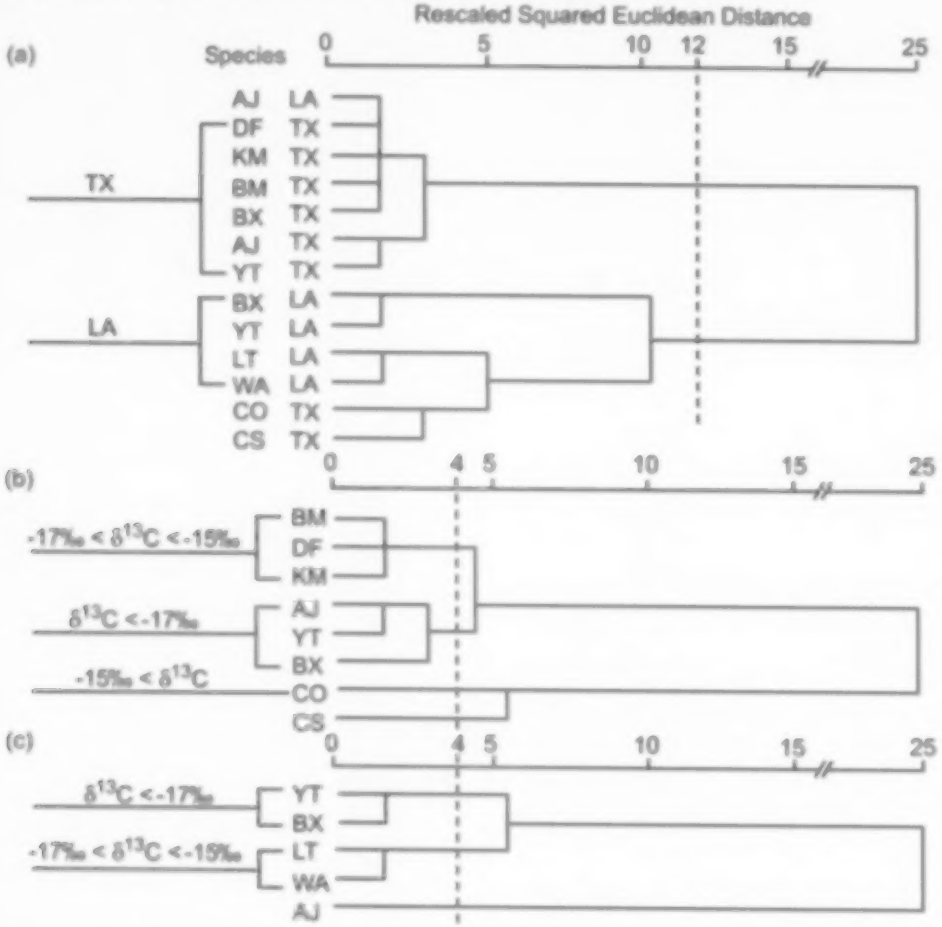

plankton signatures or other factors linked to foraging (i.e., shifts in trophic position). Regardless of the actual cause of these grouping, there did not appear to be a link to Hg bioaccumulation. For example, blue marlin and little tunny were in the high Hg group and dolphinfish was in the low Hg group. Nevertheless, all three species had similar $\delta^{13}C$ values, which may indicate the source of organic matter for these species was the same. The lack of connection between these natural groupings and the Hg pattern observed in these fishes indicated that the distinguishing factors for the groupings were not Hg accumulation in these fishes. Since the same natural groupings were obtained for both dietary markers, it not only confirmed the existence of these natural groupings but also indicated that the distinguishing factors were somewhat connected with the dietary history of these fishes. One possible explanation for the observed patterns could be linked to pelagic or benthic foraging strategies of the taxa examined. In a marine ecosystem, $\delta^{13}C$ values of benthic and pelagic prey differ; thus, consumers feeding on or near the bottom can be distinguished from consumers feeding in the water column (Hatase et al. 2002; Hobson et al. 2002). Moreover, $\delta^{13}C$ values of benthic prey of large consumers in the Gulf of Mexico are more enriched compared with their pelagic counterparts (J. Rooker, unpublished data). In the present study, cobia had the most enriched $\delta^{13}C$ value and thus appeared to feed on more benthic prey than all the other pelagic fishes in this study. Moreover, levels of one PUFA, 20:4(*n*-6), were noticeably higher in cobia than in other species examined, which may also be linked to benthic food source(s).

© 2007 NRC Canada

In this study, the classification tree based on the fatty acid profiles of pelagic fishes separated fishes from different regions (Texas vs. Louisiana). Because the fatty acid composition of the diet influences the lipid composition of tissues in fishes (Turner and Rooker 2005*a*, 2005*b*; Rooker et al. 2006), it appears that pelagic taxa within the same region share similar prey resources or a common source of organic matter in their food web. Since many of the pelagic taxa examined here are opportunistic feeders (e.g., Manooch et al. 1984; Meyer and Franks 1996; Abitia-Cardenas et al. 1999), their diets may be composed of a few dominant prey species, which vary from one region to another. Also, the primary source of organic matter supplied to primary, secondary, and tertiary consumers may vary spatially (Iverson et al. 1997*b*; Cook et al. 2000), leading to regional differences in fatty acid signatures. Although regional variability in fatty acid signatures was present, certain taxa were aligned with members of the other region. Although carcharhinid sharks and cobia from Texas were present in the Louisiana grouping, it is difficult to interpret this result, since samples of both taxa were only available from Texas. Moreover, most taxa in our assessment are highly migratory, and therefore they may utilize feeding areas in both regions. Species-specific variation in Hg levels between the two regions was negligible. The lack of agreement between fatty acid and Hg measurements (e.g., fatty acid group contained both high and low Hg taxa) appears to indicate that Hg accumulation is not tied directly to prey selection patterns. If this is true, other factors such as trophic position, age, and Hg concentrations of the entire prey community are likely the primary determinants of Hg loading. Moreover, Hg concentration is the result of a lifelong Hg accumulation process, and thus our dietary markers may not represent the cumulative lifetime feeding patterns of the consumers.

Acknowledgements

We thank Brett Falterman, Mike Lowe, and Ron Lehman for assistance in the lab and field. This work was supported with a grant from the McDaniel Charitable Foundation.

References

Abitia-Cardenas, L.A., Galvan-Magaña, F., Gutierrez-Sanchez, F.J., Rodriguz-Romero, J., Aguilar-Palomino, B., and Moehl-Hitz, A. 1999. Diet of blue marlin *Makaira mazara* off the coast of Cabo San Lucas, Baja California Sur, Mexico. Fish. Res. **44**: 95–100.

Ackman, R.G. 1972. The analysis of fatty acids and related materials by gas–liquid chromatography. *In* Progress in the chemistry of fats and other lipids. Vol. 12. *Edited by* R.T. Holman. Pergamon Press, Oxford, UK. pp. 165–284.

Ackman, R.G. 1991. Application of gas–liquid chromatography to lipid separation and analysis: qualitative and quantitative analysis. *In* Analyses of fats, oils and lipoproteins. *Edited by* E.G. Perkins. American Oil Chemists Society, Champaign, Ill. pp. 270–300.

Adams, D.H. 2004. Total mercury levels in tunas from offshore waters of the Florida Atlantic coast. Mar. Pollut. Bull. **49**: 659–663.

Adams, D.H., McMichael, R.H.J., and Henderson, G.E. 2003. Mercury levels in marine and estuarine fishes of Florida 1989–2001. 2nd ed. rev. Florida Mar. Res. Inst. Tech. Rep. TR-9.

Andersen, J.L., and Depledge, M.H. 1997. A survey of total mercury and methylmercury in edible fish and invertebrates from Azorean waters. Mar. Environ. Res. **44**: 331–350.

Bauchot, M.L. 1987. Poissons osseux. *In* Fiches FAO d'identification pour les besoins de la pêche. Rev. 1. *Edited by* W. Fischer, M.L. Bauchot, and M. Schneider. Méditerranée et mer Noire. Zone de pêche 37. Commission des Communautés Européennes and FAO, Rome. Vol. II. pp. 891–1421.

Bloom, N.S. 1998. Determination of pictogram levels of methylmercury by aqueous phase ethylation, followed by cryogenic gas chromatography with cold vapour atomic fluorescence detection. Can. J. Fish. Aquat. Sci. **46**: 1131–1140.

Bodaly, R.A., Rudd, J.W.M., Fudge, R.J.P., and Kelly, C.A. 1993. Mercury concentrations in fish related to size of remote Canadian Shield lakes. Can. J. Fish. Aquat. Sci. **50**: 980–987.

Bowles, K.C., Apte, S.C., Maher, W.A., Kawei, M., and Smith, R. 2001. Bioaccumulation and biomagnification of mercury in Lake Murray, Papua New Guinea. Can. J. Fish. Aquat. Sci. **58**: 888–897.

Brett, J.R., and Groves, T.D.D. 1979. Physiological energetics in fish physiology. *In* Fish physiology. Vol. VIII. *Edited by* W.S. Hoar, D.J. Randall, and J.R. Brett. Academic Press, New York. pp. 279–352.

Cabana, G., and Rasmussen, J.B. 1994. Modeling food chain structure and contaminant bioaccumulation using stable nitrogen isotopes. Nature (London), **372**: 255–257.

Cabana, G., Tremblay, A., Kalff, J., and Rasmussen, J.B. 1994. Pelagic food chain structure in Ontario lakes: determinant of mercury levels in lake trout (*Salvelinus namaycush*). Can. J. Fish. Aquat. Sci. **51**: 381–389.

Carty, A.J., and Malone, S.F. 1979. The chemistry of mercury in biological systems. *In* Biogeochemistry of mercury in the environment. *Edited by* J.O. Nriagu. Elsevier/North-Holland Biomedical Press, New York. pp. 433–479.

Cizdziel, J.A., Hinners, T.A., and Heithmar, E.M. 2002. Determination of total mercury in fish tissues using combustion atomic absorption spectrometry with gold amalgamation. Water Air Soil Pollut. **135**: 355–370.

Collette, B.B., and Nauen, C.E. 1983. FAO species catalogue. Vol. 2. Scombrids of the world. An annotated and illustrated catalogue of tunas, mackerels, bonitos and related species known to date. FAO Fish. Synop. **2**: 137.

Cook, E.J., Bell, M.V., Black, K.D., and Kelly, M.S. 2000. Fatty acid composition of gonald material and diets of the sea urchin, *Psammechinus miliaris*: trophic and nutritional implications. J. Exp. Mar. Biol. Ecol. **255**: 261–274.

Cook, P.L.M., Revill, A.T., Clementson, L.A., and Volkman, J.K. 2004. Carbon and nitrogen cycling on intertidal mudflats of a temperate Australian estuary. III. Sources of organic matter. Mar. Ecol. Prog. Ser. **280**: 55–72.

Deriso, R.B., Punsly, R.G., and Bayliff, W.H. 1991. A marked movement model of yellowfin tuna in the eastern Pacific Ocean and some analyses for international management. Fish. Res. **11**: 375–395.

FAO Fisheries Department. 1994. World review of highly migratory species and straddling stocks. FAO, Rome, Italy. FAO Fish. Tech. Pap. No. 337.

FDA. 2001. Consumer advisory — an important message for pregnant women and women of childbearing age who may become pregnant about the risks of mercury in fish [online]. Available from www.cfsan.fda.gov/~dms/admehg.html [updated 19 March 2004].

FDA. 2004. Mercury concentrations in fish: FDA monitoring program (1990–2004) [online]. Available from www.cfsan.fda.gov/~frf/seamehg2.html [updated 2 March 2006].

© 2007 NRC Canada

Folch, J., Lees, M., and Sloan-Stanley, G.H. 1957. A simple method for the isolation and purification of total lipids from animal tissues. J. Biol. Chem. **226**: 497–509.

Franks, J.S., Warren, J.R., and Buchanan, M.V. 1999. Age and growth of cobia, *Rachycentron canadum*, from the northeastern Gulf of Mexico. Fish. Bull. **97**: 459–471.

GBNEP. 1992. Toxic contaminant characterization of aquatic organisms in Galveston Bay: a pilot study. Galveston Bay National Estuary Program, Houston, Texas. GBNEP-20.

Georgieva, D., Rypniewski, W., Echner, H., Perbandt, M., Koker, M., Clos, J., Redecke, L., Bredehorst, R., Voelter, W., Genov, N., and Betzel, C. 2004. Synthetic human prion protein octapeptide repeat binds to the proteinase K active site. Biochem. Biophys. Res. Commun. **325**: 1406–1411.

Håkanson, L., Nilsson, A., and Andersson, T. 1988. Mercury in fish in Swedish lakes. Environ. Pollut. **49**: 145–162.

Hall, B.D., Bodaly, R.A., Fudge, R.J.P., Rudd, J.W.M., and Rosenberg, D.M. 1997. Food as the dominant pathway of methylmercury uptake by fish. Water Air Soil Pollut. **100**: 13–24.

Hatase, H., Takai, N., Matsuzawa, Y., Sakamoto, W., Omuta, K., Goto, K., Arai, N., and Fujiwara, T. 2002. Size-related differences in feeding habitat use of adult female loggerhead turtles *Caretta caretta* around Japan determined by stable isotope analyses and satellite telemetry. Mar. Ecol. Prog. Ser. **233**: 273–281.

Herzka, S.Z., and Holt, G.J. 2000. Changes in isotope composition of red drum (*Sciaenops ocellatus*) larvae in response to dietary shifts: potential applications to settlement studies. Can. J. Fish. Aquat. Sci. **57**: 137–142.

Hobson, K.A., Fisk, A., Karnovsky, N., Holst, M., Gagnon, J.M., and Fortier, M. 2002. A stable isotope ($\delta^{13}C$, $\delta^{15}N$) model for the North Water food web: implications for evaluating trophodynamics and the flow of energy and contaminants. Deep-Sea Res. Part II, **49**: 5131–5150.

Iverson, S.J., Sampugna, J., and Oftedal, O.T. 1992. Positional specificity of gastric hydrolyisis of long-chain *n*-3 polyunsaturated fatty acids of seal milk triglycerides. Lipids, **27**: 870–878.

Iverson, S.J., Arnould, J.P.Y., and Boyd, I.L. 1997*a*. Milk fatty acid signatures indicate both major and minor shifts in the diet of lactating Antarctic fur seals. Can. J. Zool. **75**: 188–197.

Iverson, S.J., Frost, K.J., and Lowry, L.F. 1997*b*. Fatty acid signatures reveal fine scale structure of foraging distribution of harbor seal and their prey in Prince William Sound, Alaska. Mar. Ecol. Prog. Ser. **151**: 255–271.

Iverson, S.J., Lang, S., and Cooper, M. 2001. Comparison of the Bligh and Dyer and Folch methods for total lipid determination in a broad range of marine tissue. Lipids, **36**: 1283–1287.

Kerstetter, D.W., Luckhurst, B.E., Prince, E.D., and Graves, J.E. 2003. Use of pop-up satellite archival tags to demonstrate survival of blue marlin (*Makaira nigricans*) released from pelagic longline gear. Fish. Bull. **101**: 939–948.

Kharlamenko, V.I., Kiyashko, S.I., Imbs, A.B., and Vyshkvartzev, D.I. 2001. Identification of food sources of invertebrates from the seagrass *Zostera marina* community using carbon and sulfur stable isotope ratio and fatty acid analyses. Mar. Ecol. Prog. Ser. **220**: 103–117.

Kidd, K.A., Hesslein, R.H., Fudge, R.J.P., and Hallard, K.A. 1995. The influence of trophic level as measured by $\delta^{15}N$ on mercury concentrations in freshwater organisms. Water Air Soil Pollut. **80**: 1011–1015.

Lyle, J.M. 1984. Mercury concentrations in four Carcharhinid and three hammerhead sharks from coastal waters of the Northern Territory. Aust. J. Mar. Freshw. Res. **35**: 441–451.

Manooch, C.S., and Potts, J.C. 1997. Age, growth, and mortality of greater amberjack from the southeastern United States. Fish. Res. **30**: 229–240.

Manooch, C.S., Mason, D.L., and Nelson, R.S. 1984. Food and gastrointestinal parasites of dolphin, *Coryphaena hippurus*, collected along the southeastern and Gulf coasts of the United States. Bull. Jap. Soc. Sci. Fish. **50**: 1511–1525.

Massuti, E., Morales-Nin, B., and Moranta, J. 1999. Otolith microstructure, age, and growth patterns of dolphin, *Coryphaena hippurus*, in the western Mediterranean. Fish. Bull. **97**: 891–899.

Meyer, G.H., and Franks, J.S. 1996. Food of cobia, *Rachycentron canadum*, from the northcentral Gulf of Mexico. Gulf Res. Rep. **9**: 161–167.

Monteiro, L.R., and Lopes, H.D. 1990. Mercury content of swordfish, *Xiphias gladius*, in relation to length, weight, age, and sex. Mar. Pollut. Bull **21**: 293–236.

Muir, D.C.G., Norstrom, R.J., and Simon, M. 1988. Organochlorine contaminants in Arctic marine food chains: accumulation of specific polychlorinated biphenyls and chlordane-related compounds. Environ. Sci. Tech. **22**: 1071–1079.

Rooker, J.R., Turner, J.P., and Holt, S.A. 2006. Trophic ecology of *Sargassum*-associated fishes in the Gulf of Mexico determined from stable isotope and fatty acid analysis. Mar. Ecol. Prog. Ser. **313**: 249–259.

Sager, D.R. 2002. Long-term variation in mercury concentrations in estuarine organisms with changes in releases into Lavaca Bay, Texas. Mar. Pollut. Bull. **44**: 807–815.

Sager, D.R. 2004. Mercury in tissues of selected estuarine fishes from minimally impacted bays of coastal Texas. Bull. Environ. Contam. Toxicol. **72**: 149–156.

Trudel, M., and Rasmussen, J.B. 1997. Modeling the elimination of mercury by fish. Environ. Sci. Technol. **31**: 1716–1722.

Turner, J.P., and Rooker, J.R. 2005*a*. Effect of diet on fatty acid signatures and turnover rates in an estuarine-dependent fish. J. Fish Biol. **67**: 1119–1138.

Turner, J.P., and Rooker, J.R. 2005*b*. Effect of dietary fatty acids on the body tissues of larval and juvenile cobia and their prey. J. Exp. Mar. Biol. Ecol. **322**: 13–27.

Turner, J.P., and Rooker, J.R. 2006. Fatty acid composition of flora and fauna associated with *Sargassum* mats in the Gulf of Mexico. Mar. Biol. **149**: 1025–1036.

US Environmental Protection Agency. 2002. National recommended water quality criteria 2002. USEPA, Washington, D.C. EPA-822-R-02-047.

US Environmental Protection Agency. 2004*a*. National listing of fish advisories. USEPA, Washington, D.C. EPA-823-F-04-016.

US Environmental Protection Agency. 2004*b*. 2004 EPA and FDA advice for women who might become pregnant, woman who are pregnant, nursing mothers, young children 2004. USEPA, Washington, D.C. EPA-823-R-04-005.

Watanabe, K.H., Desimone, F.W., Thiyagarajah, A., Hartley, W.R., and Hindrichs, A.E. 2003. Fish tissue quality in the lower Mississippi River and health risks from fish consumption. Sci. Total Environ. **302**: 109–126.

Watras, C.J., Back, R.C., Halvorsen, S., Hudson, R.J.M., Morrison, K.A., and Wente, S.P. 1998. Bioaccumulation of mercury in pelagic freshwater food webs. Sci. Total Environ. **219**: 183–208.

Wiener, J.G., and Spry, D.J. 1996. Toxicological significance of mercury in freshwater fish. *In* Environmental contaminants in wildlife: interpreting tissue concentrations. *Edited by* W.N. Beyer, G.H. Heinz, and A.W. Redmon-Norwood. Lewis Publishers, Boca Raton, Fla. pp. 297–339.

© 2007 NRC Canada

Wiener, J.G., Krabbenhoft, D.P., Heinz, G.H., and Scheuhammer, A.M. 2003. Ecotoxicology of mercury. *In* Handbook of ecotoxicology. *Edited by* D.J. Hoffman, B.A. Rattner, G.A.J. Burton, and J.J. Cairns. Lewis Publishers, New York. pp. 409–443.

Wilson, C.A., Dean, J.M., Prince, E.D., and Lee, D.W. 1991. An examination of sexual dimorphism in Atlantic and Pacific blue marlin using body-weight, sagittae weight, and age estimates. J. Exp. Mar. Biol. Ecol. **151**: 209–225.

© 2007 NRC Canada

A Bayesian hierarchical meta-analysis of growth for the genus *Sebastes* in the eastern Pacific Ocean

Thomas E. Helser, Ian J. Stewart, and Han-Lin Lai

Abstract: We conducted a meta-analysis of growth for 46 species of the genus *Sebastes* in the eastern Pacific Ocean using a Bayesian hierarchical model to estimate parameters, to investigate growth variability, and to elucidate meaningful biological covariates. Growth in terms of maximum attainable size (L_∞) ranged from 12 to 80 cm, and instantaneous growth rates varied by over an order of magnitude (K; 0.03–0.34·year^{-1}). Results from this method also confirm the theoretical, but often untested, view that growth parameters L_∞ and K are negatively correlated among populations or species of fish; Bayesian credibility intervals for correlation ranged from –0.2 to –0.7, with the posterior median of –0.4. The Bayesian hierarchical growth model showed less variability in growth parameters and lower correlations among parameters than those from standard techniques used in population ecology, suggesting that the absolute value of the correlation between L_∞ and K may be lower than the general perception in the ecological literature. Exploration of several covariates revealed that asymptotic size varied positively as a function of the size at 50% maturity. Finally, posterior probability distributions of the hyperparameters from this analysis provide plausible informative priors of growth for stock assessments of data-poor species.

Résumé : Nous entreprenons une méta-analyse de la croissance de 46 espèces du genre *Sebastes* de l'est du Pacifique à l'aide d'un modèle hiérarchique bayésien afin d'estimer les paramètres de croissance, de déterminer la variabilité de la croissance et de mettre en évidence les covariables d'intérêt biologique. La croissance, vue sous l'angle de la longueur asymptotique (L_∞), varie de 12 à 80 cm et les taux instantanés de croissance varient par un facteur de 10 (K; 0,03–0,34·an^{-1}). Les résultats obtenus par cette méthode confirment aussi la notion théorique, mais souvent non vérifiée, qu'il y a une corrélation négative entre L_∞ et K chez les populations et les espèces de poissons; les intervalles bayésiens de crédibilité pour cette corrélation vont de –0,2 à –0,7 avec une médiane a posteriori de –0,4. Le modèle de croissance bayésien montre moins de variabilité des paramètres de croissance et des corrélations plus faibles entre les paramètres que les méthodologies standard utilisées en démécologie, ce qui laisse croire que la valeur absolue de la corrélation entre L_∞ et K peut être plus faible qu'il n'apparaît dans la littérature écologique. L'examen de plusieurs covariables montre que la taille à l'asymptote varie de façon positive en fonction de la taille à 50 % de maturité. Enfin, les distributions de probabilité a posteriori des hyperparamètres obtenues dans notre analyse fournissent des distributions a priori plausibles et riches en information de la croissance pour faire des évaluations de stocks chez des espèces pour lesquelles il existe peu de données empiriques.

[Traduit par la Rédaction]

Introduction

Species of the genus *Sebastes* represent a diverse array of animals that number ~110 species worldwide, 87% of which are limited to the North Pacific and Gulf of California (Nelson 1994; Love et al. 2002). Rockfish, so named for their affinity to rocky structures, are physically characterized by hard bony structures with large spines, often on their heads. Most common in the eastern Pacific continental shelf and slope waters from Alaska to Baja California, 65 species of rockfish occupy a wide range of depths from nearshore estuarine areas to >2000 m (Eschmeyer and Herald 1983; Love et al. 2002). In addition, rockfish are among the slowest-growing teleosts, many of which live to >100 years old with delayed maturation. In response to complex and variable coastal oceanographic conditions in the eastern Pacific, these long-lived *Sebastes* exhibit a bet-hedging reproductive strategy of producing numerous pelagic larvae spread over a long reproductive life span (Love et al. 2002). However, conditions affording good survival are often rare, and successful juvenile recruitment may be sporadic at best.

Species of fish with such life history traits are often easily overexploited, even under modest fishing. Rockfish in the eastern Pacific off the US west coast have been exploited for

Received 17 May 2006. Accepted 30 October 2006. Published on the NRC Research Press Web site at http://cjfas.nrc.ca on 31 March 2007.
J19324

T.E. Helser,[1] I.J. Stewart, and H.-L. Lai. National Oceanic and Atmospheric Administration, Northwest Fisheries Science Center, 2725 Montlake Boulevard, East Seattle, WA 98112, USA.

[1]Corresponding author (e-mail: thomas.helser@noaa.gov).

 doi:10.1139/F07-024 © 2007 NRC Canada

over a century, but most substantially since 1960 with the advent of distant-water fleets, lead by Russia and Japan, targeting large aggregations over rocky outcrops (Rogers 2003). Although foreign vessels were prohibited from fishing US waters after 1976, technological developments in fishing gear and electronics allowed domestic fleets to find aggregations very effectively (Gunderson 1984) and fish deeper waters. Under increased fishing pressure, the biomass of a number of west coast rockfish has steadily declined, and recent stock assessments indicate that seven major species are currently overfished or under rebuilding plans, including canary (*S. pinniger*), bocaccio (*S. paucispinis*), widow (*S. entomelas*), Pacific ocean perch (*S. alutus*), cowcod (*S. levis*), yelloweye (*S. ruberrimus*), and darkblotched rockfish (*S. crameri*). Although these species and a few others are assessed and managed individually under the Pacific Fishery Management Council's (PFMC) Groundfish Fishery Management Plan, more than 50 others for which a quantitative assessment cannot be performed are managed under aggregate categories (PFMC 2002). Determining stock status of these species remains elusive because of limited biological and population dynamics information; however, many of these may share common life histories, population dynamics, and responses to exploitation.

We take advantage of recent methodological advances, known collectively as meta-analysis, which have emerged as an important tool for summarizing and quantifying variability of population parameters among numerous studies. Hilborn and Liermann (1998) point out that the most important advance in the current fisheries science is the application of meta-analysis. The common feature in meta-analysis is that complete data sets from all studies are used in a combined analysis or estimates from existing studies are summarized. Bayesian methods have often been used as the quantitative framework for employing meta-analysis, and numerous examples are available in the ecological (Ellison 1996; Wade 2000) and fisheries science (Hilborn and Mangel 1997; Punt and Hilborn 1997; Millar 2002) literature. Bayesian methods (Gelman et al. 2004) provide a direct means of parameter estimation and quantification of uncertainty in variance components and model parameters. Application of both hierarchical and Bayesian methods include analysis of stock and recruitment data (Myers et al. 2001; Chen and Holtby 2002), fishery population models (Meyer and Miller 1999; Millar and Methot 2002), and von Bertalanffy growth model parameters (e.g., Essington et al. 2001; Schaalje et al. 2001; Pilling et al. 2002). The last few studies that have analyzed growth of fishes using the von Bertalanffy growth model are particularly cogent to the present study. In particular, Pilling et al. (2002) estimated growth variability among individuals of a population, and Helser and Lai (2004) studied growth variability and related covariates among numerous populations within a species.

In this paper, we extend the use of a Bayesian hierarchical meta-analysis to model growth and its variability and to explore biological covariates of growth among a coherent set of species within a single genus. Furthermore, estimates of hyperparameters provide informative priors for growth of *Sebastes* species for which little or no growth information is available. This study represents the first comprehensive quantitative analysis of growth among species of the genus *Sebastes*, drawing on many available sources of published and unpublished life history data. We use a nonlinear mixed-effects model (Smith and Wakefield 1994; Davidian and Giltinan 1995), in which the functional form is the von Bertalanffy growth model, to integrate information from 46 species of *Sebastes* in the eastern Pacific Ocean.

Materials and methods

Basic data

Data consisting of age (years), total length (cm), weight (kg), sex, and sample location were obtained from the National Marine Fisheries Service (NMFS) Alaska Fishery Science Center's (AFSC) bottom trawl shelf survey (Weinberg et al. 2002), the Pacific Coast Fishery Information Network (PacFIN, commercial samples), and from numerous individual research studies conducted by university, state, and federal agencies. Fish ages were determined either from surface reading or break-and-burn methods from otoliths using generally the same procedures as specified through the Committee of Age Reading Experts (CARE, Pacific States Marine Fisheries Commission (www.psmfc.org/care). For those species for which growth information was available from both commercial and research sources, the research data were preferred unless samples were sparse (few ages represented). In this case, fishery-dependent data were then used to augment samples. From those species where age data were available from multiple stocks (i.e., west coast and Alaska Pacific ocean perch stocks), US west coast data were used to focus growth inferences for *Sebastes* from California to Washington. Of the 65 species of the *Sebastes* genus in the eastern Pacific Ocean, we obtained growth data for 46 species (71%) ranging from central California to the Gulf of Alaska (Table 1).

Sample sizes ranged from as few as nine individual age–length pairs (aurora rockfish, *S. aurora*) to as many as 8413 for widow rockfish. It should be mentioned that data for some species ranged over a number of years, as in the case for widow rockfish, whereas others were limited to a short period of time over which the study was conducted. The number (N) and range of ages sampled for a given species also varied considerably. For instance, pygmy rockfish (*S. wilsoni*) had only 10 age–length samples ranging from ages 2 to 6. In contrast, yelloweye rockfish had over 3800 samples distributed over 92 age groups. To standardize the varied data sets, the growth model was applied only to mean length-at-age for each species weighted by the associated sample size. Also, the maximum number of samples for any age was capped at 30 to prevent unwarranted domination of the model fit by a given age or species.

Nonlinear hierarchical model

A common modeling approach used in population ecology fits the von Bertalanffy growth model (von Bertalanffy 1957) to length-at-age data separately to groups or populations and then summarizes estimates of growth by means and variances. This approach treats all growth parameters as fixed, assumes a common variance for the residuals across all populations, and makes the unrealistic assumption that there is no relationship among groups. With regard to the later point,

© 2007 NRC Canada

Table 1. Source of age information used in the meta-analysis of 46 species of the genus *Sebastes* in the eastern Pacific Ocean.

Scientific name	Rockfish common name	Samples	Ages sampled	*N* ages	Sample type	Region[a]	Years	Source
S. aurora	Aurora	9	2–22	8	Research, commercial	BC	1963–1974	Westrheim and Harling 1975
S. rufus	Bank	1894	15–88	59	Commercial	CA	1977–1988	Cailliet et al. 1996
S. melanops	Black	1136	1–23	23	Research, commercial	CA, OR, WA	1979–1987	Lea et al. 1999; PacFIN
S. chrysomelas	Black-and-yellow	888	1–21	21	Research	CA	1979–1985	Lea et al. 1999; Zaitlin 1986
S. melanostomus	Blackgill	316	3–90	68	Research, commercial	CA	1998–1999	Stevens et al. 2004
S. mystinus	Blue	1696	1–44	41	Reseach, recreational	CA	1978–1998	Laidig et al. 2003
S. paucispinis	Boccacio	1874	1–37	33	Research	CA, OR, WA	1977–1995	A. MacCall[b]
S. auriculatus	Brown	206	2–46	27	Research	WA	1993–2003	J. West[c]
S. dallii	Calico	839	1–11	11	Unknown	CA	pre-1971	Chen 1971
S. pinniger	Canary	691	1–47	35	Research	CA, OR, WA	1978–1995	NMFS; Lea et al. 1999
S. goodei	Chilipepper	3241	1–22	22	Research	CA, OR, WA	1977–1995	NMFS
S. nebulosus	China	114	2–26	22	Research	Central CA	1972–1985	Lea et al. 1999
S. caurinus	Copper	1232	1–41	35	Research, commercial	CA, WA, BC	1978–2003	L. Yamanaka[d]; J. West[c]; Lea et al. 1999
S. levis	Cowcod	88	8–54	33	Commercial, recreational	CA	1975–1986	J. Butler[e]
S. crameri	Darkblotched	1616	1–91	35	Research	CA, OR, WA	1980–2001	NMFS
S. ciliatus	Dusky	1314	3–51	39	Research	AK	1996–2002	D. Hanselman[f]
S. carnatus	Gopher	555	1–24	16	Research	CA	1978–1987	Lea et al. 1999
S. rastrelliger	Grass	153	4–20	16	Research	CA	1973–1987	Lea et al. 1999
S. chlorostictus	Greenspotted	170	2–26	21	Commercial, research	CA, OR, WA	1978–1986	PacFIN; Lea et al. 1999
S. elongatus	Greenstriped	506	3–41	29	Research	AK	1995	G. Shaw[g]
S. variegatus	Harlequin	641	3–47	37	Research	AK	1996	D. Hanselman[f]
S. umbrosus	Honeycomb	1616	1–14	14	Unknown	CA	pre-1971	Chen 1971
S. atrovirens	Kelp	331	1–15	15	Research	Central CA	1978–1987	Lea et al. 1999
S. polyspinis	Northern	5729	2–72	63	Reseach	AK	1984–2002	D. Hanselman[f]
S. serranoides	Olive	405	1–14	14	Research	Central CA	1978–1985	Lea et al. 1999
S. alutus	Pacific ocean perch	5770	1–81	71	Research	CA, OR, WA	1988–2002	NMFS
S. emphaeus	Puget Sound	419	1–13	13	Research	WA	2001–2002	J. West[c]
S. wilsoni	Pygmy	10	2–6	5	Research, commercial	BC	1963–1974	Westrheim and Harling 1975
S. maliger	Quillback	1613	1–73	62	Research, recreational	WA, AK	1989–2003	L. Yamanaka[d]; J. West[c]; D. Hanselman[f]
S. babcocki	Redbanded	924	1–30	30	Research, commercial	BC	1963–1974	Westrheim and Harling 1975
S. proriger	Redstripe	301	4–34	26	Research	AK	1995	G. Shaw[g]
S. helvomaculatus	Rosethorn	194	6–64	44	Research	AK	1995	G. Shaw[g]
S. rosaceus	Rosy	159	3–14	11	Research	Central CA	1978–1982	Lea et al. 1999
S. aleutianus	Rougheye	215	3–73	45	Research	AK	1990	D. Hanselman[f]
S. zacentrus	Sharpchin	923	2–58	44	Research	WA, AK	1995–1999	G. Shaw[g]; D. Hanselman[f]
S. jordani	Shortbelly	2238	1–22	22	Research	CA, OR	1980–1988	Pearson et al. 1991
S. brevispinis	Silvergrey	844	7–75	59	Research	AK	1993–1999	D. Hanselman[f]
S. diploproa	Splitnose	4164	1–68	62	Research	CA, OR, WA	1977–1989	NMFS
S. constellatus	Starry	89	5–19	13	Research	Central CA	1978–1982	Lea et al. 1999
S. saxicola	Stripetail	45	9–20	12	Research, commercial	BC	1963–1974	Westrheim and Harling 1975

© 2007 NRC Canada

Table 1 (*concluded*).

Scientific name	Rockfish common name	Samples	Ages sampled	*N* ages	Sample type	Region[a]	Years	Source
S. ensifer	Swordspine	187	1–14	14	Unknown	CA	pre-1971	Chen 1971
S. miniatus	Vermilion	255	1–33	27	Research, commercial	CA, OR, WA	1978–1987	Lea et al. 1999; PacFIN
S. entomelas	Widow	8413	3–43	37	Commercial	CA, OR, WA	1988–2002	PacFIN
S. ruberrimus	Yelloweye	3864	4–102	92	Commercial, research	CA, OR, WA	1978–2003	L. Yamanaka[d]; PacFIN; Lea et al. 1999
S. reedi	Yelloweye	1470	4–29	26	Research, commercial	BC	1963–1974	Westrheim and Harling 1975
S. flavidus	Yellowtail	64	1–20	13	Research	Central CA	1978–1985	Lea et al. 1999

[a]BC, British Columbia; CA, California; OR, Oregon; WA, Washington; AK, Alaska; PacFIN, Pacific States Marine Fisheries Commission; NMFS, National Marine Fisheries Service.
[b]Alec MacCall, NMFS, Southwest Fisheries Science Center, 110 Shaffer Road, Santa Cruz, CA 95060, personal communication.
[c]James West, Washington Department of Fish and Wildlife, 600 Capitol Way N., Olympia, WA 98501, personal communication.
[d]Lynne Yamanaka, Fisheries and Oceans Canada, 3190 Hammond Bay Road, Nanaimo, BC V9T 6N7, Canada, personal communication.
[e]John Butler, National Marine Fisheries Service, Southwest Fisheries Science Center, 8604 La Jolla Shores Drive, La Jolla, CA 92037, personal communication.
[f]Dana Hanselman, National Marine Fisheries Service, Alaska Fisheries Science Center, Auke Bay Laboratory, 11305 Glacier Highway, Juneau AK 99801, personal communication.
[g]Gary Shaw, National Marine Fisheries Service, Alaska Fisheries Science Center,7600 Sand Point Way N.E., Building 4, Seattle, WA 98115, personal communication.

such models would tend to be over-parameterized, fit the data well, but provide inferior predictions for new data. We applied this method as a point of comparison with the hierarchical model.

For the von Bertalanffy growth model, mean lengths-at-age can be symbolized by mean lengths L_{ij} at ages T_{ij}, where $j = 1, 2, \ldots, n_i$ ages and $i = 1, 2, \ldots, N$ groups or species. In the simplest case, the lengths-at-age of species i can be fitted to its own von Bertalanffy growth model:

$$(1) \qquad L_{ij} = L_{\infty i}\left[1 - e^{-K_i(T_{ij} - t_{0i})}\right] + \varepsilon_{ij}$$

where K_i is frequently known as the Brody growth coefficient (year^{-1}), $L_{\infty i}$ is the asymptotic length (cm), t_{0i} is the x-axis intercept of the equation, and ε_{ij} is the within-group random error, assumed to be normally distributed with zero mean and common variance σ_ε^2 (i.e., $\varepsilon_{ij} \sim N(0, \sigma_\varepsilon^2)$). The growth parameter vector, $\boldsymbol{\theta}_i = (L_{\infty i}, \ln K_i, t_{0i})$, characterizes the growth of the species i.

Next, consider a mixed-effects model, which imposes additional structure on $\boldsymbol{\theta}_i$ random components of a common distribution. In the mixed-effects model, each $\boldsymbol{\theta}_i$ is assumed to be a random sample from a population of growth parameters (i.e., from all species of the genus *Sebastes* in the eastern Pacific Ocean). This population is assumed to be characterized by a multivariate normal distribution, with mean vector $\boldsymbol{\mu} = (L_\infty, \ln K, t_0)'$ and variance–covariance matrix $\boldsymbol{\Sigma}$. That is,

$$(2) \qquad \boldsymbol{\theta}_i = \begin{pmatrix} L_{\infty i} \\ \ln K_i \\ t_{0i} \end{pmatrix} \sim \text{MVN}(\boldsymbol{\mu}, \boldsymbol{\Sigma}), \quad \text{for } i = 1, 2, \ldots, N$$

where

$$(3) \qquad \boldsymbol{\Sigma} = \begin{bmatrix} \sigma_{L_\infty} & \sigma_{L_\infty \ln K} & \sigma_{L_\infty t_0} \\ \sigma_{L_\infty \ln K} & \sigma^2_{\ln K} & \sigma_{\ln K t_0} \\ \sigma_{L_\infty t_0} & \sigma_{\ln K t_0} & \sigma^2_{t_0} \end{bmatrix}$$

K is assumed to be log-normally distributed, for which $\ln K$ is the natural logarithm of K, because K on the linear scale has the potential to include negative values, as pointed out by Sainsbury (1980), which lead him to assume a gamma distribution. In a preliminary analysis, values of K from fitting the model to the data showed a pronounced right skew, which were then normalized by taking logarithm transformation. Thus, estimating $\ln K$ is preferable to K from both practical and theoretical standpoints (Pilling et al. 2002). The joint distributions among the parameters are bivariate normal–normal and normal–lognormal to accommodate both the different marginal distributions and their correlation structures. Chen and Holtby (2002) describe properties associated normal–lognormal joint distributions in hierarchical models.

Equations 2 and 3 follow a typical linear model that contains only a grand mean (Seber 1977):

$$(4) \qquad \begin{pmatrix} L_{\infty i} \\ \ln K_i \\ t_{0i} \end{pmatrix} = \begin{pmatrix} L_\infty \\ \ln K \\ t_0 \end{pmatrix} + \begin{pmatrix} e_{L_{\infty i}} \\ e_{\ln K_i} \\ e_{t_{0i}} \end{pmatrix}$$

© 2007 NRC Canada

or more conveniently in matrix form as

$$\boldsymbol{\theta}_i = \mathbf{X}_i \boldsymbol{\mu} + \boldsymbol{\varepsilon}_i \quad (5)$$

where

$$\mathbf{X}_i = \begin{pmatrix} 1 & 0 & 0 \\ 0 & 1 & 0 \\ 0 & 0 & 1 \end{pmatrix}, \quad \boldsymbol{\varepsilon}_i \sim \mathrm{MVN}(\mathbf{0}, \boldsymbol{\Sigma}), \quad \text{and } \boldsymbol{\theta} = (0, 0, 0) \quad (6)$$

Combining eqs. 1, 2, and 4 give the nonlinear mixed-effects model (Pinheiro and Bates 2000). The mean vector $\boldsymbol{\mu}$ is also referred to as the population average or population fixed effects, and the within-group and between-group errors, ε_{ij} and $\boldsymbol{\varepsilon}_i$, respectively, are the random effects (Bryk and Raudenbush 1992; Pinheiro and Bates 2000). Estimated hyperparameters are $\boldsymbol{\mu}$, $\boldsymbol{\Sigma}$, and σ_ε^2 with species-specific growth parameters $\boldsymbol{\theta}_i$.

Nonlinear hierarchical model with covariates

The existing body of literature on rockfish has suggested sexually dimorphic growth and that growth for a given species may be correlated with depth and size at maturity. While any given species may be distributed over numerous depths, we used the 50th percentile of the empirical cumulative catch-weighted depth distribution from the AFSC research survey to derive a single value, which represents the centroid of the depth distribution for each species. In addition, the estimated length at 50% maturity for many rockfish was compiled from the available literature. We first examined whether the fixed-effect parameter estimates between males and females differed enough to warrant further exploration of covariates for the sexes separately. We then reparameterized the growth parameter vector as a linear function of a given continuous covariate (x_i):

$$\boldsymbol{\theta}_i = \begin{pmatrix} L_{\infty i} \\ \ln K_i \\ t_{0i} \end{pmatrix} = \begin{pmatrix} \alpha_{1i} + \beta_{1i} x_i \\ \alpha_{2i} + \beta_{2i} x_i \\ \alpha_{3i} + \beta_{3i} x_i \end{pmatrix} + \boldsymbol{\varepsilon}_i = \mathbf{X}_i \boldsymbol{\beta} + \boldsymbol{\varepsilon}_i \quad (7)$$

where $\boldsymbol{\varepsilon}_i \sim \mathrm{MVN}(\mathbf{0}, \boldsymbol{\Sigma})$, which, expressed in a form comparable to eq. 2, is

$$\boldsymbol{\theta}_i = \begin{pmatrix} L_{\infty i} \\ \ln K_i \\ t_{0i} \end{pmatrix} \sim \mathrm{MVN}(\mathbf{X}_i \boldsymbol{\beta}, \boldsymbol{\Sigma}), \quad \text{for } i = 1, 2, \ldots, N \quad (8)$$

where $\boldsymbol{\beta} = (\alpha_1, \beta_1, \alpha_2, \beta_2, \alpha_3, \beta_3)'$ and

$$\mathbf{X}_i = \begin{bmatrix} 1 & x_i & 0 & 0 & 0 & 0 \\ 0 & 0 & 1 & x_i & 0 & 0 \\ 0 & 0 & 0 & 0 & 1 & x_i \end{bmatrix}$$

Thus, the hyperparameters to be estimated are either $\boldsymbol{\mu}$ or $\boldsymbol{\beta}$, σ_ε^2, and $\boldsymbol{\Sigma}$, with the same parameters $\boldsymbol{\theta}_i$.

Computational aspects using Bayesian inference

A Bayesian hierarchical model can be written as

$$p(\boldsymbol{\theta}, \phi | \mathbf{y}) \propto p(\phi) p(\boldsymbol{\theta} | \phi) p(\mathbf{y} | \boldsymbol{\theta}) \quad (9)$$

The joint posterior probability of the hyperparameters (ϕ) and the parameters ($\boldsymbol{\theta}$) given the data ($\mathbf{y}$) (the posterior) is proportional to the probability of the hyperparameters (the hyperprior) multiplied by the probability of the parameters given the hyperparameters (the prior) and by the probability of the data given the parameters (the likelihood). In this case, the data are individual lengths-at-age, the parameters remain $\boldsymbol{\theta}_i$ from above, and the hyperparameters are $\boldsymbol{\mu}$ or $\boldsymbol{\beta}$, σ_ε^2, and $\boldsymbol{\Sigma}$.

In the Bayesian analysis, we are interested in two types of inference: (*i*) the posterior distribution of the parameters describing the growth curve for each individual species with data in the analysis and (*ii*) inferences for a species not included in the current analysis (Minte-Vera et al. 2005). For (*i*),

$$p(\boldsymbol{\theta}_i | \mathbf{y}) \propto \int_\phi p(\boldsymbol{\theta}_i, \phi | \mathbf{y}) \, \mathrm{d}\phi \quad (10)$$

By integrating out the hyperparameters, which depend on the data for all of the species, this model framework lends strength of inference across species. Specifically, the posterior distribution for one species' parameters shrink toward the group mean when data are lacking or are uninformative. The posterior distribution of the parameters for a new species $\bar{\boldsymbol{\theta}}$ will be

$$p(\bar{\boldsymbol{\theta}}_i | \mathbf{y}) \propto \int_\phi \int_{\boldsymbol{\theta}} p(\bar{\boldsymbol{\theta}} | \phi) \, p(\boldsymbol{\theta}, \phi | \mathbf{y}) \, \mathrm{d}\boldsymbol{\theta} \, \mathrm{d}\phi \quad (11)$$

To fit the model to the data using a Bayesian approach, prior probability distributions for the hyperparameters, $\boldsymbol{\mu}$ (or $\boldsymbol{\beta}$), $\boldsymbol{\Sigma}$, and σ_ε^2, need to be specified. Smith and Wakefield (1994) suggest, that priors should be noninformative to ensure that the likelihood dominates the prior. We endorsed this approach, as no study of rockfish growth to date had elicited prior information on the growth hyperparameters. As such, the priors for $\boldsymbol{\mu}$ (or $\boldsymbol{\beta}$) were diffuse, multivariate normal distributions, with zero mean and covariance matrix with diagonal elements equal to 1000 and off-diagonal elements equal to zero. The prior for $\boldsymbol{\Sigma}$ was specified by an inverted Wishart distribution (Von Rosen 1997), with precision parameter of 10 and mean matrix $0.1 \times \mathbf{I}$. The prior for the inverse within-group variance, σ_ε^{-2}, is a gamma distribution with scale and shape parameters each equal to 0.001. These values were selected to ensure that the priors are relatively flat over relevant parameter space.

WinBUGS (Bayesian inference Using Gibbs Sampling, Thomas et al. 1992; Spiegelhalter et al. 1999) was used to fit the model to the data. The estimates of parameters were evaluated based on 1 000 000 samples, thinned to one draw every 1000th sample, from Markov chain Monte Carlo (MCMC) simulation of the joint posterior distribution. Multiple Bayesian diagnostic procedures were performed to evaluate convergence of the MCMC simulation to a stationary posterior distribution for all estimated quantities in the model (Cowles and Carlin 1996; Brooks and Gelman 1997). We monitored autocorrelation at various lags and applied both the test statistic of Heidelberger and Welch (1983) to assess whether adequate burn-in had been achieved and a test for stationarity of the mean from Geweke (1992). In addition, we examined model goodness of fit to the data and

© 2007 NRC Canada

Fig. 1. Bayesian hierarchical growth model fit to 46 species of the genus *Sebastes* in the eastern Pacific Ocean illustrating growth differences between male and female rockfish. Posterior median values of the asymptotic size (L_∞) and ln$K$ (square, females; circle, males) along with 95% credibility ellipses (broken line, females; solid line, males) about the mean fixed effects illustrate differences in growth between the sexes. Ellipses shown are derived from a Cholesky root decomposition of 1000 Markov chain Monte Carlo (MCMC) samples of the stationary posterior distribution.

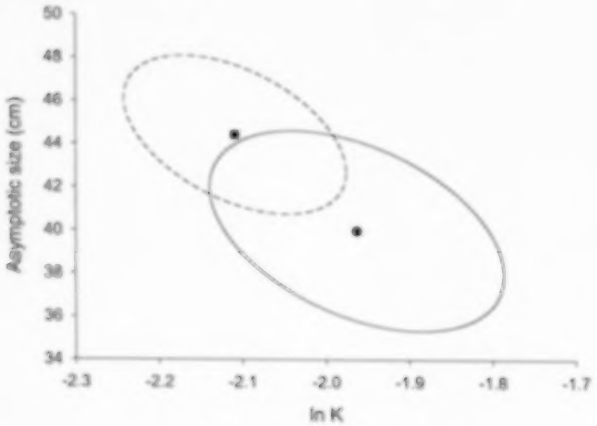

sensitivity of model results to specification of prior parameter distributions as prescribed in Gelman et al. (2004).

Results

Length-at-age data

Preliminary model exploration revealed that female rockfish grew slightly slower than males, but attained a larger asymptotic size of 45 cm vs. 40 cm for males (Fig. 1). Bayesian 95% credibility ellipses for each sex just barely encompassed the mean fixed effects of the von Bertalanffy growth parameters L_∞ and ln$K$. In fact, there is substantial probability that females grow as much as 10 cm larger than males. We posit that such differences in growth are biologically meaningful and that a separate sex model can be justified on the basis that stock assessment models commonly employ sex-specific growth functions. As such, we treat the basic growth data for the sexes separately and fit the basic hierarchical model and model with covariates accordingly.

The basic growth data, mean lengths-at-age across all species (Fig. 2), display the characteristic functional growth form of fish, where size increases with age to an asymptote. The mean lengths-at-age for each sex appear to be consistent up to ~50 years of age, with standard deviations generally equivalent after age 15. Beyond age 50, relatively few species contribute to the analysis. In general, we assume the von Bertalanffy growth model to be a reasonable approximation to these growth data and that the error variance of the model is additive.

Fig. 2. Box-and-whisker plots of mean length-at-age data (weighted by n at age) from 46 species of the genus *Sebastes* for (*a*) females and (*b*) males in the eastern Pacific Ocean used in the Bayesian hierarchical growth model.

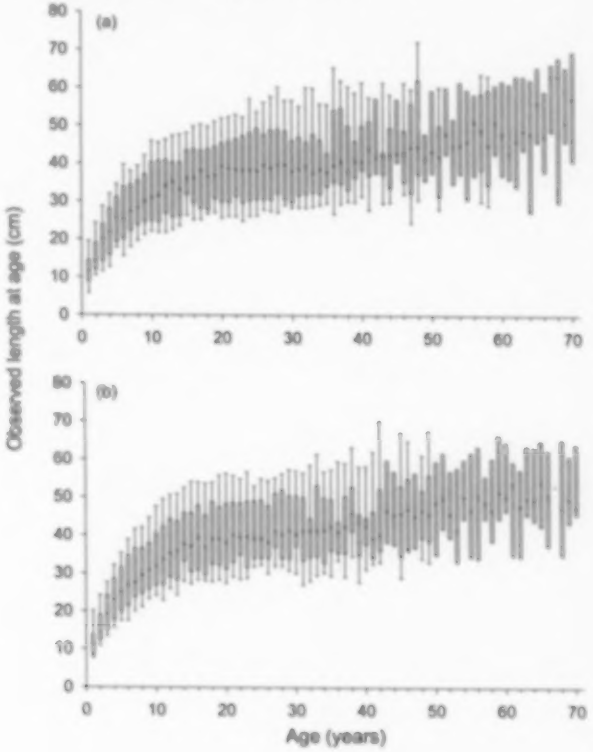

Nonlinear hierarchical model

The means of the three growth parameters from the basic method of fitting growth curves separately to each species were essentially identical to the mean fixed effects from the hierarchical nonlinear model (Table 2). The expected asymptotic size for males of species of the genus *Sebastes* in the eastern Pacific Ocean was estimated to be ~40 cm in length, with a growth rate of 0.136 cm·year^{-1} (or ln$K$ = −1.993), whereas females were 45 cm in length, with a growth rate of 0.121 cm·year^{-1} (or ln$K$ = −2.115). However, the variances associated with the three growth parameters (random effects in the model) estimated from the nonlinear hierarchical model are all substantially smaller than mean variances based on the simple overparameterized method (Table 2). This result is commonly associated with hierarchical models because the model explicitly incorporates among-population variance from the pooled data, resulting in shrinkage. The process of shrinking in hierarchical models, pulling the individual population parameter estimates toward the group mean, provides more reliable and generally lower estimates of growth variability. This is an advantage for so-called data-poor species, in which information is borrowed from the others. The estimated growth curve trajectories are given for the mean fixed effects superimposed over the individual species trajectories (Fig. 3). The graph illustrates the

© 2007 NRC Canada

Table 2. Summary statistics for the basic sex-specific Bayesian hierarchical growth model fit to 46 species of the genus *Sebastes* in the eastern Pacific Ocean.

	Male				Female			
		Hierarchical meta-analysis				Hierarchical meta-analysis		
	Means of nonlinear regression models	Bayesian credibility intervals			Means of nonlinear regression models	Bayesian credibility intervals		
Parameter	Estimate	Median	5%	95%	Estimate	Median	5%	95%
Mean								
L_∞	41.184	40.350	37.070	43.431	45.862	45.100	41.409	48.681
ln$K$	−1.969	−1.993	−2.171	−1.825	−2.115	−2.129	−2.309	−1.949
t_0	−3.356	−2.603	−3.566	−1.822	−2.909	−2.563	−3.545	−1.786
Variance								
L_∞	162.231	136.400	90.208	213.110	206.100	157.300	106.275	243.830
ln$K$	0.364	0.275	0.177	0.437	0.452	0.289	0.184	0.504
t_0	55.771	5.345	2.845	9.707	21.321	5.778	2.906	11.154
Correlation								
L_∞, ln$K$	−0.849	−0.415	−0.663	−0.091	−0.876	−0.471	−0.700	−0.205
L_∞, t_0	−0.657	−0.149	−0.470	0.187	−0.690	−0.289	−0.562	0.018
ln$K$, t_0	0.907	0.728	0.505	0.856	0.909	0.873	0.723	0.947
Error variance (σ_ε^2)	13.695	3.576	3.455	3.717	13.407	5.158	4.988	5.364

Note: Values shown compared parameter estimates from the standard approach of fitting the nonlinear growth model separately to each species (summarized by taking means) with the basic hierarchical model. Bayesian credibility intervals (5%, 50%, and 95%) are based on 1000 Markov chain Monte Carlo (MCMC) samples from a stationary posterior distribution.

Fig. 3. Fitted growth trajectories of (*a*) males and (*b*) females for 46 species of the genus *Sebastes* in the eastern Pacific Ocean estimated from the Bayesian hierarchical growth model. Curves shown were taken from the posterior median mean length-at-age for the mean fixed effects (bold lines) and for each species (thin lines) from 1000 Markov chain Monte Carlo (MCMC) samples from a stationary posterior distribution.

large amount of variability in the individual species' growth curves from the overall mean and represents the information content in the data from all species in the analysis.

Bayesian credibility intervals (5%, 50%, 95%) of the joint posterior distribution for all model parameters show that the mean fixed effects are precisely estimated (Table 2). For instance, mean fixed effects for L_∞ for males within the *Sebastes* complex narrowly ranges between 37.07 and 43.43 cm and between −2.171 and −1.825 for ln$K$. In contrast, the L_∞ for females range between 41.41 and 48.68 cm and between −2.309 and −1.949 for ln$K$. Results showing the extent that individual population growth parameter coefficients (random effects) differ from the overall mean fixed parameter coefficients for all populations (fixed effects) are quantified in term of the parameter variances, given by $\boldsymbol{\Sigma}$, and were $\sigma^2_{L_\infty}$ = 136.4 and $\sigma^2_{\ln K}$ = 0.275 for males and $\sigma^2_{L_\infty}$ = 157.3 and $\sigma^2_{\ln K}$ = 0.289 for females (Table 2). These variance components were all substantially different from zero, as indicated by 5% and 95% credibility intervals.

Correlations among the growth parameters were substantially lower from the hierarchical model than those from the basic method, which may not be completely unexpected, based on the shrinkage properties resulting in lower

© 2007 NRC Canada

Fig. 4. Bivariate posterior distributions of median, 90%, and 95% credibility ellipses for the hierarchical model fixed effects (medians, solid circles; 95% ellipse, solid lines) and random effects (medians, open circles; 90% ellipse, inner short dash; 95% ellipse, outer long dash) for asymptotic size (L_∞), transformed growth coefficient (ln$K$), and intercept (T_0). Parameter values estimated from the hierarchical model is shown for males (left panels) and females (right panels). Ellipses shown are derived from a Cholesky root decomposition of 1000 Markov chain Monte Carlo (MCMC) samples of the stationary posterior distribution.

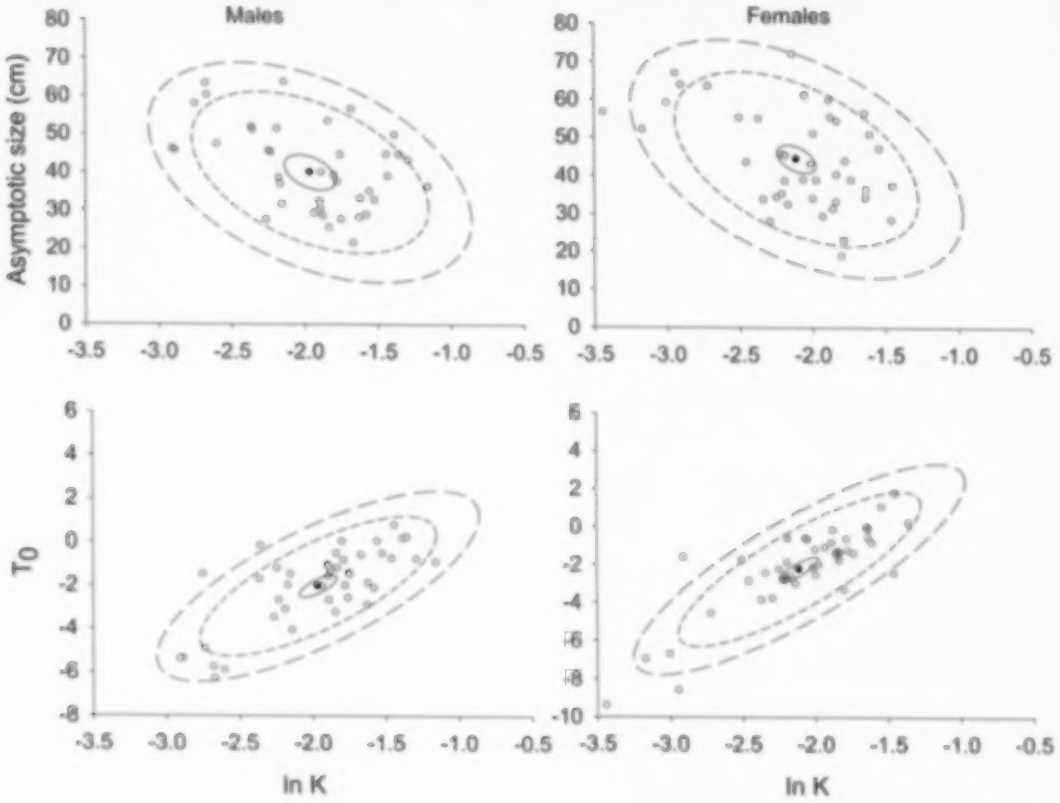

parameter variances from the hierarchical model (Table 2). Correlations between the parameters L_∞ and K, which are generally assumed to be negative in most studies on growth of fishes, were indeed estimated to be moderately negatively correlated based on both the basic method and the nonlinear hierarchical model (Fig. 4). We also found evidence of correlation between the parameters K and t_0, but not between L_∞ and t_0 for both males and females. In this analysis, Bayesian posterior modes of the individual species along with posterior credibility ellipses illustrate several important results of this analysis (Fig. 4). First, correlation between L_∞ and K from the nonlinear hierarchical model conformed to the original assumption of a normal–lognormal marginal distribution for those parameters and hence a bivariate normal–lognormal joint distribution. Second, the degree of correlation is consistent for both sexes, and the joint parameters appear to mimic a common joint distribution of random effects being modeled. These posterior modes illustrate the extent of variability in correlation between L_∞ and K likely to be encountered for species of the genus *Sebastes* in the eastern Pacific. Variability in the correlation is further quantified by credibility intervals from the Bayesian hierarchical model, which ranged between –0.663 and –0.091 for males and –0.700 and –0.205 for females. Correlation between growth parameters was substantially weaker than is frequently reported in the literature, often in the range of –0.8 to –0.9. Such inflated negative correlations between estimates of L_∞ and K likely result from estimation error in fitting the growth model to individual fish within a population of a species and statistical correlation between parameters.

Nonlinear hierarchical model with covariates

Fitting the hierarchical growth model with depth as a covariate revealed little evidence that the growth parameters vary as a function of depth (Table 3). Credibility intervals of the slope (β) parameter for L_∞ and ln$K$ and for both male and female hierarchical models showed nearly equal mass on both sides of zero. In contrast, the length at 50% maturity was an informative covariate in the hierarchical model for females. Here, the asymptotic size (L_∞) increased as a function of the length at 50% maturity, whereas ln$K$ declined (Table 3). Based on Bayesian credibility intervals, the entire mass of the marginal posterior for slope of L_∞ occurred above zero, indicating a strong positive relationship. There is, however, some mass of the

© 2007 NRC Canada

Table 3. Bayesian credibility intervals (median, 5%, 95%) from the joint posterior distribution of hyperparameters for the female and male Bayesian hierarchical meta-analysis with depth and length at 50% maturity included as covariates.

	Females covariates						Male covariates		
	Depth			Length at 50% maturity			Depth		
Parameter	Median	5%	95%	Median	5%	95%	Median	5%	95%
Fixed effect									
$L_\infty = f(\alpha + \beta\text{covariate})$									
α	45.930	39.818	52.371	15.525	10.558	21.728	41.700	36.600	46.550
β	−1.054	−6.376	4.093	0.973	0.796	1.127	−1.373	−5.645	2.773
$\ln K = f(\alpha + \beta\text{covariate})$									
α	−2.109	−2.465	−1.780	−1.673	−2.267	−1.129	−1.969	−2.264	−1.702
β	−0.009	−0.284	0.264	−0.013	−0.030	0.004	−0.014	−0.238	0.217
$t_0 = f(\alpha + \beta\text{covariate})$									
α	−2.938	−4.537	−1.510	−1.720	−4.507	0.565	−3.269	−4.512	−2.080
β	0.442	−0.852	1.651	−0.023	−0.096	0.057	0.703	−0.336	1.761
Random effect									
Variance									
L_∞	163.000	109.985	246.160	35.430	22.500	58.163	134.850	93.402	203.715
$\ln K$	0.292	0.186	0.509	0.235	0.150	0.380	0.275	0.175	0.444
t_0	5.606	3.056	11.203	5.425	2.758	10.066	4.781	2.682	8.978
Correlation									
L_∞, $\ln K$	−0.490	−0.700	−0.162	−0.353	−0.611	−0.004	−0.415	−0.643	−0.127
L_∞, t_0	−0.278	−0.556	0.098	−0.283	−0.576	0.101	−0.148	−0.457	0.220
$\ln K$, t_0	0.865	0.737	0.946	0.867	0.712	0.944	0.737	0.543	0.858
Error variance (σ_ε^2)	5.161	4.983	5.353	5.162	4.982	5.347	3.587	3.454	3.703

Note: α and β are the intercepts and slopes, respectively, of the functional relationship of each growth parameter, $f(\alpha + \beta\text{-covariate})$. Values given are based on 1000 Markov chain Monte Carlo (MCMC) samples from a stationary posterior distribution.

marginal posterior of the slope of $\ln K$ that is positive, suggesting a slightly weaker negative relationship between $\ln K$ and size at maturity; these relationships are confirmed graphically (Fig. 5).

Model diagnostics and performance

Diagnostic results of the thinned MCMC sampling chain indicated that the joint posterior distribution for all model parameters had converged to a stationary distribution. A graphical summary of the MCMC chain convergence diagnostics for all 142 model parameters for the female meta-analysis model with length-at-maturity as a covariate illustrates convergence to a stationary distribution (Fig. 6). The histograms reveal that autocorrelations at lag-one within the thinned sampling chain were less than 0.2 for all but less than 5% of the 142 parameters in the hierarchical model (Fig. 6*a*). Although this level of correlation does not necessarily provide full independence among samples in the chain, exploration of various thinning and chain lengths did not appreciably change the percentiles of the posterior distributions. This is corroborated by the effective sample sizes for most model parameters, accounting for autocorrelation, which were ≥900 (Fig. 6*b*). The distribution of Geweke statistics (which can be interpreted on the same scale as a standard normal z score) for each model parameter indicates nearly all fell within the interval ±1.96 (Fig. 6*b*). Extreme values, at a rate of 5%, would be expected because of random chance even in completely independent chain sequences. Finally, the Heidelberger and Welch statistic provides an additional check on whether a longer initial burn in phase should be trimmed from the chain; in this case, none is needed (Fig. 6*c*).

Predictive posterior checks comparing the observed percentiles (original data) and percentiles generated from the Bayesian posterior median lengths-at-age for all species in the base sex-specific models showed that the model was consistent with the data. Fiftieth, 25th, and 75th percentiles all indicated a good fit of the nonlinear hierarchical model to the data (Fig. 7). Predictive posterior median length-at-age generated from the MCMC sample of the joint posterior were consistent with the same percentiles of the original mean length-at-age data; departures in fit of the model to the observed data would be shown as deviations off a 1:1 diagonal line. Some departures are seen in the older age groups, which would not be unexpected because of fewer mean lengths-at-age data, but generally no lack of fit is particularly evident as consistent deviations either above or below the diagonal line.

As a final diagnostic check, we examined the sensitivity of this analysis to alternative assumptions for the prior probability distributions of model parameters. The hierarchical nonlinear model parameter estimates based on the joint posterior were largely insensitive to different choices of priors. For instance, an order of magnitude reduction in the variances associated with the multivariate normal distributions of the fixed parameters (precision = 100 vs. 1000 for the

© 2007 NRC Canada

Fig. 5. The functional relationships between the model's fixed-effect parameters (L_∞ and ln$K$) and the length at 50% maturity covariate for the female hierarchical growth model of the genus *Sebastes*. The solid line shows the predicted relationship generated from the models fixed-effect parameter estimates and length at 50% maturity. (*a*) Change in asymptotic size (L_∞) with size at 50% maturity: $L_\infty = \alpha + \beta L_{50}$. (*b*) Change in ln$K$ with size at 50% maturity: $\ln K = \alpha + \beta L_{50}$. Individual points show the posterior median of the random-effect parameter estimates of L_∞ and ln$K$ for each species.

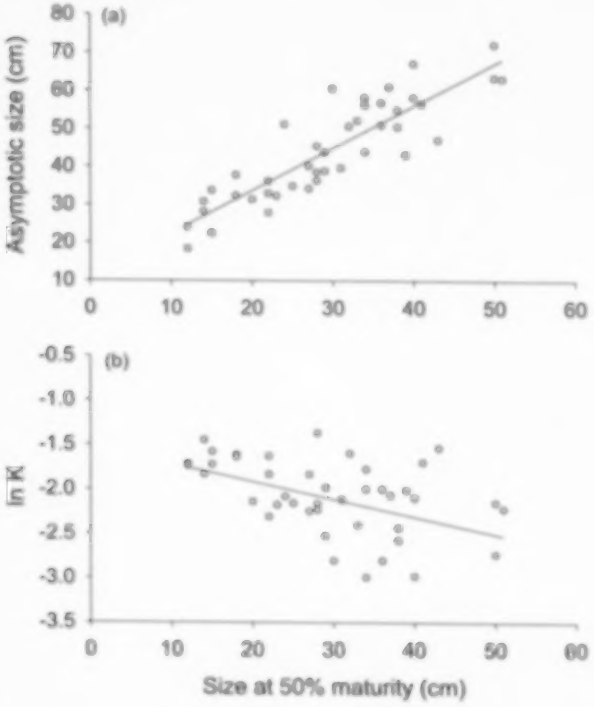

base case) and a similar reduction in the variance associated with the Wishart distribution (precision = 1 vs. 10 in the base case) resulted in less than a 4% decrease in the credibility interval of the marginal posterior distribution for any given parameter. Model results were also insensitive to an increase (order of magnitude) in precision associated with the parameters of the gamma distribution as well as using a noninformative uniform distribution on the error variance (σ_ε^2). In this analysis, the stability of the hierarchical nonlinear model under different prior assumptions indicates that the likelihood clearly dominated the priors.

Type *i* and type *ii* inferences

Posterior probability distributions were produced for males and females of each of the 46 species for which we had data; these represent the type *i* inference described above. These distributions and the covariance structure in the growth parameters are informed by a combination of the species-specific data and the data from other species through the hierarchical model structure. These posterior distributions can be used as informative priors for future growth analyses or stock assessments where the data included in this analysis will not be reused. Grass rockfish, *Sebastes rastrelliger*, illustrates how growth parameter estimates (and growth function of expected length-at-age) are updated and made more realistic in data-poor situations through the use of meta-analysis (Fig. 8). The updated growth trajectory for this species also illustrates the property of shrinkage, where parameter estimates from a data-poor situation are shrunk toward the mean generated from all species in the analysis.

For species that were not included here, the posterior distribution for an unobserved rockfish species (i.e., type *ii* inference) can be used as an informative prior for future analyses. The posterior distribution of length-at-age for unobserved male and female rockfish species are shown (Fig. 9). These curves illustrate the expected growth trajectory and plausible range of length-at-age about the mean and are fully specified by the hyperparameter estimates from the meta-analysis (Table 2). These distributions are broad, but reflect the weight of evidence for the covariance structure and plausible range of parameter values drawn from all 46 species analyzed here.

Discussion

Species of the genus *Sebastes* in the eastern Pacific Ocean have been widely studied, and dozens of von Bertalanffy growth curves have been generated for these rockfishes. Most studies have focused on a single or several geographically diverse populations of rockfish, and only a few have analyzed more than a handful of species (Chen 1971; Westrheim and Harling 1975; Lea et al. 1999). Love et al. (2002) have compiled probably the largest collection of growth curves of the rockfishes in the eastern Pacific from their work and the work of other investigators. In all these cases, growth curves were fit individually to each species, sexes were often fit separately, and little or no quantitative information on between-species variability in parameter estimates was reported. In the present study, we have revisited the analysis of rockfish growth from the perspective of simultaneously fitting the von Bertalanffy model to growth data on 46 *Sebastes* species to quantify the inherent between-species variability in parameter estimates and correlation structures and examine potential covariates with growth.

Within the genus *Sebastes*, females of a given species can be expected to grow generally larger but at slower rate than males of the same species. This is not a unique finding; other growth studies of rockfish have reported sexually dimorphic growth (Workman et al. 1998; Love et al. 2002; Laidig et al. 2003), although other studies have reported little difference in growth between sexes (O'Connell et al. 1986; Love et al. 2002). Generally, variability in the growth parameters, particularly L_∞, was greater among females than among males of *Sebastes* species. This phenomenon is not generally understood but may represent a variable response to metabolic demands for maturation and the trade-off between somatic vs. reproductive growth.

Negative correlation between L_∞ and K from this study of rockfish and studies of other fish taxa confirm conventional ecological wisdom of the negative correlation between the asymptotic size and growth. In theory, the inverse relation in

© 2007 NRC Canada

Fig. 6. Histograms of Markov chain Monte Carlo (MCMC) convergence diagnostics for all 142 model parameters indicating low autocorrelation at lag-one (*a*), Geweke statistic (*b*), effective sample size >900 for most model parameters (*c*), and Heidelberger–Welch statistic (*d*). Geweke statistic indicates no significant departure from the predicted distribution (standard normal); Heidelberger–Welch statistic indicates adequate burn-in of the MCMC chain.

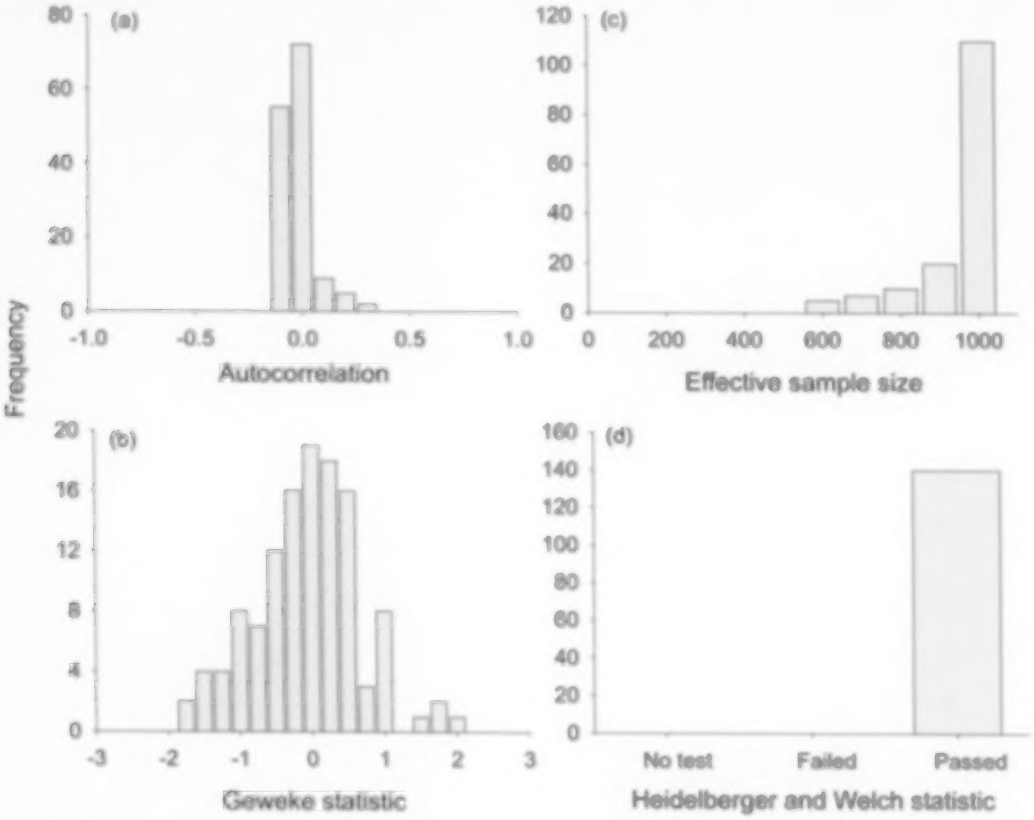

the von Bertalanffy growth parameters represents the trade-off between growth and reproduction such that high rates of growth lead to more rapid onset of maturity and ultimately smaller asymptotic sizes (von Bertalanffy 1957; Beverton 1992). However, as Pilling et al. (2002) pointed out, in practice few studies present direct evidence based on analysis of many populations or species within a taxon, and these parameters are actually negatively correlated in fish populations. In fact, most studies to date that have reported the correlation between L_∞ and K for a single population are most likely dominated by statistical correlation between the parameters and not really representing the biological correlation. Results presented in this study suggests that although correlated, the asymptotic size and growth coefficient are not as strongly related as generally perceived in the literature, often in the range of –0.8 to –0.9 (Hampton and Majkowski 1987; Quinn and Deriso 1999; He and Stewart 2001). Based on this study and several others, the more diverse the taxonomic group of fish is, the weaker the correlation becomes. For instance, Pilling et al. (2002) found the within-population correlation among individual fish to be on the order of –0.69 (or –0.42 using a hierarchical model), and Helser and Lai (2004) found the correlation between populations within a species to be approximately –0.6. In this study of between-species correlation of L_∞ and K within the broader taxonomic classification of the genus *Sebastes*, we found an even lower correlation of only –0.4. Across a still broader taxonomic classification of 85 species in numerous families of fishes, He and Stewart (2001) found a –0.2 correlation. In general, these results indicate that the correlation between L_∞ and K may be as much as 50% less when using hierarchical modeling compared with fitting populations or species separately.

Various environmental factors are known to affect growth in fishes, among them temperature and food availability (Jobling 1981). We did not find evidence that suggests depth, which may be correlated with temperature, to be correlated with growth of rockfishes. Although a number of nearshore rockfishes are generally known to be shorter-lived, and thus growth to smaller asymptotic sizes (Love et al. 2002) might imply such a relationship, the single value of depth that was used to describe the centroid of the species' distribution may be an inadequate independent covariate to capture this phenomenon. We suggest additional work is needed to explore other meaningful covariates. We did find size at 50% maturity to be a meaningful biological covariate

© 2007 NRC Canada

Fig. 7. Predictive posterior checks showing a comparison of selected observed quantiles (median: *a* and *d*; 25%: *b* and *e*; 75%: *c* and *f*) based on the original observed data and similar quantiles generated from the posterior distribution for the male (*a*, *b*, *c*) and female (*d*, *e*, *f*) *Sebastes* hierarchical growth models. Scatter of the observed mean length at age quantiles and posterior quantiles close to a 1:1 line indicate that joint posterior generated from the Markov chain Monte Carlo (MCMC) sample is consistent with the observed data, hence providing a good model fit. Percentiles of the posterior are based on 1000 MCMC samples of a stationary joint posterior.

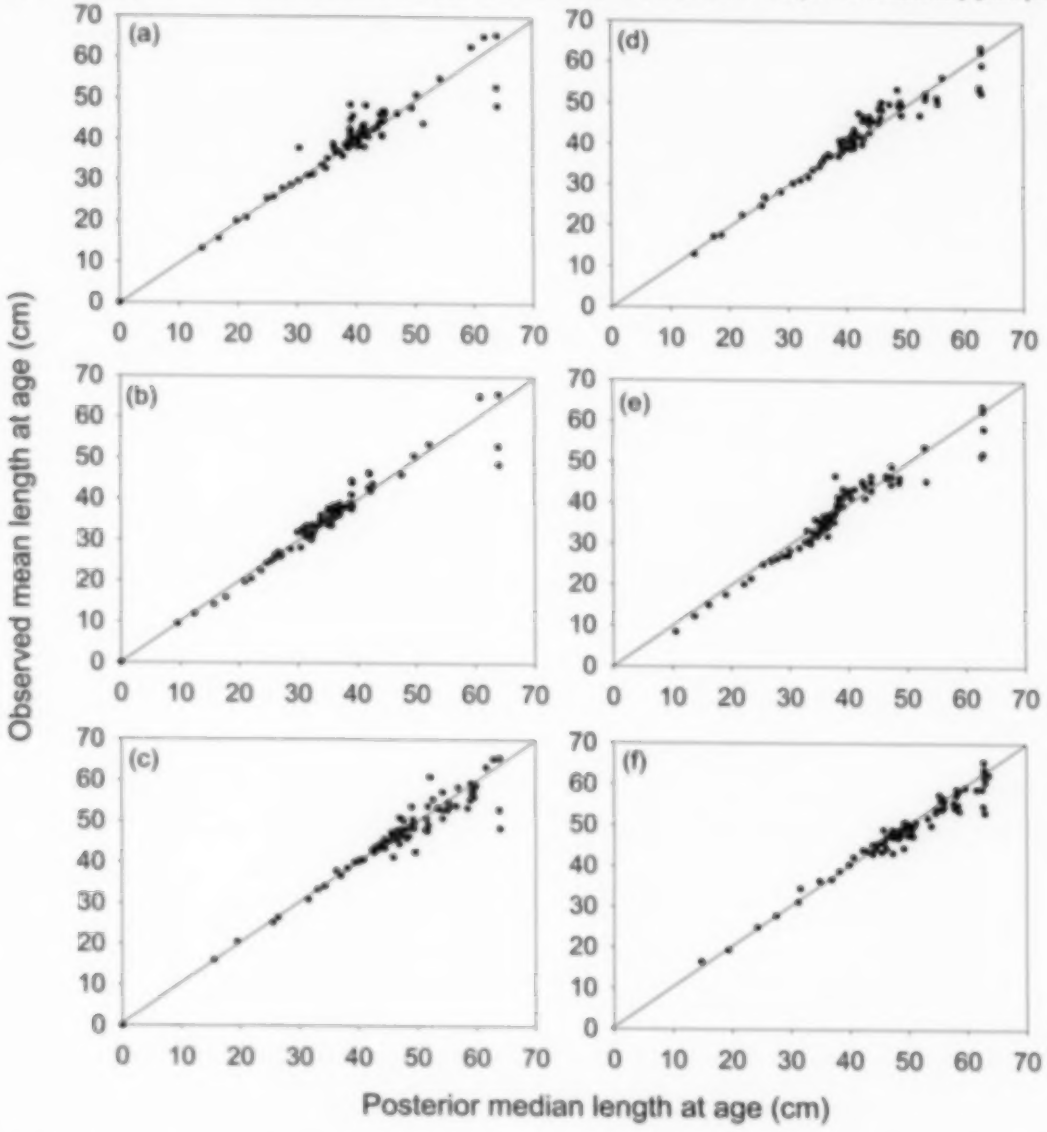

of female rockfish growth. Although there is high variation among species, it was clear that L_∞ increased as a positive linear function with size at 50% maturity, and K declined as size at maturity increased. The posterior median of the intercept and slope L_∞ was 15.25 and 0.973, respectively. This relationship implies that the proportion of L_∞ at which 50% of female rockfish mature increases rapidly (nonlinearly) as a function of their theoretical maximum size (i.e., L_∞). As such, species with a smaller theoretical maximum size mature at a much lower proportion of L_∞ than species whose maximum size is larger. This is in contrast with the published account that rockfish tend to mature at about 50% of their maximum size (Love et al. 2002).

One main conclusion from this study of fish growth is that appropriate statistical methods can be used to quantify both systematic and random components of growth variability of fish. Our use of nonlinear hierarchical meta-analysis using Bayesian inference for fish growth has the advantage of borrowing strength from other species to improve parameter estimation for a given species with weaker data (Hilborn and

© 2007 NRC Canada

Fig. 8. Comparison of von Bertalanffy growth curve fitted separately to age–length data for grass rockfish, *Sebastes rastrelliger*, and the species-specific growth curve derived from the Bayesian hierarchical meta-analysis of growth. Solid and broken lines show the median growth trajectory and 95% credibility intervals, respectively, generated from the Markov chain Monte Carlo (MCMC) sample using the hierarchical growth model fit to all 46 species of the genus *Sebastes*. Solid line with dots show the expected growth trajectory based on fitting the von Bertalanffy growth model separately to this species. The graph illustrates the degree to which estimates of growth from a data-poor species such as *S. rastrelliger* shrink toward the mean of the hierarchical model based on all species. Median and credibility intervals shown are based on 1000 MCMC samples of a stationary joint posterior.

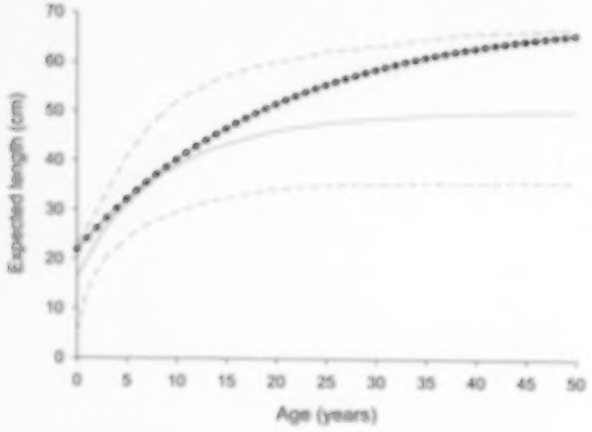

Fig. 9. Full conditional posterior predicted distributions of length-at-age for an unobserved male (*a*) and female (*b*) rockfish species of the genus *Sebastes* generated from a Markov chain Monte Carlo (MCMC) sample using the hierarchical growth model. These posterior densities were derived from the hyperparameters from the Bayesian hierarchical meta-analysis of 46 species. Posterior distributions shown are based on 1000 MCMC samples of a stationary joint posterior.

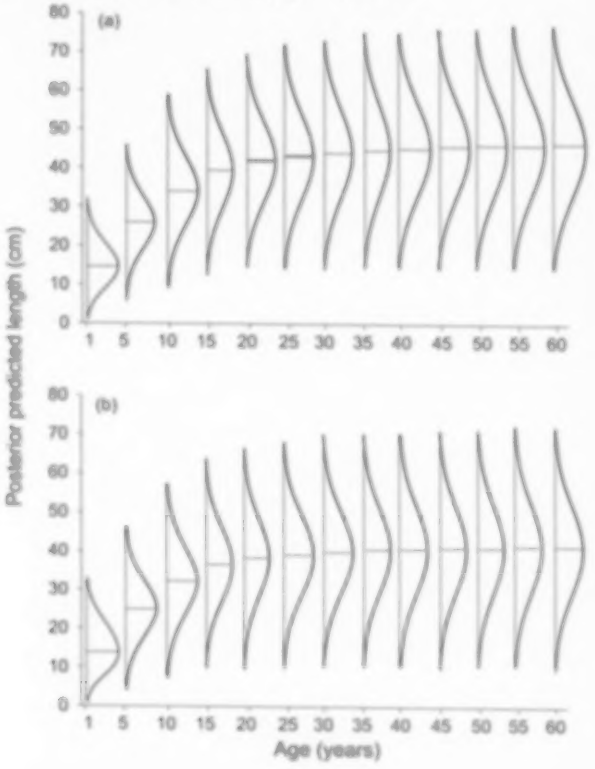

Liermann 1998; Myers and Mertz 1998) and has the flexibility to specify mixed effect parameters to fit data using a population distribution (hyperpriors in Bayesian analysis) to structure dependence into the parameters (Gelman et al. 2004) with fewer parameters. This is in contrast with the basic approach that fits the growth model to individual groups reporting only summarized means and variances (Beamesderfer and North 1995; Allen et al. 2002; MacMillian et al. 2002). Such approaches treat all effects as fixed and make the unrealistic assumption that there is no interrelation among populations. Substantial shortcomings for such methods are (*i*) estimation error associated with the individual population growth parameters is incorporated into the estimates of mean growth parameters and their variability (Lindstrom and Bates 1990), (*ii*) they provide ineffective tools for partitioning variance components in data sets with hierarchical structure, and (*iii*) they tend to place undue emphasis of inference on mean fixed effects (Gelman et al. 2004). Further, these traditional approaches that rely on oversimplified models applied to individual populations of a single species usually produce very unreliable and uncertain estimates (Hilborn and Walters 1992), especially where data are limited.

The use of sophisticated models such as Bayesian inference for complex problems are not necessarily free from technical difficulties, and practitioners (Gelman et al. 2004) have advocated model checking procedures, including (*i*) verification of convergence of the MCMC algorithm, (*ii*) sensitivity of model results to different choices of prior distributions, and (*iii*) posterior predictive check of the model fit. We applied each of these diagnostic procedures to evaluate the use of Bayesian inference for the nonlinear hierarchical meta-analysis of fish growth and in all cases concluded satisfactory results.

Although several statistical computing packages are available to fit nonlinear hierarchical or nonlinear random-effects growth models to numerous data sets simultaneously, we chose to implement the model using Bayesian inference, which can be computationally intensive. Bayesian methods have received considerable attention in the ecological and fisheries science literature (Ellison 1996; Punt and Hilborn 1997; Meyer and Millar 1999). Based on the well-developed body of statistical literature on nonlinear random-effects and hierarchical models (Lindstrom and Bates 1990; Smith and Wakefield 1994; Littell et al. 1996) and recent developments in Bayesian software (BUGS; Bayesian Inference for Gibbs sampling, Thomas et al. 1992; Spiegelhalter et al. 1999), we feel confident that our results are robust and that such tech-

© 2007 NRC Canada

niques are within the ambit of most readers. Further, the use of Bayesian inference as the framework for fitting a hierarchical von Bertalanffy growth model to age–length data was evaluated by Helser and Lai (2004) using a simulation study.

A number of technical issues and challenges remain. The underlying growth function in the hierarchical model assumes that age is measured without error (also assumed when using continuous covariates). Although careful aging method guidelines have been established by federal and state agencies, aging error can still be a problem, especially with longer-lived species. For rockfish, there is no clear generality for aging error among species or for relative age–size within species; hierarchical modeling of this process is an area for future research. Assuming age as well as maturity and depth covariates are measured without error would probably understate the true variability about parameter estimates. Additionally, we assumed that the within-error variance of length-at-age among species is equal. The basic data did not allow verification of this assumption, as many of the data sets consisted of mean length-at-age and associated sample sizes and not individual age–length observations. Further research might focus on an expanded hierarchy that estimates hyperparameters describing within-error variance. We also suggest that the appropriate sample sizes in hierarchical models that strike a balance between unwarranted domination of data-rich data sets and shrinkage to the mean is a gap in current understanding and practice of hierarchical modeling. A cap of 30 samples for a given age and species used in our analysis seemed like a reasonable compromise until simulation experiments designed to explore severely unbalanced hierarchical designs can be performed.

Finally, results of this analysis are not necessarily free from size-selective bias, particularly from fishery samples, which tend to capture larger fish of a given age. The only remedy for such a problem would be to estimate the growth curve within the context of a fully age–size structure population dynamics model such as Stock Synthesis (Methot 1989), which estimates size selectivity and growth simultaneously. However, given our intent of estimating growth and growth variability for 46 *Sebastes* species, this does not currently present a viable option. Nevertheless, the results from the hierarchical model may be less affected by selectivity because of the preponderance of research age samples in the database.

In the present analysis, we have consolidated the large body of scientific observation on growth into a quantitative framework based on a logical taxonomic grouping. We have thus provided a tool for comparing the genus *Sebastes* with other groups of fishes and for understanding the inherent variability we are likely to encounter in the remaining unstudied species of the genus. We have summarized the posterior probability distributions for 46 rockfish species for which we have some growth observations. Where many observations were available, the results here are very similar to what would have been obtained through independent analysis of a single species. However, we have updated the state of knowledge regarding many species with relatively few direct observations. By integrating out the linkage between species (the hyperparameters, eq. 10), we have shared strength of inference where data was lacking and potentially biased because of small sample size. The results of this analysis may be useful as informative priors for future growth studies and stock assessments of such data-poor species. However, the meta-analysis should only be repeated if the original data used in the meta-analysis is excluded. This would avoid contaminating the prior with the same information used in the likelihood of the future analysis (Minte-Vera et al. 2005).

For species that were not included in the current analysis, the posterior probability distributions of the hyperparameters dictate plausible species-specific growth parameter values (unobserved species, eq. 11). This distribution can serve as an informative prior to simple life-history-based analyses of productivity and relative yield. If new data are collected in the future, the current analysis can provide an informative prior that will constrain analysis until there are enough data to "speak for themselves". In many cases, there may be some catch statistics and length frequency data already available that could allow the application of a generalized, age-structured stock assessment model where the posteriors from this analysis serve as informative priors, and the uncertainty in these priors is integrated out through Bayesian analysis.

The approach presented here can be easily extended to compare other important life history parameters for better understanding and for managing rockfishes. Specifically, we imagine similar analyses for maturity, effective fecundity, and even behavior around fishing gear (selectivity) or habitat affinity across this genus. A unified approach to the synthesis of life history traits and life history invariants (Charnov 1993) will allow strong inference about productivity and serve as a guide to potentially successful management strategies in the presence of a large number of data-poor or unstudied rockfishes in the northeast Pacific Ocean.

Acknowledgements

We thank the dedicated biologists, upon who this work is based, for their tireless efforts in the field collecting data and analyzing rockfish otoliths in the laboratory. Many of those individuals have been listed in Table 1 of this paper, but we specifically mention a number of individuals who made available data sets on one or several species, including Jim West (Washington Department of Fish and Wildlife (WDFW)), Bob Lea (California Department of Fish and Game), Frank Shaw (AFSC, NMFS), Dana Henselman (Auke Bay, NMFS), Don Pearson (Southwest Fisheries Science Center (SWFSC), NMFS), Lynne Yamanaka (Fisheries and Oceans Canada (DFO)), Melissa Stevens (Monterey Bay Aquarium), Aaron King (SWFSC, NMFS), and Jody Zaitlin (Port of Oakland). Thanks also go to Don Pearson (SWFSC, NMFS) for providing rockfish maturity data. We also extend our gratitude to numerous reviewers, including Richard Methot and John Wallace (Northwest Fisheries Science Center), Andre Punt (University of Washington), Grant Thompson (AFSC, NMFS), Rick Stanley (DFO), and an anonymous reviewer.

© 2007 NRC Canada

References

Allen, M.S., Sheaffer, W., Porak, W.F., and Crawford, S. 2002. Growth and mortality of largemouth bass in Florida waters: implications for use of length limits. *In* Black bass: ecology, conservation and management. *Edited by* D.P. Philipp and M.S. Ridgway. Am. Fish. Soc. Symp. **31**: 559–566.

Beamesderfer, R.C., and North, J.A. 1995. Growth, natural mortality, and predicted response to fishing for largemouth bass and smallmouth bass populations in North America. N. Am. J. Fish. Manag. **15**: 688–704.

Beverton, R.J.H. 1992. Patterns of reproductive strategy parameters in some marine teleost fishes. J. Fish. Biol. **41**: 137–160.

Brooks, S., and Gelman, A. 1997. General methods for monitoring convergence of iterative simulations. Journal of Computational and Graphical Statistics, **7**: 434–455.

Bryk, A.S., and Raudenbush, S.W. 1992. Hierarchical linear models: applications and data analysis methods. Sage, Newbury Park, Calif.

Caillet, G.M., Botsford, L.W., Brittnacher, J.G., Ford, G., Matsubayashi, M., King, A., Watters, D.L., and Kope, R.G. 1996. Development of a computer-aided age determination system: evaluation based on otoliths of bank rockfish off California. Trans. Am. Fish. Soc. **125**: 874–888.

Charnov, E.L. 1993. Life history invariants. Some explorations of symmetry in evolutionary ecology. Oxford University Press, Oxford, England.

Chen, L.C. 1971. Systematics, variation, distribution, and biology of rockfishes of the subgenus *Sebastomus* (Pisces, Scorpaenidae, *Sebastes*). Bull. Scripps Inst. Oceanog. Univ. Calif. **18**: 1–107.

Chen, D.G., and Holtby, L.B. 2002. A regional meta-model for stock–recruitment analysis using an empirical Bayesian approach. Can. J. Fish. Aquat. Sci. **59**: 1503–1514.

Cowles, M.K., and Carlin, B.P. 1996. Markov Chain Monte Carlo convergence diagnostics: a comparative review. J. Am. Stat. Assoc. **91**: 883–904.

Davidian, M., and Giltinan, D.M. 1995. Nonlinear models for repeated measures data. Chapman and Hall, London, UK.

Ellison, A.M. 1996. An introduction to Bayesian inference for ecological research and environmental decision making. Ecol. Appl. **6**: 1036–1046.

Eschmeyer, W.N., and Herald, E.S. 1983. A field guide to Pacific coast fishes. Houghton Mifflin, Boston, Mass.

Essington, T.E., Kitchell, J.F., and Walters, C.J. 2001. The von Bertalanffy growth function, bioenergetics, and the consumption rates of fish. Can. J. Fish. Aquat. Sci. **58**: 2129–2138.

Gelman, A., Carlin, J.B., Stern, H.S., and Rubin, D.B. 2004. Bayesian data analysis. 2nd ed. Chapman and Hall, New York.

Geweke, J. 1992. Evaluating the accuracy of sampling-based approaches to the calculation of posterior moments. *In* Bayesian statistics 4. *Edited by* J.M. Bernardo, J. Berger, A.P. Dawid, and A.F.M. Smith. Oxford University Press, Oxford, England. pp. 169–193.

Gunderson, D.R. 1984. The great widow rockfish hunt of 1980–1982. N. Am. J. Fish. Manag. **4**: 465–468.

Hampton, J., and Majkowski, J. 1987. An examination of the reliability of the ELEFAN computer programs for length-based stock assessment. *In* Length-based methods in fisheries research. *Edited by* D. Pauly and G.R. Morgan. International Center for Living Aquatic Resources Management, Manila, Philippines, and Kuwait Institute for Scientific Research, Safat, Kuwait. pp. 203–215.

Heidelberger, P., and Welch, P.D. 1983. Simulation run length control in the presence of an initial transient. Operations Research, **31**: 1109–1144.

Helser, T.E., and Lai, H.-L. 2004. A Bayesian hierarchical meta-analysis of fish growth: with an example for North American largemouth bass, *Micropterus salmoides*. Ecol. Model. **178**: 399–416.

Hilborn, R., and Liermann, M. 1998. Standing on the shoulders of giants: learning from experience in fisheries. Rev. Fish Biol. Fish. **8**: 273–283.

Hilborn, R., and Mangel, M. 1997. The ecological detective: confronting models with data. Princeton University Press, Princeton, N.J.

Hilborn, R., and Walters, C.J. 1992. Quantitative fisheries stock assessment: choice, uncertainty and dynamics. Chapman and Hall, New York.

He, J.X., and Stewart, J. 2001. A stage-explicit expression of the von Bertalanffy growth model for understanding age at first reproduction of Great Lakes fishes. Can. J. Fish. Aquat. Sci. **59**: 250–261.

Jobling, M. 1981. Temperature tolerance and the final preferendum — rapid methods for the assessment of optimum growth temperatures. J. Fish. Biol. **19**: 439–455.

Laidig, T.E., Pearson, D.E., and Sinclair, L.L. 2003. Age and growth of blue rockfish (*Sebastes mystinus*) from central and northern California. Fish. Bull. **101**: 800–808.

Lea, R.N., McAllister, R.D., and VenTresca, D.A. 1999. Biological aspects of nearshore rockfishes of the genus *Sebastes* from central California. Calif. Fish Game Fish Bull. **177**: 1–109.

Lindstrom, M.J., and Bates, D.M. 1990. Nonlinear mixed effect models for repeated measures data. Biometrics, **46**: 673–678.

Littell, R.C., Milliken, G.A., Stroup, W.W., and Wolfinger, R.D. 1996. SAS system for mixed models. SAS Institute Inc., Cary, N.C.

Love, M.S., Yoklavich, M., Thorsteinson, L., and Butler, J. 2002. The rockfishes of the northeast Pacific. University of California Press, Berkeley, Calif.

MacMillan, J.L., McNeill, A.J., Heighton, R.G., and Ridgway, M.S. 2002. Life history characteristics of smallmouth bass populations in Nova Scotia based on tournament monitoring. *In* Black bass: ecology, conservation and management. *Edited by* D.P. Philipp and M.S. Ridgway. Am. Fish. Soc. Symp. **31**: 535–544.

Methot, R.D. 1989. Synthetic estimates of historical abundance and mortality for northern anchovy. *In* Mathematical analysis for fish stock dynamics: reviews, evaluations and current applications. *Edited by* E.F. Edwards and B.A. Megrey. Am. Fish. Soc. Symp. **6**: 66–82.

Meyer, R., and Millar, R.B. 1999. BUGS in Bayesian stock assessments. Can. J. Fish. Aquat. Sci. **55**: 1078–1086.

Millar, R.B. 2002. Reference priors for Bayesian fisheries models. Can. J. Fish. Aquat. Sci. **59**: 1492–1502.

Millar, R.B., and Methot, R.D. 2002. Age-structured meta-analysis of U.S. west coast rockfish populations and hierarchical modeling of trawl survey catchabilities. Can. J. Fish. Aquat. Sci. **59**: 383–392.

Minte-Vera, C.V., Branch T.A., Stewart, I.J., and Dorn, M.W. 2005. Practical application of meta-analysis results: avoiding the double use of data. Can. J. Fish. Aquat. Sci. **62**: 925–929.

Myers, R.A., and Mertz, G. 1998. Reducing uncertainty in the biological basis of fisheries management by meta-analysis of data from many populations; a synthesis. Fish. Res. **37**: 51–60.

Myers, R.A., MacKenzie, B.P., Bowen, K.G., and Barrowman, N.J. 2001. What is the carrying capacity for fish in the ocean? A meta-analysis of population dynamics of Northern Atlantic cod. Can. J. Fish. Aquat. Sci. **58**: 1464–1476.

Nelson, J.S. 1994. Fishes of the world. 3rd ed. John Wiley & Sons, New York.

© 2007 NRC Canada

O'Connell, V.M., Funk, F.C., and Melteff, B.R. 1986. Age and growth of yelloweye rockfish (*Sebastes ruberrimus*) landed in southeastern Alaska. *In* Proceedings of the International Rockfish Symposium, Lowell Wakefield Fisheries Symposium, Anchorage, Alaska, USA, 20–22 October 1986. Alaska Sea Grant Rep. No. 87-2. pp. 171–185.

PFMC. 2002. Status of the Pacific coast groundfish fishery through 2001 and acceptable biological catches for 2002: stock assessment and fishery evaluation. Pacific Fishery Management Council, Portland, Ore.

Pearson, D.E., Hightower, J.E., and Chan, J.T.H. 1991. Age, growth, and potential yield for shortbelly rockfish, *Sebastes jordani*. Fish. Bull. **89**: 403–410.

Pilling, G.M., Kirkwood, G.P., and Walker, S.G. 2002. An improved method for estimating individual growth variability in fish, and the correlation between von Bertalanffy growth parameters. Can. J. Fish. Aquat. Sci. **59**: 424–432.

Pinheiro, J.C., and Bates, D.M. 2000. Mixed effects models in S and S-Plus. Springer-Verlag, New York.

Punt, A.E., and Hilborn, R. 1997. Fisheries stock assessment and decision analysis: the Bayesian approach. Rev. Fish Biol. Fish. **7**: 35–63.

Quinn, T.J., and Deriso, R.B. 1999. Quantitative fish dynamics. Oxford University Press, New York.

Rogers, J.B. 2003. Species allocation of *Sebastes* and *Sebastolobus* sp. caught by foreign countries from 1965 through 1976 off Washington, Oregon, and California, USA. US Department of Commerce, Washington, D.C. NOAA Tech. Memo. NMFS-NWFSC-57.

Sainsbury, K.J. 1980. The effect of individual variability on the von Bertalanffy growth equation. Can. J. Fish. Aquat. Sci. **37**: 241–247.

Schaalje, G.B., Shaw, J.L., and Belk, M.C. 2001. Using nonlinear hierarchical models for analyzing annulus-based size-at-age data. Can. J. Fish. Aquat. Sci. **59**: 1524–1532.

Seber, G.A.F. 1977. Linear regression analysis. John Wiley & Sons, New York.

Smith, A., and Wakefield, J.C. 1994. The hierarchical Bayesian approach to population pharmokinetic modeling. Int. J. Bio-Med. Comput. **36**: 35–42.

Spiegelhalter, D.J., Thomas, A., and Best, N.G. 1999. WinBUGS version 1.2 user manual. Medical Research Council Biostatistics Unit, Institute of Public Health, Cambridge, UK.

Stevens, M.M., Andrews, A.H., Cailliet, G.M., Coale, K.H., and Lundstrom, C.C. 2004. Radiometric validation of age, growth, and longevity for the blackgill rockfish (*Sebastes melanostomus*) Fish. Bull. **102**: 711–722.

Thomas, A., Spiegelhalter, D.J., and Gilks, W.R. 1992. BUGS: a program to perform Bayesian statistical inference using Gibbs sampling. *In* Bayesian statistics 4. *Edited by* J.M. Bernardo, J.O. Berger, A.P. Dawid, and A.F.M. Smith. Oxford University Press, Oxford, UK. pp. 837–842.

von Bertalanffy, L. 1957. Quantitative laws in metabolism and growth. Q. Rev. Biol. **32**: 217–231.

Von Rosen, D. 1997. On moments of the inverted Wishart distribution. Statistics, **30**: 259–278.

Wade, P.R. 2000. Bayesian methods in conservation biology. Conserv. Biol. **14**: 1308–1316.

Weinberg, K.L., Wilkins, M.E., Shaw, F.R., and Zimmermann, M. 2002. The 2001 Pacific west coast bottom trawl survey of groundfish resources: estimates of distribution, abundance, and length and age composition. US Department of Commerce, Washington, D.C. NOAA Tech. Memo. NMFS-AFSC-128.

Westrheim, S.J., and Harling, W.R. 1975. Age–length relationships for 26 Scorpaenids in the northeast Pacific Ocean. Can. Tech. Rep. Fish. Aquat. Sci. **565**: 1–12.

Workman, G.D., Olsen, N., and Kronlund, A.R. 1998. Results from a bottom trawl survey of rockfish stocks off the west coast of the Queen Charlotte Islands, September 5–23, 1997. Can. Manuscr. Rep. Fish. Aquat. Sci. 2457. Fisheries and Oceans Canada, Ottawa, Ont.

Zaitlin, J.A. 1986. Geographical variation in the life history of *Sebastes chrysomelas*. M.S. thesis, San Francisco State University, Calif.

© 2007 NRC Canada

Individual variability in activity patterns of juvenile Atlantic salmon (*Salmo salar*) in Catamaran Brook, New Brunswick

Cindy Breau, Laura K. Weir, and James W.A. Grant

Abstract: The activity of juvenile salmonids in streams varies between seasons, age classes, and times of day, but few studies have quantified the magnitude of individual variation in the behaviour of wild individuals. We monitored the activity patterns of 35 young-of-the-year (YOY) (fork length: 25.6–34.6 mm) and eight 1+ (fork length: 68.2–78.7 mm) Atlantic salmon (*Salmo salar*) over an 8-week summer field season. Age 1+ salmon were more active at night than during the day, whereas YOY fish were almost exclusively active during the day. However, daytime activity did not peak at 16–20 °C, the optimal water temperature range for growth determined in laboratory studies. Rather, the activity of 1+ fish peaked at 21 °C, whereas the activity of YOY fish continued to increase until 23 °C and then leveled off between 23 and 27 °C. There was also considerable individual variability within an age class in how fish responded to environmental variables that was often obscured by the average patterns. In a multiple logistic regression analysis for the activity of the 35 YOY, 18 responded significantly to time of day, 17 to water temperature, and 16 to day of the year. The causes of this individual variability and the consequences for growth and mortality deserve further study.

Résumé : L'activité des jeunes salmonidés dans les cours d'eau varie en fonction des saisons, des classes d'âge et de l'heure de la journée; peu d'études ont cependant mesuré l'importance de la variation individuelle du comportement des poissons sauvages. Nous avons suivi les patrons d'activité de 35 jeunes saumons atlantiques (*Salmo salar*) de l'année (YOY) (longueur à la fourche: 25,6–34,6 mm) et de huit saumons d'âge 1+ (longueur à la fourche: 68,2–78,7 mm) durant une saison de terrain de huit semaines en été. Les saumons d'âge 1+ sont plus actifs la nuit que le jour, alors que les poissons YOY sont presque exclusivement actifs de jour. Cependant, l'activité de jour n'atteint pas son maximum à 16–20 °C, l'étendue des températures optimales de l'eau pour la croissance déterminée dans les études en laboratoire. Au contraire, l'activité des poissons d'âge 1+ est maximale à 21 °C, alors que celle des poissons YOY continue à augmenter jusqu'à 23 °C pour atteindre un plateau entre 23 et 27 °C. Il existe aussi au sein d'une même classe d'âge une importante variation individuelle de la réaction des poissons aux variables du milieu, qui est souvent camouflée par les patrons moyens. Dans une analyse de régression multiple logistique de l'activité des 35 poissons YOY, 18 réagissent significativement à l'heure de la journée, 17 à la température de l'eau et 16 au jour de l'année. Les causes de cette variabilité individuelle et ses conséquences sur la croissance et la mortalité requièrent des études additionnelles.

[Traduit par la Rédaction]

Introduction

Ever since the pioneering works of Kalleberg (1958) and Keenleyside (1962), juvenile stream-dwelling salmonids have been a popular model system for investigating the foraging decisions of animals. Juvenile salmonids are primarily visual foragers, so it is not surprising that their foraging efficiency declines with decreasing light intensity (Wilzbach et al. 1986; Fraser and Metcalfe 1997). Hence, juvenile salmonids in general and Atlantic salmon (*Salmo salar*) in particular were long considered to be diurnal or crepuscular feeders during the summer (Metcalfe et al. 1999). When the water temperature decreases below 10 °C in the autumn, they typically become less active and begin hiding in the substrate (Rimmer and Paim 1983), presumably until water temperatures increase in the spring.

More recent work, however, suggests that juvenile Atlantic salmon are not inactive during the winter but switch to nocturnal feeding (Fraser et al. 1993; Heggenes et al. 1993) as a result of a trade-off between lower feeding efficiency

Received 2 June 2006. Accepted 7 December 2006. Published on the NRC Research Press Web site at http://cjfas.nrc.ca on 31 March 2007.
J19347

C. Breau,[1,2] L.K. Weir,[3] and J.W.A. Grant. Department of Biology, Concordia University, 7141 Sherbrooke Street W., Montréal, QC H4B 1R6, Canada.

[1]Corresponding author (e-mail: cindy.breau@unb.ca).
[2]Present address: Department of Biology, University of New Brunswick, Bag Service 45111, Fredericton, NB E3B 6E1, Canada.
[3]Present address: Department of Biology, Life Sciences Centre, Dalhousie University, Halifax, NS B3H 4J1, Canada.

 doi:10.1139/F07-026 © 2007 NRC Canada

Table 1. Physical characteristics of the study sites in Catamaran Brook and the Little Southwest Miramichi River.

		Water temperature (°C) (n = 48–67)			Light intensity (lx) (n = 48–67)		
Study site	Area (m^2)	Median	Lower and upper quartile	Range	Median	Lower and upper quartile	Range
Mouth	24	19.5	17.1–21.4	14.2–25.0	119.0	52.4–284.0	0–464
Gorge 1	28	18.5	16.1–20.8	13.3–24.6	65.6	22.7–140.0	0–354
Gorge 2	20	18.3	16.0–20.8	13.2–24.3	66.8	26.0–184.0	0–321
Gorge 3	32	18.7	16.6–20.8	13.3–24.8	29.9	10.1–97.1	0–297
Gorge 4	24	18.3	16.2–20.7	13.4–24.6	38.3	7.6–123.5	0–255
River 1	24	22.4	20.2–24.7	16.1–27.7	167.9	84.7–288.0	0–397
River 2	24	22.0	19.1–23.4	14.8–27.7	173.0	38.1–300.3	0–442
River 3	36	22.6	20.4–24.6	15.9–27.2	90.3	34.1–205.3	0–335

(e.g., 35% of diurnal efficiency (Fraser and Metcalfe 1997)) and lower risk of predation at night (Fraser and Metcalfe 1997). Similarly, foraging behaviour during the summer is more complex than the simple story of diurnal or crepuscular feeding. For example, smaller or younger Atlantic salmon (LeDrew et al. 1996; Gries et al. 1997; Imre and Boisclair 2004) and Pacific salmon (Bradford and Higgins 2001) are relatively more active during the day than at night and vice versa for larger or older fish.

Because foraging decisions will depend on the actual trade-offs experienced by individual fish, diel activity patterns will likely vary among individuals rather than be governed by simple environmental variables (Bradford and Higgins 2001). Hence, short-term variation within and between individuals in foraging success, hunger, physiological state, and perceived predation risk may affect short-term decisions about diel activity patterns (Metcalfe et al. 1999). An additional factor that will likely affect the summer activity patterns of juvenile salmonids is water temperature. The growth rate and food consumption of juvenile Atlantic salmon are both highest between 16 and 20 °C (Elliott and Hurley 1997; Jonsson et al. 2001), at least in laboratory conditions. Given the predation hazard associated with daytime foraging, we might expect juvenile Atlantic salmon to concentrate their effort within this optimal temperature range when the payoffs from this hazardous foraging are greatest. If the magnitude of the variation within and between individuals is considerable, then it will be important to document the activity patterns of individually marked fish rather than to report averages for age classes or populations.

We undertook a field study of the activity patterns of individually marked young-of-the-year (YOY) and 1+ Atlantic salmon in the wild during the summer. Our primary goal was to document the magnitude of individual variation in the activity patterns of YOY fish using detailed information about marked individuals. Despite the anticipated variation in behaviour between individuals, we also expected two general patterns to emerge. Specifically, we tested the predictions (*i*) that smaller fish (YOY) are relatively more active during the day, whereas larger fish (1+) are relatively more active at night, as observed in previous studies, and (*ii*) whether daytime activity in the wild peaked at the optimal temperatures determined in laboratory studies. To achieve these goals, we followed the activity of 43 juvenile Atlantic salmon over an 8-week field season in Catamaran Brook, New Brunswick, Canada.

Materials and methods

Study site and population

The study was conducted during the summer of 2001 in the Little Southwest Miramichi River (fifth-order stream, mean width = 75 m), New Brunswick, and in one of its tributaries, Catamaran Brook (third-order stream, mean width = 7.2 m; see Steingrímsson and Grant (2003) for a map of the study area). Catamaran Brook has been the focus of a long-term multidisciplinary study assessing the effect of logging on the stream and its biota (Cunjak et al. 1993). In this system, Atlantic salmon, brook trout (*Salvelinus fontinalis*), eastern blacknose dace (*Rhinichthys atratulus*), creek chub (*Semotilus atromaculatus*), lake chub (*Couesius plumbeus*), white sucker (*Catostomus commersonii*), slimy sculpin (*Cottus cognatus*), and sea lamprey (*Petromyzon marinus*) are common to the stream (Cunjak et al. 1993). YOY Atlantic salmon emerge from the gravel in mid-June at a total length of about 2.6 cm (Randall 1982). They reside in the stream for a period of 2–3 years (Cunjak et al. 1993) where their diet is composed mainly of invertebrates, primarily chironomid larvae (Keeley and Grant 1997).

Eight study sites (mean area = 26 m^2, range = 20–36 m^2) were used (see Table 1) with a minimum distance of 20 m between sites. Four sites were located in the Gorge Reach (see Cunjak et al. (1993) for details), which is ~5 km upstream from the mouth of Catamaran Brook, one site was located 5 m upstream from the mouth of Catamaran Brook, and three sites were along the south river bank of the Little Southwest Miramichi River, all within 250 m of the mouth of Catamaran Brook. Hereafter, we will refer to these reaches as the Gorge, Mouth, and River, respectively. The Gorge sites were all located between Middle Pool 1 and Gorge Run 2 (see fig. 2 in Cunjak et al. 1993). In the River, site 1 was located 20 m upstream from the mouth of Catamaran Brook, whereas sites 2 and 3 were 40 and 250 m downstream of the mouth, respectively.

Tagging protocol

Seven YOY Atlantic salmon were marked per site between 25 and 29 June 2001 for a total of 56 fish. On 9 July,

© 2007 NRC Canada

two additional YOY fish were marked per site and thirteen 1+ fish were also marked: six in the Gorge, three in the Mouth, and four in the River. YOY salmon were marked approximately 2 weeks after emergence at fork lengths of 25.6–34.6 mm, whereas the 1+ salmon were 68.2–78.7 mm. Beginning below a study site, we (C. Breau and L.K. Weir) snorkeled upstream until a fish was located, observed it for 1 min to ensure that it was feeding normally, and then captured it using two aquarium dipnets. The position of each fish was marked with an identification flag that was pushed into the substrate where the fish was first seen. Each fish was anesthetized using clove oil (Keene et al. 1998) and measured for fork length to the nearest 0.1 mm using a hand-held caliper. Fish were individually marked with a subcutaneous injection of fluorescent elastomer paint (Dewey and Zigler 1996; Steingrímsson and Grant 2003) in two of eight possible tagging locations (left and right pectoral fin, front and back of the dorsal fin, and top left, bottom left, top right, and bottom right side of the caudal peduncle) with four different paint colours (yellow, red, green, and orange). The fish were allowed to recover in buckets of water for 5–15 min before being returned to their station via snorkeling. From the time of fish capture until they were returned to their territories, no fish mortalities occurred.

Using the same technique, all active fish were recaptured and remeasured in the Gorge on 31 July and in the Mouth and River on 1 August. Fading tags were retouched to minimize tag loss. The sites were sampled by a four-person crew using a 500 V Smith-Root model 12A electrofisher (Smith-Root, Inc., Vancouver, Washington) on 21–22 August; all of the marked fish that were recaptured were again measured for fork length.

Behavioural observations

Data on the activity of the individually marked fish were collected between 25 June and 22 August 2001. We attempted to observe each fish eight times over the summer in each of the eight time periods during the day (0700, 0900, 1100, 1300, 1500, 1700, 1900, and 2100) and three times at night (2300) for a total of 67 observations per individual. On any particular day, we collected data for all eight sites beginning with either the Gorge or the Mouth and River in the morning and rotating between reaches for the three time periods (e.g., Gorge, 0700–1100; Mouth and River, 1300–1700; Gorge, 1900–2300). Each observer snorkeled upstream within a site to collect the data for two of the four sites for a particular time period. The observers alternated for each time period. No observations were made in the Mouth from 15 to 22 August because the water level was too shallow for snorkeling. Each fish that was present for the complete 8-week study (see below) was observed 48–67 (mean = 51.3) times during the study period. Each time a site was snorkeled (i.e., a survey), the number of "active" (see below) juvenile Atlantic salmon (both marked and unmarked) was counted for a total of seven density measurements per time period during the day and three at night (2300); salmon density was not measured during the first of eight daytime surveys of each site.

Before entering a site, the water temperature and light intensity were measured. Water temperature was recorded at the downstream end of each site using a MultiLine P4-F/set-3/110 V digital hand-held thermometer (±0.1 °C). Light intensity was measured (±50 lx) using an Extech Instruments model 401027 light meter (range 0 – 20 000 lx). Light intensity was measured 5 cm above the water surface with the probe facing towards the water surface. Three periods of the diel cycle were defined based on light intensity: night (<0.01 lx), dawn or dusk (0.01–100 lx), and day (>100 lx) (see Valdimarsson and Metcalfe 1999). Sunrise was always before 0700, but on 51 of 260 observations conducted in the heavily forested Gorge sites, 0700 was defined as dawn. Under the more open canopy at the Mouth and River sites, 0700 was always defined as day. Similarly, 2100 was always day or dusk in the Mouth and River sites, but in the Gorge sites, 41 of 202 observations were defined as night. Marked fish were visible during nighttime observations by shining an underwater blue light on the fluorescent elastomer paint. Average, maximum, and minimum daily water temperatures varied throughout the study period but were not correlated with day of the year. Drift samples were collected in the Mouth and River sites on 27–28 July, 4 August, and 21 August 2001, whereas samples in the Gorge were collected on 26–27 July, 5 August, and 22–23 August 2001.

An observation consisted of finding or not finding an individual fish in its original site (i.e., site where marked) during a survey at a particular time of day on a particular day of the year. After locating a marked individual, the observer recorded behaviour for 5 min. The activity of marked individuals was first categorized as being active or not. A fish was scored as active if it was swimming, foraging, or holding position on or near the substrate anywhere within its original site. Individuals that were not seen were assumed to be sheltering within the substrate (see below) but may have also died or relocated. To guard against counting a dead or relocated fish as "inactive", a fish that was not observed was only scored as inactive if it was subsequently observed in its original site. The 5 min observation period allowed us to judge whether fish switched between being active or not at a small temporal scale; fish were never observed changing their level of activity during an observation.

Statistical analysis

Each fish was potentially observed at eight times of day eight times over the season (except only three times for 2300). Despite the smaller number of observations for 2300, our results were qualitatively similar whether or not they were included in the analyses. Time of day and season were always included as factors in any analysis. For each of these observations, we also monitored light intensity and water temperature.

To examine the overall patterns of activity of all fish with respect to an environmental variable, we calculated the percentage of times that an individual was active at a particular value for a particular environmental variable. For example, all 35 YOY individuals had observations for water temperatures from 17 to 21 °C. If an individual was observed 10 times at 17 °C, then its score could be 0%, 10%, 20%, 30%, 40%, 50%, 60%, 70%, 80%, 90%, or 100% active depending on the number of times that it was active out of the 10 observations. The percentage of times active for each fish was then arcsine square root transformed and used as a datum in the analysis (n = 35 for YOY, n = 8 for 1+).

© 2007 NRC Canada

Univariate analyses and individual variability in activity

For the overall analyses of time of day, a two-way analysis of variance (ANOVA) was used to determine if there was an interaction between age class and time of day. Because YOY and 1+ differed in diel activity, the daytime activity of each age-class was analyzed separately using a randomized complete block design with individual fish as blocks (repeated-measures ANOVA). Specific linear or dome-shaped trends were tested using linear and quadratic contrasts (Sokal and Rohlf 1995). Quantitative trends were described using standard linear and quadratic regression. Positive and negative trends were compared using Sign tests.

Because activity is an attribute variable (i.e., active or not, sensu Sokal and Rohlf 1995), it was analyzed separately for each individual using a simple logistic regression for the four main variables (time of day, day of the year, water temperature, and light intensity) (i.e., 43 fish × 4 variables = 172 logistic regressions). However, we present results only for time of day and water temperature because these variables had the strongest effects on behaviour. To correct for multiple comparisons, we set α at 0.0127 using the Dunn–Šidák method (Sokal and Rohlf 1995).

Multivariate analysis of activity

A multiple logistic regression was also calculated for each YOY fish to evaluate which variables were most significantly related to activity. Quadratic terms were included in the logistic regression models only if significant after the linear term was first entered in the model. Differences among sites were compared using χ^2 tests.

To meet the assumptions of parametric tests, light intensity was $\log_{10}$-transformed and the activity of fish was arcsine square root transformed. To simplify the graphical presentation, however, we used the untransformed data in all of the figures.

Results

Density

The diel patterns in the density of juvenile Atlantic salmon that were counted during snorkeling surveys differed between the two age classes (two-way ANOVA, interaction effect: $F_{[8,120]} = 12.61$, $P < 0.001$) (Fig. 1*a*). The density of YOY fish exhibited a dome-shaped relationship (ANOVA with sites as blocks, quadratic contrast: $F_{[1,63]} = 62.55$, $P < 0.001$); the number was low in the morning, peaked in the early afternoon, and then decreased at night (quadratic regression for YOY: density = 0.076 × time of day – 0.0026 × time of day^2 – 0.34; $r^2 = 0.54$, $n = 72$, $P < 0.001$). In contrast, the density of 1+ fish increased linearly over the day (ANOVA with sites as blocks, linear contrast: $F_{[1,63]} = 83.89$, $P < 0.001$) and was highest at night (linear regression for 1+: density = 0.013 × time of day – 0.055; $r^2 = 0.46$, $n = 72$, $P < 0.001$).

Univariate analyses and individual variability in activity

Of the original marked fish, 51 of 72 YOY fish and 10 of thirteen 1+ fish were seen at least once after tagging and 35 YOY (18, 13, and 4 in the Gorge, River, and Mouth, respectively) and eight 1+ fish (three, two, and three in the Gorge, River, and Mouth, respectively) were followed throughout the 8-week study period. The mean displacement from the initial tagging location to the location observed at the end of the study did not differ significantly for YOY fish (mean ± SE = 0.53 ± 0.10 m, $n = 35$, range = 0–3 m) and 1+ fish (mean ± SE = 0.39 ± 0.11 m, $n = 8$, range = 0–1 m) (two-sample t test: $t = 0.68$, df = 41, $P = 0.50$). Similarly, the probability of observing either YOY or 1+ fish did not differ, as YOY and 1+ salmon were observed on 46.1% ($n = 35$, range = 22.0–82.9) and 36.8% ($n = 8$, range = 11.9–70.2) of the snorkeling surveys over the study period (two-sample t test: $t = 1.72$, df = 41, $P = 0.093$).

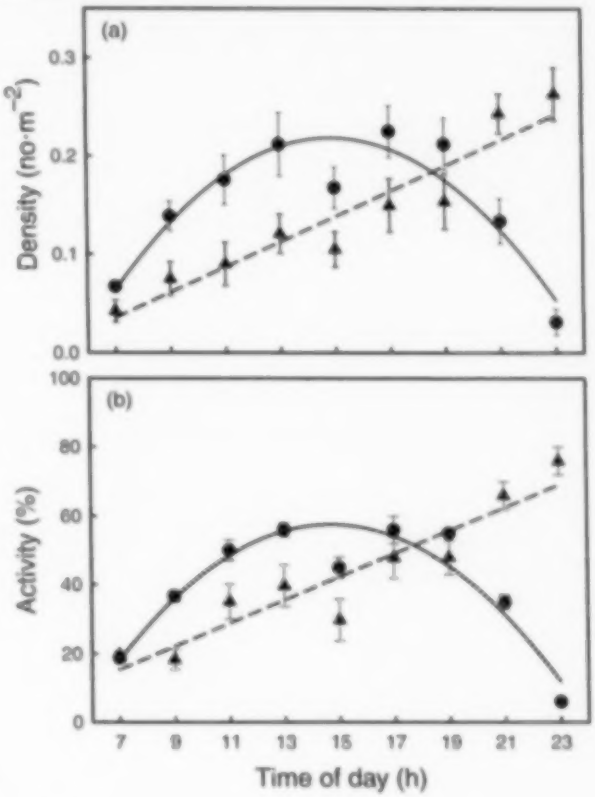

Fig. 1. (*a*) Mean density (±SE) ($n = 8$ sites) of marked and unmarked young-of-the-year (YOY) (●) and 1+ (▲) Atlantic salmon counted during snorkeling surveys at different times of the day. A datum in the analysis was the average density at a particular site and time of day based on eight counts over the season (except $n = 3$ for 2300). (*b*) Mean (±SE) percentage of snorkeling surveys in which individually marked YOY (●) ($n = 35$) and 1+ (▲) ($n = 8$) salmon were observed at various times of day. A datum in the analysis was the percentage of surveys ($n = 5$–8 over the season, except $n = 3$ for 2300) in which an individual salmon was active at a particular time of day.

Time of day

Overall, the diel patterns of activity of the marked fish (Fig. 1*b*) were similar to the diel patterns in density; the two age classes showed different diel activity patterns (two-way

© 2007 NRC Canada

Fig. 2. Logistic regressions of the diel activity of 35 YOY Atlantic salmon found in the (*a*) Gorge, (*b*) River, and (*c*) Mouth and (*d*) eight 1+ salmon found in all four sites. The solid lines represent significant linear or quadratic logistic regressions, whereas broken lines were not significant. Sample size varied between 48 and 67 observations for each fish.

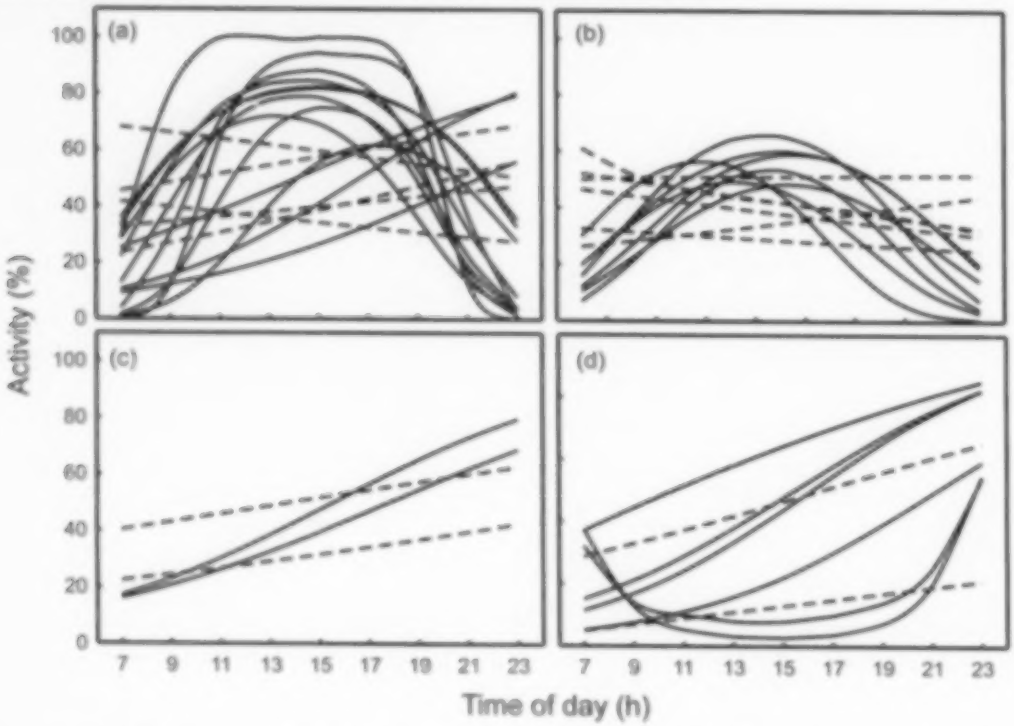

ANOVA, interaction effect: $F_{[8,360]} = 10.49$, $P < 0.001$). The YOY fish were most active in the late morning and afternoon (ANOVA with individuals as blocks, quadratic contrast: $F_{[1,272]} = 173.37$, $P < 0.001$; quadratic regression for YOY: arcsine square root activity = 0.78 × time of day – 0.026 × time of day^2 – 5.65; $r^2 = 0.33$, $n = 315$, $P < 0.001$), whereas 1+ fish were most active at night (ANOVA with individuals as blocks, linear contrast: $F_{[1,64]} = 39.90$, $P < 0.001$; linear regression for 1+: arcsine square root activity = 0.12 × time of day – 2.27; $r^2 = 0.27$, $n = 81$, $P < 0.001$).

There was considerable variation in the diel activity patterns among individuals within an age class (Fig. 2). To investigate this individual variability, separate logistic regressions were calculated for each fish. Three basic patterns of diel activity were detected for YOY fish (Figs. 2*a*–2*c*): linear increase, dome-shaped relationship, and nonsignificant relationship. Of the 35 YOY fish, 22 exhibited a significant diel activity pattern: 17 showed a significant quadratic relationship with activity peaking in the late morning or early afternoon and five showed a significant increase over the day with their activity highest at night. Of the 13 fish whose activity did not differ significantly with time of day, seven exhibited a positive trend and six a negative trend with time of day. Curiously, none of the four fish at the Mouth exhibited a dome-shaped relationship.

The diel activity patterns of 1+ fish differed from those of most YOY fish (Fig. 2*d*). Of the eight 1+ fish, six increased their activity with time of day, four of which were significant. Two fish in the Gorge exhibited a significant U-shaped relationship, being most active at dawn and at dusk–night.

In summary, the behaviour of only 17 of 35 YOY individuals conformed to the overall dome-shaped pattern, whereas four of eight 1+ individuals showed an increase in activity over the day. Furthermore, only 69% (17 significantly dome-shaped and six negative trends) of YOY individuals exhibited a decrease in activity at night, whereas all eight 1+ individuals were more active at night than during the day.

Daytime activity and water temperature

Because the activity of most YOY and 1+ fish differed between day (>100 lx) and night (<0.01 lx), only the daytime data are presented below. Overall, the daytime activity of YOY fish increased with increasing water temperature and then leveled off at about 23 °C (ANOVA with individuals as blocks, quadratic contrast: $F_{[1,365]} = 4.50$, $P = 0.035$; quadratic regression: arcsine square root activity = 10.96 × water temperature – 0.20 × water temperature^2 – 98.27; $r^2 = 0.15$, $n = 414$, $P < 0.001$) (Fig. 3). In contrast, the daytime activity of 1+ fish exhibited a dome-shaped relationship with a peak in activity at 20.7 °C (ANOVA with individuals as blocks, quadratic contrast: $F_{[1,77]} = 16.32$, $P < 0.001$; quadratic regression: arcsine square root activity = 30.71 × water temperature – 0.71 × water temperature^2 – 288.96; $r^2 = 0.31$, $n = 99$, $P < 0.001$).

Once again, there was considerable variability among the marked fish (Fig. 4). Four patterns emerged: linear increase,

© 2007 NRC Canada

Fig. 3. Mean (±SE) daytime (light intensity > 100 lx) activity of YOY (●) (n = 35 fish for 17–21 and 23–24 °C, n = 32 for 16 °C, n = 30 for 22 and 25 °C, n = 23 for 14 °C, n = 19 for 15 °C, n = 15 for 13 °C, n = 13 for 26 °C, and n = 11 for 27 °C) and 1+ (▲) (n = 8 fish for 17, 19, 21, and 23 °C and n = 3 for 13–16, 20, and 24–27 °C) Atlantic salmon in relation to water temperature. Each datum was the mean activity for each marked fish at each water temperature.

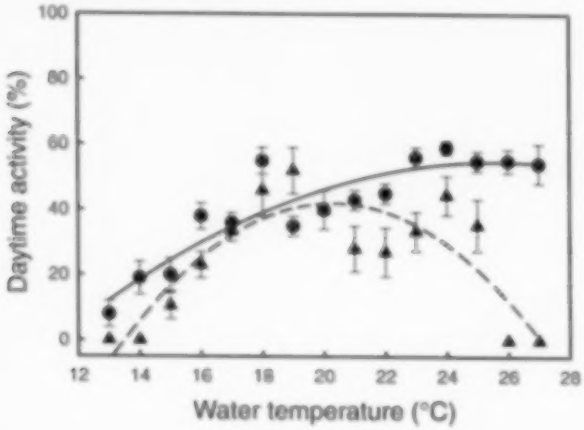

linear decrease, dome-shaped, and nonsignificant. Daytime activity was significantly related to water temperature in 18 of 35 YOY fish. Of these 18 fish, 11 fish were more active with increasing water temperature, six exhibited dome-shaped relationships with peaks in activity at about 21 °C, and one was less active with increasing water temperature. Curiously, all six fish exhibiting a dome-shaped relationship were in the Gorge. Of the 17 YOY fish whose activity was not significantly related to water temperature, 15 increased rather than decreased their activity with water temperature (Sign test: P = 0.01). Hence, 33 of 35 YOY fish increased their activity as water temperature increased from 13 to 20 °C (Sign test: $P < 0.01$).

Unlike the YOY fish, there was no consistent pattern with the 1+ fish. The activity of only four of eight 1+ fish was significantly related to water temperature: three increased their activity and one showed a dome-shaped relationship with a peak at 20 °C (Fig. 4*d*). Of the four fish with nonsignificant relationships, two were less active and two were more active with increasing water temperature.

In summary, the average patterns in activity in relation to water temperature obscured interesting variability in behaviour. The overall impression of an asymptotic increase in YOY activity until about 23 °C was caused by most fish increasing their activity coupled with six individuals that showed a marked dome-shaped response. Similarly, only one of eight 1+ individuals showed the average pattern of a dome-shaped relationship with water temperature.

Multivariate analysis of activity

Because changes in activity may be influenced by more than one environmental variable, a complete multiple logistic regression for each individual fish was used to determine which variables had significant effects on activity when entered last in the model. For the YOY fish, time of day, water temperature, and day of the year were the most important variables influencing activity (Table 2). Of the 35 fish, the activity of 18 was significantly affected by time of day. As observed in the univariate analysis, the modal pattern was a dome-shaped relationship with activity peaking in late morning or early afternoon. However, there was considerable individual variability in activity within and between sites, so that only 29% of fish showed this modal pattern of activity, nine of which were in the Gorge. Five other fish increased their activity over the day, similar to the average pattern for 1+ fish, and three fish decreased their activity over the day. The importance of time of day also varied among sites; for example, time of day had a significant effect on the activity of 15 of 18 fish in the Gorge but only 2 of 13 fish in the River (χ^2 test of independence: χ^2_1 = 14.1, $P < 0.001$).

Seventeen of 35 YOY fish responded significantly to water temperature; 14 fish increased their activity with increasing water temperature, nine of which were in the River, whereas only two fish showed a dome-shaped relationship. These latter two fish were both in the Gorge and showed peaks in activity of 83% and 72% both at 21 °C. Site differences in the importance of water temperature were also apparent; water temperature had a significant effect on the activity of 9 of 13 fish in the River but only 6 of 18 fish in the Gorge (χ^2 test of independence: χ^2_1 = 3.89, $P < 0.05$).

Sixteen of 35 YOY fish responded significantly to day of the year, but the patterns were quite variable. The modal pattern was a decrease in activity over the summer, but only eight fish showed this pattern, seven of which were in the Gorge. In contrast, four of five fish showing an increase in activity over the season were in the Mouth. Only 7 of 35 YOY fish responded significantly to light intensity. The abundance of drifting invertebrates was used in simple and multiple logistic regressions but was not a significant predictor of activity.

Discussion

The results of this study indicated that (*i*) on average, YOY fish were more active during the day than at night and vice versa for 1+ fish, (*ii*) the average activity of YOY and 1+ fish peaked at a higher temperature than the optimum based on laboratory studies, and (*iii*) there was considerable individual variability with respect to diel activity patterns both within and between sites.

The differences in the average activity patterns between YOY and 1+ Atlantic salmon in this study support the findings of previous studies. The YOY fish in Catamaran Brook were active predominantly during the day throughout their primary growth period (July and August) (Girard et al. 2004), presumably to maximize their growth rate by feeding when conditions are optimal for visual foraging (Wilzbach et al. 1986) and sustaining energy reserves (Bacon et al. 2005). Interestingly, Gries et al. (1997) found that YOY fish were almost as active at night as during the day. These divergent findings may be the result of seasonal differences in the two studies; we observed YOY salmon during the peak of their growing season, whereas Gries et al. (1997) observed fish later in the growing season.

© 2007 NRC Canada

Fig. 4. Logistic regressions of the daytime activity in relation to water temperature of 35 YOY Atlantic salmon found in the (*a*) Gorge, (*b*) River, and (*c*) Mouth and (*d*) eight 1+ salmon at all sites. The solid lines represent significant linear or quadratic logistic regressions, whereas broken lines were not significant. Sample size varied between 48 and 67 observations for each fish.

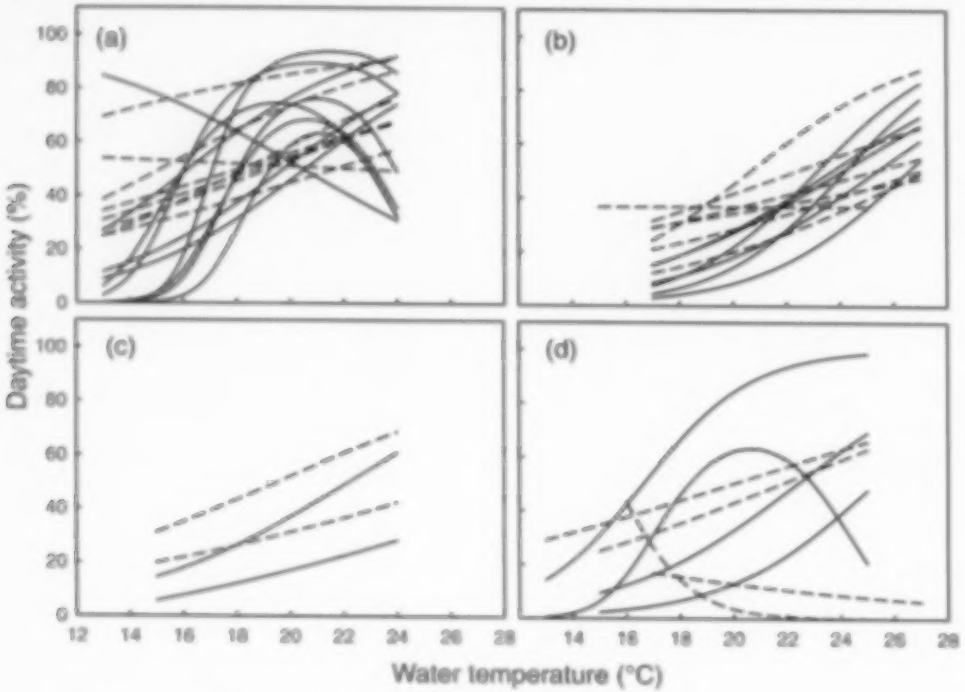

Table 2. Multiple logistic regressions of the daytime activity of 35 YOY Atlantic salmon in relation to each environmental variable.

Environmental variable[a]	Increase[b]	Decrease[b]	Dome-shaped[c]	U-shaped[c]	Modal pattern	% conforming to modal pattern[d]
Time of day (hour)	5 (4, 0, 1)	3 (2, 1, 0)	10 (9, 1, 0)	0	Dome	29
Water temperature (°C)	14 (3, 9, 2)	1 (1, 0, 0)	2 (2, 0, 0)	0	Increase	40
Day of the year	5 (5, 0, 0)	8 (0, 7, 1)	2 (0, 0, 2)	1 (1, 0, 0)	Decrease	23
Light intensity (lx)	5 (4, 0, 1)	1 (1, 0, 0)	1 (0, 0, 1)	0	Increase	14

Note: The numbers represent the number of fish for which a particular environmental variable was significantly related to activity when entered last in the model. The numbers in parentheses refer to how many of these fish were located in the Gorge, River, or Mouth, respectively.

[a]Logistic regressions are based on $\log_{10}$-transformed data for light intensity.

[b]Activity either increased or decreased in response to an environmental variable.

[c]Dome-shaped and U-shaped are significant quadratic curves with a maximum and minimum, respectively.

[d]Percentage of all fish conforming to the modal activity pattern for that age class.

In contrast, the 1+ fish were more active at night than during the day during July and August, a pattern also observed by Gries et al. (1997) later in the season (end of August and early September) and by Imre and Boisclair (2004). Age 1+ fish grow little during July and August in Catamaran Brook (also see Swansburg et al. 2002), perhaps because the abundance of invertebrate drift declines over the summer (Keeley and Grant 1997; Steingrímsson and Grant 1999; this study) or because they have reached a critical body size for overwintering. Hence, given the reduced benefits of daytime feeding, 1+ fish probably maximize their fitness by feeding mainly at night to minimize their risk of predation during the day. Further studies of nighttime activity of 1+ fish are required to properly assess this hypothesis.

It was striking how inactive the fish were during the summer, the period of active growth. During the daytime, the YOY fish were active on average only 46% of the time with a peak of 56% early in the afternoon. Similarly, 1+ fish were active on average 37% of the time, but 74% of the fish were active at night. The fish from both age classes were possibly obtaining enough food during their short bouts of activity to reach sizes sufficient to survive the winter period (Cunjak et al. 1998 and references therein), without unduly increasing their risk of predation. Taken together, the different diel activity patterns of the two age classes are consistent with the hypothesis of asset protection (Clarke 1994). Larger or older individuals, who are closer to reproductive size or age, are predicted to take fewer chances while foraging to reduce their risk of predation. Consistent with this prediction, larger, older salmonid fishes typically take fewer risks with predators by taking longer to resume foraging (Grant and Noakes 1987; Reinhardt and Healey 1999) or moving farther

© 2007 NRC Canada

(Dionne and Dodson 2002) after a disturbance or predation event.

Contrary to our expectations, YOY and 1+ fish did not show a strong daytime peak in activity at their optimal water temperature in the laboratory (16–20 °C). On average, the activity of YOY fish did not decline at water temperatures >20 °C but leveled off between 23 and 27 °C. In laboratory studies, when fish are fed to satiation, salmon begin to decrease their foraging rate and growth rate at temperatures between 22 and 25 °C (Elliott and Hurley 1997; Jonsson et al. 2001). However, under natural conditions, fish may need to continue feeding at temperatures that are not optimal for growth in order to meet a critical size. Furthermore, wild fish are generally smaller than laboratory fish at age and thus can likely metabolize more efficiently and consequently remain active at higher temperatures. For 1+ fish, a peak in daytime activity was detected at 21 °C, much higher than the preferred temperature of 17 °C under laboratory conditions (Javaid and Anderson 1967). As mentioned above, differences in body condition of the fish may influence the temperature at which optimal growth and performance occur. The decrease in observed activity of 1+ fish at water temperatures >21 °C is likely because they are sheltering to avoid excessive energy expenditure or have moved to cooler water to escape the higher metabolic demands of increased temperature (Gibson 1966).

The most striking finding of our study was the magnitude of individual variability in activity patterns. For example, the dome-shaped pattern of diel activity exhibited by the average of the 35 YOY fish was observed in only 17 and 10 fish in the univariate and multivariate analyses, respectively. In contrast with this average pattern, three YOY fish in the Gorge and two in the Mouth were most active at night, typical of 1+ fish. While only two of these fish were larger than average when they were tagged, three of these fish for which body length measurements were available from the end of the study were larger (55.0, 54.9, and 50.4 mm) than the average fish at these sites (mean = 49.7 mm). Perhaps these fish had quickly reached a body size at which it was more beneficial to trade off a higher growth rate for a lower risk of predation. Similarly, two 1+ fish exhibited a U-shaped daily activity pattern; they were active at dawn and dusk–night but were almost totally inactive during the day. These two fish were initially larger (76.7 and 79.1 mm) than the average fish (mean = 71.7 mm) and the one fish for which we have data from the end of the study was much larger (85.7 mm) than the average 1+ fish (mean = 75.5 mm). This anecdotal information suggests that some of the individual variability in daily activity patterns may be explained by body size. Small fish may be taking risks to catch up, whereas large fish may be protecting their accumulated assets.

Individual variability was also clearly related to differences among sites. The activity of YOY fish in the Gorge was most frequently affected by time of day, whereas those in the River were most frequently affected by water temperature. The median water temperature in the Gorge, ~19 °C, was within the optimal range for Atlantic salmon growth (Elliott and Hurley 1997; Jonsson et al. 2001). Hence, it was perhaps not surprising that the YOY salmon in the Gorge responded less to water temperature than to other environmental factors. In contrast, the median water temperature at the River sites was ~3 °C higher than in the Gorge, and the highest water temperatures at River sites approached the lethal temperature of 28 °C (Garside 1973; Elliott and Hurley 1997). Hence, it seems reasonable that salmon in the River would decrease their activity levels in response to these less than ideal water temperatures. Unexpectedly, however, their activity actually increased, even when water temperatures approached 27 °C. Because fish in the River sites were smaller than those in the Gorge (Breau 2003), they may have increased their activity to maximize growth rate in response to the increasing metabolic demands of the warmer water temperatures. Perhaps because of their smaller size, the YOY fish could better cope with the higher temperatures (Schmidt-Nielsen 1997). Another possibility might be that the fish were taking advantage of the fact that larger fish were not out foraging at these temperatures.

The advantage of monitoring marked individuals is the ability to detect individual variation. Sometimes, overall patterns were an accurate representation of individuals in the population. For example, most YOY fish were more active during the day than at night and vice versa for 1+ fish. In most other cases, however, overall patterns obscured important variation in activity between sites and between individuals. For example, the overall relationship between daytime activity and water temperature for 1+ fish was a dome-shaped curve, whereas only one of eight individuals exhibited such a relationship. The functional reasons for this important variation in behaviour deserve further study.

Acknowledgements

We thank Stefán Steingrímsson for developing the tagging technique and James Connop, Yannick Da Silva, and André Drapeau for help with electrofishing. We also thank Rick Cunjak of the University of New Brunswick and Peter Hardie and Daniel Caissie of the Department of Fisheries and Oceans for facilitating this research, which was financially supported by a research grant from the Natural Sciences and Engineering Research Council of Canada to J.W.A.G., a Natural Sciences and Engineering Research Council of Canada undergraduate student research award to L.K.W., and a graduate teaching assistantship from Concordia University to C.B. This paper is contribution No. 77 of the Catamaran Brook Habitat Research Project.

References

Bacon, P.J., Gurney, W.S.C., Jones, W., McLaren, I.S., and Youngson, A.F. 2005. Seasonal growth patterns of wild juvenile fish: partitioning variation among explanatory variables, based on individual growth trajectories of Atlantic salmon (*Salmo salar*) parr. J. Anim. Ecol. **74**: 1–11.

Bradford, M.J., and Higgins, P.S. 2001. Habitat-, season-, and size-specific variation in diel activity patterns of juvenile chinook salmon (*Oncorhynchus tshawytscha*) and steelhead trout (*Oncorhynchus mykiss*). Can. J. Fish. Aquat. Sci. **58**: 365–374.

Breau, C. 2003. Individual variability in activity patterns of juvenile Atlantic salmon (*Salmo salar*). M.Sc. thesis, Concordia University, Montreal, Que.

Clarke, C.W. 1994. Antipredator behaviour and the asset-protection principle. Behav. Ecol. **5**: 159–170.

© 2007 NRC Canada

Cunjak, R.A., Caissie, D., El-Jabi, N., Hardie, P., Conlon, J.H., Pollock, T.L., Giberson, D.J., and Komadina-Douthwright, S. 1993. The Catamaran Brook (New Brunswick) habitat research project: biological, physical, and chemical conditions (1990–1992). Can. Tech. Rep. Fish. Aquat. Sci. No. 1914.

Cunjak, R.A., Prowse, T.D., and Parrish, D.L. 1998. Atlantic salmon (*Salmo salar*) in winter: "the season of parr discontent"? Can. J. Fish. Aquat. Sci. **55**(Suppl. 1): 161–180.

Dewey, M.R., and Zigler, S.J. 1996. An evaluation of fluorescent elastomer for marking bluegills in experimental studies. Prog. Fish-Cult. **58**: 219–220.

Dionne, M., and Dodson, J.J. 2002. Impact of exposure to a simulated predator (*Mergus merganser*) on the activity of juvenile Atlantic salmon (*Salmo salar*) in a natural environment. Can. J. Zool. **80**: 2006–2013.

Elliott, J.M., and Hurley, M.A. 1997. A functional model for maximum growth of Atlantic salmon parr, *Salmo salar*, from two populations in northwest England. Funct. Ecol. **11**: 592–603.

Fraser, N.H.C., and Metcalfe, N.B. 1997. The cost of becoming nocturnal: feeding efficiency in relation to light intensity in juvenile Atlantic salmon. Funct. Ecol. **11**: 385–391.

Fraser, N.H.C., Metcalfe, N.B., and Thorpe, J.E. 1993. Temperature-dependent switch between diurnal and nocturnal foraging in salmon. Proc. R. Soc. Lond. B Biol. Sci. **252**: 135–139.

Garside, E.T. 1973. Ultimate upper lethal temperature of Atlantic salmon *Salmo salar* L. Can. J. Zool. **51**: 898–900.

Gibson, R.J. 1966. Some factors influencing the distributions of brook trout and young Atlantic salmon. J. Fish. Res. Board Can. **23**: 1977–1980.

Girard, I.L., Grant, J.W.A., and Steingrímsson, S.Ó. 2004. Foraging, growth and loss rate of young-of-the-year Atlantic salmon (*Salmo salar*) in relation to habitat use in Catamaran Brook, New Brunswick. Can. J. Fish. Aquat. Sci. **61**: 2339–2349.

Grant, J.W.A., and Noakes, D.L.G. 1987. Escape behaviour and use of cover by young-of-the-year brook trout, *Salvelinus fontinalis*. Can. J. Fish. Aquat. Sci. **44**: 1390–1396.

Gries, G., Whalen, K.G., Juanes, F., and Parrish, D.L. 1997. Nocturnal activity of juvenile Atlantic salmon (*Salmo salar*) in late summer: evidence of diel activity partitioning. Can. J. Fish. Aquat. Sci. **54**: 1408–1413.

Heggenes, J., Krog, O.M.W., Lindås, O.R., Dokk, J.G., and Bremnes, T. 1993. Homeostatic behavioural responses in a changing environment: brown trout (*Salmo trutta*) become nocturnal during winter. J. Anim. Ecol. **62**: 295–308.

Imre, I., and Boisclair, D. 2004. Age effects on diel activity patterns of juvenile Atlantic salmon: parr are more nocturnal than young-of-the-year. J. Fish Biol. **64**: 1731–1736.

Javaid, M.Y., and Anderson, J.M. 1967. Thermal acclimation and temperature selection in Atlantic salmon, *Salmo salar*, and rainbow trout, *S. gairdneri*. J. Fish. Res. Board Can. **24**: 1507–1513.

Jonsson, B., Forseth, T., Jensen, A.J., and Næsje, T.F. 2001. Thermal performance of juvenile Atlantic salmon, *Salmo salar* L. Funct. Ecol. **15**: 710–711.

Kalleberg, H. 1958. Observations in a stream tank of territoriality and competition in juvenile salmon and trout (*Salmo salar* L., and *S. trutta*). Inst. Freshw. Res. Drottningholm Rep. **39**: 55–98.

Keeley, E.R., and Grant, J.W.A. 1997. Allometry of diet selectivity in juvenile Atlantic salmon (*Salmo salar*). Can. J. Fish. Aquat. Sci. **54**: 1894–1902.

Keene, J.L., Noakes, D.L.G., Moccia, R.D., and Soto, C.G. 1998. The efficacy of clove oil as an anaesthetic for rainbow trout, *Oncorhynchus mykiss* (Walbaum). Aquacult. Res. **29**: 89–101.

Keenleyside, M.H.A. 1962. Skin-diving observations of Atlantic salmon and brook trout in the Miramichi River, New Brunswick. J. Fish. Res. Board Can. **19**: 625–634.

LeDrew, L.J., Scruton, D.A., McKinley, R.S., and Power, G. 1996. A comparison of habitat suitability indices developed from daytime versus nighttime observations for Atlantic salmon in a regulated Newfoundland stream. *In* Proceedings of the 2nd International Symposium on Habitat Hydraulics: Ecohydraulics 2000, June 1996, Quebec. Vol. B. *Edited by* M. Leclerc, H. Capra, S. Valentin, A. Boudreault, and Y. Côté. INRS-Eau, Québec, Que. pp. 33–44.

Metcalfe, N.B., Fraser, N.H.C., and Burns, M.D. 1999. Food availability and the nocturnal vs. diurnal foraging trade-off in juvenile salmon. J. Anim. Ecol. **68**: 371–381.

Randall, R.G. 1982. Emergence, population densities, and growth of salmon and trout fry in two New Brunswick streams. Can. J. Zool. **60**: 2239–2244.

Reinhardt, U.G., and Healey, M.C. 1999. Season and size-dependent risk taking in juvenile coho salmon: experimental evaluation of asset protection. Anim. Behav. **57**: 923–933.

Rimmer, D.M., and Paim, U. 1983. Autumnal habitat shift of juvenile Atlantic salmon (*Salmo salar*) in a small river. Can. J. Fish. Aquat. Sci. **40**: 671–680.

Schmidt-Nielsen, K. 1997. Animal physiology: adaptation and environment. 5th ed. Cambridge University Press, Cambridge, UK. pp. 217–238.

Sokal, R.R., and Rohlf, F.J. 1995. Biometry: the principles and pratice of statistics in biological research. 3rd ed. W.H. Freeman and Company, New York.

Steingrímsson, S.Ó., and Grant, J.W.A. 1999. Allometry of territory size and metabolic rate as predictors of self-thinning in young-of-the-year Atlantic salmon. J. Anim. Ecol. **68**: 17–26.

Steingrímsson, S.Ó., and Grant, J.W.A. 2003. Patterns and correlates of movement and site fidelity in individually marked young-of-the-year Atlantic salmon (*Salmo salar*). Can. J. Fish. Aquat. Sci. **60**: 193–202.

Swansburg, E., Chaput, G., Moore, D., Caissie, D., and El-Jabi, N. 2002. Size variability of juvenile Atlantic salmon: links to environmental conditions. J. Fish Biol. **61**: 661–683.

Valdimarsson, S.K., and Metcalfe, N.B. 1999. Effect of time of day, time of year, and life history strategy on time budgeting in juvenile Atlantic salmon, *Salmo salar*. Can. J. Fish. Aquat. Sci. **56**: 2397–2403.

Wilzbach, M.A., Cummins, K.W., and Hall, J.D. 1986. Influence of habitat manipulations on interactions between cutthroat trout and invertebrate drift. Ecology. **67**: 898–911.

© 2007 NRC Canada

Spatial and temporal patterns in the food web structure of a large floodplain river assessed using stable isotopes

Brian R. Herwig, David H. Wahl, John M. Dettmers, and Daniel A. Soluk

Abstract: We assessed naturally occurring stable isotope ratios of carbon ($\delta^{13}C$) and nitrogen ($\delta^{15}N$) for available food resources and consumers in the mainstream channel of the Mississippi River. Isotopic ratios were assessed for organic sources and organisms at two different sites during a fall, spring, and two summer seasons. Terrestrial C_4 plants did not appear to be an important carbon source for consumers in the mainstream channel. A mixing model, IsoSource, indicated that terrestrial C_3 vegetation, suspended algae, and epixylon were at times important food resources for large river consumers. Many consumer signatures fell outside the mixing polygon defined by these sources, indicating that there was a ^{13}C-depleted food resource for which we did not account. We could not distinguish precisely whether downstream allochthonous and autochthonous carbon, or in situ production, was the dominant food resource supporting consumers in these systems. However, our data suggest that in situ organic matter sources can be important. Consumer $\delta^{13}C$ and $\delta^{15}N$ signatures intermediate between several sources indicated widespread omnivory in the river reaches that we studied. To fully understand food web structure and energy sources in complex large river ecosystems, an integrative approach that combines related empirical data sets is needed.

Résumé : Nous avons déterminé les rapports des isotopes stables de carbone ($\delta^{13}C$) et d'azote ($\delta^{15}N$) qui existent naturellement dans les ressources alimentaires et les consommateurs dans le chenal principal du Mississippi. Nous avons déterminé les rapports isotopiques pour les sources organiques et les organismes à deux sites différents durant un automne, un printemps et deux étés. Les plantes terrestres C_4 ne semblent pas constituer une source importante de carbone pour les consommateurs dans le chenal principal. Un modèle de mélange, IsoSource, indique que la végétation terrestre C_3, les algues en suspension et l'épixylon sont à certains moments des sources alimentaires importantes pour les consommateurs dans les grandes rivières. Plusieurs signatures de consommateurs se retrouvent à l'extérieur du polygone de mélange défini à partir de ces sources, ce qui indique qu'il existe une source de nourriture pauvre en C^{13} dont nous n'avons pas tenu compte. Nous n'arrivons pas à déterminer précisément si c'est le carbone allochtone et autochtone de l'aval ou alors la production in situ qui représente la ressource alimentaire principale qui fait vivre les consommateurs dans ces systèmes. Toutefois, nos données indiquent que les sources in situ de matière organique peuvent être importantes. Les signatures $\delta^{13}C$ et $\delta^{15}N$ de consommateurs qui sont intermédiaires entre plusieurs sources montrent que l'omnivorie est répandue dans les sections de rivière étudiées. Il faut une approche intégrée qui combine les divers ensembles reliés de données empiriques pour bien comprendre la structure du réseau alimentaire et les sources d'énergie dans les écosystèmes complexes des grandes rivières.

[Traduit par la Rédaction]

Introduction

In contrast with other aquatic systems, our understanding of food webs and energy flows in large floodplain river ecosystems is limited (Johnson et al. 1995). Large floodplain rivers contain a mosaic of lotic habitats (main channel and side channel) and comparatively lentic habitats (backwater lakes, bays, some side channels, hereafter referred to as slackwater habitats) that are interconnected during periods of flooding. These interconnections allow for the exchange

Received 31 March 2006. Accepted 1 December 2006. Published on the NRC Research Press Web site at http://cjfas.nrc.ca on 5 April 2007.
J19253

B.R. Herwig.[1,2] Illinois Natural History Survey, Section for Aquatic Ecology and Conservation, 1816 S. Oak Street, Champaign, IL 61820, USA.
D.H. Wahl. Kaskaskia Biological Station, Illinois Natural History Survey, R.R. 1, Box 157, Sullivan, IL 61951, USA.
J.M. Dettmers.[3] Lake Michigan Biological Station, Illinois Natural History Survey, 400 17th Street, Zion, IL 60099, USA.
D.A. Soluk. Department of Biology, University of South Dakota, 414 E. Clark Street, Vermillion, SD 57069, USA.

[1]Corresponding author (e-mail: brian.herwig@dnr.state.mn.us).
[2]Present address: Minnesota Department of Natural Resources, Division of Fish and Wildlife – Fisheries Research, 2114 Bemidji Avenue, Bemidji, MN 56601, USA.
[3]Present address: Great Lakes Fishery Commission, 2100 Commonwealth Boulevard, Suite 100, Ann Arbor, MI 48105, USA.

 doi:10.1139/F07-023 © 2007 NRC Canada

of nutrients and organisms among habitats within these ecosystems (Welcomme 1979; Junk et al. 1989; Johnson et al. 1995).

Potential energy sources for large river ecosystems include allochthonous and autochthonous organic matter transported from upstream, allochthonous material from adjacent riparian vegetation, and autochthonous production within either the main channel or slackwater habitats. Especially during times of flooding, both autochthonous sources from backwater lakes and allochthonous inputs carried off the floodplain could be important. Three major concepts have been advanced to describe the energy sources and processes that shape biotic communities in large rivers: the river continuum concept (RCC) (Vannote et al. 1980), the flood pulse concept (Junk et al. 1989), and the riverine productivity model (Thorp and DeLong 1994). The RCC views rivers as longitudinally linked systems in which biotic assemblages and ecosystem-level properties shift in a predictable manner along the length of a river from its headwaters to reaches far downstream (Vannote et al. 1980). Subsequent revisions to the RCC for large rivers emphasize the role of site-specific influences in modifying predictions of the RCC, including constraints imposed by climate, geography, geomorphology and lithology, and anthropogenic changes (Minshall et al. 1985) as well as the degree of interaction between the river and its floodplain forest (Sedell et al. 1989). The original RCC suggests that the main energy source for large rivers is fine particulate organic matter transported from upstream areas, while riparian leaf matter inputs and in situ primary production were thought to be of little importance (Vannote et al. 1980). The flood pulse concept introduces a lateral dimension to the function of large river systems (Junk et al. 1989) and views upstream sources of organic matter to be less important than material derived from the floodplain during the annual flood pulse (Junk et al. 1989). The riverine productivity model hypothesizes that the major sources of organic matter assimilated by aquatic organisms in large rivers are either from autochthonous production in the channel or from leaf litter inputs from the riparian zone directly upstream and adjacent to the channel (Thorp and Delong 1994). Little empirical evidence indicates which of these concepts more accurately represents the energy sources and the processes that structure energy flow in large river ecosystems (but see Hamilton et al. 1992; Angradi 1994; Delong et al. 2001).

One potentially powerful approach to determining patterns of energy flow and food web linkages in ecosystems is through the use of naturally occurring stable isotopes of carbon and nitrogen (Peterson and Fry 1987; McCutchan and Lewis 2002). Investigations using multiple stable isotopes (carbon and nitrogen and sometimes sulfur) have successfully determined feeding relationships and energy flows in lakes, streams, estuaries, and marine ecosystems. Studies using naturally occurring ^{13}C and ^{15}N abundances to evaluate the relative importance of autochthonous versus allochthonous sources of energy in streams have had varied success. Some studies reported distinct signatures (Rounick and Hicks 1985; Bunn et al. 1989; Angradi 1994), whereas others could not differentiate between signatures (Rosenfeld and Roff 1992; France 1995, 1996). In the floodplain of the Orinoco River, Venezuela, Hamilton et al. (1992) demonstrated the importance of phytoplankton and epiphytic algae in floodplain food webs despite abundant aquatic vascular plants that were assumed to be important energy sources. In main channel habitats of the Ohio River, Thorp et al. (1998) concluded that bulk, ultrafine transported organic matter (≤1 μm) and dissolved organic matter were the sources most likely supporting invertebrate and fish consumers. However, the Ohio River is very highly modified and unusual because it has a constricted floodplain with few backwaters; thus, it is difficult to know whether results from this system are widely applicable to other large rivers.

In this study, we measured naturally occurring carbon and nitrogen stable isotope ratios of aquatic plants and animals in the mainstream channel of the Mississippi River, the largest floodplain river in North America. One goal of this study was to explore whether organic matter energy sources (e.g., algae, terrestrial detritus, etc.) for higher trophic levels could be distinguished from one another using combined $\delta^{13}C$ and $\delta^{15}N$ signatures. Additional goals of this study were to determine the relative importance of the ultimate basal resources supporting main channel consumers and a better understanding of seasonal and spatial variation in the trophic structure of main channel food webs. We compared stable isotope signatures of consumers and primary basal resources from two main channel sites that varied substantially in the amount of adjacent slackwater aquatic habitat and evaluated seasonal contributions of potential energy resources for consumers at both sites.

Materials and methods

Study sites and sampling design

The Mississippi River is a large floodplain–river ecosystem with a mosaic of main and side channels, backwater lakes, and seasonally inundated wetlands. Despite extensive channel and floodplain modifications (e.g., levee construction and land use conversion to agriculture), seasonal flood pulses cover the floodplain for extended periods connecting river channel, slackwater, and terrestrial habitats (Sparks et al. 1998). We sampled food webs from two main channel sites of the Upper Mississippi River that varied greatly in amount of side channel and slackwater habitat (Figs. 1*b* and 1*d*). One main channel site was located in Reach 13 (MR13) (river kilometre 872, latitude, longitude (DMS) 42°8′46″, 90°12′19″) near Savanna, Illinois (Fig. 1*c*), and another in Reach 26 (MR26) (river kilometre 359, latitude, longitude (DMS) 38°55′26″, 90°30′2″) near Grafton, Illinois (Fig. 1*e*). MR13 has extensive slackwater and side channel habitats. The spring flood pulse typically is of short duration (Figs. 1*b* and 2*a*). MR26 is relatively isolated from the floodplain by levees. As a consequence, it has few slackwater habitats and a spring flood pulse typically of long duration (Figs. 1*d* and 2*b*). Streambed sediments at our study sites consisted primarily of sand. In areas not converted to agriculture (primarily field corn (*Zea mays*) in both study areas), dominant floodplain vegetation includes maple (*Acer* spp.), cottonwood (*Populus* spp.), willow (*Salix* spp.), and floodplain grasses. Agricultural land use within the immediate floodplain of the two river reaches studied (Figs. 1*b* and 1*d*) was more than twice as extensive at MR26 (31.7 ×

© 2007 NRC Canada

Fig. 1. Map showing the regional and specific locations of our study sites: (*a*) location of Reach 13 (north) and Reach 26 of the Mississippi River, (*b*) detail of Reach 13 showing extensive slackwater habitat throughout the reach (indicated by all areas in black in addition to the mainstem channel), (*c*) specific location of the study site MR13 denoted by a white asterisk, (*d*) detail of Reach 26 showing sparse slackwater habitat throughout the reach (indicated by all areas in black in addition to the mainstem channel), and (*e*) specific location of the study site MR13 denoted by a white asterisk.

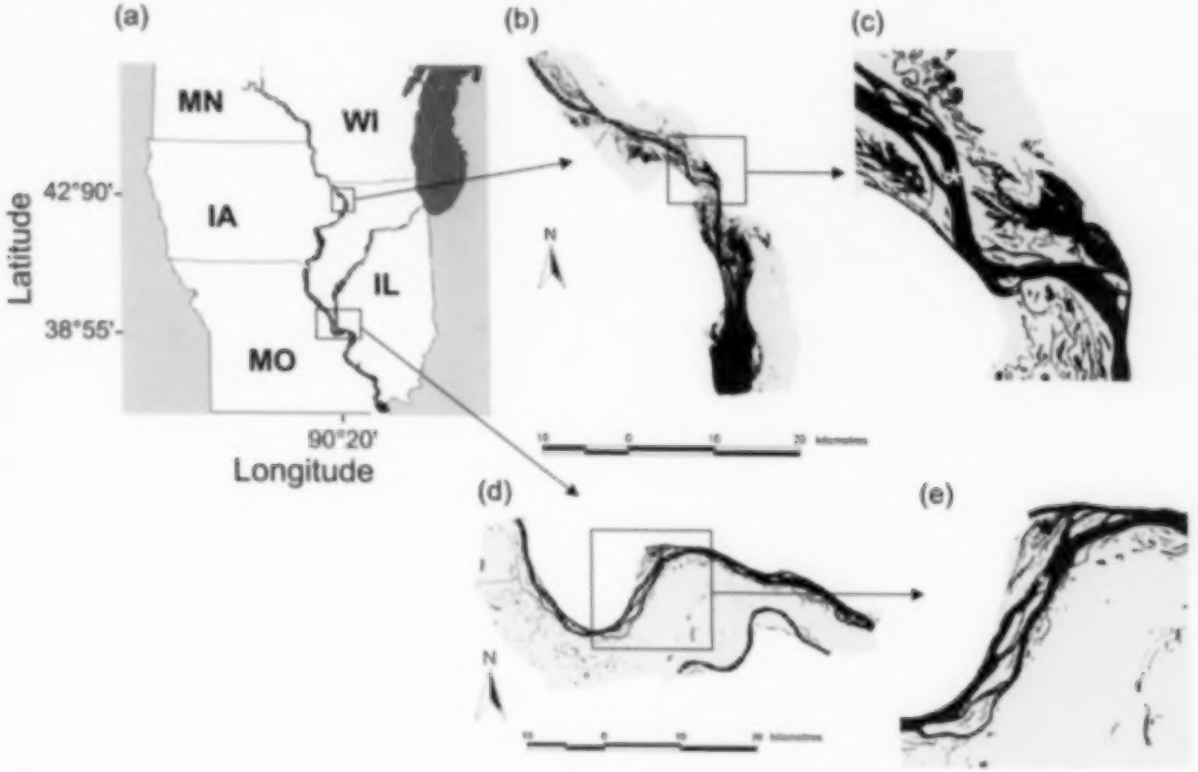

10^3 ha, or 53.4% of the river–floodplain area) than at MR13 (9.1×10^3 ha, or 35.3% of the river–floodplain area).

The specific sampling locations (for both MR13 and MR26) were located at approximately the middle of the reach (longitudinally) and were not directly adjacent to or immediately downstream of any side channel or tributary stream (Figs. 1*c* and 1*e*). These sampling locations provided us with a spatially integrated representation of all upstream aquatic (river channel and slackwater) habitats and carbon sources potentially contributing to the mainstem food web, thereby allowing us to capture broad-scale differences in floodplain characteristics between the two sites.

Food web components sampled

Organisms for stable isotope analysis were sampled in summer (July) and fall (November) in 1998 and in spring (early April) and summer (July) in 1999. When possible, up to five replicate samples were collected for each food web component (both sources and animals), although zooplankton and some macroinvertebrate groups were typically represented by a single sample. At each site, we collected suspended algae. Epixylon (microalgae attached to wood) was collected only in summer 1999; here, individual algal filaments were physically removed from detrital material and washed repeatedly with distilled water. Foliage from dominant riparian vegetation was collected from the floodplain forest and adjacent agricultural fields during summer 1998. Isotope signatures for terrestrial vegetation exhibit minimal temporal variability; thus, values from summer 1998 were used to represent these sources across seasons and years. Terrestrial C_3 plant signatures were represented by tree leaves and floodplain grasses; terrestrial C_4 plant signatures were represented by field corn. Based on $^{13}C/^{12}C$ isotope ratios of the several species of common floodplain grasses that we sampled, all apparently used the C_3 pathway for photosynthesis. This is despite C_4 grass species reportedly representing 30%–40% of the native grass flora within this region of North America (Teeri and Stowe 1976).

In the main channel and main channel border, drifting invertebrates were collected from the water column by suspending a drift net (500 µm) just beneath the surface of the water beside or behind an anchored boat for 10–15 min. Benthic macroinvertebrates in main channel sediments were collected using a Ponar grab sampler. All animals were immediately placed on ice and transported to the laboratory. Samples were then sorted, identified, and gut contents removed by dissection to eliminate any bias in the stable isotope signature from stomach content items (Hamilton et al. 1992; Angradi 1994; Junger and Planas 1994). To meet the

© 2007 NRC Canada

Fig. 2. Daily pool elevations of two reaches of the Mississippi River at (*a*) MR13 and (*b*) MR26 plotted for 1998 (solid line) and 1999 (broken line).

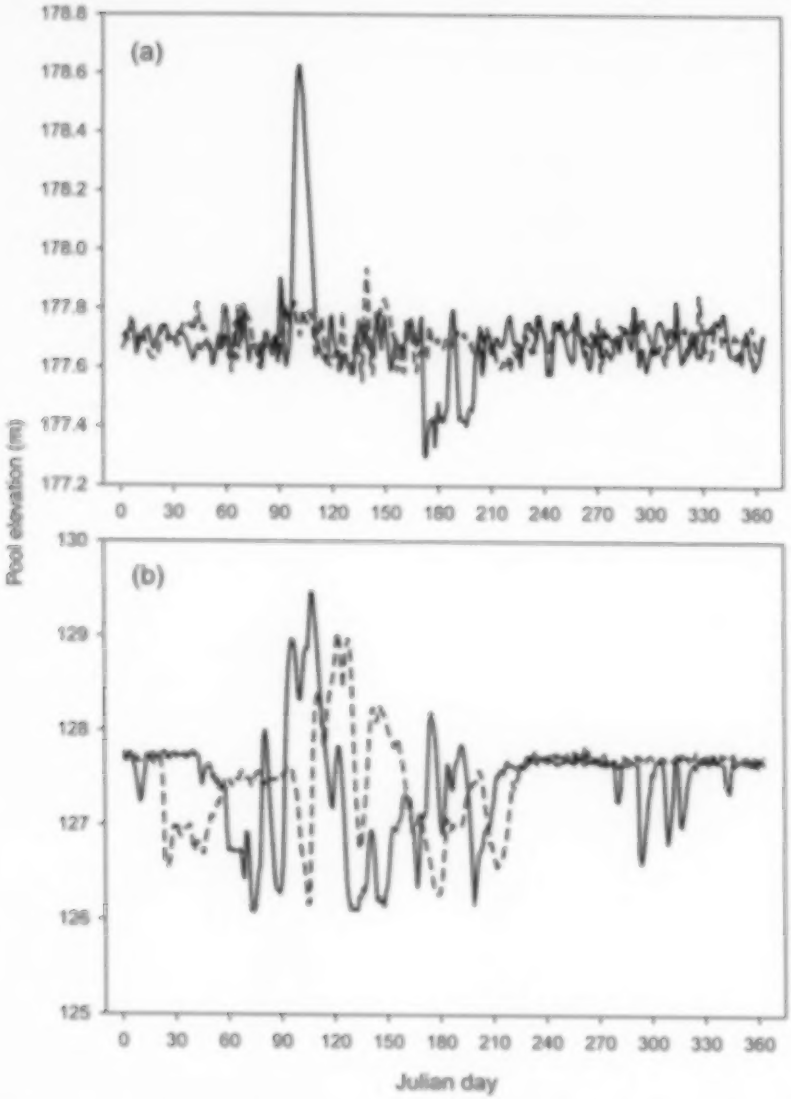

minimum sample requirement of 2 mg, stable isotope ratios for all invertebrate and zooplankton taxa were determined from composite samples containing multiple individuals.

Snails and zebra mussels (*Dreissena polymorpha*) were collected from rocks along the riverbank, when low water levels permitted collection (typically summer and fall). Only the flesh was used for stable isotope analysis because shell material is enriched in ^{13}C and does not reflect the $\delta^{13}C$ signature of food sources consumed (Mitchell et al. 1996). Zooplankton were collected from the main channel by suspending a conical zooplankton net (0.5 m diameter, 64 µm mesh) from an anchored boat beneath the surface of the water for 5–10 min. Zooplankton were placed in a Ziplock® bag, frozen, and later separated into taxonomic groups using a dissecting microscope.

During each sampling period, adult gizzard shad (*Dorosoma cepedianum*), bluegill (*Lepomis macrochirus*), and freshwater drum (*Aplodinotus grunniens*) were sampled for isotopic analysis. During the summer, additional fish species were sampled, including channel catfish (*Ictalurus punctatus*), smallmouth buffalo (*Ictiobus bubalus*), common carp (*Cyprinus carpio*), white bass (*Morone chrysops*), mooneye (*Hiodon tergisus*), and shortnose gar (*Lepisosteus platostomus*). Adult fish were collected primarily using boat-mounted electrofishing equipment supplemented by angling. Fish were collected from border areas only. Collecting in the midchannel area was not possible given the depths and flow rate. Dorsal white muscle tissue was removed from each fish, since this tissue has been shown to be representative of the overall stable isotope signature of fish (Rounick and

© 2007 NRC Canada

Fig. 3. Estimated average $\delta^{15}N$ and $\delta^{13}C$ signatures of food resources assimilated by selected common large river consumers at MR13 in (*a*) summer 1998, (*b*) fall 1998, (*c*) spring 1999, and (*d*) summer 1999. The triangle defined by the broken lines represents the mixing polygon for the three major ultimate organic matter sources in the system: C_3 terrestrial plants (C_3), C_4 terrestrial grasses (C_4), and suspended algae (alg). Suspended algae were not sampled in fall 1998; thus, we used the summer 1998 value to represent this source. During summer 1999, we also considered a fourth organic matter source, epixylon (epi). Arrow tips represent the isotopic position (average mixture) of food resources assimilated by selected consumers. When arrow tips fall within the mixing polygon, all feasible solutions of the proportion of each of the three (or four) ultimate organic sources supporting that consumer can be calculated at 1‰ increments using an isotopic mixing model. Consumers: blg, bluegill; cad, hydropsychid caddisfly; cop, copepod; chi, chironomid larvae; fwd, freshwater drum; gzd, gizzard shad; hep, heptageniid mayfly.

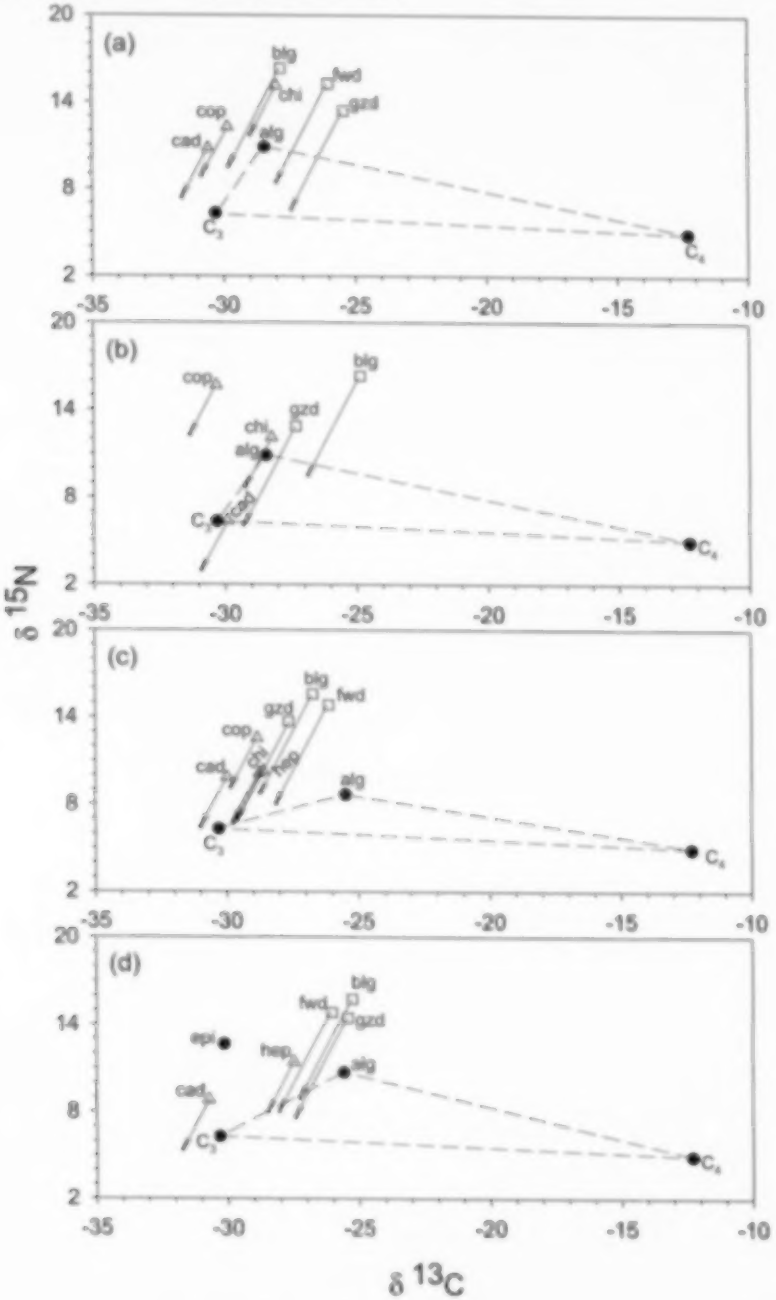

© 2007 NRC Canada

Fig. 4. Estimated average $\delta^{15}N$ and $\delta^{13}C$ signatures of food resources assimilated by selected common large river consumers at MR26 in (*a*) summer 1998, (*b*) fall 1998, (*c*) spring 1999, and (*d*) summer 1999. The triangle defined by the broken lines represents the mixing polygon for the three major ultimate organic matter sources in the system: C_3 terrestrial plants (C_3), C_4 terrestrial grasses (C_4), and suspended algae (alg). Suspended algae was not sampled in fall 1998; thus, we used the summer 1998 value to represent this source. During summer 1999, we also considered a fourth organic matter source, epixylon (epi). Arrow tips represent the isotopic position (average mixture) of food resources assimilated by selected consumers. When arrow tips fall within the mixing polygon, all feasible solutions of the proportion of each of the three (or four) ultimate organic sources supporting that consumer can be calculated at 1‰ increments using an isotopic mixing model. Consumers: blg, bluegill; cad, hydropsychid caddisfly; cop, copepod; chi, chironomid larvae; fwd, freshwater drum; gzd, gizzard shad; hep, heptagenid mayfly.

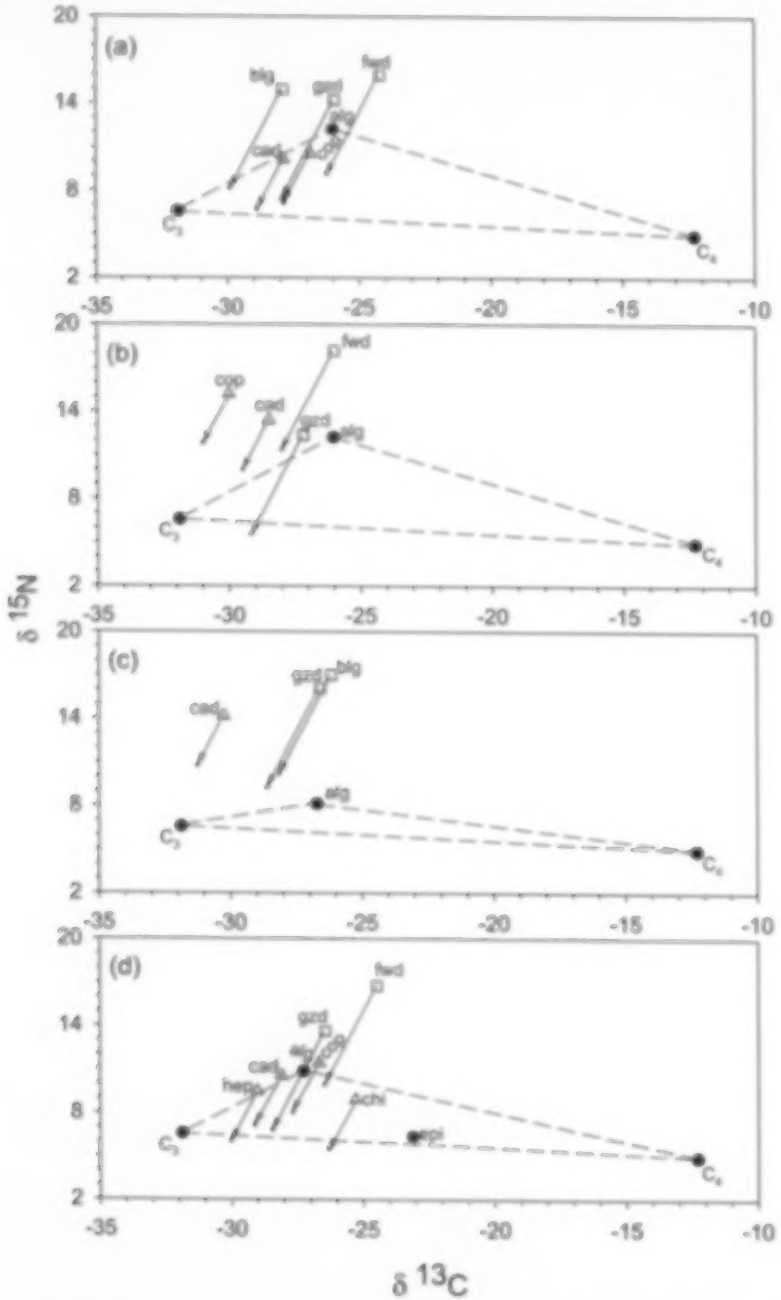

© 2007 NRC Canada

Fig. 5. Consumer $\delta^{15}N$ plotted against $\delta^{13}C$ for MR13 in (*a*) summer 1998, (*b*) fall 1998, (*c*) spring 1999, and (*d*) summer 1999. Triangles denote invertebrate consumers and squares represent fish. Error bars represent the mean ±1 SE of replicate samples. Consumers: amp, amphipod; baet, baetiscid mayfly; blg, bluegill; bmay, burrowing mayfly; cad, hydropsychid caddisfly; ccat, channel catfish; cer, ceratopogonid larvae; chi, chironomid larvae; cor, corixid; cop, copepod; *Daph*, *Daphnia* spp.; dams, damselfly larvae; drag, dragonfly larvae; fwd, freshwater drum; gzd, gizzard shad; hept, heptageniid mayfly; lv fish, larval fish; smb, smallmouth buffalo; sna, snail; taen, taeniopterygid stonefly; moeye, mooneye; wbass, white bass; zebm, zebra mussel.

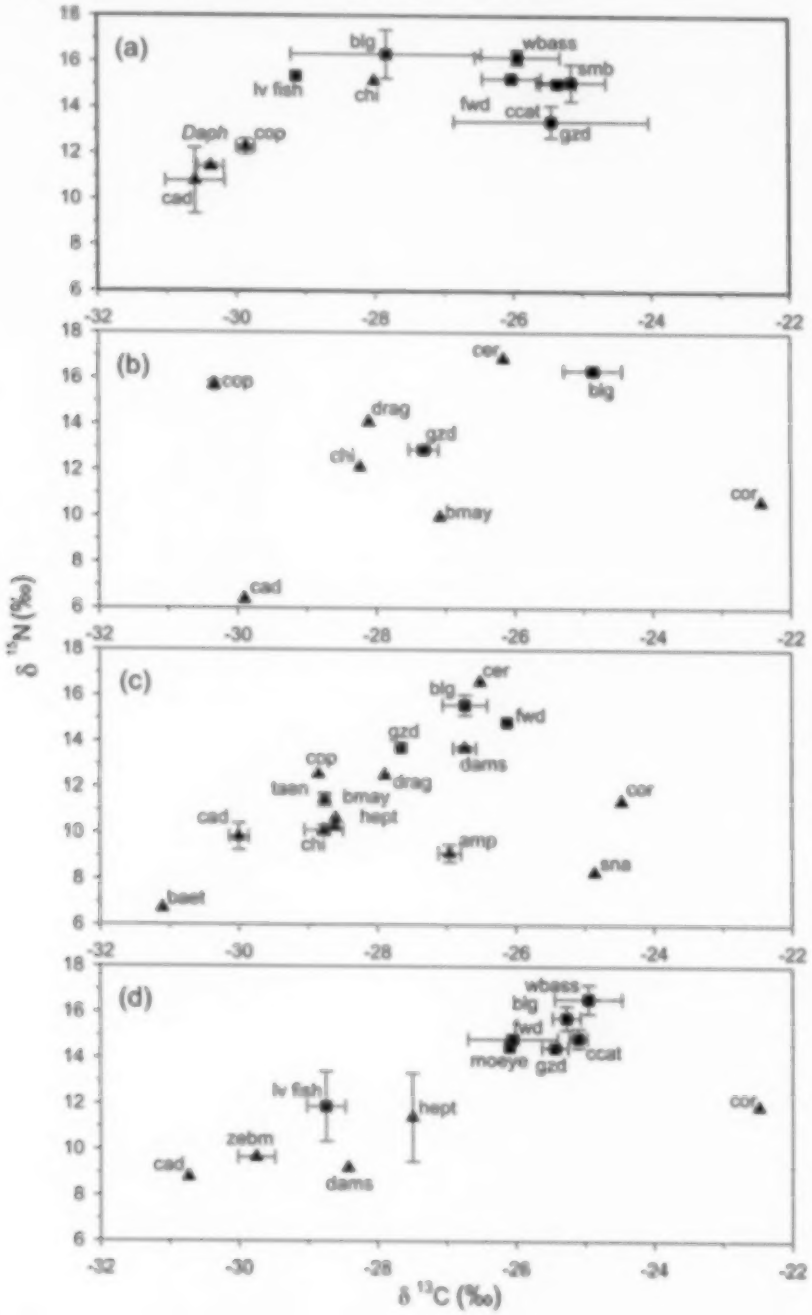

© 2007 NRC Canada

Hicks 1985; Hesslein et al. 1993) and exhibits the least variable fractionation with respect to diet compared with other tissues (Pinnegar and Polunin 1999). We also sampled larval fish during the summer by pushing bow-mounted ichthyoplankton nets (0.5 m diameter, 500 μm mesh) upstream for 10–15 min. Whole larval fish (minus the gut) were used for stable isotope analyses. This technique yields the most consistent fractionation with respect to diet for small fish (Pinnegar and Polunin 1999).

Sample preparation and isotopic analysis

After initial processing, samples were dried in scintillation vials at 60 °C until they reached a constant dry weight and then ground into a fine powder. Mass spectrometry was performed on all samples to determine $\delta^{13}C$ and $\delta^{15}N$ ratios. Samples were analyzed using a continuous-flow stable isotope mass spectrometer (Micromass; Waters Corp., Milford, Massachusetts) coupled to a Carlo Erba elemental analyzer (CHNS-O EA1108; Thermo Electron Corp., Milan, Italy). Analytical precision was ±0.2‰ for carbon and ±0.3‰ for nitrogen; thus, differences of less than 1‰ were not considered biologically meaningful (Mihuc and Toetz 1994). Stable isotope ratios are reported in del (δ) units in parts per thousand (‰) relative to the international standard for that isotope (Peterson and Fry 1987). Isotope ratios for carbon are reported relative to carbon in the PeeDee limestone deposit and for nitrogen relative to atmospheric nitrogen (Peterson and Fry 1987).

Comparative analyses

Seasonal isotopic signatures of consumers were plotted and trophic relationships evaluated based on association between food source and consumer signatures (Peterson and Fry 1987). We assumed a trophic enrichment of +1‰ $\delta^{13}C$ (DeNiro and Epstein 1978) and +3.4‰ $\delta^{15}N$ (Minagawa and Wada 1984; Post 2002) for each trophic transfer. We also calculated the average isotopic composition of the diet of several common large river consumers (copepods, hydropsychid caddisflies, chironomid larvae, heptageniid mayflies, gizzard shad, bluegill, and freshwater drum). We assumed that invertebrate consumers fed at trophic level 2 and nonpiscivorous fish at trophic level 3. Next, we constructed mixing polygons defined by potential ultimate food resources within each main channel study site; these sources included C_3 plants, C_4 terrestrial grasses, suspended algae, and epixylon (summer 1999 only). We then used the IsoSource mixing model (Phillips and Gregg 2003) to determine ranges of feasible solutions for unique combinations of source proportions. In this technique, all combinations of each source are examined in 1‰ increments; feasible solutions include all combinations that sum to the observed isotopic signature mixture within ±0.1‰.

Results

Seasonal comparison of resource and consumer signatures

Stable isotopic signatures for autochthonous basal resources were seasonally variable and difficult to differentiate. In contrast, for both sites, terrestrial C_3 vascular plants (tree leaves and grasses) had similar average signatures for $\delta^{13}C$ (–31.9‰ to –28.4‰) and for $\delta^{15}N$ (4.6‰–6.6‰) (Figs. 3 and 4). Stable isotope signatures for epixylon were variable between sites (Figs. 3 and 4) with average $\delta^{13}C$ differing by 7‰ and average $\delta^{15}N$ differing by 6.3‰. Suspended algae exhibited seasonal variation in both $\delta^{15}N$ and $\delta^{13}C$ values. For all sites and seasons, C_4 plants were separated from other sources by at least 7‰ for $\delta^{13}C$, giving them a unique signature that could be easily identified in consumers if they used this food source exclusively. Excepting C_4 plants, separations between C_3 terrestrial plants and algal source signatures were often less than 2‰ for both $\delta^{13}C$ and $\delta^{15}N$; thus, we often could not distinguish between these food sources (Figs. 3 and 4).

C_4 plants were not a dominant food source in any season for aquatic consumers at either site (Figs. 3–6). Maximal source contributions to consumers from C_4 grasses were 17% and 16% at MR13 and MR26, respectively (Tables 1 and 2). We could not distinguish precisely whether terrestrial C_3 plants or suspended algae were the primary energy sources for most invertebrate consumers and fish because $\delta^{13}C$ and $\delta^{15}N$ ratios were similar (Figs. 3 and 4). However, mixing models indicated that C_3 plants appeared to be the most important food resource for large river consumers with feasible contributions ranging from 13% to 76% at MR13 and from 35% to 80% at MR26 (Tables 1 and 2). Suspended algae were also an important source for many consumers with feasible contributions ranging from 0% to 75% at MR13 and from 0.06% to 51% at MR26. Finally, in summer 1999, epixylon also appeared as a potentially important food resource with feasible contributions of up to 46% at MR13 and 37% at MR26.

Hydropsychid caddisflies (filter-feeders) and copepods varied considerably in $\delta^{15}N$ among seasons at both MR13 and MR 26 (Figs. 3 and 4). For example, caddisflies at MR26 were depleted in ^{15}N in fall (6.4‰) but enriched in spring and summer (8.5‰–10.0‰). At this site, many filter-feeding benthic invertebrates (e.g., hydropsychid caddisflies and zebra mussels) had enriched $\delta^{15}N$ signatures in fall and spring compared with fish (Fig. 6). Suspended algae had the highest $\delta^{15}N$ signatures among the major ultimate food resources that we sampled. An unsampled planktonic algae source (similarly enriched in ^{15}N but depleted in ^{13}C) might be the main food resource assimilated by these filter-feeders and many other invertebrates at both MR13 and MR26 (Figs. 3 and 4). Water boatmen (Corixidae) and snails at MR13 had $\delta^{13}C$ signatures considerably higher than those of other invertebrate consumers, suggesting that these consumers used different carbon sources (e.g., attached algae for snails) than other primary consumers in the food web (Fig. 5). Copepods were typically depleted in $\delta^{13}C$ relative to fish, indicating that copepods were not a dominant food item for most adult fish (Figs. 3 and 4). However, fish may have used copepods as a food resource in spring at MR13 and in summer at MR26 (Figs. 3 and 4). Ceratopogonid larvae (Ceratopogonidae) were the only consumers more enriched than fish consumers and had $\delta^{15}N$ signatures 4‰–8‰ higher than chironomid (Chironomidae) larvae, which were a likely prey resource (Fig. 5). Ceratopogonids themselves were not a significant prey resource for fish given their high $\delta^{15}N$. Macroinvertebrate predators including dragonfly (Anisoptera)

© 2007 NRC Canada

Fig. 6. Consumer $\delta^{15}N$ plotted against $\delta^{13}C$ for MR26 in (*a*) summer 1998, (*b*) fall 1998, (*c*) spring 1999, and (*d*) summer 1999. Triangles denote invertebrate consumers and squares represent fish. Error bars represent the mean ±1 SE of replicate samples. Consumers: blg, bluegill; cad, hydropsychid caddisfly; cop, copepod; chi, chironomid larvae; fwd, freshwater drum; gzd, gizzard shad; hep, heptageniid mayfly; mus, bivalve mussel; perl, perlodid stonefly; sng, shortnose gar.

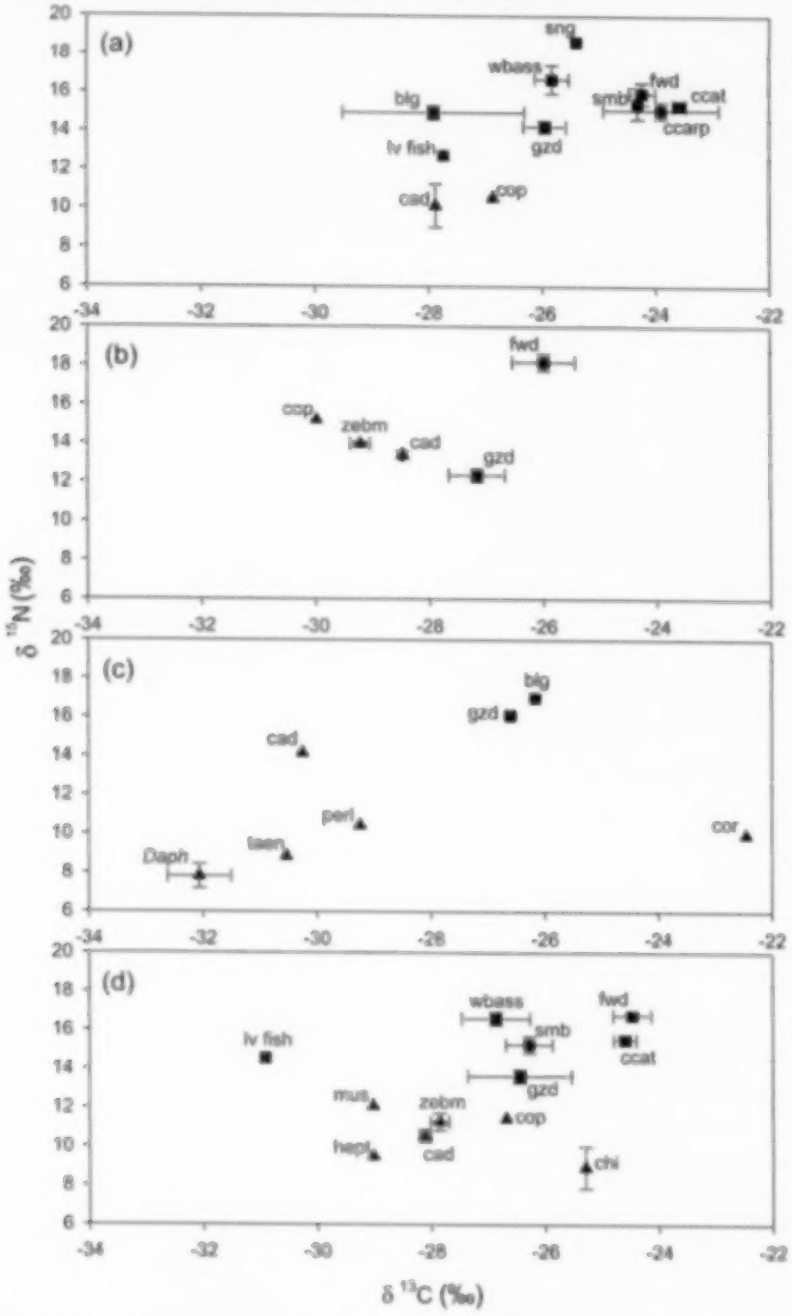

and damselfly (Zygoptera) larvae had expected $\delta^{15}N$ values intermediate to fish and primary consumers, except in summer when damselfly larvae had an unexplainably low $\delta^{15}N$ value that did not reflect their role as predators (Fig. 5).

Generally, fish had similar $\delta^{13}C$ and $\delta^{15}N$ ratios in the spring, summer, and fall at both MR13 and MR26 (within ±2‰ in each season) reflecting the time-integrated nature of fish tissues. At MR26, however, gizzard shad $\delta^{15}N$ values

© 2007 NRC Canada

Table 1. Range of feasible source contributions for selected consumers at MR13 using the IsoSource model.

	Basal resource			
Consumer	C_3 terrestrial plants	C_4 terrestrial grasses	Suspended algae[a]	Epixylon[b]
Summer 1998				
Chironomid larvae	ns	ns	ns	
Hydropsychid caddisfly larvae	ns	ns	ns	
Copepod	ns	ns	ns	
Heptageniid mayfly	—	—	—	
Bluegill	ns	ns	ns	
Freshwater drum	0.41–0.44	0.07–0.08	0.48–0.51	
Gizzard shad	0.73–0.76	0.15	0.09–0.12	
Fall 1998				
Chironomid larvae	0.46–0.48	0–0.01	0.51–0.54	
Hydropsychid caddisfly larvae	ns	ns	ns	
Copepod	ns	ns	ns	
Heptageniid mayfly	—	—	—	
Bluegill	0.13–0.16	0.11–0.12	0.72–0.75	
Freshwater drum	—	—	—	
Gizzard shad	ns	ns	ns	
Spring 1999				
Chironomid larvae	ns	ns	ns	
Hydropsychid caddisfly larvae	ns	ns	ns	
Copepod	ns	ns	ns	
Heptageniid mayfly	ns	ns	ns	
Bluegill	ns	ns	ns	
Freshwater drum	ns	ns	ns	
Gizzard shad	ns	ns	ns	
Summer 1999				
Chironomid larvae	—	—	—	—
Hydropsychid caddisfly larvae	ns	ns	ns	ns
Copepod	—	—	—	—
Heptageniid mayfly	0.60–0.63	0–0.01	0–0.39	0–0.28
Bluegill	0.36–0.39	0.01–0.17	0–0.62	0–0.46
Freshwater drum	0.56–0.59	0.02–0.12	0–0.42	0–0.3
Gizzard shad	0.58–0.61	0.07–0.16	0–0.35	0–0.26

Note: ns, no solution; —, consumer not sampled.
[a]Suspended algae not sampled in fall 1998. We used the summer 1998 value to represent suspended algae for this sampling period.
[b]Epixylon only sampled during summer 1999.

were appreciably higher in spring (16.1‰) than in either fall (12.4‰) or summer (13.6‰) (Fig. 6). This enrichment in spring could result from either the inclusion of more zooplankton (because zooplankton were enriched in $\delta^{15}N$) or a seasonal shift in detrital $\delta^{15}N$ in diets. Fish were 1.5‰–9.0‰ more enriched in $\delta^{15}N$ than benthic invertebrates, indicating that they fed one or two trophic levels higher than these invertebrates (Figs. 5 and 6). Based on combined $\delta^{13}C$ and $\delta^{15}N$ signatures, benthic invertebrates appeared to be the most important group in the transfer of energy to fish.

Interannual variability in resource and consumer signatures

While $\delta^{13}C$ and $\delta^{15}N$ signatures of C_3 and C_4 terrestrial vegetation did not vary among years, suspended algae exhibited more variability. Suspended algae were more enriched in ^{13}C in 1999 versus 1998 at MR13 (by about 3.0‰) (Fig. 3), possibly because of differences in the isotopic composition of the dissolved inorganic carbon pool, growth rates, or boundary layer effects. Suspended algae $\delta^{13}C$ and $\delta^{15}N$ signatures at MR26 did not vary appreciably (Fig. 4). Most primary consumers and fish had consistent isotopic ratios between years (Figs. 5 and 6). For both sites, invertebrate $\delta^{13}C$ and $\delta^{15}N$ signatures typically differed by less than 1.0‰ between years. One exception was hydropsychid caddisflies at MR13 that were much more enriched in ^{15}N in summer 1998, possibly reflecting variability in the $\delta^{15}N$ signatures of their food resources (Fig. 3). Most adult fish, including freshwater drum, channel catfish, gizzard shad, and white bass, had $\delta^{13}C$ and $\delta^{15}N$ ratios that varied by less than 2.0‰ between years (Figs. 5 and 6). Bluegill were 2.6‰ more enriched in $\delta^{13}C$ in 1999 than in 1998 at MR13 (Fig. 5); however, it is unclear whether this difference is meaningful because bluegill $\delta^{13}C$

© 2007 NRC Canada

Table 2. Range of feasible source contributions for selected consumers at MR26 using the IsoSource model.

Consumer	Basal resource			
	C_3 terrestrial plants	C_4 terrestrial grasses	Suspended algae[a]	Epixylon[b]
Summer 1998				
Chironomid larvae	—	—	—	
Hydropsychid caddisfly larvae	0.79–0.8	0.13–0.14	0.06–0.08	
Copepod	0.68–0.7	0.16	0.14–0.16	
Heptageniid mayfly	—	—	—	
Bluegill	0.69–0.71	0.01–0.02	0.27–0.3	
Freshwater drum	0.35–0.38	0.14	0.48–0.51	
Gizzard shad	0.65–0.67	0.14–0.15	0.18–0.21	
Fall 1998				
Chironomid larvae	—	—	—	
Hydropsychid caddisfly larvae	ns	ns	ns	
Copepod	ns	ns	ns	
Heptageniid mayfly	—	—	—	
Bluegill	—	—	—	
Freshwater drum	ns	ns	ns	
Gizzard shad	ns	ns	ns	
Spring 1999				
Chironomid larvae	—	—	—	
Hydropsychid caddisfly larvae	ns	ns	ns	
Copepod	—	—	—	
Heptageniid mayfly	—	—	—	
Bluegill	ns	ns	ns	
Freshwater drum	—	—	—	
Gizzard shad	ns	ns	ns	
Summer 1999				
Chironomid larvae	ns	ns	ns	ns
Hydropsychid caddisfly larvae	0.6–0.74	0–0.1	0.13–0.19	0–0.25
Copepod	0.34–0.5	0–0.13	0.34–0.4	0–0.31
Heptageniid mayfly	ns	ns	ns	ns
Bluegill	—	—	—	—
Freshwater drum	0.44–0.62	0–0.14	0.2–0.27	0–0.35
Gizzard shad	0.56–0.75	0–0.15	0.06–0.13	0–0.37

Note: ns, no solution; —, consumer not sampled.

[a]Suspended algae not sampled in fall 1998. We used the summer 1998 value to represent suspended algae for this sampling period.

[b]Epixylon only sampled during summer 1999.

signatures were highly variable in 1998 compared with 1999.

Discussion

We assessed seasonal and spatial variability in basal energy resources by sampling two spatially distinct main channel locations on the Mississippi River during three seasons. Lack of separation among several potential food resources made precise identification of the sources of organic matter that supported secondary production in main channel habitats of the Mississippi River difficult. Using only naturally occurring carbon and nitrogen stable isotope ratios, we could not definitively assess which of the large river theories (RCC, riverine productivity model, flood pulse concept) most accurately described energy cycling in main channel habitats of large rivers. We encountered some of the same limitations noted in other isotopic studies, including spatial and temporal variability in source signatures (Vander Zanden and Rasmussen 1999; Herwig et al. 2004) and poor separation among autochthonous and allochthonous stable isotope signatures (France 1995, 1996).

Our data indicate that terrestrial C_3 plants and algal sources (transported from upstream or from in situ production) were important for some consumers in some seasons, partially supporting both the original (Thorp and Delong 1994) and revised riverine productivity model (Thorp and Delong 2002) and the RCC (Vannote et al. 1980; Minshall et al. 1985; Sedell et al. 1989). The IsoSource mixing model of Phillips and Gregg (2003) indicated that terrestrial C_3 vegetation, suspended algae, and epixylon could all potentially be important food resources for large river consumers. Many consumer signatures fell outside the mixing polygon defined by these sources, indicating that either a ^{13}C-depleted food

© 2007 NRC Canada

resource existed for which we did not account (perhaps diatoms or smaller-sized green algae) or it is inaccurate to assume enrichment factors of +1.0‰ and +3.4‰ for ^{13}C and ^{15}N, respectively. For example, bending the lines in Figs. 3 and 4 (e.g., lower enrichment factors for $\delta^{13}C$ and $\delta^{15}N$) would produce a different interpretation of source contributions and a greater proportion of feasible solutions.

Based on their distinct (enriched) $\delta^{13}C$ signature, we ruled out terrestrial C_4 plants as an important source of carbon for large river consumers. We could not precisely distinguish relative contributions from C_3 vegetation versus "in-stream" sources. Unique stable isotope signatures were also not observed between main channel and backwater habitats (cf. Herwig et al. 2004); thus, the exact contribution of organic matter from either backwater or terrestrial habitats during floods and at other times of the year remains unclear.

The distinct (enriched) $\delta^{13}C$ signature of C_4 vegetation did not appear in any consumer sampled. Thus, terrestrial C_4 plants (e.g., native C_4 grasses and field corn) likely were not an important carbon source for large river consumers. This suggests that the large areas of floodplain wetland and forested habitat that have been converted to field corn production in the Mississippi basin do not contribute to secondary production in the river. However, because the contribution of natural floodplains to main channel consumers is poorly known, we cannot assess whether this change in land use has contributed to any reduced productivity in this system. There is some empirical support for the idea that local sources of production are most important for large river food webs (Hamilton et al. 1992; Angradi 1994; Thorp and Delong 2002).

We observed high levels of interannual variability in $\delta^{13}C$ and $\delta^{15}N$ for algal sources at both sites, a finding similar to that observed in other ecosystems (e.g., MacLeod and Barton 1998; Finlay et al. 1999; Leggett et al. 1999). Consistent with findings for both the Mississippi and Missouri rivers (Delong et al. 2001), most primary consumers showed low levels of interannual variability, indicating that there was a consistent pattern of energy flow/prey resource use between years. Fish also exhibited consistent isotopic ratios across years, which probably most strongly reflects the time-integrated nature of fish tissues. Identifying important trophic linkages for long-lived predators such as fish is difficult, since prey signatures may change more rapidly than predator signatures that integrate consumption over months to years. Isotope signatures of fish may not reflect isotope ratios of potential food sources at the time of sampling (Hesslein et al. 1993).

Omnivory is commonly observed in freshwater food webs across a number of ecosystems (Vadas 1990). Our data indicate that omnivory was common in the large river habitats that we studied. Fish $\delta^{13}C$ and $\delta^{15}N$ signatures were typically intermediate to several different prey signatures, suggesting that fish diets comprised multiple prey types from several trophic levels. Some benthic macroinvertebrate consumers also were omnivorous, based on intermediate $\delta^{13}C$ and $\delta^{15}N$ signatures. Taken together, our data indicate that many large river consumers have flexible diets and are omnivorous. In all of these cases, supplemental diet information (gut content information) will be needed to help interpret consumer stable isotope signatures, since several potential diet items had similar stable isotope signatures.

Zooplankton in the main channel was only important during the early life stages of fish and for select adult fish species. Only larval fish, and adult bluegill at one site, showed any evidence of significant zooplankton assimilation. In a stable isotope analysis of backwater lake food webs from large rivers, Herwig et al. (2004) found little evidence that fish assimilated much zooplankton; instead, it appeared that fish fed primarily on benthic macroinvertebrates. Therefore, main channel and backwater lake food webs appear to differ considerably from many lakes where empirical evidence suggests that phytoplankton–zooplankton is the most important carbon source supporting fish growth (Yoshioka et al. 1994; Gu et al. 1996). As a result, models explaining community structure in north temperate lakes (e.g., trophic cascade hypothesis: Carpenter and Kitchell 1988) may be of limited utility in explaining food web structure in large rivers.

We commonly observed filter-feeding macroinvertebrates such as hydropsychid caddisflies and zebra mussels to exhibit seasonal upward shifts in $\delta^{15}N$ of up to 3‰ in spring and fall. These differences could be attributable to a shift towards algal carbon use in spring and fall. However, inputs of dissolved inorganic or animal-derived nitrogen from the adjacent watershed enriched in $\delta^{15}N$ could explain the observed pattern (Chang et al. 2002). The resulting isotopic composition of these nitrogen sources may be incorporated seasonally into main channel food webs by floodwater and downstream transport.

We expected increased dependence on phytoplankton carbon by consumers at MR13, where channel connectedness to slackwater habitats was high as compared with MR26. Our data suggest, based on similar consumer signatures between sites, that main channel habitats with contrasting levels of floodplain connectivity and slackwater habitat do not strongly differ in terms of predominant carbon sources assimilated by secondary consumers. However, this does not mean that differences in floodplain connectivity and slackwater habitats are unimportant. Slackwater and floodplain habitats are critical as fish spawning and rearing grounds for many riverine species (Welcomme 1979; Junk et al. 1989).

Food web studies using stable isotopes often sample in only one season and in one habitat (but see Yoshioka et al. 1994; McCutchan and Lewis 2002). Food webs are dynamic over both temporal and spatial scales (Polis et al. 1996; Winemiller and Polis 1996), and among aquatic consumers, ontogenetic diet shifts and size-selective predation are common (Werner and Gilliam 1984). In many previously published stable isotope studies, only one autochthonous component is sampled (often epilithon) with little if any replication and then used to represent all autochthonous carbon. By sampling multiple sources across multiple seasons, we documented the complexity of energy sources in the mainstream channel of large rivers, demonstrating that energy provenance for large river consumers is not easily resolved.

We could not distinguish precisely whether upstream allochthonous and autochthonous carbon, or in situ production, was the dominant food resource supporting consumers. Much of this ambiguity stems from the many potential food

© 2007 NRC Canada

resources, similar source signatures, as well as the high degree of spatial and temporal complexity present in large floodplain–river systems. Taken together, our results suggest that energy pathways in large floodplain rivers are complex (also see Sedell et al. 1989; Dettmers et al. 2001), making them difficult to resolve by measuring only natural abundance ratios of $\delta^{13}C$ and $\delta^{15}N$. We suggest that the three major theories describing large river food webs should be viewed as complementary rather than contradictory. An integrative perspective using a variety of interrelated empirical data sets (e.g., hydrological, chemical, population, habitat, behavioral, and diet studies) will be needed to more completely understand the complexity of large floodplain river ecosystems.

Acknowledgements

We thank Dr. J. Tank for numerous helpful ideas in the development of this research and for her review of an earlier version of this manuscript as well as the comments of J. Thorp and two anonymous reviewers. F. Cronin and J. Stone at the Great Rivers Biological Station (Illinois Natural History Survey) and M. Bowler at the Bellevue Field Station (Iowa Department of Natural Resources) helped with fish collections. Additional samples were collected in conjunction with the project "Main channel fisheries investigations" funded by the US Army Corps of Engineers through contract NCR-94-175 with the US Geological Survey. Dr. S. Gutreuter, US Geological Survey, provided logistical and administrative support on this project. T. Mason, B. Davis, K. Dockendorf, J. Rader, C. Dolan, K. O'Gara, M. Engel, and S. Lowe provided field assistance. P. Frantz, T. Griffiths, A. Cziko, L. Baker, S. Dovalovsky, and O. Nelson III provided laboratory assistance. The Department of Natural Resources and Environmental Sciences of the University of Illinois and the Illinois Natural History Survey provided funding for this research.

References

Angradi, T.R. 1994. Trophic linkages in the lower Colorado River: multiple stable isotope evidence. J. North Am. Benthol. Soc. **13**: 479–495.

Bunn, S.E., Barton, D.R., Hynes, H.B.N., Power, G., and Pope, M.A. 1989. Stable isotope analysis of carbon flow in a tundra river system. Can. J. Fish. Aquat. Sci. **46**: 1769–1775.

Carpenter, S.C., and Kitchell, J.F. 1988. Consumer control of lake productivity. Bioscience, **38**: 764–769.

Chang, C.C.Y., Kendall, C., Silva, S.R., Battaglin, W.A., and Campbell, D.H. 2002. Nitrate stable isotopes: tools for determining nitrate sources among different land uses in the Mississippi River Basin. Can. J. Fish. Aquat. Sci. **59**: 1874–1885.

Delong, M.D., Thorp, J.H., Greenwood, K.S., and Miller, M.C. 2001. Responses of consumers and food resources to a high magnitude, unpredicted flood in the Upper Mississippi River Basin. Regul. Rivers Res. Manag. **17**: 217–234.

DeNiro, M.J., and Epstein, S. 1978. Influence of diet on the distribution of carbon isotopes in animals. Geochim. Cosmochim. Acta, **42**: 495–506.

Dettmers, J.M., Wahl, D.H., Soluk, D.A., and Gutreuter, S. 2001. Life in the fast lane: fish and food web structure in the main channel of large rivers. J. North Am. Benthol. Soc. **20**: 255–265.

Finlay, J.C., Power, M.E., and Cabana, G. 1999. Effects of water velocity on algal carbon isotope ratios: implications for river food web studies. Limnol. Oceanogr. **44**: 1198–1203.

France, R.L. 1995. Critical examination of stable isotope analysis as a means for tracing carbon pathways in stream ecosystems. Can. J. Fish. Aquat. Sci. **52**: 651–656.

France, R.L. 1996. Carbon-13 conundrums: limitations and cautions in the use of stable isotope analysis in stream ecotonal research. Can. J. Fish. Aquat. Sci. **53**: 1916–1919.

Gu, B., Schelske, C.L., and Hoyer, M.V. 1996. Stable isotopes of carbon and nitrogen as indicators of diet and trophic structure of the fish community in a shallow hypereutrophic lake. J. Fish Biol. **49**: 1233–1243.

Hamilton, S.K., Lewis, W.M., Jr., and Sipel, S.J. 1992. Energy sources for aquatic animals in the Orinoco River floodplain: evidence from stable isotopes. Oecologia, **89**: 324–330.

Herwig, B.R., Soluk, D.A., Dettmers, J.M., and Wahl, D.H. 2004. Trophic structure and energy flow in backwater lakes of two floodplain rivers assessed using stable isotopes. Can. J. Fish. Aquat. Sci. **61**: 12–22.

Hesslein, R.H., Hallard, K.A., and Ramlal, P. 1993. Replacement of sulfur, carbon, and nitrogen in tissue of growing broad whitefish (*Coregonus nasus*) in response to a change in diet traced by $\delta^{34}S$, $\delta^{13}C$, and $\delta^{15}N$. Can. J. Fish. Aquat. Sci. **50**: 2071–2076.

Johnson, B.L., Richardson, W.B., and Naimo, T.J. 1995. Past, present, and future concepts in large river ecology. Bioscience, **45**: 134–141.

Junger, M., and Planas, D. 1994. Quantitative use of stable carbon isotope analysis to determine the trophic base of invertebrate communities in a boreal forest lotic system. Can. J. Fish. Aquat. Sci. **51**: 52–61.

Junk, W.J., Bayley, P.B., and Sparks, R.E. 1989. The flood pulse concept in river–floodplain systems. *In* Proceedings of the International Large River Symposium. *Edited by* D.P. Dodge. Can. Spec. Publ. Fish. Aquat. Sci. No. 106. pp. 110–127.

Leggett, M.F., Servos, M.R., Hesslein, R., Johannsson, O., Millard, E.S., and Dixon, D.G. 1999. Biogeochemical influences on the carbon isotope signatures of Lake Ontario biota. Can. J. Fish. Aquat. Sci. **56**: 2211–2218.

MacLeod, N.A., and Barton, D.R. 1998. Effects of light intensity, water velocity, and species composition on carbon and nitrogen stable isotope ratios in periphyton. Can. J. Fish. Aquat. Sci. **55**: 1919–1925.

McCutchan, J.H., Jr., and Lewis, W.M., Jr. 2002. Relative importance of carbon sources for macroinvertebrates in a Rocky Mountain stream. Limnol. Oceanogr. **47**: 742–752.

Mihuc, T., and Toetz, D. 1994. Determination of diets of alpine aquatic insects using stable isotopes and gut analysis. Am. Midl. Nat. **131**: 146–155.

Minagawa, M., and Wada, E. 1984. Stepwise enrichment of ^{15}N along food chains: further evidence and the relation between $\delta^{15}N$ and animal age. Geochim. Cosmochim. Acta, **48**: 1135–1140.

Minshall, G.W., Cummins, K.W., Peterson, R.C., Cushing, C.E., Bruns, D.A., Sedell, J.R., and Vannote, R.L. 1985. Developments in stream ecosystem theory. Can. J. Fish. Aquat. Sci. **42**: 1045–1055.

Mitchell, M.J., Mills, E.L., Idrisi, N., and Michener, R. 1996. Stable isotopes of nitrogen and carbon in an aquatic food web recently invaded by *Dreissena polymorpha* (Pallas). Can. J. Fish. Aquat. Sci. **53**: 1445–1450.

Peterson, B.J., and Fry, B. 1987. Stable isotopes in ecosystem studies. Annu. Rev. Ecol. Syst. **18**: 293–320.

© 2007 NRC Canada

Phillips, D.L., and Gregg, J.W. 2003. Source partitioning using stable isotopes: coping with too many sources. Oecologia, **136**: 261–269.

Pinnegar, J.K., and Polunin, N.V.C. 1999. Differential fractionation of $\delta^{13}C$ and $\delta^{15}N$ among fish tissues: implications for the study of trophic interactions. Funct. Ecol. **13**: 225–231.

Polis, G.A., Holt, R.D., Menge, B.A., and Winemiller, K.O. 1996. Time, space, and life history: influences on food webs. *In* Food webs: integration of patterns and dynamics. *Edited by* G.A. Polis and K.O. Winemiller. Chapman and Hall Publishers, New York. pp. 435–460.

Post, D.M. 2002. Using stable isotopes to estimate trophic position: models, methods, and assumptions. Ecology, **83**: 703–718.

Rosenfeld, J.S., and Roff, J.C. 1992. Examination of the carbon base in southern Ontario streams using stable isotopes. J. North Am. Benthol. Soc. **11**: 1–10.

Rounick, J.S., and Hicks, B.J. 1985. The stable carbon isotope ratios of fish and their invertebrate prey in four New Zealand rivers. Freshw. Biol. **15**: 207–214.

Sedell, J.R., Richey, J.E., and Swanson, F.J. 1989. The River Continuum Concept: a basis for the expected ecosystem behavior of very large rivers? *In* Proceedings of the International Large River Symposium. *Edited by* D.P. Dodge. Can. Spec. Publ. Fish. Aquat. Sci. No. 106. pp. 49–55.

Sparks, R.E., Nelson, J.C., and Yin, Y. 1998. Naturalization of the flood regime in regulated rivers. Bioscience, **48**: 706–720.

Teeri, J.A., and Stowe, L.G. 1976. Climatic patterns and the distribution of C4 grasses in North America. Oecologia, **23**: 1–12.

Thorp, J.H., and Delong, M.D. 1994. The riverine productivity model: an heuristic view of carbon source and organic processing in large river ecosystems. Oikos, **70**: 305–308.

Thorp, J.H., and Delong, M.D. 2002. Dominance of autochthonous autotrophic carbon in food webs of heterotrophic rivers. Oikos, **96**: 543–550.

Thorp, J.H., Delong, M.D., Greenwood, K.S., and Casper, A.F. 1998. Isotopic analysis of three food web theories in constricted and floodplain regions of a large river. Oecologia, **117**: 551–563.

Vadas, R.L., Jr. 1990. The importance of omnivory and predator regulation of prey in freshwater fish assemblages of North America. Environ. Biol. Fishes, **27**: 285–302.

Vander Zanden, M.J., and Rasmussen, J.B. 1999. Primary consumer $\delta^{13}C$ and $\delta^{15}N$ and the trophic position of aquatic consumers. Ecology, **80**: 1395–1404.

Vannote, R.L., Minshall, G.W., Cummins, K.W., Sedell, J.R., and Cushing, C.E. 1980. The river continuum concept. Can. J. Fish. Aquat. Sci. **37**: 130–137.

Welcomme, R.L. 1979. Fisheries ecology of large floodplain rivers. Longman, London, UK.

Werner, E.E., and Gilliam, J.F. 1984. The ontogenetic niche and species interactions in size-structured populations. Annu. Rev. Ecol. Syst. **15**: 393–425.

Winemiller, K.O., and Polis, G.A. 1996. Food webs: what do they tell us about the world? *In* Food webs: integration of patterns and dynamics. *Edited by* G.A. Polis and K.O. Winemiller. Chapman and Hall Publishers, New York. pp. 1–22.

Yoshioka, T., Wada, E., and Hayashi, H. 1994. A stable isotope study on seasonal food web dynamics in a eutrophic lake. Ecology, **75**: 835–846.

© 2007 NRC Canada

The influence of spawning habitat restoration on juvenile brown trout (*Salmo trutta*) density

Daniel Palm, Eva Brännäs, Fabio Lepori, Kjell Nilsson, and Stefan Stridsman

Abstract: Between 1992 and 2003, we assessed the density of age-0+ brown trout (*Salmo trutta*) in a channelized stream in northern Sweden, which was restored using two different schemes. One section of the stream was restored by the addition of boulders and reconstruction of gravel beds (boulder + gravel section), whereas another section was restored through addition of boulders only (boulder-only section). In addition, we compared the substrate size composition of gravel beds and the egg-to-fry survival between the two stream sections, and we related the density of age-0+ brown trout to the area of reconstructed gravel beds. After the restoration, the density of age-0+ brown trout increased significantly in the boulder + gravel section and was positively correlated with the area of reconstructed gravel beds. By contrast, the density of age-0+ brown trout did not change in the boulder-only treatment. Egg-to-fry survival was significantly higher in the boulder + gravel section compared with the boulder-only section, probably because of the higher content of sand and fines in the gravel beds of the latter treatment. This study shows that the density of age-0+ brown trout was limited by the availability and quality of spawning substrate rather than by the structural habitat complexity.

Résumé : De 1992 à 2003, nous avons évalué la densité des truites brunes (*Salmo trutta*) d'âge 0+ dans un cours d'eau canalisé du nord de la Suède, qui a été restauré selon deux arrangements différents. Une section a été restaurée par l'addition de blocs de pierre et la reconstruction des lits de gravier (section blocs + gravier), alors qu'une autre section n'a reçu que des blocs (section blocs seuls). De plus, nous avons comparé la composition en taille du substrat dans les lits de gravier et la survie de l'oeuf à l'alevin dans les deux sections de cours d'eau; nous avons mis en relation la densité des truites brunes d'âge 0+ à la surface des lits de gravier reconstruits. Après la restauration, la densité des truites brunes d'âge 0+ a augmenté significativement dans la section blocs + gravier où elle est en corrélation positive avec la surface des lits de gravier reconstitués. Au contraire, la densité des truites d'âge 0+ n'a pas changé dans la section ayant reçu les blocs seuls. La survie de l'oeuf à l'alevin est significativement plus importante dans la section blocs + gravier que dans la section blocs seuls, probablement à cause du contenu plus grand de sable de de sédiments fins dans les lits de gravier de cette dernière section. Notre étude montre que la densité des truites d'âge 0+ est limitée par la disponibilité et la qualité des substrats de fraie plutôt que par la complexité structurale de l'habitat.

[Traduit par la Rédaction]

Introduction

Over the last two decades, the restoration of degraded streams has become an increasingly important strategy in trout fishery management (Hunter 1991). An impact that has prompted widespread attempts of habitat restoration is channelization (i.e., any modification of streams that involves channel straightening, bank reinforcement, or the dredging of flow obstructions). Channelization has been implemented worldwide for improved navigation and transport, drainage of agricultural land, or stabilization of banks against erosion. Moreover, in boreal regions across the Northern Hemisphere, streams were channelized during the nineteenth and twentieth centuries to facilitate the transport of timber. Streams were deepened and boulders and large woody debris were removed from the channel (Törnlund and Östlund 2002; Nilsson et al. 2005). Timber transport was particularly widespread in Scandinavia; by 1950, 60% (i.e., 30 000 km) of all streams in Sweden had been channelized for this purpose (Törnlund 2002; Törnlund and Östlund 2002).

Channelization has multiple impacts on salmonines. First, boulders and large woody debris are essential elements of both juvenile and adult salmomine habitat, as they provide refuge from predators and fast flows as well as hydraulically suitable feeding stations. Second, boulders retain finer particles such as gravel and sand, which would otherwise be eroded, with an armouring layer of coarse particles develop-

Received 6 July 2006. Accepted 18 January 2007. Published on the NRC Research Press Web site at http://cjfas.nrc.ca on 7 April 2007.
J19402

D. Palm[1] and E. Brännäs. Swedish University of Agricultural Sciences, 901 83 Umeå, Sweden.
F. Lepori. University of Umeå, 901 87 Umeå, Sweden.
K. Nilsson. Nilivaara Sportfishing Association, Nilivaara 108, 982 91 Gällivare, Sweden.
S. Stridsman. Swedish National Board of Fisheries, 972 38 Luleå, Sweden.

[1]Corresponding author (e-mail: daniel.palm@vabr.slu.se).

 doi:10.1139/F07-027 © 2007 NRC Canada

Fig. 1. Location of the study site (stream Hartijokki) in northern Sweden. The boulder + gravel and boulder-only treatments are marked as B + G and B, respectively. Electrofishing sites are indicated by circles.

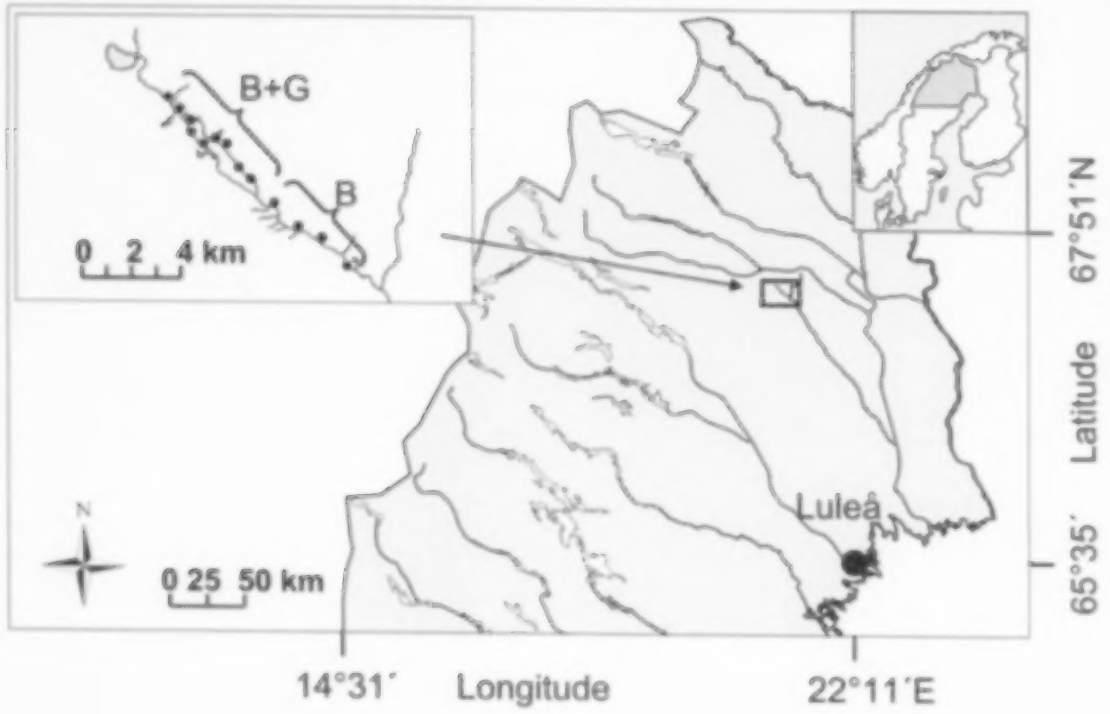

ing on the streambed (Merz et al. 2004). Given that most salmonines spawn in depressions (redds) excavated into gravel, the presence of gravel is essential for the reproduction and recruitment of these fish. Therefore, any removal of boulders as a result of channelization might reduce salmonine densities not only because of the loss of juvenile and adult habitat but also because of the loss of spawning substrate.

In Scandinavia, several channelized streams have been restored since the floating of timber ended in the 1980s to enhance stocks of the game fish brown trout (*Salmo trutta*). The restoration schemes have generally been consistent, focusing on the replacement of large boulders into the streams (Lepori et al. 2005*a*, 2005*b*). However, especially in eastern Scandinavia, the recruitment of gravel in streams is limited owing to the glacial surface geology, the abundance of lakes and low-gradients reaches that trap sediments, and the presence of stone walls (built to facilitate timber floating) that separate the channel from sediment sources along the banks (Nilsson et al. 2005). Therefore, suitable spawning substrates are unlikely to spontaneously recover in streams affected by channelization, even where the streambed has been consolidated by the addition of boulders. In spite of this, and the increasing recognition of the importance of spawning habitat in the literature on salmonines (Zeh and Donni 1994; Merz and Setka 2004; Rubin et al. 2004), spawning habitats have only rarely been restored in channelized streams in Scandinavia. Moreover, where spawning habitats have been restored, the consequences for fish have not been evaluated.

This study assesses the consequences of restoring spawning habitat for a population of brown trout in a stream in northern Sweden, which was channelized to facilitate timber floating. Two continuous sections of the stream were restored in 1993–2003 using contrasting schemes. One section was restored by replacing boulders into the stream. In the other, patches of gravel suitable for brown trout spawning were reconstructed in addition to the replacement of boulders. We compared the density of age-0+ brown trout, egg-to-fry survival, and substrate size composition of these two sections, testing the hypothesis that the restoration of spawning habitat enhanced these important features of brown trout populations more than the replacement of boulders alone.

Materials and methods

Study area

The study was conducted in a section of a third-order tributary to the River Kalix in northern Sweden (367 m above sea level, 67°24′N, 21°57′E) that, before the restoration, was channelized for timber floating (Fig. 1). At the study site, average discharge is 0.4 $m^3 \cdot s^{-1}$, with peaks of 5–14 $m^3 \cdot s^{-1}$ during snowmelt in May and June. Ice covers the stream from November to April. The average width and depth are 6.0 and 0.5 m, respectively, and the average slope is 2.3‰. The annual air temperature ranges between –35 and +30 °C (average 5 °C). The fish fauna is predominated by resident, potadromous, and anadromous brown trout and bullhead

© 2007 NRC Canada

(*Cottus gobio*), Northen pike (*Esox lucius*), minnow (*Phoxinus phoxinus*), burbot (*Lota lota*), and Atlantic salmon (*Salmo salar*) occur sparsely throughout the system. The riparian surroundings consist of managed boreal coniferous forest predominated by Scots pine (*Pinus sylvestris*) and Norway spruce (*Picea abies*).

In the study stream, channelization involved the removal of boulders and large woody debris and the straightening of the channel. An armouring layer, almost certainly developed as a consequence of channelization, was present on the streambed.

In 1992, a 10 km long section of the stream was restored by replacing ~90% of the boulders that were removed and piled along the banks back into the stream channel (Fig. 1). Roughly 600 m^3 of boulders with diameter between 40 and 70 cm were replaced. This resulted in a mean density of ~12 boulders·100 m^{-2} of wetted channel. The boulders were evenly scattered trying to mimic natural conditions. In addition, between 1992 and 2002, 85 patches of gravel were reconstructed in the uppermost 5 km of the section (Fig. 1) to provide spawning habitat using the following method. The coarse armouring layer was removed from areas of 2 m^2 to expose gravel of 1–5 cm in diameter. Sand and finer sediments were removed from the gravel to a depth of ~30 cm by manually disturbing the gravel using shovels. A cluster of boulders was placed at the downstream end of each gravel bed to prevent gravel erosion. In the lower 5 km of the stream section (Fig. 1), no gravel beds were reconstructed. Except for the consequences of the restoration, the two sections were very similar in general habitat characteristics including slope, channel width and length, and substrate type. In 1993, when brown trout were first sampled simultaneously at both sections, the densities of age-0+ individuals were low and similar in the upper and lower sections (1.6 and 1.0 individuals·100 m^{-2}, respectively). However, the relative contribution of age-0+ individuals to the total population was lower in the upper section than in the lower section (25.5% versus 50.0%). We will refer to the upper 5 km of the stream section as the boulder + gravel treatment and the lower 5 km as the boulder-only treatment.

Density of brown trout

Thirteen electrofishing sampling locations (mean area 740 m^2) were established at the study site, with nine located in the boulder + gravel treatment and four in the boulder-only treatment (Fig. 1). All electrofishing sites were separated by lentic reaches to minimize dispersal of age-0+ brown trout between sites. Electrofishing was performed yearly, in August, from 1992 through 2003 following Bohlin et al. (1989). The number of sites sampled each year varied between 5 and 13 depending on flow conditions. The fish captured were identified to species and measured to the nearest millimetre. Four distinct size-classes of brown trout (≤70, 71–120, 121–170, and ≥171 mm) were distinguished according to the length–frequency distribution of all (N = 8675) brown trout captured during the study. Brown trout of length ≥171 mm were assumed to be mature resident individuals (Näslund et al. 1998).

Egg-to-fry survival and substrate composition

On 23 October 2004, a mixture of 8000 newly fertilized and water-hardened eggs from eight pairs of wild anadromous brown trout captured in River Umeälven (located 300 km south of the study stream) were brought to the study stream. Water temperature during fertilization was 2–3 °C. During transport, the eggs were kept in a water container (volume 100 L) holding a constant temperature of 2 °C. Batches of 200 eggs were placed in each of 40 egg incubators, which were modifications of Rubin's (1995) and Flanagan's (2003) designs. Each incubator consisted of two polyvinylchloride cylinders 26 cm long and 10 cm in diameter (volume 2041 cm^3) closed at both ends. The cylinders had three 8 cm × 15 cm windows covered with plastic mesh (size 2 mm). The two cylinders were placed vertically on top of each other and were interconnected by a pipe measuring 2.5 cm in diameter, which allowed passage of fry. Brown trout eggs were placed in the lower cylinder together with gravel; after emergence, fry move into the upper cylinder, where they can start to feed. Twenty incubators, distributed in clusters of four at five different locations, were placed in each treatment within 18 h after egg fertilization. The temperature of the stream water during the placement of the incubators was 2 °C. The incubators were placed starting at the most upstream site; however, less than 3 h elapsed between the placement of the first and last incubators. Embryos tolerate handling for up to 48 h after fertilization without any significant increase in mortality (Piper et al. 1982) and no trend of increasing sensitivity of handling during the first 6 h (Krise 2001) and 72 h (Jensen and Alderdice 1983). Therefore, the order of placement was unlikely to influence the survival rates in the incubators. In the boulder + gravel treatment, incubators were placed in reconstructed gravel beds. In the boulder-only treatment, incubators where placed in the scarce patches of gravel still remaining after channelization where depth, current velocity, and surface substrate size matched those of the reconstructed gravel beds found in the boulder + gravel treatment. In the field, the eggs were gently poured into the lower cylinder of the incubators and covered with gravel. Next, the incubators were placed in the stream with the lower cylinder buried into the substrate and the upper cylinder protruding into the water column. All incubators were placed in depressions 15 cm deep, 50 cm wide, and 50 cm long excavated into the substratum. The gravel used in and around the incubators was taken just upstream from these depressions; it was lifted 30 cm above the streambed and then allowed to settle in the depression to mimic the substrate disturbance that salmonines cause when excavating and covering redds (Harris 1973; Kondolf et al. 1993). Gravel was added until the lower cylinder of the incubators was buried under 30 cm of substrate. As a control, four batches of 200 eggs each were placed in a hatchery 8 h after fertilization under normal rearing conditions and water temperature starting at 2 °C. On 19 June 2005 (i.e., after 241 days or 282 degree-days from the beginning of the study), the incubators were retrieved from the stream and the number of surviving fry was counted in both the upper and lower cylinders. To compare substrate size composition at incubation sites between the boulder + gravel and boulder-only treatments, one randomly chosen incubator from each site was brought to the laboratory and dried at 60 °C for 72 h. The dry substrate was sorted using sieves of size 16, 5.6, 1.6, 1.0, and 0.56 mm, which represent coarse gravel, fine gravel, very coarse sand,

© 2007 NRC Canada

Fig. 2. Age-0+ brown trout density (mean ± SE) in the boulder + gravel treatment (BG1–BG4) and the boulder-only treatment (B1–B4) before (open bars) and after (shaded bars) the gravel bed reconstruction.

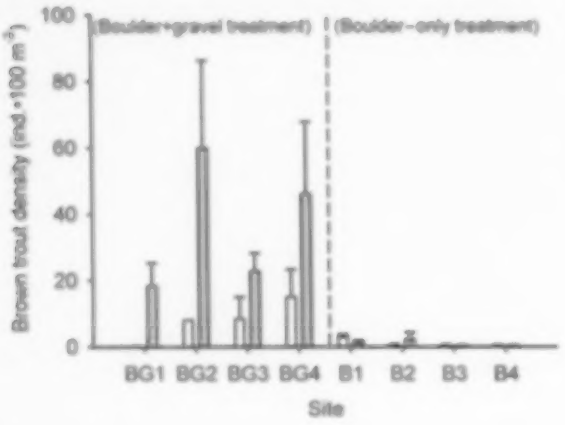

course sand, and sand and fines, respectively (Gordon et al. 1992). Each substratum fraction was weighed to the nearest 0.01 g.

Data analysis

Four of the nine electrofishing sites within the boulder + gravel treatment were electrofished on at least two occasions before (1992–1996) any gravel beds were reconstructed within these sites. At these four sites, the mean change in the density of age-0+ and mature brown trout individuals between before (1992–1996) and after (1997–2003) gravel bed reconstruction was compared with the mean change in the boulder-only treatment between the corresponding time periods using one-way analysis of variance (ANOVA). For the time periods 1992–1993, 1994–2000, and 2001–2003, the differences in age-0+ brown trout mean density in the boulder + gravel treatment were also analysed using one-way ANOVA. Linear regression analyses were used to evaluate if brown trout densities increased within any of these different time periods and to evaluate whether the area of reconstructed gravel beds per unit stream area influenced the mean density of 0+ brown trout in the boulder + gravel treatment. As spawning success influences fish density the following year, the number of reconstructed gravel beds was lagged by 1 year in this analysis. The data were log-transformed to satisfy the parametric assumptions of the tests. Egg-to-fry survival and substrate size composition were compared between treatments using one-way ANOVAs following arcsine square root transformation. All calculations were made using SPSS version 11.5 (SPSS Inc., Chicago, Illinois).

Results

Density of brown trout

The increase in density of age-0+ brown trout after gravel bed reconstruction was evident at all four sites in the boulder + gravel treatment compared with the four sites in the boulder-only treatment (Fig. 2). The mean density increase was significantly higher in the boulder + gravel treatment, 28.8 ± 8.44 individuals·100 m^{-2} (mean ± SE), compared with the boulder-only treatment, 0.0 ± 0.71 individuals·100 m^{-2} (ANOVA, $F = 15.81$, df = 1, $P = 0.007$). However, the densities of mature resident individuals were generally low at all sites and treatments (range 0.07–1.56 individuals·100 m^{-2}, mean 0.69 individual·100 m^{-2}) and did not differ between the two sections either before (ANOVA, $F = 0.84$, df = 1, $P = 0.39$) or after (ANOVA, $F = 2.88$, df = 1, $P = 0.14$) gravel bed treatment. In the boulder + gravel treatment, the percentage of age-0+ brown trout in the population increased from 36.0% to 51.5 % after gravel bed restoration, whereas at the same time, this same percentage declined from 27.9% to 23.4% in the boulder-only treatment (Table 1). Data from 11 years of continuous spawning habitat restoration showed a stepwise increase in density of age-0+ brown trout in the boulder + gravel treatment, whereas densities remained constantly low in the boulder-only treatment (Fig. 3). The mean density in the boulder-only treatment increased significantly between the three time periods 1992–1993, 1994–2000, and 2001–2003 (ANOVA, $F = 23.72$, df = 2, $P < 0.001$), with only the latter period showing an increasing trend within the time period (brown trout density = –47349 + 23.7 × year; $R^2 = 17.2$, $P = 0.031$). Linear regression analyses showed that the mean density of 0+ brown trout was positively associated with the mean area of reconstructed gravel beds per unit stream area (brown trout density = 0.583 + 0.259 × gravel bed area; $R^2 = 61.8$, $P = 0.020$) (Fig. 4).

Table 1. Size distribution and proportion of the total population (%) of brown trout caught by electrofishing in the boulder + gravel and boulder-only treatments before and after gravel bed reconstruction.

	Boulder + gravel		Boulder-only	
Size (mm)	Before treatment	After treatment	Before treatment	After treatment
≤70	36.0	51.5	29.7	23.4
71–120	37.8	34.2	23.3	32.2
121–170	21.7	10.3	27.9	24.3
≥171	4.5	4.3	19.8	20.1

Egg-to-fry survival and substrate composition

On the date of incubator retrieval, 5.6% ± 1.5% (mean ± SE) of the surviving fry had emerged. Egg-to-fry survival, including emerged and nonemerged fry, was generally low, 5.9% ± 1.9%, ranging from 0% to 47% across all incubators. In contrast, the mean survival of the control batches in the hatchery was high (76.6% ± 6.6%). Survival was significantly higher in the boulder + gravel treatment (10.3% ± 2.6%) compared with the boulder-only treatment (1.7% ± 1.1%) (ANOVA, $F = 12.53$, df = 1, $P = 0.008$). Visual observations of the recovered eggs suggested that the most likely reason for mortality was suffocation caused by fine sediments or fungal infections. The substrate size distribution in incubators differed between the treatments, with sand (0.56–1 mm) and fines (<0.56 mm) less abundant in the boulder + gravel treatment (Table 2). At the boulder + gravel sites, sand and fines represented 0.9% and 1.0%, respectively, of

© 2007 NRC Canada

Table 2. ANOVA table of the comparison of substrate size distribution between incubators in the boulder + gravel and boulder-only treatments.

	Substrate size by mass (%) (mean ± SE)		ANOVA	
Substrate size (mm)	Boulder + gravel	Boulder-only	*F*	*P*
≥16	79.8±5.0	50.3±4.3	17.42	0.003
16–5.6	12.1±2.0	19.7±1.1	9.21	0.016
5.6–1.6	5.2±2.0	13.1±1.4	9.07	0.017
1.6–1.0	1.0±0.4	6.0±1.3	20.30	0.002
1–0.56	0.9±0.5	6.8±1.8	17.74	0.003
0.56–0	1.0±0.4	4.1±1.23	8.21	0.021

Fig. 3. Cumulative area of reconstructed gravel beds (mean ± SE) in the boulder + gravel treatment (solid line) and age-0+ brown trout density (mean ± SE) in the boulder + gravel treatment (broken line) and the boulder-only treatment (dotted line) in 1992–2003.

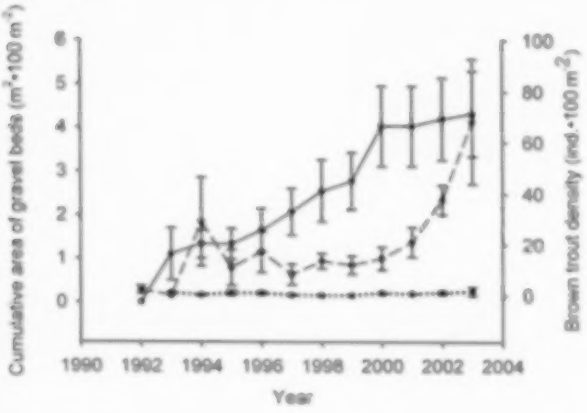

Fig. 4. Plot of the mean density of age-0+ brown trout (log-transformed) versus the mean cumulative area of gravel beds in the boulder + gravel treatment in 1992–2003 (linear regression line interpolated).

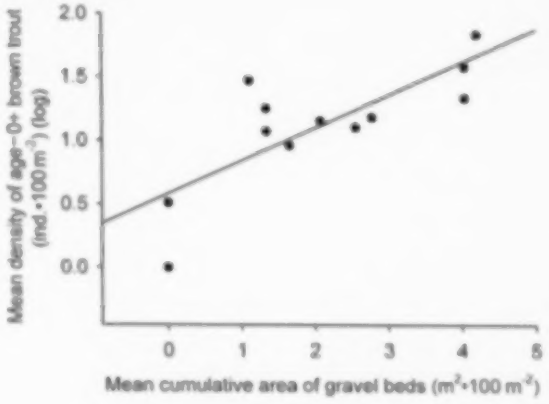

the total substrate mass compared with 6.8% and 4.1% in the boulder-only treatment.

Discussion

This study shows that, at our study site, the restoration of spawning habitat by the removal of the armoured streambed together with replacement of large boulders into the channel influenced the density of age-0+ brown trout, whereas the addition of boulders alone did not. Consistent with our results, several studies have shown that the availability of high-quality spawning substrate is one of the most important predictors of the number of redds, survival of embryos, and density of juvenile salmonines in running waters (Beard and Carline 1991; Beland 1996; Magee et al. 1996).

We suggest that the restoration of spawning habitat influenced the density of age-0+ brown trout through at least two mechanisms. First, the increased availability of spawning habitat probably reduced the mortality of embryos associated with spawning activities. Where salmonines are forced to spawn in confined areas, the redd excavated by any fish can be disturbed by overcutting from other spawners (Milner et al. 2003); the addition of spawning areas therefore allows fish to distribute less densely and avoid mutual interference during the excavation of redds. Supporting this hypothesis, in our study, the mean area of gravel beds explained a large percentage of the variation of the mean density of age-0+ brown trout. The remaining variation was, however, substantial (38.2%), which probably reflected fluctuations in the number of returning spawners or variations in nursery and rearing conditions. The existence of other sources of variation is also indicated by the stepwise increase in population size during the time periods 1992–1993, 1994–2000, and 2001–2003, which does not fully match the increase in the area of reconstructed gravel beds. Second, our incubation assay suggests that the reconstruction of spawning habitat also increased the egg-to-fry survival, which reached rates consistent with the survival in other studies where incubators were used at natural spawning sites (Bernier-Bourgault and Magnan 2002). We believe that the improved survival was mainly caused by the removal of the smothering matrix of sand and finer sediment conducted as part of the gravel bed restoration. In agreement, the cleaning of spawning gravel significantly increased the survival of brown trout embryos in four English rivers (Shackle et al. 1999), while several studies have shown that the survival of embryos tends to be low in substrates containing high amounts of sand and fines (Hausle and Coble 1976; Olsson and Persson 1988; Lapointe et al. 2004). Salmonines clean the substrate from sand and fines during the excavation of redds (Kondolf et al. 1993; Gottesfeld et al. 2004), but probably such natural disturbance of the substrate is insufficient to ensure high embryo survival where the spawning habitat has been highly de-

© 2007 NRC Canada

graded, which was probably the case in our study stream before the restoration.

In our assay, the egg-to-fry survival rate was low in both treatments. In part, the low survival might reflect artefacts resulting from the use of incubators, which tend to accumulate more sediment and impose higher mortalities to embryos than natural redds (Harshbarger and Porter 1982). The low survival might also have natural causes, such as the development of fungal infections, which might have been exacerbated by the relatively high densities of eggs in the incubators (0.1 egg·cm^{-2}). However, agglomeration of eggs is natural in salmonines, which typically lay eggs in pockets excavated into the streambed (Fleming 1996; De Gaudemar et al. 2000); moreover, in salmonines, the survival of embryos seems to be unrelated to egg density (Raddum and Fjellheim 1995; Rubin 1995). In any case, the range of survival rates observed in our study (0%–47%) was not substantially different from the range observed in other egg incubator assays at enhanced spawning sites where densities of 0.3–0.5 egg·cm^{-2} have resulted in average survival rates of 22%–51% (Rubin and Glimsäter 1996; Shackle et al. 1999; Merz et al. 2004).

Given that the restoration of spawning habitat could not be replicated and randomized at the reach scale owing to logistic and financial constraints, it is important to evaluate if any background difference between the reaches could have biased our results. For instance, the density of age-0+ brown trout was higher in the boulder + gravel treatment than in the boulder-only treatment even before the reconstruction of the gravel beds took place, and we cannot exclude that this initial discrepancy contributed to the differential increase in brown trout density observed after the restoration. However, this possibility seems unlikely. Since the abundance of mature resident brown trout was low and similar between treatments, most brown trout sampled during our study probably belonged to a migratory population. In Scandinavia, the homing behaviour of migratory brown trout is relatively inaccurate, as brown trout tend to use long stream sections (3.3–27.3 km on average) in their search for suitable spawning sites (Finstad et al. 2005; Östergren 2007). Therefore, the number of migratory brown trout returning to spawn at any of our sites was probably largely independent of the density of juveniles occurring at the same site at any prior time. Another potential concern is whether the relative position of the treatments in this study, in other words having the boulder-only treatment located downstream from the boulder + gravel treatment, could have contributed to more favourable spawning or rearing conditions at the boulder + gravel treatment. However, such a setup would more likely favour the use of the boulder-only treatment for spawning because the adult fish searching for spawning sites, which were returning from downstream areas, had to pass through the boulder-only treatment before they could reach the boulder + gravel treatment. Finally, considering that the habitat between the restored and control reaches was similar in general physiography, we believe that the increased density of juvenile brown trout was more likely to result from the gravel bed reconstruction than from any biasing factors.

The restoration of habitat is quickly becoming one of the main strategies to try to maintain self-sustaining populations of salmonines in streams and rivers in the face of growing human impact. However, doubts about the efficacy and permanence of in-stream restoration structures are widespread in the scientific community as well as the perception that restoration schemes often lack sound geomorphic or ecological foundation (Everest et al. 1991; Roni et al. 2002). These concerns, together with the ambiguity about the results achieved so far, mean that the potential benefits of habitat restoration for the management of salmonine populations remain uncertain. Our study suggests that, under the right circumstances, in-stream habitat restoration can positively influence the density of juvenile salmonines. Successful restoration for salmonines relies on the identification of the relevant limiting factors. At our study site, the density of juvenile brown trout was more strongly limited by the lack of spawning habitats than by the lack of structural complexity. We hope that the results of our study will increase the awareness of the possibility of spawning habitat restoration in future restoration projects where spawning habitat is a limiting factor.

Acknowledgments

We thank Åke Forsèn, Gunnar Åström, and Melsy Strömsten for providing brown trout eggs and Bo-Sören Wiklund, who produced the maps used in Fig. 1. We also thank two anonymous reviewers for valuable comments on the manuscript. This project was funded by the Swedish Sport Fishing Association through the Göte Borgström Foundation. The present study was approved by the Animal Ethical Board of Sweden (references A65-01 and A5-06).

References

Beard, T.D., and Carline, R.F. 1991. Influence of spawning and other stream habitat features on spatial variability of wild brown trout. Trans. Am. Fish. Soc. **6**: 711–722.

Beland, F.K. 1996. The relationship between redd counts and Atlantic salmon (*Salmo salar*) parr populations in the Dennys River, Maine. Can. J. Fish. Aquat. Sci. **53**: 513–519.

Bernier-Bourgault, I., and Magnan, P. 2002. Factors affecting redd site selection, hatching and emergence of brook charr, *Salvelinus fontinalis*, in an artificially enhanced site. Environ. Biol. Fishes, **64**: 333–341.

Bohlin, T., Hamrin, S., Heggeberget, T.G., Rasmussen, G., and Saltveit, S.J. 1989. Electrofishing — theory and practice with special emphasis on salmonids. Hydrobiologia, **173**: 9–43.

De Gaudemar, B., Schroder, S.L., and Beall, E.P. 2000. Nest placement and egg distribution in Atlantic salmon redds. Environ. Biol. Fishes, **57**: 37–47.

Everest, F.H., Sedell, J.R., and Reeves, G.H. 1991. Planning and evaluating habitat projects for anadromous salmonids. Am. Fish. Soc. Symp. **10**: 68–77.

Finstad, A.G., Okland, F., Thorstad, E.B., and Heggberget, T.G. 2005. Comparing upriver spawning migration of Atlantic salmon *Salmo salar* and sea trout *Salmo trutta*. J. Fish Biol. **67**: 919–930.

Flanagan, J.J. 2003. The impact of fine sediments and variable flow regimes on the habitat and survival of Atlantic salmon (*Salmo salar*) eggs. M.Sc. thesis, Department of Biology, University of New Brunswick, Fredricton, N.B.

© 2007 NRC Canada

Fleming, I.A. 1996. Reproductive strategies of Alantic salmon: ecology and evolution. Rev. Fish Biol. Fish. **6**: 379–416.

Gordon, N.D., McMahon, T.A., and Finlayson, B.L. 1992. Stream hydrology. An introduction for ecologists. Wiley, Chichester, UK.

Gottesfeld, A.S., Hassan, M.A., Tunnicliffe J.F., and Porier, R.W. 2004. Sediment dispersion in salmon spawning streams: the influence of floods and salmon redd construction. J. Am. Water Resour. Assoc. **40**: 1071–1086.

Harris, G.S. 1973. A simple egg box planting technique for estimating the survival of eggs deposited in stream gravel. J. Fish Biol. **5**: 85–88.

Harshbarger, T.J., and Porter, P.E. 1982. Embryo survival and fry emergence from two methods of planting brown trout eggs. N. Am. J. Fish. Manag. **2**: 84–89.

Hausle, D.A., and Coble, D.W. 1976. Influence of sand in redds on survival and emergence of brook trout (*Salvelinus fontinalis*). Trans. Am. Fish. Soc. **105**: 57–63.

Hunter, C.J. 1991. Better trout habitat. A guide to stream restoration and management. Island Press, Washington, D.C.

Jensen, J.T.O., and Alderdice, D.F. 1983. Changes in mechanical shock sensitivity of coho salmon (*Oncorhynchus kisutch*) eggs during incubation. Aquaculture, **32**: 303–312.

Kondolf, G.M., Sale, M.J., and Wolman, M.G. 1993. Modification of fluvial gravel size by spawning salmonids. Water Resour. Res. **29**: 2265–2274.

Krise, W.F. 2001. Sensesivity of Atlantic salmon eggs to mechanical shoch during the first six hours after fertilisation. N. Am. J. Aquacult. **63**: 34–37.

Lapointe, M.F., Bergeron, N.E., Bérubé, F., Pouliot, M.-A., and Johnston, P. 2004. Interactive effects of substrate sand and silt contents, redd-scale hydraulic gradients, and interstitial velocities on egg-to-emergence survival of Atlantic salmon (*Salmo salar*). Can. J. Fish. Aquat. Sci. **61**: 2271–2277.

Lepori, F., Palm, D., and Malmqvist, B. 2005*a*. Effects of stream restoration on ecosystem functioning: detritus retentiveness and decomposition. J. Appl. Ecol. **42**: 228–238.

Lepori, F., Palm, D., Brännäs, E., and Malmqvist, B. 2005*b*. Does restoration of structural heterogeneity enhance the diversity of fish and macroinvertebrates? Ecol. Appl. **15**: 2060–2071.

Magee, J.P., McMahon, T.E., and Thurow, R.F. 1996. Spatial variation in spawning habitat of cutthroat trout in a sediment-rich stream basin. Trans. Am. Fish. Soc. **125**: 768–779.

Merz, J.E., and Setka, J.D. 2004. Evaluation of a spawning habitat enhancement site for Chinook salmon in a regulated California river. N. Am. J. Fish. Manag. **24**: 397–407.

Merz, J.E., Setka, J.D., Pasternack, G.B., and Wheaton, J.M. 2004. Predicting benefits of spawning-habitat rehabilitation to salmonid (*Oncorynchus* spp.) fry production in a regulated California river. Can. J. Fish. Aquat. Sci. **61**: 1433–1446.

Milner, N.J., Elliott, J.M., Armstrong, J.D., Gardiner, R., Welton, J.S., and Ladle, M. 2003. The natural control of salmon and trout populations in streams. Fish. Res. **62**: 111–125.

Nilsson, C., Lepori, F., Malmqvist, B., Törnlund, E., Hjerdt, N., Helfield, J.M., Palm, D., Östergren, J., Jansson, R., Brännäs, E., and Lundqvist, H. 2005. Forecasting environmental responses to restoration of rivers used as log floatways: an interdisciplinary challenge. Ecosystems, **8**: 779–800.

Näslund, I., Degerman, E., and Nordwall, F. 1998. Brown trout (*Salmo trutta*) habitat use and life history in Swedish streams: possible effects of biotic interactions. Can. J. Fish. Aquat. Sci. **55**: 1034–1042.

Olsson, T.I., and Persson, B.G. 1988. Effects on deposited sand on ova survival and alevin emergence in brown trout (*Salmo trutta* L.). Arch. Hydrobiol. **113**: 621–627.

Östergren J. 2007. Migration biology and genetic population structure of *Salmo salar* and *Salmo trutta* in northern Swedish rivers. Doctoral thesis, Department of Aquaculture, Swedish University of Agricultural Science, Umeå, Sweden.

Piper, R.G., McElwain, I.B., Orme, L.E., McCraven, J., Fowler, L.G., and Leonard, J.R. 1982. Fish hatchery management. American Fisheries Society, Bethesda, Md.

Raddum, G.G., and Fjellheim, A. 1995. Artificial deposition of eggs of Atlantic salmon (*Salmo salar*) in a regulated Norwegian river — hatching, dispersal and growth of the fry. Regul. Rivers Res. Manag. **10**: 169–180.

Roni, P., Beechie, T.J., Bilby, R.E., Leonetti, F.E., Pollock, M.M., and Pess, G.R. 2002. A review of stream restoration techniques and a hierarchical strategy for prioritizing restoration in Pacific northwest watersheds. N. Am. J. Fish. Manag. **22**: 1–20.

Rubin, J.F. 1995. Estimating the success of natural spawning of salmonids in streams. J. Fish Biol. **46**: 603–622.

Rubin, J.F., and Glimsäter, C. 1996. Egg-to-fry survival of the sea trout in some streams of Gotland. J. Fish Biol. **48**: 585–606.

Rubin, J.F., Glimsäter, C., and Jarvi, T. 2004. Characteristics and rehabilitation of the spawning habitatas of the sea trout, *Salmo trutta*, in Gotland (Sweden). Fish. Manag. Ecol. **11**: 15–22.

Shackle, V.J., Hughes, S., and Lewis, V.T. 1999. The influence of three methods of gravel cleaning on brown trout, *Salmo trutta*, egg survival. Hydrol. Process. **13**: 477–486.

Törnlund, E. 2002. Flottningen dör aldrig: bäckflottningens avveckling efter Ume- och Vindelälven 1945–70. Doctoral thesis, Department of Economic History, University of Umeå, Umeå, Sweden.

Törnlund, E., and Östlund, L. 2002. The floating of timber in northern Sweden: construction of floatways and transformation of rivers. Environ. Hist. **8**: 85–106.

Zeh, M., and Donni, W. 1994. Restoration of spawning grounds for trout and grayling in the river High-Rhine. Aquat. Sci. **56**: 59–69.

© 2007 NRC Canada

Regional ecosystem variability drives the relative importance of bottom-up and top-down factors for zooplankton size spectra

Kerri Finlay, Beatrix E. Beisner, Alain Patoine, and Bernadette Pinel-Alloul

Abstract: The relative effects of top-down and bottom-up drivers of zooplankton size structure were examined in three limnologically diverse regions of Quebec, Canada. Lake productivity drove biomass of small-sized zooplankton (300–1000 µm) in the Eastern Townships and Laurentian regions, which have high total phosphorus gradients, but was not significant in the low-productivity region, Gouin. Fish species composition was found to affect biomass of large-sized (>1000 µm) zooplankton and was the primary factor affecting zooplankton size structure in the low productivity region. When size structure of the zooplankton communities were described as normalized biomass size spectra, only bottom-up factors were significant, as increasing productivity resulted in higher curve peaks and increased parabola curvature. No factors were significantly related to any parameter of the Pareto distribution to describe size spectra. Overall, bottom-up forces were stronger drivers of zooplankton size structure, particularly in regions with wide ranges in lake trophy, while fish predation was more important in regions with low productivity variability.

Résumé : Nous avons examiné les effets relatifs des facteurs explicatifs descendants et ascendants de la structure en taille du zooplancton dans trois régions du Québec, Canada, qui diffèrent par les caractéristiques limnologiques de leurs lacs. La productivité lacustre explique la biomasse du zooplancton de petite taille (300–1000 µm) dans les Cantons de l'Est et les Laurentides où il existe de forts gradients de phosphore total; elle n'est cependant pas significative dans la région de Gouin qui possède une faible productivité. La composition spécifique des poissons affecte la biomasse du zooplancton de grande taille (>1000 µm) et elle est le principal facteur à affecter la structure en taille du zooplancton dans la région de faible productivité. Lorsque la structure en taille du zooplancton est présentée sous forme de spectres de taille de la biomasse normalisée, seuls les facteurs ascendants sont significatifs, car une productivité accrue a pour effet de produire des sommets plus élevés dans la courbe et d'augmenter la courbure de la parabole. Aucun des facteurs n'est significativement relié à quelque paramètre que ce soit de la distribution de Pareto qui sert à décrire les spectres de taille. Globalement, les forces ascendantes sont de meilleurs facteurs explicatifs de la structure en taille du zooplancton, particulièrement dans les régions où il existe une forte étendue de trophie dans les lacs, alors que la prédation par les poissons est plus importante dans les régions de faible variation de la productivité.

[Traduit par la Rédaction]

Introduction

The question of whether bottom-up or top-down factors drive ecosystem dynamics has shifted in the last two decades to address instead when and under what conditions top-down or bottom-up factors dominate (Hunter and Price 1992; Power 1992). In lakes, bottom-up factors known to affect zooplankton dynamics include total phosphorus (TP) and cation concentration. Increased TP generally increases total zooplankton abundance and biomass (Hanson and Peters 1984; Yan 1986; Pinto-Coelho et al. 2005), but has often been demonstrated to disproportionately affect smaller zooplankton (Bays and Crisman 1983). Calcium is considered to be limiting for large cladocerans, and increasing cation concentration has been linked to an increase in the abundance of larger zooplankton (Tessier and Horwitz 1990; Patoine et al. 2002). Top-down predation effects of both invertebrates (*Mysis* spp.: Nero and Sprules 1986; Johannsson et al. 1994; and *Chaoborus* spp.: Kajak and Rybak 1979; Mackay et al. 1990; Ramcharan et al. 2001) and fish (Brooks and Dodson

Received 12 July 2006. Accepted 9 January 2007. Published on the NRC Research Press Web site at http://cjfas.nrc.ca on 10 April 2007.
J19416

K. Finlay.[1] Département des sciences biologiques, Université du Québec à Montréal (UQÀM), CP 8888, Succ. Centre Ville Montréal, QC H3C 3P8, Canada; Department of Biology, University of Regina, 3737 Wascana Parkway, Regina, SK S4S 0A2, Canada.
B.E. Beisner. Département des sciences biologiques, UQÀM, CP 8888, Succ. Centre Ville Montréal, QC H3C 3P8, Canada.
A. Patoine. Department of Biology, University of Regina, 3737 Wascana Parkway, Regina, SK S4S 0A2, Canada.
B. Pinel-Alloul. Département de Sciences Biologiques, Université de Montréal, Pavillon Marie-Victorin, 90 Vincent d'Indy, Montréal, QC H3C 3J7, Canada.

[1]Corresponding author (e-mail: kerri.finlay@uregina.ca).

 doi:10.1139/f07-028 © 2007 NRC Canada

1965) are well known, and the relative effects of each predator on zooplankton communities have been summarized by McQueen et al. (1986). Thus, although we currently know which factors can regulate zooplankton biomass and size structure, general trends of the relative strengths of top-down and bottom-up factors across lakes and regions remain elusive.

While a combination of both lake productivity and fish predation have been shown to be responsible for variations in zooplankton biomass and size structure, differences in the relative strengths of top-down and bottom-up factors between studies are common (e.g., Stemberger and Lazorchak 1994; Hessen et al. 1995; Pinel-Alloul et al. 1995). Differences in the relative variability of abiotic and biotic variables at different scales of observation may explain the lack of observed trends between studies and systems (Hunter and Price 1992). For example, Gasol et al. (1995) observed that heterotrophic nanoflagellates were correlated with bottom-up forces across lakes that varied greatly in resource supply, but when examining nanoflagellates within individual lakes (where variation in resource supply was lower), both bottom-up and top-down forces were important. The scale of observation has been used to explain the differences in conclusions drawn regarding the relative effects of top-down and bottom-up factors for crustacean zooplankton (Pinel-Alloul et al. 1995). Currie et al. (1999) found that resource levels most strongly affected zooplankton abundance across three regions in Quebec and Ontario, while across five regions in Quebec, Pinel-Alloul et al. (1995) found that bottom-up factors of lake chemistry were the main factors explaining zooplankton community structure. In contrast, Rodriguez et al. (1993) concluded that fish were more important when only one of the Quebec regions was studied. The range of values for physical and chemical variables as well as for predation pressure often differs considerably within and between different regions, and thus conclusions may be influenced by the scale of observation and gradients of variability present in a particular area of interest.

Here, we examine the relative strengths of top-down and bottom-up factors on different size classes of crustacean zooplankton and test for differences among three lake districts that differ in their range of limnological characteristics. We examine a region that varies widely in TP concentration because of heavy human use (Eastern Townships), one that has moderate human activity and accordingly moderate variation in nutrient concentration, but is also characterized by highly coloured dissolved organic carbon (DOC, Laurentians), and one that has very low human impact and low nutrient variability (Gouin Reservoir). We predict that those regions with greater variation in nutrient availability will have stronger bottom-up effects than the region with lower nutrient variability.

As a secondary goal, we sought to explore the relationships between bottom-up and top-down factors on size spectra descriptors. Much previous work on size structure in aquatic systems has revolved around the construction of normalized biomass size spectra (NBSS) (Platt and Denman 1978) and Pareto distributions (Vidondo et al. 1997). These models fit to organism size data and have been used to estimate productivity and energy flow through lake food webs (Thiebaux and Dickie 1992, 1993; Sprules and Goyke 1994). Most previous studies that have examined the effect of bottom-up and top-down drivers on size spectra shape have done so across multiple trophic levels from phytoplankton to fish (e.g., Sprules and Munawar 1986; Gaedke 1992; Zhou 2006), which is anticipated to follow different patterns than within trophic levels (Thiebaux and Dickie 1992, 1993; Sprules and Goyke 1994). Of those that have looked at zooplankton specifically, bottom-up and top-down factors have only been invoked anecdotally or by using a limited number of drivers. For example, in a comparison of the Great Lakes epilimnion and hypolimnion communities, Yurista et al. (2006) found that of temperature, conductivity, and chlorophyll concentration, temperature was the only significant factor driving size spectra in the Great Lakes. Moore and Suthers (2006) suggested that NBSS slopes may also reflect the relative contribution of top-down and bottom-up factors in communities of varying productivity and that oligotrophic systems may have steeper slopes because of control by top-down forces, but this was not tested directly. We therefore sought to determine whether there are consistent relationships between bottom-up and top-down forces and the biomass size structure, as well as the parabolic shape of NBSS in lake zooplankton.

The objectives of this study are twofold: (*i*) to determine the relative strengths of top-down and bottom-up factors on the biomass of different size classes of zooplankton in lakes in three regions in Quebec (Canada) that vary considerably in productivity, geology, and land use and (*ii*) to determine whether these same factors also affect NBSS and Pareto descriptions of zooplankton communities to facilitate future research in size spectrum theory.

Materials and methods

Study sites

We examined changes in biomass size structure in three different regions in Quebec: the Eastern Townships, Laurentians, and Gouin Reservoir. These three areas differ widely in their underlying geology, land use, and accordingly, their productivity (Table 1). Although the three regions were sampled in different years (1996, 2004, and 2005), all samples were taken during the month of July, and therefore those lakes that stratify will have done so at the time of sampling. 1996 and 2004 were average years in terms of climate (data from Environment Canada; www.climate.weatheroffice.ec.gc.ca/) as the mean summer temperature and precipitation were well within the 10-year averages for Montreal. 2005, however, was a particularly warm and wet year (average temperature was 1.4 °C warmer than 1996 and 2004 and had the highest precipitation in the 10-year period).

Although interannual variability in zooplankton species dynamics can be large in some lakes (e.g., Gerten and Adrian 2002), Olden et al. (2006) found that this variability has only serious consequences when making conclusions for lakes that are similar in their habitat characteristics. Since we sampled lakes within each region in the same year, we believe that variability due to interannual differences among lakes within regions will be minimal relative to the differences among these very diverse regions.

© 2007 NRC Canada

Table 1. Mean (range in parentheses) limnological lake characteristics in the three regions of Quebec.

	Region		
Variable	Eastern Townships	Laurentians	Gouin
Bottom-up			
Lake area (km^2)	2.9 (0.2–14.5)	1.2 (0.1–5.3)	0.42 (0.2–0.8)
TP ($\mu g \cdot L^{-1}$)	16.5 (5.2–45.1)	19.0 (5.4–48.0)	7.6 (4.6–15.5)
TN ($mg \cdot L^{-1}$)	0.41 (0.17–0.93)	0.31 (0.18–0.56)	0.23 (0.14–0.32)
DOC ($mg \cdot L^{-1}$)	5.8 (2.3–8.9)	5.8 (2.1–9.3)	5.1 (2.8–9.5)
Secchi disk depth (m)	3.7 (0.8–9.5)	3.9 (1.5–8.5)	4.0 (2.1–6.1)
Mean Chl *a* ($\mu g \cdot L^{-1}$)	5.2 (0.9–22.3)	2.1 (0.43–7.6)	2.2 (1.0–3.2)
Top-down			
Z_{max} (m)	20.9 (1.8–61.9)	16.9 (4.2–45.7)	13 (7–23)
Fish species (*n*)	12.2 (6–19)	9.2 (5–15)	3.7 (1–7)

Note: Bottom-up variables included in the analyses were lake area, total phosphorus (TP), total nitrogen (TN), dissolved organic carbon (DOC), Secchi disk depth, and mean chlorophyll *a* (Chl *a*) concentration. Top-down factors included the presence or absence of common fish species (number of species (*n*)), the presence or absence of *Chaoborus* predators (not included in table), and maximum lake depth (Z_{max}).

Eastern Townships lakes

Eighteen lakes in the Eastern Townships region of Quebec were sampled in July 2004 (Beisner et al. 2006). These lakes are located 100 km east of Montréal in a well-buffered, calcareous region underlain by a sedimentary geology of the St. Lawrence lowlands and characterized by elevated pH and alkalinities.

Each lake was sampled at the deep point to reflect the deep pelagic community, but may not reflect conditions throughout the entire lake. Zooplankton samples were taken using a 0.5 m diameter, 2 m long, 100 µm mesh net from 1 m above the sediment to the lake surface during daylight hours, between 1000 and 1800. Cod-end samples were collected and preserved in 75% ethanol. Secchi disk depth, pH, TP, total nitrogen (TN), DOC, dissolved inorganic carbon (DIC), and chlorophyll *a* (Chl *a*) concentration were taken at the same time as the zooplankton samples. Details of chemical analyses can be found in Beisner et al. (2006). The presence or absence of *Chaoborus* spp. was determined by visual examination of the samples collected, but because of the low densities and different behaviour of these predators we did not attempt to quantify their abundance. Data of fish species composition were obtained from the Quebec Ministry of Natural Resources and Wildlife, who have sampled these lakes sporadically since the 1930s using a variety of gill nets in each lake. For each lake, we have at least two, and at most four, sampling years. These surveys thus provide a generalized list of major fish species in each lake.

Subsamples from each preserved zooplankton sample were passed through a laser optical plankton counter (LOPC, Brooke Ocean Technology, Dartmouth, Nova Scotia; Herman et al. 2004) lab benchtop version within 1 year of collection to count and size particles. Finlay et al. (2007) demonstrated that abundance of preserved zooplankton samples is adequately estimated by the LOPC compared with traditional microscope counts and that although size as estimated by the LOPC (in equivalent spherical diameter, ESD) underestimates the size of large cladocerans, a correction factor can be used to convert ESD into accurate biomass estimates.

Laurentian lakes

We sampled 20 lakes in the Laurentians in July 2005. These lakes are located in the southeastern part of the Precambrian shield. The bedrock is mainly gneiss and granite, covered by morainic soils. A notable difference between the lakes in the Laurentians and the other study regions is the colour of their DOC. The contribution of DOC to the light extinction coefficient is much higher in the Laurentian lakes compared with those in the Eastern Townships, which is responsible for considerable differences in lake processes, such as the summer metabolic balance (Prairie et al. 2002). Data of fish species composition were also obtained from the Quebec Ministry of Natural Resources and Wildlife, but we were unable to obtain fish species composition for 4 of 20 lakes. Zooplankton and environmental conditions were sampled using the same methods and equipment as described for the Eastern Townships lakes.

Gouin lakes

Zooplankton from the Gouin region have been studied previously (Patoine et al. 2002). Patoine et al. (2002) examined the effect of watershed deforestation by logging and wildfires on the zooplankton communities for 3 months in each of 2 years following the perturbation, but for our study, we used only the data from July 1996 in reference lakes that were unaffected by logging or forest fires. The Gouin region intersects the Greenville and Superior geological provinces of the Canadian Shield (details of the lakes and region can be found in Carignan et al. 2000), and the lakes here are generally oligotrophic.

Zooplankton were sampled from the deepest site in each lake using a cantilevering net (Filion et al. 1993) fitted with a 53 µm net from 1 m above the sediments to the surface. Fish in the Gouin region were sampled in 1996 and 1997 with experimental monofilament gill nets with a fishing effort between 6 and 12 nets per night, depending on lake area (St-Onge and Magnan 2000). Details of zooplankton and environmental sampling can be found in Patoine et al. (2002), who used an optical plankton counter (OPC) to analyze zooplankton samples.

© 2007 NRC Canada

Although the zooplankton were sampled using different methods in the three regions, we do not believe that these differences substantially biased our results. The cantilevering net is designed to minimize clogging and avoidance (Filion et al. 1993) and was particularly unlikely to clog in Gouin, which has low zooplankton densities. Our plankton nets used in the Eastern Townships and Laurentians had an open area ratio of 5:1, which should minimize clogging in most lakes (Omori and Ikeda 1984). Net efficiency has been shown to vary from 32% to 100% (McQueen and Yan 1993), and thus a severely clogged net may under-represent zooplankton densities by three times. Net clogging was possible in some of our very productive lakes; however, we observed ranges in large zooplankton (>1000 µm) densities from 0 to 1000·m^{-3}, which is a difference of 1000 times. Thus we believe that the natural variability in densities between lakes overlays any potential differences that may have occurred because of a reduction in net efficiency.

The use of the OPC and LOPC is also not anticipated to contribute substantially to differences between regions. Patoine et al. (2006) compared OPC derived values with microscope estimates of zooplankton abundance and biomass, and Finlay et al. (2007) did the same comparisons for the LOPC. Thus, the output from both devices in terms of their abilities to process laboratory-fixed samples have been compared and standardized to microscope counts, and the differences between the OPC and LOPC should be minimal.

Size spectra analyses

The NBSS plots the normalized biomass of the community vs. the log biomass of the particle. The slope and intercept of the regression line or the parameters describing a parabolic fit are then compared between systems. Vidondo et al. (1997), however, proposed the use of the Pareto distribution to describe size spectra, since the Pareto parameter c is an unbiased estimator of the NBSS slope and yields a better fit to the data. Furthermore, it avoids the need to group data by log size classes and avoids the problem of empty size classes that occurs with NBSS. The Pareto type II can be used to model parabolic curves comprising the overall size spectra (Vidondo et al. 1997). We used both the NBSS and Pareto descriptions of zooplankton size spectra for our analyses.

NBSS calculations

The LOPC provides data of the number of individuals in 15 µm bins. The biomass of the midpoint of each 15 µm bin was calculated using the following equation (Sprules and Munawar 1986):

$$V = \frac{\Pi}{6}\left(\frac{\mathrm{ESD}^3}{f^2}\right) \quad (1)$$

where V is volume, which was converted to biomass assuming a specific gravity of 1; ESD is the equivalent spherical diameter of the particle as measured by the LOPC, and f is a ratio of length:width for the zooplankton samples. Previous work has found that a value of 1.72 provides the closest relationship between volume and biomass as determined by species-specific length–weight regressions in the Eastern Townships (Finlay et al. 2007). This f value fits in the range of values found by Patoine et al. (2006) and thus was used to calculate biomass in all three regions. The OPC data from the Gouin region were available as the density of particles in 100 µm ESD bins. The midpoint of each 100 µm bin was converted to biomass using the equation and conversions above.

Bin size was $\log_{10}$-transformed, and total community biomass was summed over all sizes in each 0.1 $\log_{10}$ biomass size class. Delta biomass was calculated as the difference in biomass between each 0.1 $\log_{10}$ size class (each bin was thus 1.259 times the size of the previous bin). Biomass size spectra are represented graphically as log(biomass (per m^3) / Δbiomass) vs. log biomass of size class. Calculations of NBSS followed that of Gaedke (1992). Although the LOPC measures zooplankton from 100 to 3500 µm ESD, we analyzed only those zooplankton between 300 and 2000 µm ESD. We found that bubbles in the lab circulator arrangement of the LOPC prevented accurate counts below 300 µm ESD, and an extremely low density of larger zooplankton (because of the use of a small plankton net) made counts >2000 µm ESD unreliable. This also allowed for direct comparisons with the OPC, as the lower limit of detection for this is ~250 µm ESD (Herman et al. 2004); thus, we are confident that both the OPC and LOPC were adequately counting the smallest particles included in our analyses. The zooplankton included in this 300–2000 µm window ranged from small copepodids to the largest daphnids, but excluded the microzooplankton, including copepod nauplii and rotifers, and larger predatory zooplankton such as *Mysis* spp. and *Leptodora* spp. (Finlay et al. 2007).

A parabolic fit was applied to these data using

$$y = a + 0.5c(x - b)^2 \quad (2)$$

where c is the curvature of the parabola, and a and b are the y and x coordinates of the vertex (Sprules and Goyke 1994). Parameter a is thus considered to reflect total zooplankton biomass.

Pareto calculations

The density of individuals in each 15 µm ESD size bin (as given in the LOPC output for the Eastern Townships and Laurentian regions) and 100 µm bins (from the OPC output for the Gouin data) was used to construct the Pareto distributions of the size spectra following Vidondo et al. (1997). The probability that an individual is of a given size is taken as the fraction of all individuals larger than or equal to itself (Boix et al. 2004) and is plotted against the weight of that size class, using the calculations above to convert ESD to biomass. The relationship was fit with the type II Pareto model:

$$\log[\mathrm{prob}(s \geq S)] = c\log(K + D) - c\log(S + D) \quad (3)$$

where $\log[\mathrm{prob}(s \geq S)]$ is the accumulated probability that the size variable (s) will have a value greater than the size (S) of the individual in question. c and K are the distribution's shape and scale parameters, respectively, and D is an additive constant.

© 2007 NRC Canada

Statistical analyses

The data used for ordination techniques was zooplankton biomass in bins of 100 µm (Gouin) and 105 µm ESD (Eastern Townships and Laurentians, since LOPC data are only available in 15 µm groups). Principal components analysis (PCA) using zooplankton biomass in each bin was used to evaluate the similarities between lakes and regions.

The relationship between environmental variables and biomass of zooplankton in different size classes was first analyzed using data of zooplankton biomass in 100 µm (Gouin) and 105 µm (Eastern Townships and Laurentians) bins. This allows for a direct estimate of how each environmental factor affects each size class of zooplankton using redundancy analyses (RDA). Environmental variables with non-normal distributions were log-transformed, and all variables were centered and standardized prior to ordination. Significant ($P < 0.05$) predictor variables were determined using forward selection, and significance was determined by Monte Carlo permutation (999 permutations).

To separate the relative effects of different predictor variables, the significant environmental variables representing top-down and bottom-up factors were run in separate RDAs. Top-down variables included common fish species composition (those species occurring in more than three lakes) and the presence or absence of *Chaoborus* spp., as well as lake depth, as an increase lake depth allows zooplankton to vertically migrate and avoid fish predation (Tessier and Welser 1991; Gaedke 1992). The effect of piscivores will be different than the effect of planktivores on zooplankton size spectra, but this will be reflected in the direction of the relationships in the RDA. Planktivorous fish species will have a negative relationship with large (>1000 µm) zooplankton, while piscivores that create a trophic cascade will be positively correlated with large zooplankton biomass (Brooks and Dodson 1965). *Chaoborus* spp. feed preferentially on small zooplankton (<1000 µm, Wissel et al. 2003), and thus we would expect a negative relationship between these two groups in the RDA.

Bottom-up effects included lake size, TP, TN, DOC, Secchi disk depth, Chl *a* concentration, as these all reflect potential productivity of lakes. RDAs examining both top-down and bottom-up factors together were run on the significant variables from the separate analyses. All PCAs and RDAs were performed using CANOCO version 4.5 (ter Braak 1990). The variation explained by bottom-up and top-down factors were summarized using variation partitioning (Borcard et al. 1992; Peres-Neto et al. 2006).

Relationships between environmental factors and the fitted size spectra functions were explored using multiple regression with forward selection of parameters from the NBSS (*a*, *b*, and *c* from eq. 2) and Pareto (*c*, *K*, *D* from eq. 3) to environmental variables (maximum depth, mean depth, volume, area, Secchi disk depth, pH, TP, TN, DOC, DIC, total Chl *a*). Critical α was chosen as the Bonferroni correction of 0.05/6 = 0.008 to account for multiple comparisons. To determine the effect of the presence or absence of predator species on size spectra parameters, *t* tests were used. Multiple regressions and *t* tests were performed using the statistical program JMP IN version 5.1 (SAS Institute Inc., Cary, North Carolina).

Results

An example of the three different size spectra analyses (biomass in 100 µm bins, NBSS, and Pareto distributions) in each of the three regions (Eastern Townships, Laurentians, and Gouin) is shown (Fig. 1). The lakes in this figure were chosen to demonstrate the range of variability in size spectra and how these differences are captured by the different analyses. Lake Waterloo in the Eastern Townships is eutrophic (total Chl *a* concentration = 21.9 µg·L^{-1}) and has one of the highest zooplankton biomass levels of all the lakes studied; Lake Connelly in the Laurentians is oligo–mesotrophic (Chl *a* = 2.03 µg·L^{-1}); and Lake N84 in the Gouin Reservoir is oligotrophic (Chl *a* = 1.0 µg·L^{-1}). A parabola could not be fit to Lake N84, and thus the straight-line relationship is shown here.

Most of the variability in biomass in each 105 µm size fraction for the Eastern Townships and the Laurentians was seen in the small zooplankton fractions (from 300 to 825 µm; Figs. 2*a*, 2*b*), as these small size classes oriented along the first axis of the PCA with longer vectors than the large sizes classes. In contrast, the most variability in Gouin was in the larger zooplankton fraction (1100–1700 µm; Fig. 2*c*). Overall, the variability in the zooplankton biomass–size relationship was comparable between the Eastern Townships and Laurentian regions, but the zooplankton in the Gouin region varied comparatively little. The PCA of zooplankton biomass in all regions together shows an overlap of lakes in the Eastern Townships and those from the Laurentians, while the lakes in the Gouin region all cluster very closely together near the origin (Fig. 2*d*).

Bottom-up factors affecting zooplankton biomass in 105 µm bins

TP concentration was the sole bottom-up environmental factor selected by the RDA with biomass in 105 µm bins for the Eastern Townships (Fig. 3*a*; $P = 0.002$, 52.2% variation explained) and demonstrates that the biomass of small zooplankton classes increases as TP increases. In the Laurentians, the results of the RDA between biomass in 105 µm bins and bottom-up factors demonstrated that an increase in TN concentration positively affected the biomass of small zooplankton (<1000 µm ESD) and negatively affected larger zooplankton, while the opposite relationship was found with increasing lake area (Fig. 3*b*). No significant bottom-up factors were found for the Gouin lakes or when all lakes were examined together in a single RDA.

In the Laurentian lakes, there was no relationship between TP and Chl *a* concentration (linear regression, $P > 0.05$, results not shown). There was, however, a significant relationship between TP and TN (linear regression, $P = 0.01$, $R^2_{adj} = 0.26$), suggesting that TP measurements were accurate (i.e., that sample contamination was unlikely the cause for the lack of relationship between TP and Chl *a*). Moreover, there was a significant but weak relationship between TN and Chl *a* ($P = 0.004$, $R^2_{adj} = 0.34$). In contrast, the TP–Chl *a* relationship in the Eastern Townships has $R^2_{adj} = 0.73$ ($P < 0.0001$), suggesting that additional factors in the Laurentians were affecting primary production relationships, which likely also affected relationships further up the food web.

© 2007 NRC Canada

Fig. 1. Examples of biomass in 100 µm equivalent spherical diameter (ESD) bins (*a*, *b*, *c*), normalized biomass size spectra (NBSS) (*d*, *e*, *f*), and Pareto distributions (*g*, *h*, *i*) for Lake Waterloo in the Eastern Townships (left column), Lake Connelly in the Laurentians (middle column), and Lake N84 in the Gouin Reservoir (right column). These lakes represent the range of size spectra seen in these areas. Details of lake productivity and morphometry can be found in Table 1. For the NBSS and Pareto distributions, the points represent the size spectra values, and the lines represent the curves fit to the points using a parabolic curve for the NBSS and the Pareto type II distribution.

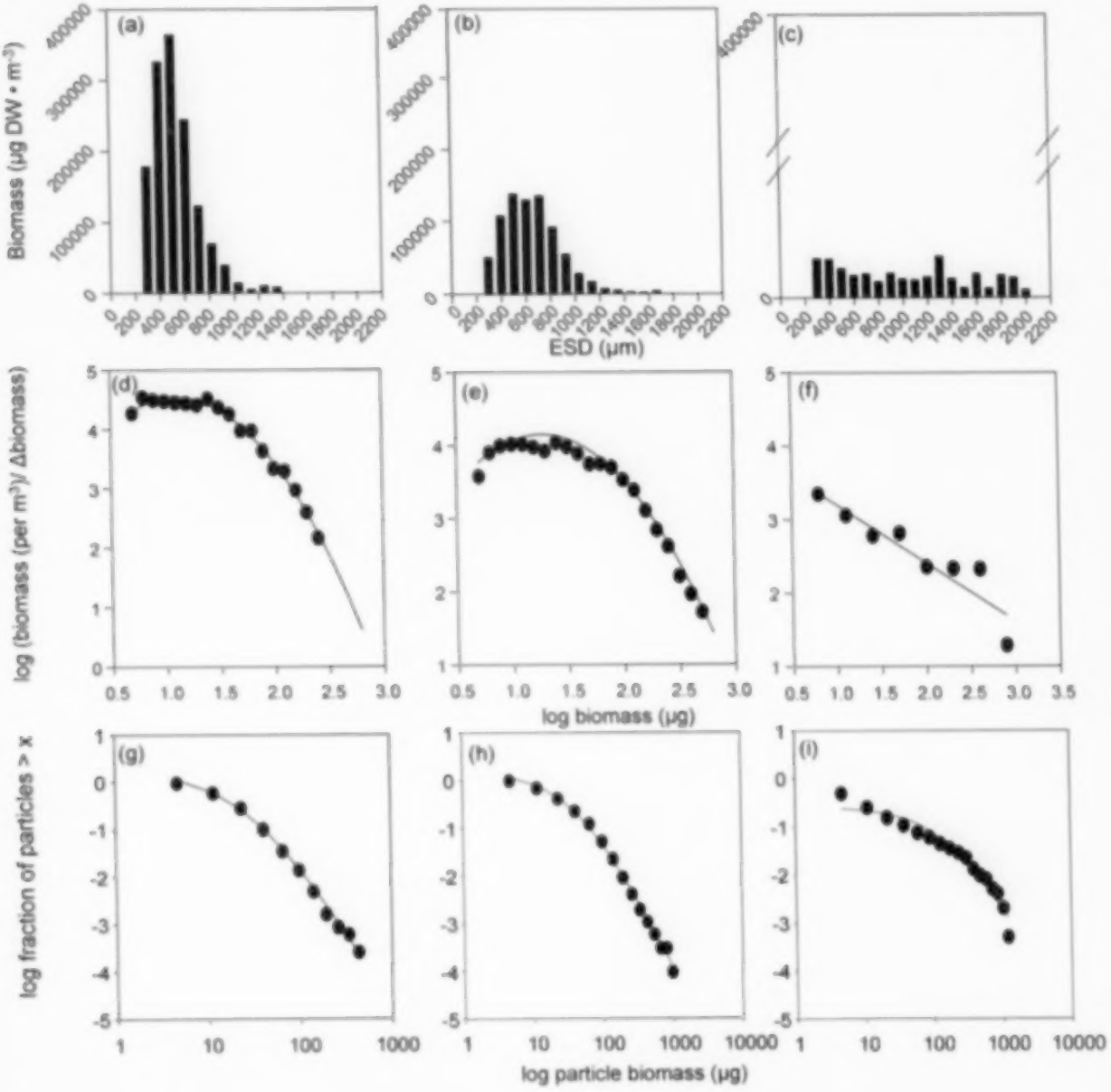

Top-down factors affecting zooplankton biomass in 105 µm bins

The presence of three fish species (rainbow smelt, *Osmerus mordax*; white sucker, *Catostomus commersonii*; and golden shiner, *Notemigonus crysoleucas*) were selected by the RDA of the biomass–size relationship with top-down variables alone in the Eastern Townships (Fig. 4*a*; $P = 0.008$, 54.5% variation explained). No top-down factors were significant in the RDAs for the Laurentians. Only top-down forces were found to significantly influence the biomass–size relationship of the zooplankton community in the Gouin region. The presence or absence of three fish spe-

© 2007 NRC Canada

Fig. 2. Ordination biplots for the principal components analyses (PCAs) of biomass in 100 µm equivalent spherical diameter (ESD) bins for the lakes in (*a*) the Eastern Townships, (*b*) the Laurentians, (*c*) the Gouin Reservoir, and (*d*) all lakes from all regions. Open symbols represent lakes from the Eastern Townships, shaded symbols are from the Laurentians, and the solid symbols represent lakes from the Gouin Reservoir. Arrows represent biomass in each bin size; for example, 300 represents biomass of zooplankton from 300 to 404 µm ESD, 405 represents the biomass of zooplankton from 405 to 509 µm ESD. These 105 µm bins were necessary, as data from the laser optical plankton counter (LOPC) are given in 15 µm intervals.

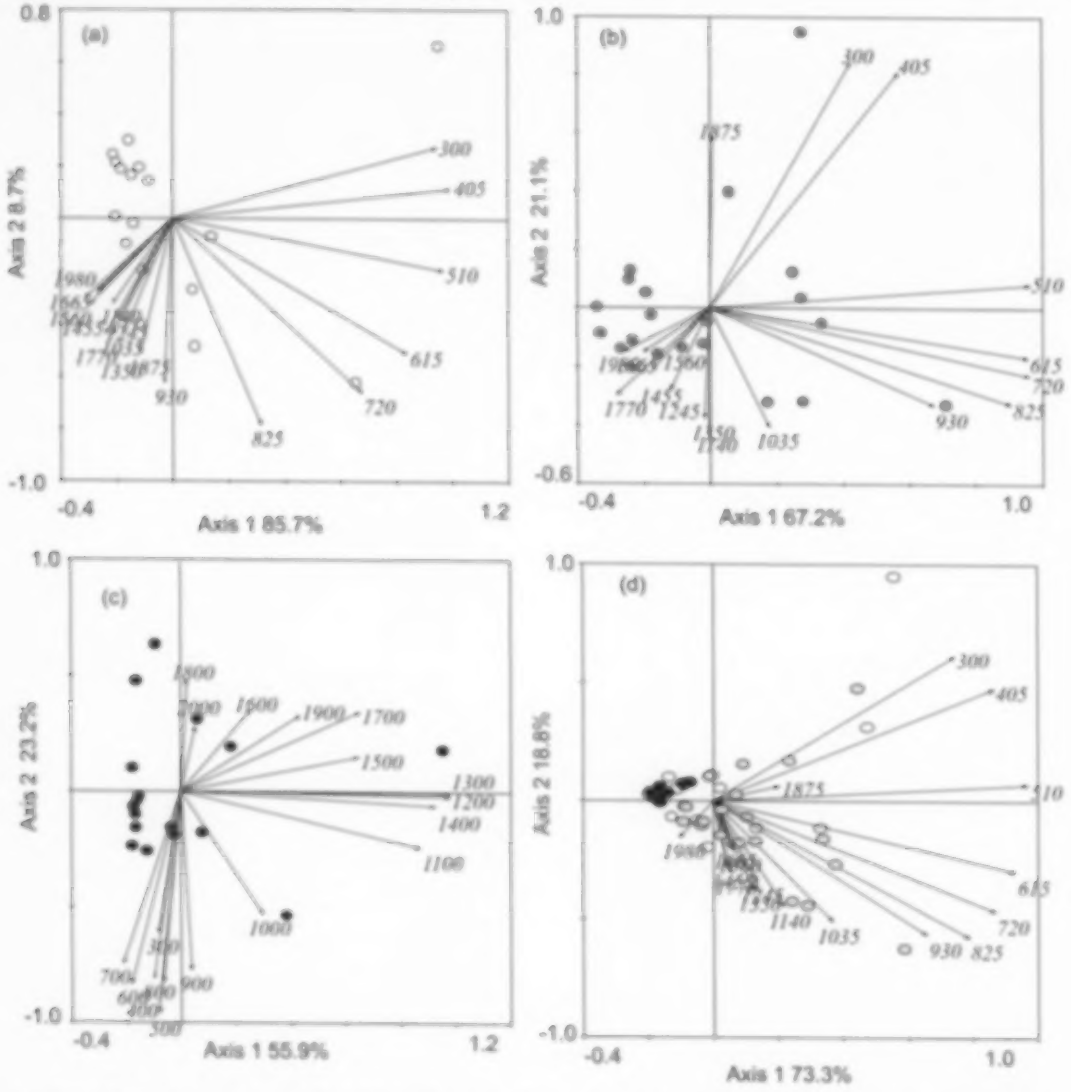

cies (brook trout (*Salvelinus fontinalus*), fallfish (*Semotilus corporalis*), and unidentified cyprinids) explained 49.3% of the variation (Fig. 4*b*; $P = 0.002$). No top-down factors were significant when all regions were examined together.

Relative strengths of top-down and bottom-up factors in 105 µm bins

When the significant top-down and bottom-up factors of the Eastern Townships lakes were entered into an RDA with forward selection, only TP and the presence of white sucker remained significant ($R^2_{adj} = 61.2\%$, $P = 0.01$). The results of variation partitioning for each region show that in the Eastern Townships, 30.1% of the variation was attributed to differences in TP concentration ($P = 0.003$), only 12.1% was attributed to the presence of white sucker ($P = 0.031$), 18.9% was due to multicollinearity between TP and white sucker presence, and 38.8% of the variation remained unexplained (Fig. 5*a*). The variation partitioning for the Laurentians and Gouin lakes was more straightforward, as these regions only had one type of environmental driver that was significant in the RDA analyses. Bottom-up factors accounted for 34.7% of the variation in the Laurentian lakes,

© 2007 NRC Canada

Fig. 3. Ordination biplots of redundancy analyses (RDAs) for the analyses of bottom-up effects on zooplankton biomass size fractions (all numbers) and environmental variables (TP, total phosphorus; TN, total nitrogen; Area, lake area) for (*a*) the Eastern Townships lakes and (*b*) the Laurentian lakes. Only TP was significant for the Eastern Townships lakes (variation explained = 52.2%, $P = 0.002$), while TN and Area were significant for the Laurentian lakes (variation explained = 41.6%, $P = 0.002$).

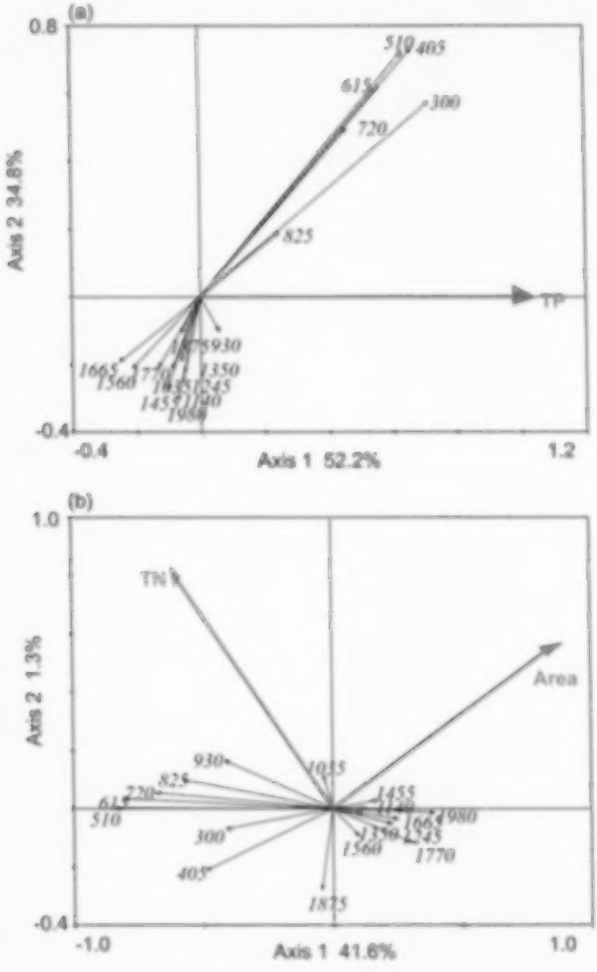

while 36.7% of variation was attributed to top-down factors in Gouin lakes (Figs. 5*b*, 5*c*; all R^2 values are adjusted).

Relative strengths of top-down and bottom-up factors on NBSS and Pareto parameters

In the Eastern Townships, parameter *a* (the *y* coordinate of the peak) of the NBSS parabolic curve was found to increase significantly with TP (Fig. 6*a*; $P < 0.0001$, $R^2_{adj} = 0.70$), and NBSS parameter *c* (the curvature of the parabola) was significantly lower with increasing TP (Fig. 6*b*; $P = 0.003$, $R^2_{adj} = 0.41$). No parameter of the Pareto distribution was significantly related to any bottom-up factor. The presence or absence of the significant fish species (as determined by the

Fig. 4. Ordination biplots of redundancy analyses (RDAs) for the analyses of top-down effects on zooplankton biomass size fractions (all numbers) and environmental variables (all listed fish species) for (*a*) the Eastern Townships lakes and (*b*) the Gouin lakes. The presence or absence of three fish species (*Catostomus commersonii*, white sucker; *Osmerus mordax*, rainbow smelt; *Notemigonus crysoleucas*, golden shiner) were significant ($P = 0.008$, variation explained = 54.5%) in the Eastern Townships, and other fish species (*Salvelinus fontinalis*, brook trout; *Semotilus corporalis*, fallfish; cyprinids) were significant ($P = 0.002$, variance explained = 49.3%) in the Gouin Reservoir.

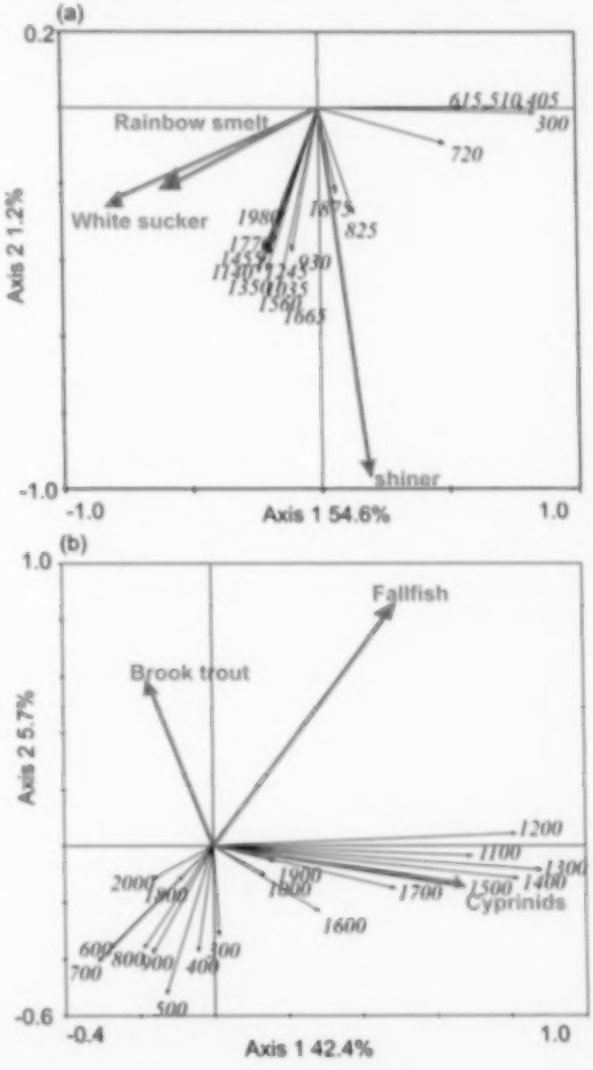

RDA analyses) did affect several parameters of both the NBSS and Pareto distributions, but this was not significant at $\alpha_{crit} = 0.008$.

In the Laurentians, parameter *a* of the NBSS was significantly negatively related to lake maximum depth (Fig. 7*a*; $P = 0.001$, $R^2_{adj} = 0.40$), while parameter *c* was found to vary

© 2007 NRC Canada

Fig. 8. Variation partitioning for top-down (open), bottom-up (solid), interaction (hatched), and unexplained (shaded) fractions explaining variability in biomass in 100 µm bins in (*a*) the Eastern Townships, (*b*) the Laurentians, and (*c*) the Gouin Reservoir. TP, total phosphorus; TN, total nitrogen; Area, lake area.

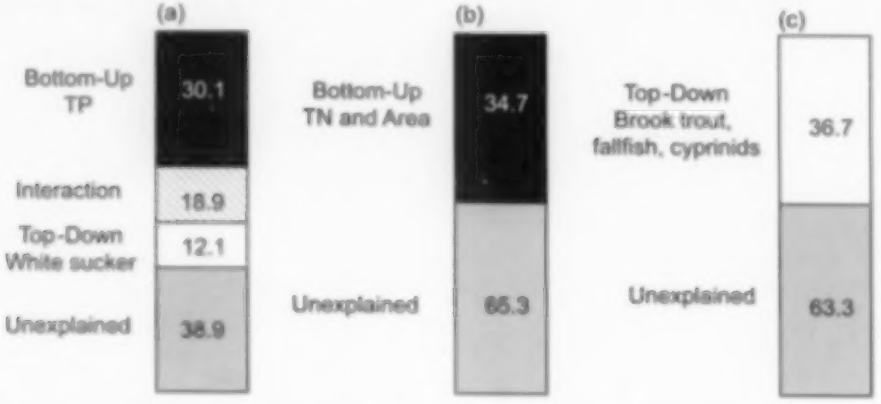

negatively with TP and positively with lake area (Figs. 7*c*, 7*d*; multiple regression $P = 0.01$, $R^2_{adj} = 0.57$). For the Pareto distribution, only parameter K was found to have any significant relationship with any environmental variable, and K decreased with increasing maximum depth (Fig. 7*b*; $P = 0.005$, $R^2_{adj} = 0.34$). No parameter values were significantly affected by the presence or absence of any fish species in this region.

Of the 17 lakes studied in the Gouin region, the size spectra of four could not be fit with a parabola, but were instead better described by a straight line. No significant relationships were found between any size spectra parameter (parabolic or linear) and any environmental variable. Data of catch per unit effort and biomass per unit effort from 1996 and 1997 were also available for the fish species communities in these lakes, but there were no significant relationships between these values and parabola parameters. When the data from all three regions were analyzed together, no significant relationships were found between NBSS or Pareto parameters and any environmental variable (all regression $P > 0.05$).

Discussion

Both bottom-up and top-down factors were found to affect zooplankton biomass and size structure in Quebec lakes, supporting the previous findings of Hessen et al. (1995) and Pinel-Alloul et al. (1995). However, the nature of the relationship between the two types of factors and size-structure varied between regions, and no factors could explain patterns in zooplankton size structure across all regions together. Our results demonstrate that lakes from a region that varies greatly in terms of potential productivity may implicate different forcing factors from lakes where fish predation varies more. This suggests that in cross-lake studies, researchers must take the limnological characteristics and degree of variation of their study lakes into account when determining whether bottom-up or top-down factors more greatly influence zooplankton community biomass.

Bottom-up factors were stronger drivers of zooplankton size structure than top-down factors in the two regions with large ranges in potential productivity (Eastern Townships and Laurentians), but was not a significant factor in Gouin, which had low productivity. Bottom-up drivers were best represented by TP in the Eastern Townships, and although Chl *a* has previously been found to be related to TP in the Laurentians (Masson et al. 2000); in 2005, we found that TN and lake area were better predictors of lake potential productivity. Increased precipitation increases DOC inputs into lakes (Schindler 1998), and coloured DOC can change the relationships between nutrients and primary productivity (Carpenter et al. 1998). Thus, the warm and wet year of 2005 may have caused a shift in the usual relationships between nutrients and productivity in the Laurentians. Regardless of the specific limiting factors in this region, we were able to detect the significant bottom-up effect on zooplankton size spectra. In both the Eastern Townships and the Laurentians, bottom-up effects were disproportionate on small zooplankton (300–1000 µm ESD), supporting Bays and Crisman (1983). Increased cyanobacterial abundance at high levels of production have been shown to reduce the densities of large cladoceran zooplankton because of feeding inhibition (Ghadouani et al. 2006), which may explain why small zooplankton in these lakes responded more strongly to bottom-up factors than larger zooplankton.

Top-down effects explained a substantial proportion of zooplankton variability in Gouin and a smaller proportion than bottom-up drivers in the Eastern Townships. Although particular fish species were not found to affect zooplankton size structure in the Laurentian lakes, we are reluctant to conclude that top-down drivers are not operating at all in this region because of the lack of sufficient fish data. The fish data available from government sources are not ideal, although we do believe that the government surveys used here were sufficient to provide an accurate list of common fish species in lakes that were sampled.

White sucker, the only fish that affected zooplankton size structure in the Eastern Townships (when both top-down and bottom-up factors were considered together), can drive other benthivores, such as brook trout, to planktivory to avoid competition (Magnan 1988). In Gouin, the presence of cyprinids accounted for the majority of the variability in zooplankton size structure. This result is contrary to predictions, since cyprinids are planktivores. However, with detailed catch-per-unit-effort data for these lakes, we were able

© 2007 NRC Canada

Fig. 6. Relationships between environmental variables and normalized biomass size spectra (NBSS) and Pareto parameters for Eastern Townships lakes. (*a*) Total phosphorus (TP) and NBSS parameter *a*; (*b*) TP and NBSS parameter *c*.

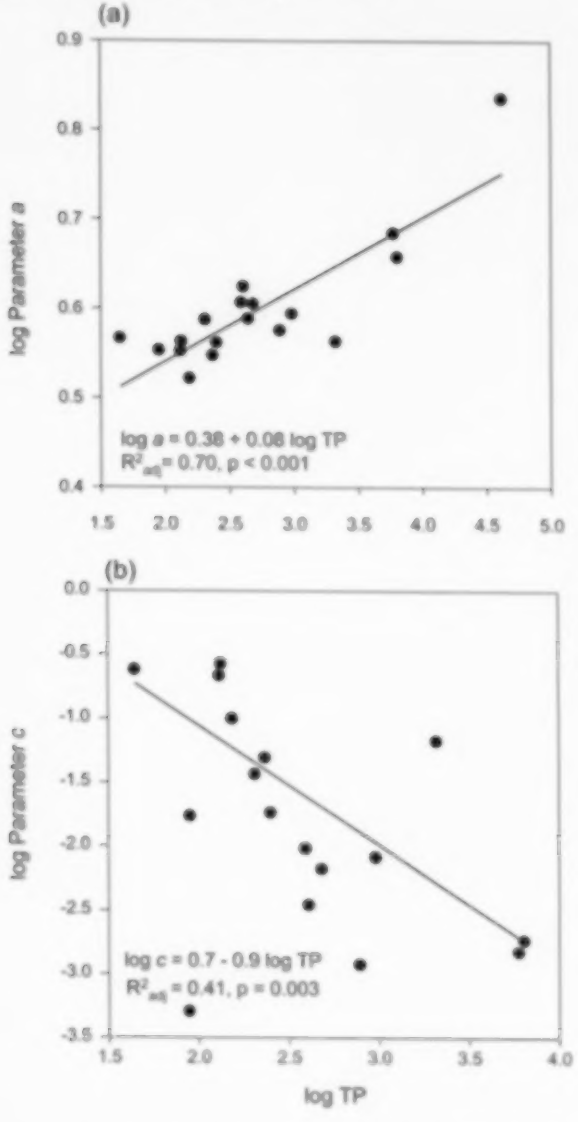

to verify that even lakes with high densities of cyprinids had high relative biomass of large-bodied zooplankton. Although cyprinids can feed on large zooplankton, they switch diets to feed preferentially on benthic macroinvertebrates once they reach a size of ~150 mm in length (Hjelm et al. 2003), usually in midsummer. Our analyses were based on samples taken in July, and lakes in the Gouin region that contained cyprinids lacked larger fish predators (data not shown). Thus, the positive relationship between large zooplankton and the presence of cyprinids likely reflects a predation release midsummer, allowing the largest zooplankton to increase in biomass. Although a detailed analysis of seasonal changes is beyond the scope of this study, preliminary analyses here found that high cyprinid biomass in June was correlated with much lower biomass of large zooplankton, supporting the midsummer predation release hypothesis.

It is somewhat surprising that the presence or absence of *Chaoborus* spp. did not have a significant effect on biomass or size spectra in any region, as previous work has found strong effects of *Chaoborus* on zooplankton size structure (Mackay et al. 1990). Instead, the lack of effect supports the predictions of McQueen et al. (1986), who suggested that invertebrate predators only have a strong regulating effect on zooplankton communities when fish predation is absent. This is further supported by the work by Steiner (2004), whose experimental work noted that *Chaoborus* may not have a strong regulating effect on *Daphnia* spp. mean body size even in the absence of fish. All lakes studied here had at least a few fish species present, which may have lessened the impact by *Chaoborus* on the zooplankton. Thus, although we did find some significant top-down effects in our study lakes, it is currently very difficult to predict which fish or invertebrate predators will exert the strongest regulating control in different lakes and regions.

Although the causes for the relative strengths of bottom-up and top-down drivers across regions may be attributed to variations in physical or chemical characteristics of the lakes, they may also be explained by the relative variability of both the drivers and the response of the zooplankton community. For example, the increased importance of top-down factors in the Gouin region may be due to the increased water clarity owing to low primary production. Clearer water would allow visual predators to feed more efficiently (Benfield and Minello 1996; Gregory 1998). Our analyses, however, suggest that bottom-up factors exert stronger regulating control over zooplankton size spectra than top-down factors over a large geographical range. The lakes in Gouin had both a small range of potential productivity and small variability in zooplankton biomass relative to the other two regions. Thus, the potential for bottom-up drivers to exert regulating effects on the zooplankton community in this region were minimized, simply because nutrient levels were uniformly low in this region. Top-down forces emerged as the primary driving factor only when productivity variability was low, but even here, the relative variability in zooplankton biomass was low compared with the other two regions. Thus, overall, bottom-up factors appear to be responsible for large changes in zooplankton size structure, but in the absence of large shifts in bottom-up factors, top-down forces can exert regulating effects over smaller variations in zooplankton biomass. This agrees with the conclusions of Carpenter et al. (1985), who suggested that primary productivity is primarily driven by nutrient levels, but trophic cascades can explain additional variability between systems. A comparison of the significant drivers and relative variability of the response variable of interest (in our case, zooplankton biomass and size structure) may aid in the comparison of studies across different systems and landscapes to obtain a hierarchy of environmental drivers.

In our study, normalized biomass size spectra parameter values were well correlated with a few bottom-up environmental drivers, while the Pareto distribution was not well described by any environmental factor. Top-down factors were never significantly related to any size spectra parameter, sug-

© 2007 NRC Canada

Fig. 7. Relationships between environmental variables and normalized biomass size spectra (NBSS) and Pareto parameters for Laurentian lakes: (*a*) lake maximum depth and NBSS parameter *a*, (*b*) lake maximum depth and Pareto parameter *K*, (*c*) and (*d*) response of NBSS parameter *c* with total phosphorus (TP) and lake area, respectively.

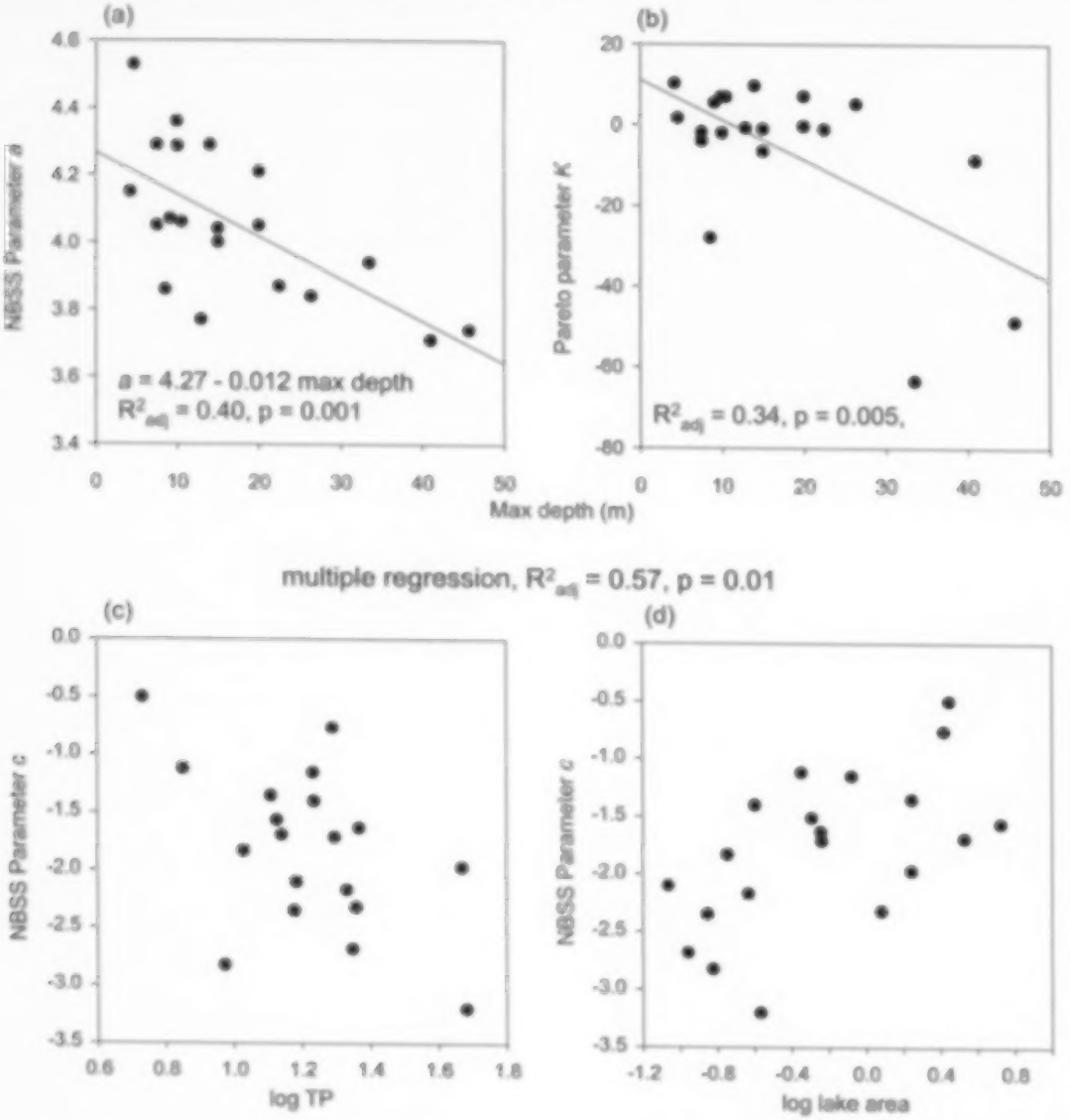

gesting that these descriptions of zooplankton size spectra are less sensitive to top-down and bottom-up effects than biomass in size-binned groups.

Parameter *a* of the NBSS reflects total biomass of the zooplankton. Thus, the significant relationship between TP and parameter *a* for the Eastern Townships supports the considerable previous research that phosphorus concentration affects zooplankton biomass (Hanson and Peters 1984; Yan 1986). Again, increased lake colour in the Laurentian lakes is the likely explanation why TP was not found to vary with parameter *a* in these lakes. The relationship between parameter *a* and lake maximum depth likely reflects the effect of potential primary productivity on zooplankton biomass, as deep lakes have lower productivity per unit volume than shallow lakes. The lack of relationship in the Gouin lakes is most likely a reflection of the low variability of TP and productivity in these lakes.

Increasing TP was also correlated with increased curvature (more negative parameter *c* values) in the Eastern Townships and Laurentians (where lake area was also significantly related to parameter *c*). Similarly, Yurista et al. (2006) found that parameter *c* of the NBSS was more negative in Lakes Erie and Ontario, the most productive of the Great Lakes, when compared with Lakes Huron, Michigan,

© 2007 NRC Canada

and Superior. It is difficult to explain the environmental or biological drivers behind a straightening of parabolic curves with decreasing lake productivity, since a straighter line could be due to a relative increase of either larger or smaller particles or to a relative decrease in midsized particles.

Top-down factors did not consistently affect either the NBSS or Pareto distribution for any region. The non-significant relationships between fish and invertebrate predator species composition and parameter values could be explained by a lack of sufficient data (for the Laurentians and Eastern Townships, we have only fish species presence or absence, and these data were collected at different times of the year and in different years). However, we did have additional data on the fish community (including catch and biomass per unit effort, sampled consistently) in the Gouin region and were still unable to find significant relationships with size-spectra-fitted lines and parabolas (data not shown). Thus, the effect of fish predation may be less severe on NBSS and Pareto distributions of zooplankton communities than it is on biomass–size distributions, which may also support the conclusion that overall, lake potential productivity is a stronger factor influencing zooplankton size structure than fish predation. Future studies examining the relationships between fish community interactions and density with zooplankton size spectra in more detail would provide valuable information to advance our understanding of zooplankton size spectra variations.

These results demonstrate that NBSS of zooplankton are influenced by bottom-up factors alone, while the Pareto distribution has no consistent relationship with any bottom-up or top-down factors. At this point, we can predict that an increase in lake productivity will increase parameter a and decrease parameter c of the NBSS parabola of zooplankton, which should help guide future work using size spectra for estimates of energy flow and production. Zooplankton biomass in binned sizes thus appears to be the most sensitive approach to establishing top-down vs. bottom-up effects. The NBSS curve still retains some biological information (e.g., parameter a represents zooplankton biomass), while the parabolic fit to the Pareto distribution has no obvious biological links. A straight-line fit to either the NBSS or Pareto may be more biologically meaningful and therefore more responsive to top-down and bottom-up forces; however, in productive systems, a straight-line fit is not always appropriate.

In conclusion, we demonstrated that the zooplankton communities in regions with wide ranges of potential productivity are driven by bottom-up effects, as seen on large latitudinal gradients (Pinto-Coelho et al. 2005). Lake potential productivity appeared to be the strongest driving factor, which was either represented by TP or TN, depending on lake colour, and increasing lake productivity results in an increase in the biomass of small (300–1000 µm ESD) zooplankton. Top-down effects of fish appear to dominate in regions with lower variability of productivity, where there is less variability in zooplankton biomass. Size spectra descriptions of zooplankton community appear to be most strongly affected by bottom-up factors, which may be useful for analyses of energy flow through aquatic communities and may provide quick estimates of lake potential primary productivity.

Acknowledgements

Funding from a Natural Sciences and Engineering Research Council of Canada (NSERC) Discovery Grant and the Canadian Foundation for Innovation (CFI) to BEB, as well as a Groupe de recherche interuniversitaire en limnologie (GRIL) postdoctoral fellowship to KF is gratefully acknowledged. We thank A. Barnett, M.L. Longhi, M. Maezo, C. Falardeau, and A. Boisvert for sample collection in the Eastern Townships and Laurentians and Patrick Lafrance, Marie-Joëlle Leblanc, Catherine Miville-Deschènes, and Isabelle Saint-Onge for sample collection and OPC analyses in Gouin. Thanks go to J. Dubé, P. Lévèsque, H. Fournier, C. Beaudoin, and L. Nadon of the Quebec Ministry of Natural Resources and Wildlife for providing access to provincial fish records. Comments from two anonymous reviewers greatly improved this manuscript.

References

Bays, J.S., and Crisman, T.L. 1983. Zooplankton and trophic state relationships in Florida lakes. Can. J. Fish. Aquat. Sci. **40**: 1813–1819.

Beisner, B.E., Peres-Neto, P.R., Lindstrom, E.S., Barnett, A., and Longhi, M.L. 2006. The role of environmental and spatial processes in structuring lake communities from bacteria to fish. Ecology, **87**(12): 2985–2991.

Benfield, M.C., and Minello, T.J. 1996. Relative effects of turbidity and light intensity on reactive distance and feeding of an estuarine fish. Environ. Biol. Fishes, **46**: 211–216.

Boix, D., Sala, J., Quintana, X., and Moreno-Amich, R. 2004. Succession of the animal community in a Mediterranean temporary pond. J. North Am. Benthol. Soc. **23**: 29–49.

Borcard, D., Legendre, P., and Drapeau, P. 1992. Partialling out the spatial component of ecological variation. Ecology, **73**: 1045–1055.

Brooks, J.L., and Dodson, S.I. 1965. Predation, body size, and composition of plankton. Science (Washington, D.C.), **150**: 28–35.

Carignan, R., D'Arcy, P., and Lamontagne, S. 2000. Comparative impacts of fire and forest harvesting on water quality in Boreal Shield lakes. Can. J. Fish. Aquat. Sci. **57**(Suppl. 2): 105–117.

Carpenter, S.R., Kitchell, J.F., and Hodgson, J.R. 1985. Cascading trophic interactions and lake productivity. Bioscience, **35**: 634–639.

Carpenter, S.R., Cole, J.J., Kitchell, J.F., and Pace, M.L. 1998. Impact of dissolved organic carbon, phosphorus, and grazing on phytoplankton biomass and production in experimental lakes. Limnol. Oceanogr. **43**: 73–80.

Currie, D.J., Dilworth-Christie, P., and Chapleau, F. 1999. Assessing the strength of top-down influences on plankton abundance in unmanipulated lakes. Can. J. Fish. Aquat. Sci. **56**: 427–436.

Filion, J.-M., Chain, P., and Futter, M. 1993. Cantilevering vertical tow nets to reduce tow-line-induced zooplankton avoidance. J. Plankton Res. **15**: 581–587.

Finlay, K., Beisner, B.E., and Barnett, A.J.D. 2007. The use of the Laser Optical Plankton Counter to measure zooplankton size, abundance, and biomass in small freshwater lakes. Limnol. Oceanogr. Methods, **5**: 41–49.

Gaedke, U. 1992. The size distribution of plankton biomass in a large lake and its seasonal variability. Limnol. Oceanogr. **37**: 1202–1220.

Gasol, J.M., Simons, A.M., and Kalff, J. 1995. Patterns in the top-down versus bottom-up regulation of heterotrophic nanoflagellates in temperate lakes. J. Plankton Res. **17**: 1879–1903.

© 2007 NRC Canada

Gerten, D., and Adrian, A.R. 2002. Species-specific changes in the phenology and peak abundance of freshwater copepods in response to warm summers. Freshw. Biol. **47**: 2163–2173.

Ghadouani, A., Pinel-Alloul, B., and Prepas, E.E. 2006. Could increased cyanobacterial biomass following forest harvesting cause a reduction in zooplankton body size structure? Can. J. Fish. Aquat. Sci. **63**: 2308–2317.

Gregory, R.S. 1998. Turbidity reduces predation on migrating juvenile pacific salmon. Trans. Am. Fish. Soc. **127**: 275–285.

Hanson, J.M., and Peters, R.H. 1984. Empirical prediction of crustacean zooplankton biomass and profundal macrobenthos biomass in lakes. Can. J. Fish. Aquat. Sci. **41**: 439–445.

Herman, A.W., Beanlands, B., and Phillips, E.F. 2004. The next generation of Optical Plankton Counter: the Laser OPC. J. Plankton Res. **26**: 1135–1145.

Hessen, D.O., Faafeng, B.A., and Anderson, T. 1995. Replacement of herbivore zooplankton species along gradients of ecosystem productivity and fish predation pressure. Can. J. Fish. Aquat. Sci. **52**: 733–742.

Hjelm, J., van de Weerd, G.H., and Sibbing, F.A. 2003. Functional link between foraging performance, functional morphology, and diet shift in roach (*Rutilus rutilus*). Can. J. Fish. Aquat. Sci. **60**: 700–709.

Hunter, M.D., and Price, P.W. 1992. Playing chutes and ladders: heterogeneity and the relative roles of bottom-up and top-down forces in natural communities. Ecology, **73**: 724–732.

Johannsson, O.E., Rudstam, L.G., and Lasenby, D.C. 1994. Assessment of metalimnetic feeding and implications for competition with fish in lakes Ontario and Michigan. Can. J. Fish. Aquat. Sci. **51**: 2591–2602.

Kajak, Z., and Rybak, T. 1979. The feeding of *Chaoborus flavicans* Meigen (Diptera, Chaoboridae) and its predation on lake zooplankton. Int. Rev. Hydrobiol. **64**: 361–378.

Mackay, N.A., Carpenter, S.R., Soranno, P.A., and Vanni, M.J. 1990. The impact of two *Chaoborus* species on a zooplankton community. Can. J. Zool. **68**: 981–985.

Magnan, P. 1988. Interactions between brook charr, *Salvelinus fontinalis*, and nonsalmonid species: ecological shift, morphological shift, and their impact on zooplankton communities. Can. J. Fish. Aquat. Sci. **45**: 999–1009.

Masson, S., Pinel-Alloul, B., and Smith, V.H. 2000. Total phosphorus–chlorophyll *a* size fraction relationships in southern Quebec lakes. Limnol. Oceanogr. **45**: 732–740.

McQueen, D.J., and Yan, N.D. 1993. Metering filtration efficiency of freshwater zooplankton hauls: reminders from the past. J. Plankton Res. **15**: 57–65.

McQueen, D.J., Post, J.R., and Mills, E.L. 1986. Trophic relationships in freshwater pelagic ecosystems. Can. J. Fish. Aquat. Sci. **43**: 1571–1581.

Moore, S.K., and Suthers, I.M. 2006. Evaluation and correction of subresolved particles by the Optical Plankton Counter in three Australian estuaries with pristine and highly modified catchments. J. Geophys. Res. **111**: C05S04.

Nero, R.W., and Sprules, W.G. 1986. Zooplankton species abundance and biomass in relation to occurrence of *Mysis relicta*. Can. J. Fish. Aquat. Sci. **43**: 420–434.

Olden, J.D., Jensen, O.P., and Vander Zanden, M.J. 2006. Implications of long-term dynamics of fish and zooplankton communities for among-lake comparisons. Can. J. Fish. Aquat. Sci. **63**: 1812–1821.

Omori, M., and Ikeda, T. 1984. Methods in marine zooplankton ecology. John Wiley and Sons, Inc., New York.

Patoine, A., Pinel-Alloul, B., and Prepas, E.E. 2002. Influence of catchment deforestation by logging and natural forest fires on crustacean community size structure in lakes of the Eastern Boreal Canadian forest. J. Plankton Res. **24**: 601–616.

Patoine, A., Pinel-Alloul, B., Méthot, G., and Leblanc, M.-J. 2006. Correspondence among methods of zooplankton biomass measurement in lakes: effect of community composition on optical plankton counter and size-fractionated data. J. Plankton Res. **28**: 695–705.

Peres-Neto, P.R., Legendre, P., Dray, S., and Borcard, D. 2006. Variation partitioning of species data matrices: estimation and comparison of fractions. Ecology, **87**: 2614–2625.

Pinel-Alloul, B., Niyonsenga, T., and Legendre, P. 1995. Spatial and environmental components of freshwater zooplankton structure. Ecoscience, **2**(1): 1–19.

Pinto-Coelho, R., Pinel-Alloul, B., Methot, G., and Havens, K.E. 2005. Crustacean zooplankton in lakes and reservoirs of temperate and tropical regions: variation with trophic status. Can. J. Fish. Aquat. Sci. **62**: 348–361.

Platt, T., and Denman, K. 1978. The structure of pelagic marine ecosystems. Rapp. P.-V. Reun. Cons. Int. Explor. Mer, **173**: 60–65.

Power, M.E. 1992. Top-down and bottom-up forces in food webs: do plants have primacy? Ecology, **73**: 733–746.

Prairie, Y.T., Bird, D.F., and Cole, J.J. 2002. The summer metabolic balance in the epilimnion of southeastern Quebec lakes. Limnol. Oceanogr. **47**: 316–321.

Ramcharan, C.W., Yan, N.D., McQueen, D.J., Perez-Fuentetaja, A., Demers, E., and Rusak, J.A. 2001. Complex responses of *Chaoborus* to changes in fish populations. Arch. Hydrobiol. Spec. Issues Adv. Limnol. **56**: 81–100.

Rodriguez, M.A., Magnan, P., and Lacasse, S. 1993. Fish species composition and lake abiotic variabiles in relation to the abundance and size structure of cladoceran zooplankton. Can. J. Fish. Aquat. Sci. **50**: 638–647.

Schindler, D.W. 1998. A dim future for boreal waters and landscapes. Bioscience, **48**: 157–164.

Sprules, W.G., and Goyke, A.P. 1994. Size-based structure and production in the pelagia of Lakes Ontario and Michigan. Can. J. Fish. Aquat. Sci. **51**: 2603–2611.

Sprules, W.G., and Munawar, M. 1986. Plankton size spectra in relation to ecosystem productivity, size, and perturbation. Can. J. Fish. Aquat. Sci. **43**: 1789–1794.

Steiner, C.F. 2004. *Daphnia* dominance and zooplankton community structure in fishless ponds. J. Plankton Res. **26**: 799–810.

Stemberger, R.S., and Lazorchak, M. 1994. Zooplankton assemblages responses to disturbance gradients. Can. J. Fish. Aquat. Sci. **51**: 2435–2447.

St-Onge, I., and Magnan, P. 2000. Impact of logging and natural fires on fish communities of Laurentian Shield lakes. Can. J. Fish. Aquat. Sci. **57**(Suppl. 2): 165–174.

ter Braak, C.J.F. 1990. Update notes: CANOCO version 3.10. Agricultural Mathematics Group, Wageningen, The Netherlands.

Tessier, A.J., and Horwitz, R.J. 1990. Influence of water chemistry on size structure of zooplankton assemblages. Can. J. Fish. Aquat. Sci. **47**: 1937–1943.

Tessier, A.J., and Welser, J. 1991. Cladoceran assemblages, seasonal succession and the importance of a hypolimnetic refuge. Freshw. Biol. **25**: 85–95.

Thiebaux, M.L., and Dickie, L.M. 1992. Models of aquatic biomass size spectra and the common structure of their solutions. J. Theor. Biol. **159**: 147–161.

Thiebaux, M.L., and Dickie, L.M. 1993. Structure of the body-size spectrum of the biomass in aquatic ecosystems: a consequence

© 2007 NRC Canada

of allometry in predator–prey interactions. Can. J. Fish. Aquat. Sci. **50**: 1308–1317.

Vidondo, B., Prairie, Y.T., Blanco, J.M., and Duarte, C.M. 1997. Some aspects of the analysis of size spectra in aquatic ecology. Limnol. Oceanogr. **42**: 184–192.

Wissel, B., Boeing, W.J., and Ramcharan, C.W. 2003. Effects of water color on predation regimes and zooplankton assemblages in freshwater lakes. Limnol. Oceanogr. **48**: 1965–1976.

Yan, N.D. 1986. Empirical prediction of crustacean zooplankton biomass in nutrient-poor Canadian Shield lakes. Can. J. Fish. Aquat. Sci. **43**: 788–796.

Yurista, P., Kelly, J.R., and Miller, S.E. 2006. Comparisons of zooplankton community size structure in the Great Lakes. J. Geophys. Res. **111**: C05S08.

Zhou, M. 2006. What determines the slope of a plankton biomass spectrum? J. Plankton Res. **28**: 437–448.

© 2007 NRC Canada

Rate of species introductions in the Great Lakes via ships' ballast water and sediments

John M. Drake and David M. Lodge

Abstract: We report results from a study of species in ballast tanks of ships entering the Great Lakes between 2000 and 2002. We collected 1349 individuals from at least 93 unique taxonomic groups, of which approximately half were identified to species. We estimated that the zooplankton assemblage in ballast water destined for the Great Lakes comprised from 200 to 1000 unique taxa consisting of both freshwater and marine species. Between 14 and 39 of these taxa have not yet been recorded from the Great Lakes. Further, 13.9% of individual specimens identified to the species level were from species not previously collected from the Great Lakes. We collected seven nonindigenous freshwater species not currently found in the Great Lakes: *Brachionus plicatilis*, *Cyclocypria kinkaidia*, *Maruenobiotus insignipes*, *Micnocyclops rubellus*, *Micnocyclops varicans*, *Neomysis awatchensis*, and *Paracyclops chiltoni*. We found no evidence that ship age, seasonal timing, or age of ballast water affected the abundance of individuals or species in the ballast tanks. To our knowledge, these are the first extrapolations of data from ballast water collections to estimate the rate of species introduction to any ecosystem.

Résumé : Nous présentons les résultats d'une étude des espèces trouvées dans les ballasts de navires qui ont pénétré dans les Grands Lacs entre 2000 et 2002. Nous avons récolté 1349 individus appartenant à au moins 93 groupes taxonomiques particuliers, dont environ la moitié ont pu être identifiés à l'espèce. Nous estimons que le peuplement de zooplancton dans l'eau de ballastage destinée aux Grands Lacs consiste en 200 à 1000 taxons particuliers, tant d'espèces d'eau douce que d'espèces marines. Entre 14 et 39 de ces taxons n'ont pas encore été signalés dans les Grands Lacs. De plus, 13,9 % des spécimens individuels identifiés à l'espèce appartiennent à des espèces non encore inventoriées dans les Grands Lacs. Nous avons récolté sept espèces non indigènes qui ne se retrouvent pas actuellement dans les Grands Lacs : *Brachionus plicatilis*, *Cyclocypria kinkaidia*, *Maruenobiotus insignipes*, *Micnocyclops rubellus*, *Micnocyclops varicans*, *Neomysis awatchensis* et *Paracyclops chiltoni*. Nous ne trouvons aucune indication que l'âge du navire, la saison de l'année et l'âge de l'eau de ballastage affectent l'abondance des individus ou des espèces dans les ballasts. À notre connaissance, il s'agit de la première fois que l'on extrapole des données de récoltes dans l'eau de ballastage dans le but d'estimer le taux d'introduction des espèces dans un écosystème.

[Traduit par la Rédaction]

Introduction

Invasive aquatic species are a leading environmental concern for freshwater ecosystems worldwide (Kolar and Lodge 2000; Rahel 2002; Simon and Townsend 2003). In the North American Great Lakes and other navigable freshwaters, ballast water discharged from ships is the primary source of nonindigenous, potentially invasive species (National Research Council 1996; Bailey et al. 2004). To develop environmental policy and monitor its effectiveness, a good understanding of several aspects of the invasion process is crucial, including historical and contemporary propagule pressures, the rate at which introduction results in successful establishment, and the relative importance of ballast water, residual sediments, and hull fouling as pathways associated with shipping. An especially important aspect is the rate at which new species (versus additional individuals of previously introduced same species) are introduced.

Introduction of species to the Great Lakes in ballast water has been studied previously, but the overall richness of species introductions has not been estimated. Early on, Locke et al. (1991, 1993) concluded that mid-ocean ballast water exchange reduced, but did not eliminate, the risk of species invasion from ballast water. Recent studies have confirmed that new species continue to be introduced (Duggan et al. 2005) and particularly that resting eggs of invertebrate species in residual ballast sediments may expose the Great Lakes to considerable invasion risk despite mid-ocean exchange (e.g., Bailey et al. 2003, 2005; Gray et al. 2005). Thus, for instance, Bailey et al. (2005) identified 21 nonindig-

Received 10 May 2006. Accepted 14 December 2006. Published on the NRC Research Press Web site at http://cjfas.nrc.ca on 12 April 2007.
J19315

J.M. Drake.[1,2] Department of Biological Sciences, University of Notre Dame, Notre Dame, IN 46556, USA, and National Center for Ecological Analysis and Synthesis, 735 State Street, Suite 300, Santa Barbara, CA 93101, USA.
D.M. Lodge. Department of Biological Sciences, University of Notre Dame, Notre Dame, IN 46556, USA.

[1]Corresponding author (e-mail: jdrake@uga.edu).
[2]Present address: Institute of Ecology, University of Georgia, 517 Bioscience Building, Athens, GA 30602, USA.

 doi:10.1139/F07-029 © 2007 NRC Canada

enous species of cladocera and rotifers from 39 ships entering the Great Lakes, and Gray et al. (2005) established that egg viability was not affected by exposure to high salinity (32 ppt) water, the presumed lethal step of exchange. It is possible, therefore, that mandatory mid-ocean ballast water exchange has been ineffective at reducing invasion rates in the Great Lakes (Holeck et al. 2004; Costello et al. 2007), though we believe that there is insufficient information to draw a conclusion either way (Drake et al. 2005; Costello et al. 2007). Thus, the present exposure of the Great Lakes to invasion risk is still largely unknown. Resolving these outstanding questions remains a high priority for research.

To estimate the rate of species introduction, we sampled ballast tanks of vessels entering the North American Great Lakes. We estimated both the total number of species in the ballast water pathway and the number of nonindigenous species. Unfortunately, it was not feasible to obtain a proper random sample of the total source assemblage, i.e., the aggregation of the multiple species pools from which species entrained in ballast water are drawn. However, by virtue of our sampling process, the sampled assemblage is a subset of the total source pool and our estimate can therefore be interpreted as a lower bound. Previous studies have suggested that features of particular shipping routes, patterns of discharge, or ship maintenance behaviors, including ship age, the timing of discharge, and the duration of the voyage, may affect the risk of invasion. Accordingly, we tested for effects of ship age on species richness and abundance of sampled organisms. We also tested for associations between the date of sampling and individual abundance (to look for effects of timing), and correlations between the age of ballast water and species richness. To conclude, we compare our results with studies conducted elsewhere, we contrast the relative risk of different pathways associated with shipping (primarily hull fouling), and we reflect on the implications of these findings for environmental policy and ballast water management.

Materials and methods

Sample collection

During December 2000 to August 2002, we sampled ballast tanks of 41 vessels entering the North American Great Lakes ($n_{2000} = 1$, $n_{2001} = 25$, $n_{2002} = 15$). Logistical obstacles precluded sampling according to a statistically designed survey, e.g., stratified random sampling. Rather, during the period of our study (December 2000 to August 2002), we obtained specimens from any accessible vessels we encountered. We sampled ballast water from 62 tanks and sediment from 41 tanks that had been emptied of ballast water. Approximate total residual ballast sediments and residual ballast water were estimated for each ship in consultation with the ship operator. In some cases, samples of water and sediment were obtained from the same tank when residual, unpumpable ballast water was retained after discharge. Water samples (20 L) were collected through sounding tubes using a modified inertial pump and filtered through a 63 µm mesh plankton net. Sediment samples (~1 L) were collected by hand with a shovel. Water samples were preserved with sugared formalin or 70% or 95% ethanol; sediment samples were preserved with 70% or 95% ethanol. To obtain a homogeneous subsample from the ethanol-saturated sediment, each sample was distributed to graduated cylinders and allowed to sit undisturbed for up to 2 days to allow particulate matter to settle. The ethanol supernatant was poured off and the remaining matter was homogenized to record the estimated weight. A subsample of 100, 200, or 250 mL was retained for analysis. The subsample was sieved through a stacked set of 250, 125, and 63 µm sieves using a sink sprayer and water to separate organisms, including resting stages, by size. Sediment and organisms were rinsed off the sieves into 50 mL sterile tubes using 95% ethanol. Samples containing an unidentified petroleum compound were soaked in butanol and washed through stacked sieves to remove the oil.

To extract organisms (including resting stages) from the sediment, the sieving process was repeated to remove any residual ethanol, and all material was rinsed into centrifuge tubes using distilled water. Ludox HS-40 colloidal silica (SiO_2; Aldrich 42-081-6) and a protocol modified from Burgess (2001) were used to separate and retain organic matter (Supplemental Appendix S1).[3] All organisms were then examined under a microscope; adults, juveniles, and resting eggs were picked out using a pipette or forceps and preserved in 95% ethanol. The remainder of this paper considers the species richness and abundance of organisms collected from these samples, excluding copepod nauplii and resting stages. Specimens were counted and identified to the lowest feasible taxonomic level ("unique taxa") using published keys (Supplemental Appendix S2).[3]

Statistical analysis

Several features of our sampling design bias our results so that our estimates are lower bounds on the species richness of the source pool. First, we never sampled all tanks from a ship or all ships from a particular source ecosystem, and moreover, the total duration of our study was relatively short (~2 years) so that our collection is some unknown fraction of the total source pool. Second, some microplankton (<63 µm) will not have been captured on our finest sieve. Third, we excluded resting eggs and copepod nauplii from species counts. Finally, not all collected individuals were identified to the species level; our designation of "unique taxa" most likely lumps some species. We conclude that our estimates should have a negative bias.

Ecologists have long used a variety of methods for estimating the species richness of a partially sampled assemblage (Chao 2004). Here we apply methods that are commonly used for biodiversity surveys to estimate the species richness of the source pool from which the species in our samples are drawn. Specifically, we estimated richness of unique taxa collected in each sample using the M_{th} incidence-based coverage estimator of Lee and Chao (1994). Like many nonparametric methods for estimating species richness, the incidence-based coverage estimator is based on

[3] Supplementary data for this article are available on the journal Web site (http://cjfas.nrc.ca) or may be purchased from the Depository of Unpublished Data, Document Delivery, CISTI, National Research Council Canada, Building M-55, 1200 Montreal Road, Ottawa, ON K1A 0R6, Canada. DUD 5151. For more information on obtaining material refer to http://cisti-icist.nrc-cnrc.gc.ca/irm/unpub_e.shtml.

© 2007 NRC Canada

Table 1. Nonindigenous animal species collected from ships entering the Great Lakes.

Phylum	Class	Order	Family	Genus	Species	Sample	Abundance
Rotifera	Monogononta	Ploima	Brachionidae	*Brachionus*	*plicatilis*†	w	1
Arthropoda	Branchiopoda	Cladocera	Bosminidae	*Bosmina*	*coregoni**†	w	66
Arthropoda	Ostracoda	Podocopida	Cyprididae	*Cyclocypria*	*kinkaidia*†	s	5
Arthropoda	Maxillopoda	Calanoida	Centropagidae	*Centropages*	*furcatus*	w	1
Arthropoda	Maxillopoda	Harpacticoida	Ectinosomatidae	*Microsetella*	*norvegica*	w	12
Arthropoda	Maxillopoda	Harpacticoida	Harpacticidae	*Harpacticus*	*chelifer*	s	2
Arthropoda	Maxillopoda	Poecilostomatoida	Oncaeidae	*Oncaea*	*mediterranea*	w	1
Arthropoda	Maxillopoda	Poecilostomatoida	Corycaeidae	*Farranula*	*carinata*	s	3
Arthropoda	Maxillopoda	Cyclopoida	Cyclopidae	*Cyclops*	*strenuus**†	w	1
Arthropoda	Maxillopoda	Cyclopoida	Cyclopidae	*Megacyclops*	*viridis**†	s	15
Arthropoda	Maxillopoda	Cyclopoida	Cyclopidae	*Microcyclops*	*varicans*†	w	58
Arthropoda	Maxillopoda	Cyclopoida	Oithonidae	*Oithona*	*robusta*	w	2
Arthropoda	Malacostraca	Mysida	Mysidae	*Neomysis*	*awatchensis*†	s	1
Arthropoda	Maxillopoda	Cyclopoida	Cyclopidae	*Microcyclops*	*rubellus*†	ws	2
Arthropoda	Maxillopoda	Cyclopoida	Cyclopidae	*Paracyclops*	*chiltoni*†	s	6
Arthropoda	Maxillopoda	Harpacticoida	Ameiridae	*Nitokra*	*hibernica**†	w	1
Arthropoda	Maxillopoda	Harpacticoida	Canthocamptidae	*Maraenobiotus*	*insignipes*†	w	1

Note: Sample: s, sediment; w, water.
*Already established in the Great Lakes.
†Known to tolerate freshwater environments.

an analogy between species richness estimation and capture–recapture estimation of population size: capture probability in the capture–recapture model corresponds to species detection probability in richness estimation, i.e., the chance that at least one individual of a given species will appear in the sample. Thus, this estimator allows that detection probability differs both among species and among samples. Following Chao and Shen (2005), we used cutoff parameter $k = 10$. This procedure obtains an estimate of species richness that is greater than the estimate obtained from the more familiar Chao2 estimator (Chao 1987), which is regarded as a lower bound (Chao and Shen 2005). As the estimated coefficient of variation in the infrequent class typically exceeded 0.8, we used the modified M_{th} estimator (i.e., $M_{th,1}$ in the notation of Chao and Shen 2005) in which the estimated sample coverage for the infrequent class is given by the formula of Shen (2003) for highly heterogeneous data (as referenced in Chao and Shen 2005). The quantity estimated with these methods is the richness of the total sampled assemblage, including species indigenous to the Great Lakes and species nonindigenous to the Great Lakes but already established.

For nonindigenous species, the number of taxa actually collected in any sample was too small to use the incidence-based coverage estimator. We therefore combined species from all samples to obtain a species-abundance distribution restricted to just nonindigenous species. Then, we estimated the total richness of this source assemblage using the Chao1 estimator (Chao 1984). The Chao1 estimator is based on the idea that rare species contain most of the information about species richness. This can be considered as a lower bound (Chao 2004) but has also been justified as a point estimate for extremely heterogeneous cases (i.e., like ours) under the assumption that species appearing only once in the sample have the same relative abundance in the assemblage (Shen et al. 2003). All calculations were performed using SPADE v2.1 (Chao and Shen 2005).

To test the hypothesis that older ships pose greater risk of invasion, we fit linear mixed models of total abundance of individuals (after $\log_{10}$ transformation) and species richness in each tank sampled to ship age using ship as a hierarchical grouping variable. Separate models were estimated for samples collected from ballast water versus samples collected from sediments. Mixed models are appropriate for fitting hierarchical data such as these, where abundance and species richness were measured independently for each tank but where tanks belong to the same ship and therefore were also built at the same time (Venables and Ripley 2002).

To test for an effect of seasonal timing on invasion risk (as found for diatoms and dinoflagellates by Zhang and Dickman (1999)), we performed linear regression using total individual abundance as the dependent variable and Julian date as the independent variable.

Chu et al. (1997) and Wonham et al. (2001) also found that the age of ballast water (ranging from 1 day to 1 year in the observational study of Chu et al. (1997) and from 1 day to 17 days in the experimental study of Wonham et al. (2001)) was a significant predictor of diatom and dinoflagellate species richness. We tested for an effect of ballast water age on species richness in ballast water samples using nonparametric correlation. Ballast water age was calculated as the time difference, rounded to the nearest day, between ballast water uptake (recorded in ship log and reported to us when samples were collected) and sampling.

Results

Taxonomic identification

We collected 73 unique taxa from water samples and 34 unique taxa from sediment samples for a total of 97 unique taxa overall (Supplemental Appendix S3)[3]. Of these, 33 were identified to the species level, of which 17 species are not native to the Great Lakes and 13 are not presently found in the Great Lakes (Table 1). Overall, 695 of 1349 (51.5%) individuals were identified to species. Of these, 95 (13.7%) belonged to the 13 species in Table 1 not yet established in the Great Lakes. The majority of ships sampled in our study

© 2007 NRC Canada

Fig. 1. Origins of ships sampled in this study by last port of call (squares) and last ballasting (circles).

Fig. 2. Frequency histogram of the total ballast capacity of ships surveyed in this study.

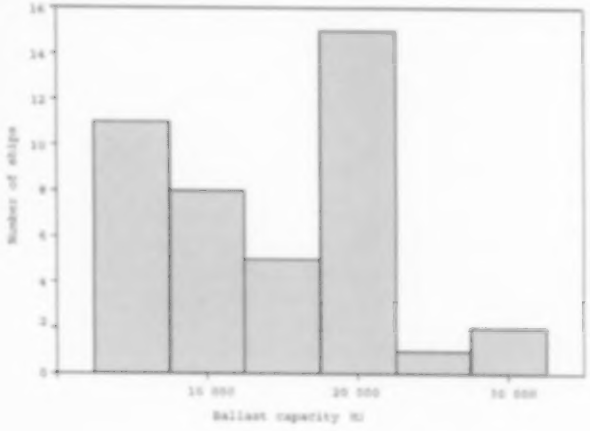

Fig. 3. Residual (unpumpable) ballast in 16 ships declaring no ballast on board (NOBOB) surveyed in this study.

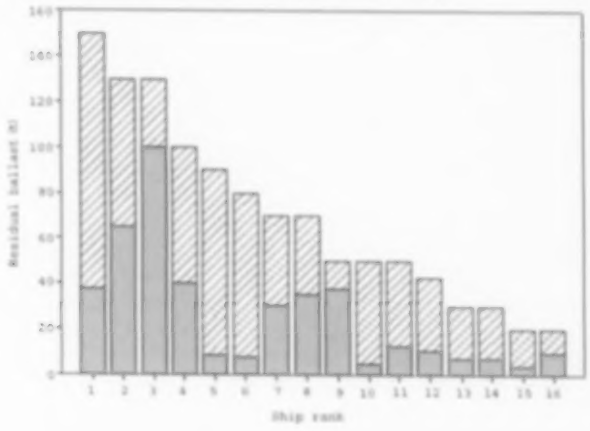

last called on ports in North America (n = 20) or Europe (n = 18, including one ship calling on the port of Gemlik in Turkey), with fewer ships coming from South America (n = 3) and southeast Asia (n = 2; last port of call not documented for two vessels; Fig. 1). These ships represented total ballast capacities ranging from 1.5×10^3 to 2.6×10^4 tonnes (t) (Fig. 2). Estimates of residual ballast ranged over an order of magnitude for ships for which this information was available (Fig. 3).

Species richness

The rank-abundance histogram for all collected specimens is fat-tailed (Fig. 4*a*), with most taxa represented by only one or two individuals. The estimated number of unique taxa in ballast water was 536 (95% confidence interval (CI) [222, 1510]), whereas the estimated number of unique taxa in residual sediments was 105 (95% CI [50, 357]). The estimated richness of the total sampled assemblage (obtained by pooling water and sediment samples) was 461 (95% CI [235, 1056]). We also estimated the richness of the total sampled assemblage pooling samples within ships obtaining an estimate of 465 (95% CI [237, 1064]). The agreement between these last two estimates suggests that intertank differences contribute relatively little to overall heterogeneity. The corresponding estimates obtained using the Chao2 estimator (i.e., providing a lower bound) were 250 unique taxa in ballast water (95% CI [149, 486]), 66 unique taxa in residual sediment (95% CI [44, 134]), 231 by pooling samples (95% CI [164, 368]), and 238 by pooling within ships (95% CI [167, 380]).

© 2007 NRC Canada

Fig. 4. (*a*) Rank abundance histogram of unique taxonomic groups collected in this study, pooled across samples. Nearly half of taxonomic groups sampled were represented by a single specimen, indicating that the population from which these species were sampled has high diversity. (*b*) Rank abundance histogram of the nonindigenous species not previously established in the Great Lakes, pooled across samples.

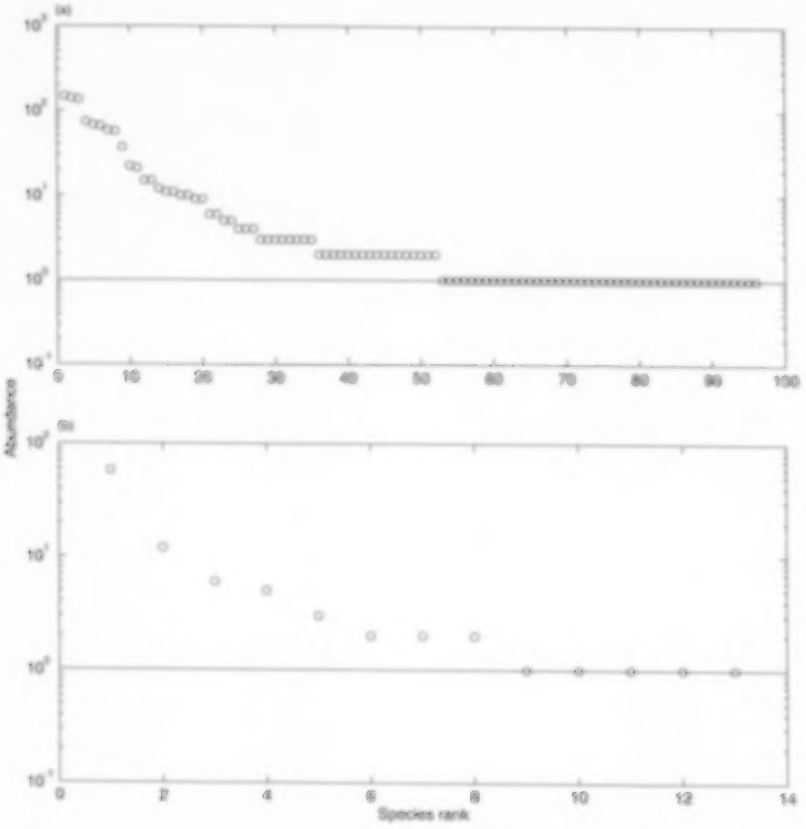

The rank-abundance histogram for nonindigenous species was also fat-tailed (Fig. 4*b*), with 5 out of 13 (38.5%) species represented by a single individual and 8 out of 13 (61.5%) represented by only one or two individuals. The estimated species richness of this potentially invasive assemblage is 17.2 (95% CI [13.7, 38.8]).

Ship age was not a significant predictor of individual abundance (Figs. 5*a*, 5*b*) in water ($p = 0.189$) or sediments ($p = 0.341$) or of observed species richness (Figs. 5*c*, 5*d*) in water ($p = 0.872$) or sediments ($p = 0.433$). There was no evidence that total abundance of individuals ($\log_{10}$-transformed) was related to Julian date (Fig. 6) in either water ($p = 0.496$, $R^2 < 0.018$) or sediments ($p = 0.921$, $R^2 < 0.001$). Ballast water in our samples ranged in age from 15 days to 98 days with a median of 33 days. Correlations between the age of ballast water and species richness were weak (Spearman's ρ, –0.22; Kendall's τ, –0.16) and not statistically significant ($p_{Spearman} = 0.22$, $p_{Kendall} = 0.20$).

Discussion

Despite policy requiring mid-ocean exchange of ballast water, nonindigenous species continue to be introduced to the Great Lakes through ballast water discharge. Using a new data set, we estimated that the size of the potentially invasive assemblage during the years 2000–2002 was at least 17 unique taxa. This is only a small fraction of the source pool, the remainder of which is indigenous to the Great Lakes or comprises nonindigenous species already established in the Great Lakes.

We believe that our sampling and analytical protocols are conservative, so that our estimate of source pool species richness represents a lower bound. Four sources of probable error bias our estimates in this direction. First, because the source pool is stratified by ships, the subset of the assemblage actually sampled is probably a subset of the total assemblage. Second, many protists, algae, and other microorganisms would have escaped our finest mesh size (63 µm), and with the exception of two protists (Supplemental Appendix S3),[3] we did not attempt to identify those that were captured. Third, as in previous studies (Bailey et al. 2005), animal resting stages were numerous in many samples, some of which may have represented additional species. (We did not attempt to identify plant seeds.) Fourth, even for those taxa for which we sought identification, we were not always able to identify specimens to the species level. Thus, our designation "unique taxa" probably groups species and is a minimal estimate of the number of true species. Each of

© 2007 NRC Canada

Fig. 5. Relationship between density and species richness in samples collected from ballast tanks and the age of the ship.

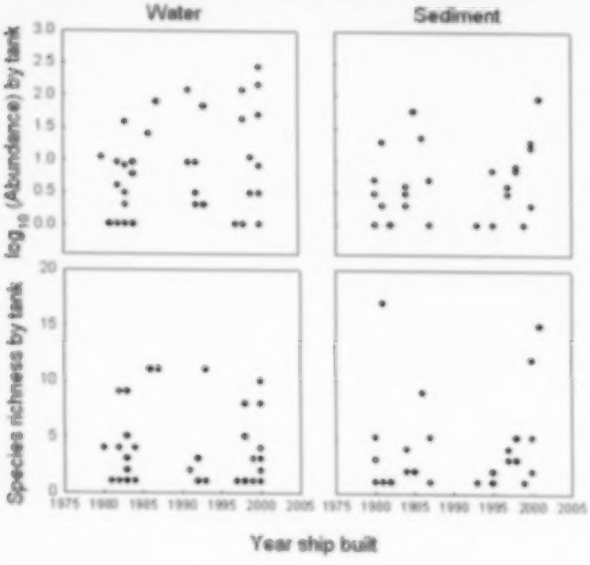

Fig. 6. Seasonal pattern in the density of organisms in samples collected from (*a*) residual ballast sediments and (*b*) ballast water.

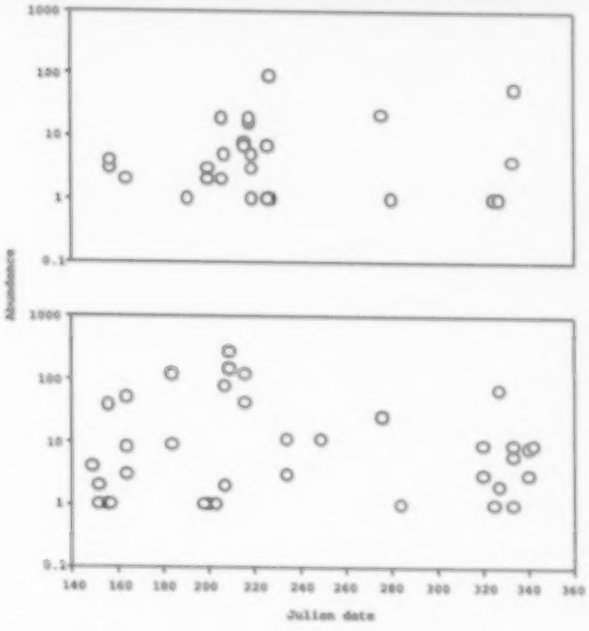

these sources of bias underestimates the species richness of the total source pool.

Only one obvious source of bias in our methods runs in the opposite direction: as in previous studies, our samples were taken from the assemblage held in a ballast tank, not from actually discharged ballast water. To our knowledge, no direct comparisons exist between what taxa exist in ballast tanks and what taxa are discharged, though it is plausible that some species collected from ballast tanks would not be discharged, particularly meiofauna and nonplanktonic fouling organisms. However, we observe that of the 97 unique taxa we collected, only 24 were obtained only from sediment samples (Supplemental Appendix S3),[3] and of these, very few are restricted to meiofaunal habitats. Ostracods in particular were overrepresented in sediment samples, with only two out of nine taxa collected from the water. Of the 13 potentially invasive species sampled, only four were collected exclusively from sediments. The extent to which species collected from ballast tanks are representative of discharged species therefore remains an open question. Unfortunately, the practical difficulties of obtaining samples of discharged ballast water are large. We suspect that this potential bias in the direction of overestimating the source pool is outweighed by the aggregate of the four conservative biases listed above. Thus we suggest that our estimates should be regarded as a lower bound.

Our findings are comparable to those of previous studies in terms of species richness but different in terms of species identity. Whereas Locke et al. (1993) collected four nonindigenous, not previously established, freshwater species (*Acanthocyclops americanus*, *Acanthocyclops robustus*, *Bosmina hagmani*, and *Daphnia rosea*) from 86 vessels entering the Great Lakes during the year 1990, we collected seven species that met the same criteria in specimens collected from 41 ships over approximately 2 years. By contrast, collections from 105 vessels entering the Great Lakes in 1995 contained no nonindigenous freshwater organisms (Aquatic Sciences Inc. 1996). Finally, the most comparable reported study, by Duggan et al. (2005), was performed during the same years. Indeed, because both studies contracted the same consultant, we probably sampled some of the same ships. Excluding nematodes (for which Duggan et al. (2005) provide much more detail, they found 48 unique taxa), both studies found about the same number of species. However, excluding species already established, both studies obtained entirely disjoint sets of copepods and cladocera. In the study of Duggan et al. (2005), all but one of these species were collected only from one ship. Our results taken together with those of Duggan et al. (2005) imply that the assemblage of species introduced in ballast water is extremely heterogeneous across ships and over time. It is unlikely, therefore, that species introduction to the Great Lakes is saturated, i.e., that all species likely to establish have already been introduced at one time or another. Thus, the number of identified nonindigenous species is probably quite small compared with the total number of species introduced.

We emphasize that not all potentially invasive species will be sampled, which is why we estimated the richness of the total source pool using a statistical model. In contrast to previous studies, our estimate of the total source pool includes both marine and freshwater species. Overall, 11 out of 17 nonindigenous species (64.7%) are known to tolerate fresh waters. We remark that many marine species are euryhaline and relatively little is known about the freshwater tolerances of marine zooplankton. Notably, one recent study found that viability of diapausing eggs of oligohaline species was largely unaffected by exposure to salt water (Gray et al. 2005), and to a lesser extent, wide tolerances may extend to adult stages of some taxa. Consequently, we contend that invasion risk by marine species should not be discounted on

© 2007 NRC Canada

the basis of a lack of information as too little is known about the environmental tolerances of most zooplankton.

The nonindigenous freshwater species collected by Locke et al. (1991, 1993) and those reported here are entirely different: we collected no nonindigenous species collected by Locke and colleagues and they collected no species collected by us. Whether the source pool changed over time or whether these studies represent different subsets of a constant source pool is unknown. This is an important question for research. If the source pool is changing, then the rate of new invasions is not expected to decline over time. Indeed, it could even rise as connections are made to new source pools. The rate at which introductions have been discovered has been relatively constant over the past two decades (Drake et al. 2005; Costello et al. 2007). If we consider the rate of invasion to be the ratio of species discovered to the total source pool, the size of the total source pool would matter very much for estimating invasion rates and therefore also for estimating the effectiveness of mid-ocean ballast water exchange. Supposing species have established at approximately the rate of 0.92 per year (cf. Drake et al. 2005) and approximating the duration of our study as 2 years, we then roughly estimate the base rate of establishment at $(0.92 \times 2/17.2) = 11\%$.

This is the first study to extrapolate from the observed number of taxa in ballast to estimate the unobserved richness of the total source pool. Here we compare the number of observed taxa in our study with numbers reported from comparable studies. The number of unique taxa we observed is consistent with the range of species richness of ballast water collections from other ecosystems. Chu et al. (1997) collected 81 species (representing eight animal phyla and five protist phyla) from five container ships entering Hong Kong during 1994 and 1995. A collection of ballast water, sediment, and hull-fouling samples collected from 186 vessels in German waters during the years 1992–1996 obtained 257 different species (Gollasch 2002). Of these, 98 species were obtained from water samples and 110 species were obtained from sediment samples. Thus, whereas nearly twice as many species were represented in our water samples compared with our sediment samples, in the German study more species were collected from sediment than water. Finally, Carlton and Geller (1993) collected 230 zooplankton species from water samples taken from 159 vessels arriving in Coos Bay, Oregon. At the high end, Wonham et al. (2001) collected at least 44 zooplankton species in a single ship over the course of a 16-day voyage. Thus, accounting for differences in sampling intensity and level of taxonomic identification, it appears that the species richness in these studies are of the same order (at most a couple of hundreds) as reported here for the Great Lakes.

Discharged ballast water is only one source of aquatic nonindigenous species, even when only the shipping pathway is considered. Recent studies of biofouling communities on the exterior surfaces of ships have demonstrated that these are a large potential source of biological propagules (Fofonoff et al. 2003; Minchin and Gollasch 2003; Coutts and Taylor 2004), and recent experimental studies have shown that the primary nontributyltin methods for controlling fouling (antifouling paint and manual cleaning) are relatively ineffective (Floerl et al. 2005). The accumulating evidence suggests that biofouling may be an even greater source of species in higher abundances than ballast water discharge. For instance, of the 257 species collected by Gollasch (2002), 110 (42.8%) were collected from fouling communities. In a parallel study, we collected 74 unique taxa from the hull of a single vessel entering the Great Lakes, almost equal to the total number of unique taxa reported here for all ships and greater than the number of species collected by Wonham et al. (2001) discussed above (J.M. Drake and D.M. Lodge, unpublished data).

Even if the hull-fouling component of ship-mediated invasions is ignored, effectively managing risk of invasion from ballast water discharge continues to challenge policymakers at global (Endresen et al. 2004; Firestone and Corbett 2005) and regional (Bailey et al. 2004) levels. Endresen et al. (2004) estimated that the annual global volume of discharged ballast water is approximately 3.5×10^9 tonnes. Given typical densities of zooplankton in ballast water of thousands to tens of thousands·m^{-3} (Minton et al. 2005), this represents the relocation of probably trillions of individual organisms worldwide annually. Ballast water discharge has also been the most important source of introduced species in the Great Lakes, accounting for 46 out of 71 (64.8%) nonindigenous species reported since 1959, when the St. Lawrence Seaway was opened to give transoceanic vessels inland access (Bailey et al. 2004). Despite a voluntary ballast water management plan implemented in Canada in 1989 (Niimi and Reid 2003) and increasingly stringent policies for reducing invasions in the Great Lakes introduced throughout the 1990s (Cangelosi 2002), no reduction in the rate of invasion has yet been detected (Ricciardi 2001; Bailey et al. 2004; Holeck et al. 2004). Reasons why mid-ocean ballast water exchange might be ineffective include incomplete exchange, high salinity tolerance of particular species, and that the majority of ships entering the Great Lakes are declared "no ballast on board" (NOBOB) and are therefore unregulated (Niimi and Reid 2003; Bailey et al. 2004). Accordingly, further development of domestic policy and regional agreements will be required to protect the Great Lakes (Cangelosi 2004). A future study repeating these methods would constitute a test of whether newly enforced salinity tests of every vessel entering the lakes will lead to reductions of potentially invasive species in ballast tanks.

The mechanisms reviewed above by which nonindigenous species survive efforts aimed at reducing invasion in the Great Lakes will likely diminish the effectiveness of other policies too. The recent International Convention on the Control and Management of Ships Ballast Water and Sediment focuses on water quality standards and is therefore a promising instrument for controlling invasion risk. However, it remains to be seen whether the flexibility of the convention compromises its effectiveness by serving neither as a "ceiling nor a floor for port-state action" (Cangelosi 2004) or if its relationship to the United Nations Convention on the Law of the Sea can in fact be leveraged to increase its global reach and applicability (Firestone and Corbett 2005). In either case, we believe the convention should represent only one instrument in a broader toolbox that includes increased monitoring, research, and development, private investment in technologies for ballast water treatment, capacity for rapid response to introduced species once they are detected, and a

© 2007 NRC Canada

range of domestic policies and regional and international agreements that scale with the legal, economic, and social dimensions in which species introductions occur.

Acknowledgements

Philip Jenkins and Aquatic Sciences Incorporated sampled the ships. Rachel Schwartz processed the samples. Taxonomic identification was performed through a contract with Dr. James Vancil (Knoxville, Tenn., USA). Funding was provided by EPA STAR (to DML), the Great Lakes Fisheries Commission (to DML), the NSF-funded (DEB 02-13698) Integrated Systems for Invasive Species project (to DML), a National Center for Ecological Analysis and Synthesis (NCEAS) Sabbatical Fellowship (to DML), and an EPA STAR Graduate Research Fellowship (to JMD). This paper was written while Drake was a Postdoctoral Associate at the NCEAS, a center funded by NSF (DEB-0072909), the University of California, and the Santa Barbara campus. Although the research described in this article has been funded in part by the US Environmental Protection Agency through a STAR grant / cooperative agreement to DML, it has not been subjected to the Agency's peer and policy review and, therefore, does not necessarily reflect the views of the Agency and no official endorsement should be inferred.

References

Aquatic Sciences, Inc. 1996. Examination of aquatic nuisance species introductions to the Great Lakes through commercial shipping ballast water and assessment of control options. Final Report. Aquatic Science, Inc., St. Catharines, Ontario, Canada.

Bailey, S.A., Duggan, I.C., van Overdijk, C.D.A., Jenkins, P.T., and MacIsaac, H.J. 2003. Viability of invertebrate diapausing eggs collected from residual ballast sediment. Limnol. Oceanogr. **48**: 1701–1710.

Bailey, S.A., Reid, D.F., Colautti, R.I., Therriault, T., and MacIsaac, H. 2004. Management options for control of nonindigenous species in the Great Lakes. Tol. J. Great Lakes L. Sci. Pol. **5**: 101–112.

Bailey, S.A., Duggan, I.C., Jenkins, P.T., and MacIsaac, H.J. 2005. Invertebrate resting stages in residual ballast sediment of transoceanic ships. Can. J. Fish. Aquat. Sci. **62**: 1090–1103.

Burgess, R. 2001. An improved protocol for separating meiofauna from sediments using colloidal silica sols. Mar. Ecol. Prog. Ser. **214**: 161–165.

Cangelosi, A. 2002. Blocking invasive aquatic species. *In* Issues in Science and Technology, Winter 2002–2003. The University of Texas at Dallas, Richardson, TX 75083-0688. pp. 69–74.

Cangelosi, A. 2004. Invasive species: global treaty is not enough. NE-MW Economic Review, Spring 2004. Northeast Midwest Institute, Washington, DC 20003. pp. 8–11.

Carlton, J.T., and Geller, J.B. 1993. Ecological roulette: the global transport of nonindigenous marine organisms. Science (Washington, D.C.), **261**: 78–82.

Chao, A. 1984. Nonparametric estimation of the number of classes in a population. Scand. J. Stat. **11**: 265–270.

Chao, A. 1987. Estimating the population size for capture–recapture data with unequal catchability. Biometrics, **43**: 783–791.

Chao, A. 2004. Species richness estimation. *In* Encyclopedia of statistical sciences. 2nd ed. *Edited by* N. Balakrishnan, C.B. Read, and B. Vidakovic. Wiley, New York.

Chao, A., and Shen, T.-J. 2005. Program SPADE (Species Prediction And Diversity Estimation). Program and User's Guide published at http://chao.stat.nthu.edu.tw.

Chu, K.H., Tam, P.F., Fung, C.H., and Chen, Q.C. 1997. A biological survey of ballast water in container ships entering Hong Kong. Hydrobiologia, **352**: 201–206.

Costello, C., Drake, J.M., and Lodge, D.M. 2007. Evaluating the effectiveness of an environmental policy: ballast water exchange and invasive species in the North American Great Lakes. Ecol. Appl. In press.

Coutts, A.D.M., and Taylor, M.D. 2004. A preliminary investigation of biosecurity risks associated with biofouling on merchant vessels in New Zealand. N.Z. J. Mar. Freshw. Res. **38**: 215–229.

Drake, J.M., Costello, C., and Lodge, D.M. 2005. When did the discovery rate for invasive species in the North American Great Lakes accelerate? Bioscience, **55**: 4.

Duggan, I.C., van Overdijk, C.D.A., Bailey, S.A., Jenkins, P.T., Limén, H., and MacIsaac, H.J. 2005. Invertebrates associated with residual ballast water and sediments of cargo carrying ships entering the Great Lakes. Can. J. Fish. Aquat. Sci. **62**: 2463–2474.

Endresen, Ø., Behrens, H.L., Bymestad, S., Andersen, A.B., and Skjong, R. 2004. Challenges in global ballast water management. Mar. Poll. Bull. **48**: 615–623.

Firestone, J., and Corbett, J.J. 2005. Coastal and port environments: international legal and policy responses to reduce ballast water and introductions of potentially invasive species. Ocean Development & International Law, **36**: 291–316.

Floerl., O., Inglis, G.J., and Marsh, H.M. 2005. Selectivity in vector management: an investigation of the effectiveness of measures used to prevent transport on non-indigenous species. Biol. Invasions, **7**: 459–475.

Fofonoff, P.W., Ruiz, G.M., Steves, B., and Carlton, J.T. 2003. In ships or on ships? Mechanisms of transfer and invasion for nonnative species to the coasts of North America. *In* Invasive species: vectors and management strategies. *Edited by* G.M. Ruiz and J.T. Carlton. Island Press, Washington, D.C. pp. 152–182.

Gollasch, S. 2002. The importance of ship hull fouling as a vector of species introductions into the North Sea. Biofouling, **18**: 105–121.

Gray, D.K., Bailey, S.A., Duggan, I.C., and MacIsaac, H.J. 2005. Viability of invertebrate diapausing eggs exposed to saltwater: implications for Great Lakes' ship ballast management. Biol. Invasions, **7**: 531–539.

Holeck, K.T., Mills, E.L., MacIsaac, H.J., Dochoda, M.R., Colautti, R.I., and Ricciardi, A. 2004. Bridging troubled waters: biological invasions, transoceanic shipping, and the Laurentian Great Lakes. Bioscience, **54**: 919–929.

Kolar, C.S., and Lodge, D.M. 2000. Freshwater nonindigenous species: interactions with other global changes. *In* Invasive species in a changing world. *Edited by* H.A. Mooney and R.J. Hobbs. Island Press, Washington, D.C. pp. 3–30.

Lee, S.-M., and Chao, A. 1994. Estimating population size via sample coverage for closed capture–recapture models. Biometrics, **50**: 88–97.

Locke, A., Reid, D.M., Sprules, W.G., Carlton, J.T., and van Leeuwen, H.C. 1991. Effectiveness of mid-ocean exchange in controlling freshwater and coastal zooplankton in ballast water. Can. Tech. Rep. Fish. Aquat. Sci. No. 1822.

Locke, A., Reid, D.M., van Leeuwen, H.C., Sprules, W.G., and Carlton, J.T. 1993. Ballast water exchange as a means of controlling dispersal of freshwater organisms by ships. Can. J. Fish. Aquat. Sci. **50**: 2086–2093.

Minchin, D., and Gollasch, S. 2003. Fouling and ships' hulls: how changing circumstances and spawning events may result in the spread of exotic species. Biofouling, **19**(Suppl.): 111–122.

© 2007 NRC Canada

Minton, M.S., Verling, E., Miller, A.W., and Ruiz, G.M. 2005. Reducing propagule supply and coastal invasions via ships: effects of emerging strategies. Front. Ecol. Env. **3**: 304–308.

National Research Council. 1996. Stemming the tide: controlling introductions of nonindigenous species by ships' ballast water. National Academy of Sciences, Washington, D.C.

Niimi, A.J., and Reid, D.M. 2003. Low salinity residual ballast discharge and exotic species introductions to the North American Great Lakes. Mar. Poll. Bull. **46**: 1334–1340.

Rahel, F.J. 2002. Homogenization of freshwater faunas. Annu. Rev. Ecol. Syst. **33**: 291–315.

Ricciardi, A. 2001. Facilitative interactions among aquatic invaders: is an "invasional meltdown" occurring in the Great Lakes? Can. J. Fish. Aquat. Sci. **58**: 2513–2525.

Shen, T.-J. 2003. Prediction of biodiversity. Ph.D. dissertation, National Tsing-Hua University, Hsin-Chu, Taiwan.

Shen, T.-J., Chao, A., and Lin, C.-F. 2003. Predicting the number of new species in further taxonomic sampling. Ecology, **84**: 798–804.

Simon, K.S., and Townsend, C.R. 2003. Impacts of freshwater invaders at different levels of ecological organisation, with emphasis on salmonids and ecosystem consequences. Freshw. Biol. **48**: 982–994.

Venables, W.N., and Ripley, B.D. 2002. Modern applied statistics with S. 4th ed. Springer-Verlag, New York.

Wonham, M.J., Walton, W.C., Ruiz, G.M., Frese, A.M., and Galil, B.S. 2001. Going to the source: role of the invasion pathway in determining potential invaders. Mar. Ecol. Prog. Ser. **215**: 1–12.

Zhang, F., and Dickman, M. 1999. Mid-ocean exchange of container vessel ballast water. 1. Seasonal factors affecting the transport of harmful diatoms and dinoflagellates. Mar. Ecol. Prog. Ser. **176**: 243–251.

© 2007 NRC Canada

Characterization of stage-classified biological processes using multinomial models: a case study of anchovy (*Engraulis encrasicolus*) eggs in the Bay of Biscay

Leire Ibaibarriaga, Miguel Bernal, Lorenzo Motos, Andrés Uriarte, David L. Borchers, Mike E. Lonergan, and Simon N. Wood

Abstract: This paper describes how multinomial models can be used to study developmental rates of biological processes and how these are affected by different factors such as temperature or parental effects. First, the most common multinomial models for ordinal categorical data (namely, proportional odds, continuation-ratio, and extended continuation-ratio models) are described within the particular framework of developmental rates for discrete and ordered stage classified biological processes. Then, the extraction from the fitted models of a series of biologically meaningful parameters is proposed. In particular, maximum probable age and several alternative definitions for stage duration are presented and pros and cons of each of them are discussed. As an example, the methodology is applied to analyze the temperature dependent development of anchovy (*Engraulis encrasicolus*) eggs in the Bay of Biscay.

Résumé : Nous décrivons comment les modèles multinomiaux peuvent servir à étudier les taux de développement des processus biologiques et comment ces derniers peuvent être affectés par divers facteurs, tels que la température et les effets parentaux. Nous décrivons d'abord les modèles multinomiaux le plus couramment utilisés pour les données catégorielles ordinales (c'est-à-dire, les modèles de cotes proportionnelles, de rapport de continuité et de rapport de continuité étendu) dans le cadre particulier des taux de développement des processus biologiques discrets et ordonnés par classes de stades. Nous proposons ensuite l'extraction d'une série de paramètres d'intérêt biologique de ces modèles ajustés. Nous présentons, en particulier, l'âge maximal probable et plusieurs définitions de rechange de la durée des stades et nous discutons des avantages et des désavantages de chacun des paramètres. Comme illustration, nous utilisons notre méthodologie pour analyser le développement des oeufs des anchois (*Engraulis encrasicolus*) du golfe de Gascogne qui est sous le contrôle de la température.

[Traduit par la Rédaction]

Introduction

Biological developmental processes are usually characterized in terms of a series of ordered stages or categories based on morphological features. For those processes, one of the major interests for scientists is to study developmental rates and how these might be affected by different factors (e.g., temperature, salinity, parental effects, or food availability). There are many examples of biological processes in which the continuous changes that happen during development are classified in discrete stages using morphological or other biological characteristics: the life cycle of copepod species is classified in stages based on morphological characteristics of the individual (McLaren et al. 1987; Miller and Tande 1993; Mauchline 1998); development of fish eggs is classified in stages according to cell divisions or morphological properties of the embryo (Russell 1976; Ahlstrom and Moser 1980; Moser and Ahlstrom 1985); fish larvae are classified depending on mouth opening, yolk sac size, eye pigmentation, etc. (Lasker 1981; Chambers and Tripple

Received 9 February 2006. Accepted 13 December 2006. Published on the NRC Research Press Web site at http://cjfas.nrc.ca on 17 April 2007.
J19162

L. Ibaibarriaga,[1] **L. Motos, and A. Uriarte.** AZTI-Tecnalia, Marine Research Unit, Herrera Kaia Portualdea z/g, 20110, Pasaia, Basque Country, Spain.
M. Bernal. Instituto Español de Oceanografía (IEO), Estación Pesquera de Cádiz, Centro Andaluz de Ciencia y tecnología (CACYTMAR), República Saharaui s/n, Campus Río San Pedro, 11510, Puerto Real, Cádiz, Spain.
D.L. Borchers. Research Unit for Wildlife Population Assessment (RUWPA), University of St. Andrews, The Observatory, Buchanan Gardens, St. Andrews, Fife, KY16 9LZ, Scotland, United Kingdom.
M.E. Lonergan. Sea Mammal Research Unit (SMRU), Gatty Marine Research Institute, University of St. Andrews, St. Andrews, Fife, KY16 8LB, Scotland, United Kingdom.
S.N. Wood. Mathematical Sciences, University of Bath, Bath, BA27AY, United Kingdom.

[1]Corresponding author (e-mail: libaibarriaga@pas.azti.es).

 doi:10.1139/F07-030 © 2007 NRC Canada

1997; Fuiman and Werner 2002); and other internal processes like degeneration of postovulatory follicles in the fish ovary are also described using a stage classification based on morphological characteristics (Hunter and Macewicz 1985; Murua et al. 2003).

To study the developmental process, estimate developmental rates, and if necessary, assign ages to the different morphological stages, it is common to perform different experiments under controlled conditions in which sampling is done at fixed time intervals and stages are recorded. The number of individuals found at each stage follow a multinomial distribution, with a certain probability of being in any given stage. These probabilities can be expressed as a function of age and of possible additional variables affecting the developmental process. Moreover, by modeling the multinomial distribution of stages, the characteristics of the developmental process can be quantified and analyzed. In other words, when only two stages are used to characterize development, the distribution of the output reduces to a binomial distribution and can be fitted using binomial models, such as the logistic or probit models (McCullagh and Nelder 1989). When there are more than two stages, this approach could be generalized, and multinomial models such as proportional odds or continuation-ratio-based models could be used (Agresti 1990; Ananth and Kleinbaum 1997). However, multinomial models are relatively new (McCullagh 1980; Anderson 1984; Peterson and Harrell 1990), and up to now, they have not been used to study developmental experiments.

One kind of developmental experiment of special importance in the framework of fisheries is the analysis of fish egg development, which provides the information necessary to assign ages to staged eggs and afterwards use them to estimate egg production (see for example a review in Stratoudakis et al. 2006). Up to now, the most common approach to analyse egg development experimental data is that of Lo (1985), in which the mean elapsed time from the beginning of the experiment of the individuals found at each stage under certain controlled conditions is modeled as a function of stage and the additional variables.

This paper describes how multinomial models can be used to analyze data from a developmental experiment by modeling the probability of being in one of a series of ordered stages as a function of the variables that control the developmental process, for example, age and temperature. Firstly, some of the most commonly used multinomial models are described, and some outputs that could be used to characterize and analyze the developmental rates of biological processes that are categorized into morphological stages are enumerated. For illustration, the development of Bay of Biscay anchovy (*Engraulis encrasicolus*) eggs and how it varies according to the incubation temperature is studied using data from an incubation experiment conducted in 1992 (Motos 1994). Finally, the results obtained and the advantages and disadvantages of this approach are discussed.

Material and methods

Let development in a given biological process be classified into k ordered stages according to some morphological characteristics. In an experiment under controlled conditions, samples are taken at given time intervals, frequent enough as to track the changes from one stage to the next. At each sampling event, let n denote the total number of individuals sampled, from which n_1 are in the first stage, n_2 are in the second stage, ..., and n_k are in the last kth stage. The stage classification at each sampling event follows a multinomial distribution with k ordered categories:

$$(1) \qquad (n_1, n_2, \ldots, n_k) \sim \text{Multi}(n, \pi_1, \pi_2, \ldots, \pi_k)$$

where $\pi_i = P(\text{Stage} = i)$ denote the individual probability of an individual of being in stage i. These probabilities depend on the age a of the individual, which is defined as the elapsed time from the beginning of the experiment to the sampling event. Furthermore, there might be some other covariate(s) that could also affect the developmental rates and form part of the controlled conditions of the experiment. Let $\boldsymbol{x} = (x_1, \ldots, x_p)$ denote the vector of these additional covariates.

There are two main approaches for modeling multinomial distributions of categorical ordered data incorporating the natural ordering of the response (Agresti 1990). Basically, they differ in the type of probabilities that will be modeled as a function of the covariates a and $\boldsymbol{x}$. On the first approach, the cumulative probability of the stages (i.e., the probability of an individual of being in a given stage or above) is modeled, whereas on the second approach the conditional probability (i.e., the probability of an individual of having arrived to a given stage but not yet developed to the next one) is modeled. The individual probability of being in a given stage can be easily computed from either the cumulative or conditional probabilities modeled.

Modeling cumulative probabilities

The first approach models the cumulative probabilities of the stages. Let $\gamma_i = P(\text{Stage} \geq i)$ denote the probability of an individual of being in stage i or higher. The cumulative probability can be modeled by means of a generalized linear model (GLM) (McCullagh and Nelder 1989) as follows:

$$(2) \qquad g(\gamma_i) = \alpha_i + \eta_i(a, \boldsymbol{x})$$

$$= \alpha_i + \beta_i a + \sum_{j=1}^{p} \lambda_{ij} x_j + \sum_{j=1}^{p} \xi_{ij}(x_j : a)$$

$$\text{for } i = 1, \ldots, k-1$$

where $g(\cdot)$ denotes the link function, and the linear predictor $\eta_i(a, \boldsymbol{x})$ is a linear function of age a and the set of additional covariates affecting development $\boldsymbol{x}$. In principle, the coefficients of age a (i.e., β_i) of the other covariates x_j for $j = 1, \ldots, p$ (i.e., λ_{ij}) and of their interaction $a : x_j$ (i.e., ξ_{ij}) are allowed to be different for each stage i.

One of the special features of this model is that it can be interpreted in terms of a latent variable. Suppose that the response variable Stage results from grouping an underlying continuous variable Z, say development, using cut points: $-\infty = \alpha_1 < \alpha_2 < \ldots < \alpha_k < \alpha_{k+1} = \infty$. That is,

$$(3) \qquad \text{State} = i \Leftrightarrow \alpha_i \leq Z < \alpha_{i+1} \qquad \text{for } i = 1, \ldots, k$$

© 2007 NRC Canada

Assuming that $Z = -\eta_i(a, \boldsymbol{x}) + \varepsilon$, where $\eta_i(a, \boldsymbol{x})$ is a linear function of the covariates a and $\boldsymbol{x}$, and ε is an error term that has the cumulative density function $F(\cdot)$, it follows that

$$\gamma_i = P(\text{State} \geq i) = P(Z \geq \alpha_i) = P[\varepsilon \geq \alpha_i + \eta_i(a, \boldsymbol{x})] = F[\alpha_i + \eta_i(a, \boldsymbol{x})] \quad (4)$$

which is the same as eq. 2.

When the link function is the logit and the regression coefficients of age and the rest of the explanatory variables are equal for all the stages — $\beta_i = \beta$, $\lambda_{ij} = \lambda_j$, and $\xi_{ij} = \xi_j$ (i.e., $\eta_i(a, \boldsymbol{x}) = \eta(a, \boldsymbol{x})$ for all i) — the model is called proportional odds (PO) model. The name comes from the fact that given two individuals with explanatory variables a_1, $\boldsymbol{x}_1 = (x_{11}, \ldots, x_{1p})$ and a_2, $\boldsymbol{x}_2 = (x_{21}, \ldots, x_{2p})$, respectively, the logarithm of the cumulative odds ratio is proportional to the distance between the values of the explanatory variables and does not depend on the response category i:

$$\log\left\{\frac{\gamma_i(a_1, \boldsymbol{x}_1)/[1-\gamma_i(a_1, \boldsymbol{x}_1)]}{\gamma_i(a_2, \boldsymbol{x}_2)/[1-\gamma_i(a_2, \boldsymbol{x}_2)]}\right\} = \beta(a_2 + a_1) + \sum_{j=1}^{p} \lambda_j(x_{2j} - x_{1j}) + \sum_{j=1}^{p} \xi_j(x_{2j}:a_2 - x_{1j}:a_1) \quad (5)$$

Among the appealing features of the PO model are invariability under collapsibility of the response categories (i.e., collapsing stage categories into bigger ones) and under reversal of the categories codes.

Modeling conditional probabilities

The second approach consists of modeling the conditional probabilities of stages. Let $\rho_i = P(\text{Stage} = i | \text{Stage} \geq i)$ denote the probability of an individual of being in stage i given that it is in stage i or higher, that is, the proportion of individuals in at least stage i that have not developed to the next stage $i + 1$. These can be modeled as

$$g(\rho_i) = \alpha_i + \eta_i(a, \boldsymbol{x}) = \alpha_i + \beta_i a + \sum_{j=1}^{p} \lambda_{ij} x_j + \sum_{j=1}^{p} \xi_{ij}(x_j:a) \qquad \text{for } i = 1, \ldots, k-1 \quad (6)$$

where $g(\cdot)$ denotes the link function, and $\eta_i(a, \boldsymbol{x})$ is the linear predictor that depends on age a and the possible rest of explanatory variables $\boldsymbol{x}$. As before, the coefficients of age and the rest of explanatory variables are allowed to vary between stages.

In case the link function is the logit and the coefficients of the linear predictor don't change between stages (only the intercept changes), the model is called continuation-ratio (CR) model. When the assumption of equal slopes for the explanatory variables is relaxed, the model is referred to as extended continuation-ratio (ECR) model.

One of the advantages of the conditional probabilities is that the multinomial response can be expressed as the product of conditionally independent binomial distributions:

$$\text{Multi}(n_1, n_2, \ldots, n_k | n, \pi_1, \pi_2, \ldots, \pi_k) = \text{Bin}(n_1 | n, \rho_1)\text{Bin}(n_2 | n - n_1, \rho_2) \ldots \times \text{Bin}(n_{k-1} | n - n_1 - \ldots - n_{k-2}, \rho_{k-1}) \quad (7)$$

So, the model can be easily fitted using the procedures developed for fitting binary regression models, the likelihood being the product of the likelihood of the binomial models, and the deviance being the sum of the deviance of the binomial models.

Extracting information on development from the model

From all the above models, it is necessary to select the one that best represents the data, checking that the underlying model assumptions are correct. Afterwards, the major interest is on extracting from the fitted model as much meaningful information about development as possible.

Firstly, the individual probabilities of being in any stage can be reconstructed from either the conditional or the cumulative probabilities fitted in the model chosen. From the fitted conditional probabilities $\hat{\rho}_i$, the cumulative probabilities can be calculated as

$$\hat{\gamma}_i = \prod_{l=1}^{i-1}(1 - \hat{\rho}_l) \quad (8)$$

and then, from the cumulative probabilities, the individual probabilities for each stage are derived as

$$\hat{\pi}_i = \hat{\gamma}_i - \hat{\gamma}_{i-1} \quad (9)$$

Plotting the individual probabilities against age, conditioned on the rest of covariates, provides a first general view on the developmental process and on how the rest of the covariates affect them.

Traditionally, there are some quantities useful to describe development, namely, stage duration and descriptive statistics of age for each stage (e.g., mean age). When any other covariate apart from age is used, the effect of each covariate on stage duration is also important to understand development. Estimates of those quantities can be obtained from the fitted model as follows: Fitted coefficients of age a and the rest of covariates $\boldsymbol{x}$ gives information on the effect of each covariate on the developmental rates. Interpretation will be different depending on the model utilized and its parameterization. Also, this information is necessary to test if the equal slope assumption is fulfilled, in which case simpler models are preferable. Modal age conditioned on the rest of covariates $\boldsymbol{x}$ can be defined as the age at which a given stage attains its maximum probability (i.e., age a such that $\hat{P}(\text{Stage} = i | a, \boldsymbol{x}) = \max_a \hat{P}(\text{Stage} = i | a, \boldsymbol{x})$) (see Fig. 1). Duration of a given stage i conditioned on the set of covariates $\boldsymbol{x}$ can be defined in three different ways: (1) as the length of the range of ages at which the individual fitted probabilities $\hat{P}(\text{Stage} = i | a, \boldsymbol{x})$ are above certain fixed value q, (2) as the length of the range of ages at which stage i is more probable than any other stage (i.e., the range of a such that $\hat{P}(\text{Stage} = i | a, \boldsymbol{x}) = \max_j \hat{P}(\text{Stage} = j | a, \boldsymbol{x})$, and (3) using conditional probabilities, as the length of the age range in which the transition

© 2007 NRC Canada

Fig. 1. Illustration of (*a*) modal age (circles), defined as the age at which the individual probability of a given stage is maximum; (*b*) stage duration (horizontal solid lines along the top), defined as the range of ages for which the probability of being in that stage is above a certain value, represented by the horizontal line at $q = 0.1$ (along the bottom); (*c*) stage duration (horizontal solid lines along the top), defined as the range of ages for which the stage is most likely than any other stage; and (*d*) stage duration (horizontal solid lines along the top), defined as the time for which the conditional probabilities from the previous stage are above 50% and the probabilities to the next stage are below 50%. Continuous lines in (*a*), (*b*), and (*c*) represent the fitted individual probabilities of each stage depending on age given the rest of covariates; in (*d*), the continuous lines represent the conditional probability of being in a given stage, given that it has arrived at least to the previous one. Vertical broken lines in (*b*), (*c*), and (*d*) show the derivation of the stage durations from the fitted multinomial model.

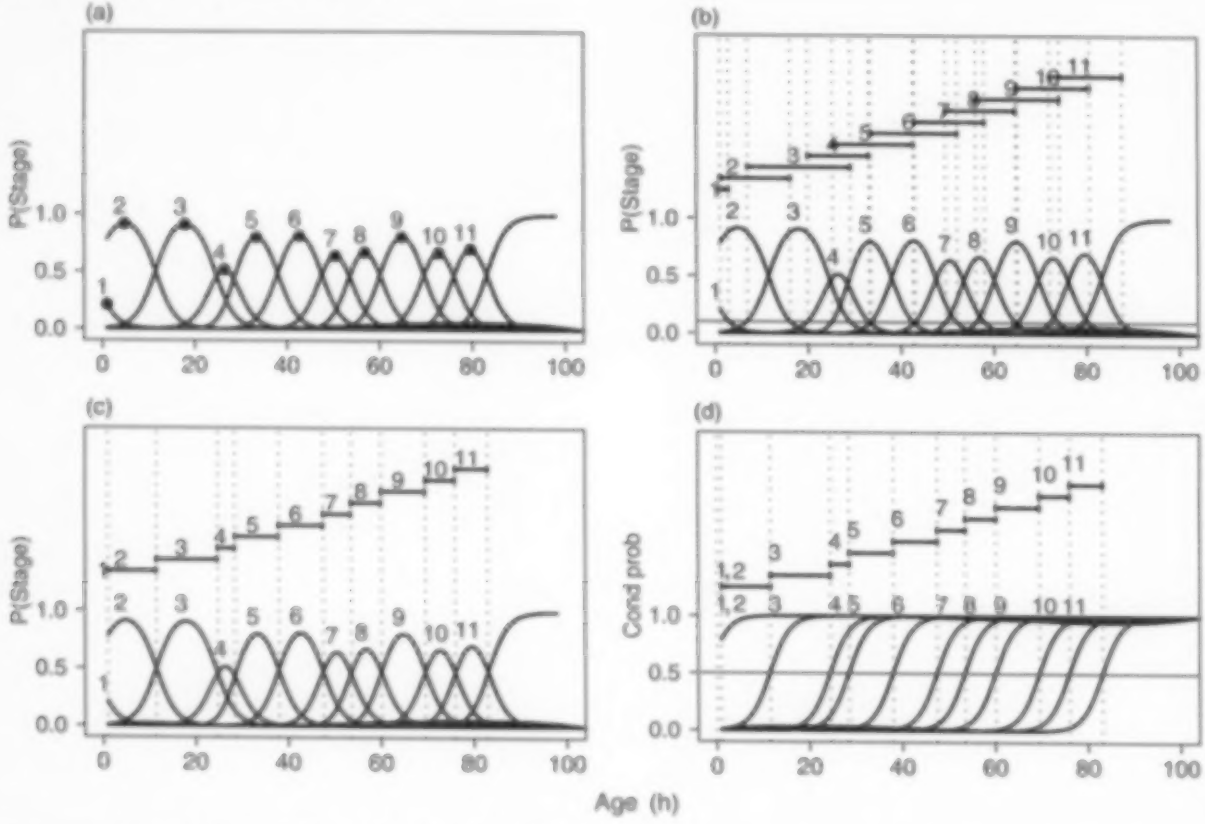

probability from the previous stage is larger than 50% and the transition probability to the next stage is smaller than 50% (i.e., the length of the age range for which it is more probable to develop from the previous stage but not to develop to the next one). The construction and the meaning of each of these alternative definitions is illustrated (Fig. 1). In addition, if the model chosen is the PO model, it's straightforward to interpret the model in terms of a latent variable and to represent the duration of a given stage i as the difference between the cut points of the underlying continuous variable that define the stage i, that is $\alpha_{i+1} - \alpha_i$. Note that this is independent of both age a and the rest of covariates $\boldsymbol{x}$.

Other statistics, like the age at which the cumulative or the conditional probability (depending on the model used) attains some probability q conditioned on the rest of covariates $\boldsymbol{x}$, might also be of interest. In CR-based models, it implicates the age at which q percentage of the individuals that are at least in a given stage will develop further to the next stage. For example, this type of statistic can be used to

Fig. 2. Elapsed time from the beginning of the experiment to the sampling events from the tubes at different temperatures.

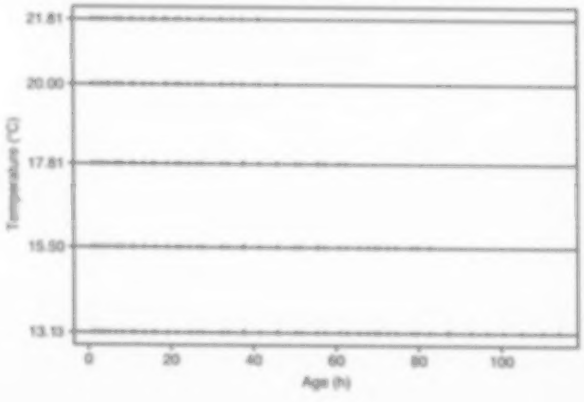

© 2007 NRC Canada

Fig. 3. Stages found at each tube at different sampling events. The size of the circle is proportional to the percentage of eggs found in each stage at each sampling event.

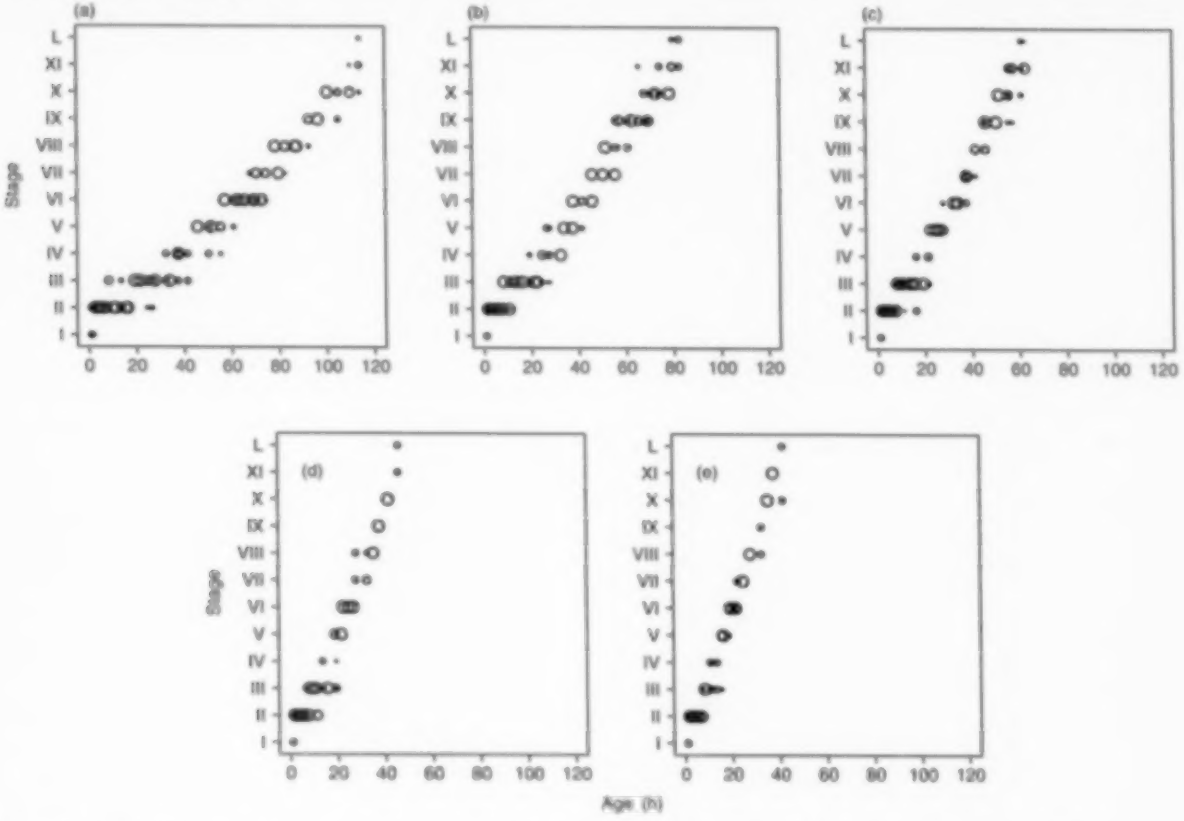

define hatching time as the age at which q percent of the eggs that were at least in the last stage have hatched and to study how the covariates influence it.

Depending on the selected model, most of these statistics can be extracted either directly from the model summary or easily from the model properties. In the Discussion, the meaning and the pros and cons of each of these quantities will be discussed. All the above statistics are based on the fitted probability of stage given age and other possible additional covariates. However, other statistics of interest can be extracted by applying Bayesian methods and extracting the posterior distribution of ages given stage (ICES 2004).

Software

All the analysis shown in this paper were done in R (www.r-project.org). The new ageing method and a function for modelling the conditional probabilities of stages $\rho_i' = 1 - \rho_i = P(\text{Stage} \geq i | \text{Stage} \geq i - 1)$ from the incubation experiment data was implemented as part as an R library called "egg" (www.ruwpa.st-andrews.ac.uk/depm) and was developed during the European project (EU Study 99/080).

There are other libraries in R that allow fitting different multinomial models. For example, function polr in the library Mass fits PO models and the function lrm in libraries Hmisc and Design fits PO and CR models. A revision of the code in S-plus and SAS to fit ordinal regression models can be found in Bender and Benner (2000).

Results: a case study on anchovy incubation

Since 1987, the Bay of Biscay anchovy (*E. encrasicolus*) is assessed yearly using the daily egg production method (Parker 1980; Santiago and Sanz 1992; Motos 1994), which consists of back-transforming the daily egg production estimate into spawning stock biomass via the daily specific fecundity estimate.

To estimate the daily egg production, the anchovy eggs collected during the ichtyoplankton survey (Gunderson 1993) are classified into 11 developmental stages (I, II,...,XI) according to Moser and Ahlstrom (1985) and have to be aged to allocate them into daily cohorts. For the ageing to be achieved, it is necessary to study the developmental rates of anchovy eggs and how this might be affected by different variables.

In general, it is known that egg development rate is affected by temperature (Ahlstrom 1943), oxygen tension, and to a lesser extent, salinity (Hempel 1979). The developmental rate of early life history stages increases as incubation temperature increases (Pepin 1991) and may also have different optimal temperatures depending on field temporal and

© 2007 NRC Canada

Table 1. Summary of fitted multinomial models.

		Cumulative probability		Conditional probability				
	Stage	PO_0	PO_1	CR_0	CR_1	ECR_{1a}	ECR_{1b}	ECR_{1c}
Intercept		−6.93 (0.000)	2.39 (0.012)	6.72 (0.000)	−2.32 (0.011)	−2.75 (0.156)	2.88 (0.166)	3.47 (0.269)
	III	−11.47 (0.000)	−3.92 (0.000)	4.52 (0.000)	6.09 (0.000)	5.29 (0.020)	2.02 (0.228)	−4.16 (0.232)
	IV	−13.31 (0.000)	−9.56 (0.000)	5.77 (0.000)	11.45 (0.000)	13.94 (0.000)	7.76 (0.000)	2.16 (0.649)
	V	−14.07 (0.000)	−11.54 (0.000)	5.72 (0.000)	12.87 (0.000)	21.21 (0.000)	7.62 (0.0000)	12.59 (0.035)
	VI	−15.42 (0.000)	−15.31 (0.000)	7.30 (0.000)	16.69 (0.000)	27.09 (0.000)	11.61 (0.000)	39.65 (0.000)
	VII	−16.86 (0.000)	−19.75 (0.000)	8.54 (0.000)	20.91 (0.000)	32.20 (0.000)	15.53 (0.000)	28.70 (0.001)
	VIII	−17.94 (0.000)	−22.71 (0.000)	9.06 (0.000)	23.59 (0.000)	33.04 (0.000)	20.11 (0.000)	42.40 (0.000)
	IX	−19.05 (0.000)	−25.83 (0.000)	9.97 (0.000)	26.49 (0.000)	38.77 (0.000)	20.82 (0.000)	14.41 (0.063)
	X	−20.35 (0.000)	−30.02 (0.000)	10.94 (0.000)	30.97 (0.000)	44.77 (0.000)	25.56 (0.000)	58.30 (0.000)
	XI	−21.58 (0.000)	−32.85 (0.000)	11.86 (0.000)	32.97 (0.000)	50.77 (0.000)	25.99 (0.000)	44.32 (0.000)
	L	−23.74 (0.000)	−36.87 (0.000)	13.74 (0.000)	36.98 (0.000)	50.13 (0.000)	33.11 (0.000)	93.61 (0.000)
Age		0.15 (0.000)	−0.59 (0.000)	−0.13 (0.000)	0.56 (0.000)	0.43 (0.000)	−2.42 (0.082)	−2.41 (0.091)
	III						2.91 (0.036)	3.04 (0.033)
	IV						2.90 (0.037)	3.00 (0.035)
	V						2.96 (0.033)	2.95 (0.038)
	VI						2.95 (0.034)	2.76 (0.053)
	VII						2.95 (0.034)	2.90 (0.042)
	VIII						2.92 (0.036)	2.82 (0.047)
	IX						2.95 (0.034)	3.02 (0.034)
	X						2.94 (0.035)	2.82 (0.048)
	XI						2.96 (0.033)	2.92 (0.040)
	L						2.92 (0.036)	2.69 (0.059)
Temperature		0.58 (0.000)	−0.10 (0.058)	−0.58 (0.000)	0.09 (0.071)	0.12 (0.273)	0.036 (0.604)	0.01 (0.964)
	III					0.06 (0.654)		0.32 (0.046)
	IV					−0.11 (0.472)		0.28 (0.194)
	V					−0.46 (0.007)		−0.18 (0.502)
	VI					−0.55 (0.001)		−1.12 (0.007)
	VII					−0.59 (0.001)		−0.49 (0.190)
	VIII					−0.47 (0.023)		−0.87 (0.068)
	IX					−0.64 (0.005)		0.37 (0.289)
	X					−0.74 (0.001)		−1.27 (0.009)
	XI					−0.93 (0.000)		−0.65 (0.143)
	L					−0.66 (0.037)		−2.35 (0.016)
Age:Temperature			0.07 (0.000)		−0.06 (0.000)	−0.06 (0.000)	−0.06 (0.000)	−0.07 (0.000)
Null deviance		2621.61	2621.61	2569.00	2569.00	2569.00	2569.00	2569.00
Residual deviance		1694.14	833.09	1294.32	502.58	462.23	474.72	417.75
% deviance		35.38	66.32	49.62	80.44	82.01	81.52	83.74
AIC		1720.14	911.09	1454.76	665.02	644.67	657.16	620.19

Note: PO refers to the proportional odds model; CR refers to the continuation-ratio model; ECR refers to the extended continuation-ratio model, where unequal slopes are allowed.

© 2007 NRC Canada

spatial distribution (Gadomski and Caddell 1991). Developmental rates of eggs depending on temperature can be obtained through incubation experiments (Lockwood et al. 1977; Lo 1985; Motos 1994). These experiments consist of incubating a number of eggs with known spawning time in tubes each at a different controlled temperature. At periodic time intervals, some eggs are sampled and staged. The most common approach to model these data is to compute the mean elapsed time from the beginning of the experiment and its standard deviation of all the individuals found at each stage under each controlled temperature and to fit a model depending on stage and temperature. In the next sections, the incubation experiment conducted in 1992 for the Bay of Biscay anchovy is described and the application of multinomial models to these data is illustrated.

Incubation experiments for the Bay of Biscay anchovy

An incubation experiment for the Bay of Biscay anchovy was carried out in May–June 1992 during the annual daily egg production method survey on board R/V *Cornide de Saavedra*. Two incubations, in two different stations, were performed, each using five completely hydrated females and five mature males selected from the pelagic trawl tow. Hydrated oocytes were extracted from the females by an abdominal massage and were put into a bowl with clean seawater. Then, sperm from the five males was added and both oocytes and sperm were gently mixed and left for 45 min to allow for fertilization. When the first cellular divisions were detected, batches of about 200 eggs were placed with 35 mL filtered seawater in 50 mL glass tubes in an incubator block (modified from Thomas et al. 1963). Two rows of seven tubes were prepared and positioned across the block covering a temperature range from 8 to 22 °C (in particular, the seven average temperatures were 8.49, 10.79, 13.13, 15.5, 17.81, and 21.81 °C). Periodically some eggs were randomly sampled from each tube (the number of eggs sampled varied between 1 and 14 eggs with an average of 3 eggs). Sampling intervals were increased as the experiment carried on. Intervals were 1 hour during the first 6 h of incubation, 4 h during the following 42 h, and every 6 h afterwards (Fig. 2). At each sampling event, the elapsed time from the beginning of the experiment, the temperature, and the number of eggs in each developmental stage (Ahlstrom and Moser 1985) were recorded. The sampling from each tube finished when eggs had begun hatching or when there were no more eggs to sample (i.e., all the eggs were already sampled or dead).

Motos (1994) followed the same approach as Lo (1985) to model the mean age of the eggs found at each stage and temperature as a function of stage and temperature and assuming that the standard deviation of age given stage and temperature was constant across temperatures.

Multinomial models

From the data collected in the incubation experiments, only the tubes with temperatures at which hatching was observed were used in the analysis, namely, temperatures above 13 °C. Information on stage I was considered unreliable, since identification problems between the nonfertilized and stage I eggs were encountered. Therefore, it was assumed that when eggs were put into the tubes (1 hour from the fertilization), eggs were in stage I or II with equal probability, but that no more stage I eggs were found in the following sampling events. In addition, information on the number of hatched eggs sampled was not recorded. So it was assumed that at the last sampling event of each of the tubes, the number of hatched eggs was the same as the number of eggs in the last stage (XI) and that at the next sampling event, all the eggs were already hatched. Note that the results obtained on these two stages will be dependent on these assumptions and may not be valid under different situations. These assumptions are only to enhance the data for illustrative purposes, and in a real case, either the experiment should be performed to ensure avoidance of those assumptions or else a careful check of its validity should be performed.

Fig. 4. Relative duration from proportional odds models PO_0 (solid line) and PO_1 (broken line) as the difference between the cut points ($\alpha_{i+1} - \alpha_i$) scaled by the total duration up to hatching according to each model.

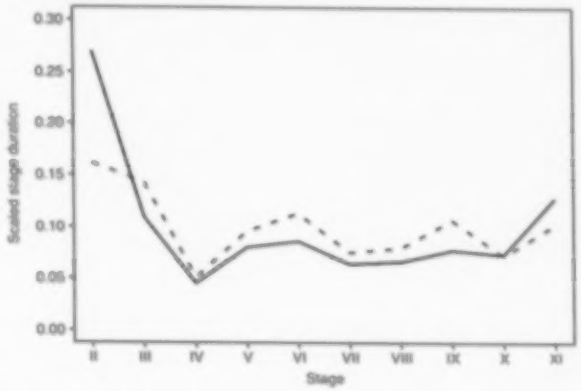

The number of eggs found at each stage at each sampling event per tube (Fig. 3) was used to fit the various multinomial models described in the previous section using age and temperature as covariates and egg stage as the response with 12 categories (11 egg stages and larvae). More precisely, PO models, as well as CR and ECR models, were fitted to the data from the incubation experiment, and main results are summarized in Table 1.

Cumulative probabilities were fitted using PO models. Two models were attempted: the first one (PO_0) having only age and temperature as covariates and the second one (PO_1) including also their interaction (first and second columns in Table 1). The interaction was significative ($p < 0.001$). Moreover, PO_1 showed a better fit with smaller Akaike's information criterion (AIC) (911.09 for PO_1 and 1720.14 for PO_0) and explained ~30% more of the null deviance (Table 1).

The relative duration of stages from the PO models computed as the difference between the intercepts in the fitted models scaled by the total duration up to hatching follow the same pattern, except for stages II and XI (Fig. 4). Without considering stage I, stages II and IV were the longest and the shortest ones, respectively.

Similarly, conditional probabilities were initially fitted without and with the age and temperature interaction (de-

© 2007 NRC Canada

Fig. 5. Fitted (lines) and observed (numbers) individual probabilities of being in a given stage at a combination of age (*x* axis) and temperature at (*a*) 13.13 °C, (*b*) 15.5 °C, (*c*) 17.81 °C, (*d*) 20 °C, and (*e*) 21.81 °C.

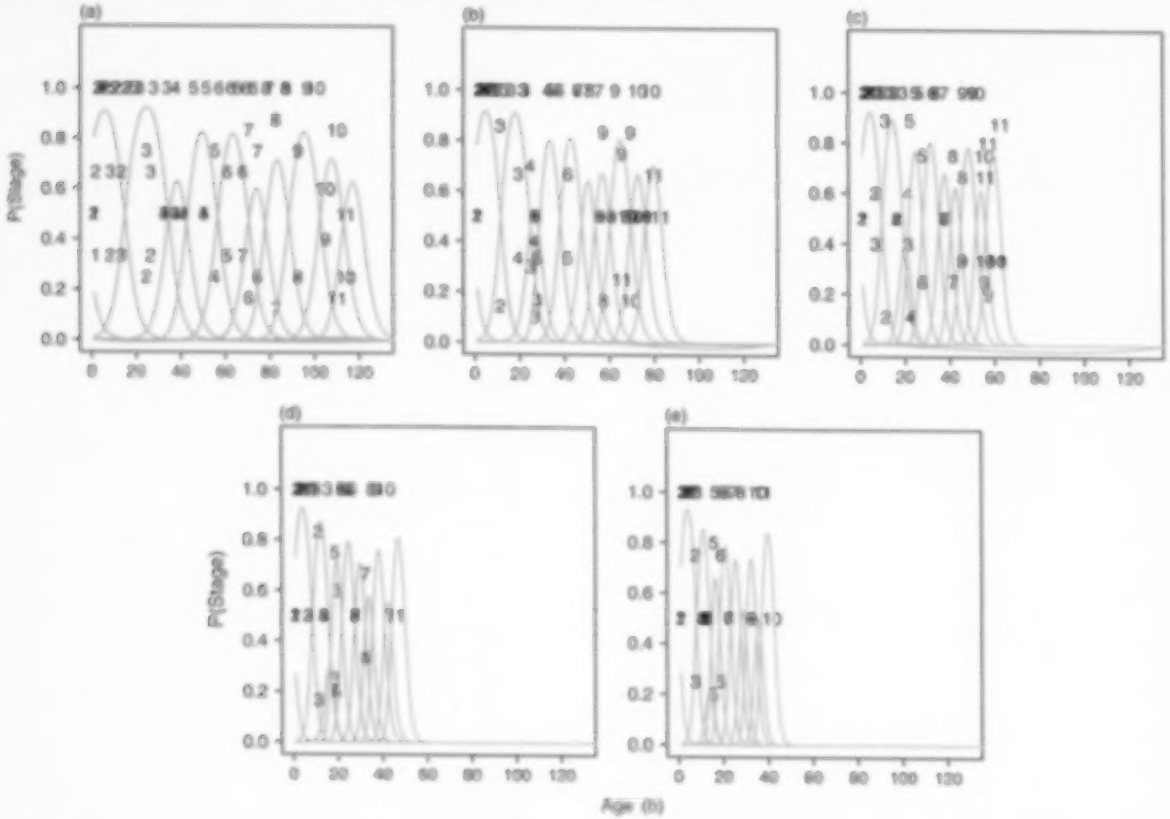

noted in what follows as models CR_0 and CR_1, respectively). Again, the model including the interaction, CR_1, resulted in a better fit with AIC = 665.02 (AIC for CR_0 = 1454.76) and 80% of the null deviance explained (30% more than in CR_0) (Table 1).

Among the two above alternatives (cumulative probabilities or conditional probabilities), the second one was considered more adequate for this particular case. Stage development is a sequential process, and conditional ratios are more useful to interpret in biological terms the probability of developing from one stage to the next and to ascertain the effects of the covariates on that progression. Since the conditional probabilities can be decomposed as the product of conditionally independent binomial distributions, the model can be fitted using the routines for binary regression, allowing the unequal slopes case to be fitted easily.

The equal slope assumption in the CR_1 model that includes the interaction between age and temperature was relaxed, and different ECR models were fitted. The model with the temperature coefficient changing for each stage is ECR_{1a}, the one with the coefficient of age changing for each stage is ECR_{1b}, and the model with both age and temperature changing for each stage is represented by ECR_{1c} (Table 1). The best of these models in terms of the lowest AIC and the largest percentage of deviance explained was ECR_{1c} (Table 1). However, most of the coefficients of age and temperature for different stages were nonsignificant ($p > 0.01$), and the model was considered to be possibly overparameterized. Thus, the other two model extensions of CR_1, namely ECR_{1a} and ECR_{1b}, were explored. From those models, ECR_{1a}, which allows the effect of temperature to change for stages, was taken as the most adequate for this case study based on the AIC, the percentage of deviance explained, and the significance of the coefficients (Table 1). In addition, the performance of this model was close to model ECR_{1c}, explaining only 1% less of the deviance than ECR_{1c}. The fitted individual probabilities for ECR_{1a} are shown (Fig. 5).

Statistics describing development were computed from model ECR_{1a}. Modal age, defined as the age at which the individual probability of a given stage was maximum, was computed. Stage duration was computed according to the three different definitions given in the previous section (i.e., definitions (1), (2), and (3) in Extracting information on development from the model, Materials and methods; results are summarized in Table 2). Stage duration for all stages and each temperature computed with the different approaches presented in this paper are compared (Fig. 6). Stage durations 2, based on the individual probabilities, and 3, based on the conditional probabilities, are equivalent in this case. In general, absolute stage duration decreased as temperature increased. Stages I and III were the shortest and the largest

© 2007 NRC Canada

Table 2. Stage durations (h) for each temperature from the fitted multinomial model ECR_{Le}.

	Temperature (°C)				
Stage	13.13	15.50	17.81	20.00	21.82
Modal age					
I	0	0	0	0	0
II	5.7	4.8	4.3	4.0	3.9
III	24.6	17.9	14.3	12.1	10.8
IV	38.4	26.4	20.0	16	13.7
V	49.7	33.4	24.7	19.4	16.4
VI	63.5	42.7	31.5	24.7	20.6
VII	74.1	50.4	37.7	29.9	25.3
VIII	83.3	56.8	42.6	33.9	28.7
IX	95.5	64.8	48.3	38.2	32.2
X	107.7	72.7	53.9	42.4	35.5
XI	117.1	79.6	59.3	47.0	39.7
Duration 1					
I	(0, 3.1)	(0, 2.8)	(0, 2.7)	(0, 2.6)	(0, 2.5)
II	(0, 21.5)	(0, 16.1)	(0, 13.2)	(0, 11.5)	(0, 10.4)
III	(8.4, 40.9)	(6.9, 29.1)	(6.0, 22.7)	(5.5, 18.8)	(5.3, 16.4)
IV	(27.8, 49.1)	(19.9, 33.1)	(15.6, 24.4)	(13.0, 19.1)	(11.5, 15.8)
V	(37.1, 63.2)	(25.2, 42.6)	(18.8, 31.5)	(15.0, 24.7)	(12.8, 20.7)
VI	(50.3, 76.9)	(33.5, 52.1)	(24.5, 38.7)	(19.1, 30.6)	(15.9, 25.7)
VII	(64.0, 84.4)	(43.0, 58.0)	(31.7, 43.8)	(24.8, 35.2)	(20.7, 30.0)
VIII	(72.6, 95.0)	(49.6, 64.7)	(37.2, 48.4)	(29.6, 38.4)	(25.1, 32.4)
IX	(82.6, 109.0)	(56.1, 74.1)	(41.8, 55.3)	(33.2, 43.8)	(28.0, 37.0)
X	(96.1, 119.5)	(65.1, 80.6)	(48.3, 59.6)	(38.1, 46.8)	(32.1, 39.1)
XI	(107.1, 127.8)	(72.0, 87.7)	(53.1, 66.1)	(41.6, 53.0)	(34.8, 45.1)
Duration 2					
I	—	—	—	—	—
II	(0, 14.8)	(0, 11.4)	(0, 9.6)	(0, 8.5)	(0, 7.8)
III	(14.9, 34.5)	(11.5, 24.7)	(9.7, 19.7)	(8.6, 16.5)	(7.9, 14.3)
IV	(34.6, 42.5)	(24.8, 28.4)	(19.8, 20.8)	—	—
V	(42.6, 56.6)	(28.5, 37.9)	(20.9, 27.9)	(16.6, 21.7)	(14.4, 18.1)
VI	(56.7, 70.5)	(38.0, 47.5)	(28.0, 35.1)	(21.8, 27.6)	(18.2, 23.1)
VII	(70.6, 77.9)	(47.6, 53.5)	(35.2, 40.3)	(27.7, 32.3)	(23.2, 27.5)
VIII	(78.0, 88.4)	(53.6, 60.0)	(40.4, 44.7)	(32.4, 35.4)	(27.6, 29.8)
IX	(88.5, 102.5)	(60.1, 69.5)	(44.8, 51.8)	(35.5, 41.0)	(29.9, 34.6)
X	(102.6, 113.1)	(69.6, 75.9)	(51.9, 56.0)	(41.1, 43.8)	(34.7, 36.5)
XI	(113.2, 121.2)	(76.0, 83.0)	(56.1, 62.5)	(43.9, 50.0)	(36.6, 42.5)
Duration 3					
I	—	—	—	—	—
II	(0, 14.9)	(0, 11.5)	(0, 9.7)	(0, 8.5)	(0, 7.9)
III	(14.9, 34.4)	(11.5, 24.5)	(9.7, 19.1)	(8.5, 15.8)	(7.9, 13.9)
IV	(34.4, 42.6)	(24.5, 28.5)	(19.1, 20.9)	(15.8, 16.3)	—
V	(42.6, 56.6)	(28.5, 38.0)	(20.9, 27.9)	(16.3, 21.8)	(13.5, 18.2)
VI	(56.6, 70.3)	(38.0, 47.5)	(27.9, 35.1)	(21.8, 27.6)	(18.2, 23.2)
VII	(70.3, 77.9)	(47.5, 53.5)	(35.1, 40.3)	(27.6, 32.3)	(23.2, 27.5)
VIII	(77.9, 88.5)	(53.5, 60.1)	(40.3, 44.8)	(32.3, 35.5)	(27.5, 29.9)
IX	(88.5, 102.5)	(60.1, 69.5)	(44.8, 51.7)	(35.5, 40.9)	(29.9, 34.4)
X	(102.5, 113.0)	(69.5, 76.0)	(51.7, 56.0)	(40.9, 43.9)	(34.4, 36.6)
XI	(113.0, 121.3)	(76.0, 83.1)	(56.0, 62.6)	(43.9, 50.1)	(36.6, 42.6)

Note: Duration 1 is the age range for which the individual probability of being in a given stage is larger than $q \approx 0.1$. Duration 2 is the age range in which a given stage is the more probable one. Duration 3 is the age range for which it is more probable to develop from the previous stage but not to develop to the next one.

© 2007 NRC Canada

Fig. 6. Different durations from model ECR_{Lo} at (*a*) 13.13 °C, (*b*) 15.5 °C, (*c*) 17.81 °C, (*d*) 20 °C, and (*e*) 21.81 °C. The dotted lines correspond to duration as the length of the range at which the *P*(Stage) is above *q*, for $q = 0.1$. The dashed lines show duration as the age range at which this stage is more probable than any other. The solid line is the length of the age range for which the transition probability from the previous stage is above 0.5 and the probability to the next stage is below 0.50.

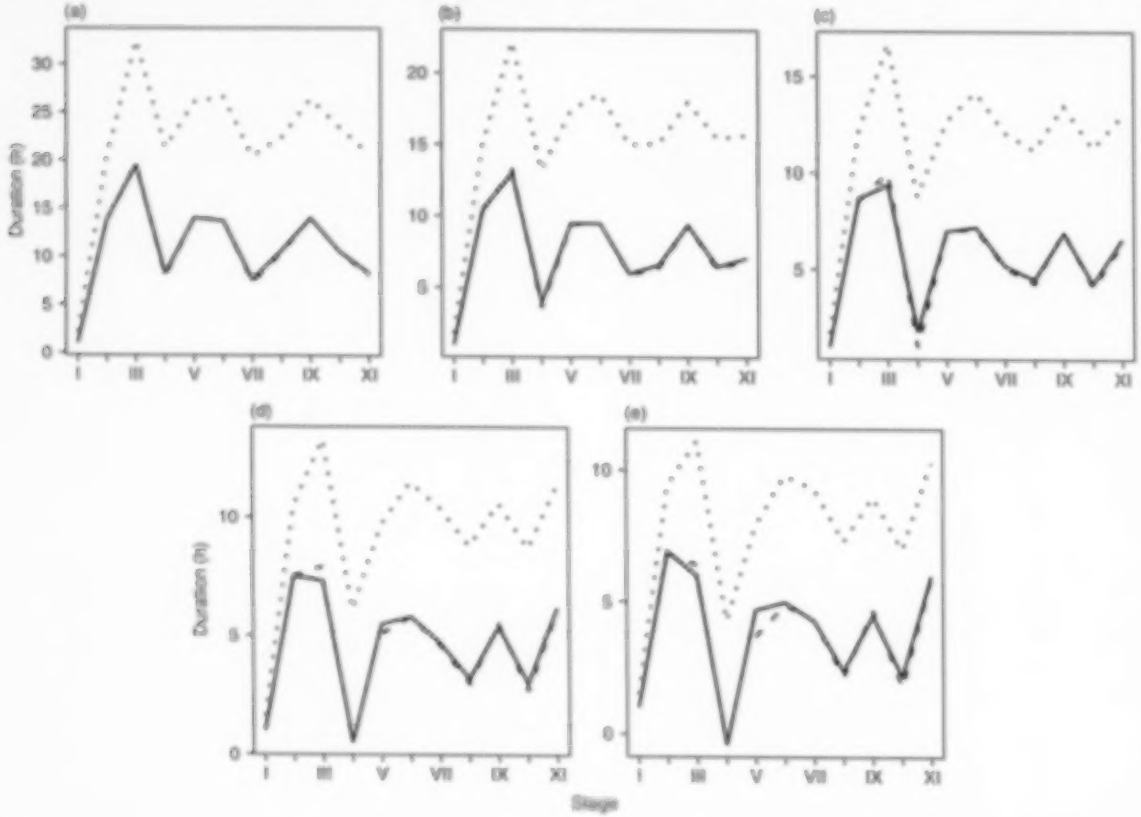

ones, respectively, for the three lowest temperatures. Stage IV also appeared to be short, but whereas the relative duration of the rest of the stages did not vary with temperature, Stage IV was relatively shorter for higher temperatures. Furthermore, the duration of stage IV as the length of the age ranges for which this stage was more probable than other stages could not be computed for the temperatures above 20 °C, as this was never the case; and the duration of stage IV defined as a function of transition probabilities (duration 3) for the highest temperature (21.81 °C) resulted in a negative value, indicating that the age at which transition probability to stage IV equals 50% is larger than the age at which transition probability from stage IV equals 50%, therefore preventing the use of this duration.

The observed ages at which eggs in each stage and temperature were recorded in the incubation experiment were encompassed within the stage durations (duration 1) for $q = 0.1$ (Fig. 7). In addition, estimated stage mean age from the multinomial model was close to the median of the observed ages (Fig. 7). Stage duration estimated from both durations 2 and 3 approaches are almost identical and are compared with the observed range of observed ages in Fig. 8. For these approaches, stage duration was shorter than for duration 1 through all stages and similar to the quantiles of ages observed in the experiment, although sometimes smaller.

In comparison with the mean age and the stage duration computed using Lo's model (Lo 1985; Motos 1994), the mean age and the stage durations computed from the multinomial model described better the distribution of the observations (Figs. 7 and 8). The mean age from Lo is underestimated at 13.13 °C and at the oldest stages, and the assumption of constant standard deviation, regardless of the temperature, seems to be inappropriate (Figs. 7 and 8).

Transition probability from one stage to the next depending on temperature was analyzed by computing the ages at which the conditional fitted probabilities were 5%, 50%, and 95% (Fig. 9). In all cases, it is obvious that the duration of the egg phase decreases for increasing temperatures; nevertheless, the absolute value of the total duration of the egg phase increases depending on the criteria used, ranging from ~110 h to near 130 h.

Several statistics describing the hatching process are summarized (Table 3). The age at which the probability of having hatched is 50% and 99% was computed. The difference between these two quantities decreased as temperature increased, with the difference being 14 h at 13.13 °C decreas-

© 2007 NRC Canada

Fig. 7. Observed ages for each stage (circles) and mean age and stage duration (open square and solid line, respectively) as derived from Lo's (1985) model and modal age and stage duration (X and solid line, respectively), defined as the length of the range at which the P(Stage) is above $q = 0.1$, derived from the multinomial model ECR_{1a} at (*a*) 13.13 °C, (*b*) 15.5 °C, (*c*) 17.81 °C, (*d*) 20 °C, and (*e*) 21.81 °C.

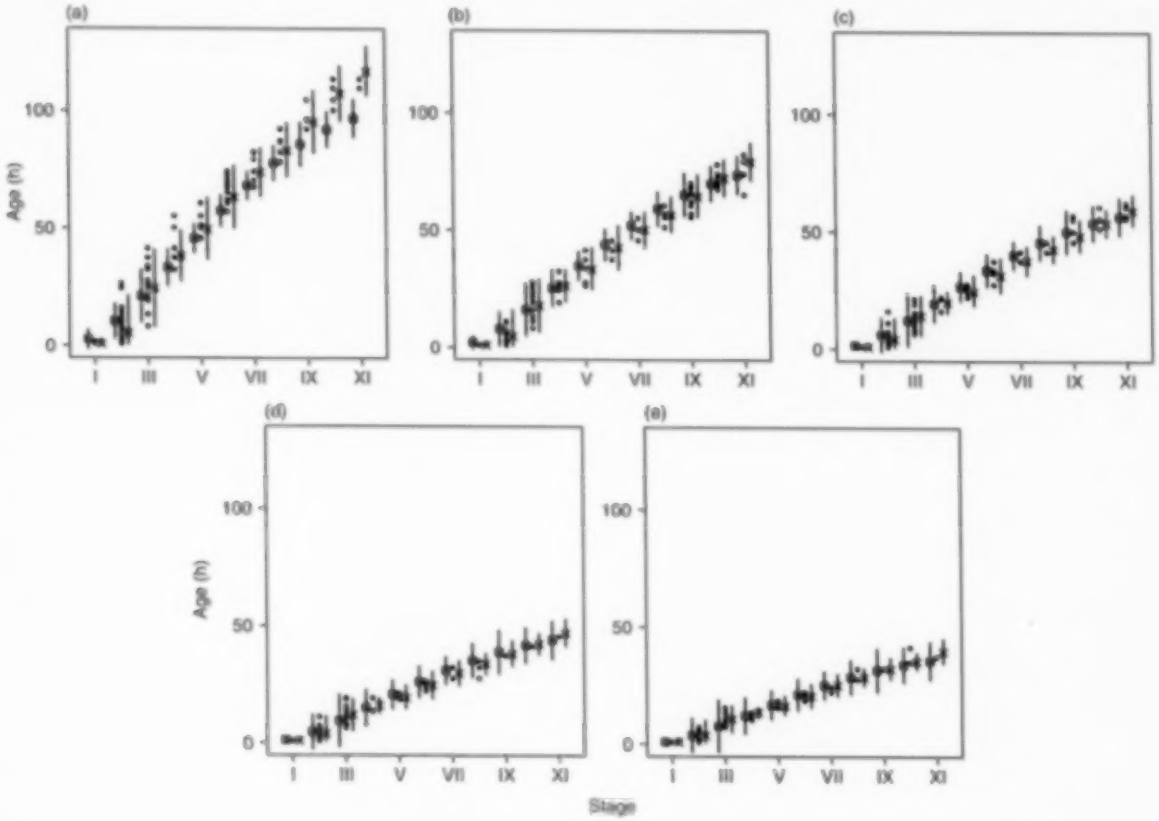

ing to a difference of 6 h at 21.81 °C. The age at which the individual probabilities for larvae were larger than any other stage were very close to the age at which the individual probabilities were 50%. On the other hand, conditional probabilities allow estimating the age at which P(Larvae|XI or Larvae) = 0.5. For the lowest temperature, 13.13 °C, this age was younger than the other quantities calculated, whereas the age for all the other temperatures was older (except for P(Larvae) = 0.99 at 15.50 °C). This suggests that for mid–high temperatures, hatching starts very quickly, though the whole process needs time to finish.

Discussion

Multinomial models for categorical ordered data are relatively new (Agresti 1990 and references therein). In most of cases, they broaden GLMs for binomially distributed responses like logistic model to the case of multinomial ordinal variables using either cumulative or conditional probabilities. Different applications can be found in psychology, medicine, and ecology (Armstrong and Sloan 1989; Bender and Grouven 1998; Guisan and Harrell 2000). In fisheries, multinomial models have been used for studying the age composition of the catches based on the length classes (Kvist et al. 2000; Rindorf and Lewy 2001).

This paper shows how multinomial models turn up naturally to model stage-classified biological processes. They present a solid and well-founded alternative to previously used approaches that were not fully appropriate from a statistical point of view. For example, in Lo (1985), observed mean age from an incubation experiment similar to the one presented in the Results section was taken as the response variable. In the temperature-dependent egg development model of Atlantic mackerel (*Scomber scombrus*) presented in Lockwood et al. (1977), the response variable was the last age at which a given stage was observed. In both approaches, some time-related statistic (mean age or maximum age) is modeled as a function of stage and temperature. However, the actual response variable is the stage classification observed given age and the additional controlled variables as temperature, for which multinomial models would be utilized. Moreover, within this framework, statistical inference can easily be conducted: different models can be compared, assumptions on the fitted coefficients can be tested, and the effect of different covariates can be studied. Hence, a large variety of data sets, such as classification of

© 2007 NRC Canada

Fig. 8. Observed ages for each stage (circles) and mean age and stage duration (open square and solid line, respectively) as derived from Lo's (1985) model and modal age and stage duration (X and solid line, respectively), defined as the age range at which this stage is more probable than any other or equivalently (in this case) as the length of the age range for which the transition probability from the previous stage is above 0.5 and the probability to the next stage is below 0.50, derived from the multinomial model ECR_{Lo} at (*a*) 13.13 °C, (*b*) 15.5 °C, (*c*) 17.81 °C, (*d*) 20 °C, and (*e*) 21.81 °C.

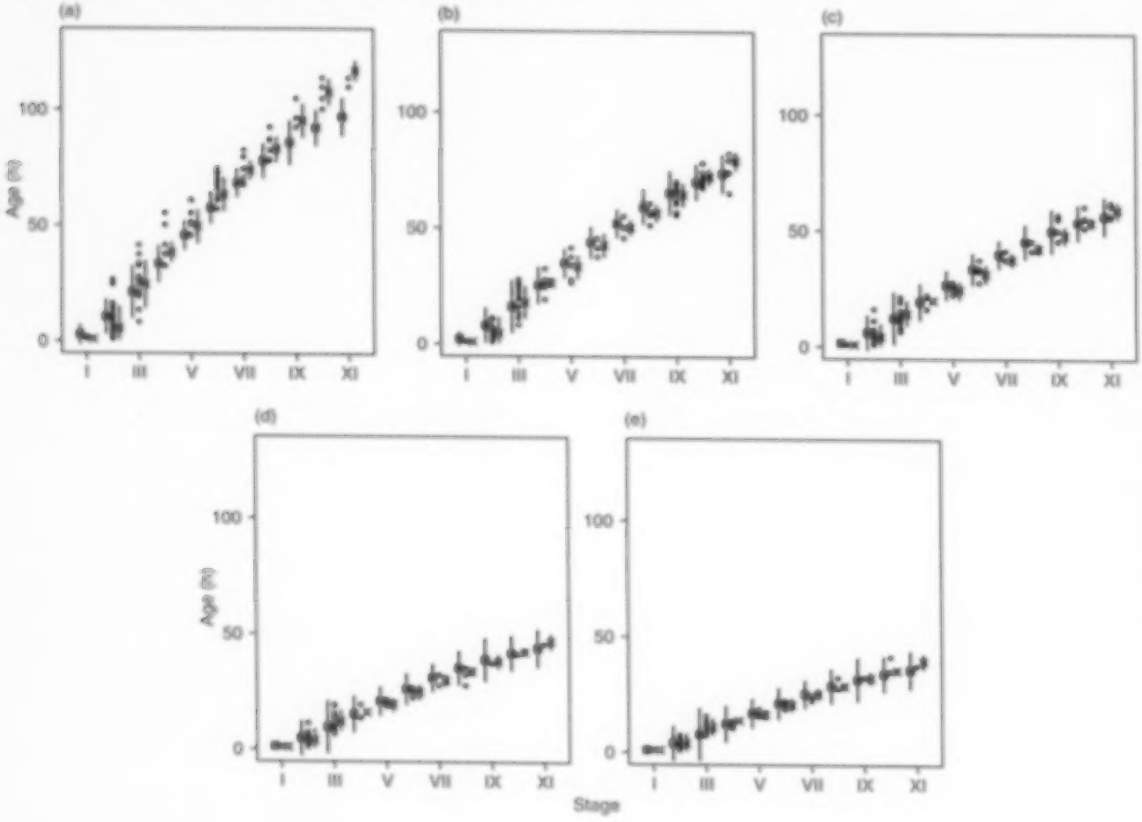

gonads according to their maturity stage or development of copepods or transition from larvae to juvenile fish, among others, could be examined using multinomial models.

Among the two alternative types of multinomial models for categorical ordered data reviewed in this paper, the ones based on conditional probabilities are recommended better than those based on cumulative probabilities. CR logits are more adequate to model sequential developmental processes and allow the analysis of the probability of developing from one stage to the the next and the influence of various covariates in that transition. In addition, in CR logit models, the assumption of equal effect of the covariates for all the stages can be easily implemented and tested.

Other models than the ones presented in this paper that could also be explored encompass choice of different link functions, as for instance probit or complementary log–log, more flexible models allowing nonlinear effects and mixed models for random effects for the case of several developmental experiments or nonparametric regression models.

One of the appealing features of this approach is that it sets the base to define several statistics of biological interest in a formal way. Based on the individual probabilities calculated from the fitted model, stage duration can be defined in three different ways: as the age interval in which the occurrence of a given stage has a probability larger than a certain threshold, as the age interval in which a given stage is more likely than any other stage in that age range, or as the length of the age range for which it is more likely to develop from the previous stage but not to develop for the next one. The first approach is equivalent to the one used by Lo (1985) to describe stage duration in anchovy eggs, by defining stage duration as the 95% quantiles of the sampled distribution of ages for a given stage, weighted by the percentage of eggs in that specific stage. When estimating this quantity from an incubation experiment of a population of eggs, the age range of consecutive stages may overlap, as eggs have different developmental rates. Furthermore, at some ages more than two stages can be found. The overlap between the stages gives an idea of the individual variability in the developmental process. If no overlapping of age range is desired, the second approach can be used, which ensures no overlapping of ages between age range of each stage. Thus, the sum of all the durations results in the total time up to hatching. In case stage durations have to be compared, say for example stage durations according to different definitions, corresponding to different temperatures or individuals of different

© 2007 NRC Canada

Fig. 9. Age at which (*a*) 5%, (*b*) 50%, and (*c*) 95% of the eggs have developed from the previous stage depending on temperature according to model ECR_{1a}.

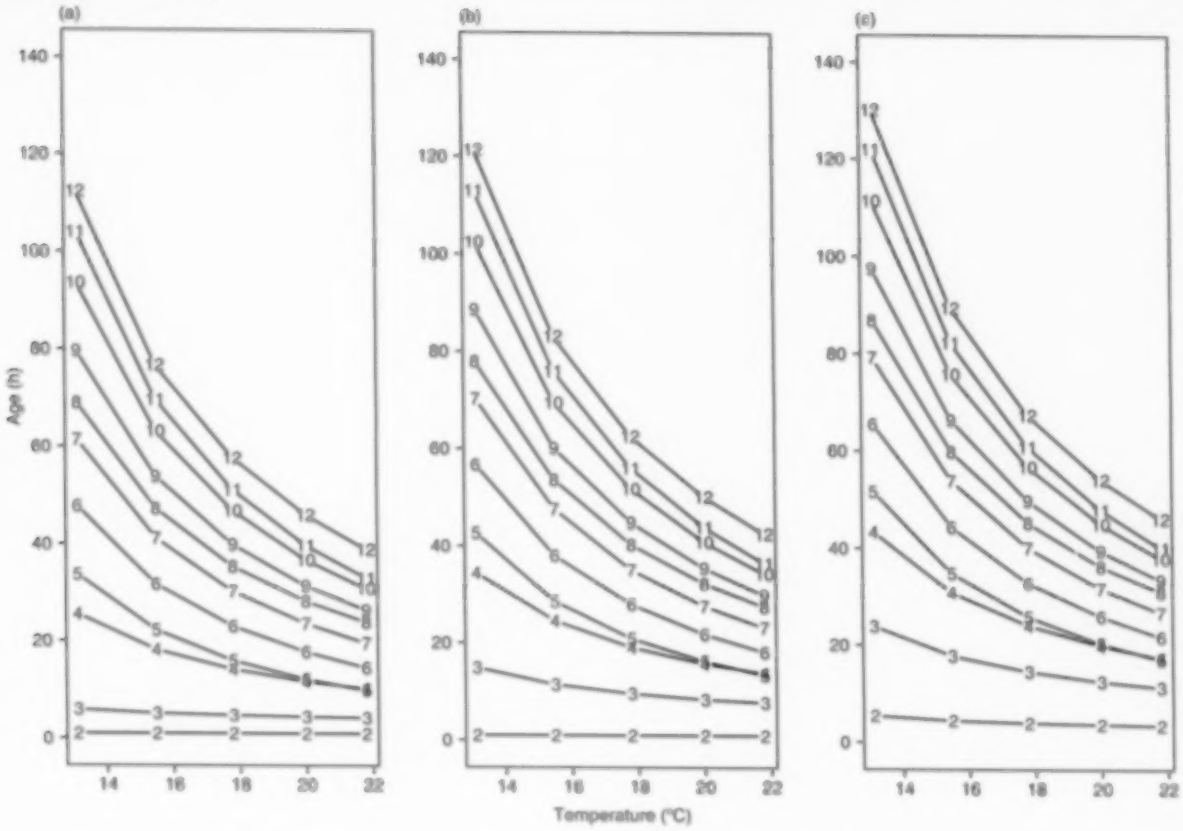

Table 3. Hatching times (h) depending on temperature from the fitted multinomial model ECR_{1a}.

	Temperature (°C)				
	13.13	15.50	17.81	20.00	21.81
P(Larvae) = 0.5	121.6	83.3	62.7	50.1	42.6
P(Larvae) = 0.99	135.3	93	70.3	56.4	48.1
P(Larvae) > *P*(Stage)	121.3	83.1	62.6	50.1	42.6
P(LarvaeIXI or Larvae) = 0.5	98.3	88	77.9	68.3	60.4

Note: *P*(Larvae) = 0.5 refers to the age at which 50% of the eggs have hatched; *P*(Larvae) = 0.99 refers to the age at which 99% of the eggs have hatched.

groups or experiments, relative stage durations (stage duration divided by the sum of the durations of all the stages) could be used. The third stage duration definition was based on the transition probabilities from one stage to the next. In some cases (as in our case study), this definition is equivalent to the second one. However, whereas sometimes a given stage can never be more probable than any other stage and thus the second definition cannot be applied, the transition probabilities can always be explored, even if duration cannot be derived, as it happened in the case study for stage IV and temperature 21.81 °C.

Apart from the approach described in this paper in which the statistics of interest are defined based on the fitted distribution of stage given age and the rest of explanatory variables, another approach will be to obtain the posterior distribution of ages given stage using Bayes' theorem and then extract the desired parameters from this posterior distribution (work in progress, some ideas presented in ICES 2004 and Stratoudakis et al. 2006). However, as how to extract parameters from a posterior distribution is well documented elsewhere, and it requires the assumption of a prior distribution of ages; therefore, this approach is not pursued in this paper.

Often, data coming from experiments are not complete, because the experiment finishes before planned because of errors or unexpected facts. For these data sets, multinomial

© 2007 NRC Canada

models provide a framework to safely explore the data by allowing the estimation of parameter significances and thus extract as much information as possible.

In particular, in the case study on anchovy incubation, ECR models were the best models of the ones tried out. Developmental properties estimated from the fitted models represented the data adequately and extracted main features of the egg development process. Fitted coefficients showed that the higher the incubation temperature, the faster the progression to the next stage. Besides the first stage that lasted ~1 h from the fertilization to the first cellular division, stage IV turned out to be the shortest one, especially for warmer temperatures (≥20 °C). Time to hatching defined as the age at which 99% of the eggs had already hatched was between 135 and 48 h for temperatures between 13 and 22 °C. The mean temperature in the Bay of Biscay during the main spawning period (May–June) is ~16.22 °C, corresponding to 81.65 h (3.4 days) for hatching. For the experiment used in this paper, neither the number of dead eggs nor the larval abundance were recorded. In case these data were available, survival from one stage to the next could also be studied.

Further work currently in progress regarding both sardines (*Sardinops pilchardus*) and anchovies incorporates the fitted multinomial model into a general Bayesian framework that allows to age each individual sampled at sea when only the developmental stage is observed.

Acknowledgements

Thanks are due to the crew of the R/V *Cornide de Saavedra*, where the incubation experiment was carried out. We are especially indebted to Amor Solá and Inmaculada Martín, who helped in the sampling and staging of eggs. Part of this work has been conducted within the EU FAR and AIR program Project MA-2495 and the EU Programme of Studies in Support of the Common Fisheries Policies Project No. 99/080, with the additional financial aid of the Department of Agriculture and Fisheries of the Basque government.The authors thank all participants in these projects for useful comments and discussions. The work of L. Ibaibarriaga was partly funded by the Agriculture and Fisheries Department of the Basque government. This paper is contribution No. 365 from AZTI-Tecnalia (Marine Research Unit).

References

Agresti, A. 1990. Categorical data analysis. John Wiley & Sons, Inc., New York.

Ahlstrom, E.H. 1943. Studies on the Pacific pilchard or sardine (*Sardinops caerula*). Influence of temperature on the rate of development of pilchard eggs in nature. US Fish. Wildl. Serv. Spec. Sci. Rep. 23.

Ahlstrom, E.H., and Moser, H.G. 1980. Characters useful in identification of pelagic marine fish eggs. Calif. Coop. Oceanic Fish. Investig. Rep. **21**: 121–131.

Ananth, C.V., and Kleinbaum, D.G. 1997. Regression models for ordinal responses: a review of methods and applications. Int. J. Epidemiol. **26**: 1323–1333.

Anderson, J.A. 1984. Regression and ordered categorical variables (with discussion). J. R. Stat. Soc. B, **46**: 1–30.

Armstrong, B.G., and Sloan, M. 1989. Ordinal regression models for epidemiological data. Am. J. Epidemiol. **129**: 191–204.

Bender, R., and Benner, A. 2000. Calculating ordinal regression models in SAS and S-plus. Biom. J. **42**: 677–699.

Bender, R., and Grouven, U. 1998. Using binary logistic regression models for ordinal data with non-proportional odds. J. Clin. Epidemiol. **51**: 809–816.

Chambers, R.C., and Tripple, E.A. 1997. Early life history and recruitment in fish populations. Chapman and Hall, London.

Fuiman, L.A., and Werner, R.G. 2002. Fisheries science: the unique contribution of early life stages. Blackwell Publishing, Oxford.

Gadomski, D.M., and Caddell, S.M. 1991. Effects of temperature on early-life-history stages of California halibut, *Paralichthys californicus*. Fish. Bull. **89**: 567–576.

Guisan, A., and Harrell, F.E. 2000. Ordinal response regression models in ecology. J. Veg. Sci. **11**: 617–626.

Gunderson, D.R. 1993. Survey of fisheries resources. John Wiley & Sons, Inc., New York.

Hempel, G. 1979. Early life history of marine fish: the egg stage. University of Washington Press, Seattle.

Hunter, J.R., and Macewicz, B.J. 1985. Measurement of spawning frequency in multiple spawning fishes. NMFS NOAA Tech. Rep. 36. pp. 79–94.

ICES. 2004. The DEPM estimation of spawning stock biomass for sardine and anchovy. ICES Coop. Res. Rep. 268.

Kvist, T., Gislason, H., and Thyregod, P. 2000. Using continuation-ratio logits to analyze the variation of the age composition of fish catches. J. Appl. Stat. **27**: 303–319.

Lasker, R. 1981. Marine fish larvae: morphology, ecology, and relation to fisheries. Washington Sea Grant Program, University of Washington Press, Seattle.

Lo, N.C.H. 1985. A model for temperature-dependent northern anchovy egg development and an automated procedure for the assignment of age to staged eggs. NMFS NOAA Tech. Rep. 36. pp. 43–50.

Lockwood, S.J., Nichols, J.H., and Coombs, S.H. 1977. The development rates of mackerel (*Scomber scombrus* L.) eggs over a range of temperatures. ICES CM. 1977/J:13.

Mauchline, J. 1998. The biology of calanoid copepods. Adv. Mar. Biol. Ser. 33. Academic Press, New York.

McCullagh, P. 1980. Regression models for ordinal data (with discussion). J. R. Stat. Soc. B, **42**: 109–142.

McCullagh, P., and Nelder, J.A. 1989. Generalized linear models. 2nd ed. Chapman and Hall, London.

McLaren, I.A., Sévigny, J.M., and Corkett, C.J. 1987. Temperature-dependent development in *Pseudocalanus* species. Can. J. Zool. **67**: 559–564.

Miller, C.B., and Tande, K.S. 1993. Stage duration estimation for *Calanus* populations, a modelling study. Mar. Ecol. Prog. Ser. **102**: 15–34.

Moser, M.H., and Ahlstrom, E.H. 1985. Staging anchovy eggs. NMFS NOAA Tech. Rep. 36. pp. 37–42.

Motos, L. 1994. Estimación de la biomasa desovante de la anchoa en el Golfo de Vizcaya, *Engraulis encrasicolus*, a partir de su producción de huevos. Bases metodológicas y aplicación. Ph.D. thesis, University of the Basque Country, Leioa, Spain.

Murua, H., Kraus, G., Saborido-Rey, F., Witthames, P.R., Thorsen, A., and Junquera, S. 2003. Procedures to estimate fecundity of marine fish species in relation to their reproductive strategy. J. Northwest Atl. Fish. Sci. **33**: 33–54.

Parker, K. 1980. A direct method for estimating northern anchovy, *Engraulis mordax*, spawning biomass. Fish. Bull. **78**: 541–544.

© 2007 NRC Canada

Pepin, P. 1991. Effect of temperature and size on development, mortality, and survival rates of the pelagic early life history stages of marine fish. Can. J. Fish. Aquat. Sci. **48**: 503–518.

Peterson, B., and Harrell, F.E., Jr. 1990. Partial proportional odds models for ordinal response variables. Appl. Stat. **39**: 205–217.

Rindorf, A., and Lewy, P. 2001. Analyses of length and age distributions using continuation-ratio logits. Can. J. Fish. Aquat. Sci. **58**: 1141–1152.

Russell, F.S. 1976. The eggs and planktonic stages of British marine fishes. Academic Press, New York.

Santiago, J., and Sanz, A. 1992. Egg production estimates of the Bay of Biscay anchovy, *Engraulis encrasicolus* (L.), spawning stock in 1987 and 1988. Bol. Inst. Esp. Oceanogr. **8**: 225–230.

Stratoudakis, Y., Bernal, M., Ganias, K., and Uriarte, A. 2006. The daily egg production method: recent advances, current applications and future challenges. Fish Fish. **7**(1): 35–57.

Thomas, W.H., Scotten, H.L., and Bradshaw, J.S. 1963. Thermal gradient incubators for small aquatic organisms. Limnol. Oceanogr. **8**: 357–360.

© 2007 NRC Canada

Estimating larval fish growth under size-dependent mortality: a numerical analysis of bias

Tian Tian, Øyvind Fiksen, and Arild Folkvord

Abstract: The early larval phase is characterized by high growth and mortality rates. Estimates of growth from both population (cross-sectional) and individual (longitudinal) data may be biased when mortality is size-dependent. Here, we use a simple individual-based model to assess the range of bias in estimates of growth under various size-dependent patterns of growth and mortality rates. A series of simulations indicate that size distribution of individuals in the population may contribute significantly to bias in growth estimates, but that typical size-dependent growth patterns have minor effects. Growth rate estimates from longitudinal data (otolith readings) are closer to true values than estimates from cross-sectional data (population growth rates). The latter may produce bias in growth estimation of about 0.03 day^{-1} (in instantaneous, specific growth rate) or >40% difference in some situations. Four potential patterns of size-dependent mortality are tested and analyzed for their impact on growth estimates. The bias is shown to yield large differences in estimated cohort survival rates. High autocorrelation and variance in growth rates tend to increase growth estimates and bias, as well as recruitment success. We also found that autocorrelated growth patterns, reflecting environmental variance structure, had strong impact on recruitment success of a cohort.

Résumé : Le début de la phase larvaire se caractérise par des taux élevés de croissance et de mortalité. L'estimation de la croissance à l'aide de données provenant de la population (transversales) et des individus (longitudinales) peut être faussée lorsque la mortalité est dépendante de la taille. Nous utilisons ici un modèle simple basé sur l'individu afin d'évaluer l'étendue de l'erreur dans les estimations de croissance sous divers patrons de taux de croissance et de mortalité reliés à la taille. Une série de simulations indique que la distribution en taille des individus dans la population peut contribuer significativement à l'erreur des estimations de croissance, mais que les patrons typiques de croissance dépendant de la taille n'ont que des effets mineurs. Les estimations de la croissance à partir de données longitudinales (lectures d'otolithes) sont plus près des valeurs réelles que les estimations à partir de données transversales (taux de croissance de la population). Ces dernières peuvent générer une erreur dans l'estimation de la croissance d'environ 0,03 jour^{-1} (taux spécifique instantané de croissance) ou une différence de >40 % dans certains cas. Nous testons quatre patrons potentiels de mortalité taille dépendante et analysons leur impact sur les estimations de croissance. Nous montrons que cette erreur produit d'importantes différences dans les estimations de taux de survie de la cohorte. Une autocorrélation et une variance importantes des taux de croissance ont tendance à faire augmenter les estimations de la croissance, l'erreur ainsi que le succès du recrutement. Nous observons également que les patrons de croissance autocorrélés, qui représentent la structure de la variance environnementale, ont un fort impact sur le succès du recrutement d'une cohorte.

[Traduit par la Rédaction]

Introduction

The early life history of fish is characterized by high rates of mortality (Cushing 1975; Bailey and Houde 1989; Leggett and Deblois 1994). Survival of marine pelagic organisms (e.g., eggs and larvae) change with size: larger individuals typically have lower risk of mortality (Peterson and Wroblewski 1984; McGurk 1986). The "growth–mortality" hypothesis argues that faster-growing and -developing larvae are more likely to pass through each stage rapidly, thereby lowering the cumulated mortality during early stages (Bailey and Houde 1989). Many fish species have allometric, dome-shaped specific growth rates, increasing during early ontogeny, leveling off, and eventually decreasing with size (Fonds et al. 1992; Folkvord 2005). The interaction between size-dependent growth and mortality affects the size distribution of larval survivors (Huston et al. 1988) and necessitates a distinction between population growth rates and true mean growth rates of individual fish (Ricker 1975), but it is known that bias is introduced when using mean values of population data under high mortality rates (e.g., Otterå 1992).

Received 22 June 2006. Accepted 13 December 2006. Published on the NRC Research Press Web site at http://cjfas.nrc.ca on 14 April 2007.
J19381

T. Tian,[1,2] Ø. Fiksen, and A. Folkvord. Department of Biology, University of Bergen, P.O. Box 7800, 5020 Bergen, Norway.

[1]Corresponding author (e-mail: tian.tian@gkss.de).

[2]Present address: Institute for Coastal Research, GKSS Research Center, Max Planck Street 1, Building 11 (KOE), 21502 Geesthacht, Germany.

 doi:10.1139/F07-031 © 2007 NRC Canada

One way to estimate growth is to group discrete population samples and compare mean size of surviving fish at successive ages. This is termed "cross-sectional" data analysis for population growth rate. Such analysis assumes no size-biased sampling or mortality between sampling intervals (Ricker 1975). Alternatively, "longitudinal" data from otolith readings use individual growth trajectories of sampled larvae (Chambers and Miller 1995). However, longitudinal growth estimates of survivors from the same cohort sampled at different times will differ under significant size-dependent mortality as some size fractions are less likely to be included in subsequent samples. The classical example is when bias emerges as a result of size selection by a fishery ("Lee's phenomenon"; Ricker 1975).

Given the absence of correction for size-dependent mortality in larval fish growth estimates, it is instructive to know under which conditions bias occurs. Both growth and mortality are highly nonlinear processes and the interactions between them are far from trivial. Huston and DeAngelis (1987) listed four critical factors responsible for changes in size distributions as individuals develop: (*i*) the initial size distribution; (*ii*) the distribution of growth rates among the individuals; (*iii*) the size and time dependence of the growth rate of each individual; and (*iv*) size-dependent mortality. Furthermore, short-term, small-scale environmental variability are expected to affect cohort survival rate (Letcher and Rice 1997; Pitchford and Brindley 2001; Pitchford et al. 2005), and thus the mean properties from population data may not accurately predict development and survival of fish populations (Rice et al. 1993; Gallego et al. 1996; Pepin 2004).

The many advantages of individual-based models (IBMs) in ecology have been discussed by various authors (Huston et al. 1988; DeAngelis and Gross 1992; Grimm and Railsback 2005). Here we use an IBM to trace growth and survival of a larval cohort through early life stages under various scenarios of size-dependent growth and mortality rates. Knowing the growth rates of survivors, we then estimate daily growth rates of the developing population with cross-sectional or longitudinal methods (Ricker 1975; Chambers and Miller 1995). The biases are obtained by comparing average growth rates of individuals at successive ages with the average growth rates of final survivors. The potential magnitudes and patterns of bias are evaluated according to three patterns or mechanisms of size-dependent mortality rate: (*i*) decreasing with size (Peterson and Wroblewski 1984; McGurk 1986); (*ii*) increasing with size (visual predation); and (*iii*) threshold size dependence in escape (e.g., gape-limited intracohort cannibalism). Two species with different allometric growth patterns (larval Atlantic cod (*Gadus morhua*) and Atlantic herring (*Clupea harengus*)) are chosen as model organisms. Cod larvae have a dome-shaped growth potential with size (Otterlei et al. 1999), whereas growth rate in larval herring is relatively independent of size (Fiksen and Folkvord 1999). We also investigate bias under variable and autocorrelated growth rates, which is anticipated for patchy environments, and how this environmental structure affects cohort survival in the model. In summary, we wish to determine (*i*) the magnitude of bias induced by using mean values of population data; (*ii*) how potential bias of growth varies with larval size, initial size distribution, and the allometric patterns of growth- and size-dependent mortality regimes; and (*iii*) the effects of environmental variability on larval survival and growth estimates.

Materials and methods

The individual-based model is initialized with a cohort of 2-day-old yolk-sac larval cod. Population size declines dramatically as the result of size-dependent mortality, therefore the "super-individual" concept (Scheffer et al. 1995) is applied (grouping together many individuals with identical attributes). We let 10^4 super-individuals represent the larval cohort. Four attributes characterize each super-individual i over time: dry weight (DW_i, mg), standard length (SL_i, mm), probability of survival (Ps_i), and the number of identical individual survivors (N_i) represented by each super-individual. (Appendix A defines all symbols used for growth estimates in the IBM.) Age is implicit as only a single cohort is traced. Simulations run until larvae reach an age of 60 days posthatch (DPH) in time steps of 1 h. Data of all super-individuals are stored once each day and compared with population assessments.

Larval growth models

Daily growth (SGR, %·day^{-1}) of larval Norwegian coastal cod (*Gadus morhua*) under optimal conditions in the lab is a function of dry body mass (DW, mg) and water temperature (T, °C) (Otterlei et al. 1999; Folkvord 2005):

$$\text{(1)}\quad \mathrm{SGR}(T,\mathrm{DW}) = 1.20 + 1.80\,T - 0.078\,T(\ln \mathrm{DW}) - 0.0946\,T(\ln \mathrm{DW})^2 + 0.0105\,T(\ln \mathrm{DW})^3$$

Here, we keep the temperature fixed at 6 °C, and then this translates to a specific instantaneous growth rate $g_{c,i}(\mathrm{DW}_i)$ of larval cod i with body mass DW_i:

$$\text{(2)}\quad g_{c,i}(\mathrm{DW}_i) = \ln\left[\frac{\mathrm{SGR}(6,\mathrm{DW}_i)}{100} + 1\right]$$

For herring-like species, instantaneous growth rate $g_{h,i}$ is independent of size, and because temperature is fixed at 6 °C, growth is a constant (Fiksen and Folkvord 1999):

$$\text{(3)}\quad g_{h,i} = -0.024 + 0.012 \times 6 = 0.048$$

Environmental stochasticity in growth $\tilde{g}_{c,i}(\mathrm{DW}_i, t)$ was modeled as an autocorrelated process (Ripa and Lundberg 1996):

$$\text{(4)}\quad \tilde{g}_{c,i}(\mathrm{DW}_i,t) = g_{c,i}(\mathrm{DW}_i) + e_i(t)\,g_{c,i}(\mathrm{DW}_i)$$
$$e_i(t) = \alpha \cdot e_i(t-1) + \sigma \cdot n(0,1) \cdot \sqrt{1-\alpha^2}$$

where t is time in hours (e_i was reset once each day), $n(0,1)$ is a random number drawn from a standard normal distribution, α is the autocorrelation coefficient ($0 \le \alpha \le 1$), and σ is standard deviation (variance = σ^2). The growth rate $\tilde{g}_{c,i}(\mathrm{DW}_i,t)$ was not allowed to exceed 50% of the expected growth rate at any age, or to be less than 0. Equation 4 is practical in generating variability into individual growth trajectories, with no ($\alpha = 0$) or high autocorrelation (α approach 1) in time. For larval fish, this mimics a situation where growth rates of individuals are influenced by a patchy environment resulting from patchy prey, temperature, or other environ-

© 2007 NRC Canada

mental factors affecting growth. Low autocorrelation would simulate a fine-grained environment in which the likelihood of switching between good and bad environments on short time scales is high. High autocorrelation mimics more coarse-grained environments, so that a larva in a good or bad environment is likely to remain in this condition for some time. The structure of the environment may have implications for emerging size distributions of larval cohorts through distribution of growth rates among individuals and, consequently, their survival probabilities and bias of growth estimates.

Larval mortality rates

Mortality or predation rates of larval fish are typically highly size-dependent. If invertebrate predators are the dominating predators, risk of predation tends to decrease with size, but if visual predators are important, risk of predation may increase with size (Bailey and Houde 1989). Here, we have applied four basic models of changes in mortality rates with size, two empirical models in which mortality drops with size, one in which risk increases, and one that chops off the smaller fraction of the cohort every week.

The daily natural mortality rates M_P (day^{-1}) of pelagic organisms are observed to be dependent on body mass (Peterson and Wroblewski 1984):

$$(5) \qquad M_P = 5.3\times10^{-3}(10^{-3}\,\mathrm{DW})^{-0.25}$$

McGurk (1986) found mortality rates M_M (day^{-1}) of fish eggs and larvae to be even more size-dependent:

$$(6) \qquad M_M = 2.2\times10^{-4}(10^{-3}\,\mathrm{DW})^{-0.85}$$

Predation rate from fish M_f (day^{-1}) is assumed to be an increasing function of larval SL if other factors such as light, larval behavior, or depth of occurrence are held constant (Fiksen et al. 2002):

$$(7) \qquad M_f = 5.5\times10^{-4}\,\mathrm{SL}^2$$

In some situations, such as during intensive cannibalism or predation from an abundant gape-limited predator, all larvae below a given size may be removed from the population. In some situations, this could generate strong bias in growth estimates (Folkvord 1997). We remove larvae shorter than the average body length from the population at weekly intervals and refer to this mortality as M_c. SL (mm) as a function of body mass is $\mathrm{SL} = \exp[2.296 + 0.277(\ln\mathrm{DW}) - 0.005128(\ln\mathrm{DW})^3]$ for larval cod (Folkvord 2005) and $\mathrm{SL} = 4.76[\ln(10^3\,\mathrm{DW}) - 2.9]$ for larval herring (Fiksen and Folkvord 1999).

Given a size-dependent mortality rate $M[\mathrm{DW}_i(t)]$ (i.e., M_P, M_M, M_f, or M_c), the probability $Ps_i(t)$ of surviving one day (Δt) for each super-individual i depends on body mass and size dependency in mortality:

$$(8) \qquad Ps_i(t) = e^{-M[\mathrm{DW}_i(t)]\Delta t}$$

The number of individual survivors represented by each super-individual N_i will decrease with $Ps_i(t)$, such that each super-individual i represents fewer individuals over time. Super-individuals (10^5 individuals) are followed (60 days), each initially representing 10^6 (cod-like growth pattern) or 10^9 individuals (herring-like growth pattern).

Estimating population growth and defining bias

Population growth rate $g_{cs}(t)$ at time t (= age of cohort) from cross-sectional methods is estimated by using mean weight of individual larvae at successive days (Folkvord 1997):

$$(9) \qquad g_{cs}(t) = \frac{\ln\overline{\mathrm{DW}}(t) - \ln\overline{\mathrm{DW}}(t-1)}{\Delta t}$$

where $\overline{\mathrm{DW}}(t)$ and $\overline{\mathrm{DW}}(t-1)$ are the mean body sizes (mg dry weight) of all individuals at days t and $t-1$ (time interval $\Delta t = 1$ day) from

$$(10) \qquad \overline{\mathrm{DW}}(t) = \frac{\sum_{i=1}^{10000} \mathrm{DW}_i(t)\cdot N_i(t-1)\cdot Ps_i(t)}{\sum_{i=1}^{10000} N_i(t-1)\cdot Ps_i(t)}$$

The total abundance $\sum_{i=1}^{10000} N_i(t)$ at t differs from that at $t-1$ as some individuals die during this time interval as a result of size-dependent mortality. However, estimates of true mean growth rates (as defined by us) require initial and final mean weights from the same individuals (Fig. 1*a*). To follow the growth rates of survivors only, we first ran the model forward for 60 days, stored the size development of the final surviving larvae, and calculated what we defined as true daily mean growth rate g_{TMG}:

$$(11) \qquad g_{\mathrm{TMG}}(t) = \frac{\sum_{i=1}^{10000} N_i(60)\cdot g_i(\mathrm{DW}_i,t)}{\sum_{i=1}^{10000} N_i(60)}$$

With longitudinal data, the use of otoliths can yield information about individual growth trajectories that reflect true growth rates of survivors from samples at time $t+1$:

$$(12) \qquad g_{\mathrm{lon}}(t) = \frac{\sum_{i=1}^{10000} N_i(t+1)\cdot g_{c,i}(\mathrm{DW}_i,t)}{\sum_{i=1}^{10000} N_i(t+1)}$$

However, a sample of individuals from any time (or cohort age) t ($2 < t < 60$ DPH in the model) will give different growth histories compared with the final cohort under size-dependent mortality. This is because the final sample will consist of a size-biased subsample of all previous samples. We define bias inherent in longitudinal estimates as the difference in growth at age between a sample of survivors at 60 DPH and any sample from $t < 60$ DPH. Technically, the bias from cross-sectional ε_{cs} or longitudinal ε_{lon} data (Fig. 1*b*) is given by

$$(13) \qquad \varepsilon_{cs} = g_{cs} - g_{\mathrm{TMG}} \text{ and } \varepsilon_{lon} = g_{lon} - g_{\mathrm{TMG}}$$

Note that there will be no bias in any estimate if mortality is not dependent on larval size (constant mortality rate).

© 2007 NRC Canada

Fig. 1. (*a*) Illustration of the bias induced by size-dependent mortality and cross-sectional data with a sampling interval of 1 week. The bars represent three different initial populations, and the solid lines represent the second sample (i.e., final population). Dotted lines represent the size frequency of individuals back-calculated from the second samples assuming no mortality. Solid triangles on the abscissa indicate the average weight (0.034, 0.3, and 3.0 mg dry weight) of initial populations, and the y axis represents larval size frequency in population biomass. (*b*) The instantaneous growth rate (day^{-1}) estimated from cross-sectional or longitudinal data (continuously sampled) and the true mean growth rate back-calculated from 60 DPH.

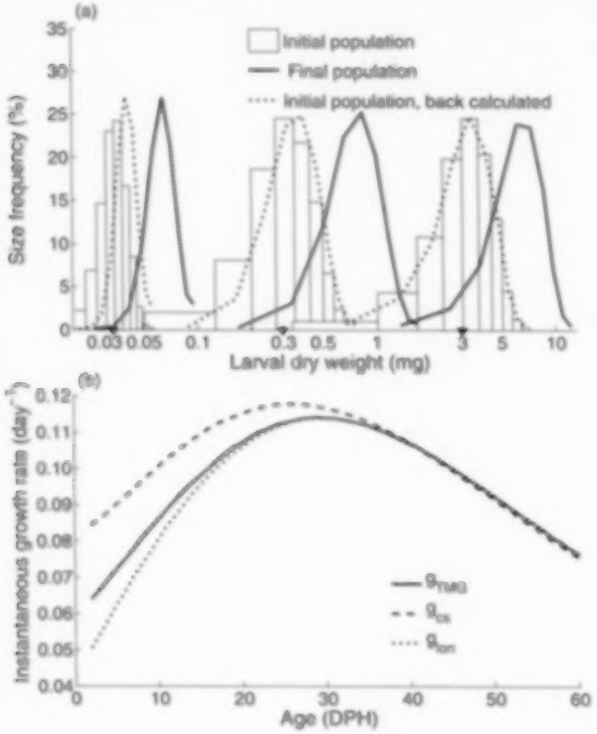

Overview of simulations

Unless specified otherwise, the initial dry weight of each super-individual is a normal deviate from a size distribution with mean dry weight (± standard deviation, SD) of 0.034 ± 0.006 mg (restricted downwards to 0.02 mg) as in the rearing experiment of Otterlei et al. (1999). As a standard, the growth pattern is dome-shaped with size (eq. 1), temperature is fixed at 6 °C, the mortality rate M_M from McGurk (1986) is used, and bias is given from cross-sectional assessment, with sampling intervals of 1 day.

We investigated the following potential candidates for bias in growth estimates.

Experiment 1: initial size distribution

We simulated growth estimates using initial body sizes from a normal (0.034 ± 0.006 mg) and a uniform (0.034 ± 0.01 mg) distribution with a fixed coefficient of variation (CV) of 17%. Cohort variance in weight distribution develops naturally from growth and mortality processes.

Experiment 2: initial body size and size variability

We initiated 10 cohorts with increasing mean weights (i.e., 0.034, 0.05, 0.1, 0.3, 0.5, 1.0, 3.0, 5.0, 10.0, and 30.0 mg). The cohorts were given CVs either fixed at 17% (populations were regenerated at each size category) or emerging naturally from a developing cohort. The estimated emergent CVs for each cohort in this case were 17%, 24%, 32%, 39%, 41%, 41%, 38%, 35%, 31%, and 24%, respectively. In this case, bias is obtained by comparing the population growth rate at 1-week intervals, and each cohort is assessed only once to mimic discrete sampling in the field.

Experiment 3: growth pattern

We simulated one cohort with dome-shaped growth rates (g_c, eq. 2) and one with constant specific growth rates (g_b, eq. 3) starting from the same initial population.

Experiment 4: size-dependent mortality rate

Each mortality model (M_M, M_P, M_t, and M_c) was assessed for effects on bias.

Experiment 5: demographic and environmental stochasticity

The stochasticity parameters α and σ (eq. 4) were varied and both bias and recruitment success were compared with deterministic simulations.

Results

Experiment 1: initial size distribution

Bias decreases near exponentially with age for both normal and uniform initial size distributions (Fig. 2*a*). A uniformly distributed larval cohort is more biased initially, but the normally distributed cohort becomes more biased after about 1 week. The maximal bias of 0.027 day^{-1} is about 40% of the true mean growth rate of 0.06 day^{-1}, but the bias decreases to less than 0.01 day^{-1} within 10 days.

Experiment 2: initial body size and size variability

For initial populations of increasing average weight but constant CV of 17%, bias peaks at 0.024 day^{-1} and decreases exponentially with weight (Fig. 2*b*). For initial populations with varying CVs, bias peaks at around 0.1 mg (0.03 day^{-1}). The size variation increases from 17% of the first initial population (smallest average size) to 32% of the third initial population owing to the dome-shaped growth pattern. The CV peaks (41%) at 0.5–1.0 mg, but the bias of growth estimates declines before this because mortality rate drops with weight and supersedes the effect of increasing variance. The mean body size of the initial population has some influence owing to the size-specific mortality function M_M, but the main factor generating biased estimates is weight variability of initial population (i.e., CV).

Experiment 3: growth pattern

When applying a size-independent growth rate (Fig. 2*c*), the constant CV of the size distribution will be preserved (as in experiment 2) and growth estimates are biased only by

© 2007 NRC Canada

Fig. 2. Bias (ε_{g_a}, in terms of specific growth per day, see eq. 13) induced by size-dependent mortality estimated in four numerical experiments. (*a*) Experiment 1: bias with different initial length distributions, uniform (solid line) and normally distributed (shaded line), respectively. The initial populations are illustrated in the inset: uniform distribution (open bars) and normal distribution (shaded bars). (*b*) Bias depending on mean weight of initial populations and initial size distribution. The CV of the initial populations is either constant (start populations are reset at each mean size (shaded line)) or varying (CVs emerge from cohort development (solid line)). Bars in the inset illustrate 3 of 10 initial populations with constant (shaded bars) or varying (open bars) CVs, respectively. (*c*) True and estimated growth rate and bias (day^{-1}) for larvae with constant growth (g_a) and size-dependent mortality M_M. (*d*) Bias in growth estimate from four models of size-dependent mortality rate (M_M, M_P, M_I, and M_c).

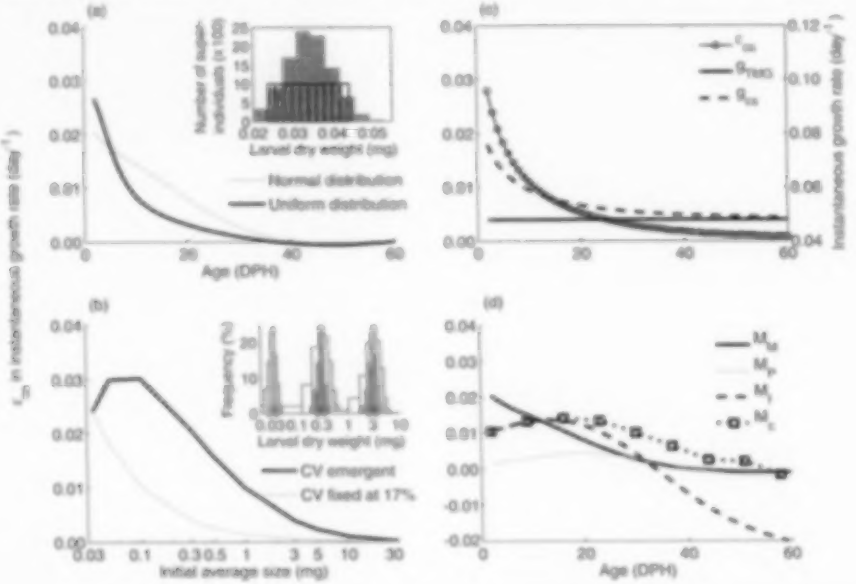

size-dependent mortality rate. The maximal bias for constant growth is 0.028 day^{-1} compared with the true growth rate of 0.048 day^{-1}. This suggests that initial size distribution is more important than growth pattern when the size-dependent mortality rate is high.

Experiment 4: size-dependent mortality regimes

Estimates of growth rates are sensitive to the pattern of size-dependent mortality (Fig. 2*d*). The mortality model M_M can yield population growth rates 0.02 day^{-1} above true values, whereas the weaker size dependence from the Peterson and Wroblewski (1984) model M_P give almost no bias. Visual predators are positively size selective, producing an underestimation of growth rate that is negligible when larvae are small but more evident as the larvae grow. The initial positive bias under visual predation is a result of the dome-shaped (initially increasing) growth pattern with size. Gape-limited selection for the smallest larvae is simulated by culling larvae shorter than average length from the population weekly. The maximum bias is still less than 0.02 day^{-1}.

Experiment 5: demographic stochasticity and environmental grain

Here we test effects on growth estimates from varying the autocorrelation coefficient α and variance σ^2. Generally the inclusion of stochasticity leads to similar maximum magnitudes of bias as in the deterministic case (≤0.02 day^{-1}). However, stochasticity itself changes both estimated population growth rates and true mean growth rates. With no autocorrelation ($\alpha = 0$), the survivors grow similarly to those in the deterministic growth pattern (Fig. 3). With autocorrelation, both estimated population growth rates and true mean growth rates increase above deterministic values, and consequently, the dome-shaped growth patterns peak earlier (Fig. 3). High autocorrelation ($\alpha = 0.9$) and higher variance (σ^2) allow some individuals to be more lucky initially and grow at high rates in the early phase with correspondingly high probability to be among the final survivors (Fig. 4). With strong size dependence in mortality, environmental stochasticity, and temporal autocorrelation (coarse-grained environments), survivors are those entrained in favorable environments in the early larval phase. This higher growth rate will shift up the size distribution of the cohort and lead to lower growth at higher ages owing to the dome-shaped growth pattern.

Implications of growth and mortality rates for cohort development

What is the implication of using biased (population estimates) rather than true growth rates (individual survivors) to assess cohort success? Applying the biased rather than the true rates of growth could cause two or more orders of magnitude differences in numbers reaching a given size (Table 1), or one order of magnitude difference when size-dependent mortality rate M_M is reduced by 10%. The importance of rapid growth in lowering cumulated mortality (e.g.,

© 2007 NRC Canada

Fig. 3. True mean growth rate (day^{-1}) of 60 DPH larval cod under three simulated stochastic environments (lines with symbols) compared with the deterministic model (solid line). Autocorrelation and variance in the environment reflects the degree of patchiness in the environment. Note that growth rates feed back on the size structure at age, which then feeds back on growth rates because of the dome-shaped growth pattern with size; therefore relatively high growth rate at early age necessarily leads to lower growth rates at higher age.

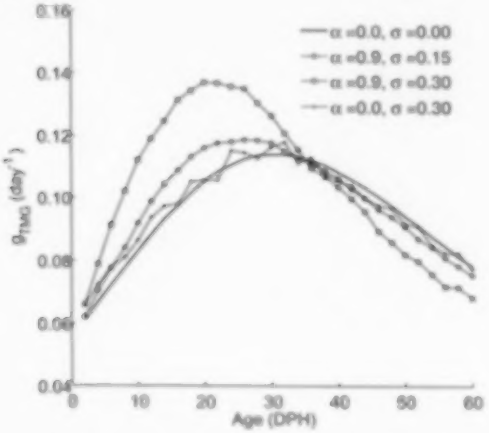

Fig. 4. Growth rate trajectories of 1000 super-individuals (shaded lines) of the cohort and the final survivors (solid lines) after 60 DPH for four scenarios: (*a*) $\alpha = 0.0$ and $\sigma = 0.0$, five super-individuals survived; (*b*) $\alpha = 0.0$ and $\sigma = 0.30$, eight super-individuals survived; (*c*) $\alpha = 0.9$ and $\sigma = 0.15$, 10 super-individuals survived; (*d*) $\alpha = 0.9$ and $\sigma = 0.30$, 32 super-individuals survived.

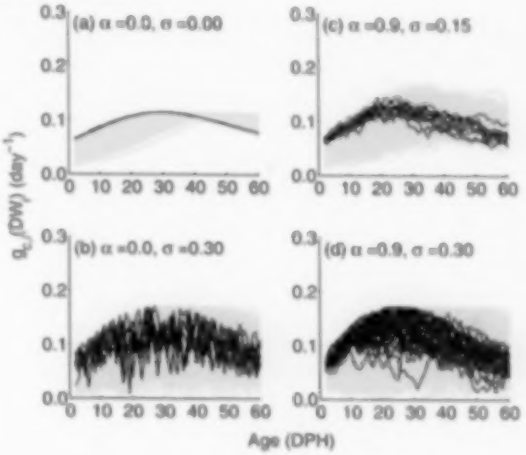

Chambers and Trippel 1997) is also clear from this example. Applying M_M leaves only 7 survivors of 10^{10} after 48 days (Table 1), whereas M_P leaves 10^9 individuals.

Environmental variance structure and recruitment success

How will environmental variance structure affect larval survival? How important is the variability experienced in growth conditions between individuals for recruitment? The individual growth trajectories of survivors (Fig. 4) illustrate the importance of rapid growth in early life. Using the standard version of the model, we evaluate recruitment success as the number of surviving individual larva reaching 3.0 mg dry weight under different stochasticity schemes (autocorrelation and variance in growth determined by sets of parameters α and σ^2). Recruitment increases markedly with autocorrelation when $\sigma > 0.3$ and with σ when $\alpha > 0.4$ (Fig. 5). Generally, higher autocorrelation and variance leads to higher recruitment.

Discussion

The correction for size-dependent mortality in growth estimation, whether in the laboratory or field, is important but difficult to carry out in practice. It is therefore essential to know the magnitude and pattern of bias and to understand which factors and methods could generate biased estimates from data analysis. This study aims not to predict the exact errors involved in field or enclosures studies, but rather to theoretically explore the mechanisms under which the potential bias is likely to be significant.

Our results confirmed that growth estimates from individual-based longitudinal data are more accurate than rates obtained from cross-sectional data. However, it is important to realize that even longitudinal estimates (e.g., otolith-based) can be biased when mortality rate is size-dependent. Significant bias is most likely to occur during the first 30 days of larval life. Estimates of growth rate may vary considerably depending on the initial size distribution. In particular, special attention should be paid to size distribution of similar-aged groups of small larvae when cross-sectional data are used to estimate growth (Folkvord et al. 1994). Allometric growth patterns did not affect growth estimates. Generally, the lower the growth rates of individuals, the higher is the bias induced by higher mortality rates. Based on our results, we recommend that ecological interpretations of differences less than 0.03 day^{-1} in estimated specific growth rates of larval fish be treated with caution as these differences can arise from estimation bias alone.

The model predicts that autocorrelated growth rates at the level of individuals will increase recruitment success. Some investigations report that prey species of larval fishes exhibit strong patchiness at spatial scales ranging from tens of kilometres to less than 10 m (e.g., Currie et al. 1998; Tokarev et al. 1998). It has been discussed for some time that prey patchiness may have a large effect on individual growth rates of fish larvae by causing variable encounter rates with prey over time, which could therefore have a wide range of effects on individual and cohort survival, depending on the scale and the intensity of patchiness and how the larval individuals react in the field (Pitchford and Brindley 2001; Pitchford et al. 2003; Pepin 2004). Individual growth both in otoliths and length are observed with significant serial autocorrelation (Folkvord et al. 2000; Pepin et al. 2001). The importance of environmental variability (e.g., temperature, food concentration, light, and turbulence) in regulating cohort survival rate has also been demonstrated in simulation studies (Gallego and Heath 1997; Letcher and Rice 1997;

© 2007 NRC Canada

Table 1. Recruitment variability predicted from true mean growth rate (TMG) (dome-shaped growth pattern), biased estimates, and various mortality formulations.

Growth rate (day^{-1})	Mortality rate (day^{-1})	Stage duration as recruits (days)	No. of recruits
g_{TMG}*	$1.0 \times M_M$	48	7
g_{TMG}*	$0.9 \times M_M$	48	59
$g_{TMG} + \varepsilon_{cv}$†	$1.0 \times M_M$	42	1 302
$g_{TMG} + \varepsilon_{cv}$†	$0.9 \times M_M$	42	6 357
$g_{TMG} + \varepsilon_{cv}$‡	$1.0 \times M_M$	38	12 245
$g_{TMG} + \varepsilon_{cv}$‡	$0.9 \times M_M$	38	47 769

Note: Average initial size is 0.034 mg dry weight for 10^{10} individuals and recruitment is defined as the number of surviving individuals reaching 3.0 mg dry weight. Stage duration: time to reach 3.0 mg dry weight as recruits.

*Model from Folkvord (2005); see eqs. 1 and 2.

†Biased growth rate from a cohort with normal initial size distribution (Fig. 2a).

‡Biased growth rate from discrete samples with varying CVs (Fig. 2b).

Fig. 5. Recruitment variability related to environmental stochasticity and spatial–temporal structure. Recruitment is defined as the total number of individual survivors up to 3.0 mg dry weight as predicted by the standard version of the model in all cases of stochastic schemes (experiment 5). The number of survivors in the deterministic case is 561.

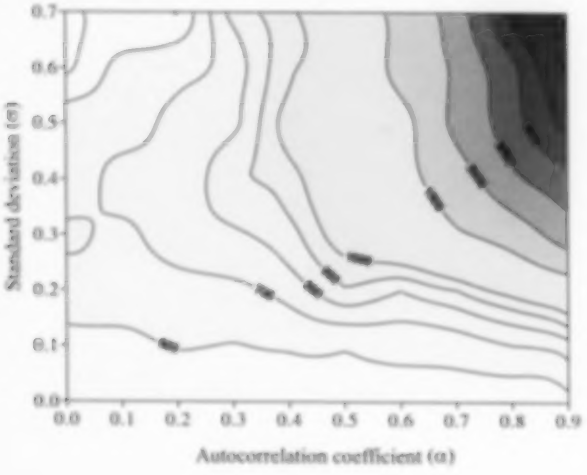

Lough et al. 2005). Gallego et al. (1996) suggest that daily growth variation in length are likely to reflect changes in the growth environment more closely during the larval stage because of relative low amounts of reserves and that small-scale spatial and temporal environmental variability in food availability influenced by, e.g., turbulence or light could be more important for larval survival than large-scale variation.

Our more abstract model confirms this general result and shows clearly how environmental variability structure may generate deviations between the survivors and the average individual. An implication is that the environmental variability will increase growth rate of survivors relative to the average individual under size-dependent mortality (Gallego and Heath 1997; Pepin et al. 2001; Dower et al. 2002). We simulated the relative scale between an individual and a patch by the autocorrelation coefficient. Low autocorrelation implies that patchiness is so small that individuals frequently switch between good and bad conditions. Higher autocorrelation will keep individuals in good or bad environments over longer times, sorting out clear winners and losers, where winners will be fast-growing larvae with high chance of survival.

Accurate estimates of both growth and mortality rates are necessary to evaluate causes of recruitment failure and success in larval fish (Ricker 1975; Buckley et al. 2000; Govoni 2005). Back-calculation based on otolith readings offers greater potential accuracy than traditional techniques (Campana 1990; Anderson 1995). Besides, otolith techniques make the trajectories of fish early life history identifiable individually and then provide critical means to determine whether mortalities are at random or not (Chambers and Miller 1995). However, as Suthers et al. (1999) and Folkvord et al. (2000) pointed out, the precision of otolith growth history determination is restricted to periods with increment widths above 1–2 μm. In several species in the temperate waters, larval growth in the first 2–3 weeks posthatch is characterized by increments around 1 μm, which leads to the inaccuracy of mean growth rate estimated by individual-level historical growth in the field (Pepin et al. 2001).

An interesting topic for the future will be to make our model spatially explicit to further increase the understanding of spatially and temporally patchy environmental effects (e.g., frontal zones, prey patchiness, and temperature variability on various scales) on larval growth and survival and to quantify autocorrelation coefficients and the variance of stochastic factors relevant to individual larval growth in the field. Such analyses could also cast some light on potential benefits of extensive spawning periods, batch spawning, or the selection of spawning grounds in a variety of fishes.

Acknowledgements

This is a contribution to GLOBEC Norway, ECOBE. T. Tian was funded by the Erasmus Mundus Programme, and Ø. Fiksen and A. Folkvord acknowledge the Norwegian Research Council for financial support. The manuscript benefited from comments made by two anonymous reviewers.

© 2007 NRC Canada

References

Anderson, C.S. 1995. Calculating size-dependent relative survival from samples taken before and after selection. *In* Recent developments in fish otolith research. *Edited by* D.H. Secor, J.M. Dean, and S.E. Campana. University of South Carolina Press, Columbia, S.C. pp. 455–466.

Bailey, K.M., and Houde, E.D. 1989. Predation on eggs and larvae of marine fishes and the recruitment problem. Adv. Mar. Biol. **25**: 1–83.

Buckley, L.J., Lough, R.G., Peck, M.A., and Werner, F.E. 2000. Comment: larval Atlantic cod and haddock growth models, metabolism, ingestion, and temperature effects. Can. J. Fish. Aquat. Sci. **57**: 1957–1960.

Campana, S.E. 1990. How reliable are growth back-calculations based on otoliths. Can. J. Fish. Aquat. Sci. **47**: 2219–2227.

Chambers, R.C., and Miller, T.J. 1995. Evaluating fish growth by means of otolith increment analysis: special properties of individual-level longitudinal data. *In* Recent developments in fish otolith research. *Edited by* D.H. Secor, J.M. Dean, and S.E. Campana. University of South Carolina Press, Columbia, S.C. pp. 155–175.

Chambers, R.C., and Trippel, E.A. 1997. Early life history and recruitment in fish populations. Chapman and Hall Ltd., London, UK.

Currie, W.J.S., Claereboudt, M.R., and Roff, J.C. 1998. Gaps and patches in the ocean: a one-dimensional analysis of planktonic distributions. Mar. Ecol. Prog. Ser. **171**: 15–21.

Cushing, D.H. 1975. Marine ecology and fisheries. Cambridge University Press, Cambridge, UK.

DeAngelis, D.L., and Gross, L.J. 1992. Individual based models and approaches in ecology: concepts and models. Routledge, Chapman and Hall, New York.

Dower, J.F., Pepin, P., and Leggett, W.C. 2002. Using patch studies to link mesoscale patterns of feeding and growth in larval fish to environmental variability. Fish. Oceanogr. **11**: 219–232.

Fiksen, Ø., and Folkvord, A. 1999. Modelling growth and ingestion processes in herring *Clupea harengus* larvae. Mar. Ecol. Prog. Ser. **184**: 273–289.

Fiksen, Ø., Aksnes, D.L., Flyum, M.H., and Giske, J. 2002. The influence of turbidity on growth and survival of fish larvae: a numerical analysis. Hydrobiologia, **484**: 49–59.

Folkvord, A. 1997. Ontogeny of cannibalism in larval and juvenile fish with special emphasis on Atlantic cod, *Gadus morhua* L. *In* Early life history and recruitment in fish populations. *Edited by* R.C. Chambers and E.A. Trippel. Chapman and Hall Ltd., London, UK. pp. 251–278.

Folkvord, A. 2005. Comparison of size-at-age of larval Atlantic cod (*Gadus morhua*) from different populations based on size- and temperature-dependent growth models. Can. J. Fish. Aquat. Sci. **62**: 1037–1052.

Folkvord, A., Øiestad, V., and Kvenseth, P.G. 1994. Growth patterns of three cohorts of Atlantic cod larvae (*Gadus morhua* L.) studied in a macrocosm. ICES J. Mar. Sci. **51**: 325–336.

Folkvord, A., Blom, G., Johannessen, A., and Moksness, E. 2000. Growth-dependent age estimation in herring (*Clupea harengus* L.) larvae. Fish. Res. **46**: 91–103.

Fonds, M., Cronie, R., Vethaak, A.D., and Van der Puyl, P. 1992. Metabolism, food consumption and growth of plaice (*Pleuronectes platessa*) and flounder (*Platichthys flesus*) in relation to fish size and temperature. Neth. J. Sea Res. **29:** 127–143.

Gallego, A., and Heath, M. 1997. The effect of growth-dependent mortality, external environment and internal dynamics on larval fish otolith growth: an individual-based modelling approach. J. Fish Biol. **51**(Suppl. A): 121–134.

Gallego, A., Heath, M.R., McKenzie, E., and Cargill, L.H. 1996. Environmentally induced short-term variability in the growth rates of larval herring. Mar. Ecol. Prog. Ser. **137**: 11–23.

Govoni, J.J. 2005. Fisheries oceanography and the ecology of early life histories of fishes: a perspective over fifty years. Sci. Mar. **69**: 125–137.

Grimm, V., and Railsback, S.F. 2005. Individual-based modeling and ecology. Princeton Univeristy Press, Princeton, N.J.

Huston, M.A., and DeAngelis, D.L. 1987. Size bimodality in monospecific populations: a critical review of potential mechanisms. Am. Nat. **129**: 678–707.

Huston, M.A., DeAngelis, D.L., and Post, W. 1988. New computer models unify ecological theory. Bioscience, **38**: 682–691.

Leggett, W.C., and Deblois, E. 1994. Recruitment in marine fishes — is it regulated by starvation and predation in the egg and larval stages. Neth. J. Sea Res. **32**: 119–134.

Letcher, B.H., and Rice, J.A. 1997. Prey patchiness and larval fish growth and survival: inferences from an individual-based model. Ecol. Model. **95**: 29–43.

Lough, R.G., Buckley, L.J., Werner, F.E., Quinlan, J.A., and Edwards, K.P. 2005. A general biophysical model of larval cod (*Gadus morhua*) growth applied to populations on Georges Bank. Fish. Oceanogr. **14:** 241–262.

McGurk, M.D. 1986. Natural mortality of marine pelagic fish eggs and larvae: role of spatial patchiness. Mar. Ecol. Prog. Ser. **34**: 227–242.

Otterlei, E., Nyhammer, G., Folkvord, A., and Stefansson, S.O. 1999. Temperature- and size-dependent growth of larval and early juvenile Atlantic cod (*Gadus morhua*): a comparative study of Norwegian coastal cod and northeast Arctic cod. Can. J. Fish. Aquat. Sci. **56**: 2099–2111.

Otterå, H. 1992. Bias in calculating growth rates in cod (*Gadus morhua* L.) due to size selective growth and mortality. J. Fish Biol. **40**: 465–467.

Pepin, P. 2004. Early life history studies of prey–predator interactions: quantifying the stochastic individual responses to environmental variability. Can. J. Fish. Aquat. Sci. **61**: 659–671.

Pepin, P., Dower, J.F., and Benoet, H.P. 2001. The role of measurement error on the interpretation of otolith increment width in the study of growth in larval fish. Can. J. Fish. Aquat. Sci. **58**: 2204–2212.

Peterson, I., and Wroblewski, J.S. 1984. Mortality rate of fishes in the pelagic ecosystem. Can. J. Fish. Aquat. Sci. **41**: 1117–1120.

Pitchford, J.W., and Brindley, J. 2001. Prey patchiness, predator survival and fish recruitment. Bull. Math. Biol. **63:** 527–546.

Pitchford, J.W., James, A., and Brindley, J. 2003. Optimal foraging in patchy turbulent environments. Mar. Ecol. Prog. Ser. **256**: 99–110.

Pitchford, J.W., James, A., and Brindley, J. 2005. Quantifying the effects of individual and environmental variability in fish recruitment. Fish. Oceanogr. **14**: 156–160.

Rice, J.A., Miller, T.J., Rose, K.A. Crowder, L.B., Marschall, E.A., Trebitz, A.S., and DeAngelis, D.L. 1993. Growth rate variation and larval survival: inferences from an individual-based size-dependent predation model. Can. J. Fish. Aquat. Sci. **50**: 133–142.

Ricker, W.E. 1975. Computation and interpretation of biological statistics of fish populations. Bull. Fish. Res. Board Can. No. 191.

Ripa, J., and Lundberg, P. 1996. Noise colour and the risk of population extinctions. Proc. R. Soc. Lond. B, **263**: 1751–1753.

© 2007 NRC Canada

Scheffer, M., Baveco, J.M., Deangelis, D.L., Rose, K.A., and Vannes, E.H. 1995. Super-individuals: a simple solution for modeling large populations on an individual basis. Ecol. Model. **80**: 161–170.

Suthers, I.M., van der Meeren, T., and Jorstad, K.E. 1999. Growth histories derived from otolith microstructure of three Norwegian cod stocks co-reared in mesocosms: effect of initial size and prey size changes. ICES J. Mar. Sci. **56**: 658–672.

Tokarev, Y.N., Williams, R., and Piontkovski, S.A. 1998. Small-scale plankton patchiness in the Black Sea euphotic layer. Hydrobiologia, **376**: 363–367.

Appendix A

Table A1. Symbols used for growth estimates in the individual-based model.

Symbols	Value and unit	Description
DW_i	mg dry weight	Dry weight
SL_i	mm	Standard length
Ps_i	—	Probability of survival
N_i	Individuals	The number of identical individual survivors represented by each super-individual. Initially 10^6 and 10^8 for cod- or herring-like species
SGR_i	%-day^{-1}	Size-specific growth rate of larval Norwegian coastal cod (*Gadus morhua*)
g_i ($g_{c,i}$ or $g_{h,i}$)	day^{-1}	Instantaneous growth rate for cod- or herring-like species
$\tilde{g}_{c,i}$	day^{-1}	Instantaneous growth rate with environmental stochasticity for cod-like species
e_i		Error term
α	[0, 1]	Autocorrelation coefficient
σ	[0, 0.7]	Standard deviation
$M_p(DW_i)$	day^{-1}	Mortality rate dependent on body mass (Peterson and Wroblewski 1984)
$M_M(DW_i)$	day^{-1}	Mortality rate dependent on body mass (McGurk 1986)
$M_f(SL_i)$	day^{-1}	Predation rate increasing with standard length
$M_c(SL_i)$	week^{-1}	Cannibalism predation rate dependent on relative standard length among the cohort
g_{cs}	day^{-1}	Instantaneous population growth rate from cross-sectional data
g_{lon}	day^{-1}	Instantaneous population growth rate from longitudinal data
g_{TMG}	day^{-1}	True mean growth rate of 60 DPH larvae
$\overline{DW}$	mg dry weight	Mean body mass of a cohort
e_{cs}	day^{-1}	Bias from cross-sectional data
e_{lon}	day^{-1}	Bias from longitudinal data

© 2007 NRC Canada

Relationship of upstream migrating adult Atlantic salmon (*Salmo salar*) and stream discharge within Catamaran Brook, New Brunswick

Sean C. Mitchell and Richard A. Cunjak

Abstract: Stream discharge has long been associated with abundance of returning adult spawning salmonids to streams and may also affect body size distribution of adult salmon as low flows interfere with returns of larger-bodied fish. We examined these relationships of abundance and body size within Catamaran Brook, a third-order tributary to the Miramichi River system of New Brunswick, Canada, to investigate the causes of a declining trend in annual returns of Atlantic salmon (*Salmo salar*) to this stream. Regression models of adult abundance, proportion of the run as grilse, and body size of returning adults as functions of maximum daily stream discharge during the period of upstream spawner migration were constructed. Adult abundance shows a logarithmic relationship with stream discharge and provides good predictive ability, while appearing to not be significantly related to adult abundance in the larger Miramichi system. The proportion as grilse in the run and female body size are also logarithmically related to stream discharge, with low flow years being very influential in the regressions. These relationships of Atlantic salmon population abundance and body size characteristics have implications with respect to stock integrity and production of the following generation.

Résumé : On associe depuis longtemps le débit des cours d'eau et l'abondance des saumons adultes qui reviennent y frayer; le débit peut aussi affecter la distribution des tailles des saumons adultes parce que les débits faibles nuisent au retour des poissons de plus grande taille. Nous avons examiné ces relations de l'abondance et de la taille dans Catamaran Brook, un tributaire d'ordre trois du système hydrographique de la Miramichi au Nouveau-Brunswick, afin d'étudier les causes d'une tendance au déclin des retours annuels des saumons atlantiques (*Salmo salar*) dans ce cours d'eau. Nous avons élaboré des modèles de régression de l'abondance des adultes, de la proportion de la montaison représentée par les madeleineaux et de la taille des adultes qui reviennent en fonction du débit journalier maximal durant la période de migration des reproducteurs vers l'amont. Il existe une relation logarithmique entre l'abondance des adultes et le débit du cours d'eau qui permet de faire de bonnes prédictions, alors qu'il ne semble pas y avoir de relation significative avec l'abondance des adultes dans l'ensemble du bassin versant de la Miramichi. Il y a aussi une relation logarithmique entre la proportion de madeleineaux dans la montaison et de la taille des femelles, d'une part, et le débit du cours d'eau, d'autre part; les années de faible débit ont une très forte influence sur les régressions. Ces relations de l'abondance et des caractéristiques de taille des populations de saumons atlantiques ont des conséquences sur l'intégrité des stocks et sur la production de la génération suivante.

[Traduit par la Rédaction]

Introduction

The abundance and certain population attributes (i.e., body size distribution and sex ratio) of upstream migrating adult anadromous salmon have long been known to be associated with river discharge. Pritchard (1936) commented that this relationship had been recognized qualitatively by nearly every investigator and reported the number of pink salmon (*Oncorhynchus gorbuscha*) to be related to water level in a small coastal stream of British Columbia. Hunter (1959) also maintained that stream discharge was an important factor controlling upstream movement of pink and chum (*Oncorhynchus keta*) salmon in another coastal British Columbia stream. Huntsman (1939, 1948) reported on the importance of high flow events in attracting Atlantic salmon (*Salmo salar*) and sea-run brook trout (*Salvelinus fontinalis*) into rivers of Nova Scotia, and Hayes (1953) conducted successful experimental manipulation of river flows in a large drainage within that province to affect salmon migration. In a Prince Edward Island stream, discharge was concluded to

Received 16 June 2006. Accepted 16 March 2007. Published on the NRC Research Press Web site at http://cjfas.nrc.ca on 18 April 2007.
J19367

S.C. Mitchell.[1] Canadian Rivers Institute, Department of Biology, University of New Brunswick, 55 MacKinnon Street, Antigonish, NS B2G 1M3, Canada.
R.A. Cunjak. Canadian Rivers Institute, Department of Biology, University of New Brunswick, Bag Service 45111, Fredericton, NB E3B 6E1, Canada.

[1]Corresponding author (e-mail: smitchel@stfx.ca).

 doi:10.1139/F07-032 © 2007 NRC Canada

be the dominant control on adult Atlantic salmon abundance (Saunders 1960). Banks (1969) reviewed the material to that time and Jonsson (1991) updated the review; both authors concluded that spawning migrations are associated with increased water flows.

There is, however, some contradictory evidence. Davidson et al. (1943) found no indication of a relationship between abundance and discharge in two pink salmon streams of Alaska, and Alabaster (1970) reported a correlation between abundance and flow for one Atlantic salmon stream in England but not in a second. Trépanier et al. (1996) found no correlation between run size and stream discharge for landlocked Atlantic salmon (ouananiche) and also listed several studies from the secondary literature providing contradictory findings. Davidson et al. (1943) observed that those pink salmon streams for which flows showed a relationship with abundance were those in which the salmon were sexually mature and staging near the river mouth, waiting to move in on high streamflow. Salmon stocks in other systems do not approach the river mouth until the fish are sexually mature, and these fish then enter the stream irrespective of flow. Huntsman (1939) suggested the hypothesis (yet untested) that the interaction of stream discharge, tidal action, and wind may act to guide Atlantic salmon from nearshore waters to their ultimate upriver destination. Thus, although the concept of a discharge–abundance relationship for adult migrants is popular, the existing evidence is somewhat ambiguous.

The distribution of adult body size has also received attention with respect to the influence of stream discharge. It has been suggested that low flows may impede access by larger-bodied salmon (van den Berghe and Gross 1989; Jonsson et al. 1990), thereby inflating the proportion of smaller fish in a run. Adult Atlantic salmon show a bimodal frequency in body size, with smaller fish (grilse) representing those that have spent only one winter at sea and larger fish having been at sea for more than one winter (multi-sea-winter, MSW). As fecundity is related to female body size (Scott and Crossman 1989), increasing the proportion of grilse in a population may clearly have consequences for production of the following generation. The proportion of grilse in a run has been linked to discharge for some populations of Atlantic salmon (Power 1981; Jonsson et al. 1990, 1991). In Iceland, however, Scarnecchia (1983) found only very low correlation between grilse proportion and streamflow for each sex. The body size distribution of female coho salmon (*Oncorhynchus kisutch*) was reported to correlate positively with streamflow in a Washington State stream by van den Berghe and Gross (1989). Similar to a discharge–abundance relationship, the interaction of body size and discharge appears to be stream- or study-specific.

Bardonnet and Baglinière (2000) explicitly identified three phases of upstream migration by Atlantic salmon. There is an initial upstream movement of fish from the sea to a location close to their ultimate spawning destination. The second phase is a relatively long residency period. Finally another ascending period takes place shortly before spawning. In Atlantic Canada, the first phase often occurs in the summer months (June–August) with adult salmon moving into larger rivers, estuaries, or small catchments with lacustrine areas. The fish then remain in these systems

Fig. 1. Estimated number of adult Atlantic salmon (*Salmo salar*) (Petersen estimates) returning to Catamaran Brook each year from 1990 to 2005. Error bars are 95% confidence intervals. Regression line: number of adults = –8.00 (±2.90) × year + 201.92 (±28.02), $r^2 = 0.352$, $p = 0.015$. Note regression is on year number (1–16), not calendar year (1990–2005).

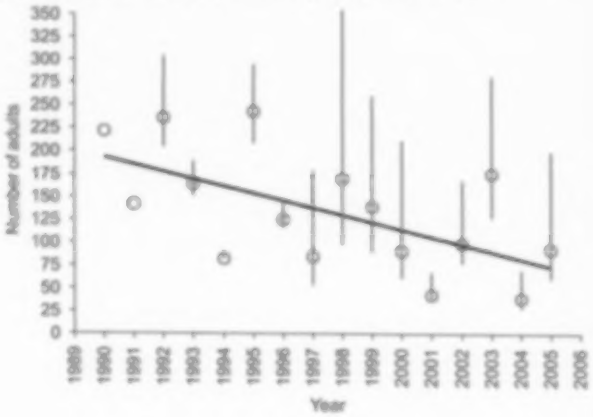

(phase 2) until late autumn (October–November) when they move farther upstream in the main river channel or into smaller-order streams (phase 3) for spawning. Owing to management objective to control river angling effort (occurring through summer and early autumn), the emphasis in trying to understand salmon–discharge relationships has largely focussed on phase 1, the immigration into river systems in summer months. Relatively little work has been done on the relationship during phase 3 (autumn months) within Atlantic Canada.

Records of adult returns through a fish-counting fence at the mouth of Catamaran Brook, a small subbasin of the Miramichi River system in New Brunswick, Canada, have indicated a general decline in adult salmon returns over the last 16 years (Fig. 1). Coincident with this decline has been lower than average streamflows during the autumn months. We hypothesized that the number of returning adults may be a function of stream discharge in this brook and not necessarily represent a real decline in the wider (meta-) population. The purpose of this research was to determine whether annual adult salmon abundance could be explained as a function of hydrological conditions and to assess how these conditions affect population characteristics, specifically the grilse component and fish body size.

Materials and methods

Study area

Catamaran Brook (46°52.7′N, 66°06.0′W) is a third-order stream (drainage area 52 km^2) tributary to the Little Southwest Miramichi River within the Miramichi River system (drainage area 14 000 km^2) of central New Brunswick, Canada (Fig. 2; see also Cunjak et al. (1990), Giberson and Caissie (1998), and Caissie et al. (2002) for a more detailed description of study area). The stream is approximately 90 km upstream of salt water and has a mainstem length of 18.4 km. This system has been the subject of a long-term research program evaluating forest-harvesting impacts and At-

© 2007 NRC Canada

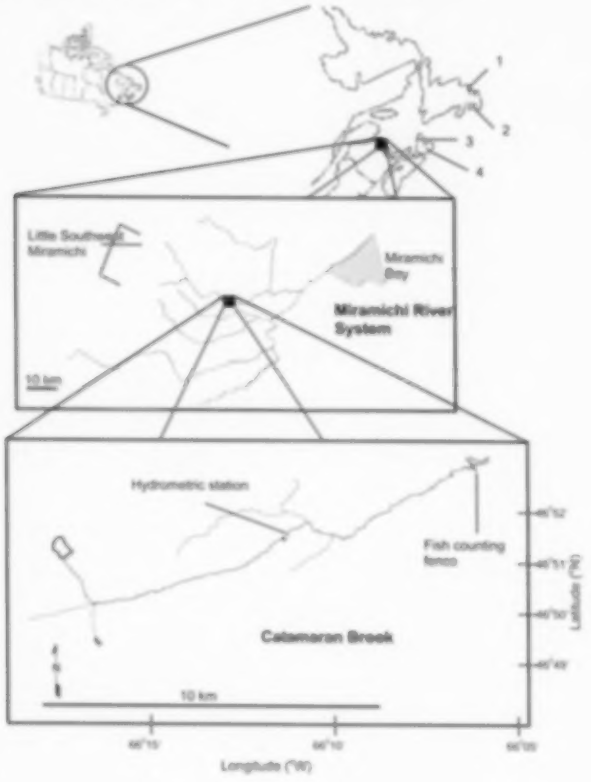

Fig. 2. Location of Catamaran Brook and the Miramichi River system in Atlantic Canada. Scale bar in each inset represents approximately 10 km. Numbered locations refer to other areas mentioned in the text: (1) Middle River, (2) Northeast Brook, Trepassey, (3) Lake O'Law Brook, (4) Grand River.

lantic salmon ecology (Cunjak and Therrien 1998; Caissie et al. 2002; Cunjak et al. 2004) and has included monitoring of the adult Atlantic salmon population since 1990. Adult salmon migrate into the Miramichi River system between June and October (Randall et al. 1989) as phase 1 and then stage in the estuary or deep pools within the larger mainstem branches (phase 2). The fish then move from these holding areas into small streams, including Catamaran Brook, to spawn during October and November of the year. Annual operation of a fish-counting fence has documented run timing to this brook to begin as early as 16 September (1990) and as late as 3 November (1997) (Table 1). The run is composed primarily of grilse. Estimated mean annual flow (MAF) of Catamaran Brook is 1.3 $m^3 \cdot s^{-1}$ with a bankfull discharge of 5.0 $m^3 \cdot s^{-1}$ at a point 9 km upstream of the mouth (Giberson and Caissie 1998). Stream discharge is generally low in September (i.e., maximum value less than MAF except in 1991, 1996, and 1999), increasing in late October and November as the result of autumn rains (Fig. 3).

Field sampling

Stream discharge was summarized for the period of 15 September to 30 November of each year as this is the period during which adult salmon have been recorded on their spawning ascent into Catamaran Brook (Table 1). The data are prorated to represent the discharge at the stream mouth, based on the discharge recorded at a hydrometric station 9 km upstream of the fish-counting fence and encompassing a drainage area of 27 km^2 (i.e., one-half the catchment). From 53-point sample estimates of discharge at the stream mouth (Q_{mouth}) between 1991 and 2004, we regressed discharge at the mouth against discharge at the hydrometric station ($Q_{station}$) for that date with the resulting relationship:

$$(1) \quad Q_{mouth} = 1.852(\pm 0.042\,(\text{standard error, SE})) \times Q_{station} + 0.039(\pm 0.034),\ r^2 = 0.973,\ P < 0.0001$$

This was then used to calculate discharge at the stream mouth for all records, and all analyses are based on these data. Data from 1990–2004 are presented here; discharge for 2005 has not yet been calculated from water level by Water Survey of Canada. Hydrologic conditions within this brook have been reported previously (Cunjak et al. 1993; Giberson and Caissie 1998; Caissie et al. 2002). We calculated the flood frequency for the period 15 September – 30 November. This was done by fitting an exponential curve to the annual flood frequency plot of streamflow for the September–November period of the 15 years and using this curve to estimate 1-in-2 (50th percentile), 1-in-5 (80th percentile), 1-in-10 (90th percentile), and 1-in-20 (95th percentile) year return flows.

The number of adult salmon returning to Catamaran Brook each year between 1990 and 2005 was estimated at a fish-counting fence. In 1990 the fence was 50 m upstream of the stream mouth, but this was found to be unsuitable and so was moved to a new position 200 m upstream for all subsequent years. Description of the fence may be found in Cunjak et al. (1993). Captured fish were identified to sex, measured (fork length, FL) for classification as grilse (<63 cm FL) or MSW salmon (>63 cm, terminology from Allan and Ritter 1977), and tagged with Carlin tags to allow individual identification. The annual spawning run estimate was calculated using the Petersen methodology for the years 1992–2005, and 95% confidence intervals on the estimates were constructed from the graph of binomial confidence limits in Krebs (1989; p. 21). Fish were tagged (M according to Krebs' notation) on their upstream passage through the fence, and the recapture phase consisted of those fish moving downstream through the fence after spawning. These fish were identified as tagged (R) or not tagged (this final group + R, represents C, the total number of individuals captured in the second sample). Precision of these estimates, when presented as percentage, is calculated as ([upper confidence limit – estimate]/estimate × 100). Data in the years 1990 and 1991 were not suitable for the Petersen methodology owing to ambiguity of individual fish identification and so population estimates in these years were determined as the counted number of adults through the fence multiplied by annual fence efficiency as determined by mark–recapture analysis of downstream migrating kelts each year (i.e., a tagged-to-untagged ratio of downstream migrating kelts). This was the method used by Cunjak and Therrein (1998). Estimated fence efficiency was 50% in 1990 and 90% in 1991 (Cunjak and Therrein 1998). The low efficiency of 1990 prompted the change in location of the fence. In addition to the Cata-

© 2007 NRC Canada

Table 1. Estimated annual stream discharge characteristics ($m^3 \cdot s^{-1}$) at the stream mouth for 15 September – 30 November of each year from 1990 to 2004 and timing and maximum discharge (Q_{max}) during period of upstream adult salmon migration (1990–2005) in Catamaran Brook, New Brunswick. The estimated autumn flood flow return periods[a] are provided in the lower part of the table.

	Estimated annual stream discharge ($m^3 \cdot s^{-1}$)					Adult movement upstream	
Year	Q_{50}	Q_{25}	Q_{75}	Minimum	Maximum	Timing	Q_{max} ($m^3 \cdot s^{-1}$)
1990	1.42	0.87	2.02	0.3	9.89	16 Sept.–24 Oct.	9.89
1991	1.54	1.21	2.02	0.37	8.31	28 Sept.–9 Nov.	5.39
1992	0.66	0.21	1.09	0.1	7.11	10 Oct.–14 Nov.	7.11
1993	0.96	0.27	1.19	0.11	3.79	13 Oct.–6 Nov.	3.79
1994	0.19	0.12	0.38	0.08	1.63	21 Oct.–17 Nov.	1.63
1995	0.25	0.12	1.34	0.11	6.15	8 Oct.–8 Nov.	6.15
1996	0.75	0.33	1.06	0.22	5.03	9 Oct.–10 Nov.	3.7
1997	0.3	0.13	0.45	0.09	2.87	3 Nov.–13 Nov.	2.87
1998	0.79	0.6	1	0.41	3.94	5 Oct.–11 Nov.	1.81
1999	0.84	0.45	1.27	0.1	4.15	22 Sept.–8 Nov.	4.15
2000	0.55	0.3	0.92	0.13	2.92	13 Oct.–15 Nov.	2.13
2001	0.26	0.14	0.37	0.08	1.56	17 Oct.–16 Nov.	1.55
2002	0.39	0.22	1.03	0.13	3.05	17 Oct.–18 Nov.	2.33
2003	0.45	0.24	1.34	0.19	13.78	15 Oct.–22 Nov.	13.78
2004	0.15	0.13	0.22	0.11	1.77	13 Oct.–7 Nov.	0.53
2005	N/A	N/A	N/A	N/A	N/A	27 Sept.–7 Nov.	3.94 (est.)
Mean	0.63	0.36	1.05	0.17	5.06	9 Oct.–11 Nov.	4.42
SD	0.42	0.31	0.53	0.1	3.45		3.46
Flood return interval			1-in-2 year		1-in-5 year	1-in-10 year	1-in-20 year
Maximum discharge ($m^3 \cdot s^{-1}$)			3.83		7.34	9.12	10.16

Note: Q_{50}, median discharge; Q_{25}, value of 25th percentile of discharge; Q_{75}, value of 75th percentile of discharge; SD, standard deviation; N/A, not available; est., estimated.

[a]Flood flow frequency estimated by fitting exponential curve ($Y = 1.295e^{2.3X}$, $r^2 = 0.976$, where Y = stream discharge and X = cumulative percentile) to flood frequency plot.

maran Brook adult returns, we also incorporated estimated adult returns to the entire Miramichi River system in parts of our analysis. These data were provided by D. Moore of the Department of Fisheries and Oceans. Methodology for their calculation is provided in Chaput et al. (2001).

Statistical analysis

To examine adult returns as a function of stream discharge, the estimated number of adults returning in a year was regressed on maximum daily discharge (Q_{max}, $m^3 \cdot s^{-1}$) during the interval of adult returns for that year. Q_{max} was selected as the hydrological variable of interest as we hypothesized that adult abundance has a relationship with water quantity, and knowing that adult salmon tend to ascend streams during high water periods (e.g., Jensen et al. 1986; Jonsson 1991; Smith et al. 1994), it was reasonable to use maximum discharge during the period when the fish are in the stream as the independent variable representing water quantity. Owing to 2005 discharge data not being available at the time of analysis, we used the median Q_{max} from 1990–2004 as the estimate for 2005; this value may be in error and is subject to modification as the 2005 discharge data become available.

Regression modeling was conducted examining number of returning adults, proportion of population as grilse, and body size of returning fish as functions of Q_{max}. A data-splitting approach (Myers 1990) was used that allowed validation of derived models. The number of returning adults each year was split chronologically (i.e., 1990–2001, or 75% of the data, used in model building, with the data from 2002–2005 as validation), rather than by random selection of years. This provided an indication of the forecasting ability of derived relationships (Myers 1990). Splitting of the body size and grilse proportion data sets differed from the abundance data in that the interest was in capturing the variability of the extremes of flow in the model-building data, particularly the extreme low flows as these are hypothesized to influence body size distribution. Therefore, Q_{max} was ranked and every fourth datum (years of 1991, 1996, 1998, 2003) was excluded for use as validation (i.e., systematic sampling; Scheaffer et al. 1990). The sensitivity of these models to individual component years was assessed by the prediction sum of squares (PRESS) statistic (Myers 1990), involving a "leave-one-out" analysis in which each year's datum is sequentially excluded from the data set and a new model is fit to the data, creating a series of n models each of sample size $n - 1$. Those data points that are not consistent with all other data become evident as the model of that year is very different from all other models. The PRESS statistic is then simply the sum over n years of (observed – predicted)^2, where predicted is the value predicted in year i by the model excluding the ith datum. Peters (1991) and Murray (2001) present compelling arguments that predictive ability should be the key feature by which we judge all ecological theories and concepts. For this reason, emphasis is placed on predictive ability of models rather than simply goodness of fit. Final models presented include entire data sets, both model and validation sets, as recommended by Myers (1990). All

© 2007 NRC Canada

Fig. 3. (*a*) Autumn (15 September – 30 November) hydrograph of Catamaran Brook discharge. Line represents daily median flow over 15 years (1990–2004), and error bars represent the range of central 50th percentile of flows (i.e., 25th to 75th percentiles). (*b*) Maximum stream discharge between 15 September and 30 November each year in Catamaran Brook as departure from 15-year median (3.95 $m^3 \cdot s^{-1}$). Values represent recorded discharge.

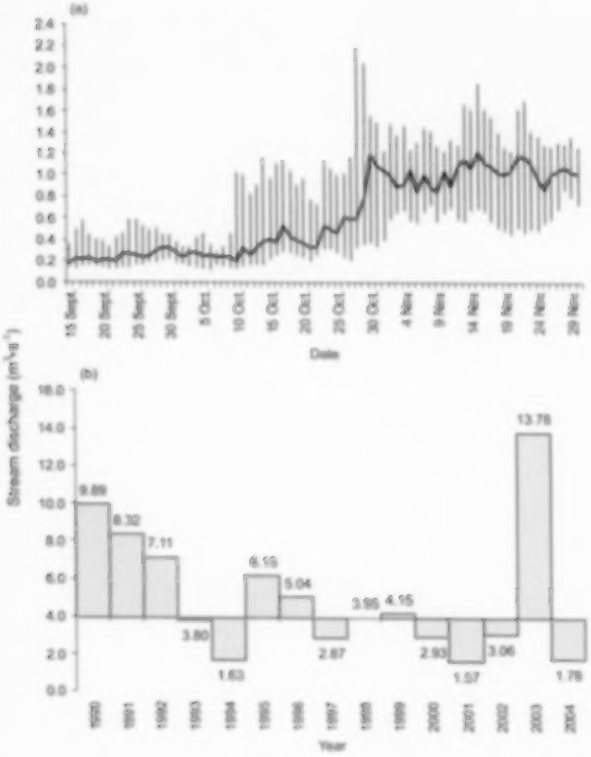

models were fit using Microsoft Excel XP or Systat 6.0 (Systat Software Inc., Point Richmond, California).

To investigate geographic generality and robustness of results to the phase of the salmon migration, a similar analysis to that conducted for Catamaran Brook was also done on four other Canadian east coast streams with fish-counting fences (Fig. 2). These were Grand River (1988–1994; data from Marshall et al. 2000) and Lake O'Law Brook (1989–1993; data from Davidson et al. 1995) in Nova Scotia and Middle Brook (1974–1975, 1978–2000) and Northeast Brook, Trepassey (1984–2000), in Newfoundland (data for both of these are from O'Connell et al. 2001). These streams represent a range of drainage areas from 21 km^2 (Northeast Brook, Trepassey) to 275 km^2 (Middle Brook), and all represent streams flowing either directly into the ocean or only a short distance above head of tide. Discharge data from each of these streams were accessed from Water Survey of Canada (2005). Of these, all but Lake O'Law Brook had salmon counted during phase 1 of the upstream migration (months of June–July). Within Lake O'Law Brook, the fish were counted during October–November as they moved to spawning grounds.

Table 2. Size and sex distribution of returning adult Atlantic salmon passing through the fish-counting fence at Catamaran Brook for each year between 1990 and 2005.

Year	Grilse (%)	Females (%)	Grilse as female (%)	MSW salmon as female (%)
1990	63.75	31.53	9.80	53.44
1991	60.97	41.02	20.00	68.75
1992	66.83	32.76	11.27	65.15
1993	71.52	32.45	11.11	86.04
1994	69.13	26.58	12.50	56.00
1995	62.96	41.08	14.28	84.28
1996	65.51	31.03	3.94	82.50
1997	62.00	28.57	3.22	68.42
1998	60.00	41.93	12.82	80.76
1999	69.73	28.94	16.98	56.52
2000	84.21	14.03	6.25	55.55
2001	69.44	40.00	32.00	54.54
2002	81.81	19.48	12.69	50.00
2003	55.31	31.18	5.76	61.90
2004	92.85	26.92	23.07	50.00
2005	68.62	39.21	11.42	100.00
Mean	69.04	31.67	12.94	67.11
SD	9.77	7.89	7.41	15.26

Note: MSW, multi-sea-winter; SD, standard deviation.

In the following, the measure of precision for a point estimate is given as ± SE unless noted otherwise. Coefficient of variation (CV), when presented, is $SD / \bar{x} \times 100$, and statistical tests between two means were conducted using one-tailed, unequal variance Student's *t* test with $\alpha = 0.10$. *p* values for regressions are only provided when it is not obvious that the relationships are statistically significant (i.e., in general when $r^2 < 0.50$).

Results

Stream discharge between 15 September and 30 October within Catamaran Brook is low (i.e., generally <1.0 $m^3 \cdot s^{-1}$) before rising thereafter to relatively moderate flows through November (Fig. 3), with high water events punctuating these otherwise low flow conditions. The 15-year mean median flow for the 11-week period of 15 September to 30 November is 0.64 $m^3 \cdot s^{-1}$ (±0.11), and on a yearly basis, median flow between these dates has ranged from a low of 0.15 (2004) to 1.54 $m^3 \cdot s^{-1}$ (1991) (Table 1). Maximum daily streamflow in a year within this period has averaged 5.07 $m^3 \cdot s^{-1}$ (±0.89), ranging from 1.56 (2001) to 13.78 $m^3 \cdot s^{-1}$ (2003). Estimated flood return frequencies are shown in Table 1 from which it may be seen that autumn bankfull flows are relatively rare events (return period of >10 years). Years of lowest autumn flows (maximum discharge <2 $m^3 \cdot s^{-1}$) are 1994, 2001, and 2004, whereas years of greatest flow (maximum discharge >1-in-10 year return period) occurred in 1990 and 2003 (Fig. 3).

The estimated number of adult salmon returning to Catamaran Brook each year from 1990 to 2005 ranged between 39 (2004) and 244 (1995), with indication of a decline over the period of record (Fig. 1). The mean number of salmon returning to the brook annually has been 133.9 (±16.04). Precision of the Petersen estimates has ranged between 8.5%

© 2007 NRC Canada

Table 3. Mean fork length (cm) of returning adult Atlantic salmon passing through the fish-counting fence at Catamaran Brook for each year between 1990 and 2005.

	Grilse		MSW salmon		Grilse + MSW salmon combined	
Year	Female	Male	Female	Male	Female	Male
1990	53.54 (2.63)	56.32 (2.74)	80.41 (8.93)	79.65 (7.75)	73.85 (14.06)	59.21 (8.54)
1991	55.23 (3.2)	55.72 (2.61)	82.71 (10.03)	74.5 (6.77)	74.12 (15.4)	59.26 (8.26)
1992	54.8 (3.23)	56.61 (2.69)	81.62 (8.87)	79.04 (9.67)	75.04 (14.04)	59.65 (8.82)
1993	53.15 (2.33)	56.22 (2.88)	76.61 (6.34)	68.22 (7.99)	70.62 (11.74)	56.85 (4.22)
1994	54.48 (2.27)	56.55 (2.68)	78.28 (6.92)	76.75 (5.67)	70.35 (12.84)	59.92 (8.28)
1995	54.55 (2.6)	55.29 (2.52)	75.43 (5.07)	76.69 (3.78)	70.13 (10.23)	57.61 (7.2)
1996	54.5[a]	56.15 (2.71)	76.56 (5.16)	79.62 (9.86)	75.18 (7.37)	58.32 (7.81)
1997	55.2[b]	57.76 (2.48)	79.74 (6.16)	69.43 (7.6)	77.85 (9)	58.86 (4.6)
1998	53.57 (6.92)	56.72 (3.21)	80.07 (6.41)	75.32 (15.74)	75.65 (11.91)	58.84 (8.19)
1999	56.76 (3.46)	58.14 (2.71)	80.3 (6.8)	67.68 (3.37)	70.21 (13.14)	60.09 (4.8)
2000	54.85 (2.61)	55.93 (10.45)	74.22 (3.37)	77.25 (13.03)	67.76 (10.4)	58.24 (12.5)
2001	57.52 (2.54)	56.12 (4.39)	77.02 (8.75)	72.97 (3.55)	65.02 (11.25)	60.08 (8.43)
2002	55.71 (2.21)	56.96 (5.01)	82.83 (6.88)	75.64 (6.62)	67.33 (14.65)	58.6 (7.37)
2003	58.36 (3.13)	58.46 (2.11)	79.95 (7.49)	78.46 (10.2)	77.36 (10.06)	63.19 (10)
2004	55.41 (2.9)	56.43 (2.41)	75.0[b]	77.3[b]	58.21 (7.86)	57.65 (5.57)
2005	54.62 (2.86)	57.92 (2.22)	80.1 (7.14)	[c]	75.01 (12.28)	57.92 (2.22)
Mean	55.14	56.71	78.8	75.23	71.48	59.02
SD	1.4	0.91	2.7	3.98	5.15	1.46

Note: Fork length reported as mean size with standard deviation in parentheses. MSW, multi-sea-winter.
[a]Two fish in this category, both 54.5 cm.
[b]Only one fish in this category.
[c]No fish in this category.

(1994) and 195% (1998) (mean 72.9% ± 14.4%). The adults return primarily as grilse (Table 2), forming a mean proportion of 69% of the run (±2.4%). Maximum and minimum grilse presence as the proportion of the run occurred in 2004 (92.8%) and 2003 (55.3%), respectively. The proportion of the returns as females has remained stable over the 16 years of record (31.7% ± 1.9%; Table 2). The two years in which females formed the lowest proportion of the run were 2000 (14.0%) and 2002 (19.5%); in all other years, females formed between 25% and 42% of the run. Though grilse form the majority of the run, few of these fish are female (12.9% ± 1.8%), whereas this sex forms the majority of MSW salmon (67.1% ± 3.8%).

Over the 16 years of record, male grilse had a mean FL greater than that of female grilse ($P < 0.001$; Table 3). In contrast, the mean FL of female MSW salmon was greater than that of males ($P < 0.01$). In examining FL of all fish by sex, without discriminating as grilse or MSW salmon, the mean FLs fluctuate between years to a lesser extent (CV = 2.5%) in males than in females (CV = 7.2%). In particular, females show small body size (<69 cm; i.e., >2 SE below long-term mean) in 2000, 2001, 2002, and 2004.

Regression of number of returning adults against Q_{max} (Fig. 4*a*) indicates a logarithmic relationship for the years 1990–2001. A "leave-one-out" analysis yielded a PRESS statistic of 16 272.8 and highlighted the year 1998 as contributing 42% of this statistic. All other years contributed 16% or less to this statistic. This model predicts that at $Q_{max} < 0.66$ m^3·s^{-1} adult returns will be zero. That is, below this value, stream discharge is sufficiently low to preclude upstream movement. Below 0.66 m^3·s^{-1}, the model returns negative values for adult returns; these are truncated to zero in the following analysis. Validation of the model using the years 2002–2005 is provided (Fig. 4*b*). Number of adults was very well estimated in 2002 (within 10 fish or 10% of observed) and reasonably well estimated in 2003 (87 fish or 33%) given that it is an extrapolation well outside the limits of the original model that was based on $Q_{max} \leq 9.89$ m^3·s^{-1}. The year 2004 is likewise outside the original limits and is underpredicted in that the model suggests zero fish for that stream discharge. In 2005, adult returns were overpredicted relative to observed (62 fish or 40%). The final model, using all of the data (1990–2005), is

$$\text{(2)}\quad \text{No. of salmon} = 61.89(\pm 13.51) \times \ln(Q_{max}) + 58.97(\pm 19.45),\ r^2 = 0.60$$

which is not significantly different from the 1990–2001 model based on 90% confidence intervals (i.e., ±2 SE) of the parameter estimates.

Attempts at linking adult salmon abundance and some measure of mean or median streamflow have commonly been done (see Discussion). For comparison, we regressed annual adult returns of Catamaran Brook salmon on seasonal median discharge (Q_{50}) during upstream migration for 1990–2004. The resulting model has greatly reduced predictive capacity and is

$$\text{(3)}\quad \text{No. of salmon} = 47.23(\pm 21.77) \times \ln(Q_{50}) + 168.84(\pm 21.09),\ r^2 = 0.266,\ P < 0.001$$

Given that Q_{max} appears to account for a large proportion of the variation in interannual populations of adult salmon in Catamaran Brook, we were interested in whether interannual fluctuations in the Miramichi River adult returns may ex-

© 2007 NRC Canada

Fig. 4. (*a*) Estimated number of adult Atlantic salmon (*Salmo salar*) per year in Catamaran Brook as function of maximum stream discharge during period of upstream migration (Q_{max}). Regression equation: number of adults = 86.16 (±20.00) × $\ln(Q_{max})$ + 35.92 (±27.84), $r^2 = 0.65$. (*b*) Model estimates of number of returning adults as function of Q_{max} (model standard error as broken lines) and validation years of 2002–2005. In both panels, error bars are 95% confidence intervals on population estimates.

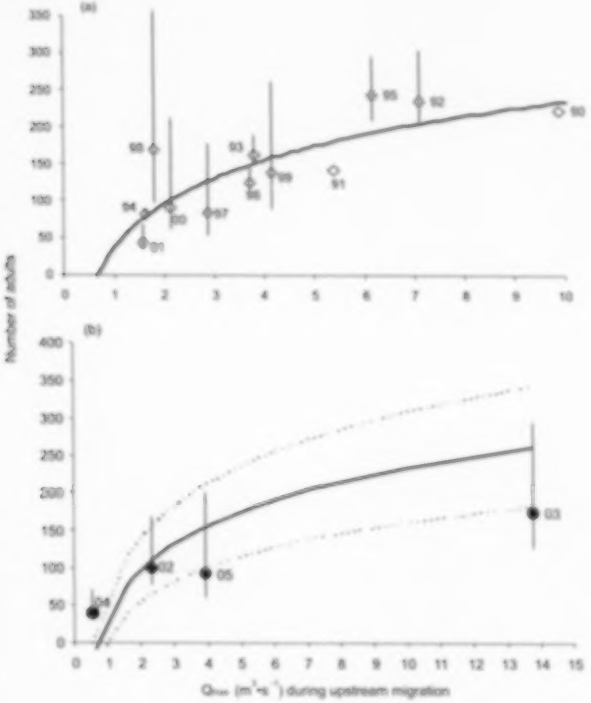

plain a significant proportion of the remaining variability. Annual adult returns to Catamaran Brook are correlated with Miramichi returns ($r = 0.58$) for the period 1990–2005, with a regression slope between the two not significantly different from unity.

$$\text{(4)}\quad \text{Catamaran (individuals)} = 0.90(\pm 0.34) \times \text{Miramichi } (\times 10^3) + 69.97(\pm 27.51),\quad r^2 = 0.34,\ P = 0.018$$

However, inclusion of the Miramichi returns as a linear function in the previous discharge model (utilizing all years of data, 1990–2005) only assisted in understanding the single point 1992 in which Catamaran returns appear to be a function of both stream discharge and adults in the Miramichi; in all other years, the two models performed equally well (Fig. 5). The sums of the residuals were –0.47 for the discharge model and –0.10 for the discharge + Miramichi adults model. Thus, inclusion of adult returns to the Miramichi River is not considered to contribute consistently to explaining annual variation in returns to Catamaran Brook over and above that explained by Q_{max} alone.

Fig. 5. Results of two models (discharge model, solid diamonds; discharge + Miramichi adult returns, open squares) of adult returns to Catamaran Brook relative to observed returns (Petersen estimates, shaded circles). The discharge model is given in the text (eq. 2). The discharge + Miramichi adult returns model: number of adults (individuals) = 51.77 (±13.10) × $\ln(Q_{max})$ + 0.53 (±0.25) × number of Miramichi adults ($\times 10^3$) + 33.28 (±21.24), $r^2 = 0.70$.

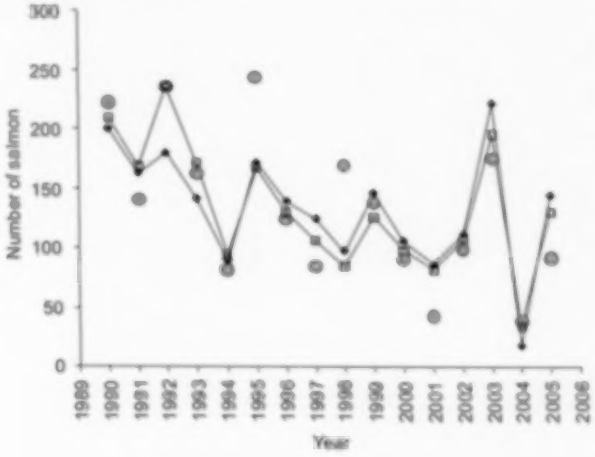

The proportion of the run as grilse shows a relationship with Q_{max} (Fig. 6). The PRESS statistic for this relationship is 0.049, with the years contributing the greatest to the statistic being 1997 (14.1%), 2000 (26.7%), 2002 (19.4%), and 2004 (13.2%); all other years contribute <8% to PRESS. These four years are very influential in forming this relationship, together accounting for 73.4% of the PRESS statistic. This suggests that the relationship is quite sensitive to these few low-flow years. The proportion of grilse in Catamaran Brook is weakly correlated ($r = 0.41$, $0.05 < P < 0.10$) with the proportion of grilse in the Miramichi. The proportion grilse in the validation years is consistently overpredicted, ranging from 2.2% difference (1996) to 15.7% (1998). The final model, using all of the data (1990–2005), is

$$\text{(5)}\quad \text{Proportion grilse} = -0.08(\pm 0.02) \times \ln(Q_{max}) + 0.79(\pm 0.03),\ r^2 = 0.50,\ P < 0.001$$

which is not significantly different from the model excluding the validation points based on the SE of the parameter estimates. The mean proportion of grilse in the Miramichi River over the period 1990–2005 was 66.1% (±0.02%).

Body size of male salmon does not show a relation to Q_{max} (Fig. 7),whereas females do illustrate a relationship and a greater response of FL to streamflow. Female body size is particularly affected at $Q_{max} < 1.25$ $m^3 \cdot s^{-1}$. The PRESS statistic associated with the female regression was 268.1 and highlighted the year 1997 as contributing 50% of this statistic. The years 1990 and 2004 contributed 16% and 28%, respectively, and all other years contributed <12% to this statistic. Validation of the model using the years 1991, 1996, 1998, and 2003 is provided (Fig. 7). The FLs estimated in the years 1991, 1996, and 2003 were all within ±6 cm (8%) of observed; estimated FL in 1998 was in error by 8.0 cm

© 2007 NRC Canada

Fig. 6. Relationship of proportion of run as grilse with Q_{max} in Catamaran Brook, 1990–2005. Regression equation: proportion grilse = –0.09 (±0.02) × ln(Q_{max}) + 0.82 (±0.03), r^2 = 0.55. Model-building data are presented as open symbols, validation data are presented as solid symbols. Years are presented in two-digit form for clarity of figure.

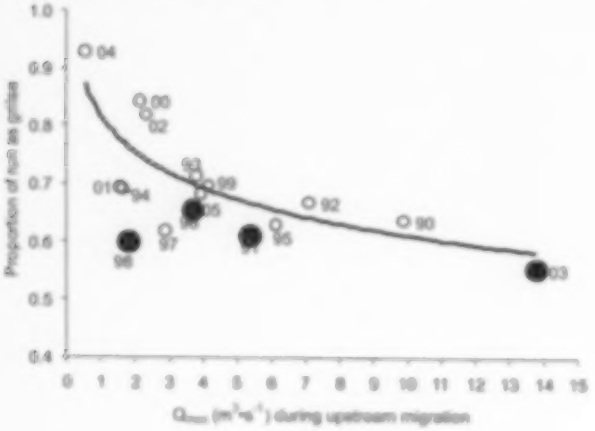

Fig. 7. Relationship of mean fork length of returning Atlantic salmon (*Salmo salar*) (by sex) with Q_{max} in Catamaran Brook, 1990–2005. Regression equations: male FL (cm) = 0.06 (±0.23) × Q_{max} + 58.61 (±0.53), r^2 = 0.000, p = 0.81; female FL (cm) = 5.02 (±1.31) × ln(Q_{max}) + 67.79 (±1.18), r^2 = 0.596. Model-building data are presented as open symbols, validation data are presented as solid symbols. Years are presented in two-digit form for clarity of figure.

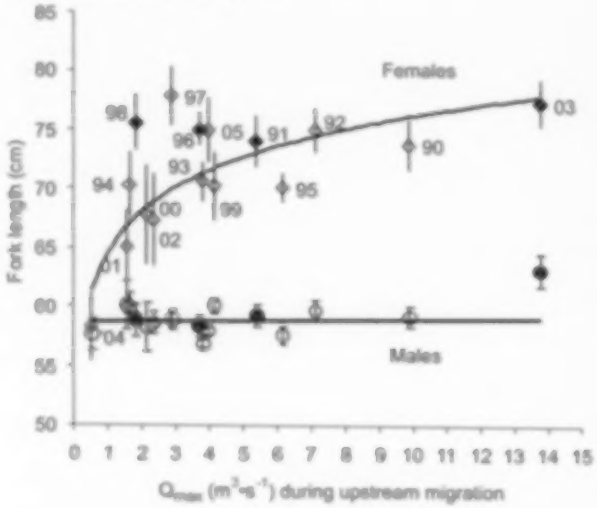

(12%) relative to observed FL. FL in the year 2003 was very well estimated considering that the stream discharge in this year was well outside the range of the original model. The final model, using all of the data (1990–2005), is

$$\text{Mean female FL (cm)} = 4.30\ (\pm 1.66) \times \ln(Q_{max}) + 65.20\ (\pm 2.39),\ r^2 = 0.52 \quad (6)$$

which is not significantly different from the model excluding the validation points based on the SE of the parameter estimates. Of note is the convergence on body size at approximately 58 cm by both female and male salmon at the lowest flows.

To assess whether the relationships here represented other populations, a similar analysis was conducted on four other streams in eastern Canada with data available comparable to those of Catamaran Brook. In the three streams with phase 1 migrants, there were nonsignificant and inconsistent correlations between abundance and Q_{max} during the migration period (Grand River, r = 0.096, $P > 0.5$; Middle Brook, r = –0.17, $P > 0.5$; Northeast Brook, Trepassey, r = 0.25, $0.20 < P < 0.50$). Within Lake O'Law Brook, the results were ambiguous. The year 1990 saw the fish-counting fence removed apparently before the run was complete and so the resulting abundance may not be reliable. Exclusion of this year as an underestimate yields a correlation of r = 0.47 ($P > 0.5$) between number of spawners and Q_{max}, whereas including it yields a much lower correlation of opposite sign (r = –0.27, $P > 0.5$); neither correlation is statistically significant.

Discussion

This analysis of adult Atlantic salmon migrant abundance and stream discharge has provided one of the most unambiguous relationships yet reported in the literature. Our models include relatively large magnitude coefficients of determination and, more importantly, are validated with independent data, a fundamental modeling procedure often lacking in the fisheries literature. Many previous efforts investigating relationships between aspects of salmonid migration and streamflow have used some measure of central tendency (e.g., mean or median flow; Jonsson et al. 1991; Moir et al. 1998; Svendsen et al. 2004) and have resulted in relationships more vague than that presented here. Our comparison of the use of Q_{max} versus Q_{50} suggests that high water flow events are much better correlated with adult returns than is median discharge.

Our data showed a strong relationship between the total number of adult salmon returning within a year and maximum discharge during that period, and our validation approach suggests that this relationship has reasonable predictive ability (i.e., ±40% and within confidence intervals of observed estimates; at least at $Q_{max} > 1.4$ $m^3 \cdot s^{-1}$). Within the model-building data, the year 1998 was identified as contributing much to the residuals of the model. This year was of the lowest precision in the Petersen estimate of adult abundance and so contributes to the inflated residuals. The mechanism underlying this relationship is uncertain. Migratory movements by Atlantic salmon are established to be related to stream discharge cues (Banks 1969; Alabaster 1970; Smith et al. 1994). Thus it is possible that the smaller number of fish at lower discharge is due to an insufficient discharge cue to the waiting fish. Further evidence that salmon move into Catamaran Brook in response to streamflow cues are two anomalous migration events. Six MSW salmon and four grilse were captured moving upstream in July of 1990 and 1995, respectively. In each of these years high water flow events (Q_{max}, 3.87 $m^3 \cdot s^{-1}$ on 25 July 1990; 2.24 $m^3 \cdot s^{-1}$ on 26 July 1995) from localized precipitation in

© 2007 NRC Canada

the subbasin preceded these adult salmon movements; in each case, the adult salmon emigrated from the brook as water levels receded. These anomalies show that salmon will enter these small brooks during high water flow events despite other environmental cues (e.g., photoperiod, water temperature) being inappropriate. That discharge is indeed the important variable is supported by the comparison of Catamaran Brook and the larger Miramichi population. The adult returns to Catamaran Brook showed a correlation with the larger Miramichi population, but inclusion of the Miramichi population estimates did not improve the explanatory capability of the model with the exception of 1992. This year saw a record return year to the Miramichi (estimated 190 000 salmon) over this 16-year period (next highest year (131 000 salmon) was 1993), and so when returns to the Miramichi are very high, this abundance may be an important factor to consider in addition to Q_{max} in understanding adult returns to Catamaran Brook. However, in most years, when returns to the Miramichi are less than maximal, it is not a useful variable in explaining more than Q_{max} does alone. This suggests that at the local stream scale, discharge is the overriding variable of concern affecting adult returns, not the larger river population.

The apparent decline in the salmon counts over time in Catamaran Brook may be partly explained as a local response to streamflow rather than a long-term decrease in the wider population. This is significant in that it is clearly necessary to understand how streamflow affects the behaviour of the adults in the population to appropriately interpret long-term population trends in small streams and tributaries (subbasins). Streamflow does not account for the entire decline, as there has also been a decline in the estimates for the entire Miramichi salmon population between the early 1990s and 2000 (Chaput et al. 2001). However, at a smaller scale, streamflow does explain a great amount of year-to-year variation in abundance. Further, the observed relationship between salmon abundance and discharge carries implications for the concept of stock integrity among spawning salmon, assuming Ricker's (1972) definition of stocks as spatially or temporally reproductively isolated groups. If the fish are not entering tributaries (their presumed natal streams) due to low stream discharge, they have two options: either refrain from spawning altogether or spawn elsewhere. Conceptually, low flows in several proximal tributaries would encourage spawning by these salmon in fewer areas of high density (e.g., in mainstem of the larger river to which these streams are tributary). Such a congregation may result in considerable mixing of separate stocks thereby contributing to gene flow between various tributaries. Within Catamaran Brook, "partly spent" adult salmon are regularly captured migrating upstream (R. Cunjak, unpublished data), suggesting that they may be spawning in other locations (possibly within the Little Southwest Miramichi River) before moving into Catamaran Brook itself. Banks (1969) suggested that owing to the year-to-year variability in streamflow, salmon may be much more flexible in their homing tendencies than we have been accustomed to expect. Therefore, as a result of hydrologic conditions, salmon stocks may not be as neatly discrete as we have traditionally viewed them to be.

One of the factors contributing to our high-quality abundance–discharge regression is that Catamaran fish are entering the third and final phase of their upstream migration; therefore, their behaviour and reaction to flow are likely much more tightly constrained than in most previous studies that have examined phases 1 and 2 spawning migrations. By phase 3, the fish are waiting for the water to rise to enter the smaller streams and so are more tightly coupled to streamflow than in the summer. Comparison of our results with those of other systems (Grand River, Lake O'Law Brook, Middle Brook, Northeast Brook, Trepassey) show clearly that the relationship from Catamaran Brook does not apply to phase 1 salmon, and it remains uncertain how well they apply to the Lake O'Law phase 3 fish. Unfortunately, few systems in Atlantic Canada have coincident long records of stream discharge and reliable estimates of adult salmon returns to further test the geographic generality of our results. At this point we suggest that our results are likely applicable only to tributary spawning streams into which adult salmon are moving during the final phase of their migration. Further work is required on phase 3 of populations to extend the geographic generality of the results presented here.

The proportion of the run as grilse is, at least at low flows, a function of Q_{max}, with low flows favoring the grilse over MSW salmon. The mechanism of this relationship of proportion grilse and Q_{max} is likely that low flows prevent entry of large-bodied salmon and so inflate the proportion of grilse that are not constrained at these low flows. Extreme examples of this are provided in 2003 (greatest Q_{max} and lowest proportion of grilse) and 2004 (very low Q_{max} and highest proportion of grilse). Over much of the range of Q_{max} (i.e., 1.0–5.5 $m^3 \cdot s^{-1}$), however, the proportion of grilse is constant, and it is only at continued low flows through the autumn months that the proportion of the run as grilse is affected.

The significance of the grilse response to Q_{max} is that the majority of grilse in Catamaran Brook are male, whereas the majority of MSW salmon are female. Thus, low streamflow results in low abundance of females and hence low egg deposition. The male dominance of grilse also explains the low proportion of the run as female (only about one-third of the population). The very low proportion of females in 2000 and 2002 may be a function of relatively low Q_{max} in Catamaran Brook in those years combined with high grilse proportions of the Miramichi River in those years (fifth and second highest, respectively, in the 16 years of 1990–2005). Though females are less abundant than males, they predominate in the MSW salmon category. This is likely due to differential mortality between maiden and repeat spawners, with males showing lower survival to repeat spawning (Quinn 2005).

Female salmon (grilse + MSW salmon combined) were considerably smaller in 2000, 2001, 2002, and 2004 than the long-term mean FL. This is most likely a function of the proportion of grilse (or, conversely, of MSW salmon) in the run. In 2001, the proportion of grilse returning was equivalent to the long-term average, but the proportion of grilse as females was highest on record (32%) and proportion of MSW females was below average. Thus, the abundance of female grilse shifted mean size downward. The other three years of small-bodied females represented the three years of greatest proportion of grilse returns (proportion of grilse >80% of run) again shifting mean size down. Owing to the

© 2007 NRC Canada

unequal distribution of sex between grilse and MSW salmon, with females being predominantly MSW, the females are more affected by low stream discharge than males. Thus the females that do ascend in years of very low flow tend to be smaller (and hence of lower fecundity) than in years of high flow. Therefore, the importance of autumn streamflow conditions is not only in affecting number of returning salmon, but also in size distribution of the egg-carrying females. Clearly, this may have profound implications on subsequent juvenile production. Our distribution of female body size with Q_{min} agrees with those of van den Berge and Gross (1989) and Jonsson et al. (1990, 1991), who speculated that low flows act as impediments to large fish, which would in turn reduce the abundance of spawners. However, it appears that only at the absolutely lowest flows are larger salmon impeded. The convergence of male and female body size on a common length at the lowest flows is an intriguing observation and consistent with what we expect on the premise that low streamflow does indeed influence body size distribution, at least of the female salmon.

Acknowledgements

We thank Steve Heard (University of New Brunswick) and Bob Randall and Dave Scruton (Canada Department of Fisheries and Oceans) for reviews of an earlier draft of this work. Dave Moore (Canada Department of Fisheries and Oceans) provided data on the Miramichi salmon population for our use. We also acknowledge the comments and suggestions of three anonymous reviewers and thank them for their efforts. Funding for this research was provided by the Natural Sciences and Engineering Research Council of Canada (NSERC).

References

Alabaster, J.S. 1970. River flow and upstream movement and catch of migratory salmonids. J. Fish Biol. **2**: 1–13.

Allan, I.R.H., and Ritter, J.A. 1977. Salmonid terminology. J. Cons. Int. Explor. Mer, **37**: 293–299.

Banks, J.W. 1969. A review of the literature on the upstream migration of adult salmonids. J. Fish Biol. **1**: 85–136.

Bardonnet, A., and Baglinière, J.L. 2000. Freshwater habitat of Atlantic salmon (*Salmo salar*). Can. J. Fish. Aquat. Sci. **57**: 497–506.

Caissie, D., Jolicoeur, S., Bouchard, M., and Poncet, E. 2002. Comparison of streamflow pre- and post-timber harvesting in Catamaran Brook (Canada). J. Hydrol. **258**: 232–248.

Chaput, G., Moore, D., Hayward, J., Sheasgreen, J., and Dubee, B. 2001. Stock status of Atlantic salmon (*Salmo salar*) in the Miramichi River, 2000. Canadian Science Advisory Secretariat Research Document No. 2001/008.

Cunjak, R.A., and Therrein, J. 1998. Inter-stage survival of wild juvenile Atlantic salmon, *Salmo salar* L. Fish. Manag. Ecol. **5**: 209–223.

Cunjak, R.A., Caissie, D., and El-Jabi, N. 1990. The Catamaran Brook Habitat Research Project: description and general design of study. Can. Tech. Rep. Fish. Aquat. Sci. No. 1751.

Cunjak, R.A., Caissie, D., El-Jabi, N., Hardie, P., Conlon, J.H., Pollock, T.L., Giberson, D.J., and Komadina-Douthwright, S. 1993. The Catamaran Brook (New Brunswick) Habitat Research Project: biological, physical and chemical conditions (1990–1992). Can. Tech. Rep. Fish. Aquat. Sci. No. 1914.

Cunjak, R.A., Curry, R.A., Scruton, D.A., and Clarke, K.D. 2004. Fish–forestry interactions in freshwaters of Atlantic Canada. Chapter 20. *In* Fishes and forestry: worldwide watershed interactions and management. Blackwell Science, Oxford. pp. 439–462.

Davidson, F.A., Vaughn, E., and Hutchinson, S.J. 1943. Factors influencing the upstream migration of the pink salmon (*Oncorhynchus gorbuscha*). Ecology, **24**: 149–168.

Davidson, K., Niles, M., Swan, P., and Forsyth, L. 1995. The Lake O'Law Project, Cape Breton, Nova Scotia: 1989–1993. Can. Tech. Rep. Fish. Aquat. Sci. No. 2053.

Giberson, D.J., and Caissie, D. 1998. Stream habitat hydraulics: interannual variability in three reaches of Catamaran Brook, New Brunswick. Can. J. Fish. Aquat. Sci. **55**: 485–494.

Hayes, F.R. 1953. Artificial freshets and other factors controlling the ascent and population of Atlantic salmon in the LeHave River, N.S. Bull. Fish. Res. Board Can. No. 99.

Hunter, J.G. 1959. Survival and production of pink and chum salmon in a coastal stream. J. Fish. Res. Board Can. **16**: 835–886.

Huntsman, A.G. 1939. Salmon for angling in the Margaree River. Bull. Fish. Res. Board Can. No. 57.

Huntsman, A.G. 1948. Freshets and fish. Trans. Am. Fish. Soc. **75**: 257–266.

Jensen, A.J., Heggberget, T.G., and Johnsen, B.O. 1986. Upstream migration of adult salmon, *Salmo salar* L., in the River Vefsna, northern Norway. J. Fish Biol. **29**: 459–465.

Jonsson, N. 1991. Influence of water flow, water temperature and light on fish migration in rivers. Nord. J. Freshw. Res. **66**: 20–35.

Jonsson, N., Jonsson, B., and Hansen, L.P. 1990. Partial segregation in the timing of migration of Atlantic salmon of different ages. Anim. Behav. **40**: 313–321.

Jonsson, N., Hansen, L.P., and Jonsson, B. 1991. Variation in age, size and repeat spawning of adult Atlantic salmon in relation to river discharge. J. Anim. Ecol. **60**: 937–947.

Krebs, C.J. 1989. Ecological methodology. Harper Collins Publishers, New York.

Marshall, T.L., LeBlanc, P.H., Rutherford, K.A., and Jones, R.A. 2000. Assessments of Atlantic salmon stocks in selected rivers of Cape Breton Island 1999. Canadian Stock Assessment Secretariat Research Document No. 2000/008.

Moir, H.J., Soulsby, C., and Youngson, A. 1998. Hydraulic and sedimentary characteristics of habitat utilized by Atlantic salmon for spawning in the Girnock Burn, Scotland. Fish. Manag. Ecol. **5**: 241–254.

Murray, B.G. 2001. Are ecological and evolutionary ideas scientific? Biol. Rev. **76**: 255–289.

Myers, R.H. 1990. Classical and modern regression with applications. 2nd ed. PWS–Kent Publishing, Boston, Mass.

O'Connell, M.F., Walsh, A., and Cochrane, N.M. 2001. Status of Atlantic salmon (*Salmo salar* L.) in Middle Brook (SFA 5), Northeast Brook, Trepassey (SFA 9), and Northeast River, Placentia (SFA 10), Newfoundland, in 2000. Canadian Science Advisory Secretariat Research Document No. 2001/042.

Peters, R.H. 1991. A critique for ecology. Cambridge University Press, Cambridge, UK.

Power, G. 1981. Stock characteristics and catches of Atlantic salmon (*Salmo salar*) in Quebec and Newfoundland and Labrador in relation to environmental variables. Can. J. Fish. Aquat. Sci. **38**: 1601–1611.

Pritchard, A.L. 1936. Factors influencing the upstream spawning migration of the pink salmon, *Oncorhynchus gorbuscha* (Walbaum). J. Biol. Board Can. **2**: 383–389.

Quinn, T.P. 2005. The behaviour and ecology of Pacific salmon and trout. American Fisheries Society and UBC Press, Vancouver, British Columbia.

© 2007 NRC Canada

Randall, R.G., O'Connell, M.F., and Chadwick, E.M.P. 1989. Fish production in two large Atlantic coast rivers: Miramichi and Exploits. *In* Proceedings of the International Large River Symposium. Can. Spec. Publ. Fish. Aquat. Sci. No. 106. pp. 292–308.

Ricker, W.E. 1972. Hereditary and environmental factors affecting certain salmonid populations. *In* The stock concept in Pacific salmon. H.R. MacMillan Lectures in Fisheries, University of British Columbia, Vancouver, B.C. pp. 27–160.

Saunders, J.W. 1960. The effect of impoundment on the population and movement of Atlantic salmon in Ellerslie Brook, Prince Edward Island. J. Fish. Res. Board Can. **17**: 453–473.

Scarnecchia, D.L. 1983. Age at sexual maturity in Icelandic stocks of Atlantic salmon (*Salmo salar*). Can. J. Fish. Aquat. Sci. **40**: 1456–1468.

Scheaffer, R.L., Mendenhall, W., and Ott, L. 1990. Elementary survey sampling. 4th ed. PWS–Kent Publishing Company, Boston, Mass.

Scott, W.B., and Crossman, E.J. 1989. Freshwater fishes of Canada. Bull. Fish. Res. Board Can. No. 184.

Smith, G.W., Smith, I.P., and Armstrong, S.M. 1994. The relationship between river flow and entry to the Aberdeenshire Dee by returning adult Atlantic salmon. J. Fish Biol. **45**: 953–960.

Svendsen, J.C., Koed, A., and Aarestup, K. 2004. Factors influencing the spawning migration of female anadromous brown trout. J. Fish Biol. **64**: 528–540.

Trépanier, S., Rodríguez, M.A., and Magnan, P. 1996. Spawning migrations in landlocked Atlantic salmon: time series modelling of river discharge and water temperature effects. J. Fish Biol. **48**: 925–936.

van den Berghe, E.P., and Gross, M.R. 1989. Natural selection resulting from female breeding competition in a Pacific salmon (coho: *Oncohynchus kisutch*). Evolution, **43**: 125–140.

Water Survey of Canada. 2005. Archived hydrometric data. Accessed at http://www.wsc.ec.gc.ca/hydat/H2O/.

© 2007 NRC Canada

Density, climate, and the processes of prespawning mortality and egg retention in Pacific salmon (*Oncorhynchus* spp.)

T.P. Quinn, D.M. Eggers, J.H. Clark, and H.B. Rich, Jr.

Abstract: In 2004 and 2005, exceptionally large runs of sockeye salmon (*Oncorhynchus nerka*) to the Alagnak River system in Bristol Bay, Alaska, coincided with weak runs to the nearby Kvichak River system. Restricted fishing to protect the Kvichak populations resulted in densities on the Alagnak River system's spawning grounds that were 11.5-fold (in 2004) and 9.0-fold (in 2005) above the long-term (1956–2003) average. Carcass sampling indicated that 23% (2004) and 44% (2005) of the potential egg deposition was lost to prespawning mortality or incomplete spawning in the Alagnak populations. Much lower levels of egg retentions were observed in spawning populations in the Kvichak River and Wood River systems, where the runs did not appreciably exceed the escapement goals, indicating that density-dependent spawning failure may have occurred. However, in 2005, significantly higher egg retention rates were observed in the Alagnak River system despite slightly lower densities than in 2004, indicating that environmental processes (probably low river levels and high temperatures) influenced prespawning mortality as well. More limited sampling in 2006 revealed only 3% egg retention in one of the Alagnak populations, but the combination of lower density and cooler conditions did not allow us to determine the relative contributions of these two factors to spawning failure.

Résumé : En 2004 et 2005, des montaisons exceptionnellement importantes de saumons rouges (*Oncorhynchus nerka*) dans le bassin de la rivière Alagnak dans la baie de Bristol ont coïncidé avec des montaisons faibles dans le bassin adjacent de la Kvichak. Des restrictions de pêche pour protéger les populations de la Kvichak ont eu pour conséquence que les densités sur les zones de reproduction de l'Alagnak étaient 11,5 fois (en 2004) et 9,0 fois (en 2005) plus importantes que la moyenne à long terme (1956–2003). Un échantillonnage des carcasses révèle que 23 % (2004) et 44 % (2005) de la ponte potentielle des oeufs a été perdue à cause de la mortalité avant la fraie et de fraies incomplètes dans les populations de l'Alagnak. Nous avons observé des taux beaucoup plus bas de rétention des oeufs dans les populations reproductives des bassins versants de la Kvichak et de la Wood, où les montaisons n'ont pas dépassé de façon appréciable les objectifs de l'échappement; cela indique qu'il s'est peut-être produit un insuccès de la fraie relié à la densité. Cependant, en 2005, nous avons noté des taux significativement supérieurs de rétention des oeufs dans le bassin versant de l'Alagnak malgré des densités un peu plus faibles qu'en 2004, ce qui indique que des processus environnementaux (probablement des niveaux d'eau bas et des températures élevées) ont influencé aussi la mortalité avant la fraie. Un échantillonnage plus restreint en 2006 indique une rétention de seulement 3 % dans l'une des populations de l'Alagnak, mais la combinaison d'une faible densité et des conditions plus fraîches ne nous a pas permis de déterminer les contributions relatives de ces deux facteurs à l'insuccès de la fraie.

[Traduit par la Rédaction]

Introduction

The tendency for populations to decline in productivity as they increase in density, often referred to simply as density dependence, is fundamental to both our understanding of population ecology and natural resource management. The concepts of maximum sustainable yield and harvestable surplus are predicated on the idea that the populations in question would experience higher per capita mortality or lower reproductive success at high densities, although productivity may also be depressed at very low densities (Liermann and Hilborn 2001). Therefore, not only can populations sustain some level of fishing mortality, but mortality actually increases productivity (Ricker 1954, 1975; Beverton and Holt 1957).

The management of Pacific salmon (*Oncorhynchus* spp.) is based on the concept of escapement goals, the number of salmon of a given species that will maximize the level of surplus production from a given river system. Ideally, the fisheries are regulated to allow this number of salmon to

Received 24 May 2006. Accepted 22 December 2006. Published on the NRC Research Press Web site at http://cjfas.nrc.ca on 18 April 2007.
J19337

T.P. Quinn[1] and H.B. Rich, Jr. School of Aquatic and Fishery Sciences, Box 355020, University of Washington, Seattle, WA 98195, USA.
D.M. Eggers and J.H. Clark. Alaska Department of Fish and Game, P.O. Box 25526, Juneau, AK 99802-5526, USA.

[1]Corresponding author (e-mail: tquinn@u.washington.edu).

 doi:10.1139/F07-035 © 2007 NRC Canada

spawn. The biological basis of the escapement goals depends on the life history of the salmon species (Groot and Margolis 1991; Quinn 2005). Coho salmon (*Oncorhynchus kisutch*), Chinook salmon (*Oncorhynchus tshawytscha*), and steelhead trout (*Oncorhynchus mykiss*) generally spawn at relatively low densities and produce offspring that rear in streams. The capacity of streams for breeding and incubation of embryos exceeds their capacity to support juvenile salmon, and so food and rearing space have long been believed to control the populations of these species (Chapman 1966). The production of smolts from such populations is largely determined by the quantity and quality of habitat for rearing (Bradford et al. 1997; Sharma and Hilborn 2001).

Pink (*Oncorhynchus gorbuscha*), chum (*Oncorhynchus keta*), and sockeye salmon (*Oncorhynchus nerka*) are more numerous and tend to spawn at higher densities (Quinn 2005), likely because their offspring migrate from the unproductive spawning stream to feed in the ocean (pink and chum salmon) or to a lake (sockeye salmon). Density dependence in these species (and stream-rearing salmonids as well, though perhaps to a lesser extent) may result from several processes on the spawning grounds. First, competition among females for ideal nesting sites may cause late-arriving or competitively inferior females to spawn in locations with fine sediment, vulnerability to streambed scour, or other physical factors not conducive to embryo survival (Chapman 1988; Rennie and Millar 2000; Schuett-Hames et al. 2000). Second, females that spawn late in the season may superimpose their redds over those of females that spawned earlier and died, thereby dislodging the fertilized eggs of the prior occupants (McNeil 1964; Fukushima et al. 1998). Both of these processes are supported by behavioral observations. Female chum salmon possessing territories successfully resisted eviction by newly arrived females, forcing the intruders to spawn at suboptimal sites (Schroder 1981). However, females nearing death were evicted by later-arriving intruders, and when densities were high, territory size decreased, presumably increasing vulnerability to disturbance by nearby females. In addition to these processes during the spawning period, embryos and alevins may die during development, perhaps from low levels of dissolved oxygen, when densities are very high (Heard 1978).

Another possibility, that females may fail to deposit all of their eggs before death, has been discussed in the literature for decades without a clear consensus. Experiments on pink salmon indicated that "crowding reduces the survival rate by increasing the retention of eggs" (Hanavan 1954, p. 176), and experiments with sockeye salmon showed higher rates of egg retention early in the season when densities were high than later when densities were lower (Parenskiy 1990). On the other hand, only 6.5% of the eggs were retained at death by sockeye salmon in British Columbia, and only 1.6% of the females died before spawning any eggs (Manzer and Miki 1985). Egg retention may be related to delay in commencing spawning. Female chum salmon that started their nests on the first through fifth days after arrival retained, on average, 52, 95, 101, 177, and 1182 eggs, respectively (Schroder 1973). Such delay might result from high densities, but egg retention was not a factor in the density-dependent reduction in productivity of sockeye salmon at the Weaver Creek Spawning Channel (Essington et al. 2000). Because females compete for spawning sites, early-arriving females should be more likely to spawn completely, whereas later-arriving females might not be able to establish territories. In addition, smaller females might experience egg retention and spawning failure to a greater extent, both because they might not compete successfully with larger females (van den Berghe and Gross 1989) and because they often arrive later than larger females (Hendry et al. 1999). On the other hand, egg retention in Auke Creek, Alaska, pink salmon was highest early in the season, coincident with high temperatures, and declined later (Fukushima and Smoker 1997).

In the millennia before heavy fishing by humans, densities of salmon on the spawning grounds would routinely have exceeded their carrying capacity, so Pacific salmon evolved under conditions of strong density dependence. Indeed, analyses of sediment cores indicated large runs in some prehistoric periods, though abundance varied greatly over long time scales (Finney et al. 2002; Schindler et al. 2005). However, most current management regimes prevent such "overescapement" because the salmon are so valuable, making it difficult to observe the natural processes related to high salmon densities. Nevertheless, the need to protect one population sometimes necessitates very limited fishing on another population if their spatial and temporal overlap is too great to permit selective fisheries. This paper reports an opportunistic investigation of one such situation that took place in Bristol Bay, Alaska, in 2004 and 2005 when exceptionally large runs of sockeye salmon were returned to the Alagnak (also known as the Branch) River system, coinciding with warm, dry conditions in the region. Our primary goal was to quantify the prevalence of prespawning mortality and incomplete spawning, comparing the levels in Alagnak River system populations with populations elsewhere in Bristol Bay where salmon runs approximated the escapement goals. Our secondary goal was to test the hypothesis that larger females would have a lower frequency of incomplete spawning and spawning failure. We assumed that they would be competitively superior to smaller females and also tend to arrive earlier than smaller females and so should be more likely to complete spawning.

Materials and methods

Site descriptions

The many lake systems of Bristol Bay in southwestern Alaska make this region a center of distribution of sockeye salmon. The fisheries (almost exclusively gillnets) are organized into five major districts (Minard and Meacham 1987) centered around the mouths of large rivers draining one or more lakes. Over most of the 20th century, the most important was the Naknek–Kvichak district (Hilborn et al. 2003). The Kvichak River system (including Iliamna Lake and Lake Clark) dominated, producing about 60% of the district's total since 1956, and the Naknek River system contributed about 31%. The remaining 9% came from the Alagnak River system, draining into the lower reaches of the Kvichak River, just above Kvichak Bay (Fig. 1). In these and other systems in Bristol Bay, most sockeye salmon spawning takes place from late July to mid-September in a

© 2007 NRC Canada

Fig. 1. Map of western Alaska, USA, showing the locations in the Wood River (1, Little Togiak Lake, including A Creek, C Creek, and the Little Togiak River; 2, Pick Creek; 3, Lynx Creek; 4, Ice Creek; 5, Yako Creek; 6, Bear Creek; 7, Happy Creek), Kvichak River (8, Pedro Bay ponds; 9, Chinkelyes Creek; 10, Copper River; 11, Gibraltar Creek; 12, Dream Creek; 13, Upper Talarik Creek), and Alagnak River (14, Moraine Creek and Funnel Creek; 15, Battle River; 16, Nanuktuk Creek; 17, Kulik River) systems where female sockeye salmon (*Oncorhynchus nerka*) were sampled for egg retention. Inset shows location in western North America.

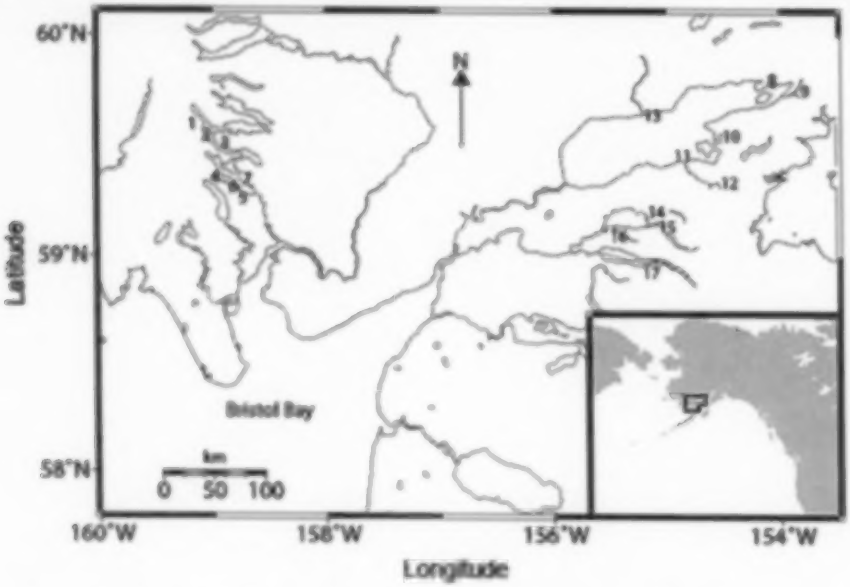

variety of creeks and rivers and along beaches of the lakes themselves.

The total escapements have been intensively monitored with tower counts by the Alaska Department of Fish and Game for the Kvichak River and Naknek River systems since 1956 and for the Alagnak River system from 1956–1976 and since 2001. Total escapement has averaged 5.2 (standard deviation (SD) = 5.3) million to the Kvichak and 1.3 (SD = 0.6) million to the Naknek from 1956 through 2006. Alagnak River system escapements, based on tower counts and expanded aerial survey estimates, averaged 0.7 (SD = 1.0) million through 2006 (Clark 2005). Virtually all of the spawning in the Alagnak River system takes place in four spawning areas (Fig. 1): two lake tributaries where salmon spawn early (Nanuktuk and Moraine creeks), and two lake outlet rivers where salmon spawn later (Battle and Kulik rivers). In 2003, an unusually large escapement of 3.7 million sockeye salmon returned to the Alagnak River system, and in 2004 and 2005, even larger runs of 5.4 million and 4.2 million, respectively, returned. For reasons that are not clear (and beyond the scope of this paper), this period of increased production in the Alagnak River system coincided with low returns to the Kvichak River system. Runs to the Kvichak River system have been consistently weak since the early 1990s, and to protect the Kvichak River populations, fishing in the Naknek–Kvichak District has been restricted to the Naknek River Special Harvest Area in most of the last 10 years. These restrictions have resulted in low exploitation on the Alagnak River populations. The combination of exceptionally large returns (without precedent in 50 years) and low fishing rates resulted in salmon densities on the Alagnak River system's spawning grounds that were about 11.5-fold (in 2004) and 9.0-fold (in 2005) greater than the average through 2003. In 2006, the run to the Alagnak River system (1.8 million) was above average but smaller than in the previous two years. The extraordinary Alagnak River overescapements in 2004 and 2005 and the contrasting runs there in 2006 and in the other Bristol Bay systems provided a rare opportunity to assess the prevalence of egg retention and spawning failure.

Sampling was conducted in the 2004 and 2005 spawning seasons at the four principal spawning sites in the Alagnak system (Battle and Kulik rivers, Nanuktuk Creek, and the area at the confluence of Moraine and Funnel creeks). A fifth site (Battle Lake Beach) was sampled only in 2004 (Fig. 1), and in 2006, only the Moraine–Funnel site was sampled. We compared the site-specific peak aerial survey index count (Clark 2005) in the year of sampling with the long-term (1978–2002) average peak aerial survey index count. Sites elsewhere in Bristol Bay, in the Wood River and Kvichak River systems, were sampled as "pseudocontrols" for comparison with the Alagnak River. Differences in habitat quality and lack of directly comparable data preclude objective assessment of density among these different sites, but the Wood River and Iliamna Lake systems did not experience levels of overescapement comparable with those in the Alagnak River in these years. For the Wood River populations, we used the annual counts from foot surveys at the peak of the run and compared the abundance in the year when egg retention was estimated with the long-term average (from 1947 to 2002 in most cases, with occasional missing years). Aerial and foot surveys have well-established weaknesses (Knudsen 2000; Stewart et al. 2003), so the data are presented graphically rather than analyzed statistically.

© 2007 NRC Canada

Table 1. Numbers of female sockeye salmon sampled (*N*) and the mean rate of egg retention in the Alagnak River, Kvichak River, and Wood River systems of Bristol Bay, Alaska.

	2004		2005		2006	
Region and site	*N*	Retention	*N*	Retention	*N*	Retention
Alagnak River						
Battle Lake	162	0.009				
Battle River	491	0.286	543	0.461		
Kulik River	328	0.016	477	0.176		
Moraine Creek	849	0.104	425	0.401	254	0.030
Nanuktuk Creek	536	0.493	398	0.604		
Kvichak River						
Chinkelyes Creek	200	0.025	237	0.071	78	0.023
Copper River	172	0.024	62	0.136	99	0.000
Dream Creek	201	0.140	96	0.216		
Gibraltar Creek	100	0.040	96	0.388	40	0.062
Pedro Bay ponds	157	0.103			117	0.027
Upper Talarik Creek	126	0.033				
Wood River						
A Creek			96	0.067		
Bear Creek			100	0.055	90	0.061
C Creek			67	0.030		
Happy Creek	103	0.023	195	0.051	75	0.036
Ice Creek	108	0.000				
Little Togiak River	177	0.002	50	0.003		
Lynx Creek	130	0.012				
Pick Creek	201	0.005	74	0.018		
Yako Creek			172	0.038	96	0.022

Nevertheless, they provide some perspective on the relative densities of salmon at the sites we sampled. The Kvichak River system populations were not surveyed for abundance in 2004–2006 so we could not include them in the analysis of density, but the escapements to the system as a whole were 5.5 million in 2004, 2.3 million in 2005, and 3.1 million in 2006.

Field methods

We sampled each site during the period of heavy spawning activity, based on our personal experience, that of other regional biologists, and catalogs of the areas (Demory et al. 1964; Marriott 1964). Field personnel removed carcasses of female salmon from the water and margins of the streams. We were interested in the extent to which females died of "natural causes" before completing spawning. We therefore did not sample fish that had been killed by bears (Quinn et al. 2003) or if external signs of pecking or missing internal organs and egg skeins indicated that scavenging by gulls or other birds had taken place (Quinn and Buck 2000), as those data would not represent the fish's condition at death.

Females that were suitable for sampling were measured for length from the middle of the orbit of the eye to the end of the hypural plate, and the body cavity was slit open. If visual assessment indicated that there were <100 eggs in the body cavity, the fish was designated "completely spawned" and no further data were recorded. If >100 eggs were estimated, then all eggs were removed by hand from the body cavity. Females with intact egg skeins (i.e., eggs not loose in the body cavity) were noted as spawning failures but otherwise processed similarly to samples with loose eggs. The entire egg mass was placed into a plastic colander, allowing ovarian fluid to drain away, and the volume was measured by displacement of water in a 500 mL graduated cylinder.

To estimate the number of eggs retained from our data on egg volume, we took subsamples of the retained eggs from 20–30 females at each site and calculated average egg weight from a subsample of 30 eggs from each female (Quinn et al. 1995). These egg weights were used to estimate the volume retained by that fish, and we also developed population-specific regressions of body length and egg weight to convert the egg volumes to numbers of retained eggs for fish with eggs that were not weighed. In addition, population-specific regressions of fecundity and body length were estimated from the females classified as spawning failures. These regressions were used to standardize the measured volume of retained eggs to an egg retention rate (i.e., retained eggs as proportion of the individual's total fecundity).

In the Wood River and Kvichak River systems, there were so few females classified as spawning failures that we could not estimate population-specific relationships between body length and fecundity (Table 1). Therefore, egg weight data and fecundity data were pooled among the populations within each of these two systems to estimate egg weight – body length and fecundity – body length regressions. Within the Alagnak River system, samples were sufficient to produce population-specific estimates of egg weight – body length and fecundity – body length regressions. Pooled regressions were estimated for cases where there were no

© 2007 NRC Canada

between-year or between-stock differences in these regressions. A three-stock, pooled-year model was the most parsimonious (analysis of covariance (ANCOVA), $p < 0.05$) and indicated differences between Nanuktuk Creek and Moraine Creek but not between Battle River and Kulik River (so these data were pooled). This model was then used to estimate number of eggs retained and egg retention rate for individual females sampled.

Results

All four of the major spawning areas in the Alagnak River system were sampled in 2004 and 2005 and the Moraine–Funnel site was sampled again in 2006 for a total of 4041 carcasses examined (Table 1). In 2004, sampling was conducted throughout the spawning period in the Nanuktuk and Moraine creeks (Fig. 2). The sockeye salmon enter these creeks in late July and spawning is completed in early September. Egg retention rates were very low in these creeks during the early sampling periods but were high later, when high densities of dead fish were observed, ranging from 0.04 to 0.64 and 0.01 to 0.18, respectively, among sampling events. The egg retention rates, weighted by escapement density to represent overall estimates of the annual retention, were 0.23 for Nanuktuk Creek and 0.43 for Moraine Creek.

In 2004, egg retention rate in the Battle River was only estimated once, during the peak of spawning, and the value was high (0.29). The egg retention rate in the Kulik River, observed during a single sampling event early in the spawning period, was relatively low (0.02). We estimated that 23% of the 2004 Alagnak River's potential egg deposition was lost as a result of prespawning mortality or incomplete spawning in 2004, based on the average of the egg retention rates for individual spawning areas, weighted by the peak aerial survey counts for each area.

In 2005, sampling was conducted twice in the each of the four main spawning areas. During periods of heavy spawning, egg retention rates were high in Nanuktuk Creek (0.69), Moraine Creek (0.40), and the Battle River (0.50). In 2005, both sampling events in the Kulik River were early in the spawning period and egg retention rates (0.19) were lower than in the other areas. We estimated that 43% of the Alagnak River's potential egg deposition in 2005 was lost owing to prespawning mortality or incomplete spawning. The 2006 sampling on a single day at Moraine Creek was not adequate to estimate overall egg retention, but the rate was markedly lower than that of the previous years (0.03).

In 2004, the spawning density in each of the four principal spawning areas within the Alagnak River was the highest observed since aerial surveys were initiated, with observed peak aerial counts ranging from 6 to 20 times the historical averages through 2002. Spawning densities were lower in 2005 than in 2004 but still higher than observed before 2004; peak counts ranged from 5 to 10 times the historical average. In both years, the egg retention rate among spawning areas increased with increasing escapement density among spawning areas (Fig. 3). Egg retention rates were the highest in Nanuktuk Creek and Battle River, areas that had the highest spawning densities. In 2006, the aerial survey of Moraine Creek indicated a density 4.51 times the long-term average.

Fig. 2. Aerial survey counts of live (solid circles) and dead (open circles) sockeye salmon (*Oncorhynchus nerka*) and estimated egg retention rates (open squares) in 2004 in (*a*) Nanuktuk Creek and (*b*) Moraine Creek including its tributary, Funnel Creek.

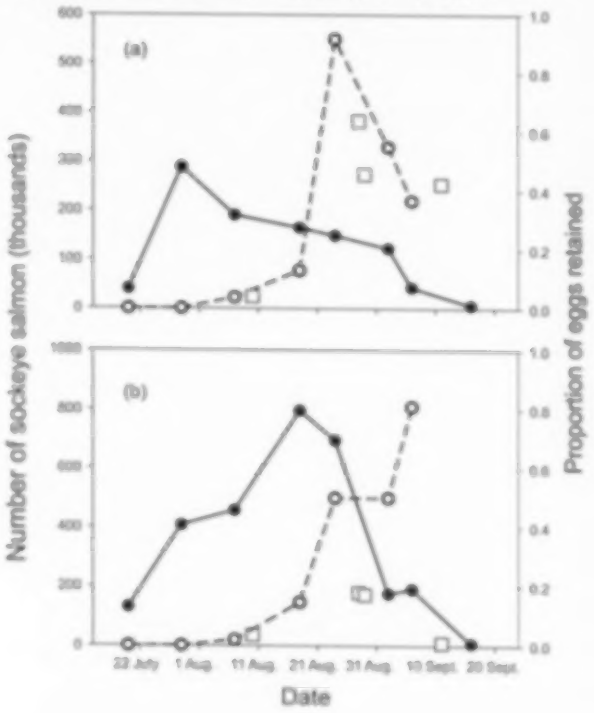

Egg retention rates observed in the Alagnak River system spawning area were well above those in the other spawning areas (Fig. 3). Spawning densities were near average levels in the Kvichak River system (total escapement density was 1.1 in 2004 and 0.4 in 2005, relative to the long-term average) and somewhat above average in the Wood River system (Fig. 3). Five spawning areas were sampled in the Wood River system in 2004, seven in 2005, and three in 2006 (Table 1). Based on the pooled egg weight – body length and fecundity – body length regressions and the observed egg retention volumes, egg retention rates averaged 0.01 in 2004 (range = 0 to 0.02), 0.04 in 2005 (range = 0 to 0.08), and 0.04 in 2006 (range = 0.02 to 0.06). Seven spawning areas were sampled in the Kvichak River system in 2004 and four spawning areas were sampled in 2005 and 2006 (Table 1). Based on the pooled egg weight – body length and fecundity – body length regressions and the observed egg retention volumes, egg retention rates in the Kvichak River system in 2004 averaged 0.05 and ranged from 0.0 to 0.17. In 2005, the egg retention rates were higher (average = 0.20, range = 0.07 to 0.39), but in 2006, they were low (0.03).

To test the hypothesis that larger females would experience lower rates of egg retention than smaller females, we reduced the data set to 17 combinations of population and year with at least 80 females and at least 10% with either partial or complete spawning failure for analysis. Then we conducted linear regressions with body length as the independent variable and retention rate as the dependent vari-

© 2007 NRC Canada

Fig. 3. Proportion of eggs retained by female sockeye salmon (*Oncorhynchus nerka*) as a function of the spawning site's escapement relative to long-term averages: (*a*) Wood River and Alagnak River populations (solid triangles, Alagnak in 2004; solid circles, Alagnak in 2005; solid square, Alagnak in 2006; open diamonds, Wood River in all years combined) and (*b*) Wood River (numerals 04, 05, and 06 refer to the sampling years 2004, 2005, and 2006, respectively). Note the differences in scale on the axes of the two panels.

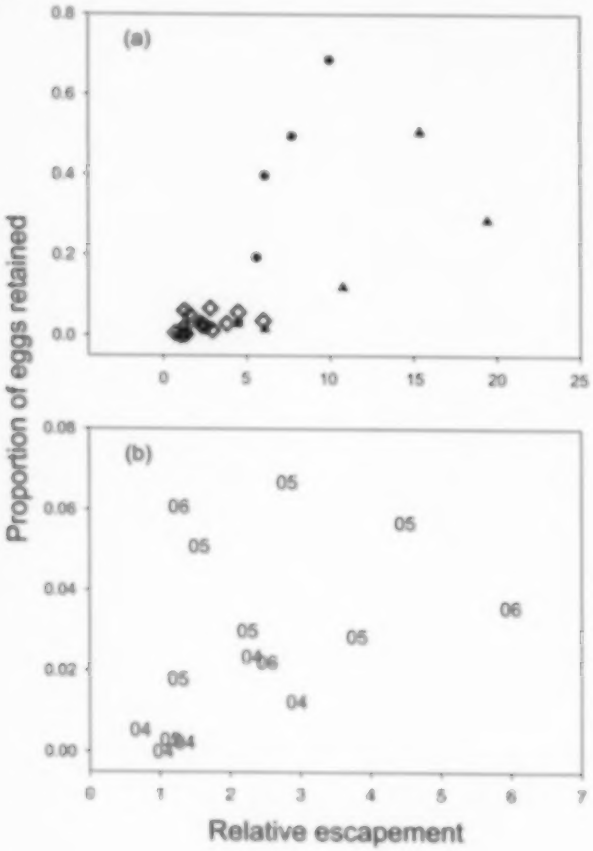

able. After correction for multiple comparisons, there were two cases in which larger females experienced higher rates of egg retention than small ones (Battle River and Dream Creek in 2004) and one case in which smaller females experienced higher retention rates (Nanuktuk Creek in 2005). However, length explained almost none of the variation in egg retention ($r^2 < 0.06$ in all these cases), and in the other 14 population–year combinations, there was no significant correlation after correction for multiple comparisons.

Discussion

We observed very high levels of egg retention in Alagnak River spawning populations during 2004 and 2005 in the face of the highest spawning densities observed since escapement enumeration programs began in the 1950s. For the three largest populations (Nanuktuk Creek, Moraine Creek, and Battle River) in the Alagnak River system, extensive sampling in both years coincided with the period of heavy spawning and high densities. It was estimated that 23% and 44% of the potential egg deposition was lost to prespawning mortality or incomplete spawning in 2004 and 2005, respectively. These levels of egg retention were much higher than those observed in spawning populations in the Kvichak River and Wood River systems where spawning densities were near normal. Based on our review of the literature, egg retentions of this magnitude have not been documented in natural spawning populations of salmon and would be a significant component of the overall spawner–recruit relationship. Much lower egg retention rates were observed in the Kulik River. However, we were not able to sample late enough to encompass the period of peak spawning and the estimated egg retentions rates may be lower than the true values for the population.

Our working hypothesis was that density of spawning would be positively associated with egg retention, both through spawning failure and incomplete spawning. Consistent with this hypothesis, the Alagnak River populations had much higher densities, relative to their long-term averages, and higher rates of egg retention than the Wood River and Kvichak River populations. Furthermore, sampling in Moraine and Nanuktuk creeks in 2004 indicated that rates of egg retention generally increased and then decreased with salmon density. In addition, the rate of egg retention tended to increase with relative escapement among the Alagnak populations in both years and among the Wood River populations. However, all four of the Alagnak River populations experienced higher rates of egg retention in 2005 than in 2004, despite lower densities, a result inconsistent with the hypothesis of density dependence. Moreover, the first sampling events of the 2005 season in Moraine Creek and to an even greater extent in Nanuktuk Creek saw very high rates of egg retention, even though sampling at the same time of year in 2004 saw much lower rates. Finally, egg retention rates observed in the Wood River and Kvichak River populations were also higher in 2005 despite generally similar spawning densities in Wood River and lower escapement levels in Kvichak River (Kvichak escapement was 5.5 million and 2.32 million in 2004 and 2005, respectively). These results were inconsistent with our hypothesis and cause us to believe that significant environmental factors interacted with density to affect prespawning mortality.

In general, the summers of both 2004 and 2005 (and 2003) were characterized by warm, dry conditions in this region. Records from King Salmon, on the nearby Naknek River system, indicated that August 2004 was the warmest on average since records began in 1948 and also had the second-lowest level of precipitation. Records from Iliamna village, on Iliamna Lake, also indicated that 2004 was warm throughout the summer; average daily temperatures were warmer in both July and August in 2004 than in any other year since records began in 1950. In 2005, August temperatures at King Salmon were warm but not exceptionally so (average was ranked 11th warmest out of 59 years) and precipitation was very close to the long-term average. At Iliamna, August 2005 temperatures averaged 1.3 °C above the 1950–2006 average (tied for 5th warmest year). In terms of maximum temperatures, 2004, 2003, and 1968 were tied

© 2007 NRC Canada

for the warmest on record at Iliamna in August (20.6 °C, 1.2 °C warmer than the next warmest). The average daily maximum in 2005 was 18.3 °C.

All these lines of evidence point to exceptionally warm conditions in 2004 but less warm in 2005, when prespawning mortality was even more prevalent. However, the salmon swimming upriver from Bristol Bay and holding in the lakes before spawning would be exposed to temperatures in the lakes, and these showed a different pattern. We have no long-term temperature records from the Alagnak system's lakes, but our data reveal that Iliamna Lake was much warmer in 2005 than in 2004 or 2003. Mid-August temperatures at a depth of 5 m in Knutson Bay were 11.2 °C in 2003, 13.8 °C in 2004, and 16.4 °C in 2005. At a depth of 10 m, the water was 11.1 °C in 2003, 13.2 °C in 2004, and 15.4 °C in 2005. Other stations recorded the same pattern — exceptionally warm water in 2005, not just on the very surface, as might indicate a calm, sunny day, but over the entire epilimnion for the month. By way of comparison, water temperatures in Knutson Bay averaged over 10 years between 1968 and 1984 were 11.3 °C at 5 m and 10.0 °C at 10 m, or about 5 °C cooler than in 2005, and other stations in the lake were similarly cooler in the past than in 2005. There are no long-term records of egg retention in any of these populations but the very large escapements in the Kvichak River system in 1960 (14.6 million) and 1965 (24.3 million) motivated some sampling, and fewer than 10% of the females retained >100 eggs (unpublished records and annual reports of the College of Fisheries, University of Washington). Interestingly, the August air temperatures in both of these years were below the long-term average.

The air temperature records do not clearly explain why the fish experienced such high rates of prespawning mortality and egg retention in 2005, though the water temperature records (at least in Iliamna Lake) suggested unusually warm water. In our early season surveys of Moraine and Nanuktuk creeks, and especially Nanuktuk in 2005, we observed many salmon that had just arrived on the spawning grounds, as indicated by the absence of scars from fighting and digging that characterize Pacific salmon after a few days of reproductive activity. Nevertheless, these fish were listless and barely able to maintain themselves against the flow of the river and some died as we watched them, including some in the lake itself below the creek. Examination of the gills revealed extensive fungus in many cases, and the fish may have been deprived of oxygen by a combination of warm water and impaired gill function. In addition, although discharge records are not available for these streams, the flows seemed to be very low for the general width and configuration of the streams. That is, there were large areas of exposed gravel that were devoid of vegetation, suggesting that they are normally in the wetted part of the channel. Discharge will reflect a combination of recent precipitation and also accumulation and runoff of snow from the winter. If the fish were exposed to crowding from high abundance and low water levels and stress from high temperatures and oxygen depletion, they might be susceptible to pathogens.

Conditions in 2006 were much cooler and wetter than in the previous two years in the Bristol Bay region. The mean August air temperature at Iliamna was 11.6 °C, the 11th coolest year since 1950. August of 2006 was the second wettest in the 52-year period of record at King Salmon, and it was the fifth wettest in the 57 years of records at Iliamna village. Similarly, in mid-August, Iliamna Lake was much cooler in 2006 than in 2004 and 2005 (10.1 °C at 5 m depth in Knutson Bay and 10.0 °C at 10 m depth). The lower rates of egg retention in 2006 than in 2005 in the Alagnak River system's Moraine Creek population might be explained by either the lower density or lower temperatures, but the lower rates in the Iliamna Lake populations, where density was, if anything, higher in 2006, seem best explained by the cooler, wetter conditions.

Our analysis of the data on female length and egg retention did not support our hypothesis that large (presumably competitively superior) females would be more successful in spawning. Our observations indicated that many females died without attempting to dig redds, as their tails and caudal regions displayed none of the fraying and scarring typical of females that have been digging and their bodies were not scarred from intrasexual competition. These observations suggested that stressful conditions rather than competitive inferiority played a role in at least some cases. We also did not see a consistent pattern of larger females in the earlier samples within a given season, though this did occur in some cases.

In conclusion, our results clearly demonstrated that under extreme but natural conditions, high rates of egg retention can occur in salmon on the spawning grounds. Recent examination of $\delta^{15}N$ in a sediment core from Kukaklek Lake indicated that this system has experienced alternating brief periods of high salmon abundance followed by longer periods of lower abundance roughly every 100 years during the last five centuries (Schindler et al. 2006). Thus the recent levels of abundance are extreme but probably not unprecedented. However, density seems to have contributed to the prespawning mortality in 2004 and 2005, but it was not simply a matter of late-arriving fish being unable to obtain suitable spawning sites; environmental conditions apparently played an important role. Adult sockeye salmon avoid high temperatures (Hyatt et al. 2003; Newell and Quinn 2005), and high temperatures can contribute to elevated mortality during the lengthy upriver migration of sockeye salmon in the Fraser (Gilhousen 1990) and Columbia (Naughton et al. 2005) rivers. We conclude that some interaction between density, environmental conditions, and perhaps also pathogens caused the mortality. There is a clear warming trend in this region, as indicated by average air temperatures in Iliamna, so such interactions may occur again. The trend is most pronounced in July (0.023 °C per year increase from 1950–2006, $r^2 = 0.16$), with weaker patterns in August (0.022 °C per year, $r^2 = 0.12$) and September (0.016 °C per year, $r^2 = 0.07$).

Acknowledgements

Funding for this research was provided by the Alaska Department of Fish and Game (ADF&G), a grant from the Governor's Office to ADF&G, a consortium of seafood processing companies operating in Bristol Bay, the National Science Foundation's Biocomplexity Program, the Bristol Bay Science and Research Institute, and the Gordon and Betty Moore Foundation. Field assistance was provided by

© 2007 NRC Canada

many people but especially Fred West, Lowell Fair, Dave Gaudet, Ed Jones, Ron Josepheson, Slim Morstad, Andy McGregor, Mike Tracy, Chris Boatright, Daniel Schindler, Keith Denton, Neala Kendall, and Tanya Kleisborg. We thank Stephanie Carlson for assistance with statistical analysis and comments on the paper and the National Park Service for permission to sample in Katmai National Park.

References

Beverton, R.J.H., and Holt, S.J. 1957. On the dynamics of exploited fish populations. His Majesty's Stationary Office, London, UK.

Bradford, M.J., Taylor, G.C., and Allan, J.A. 1997. Empirical review of coho salmon smolt abundance and the prediction of smolt production at the regional level. Trans. Am. Fish. Soc. **126**: 49–64.

Chapman, D.W. 1966. Food and space as regulators of salmonid populations in streams. Am. Nat. **100**: 345–357.

Chapman, D.W. 1988. Critical review of variables used to define effects of fines in redds of large salmonids. Trans. Am. Fish. Soc. **117**: 1–21.

Clark, J.H. 2005. Abundance of sockeye salmon in the Alagnak River system of Bristol Bay Alaska. Fishery Manuscript Report No. 05-01, Alaska Department of Fish and Game, Anchorage, Alaska.

Demory, R.L., Orrell, R.F., and Heinle, D.R. 1964. Spawning ground catalog of the Kvichak River system, Bristol Bay, Alaska. US Fish and Wildlife Service, Washington, D.C. Report No. 488.

Essington, T.E., Quinn, T.P., and Ewert, V.E. 2000. Intra- and interspecific competition and the reproductive success of sympatric Pacific salmon. Can. J. Fish. Aquat. Sci. **57**: 205–213.

Finney, B.P., Gregory-Eaves, I., Douglas, M.S.V., and Smol, J.P. 2002. Fisheries productivity in the northeastern Pacific Ocean over the past 2,200 years. Nature (London), **416**: 729–733.

Fukushima, M., and Smoker, W.W. 1997. Determinants of stream life, spawning efficiency, and spawning habitat in pink salmon in the Auke Lake system, Alaska. Can. J. Fish. Aquat. Sci. **54**: 96–104.

Fukushima, M., Quinn, T.J., and Smoker, W.W. 1998. Estimation of eggs lost from superimposed pink salmon (*Oncorhynchus gorbuscha*) redds. Can. J. Fish. Aquat. Sci. **55**: 618–625.

Gilhousen, P. 1990. Prespawning mortalities of sockeye salmon in the Fraser River system and possible causal factors. Int. Pac. Salmon Fish. Comm. Bull. **26**: 1–58.

Groot, C., and Margolis, L. 1991. Pacific salmon life histories. University of British Columbia Press, Vancouver, British Columbia.

Hanavan, M.G. 1954. Survival of pink-salmon spawn in an intertidal area with special reference to influence of crowding. Fish. Bull. **56**: 167–176.

Heard, W.R. 1978. Probable case of streambed overseeding — 1967 pink salmon, *Oncorhynchus gorbuscha*, spawners and survival of their progeny in Sashin Creek, southeastern Alaska. Fish. Bull. **76**: 569–582.

Hendry, A.P., Berg, O.K., and Quinn, T.P. 1999. Condition dependence and adaptation-by-time: breeding date, life history, and energy allocation within a population of salmon. Oikos, **85**: 499–514.

Hilborn, R., Quinn, T.P., Schindler, D.E., and Rogers, D.E. 2003. Biocomplexity and fisheries sustainability. Proc. Nat. Acad. Sci. **100**: 6564–6568.

Hyatt, K.D., Stockwell, M.M., and Rankin, D.P. 2003. Impact and adaptation responses of Okanagan River sockeye salmon (*Oncorhynchus nerka*) to climate variation and change effects during freshwater migration: stock restoration and fisheries management implications. Can. Water Res. J. **28**: 689–713.

Knudsen, E.E. 2000. Managing Pacific salmon escapements: the gaps between theory and reality. *In* Sustainable fisheries management: Pacific salmon. *Edited by* E.E. Knudsen, C.R. Steward, D.D. MacDonald, J.E. Williams, and D.W. Reiser. Lewis Publishers, Boca Raton, Florida. pp. 237–272.

Liermann, M., and Hilborn, R. 2001. Depensation, evidence, models and implications. Fish Fish. **2**: 33–58.

Manzer, J.I., and Miki, I. 1985. Fecundity and egg retention of some sockeye salmon *(Oncorhynchus nerka)* stocks in British Columbia. Can. J. Fish. Aquat. Sci. **43**: 1643–1655.

Marriott, R.A. 1964. Stream catalog of the Wood River lake system, Bristol Bay, Alaska. US Fish and Wildlife Service, Washington, D.C. Report No. 494.

McNeil, W.J. 1964. Redd superimposition and egg capacity of pink salmon spawning beds. J. Fish. Res. Board Can. **21**: 1385–1396.

Minard, R.E., and Meacham, C.P. 1987. Sockeye salmon (*Oncorhynchus nerka*) management in Bristol Bay, Alaska. Can. Spec. Publ. Fish. Aquat. Sci. **96**: 336–342.

Naughton, G.P., Caudill, C.C., Keefer, M.L., Bjornn, T.C., Stuehrenberg, L.C., and Peery, C.A. 2005. Late-season mortality during migration of radio-tagged adult sockeye salmon (*Oncorhynchus nerka*) in the Columbia River. Can. J. Fish. Aquat. Sci. **62**: 30–47.

Newell, J., and Quinn, T.P. 2005. Behavioral thermoregulation by maturing adult sockeye salmon (*Oncorhynchus nerka*) in a stratified lake prior to spawning. Can. J. Zool. **83**: 1232–1239.

Parenskiy, V.A. 1990. Relation between the spawning success of sockeye salmon, *Oncorhynchus nerka*, and the behavior on spawning grounds. J. Ichthyol. **30**: 48–58.

Quinn, T.P. 2005. The behavior and ecology of Pacific salmon and trout. University of Washington Press, Seattle, Washington.

Quinn, T.P., and Buck, G.B. 2000. Scavenging by brown bears, *Ursus arctos*, and glaucous-winged gulls, *Larus glaucescens*, on adult sockeye salmon, *Oncorhynchus nerka*. Can. Field-Nat. **114**: 217–223.

Quinn, T.P., Hendry, A.P., and Wetzel, L.A. 1995. The influence of life history trade-offs and the size of incubation gravels on egg size variation in sockeye salmon (*Oncorhynchus nerka*). Oikos, **74**: 425–438.

Quinn, T.P., Gende, S.M., Ruggerone, G.T., and Rogers, D.E. 2003. Density-dependent predation by brown bears (*Ursus arctos*) on sockeye salmon (*Oncorhynchus nerka*). Can. J. Fish. Aquat. Sci. **60**: 553–562.

Rennie, C.D., and Millar, R.G. 2000. Spatial variability of stream bed scour and fill: a comparison of scour depth in chum salmon (*Oncorhynchus keta*) redds and adjacent bed. Can. J. Fish. Aquat. Sci. **57**: 928–938.

Ricker, W.E. 1954. Stock and recruitment. J. Fish. Res. Board Can. **11**: 559–623.

Ricker, W.E. 1975. Computation and interpretation of biological statistics of fish populations. Bull. Fish. Res. Board Can. **191**: 1–382.

Schindler, D.E., Leavitt, P.R., Brock, C.S., Johnson, S.P., and Quay, P.D. 2005. Marine-derived nutrients, commercial fisheries, and production of salmon and lake algae in Alaska. Ecology, **86**: 3225–3231.

Schindler, D.E., Leavitt, P.R., Johnson, S.P., and Brock, C.S. 2006. A 500-year context for the recent surge in sockeye salmon

© 2007 NRC Canada

(*Oncorhynchus nerka*) abundance in the Alagnak River, Alaska. Can. J. Fish. Aquat. Sci. **63**: 1439–1444.

Schroder, S.L. 1973. Effects of density on the spawning success of chum salmon (*Oncorhynchus keta*) in an artificial spawning channel. College of Fisheries, University of Washington, Seattle, Washington.

Schroder, S.L. 1981. The role of sexual selection in determining the overall mating patterns and mate choice in chum salmon. School of Fisheries, University of Washington, Seattle, Washington.

Schuett-Hames, D.E., Peterson, N.P., Conrad, R., and Quinn, T.P. 2000. Patterns of gravel scour and fill after spawning by chum salmon in a western Washington stream. N. Am. J. Fish. Manag. **20**: 610–617.

Sharma, R., and Hilborn, R. 2001. Empirical relationships between watershed characteristics and coho salmon (*Oncorhynchus kisutch*) smolt abundance in 14 western Washington streams. Can. J. Fish. Aquat. Sci. **58**: 1453–1463.

Stewart, I.J., Hilborn, R., and Quinn, T.P. 2003. Coherence of observed adult sockeye salmon abundance within and among spawning habitats in the Kvichak River watershed. Alaska Fish. Res. Bull. **10**: 28–41.

van den Berghe, E.P., and Gross, M.R. 1989. Natural selection resulting from female breeding competition in a Pacific salmon (coho: *Oncorhynchus kisutch*). Evolution, **43**: 125–140.

© 2007 NRC Canada

ERRATUM / ERRATUM

Erratum: Comparison of size-at-age of larval Atlantic cod (*Gadus morhua*) from different populations based on size- and temperature-dependent growth models

A. Folkvord

Ref.: Can. J. Fish. Aquat. Sci. **62**(5): 1037–1052 (2005).

Several lines of data were missing from Table 1, namely those for Mesocosm studies E8–E12. This information is now correctly shown in Table 1 on pages 584–585.

Additionally, eq. 2 was incorrectly written as $SGR = 100 - (e^g - 1)$. The correct eq. 2 is $SGR = 100(e^g - 1)$.

Equations 5 and 6 were also incorrectly included as

(5) $$\ln DW = -9.38 + 4.55 \ln SL - 0.2046(\log SL)^2$$

(6) $$\ln SL = 2.296 + 0.277 \ln DW - 0.005128(\log DW)^2$$

The correct eqs. 5 and 6 should have the final log terms replaced with ln:

(5) $$\ln DW = -9.38 + 4.55 \ln SL - 0.2046(\ln SL)^2$$

(6) $$\ln SL = 2.296 + 0.277 \ln DW - 0.005128(\ln DW)^2$$

Received 4 April 2007. Accepted 4 April 2007. Published on the NRC Research Press Web site at http://cjfas.nrc.ca on 18 April 2007.
J18084E

A. Folkvord. Department of Biology, University of Bergen, 5020 Bergen, Norway (e-mail: arild.folkvord@bio.uib.no).

 doi:10.1139/F07-045 © 2007 NRC Canada

Table 1. Sources of growth- and size-at-age data of larval and juvenile cod (*Gadus morhua*) used in the study.

Reference	Study code	Area or place of study	Temperature (°C)	Initial DW used (µg)	Duration (days)	Fixation and measures	Comments (temperature data from paper unless specified otherwise)
Laboratory studies							
Laurence 1978	L1	Rhode Island, USA	4, 7, 10	36–43 on day 0	35–49	Not specified	First pioneering laboratory growth study on larval cod
Laurence et al. 1981	L2	Rhode Island, USA	7	44 on day 0	42	Fixed in formalin	Low survival in highest prey density group (sampled to extinction)
Buckley et al. 1993	L3	Rhode Island, USA	7[a]	35 on day 0	42	Fresh for SL, frozen for DW	31%–44% survival in high prey density group
Otterlei et al. 1999	L4	Bergen, Norway	6, 10 (4, 8, 12, 14 not shown here)	30 on day 0	56	Fresh for SL, frozen for DW	5%–45% survival, basis for growth models, otoliths removed before DW measurements, only NC cod data shown here
Folkvord et al. 1999	L5	Bergen, Norway	8	38 on day 0	56	Fresh for SL, frozen for DW	47%–65% survival of NA cod, six replicates, used SL–DW relationship from this study
Baskerville-Bridges and Kling 2000	L6	Maine, USA	10–11, experiment I	30 on day 0	44	Fresh for SL, frozen for DW	Fed rotifers and *Artemia* (from day 22 or 16), 29%–36% survival (experiments I and II in paper)
			7–8, experiment II		36		
Puvanendran and Brown 2002	L7	Newfoundland, Canada	8	48 on day 0	42	Fresh for SL and DW	High light intensity and 24:0 light cycle gave best growth, 30%–40% survival
Mesocosm studies							
Ellertsen et al. 1981	E1	Flødevigen, Norway	4.5–9.9	50 on day 11	52	4% buffered formaldehyde	First group 1976, first mesocosm study of NC larval cod growth in a century, 10% survival
Pedersen et al. 1989	E2	Tromsø, Norway	2.0–11.5 (max. temperature)	34 on day 4	50	4% buffered formaldehyde	Low initial temperatures in 1987, 7% survival, several releases[b]
Olsen et al. 1991	E3	Tromsø, Norway	6.1–14.7 (mean temperature)	75 on day 11	70	4% buffered formaldehyde	Rapid growth in 1989, larval DW estimated from SL[b]
Blom et al. 1991	E4	Øygarden, Norway	3.7–11.9 (mean temperature)	61 on day 6	80	4% buffered formaldehyde	1988 NC cod data, last samples taken with dip net, 23% survival to metamorphosis
Blom et al. 1994	E5	Øygarden, Norway	5.8–9.8	32 on day 2	45	4% buffered formaldehyde	Average of two strains of NC cod in 1991, 23% survival[c]
Folkvord et al. 1994	E6	Austevoll, Norway	6.8–11.2 (max. temperature)	33 and 34 on day 4 and day 5	40, 29	4% buffered formaldehyde	1985 cohorts 1 and 2 with NC cod, 40% and 15% survival
van der Meeren et al. 1994	E7	Austevoll, Norway	4.4–12.2, 7.4–12.3	44 and 42, 42 and 40 on day 2	48, 36	Fresh for WW and DW	1993 data (experiments I and II) on NC and NA cod, 28%–83% survival
Suthers et al. 1999	E8	Austevoll, Norway	7.6–16.0	39 and 56 on day 0	37	Fresh for WW and DW	NC and NA cod, bags 2–4, 30%–50% survival, release 1 week later than study E9
van der Meeren and Jørstad 2001	E9	Austevoll, Norway	7.4–13.4	46 and 62 on day 2	36	Frozen	NC and NA cod, natural light groups from 1994, 29%–83% survival
Finn et al. 2002	E10	Austevoll, Norway	7.9–17.3 (max. temperature)	50 on day 4	52	Fresh for SL, frozen for DW	Series 1 from 1993, NC cod, survival > 30% to 30 days posthatching
Clemmesen et al. 2003	E11	Flødevigen, Norway	4.2–12.7, 5.0–14.5	45 on day 1	46 and 49	Frozen	Larvae of repeat and recruit NA spawners in each of two mesocosms, 10% survival

© 2007 NRC Canada

Table 1 (*concluded*).

Reference	Study code	Area or place of study	Temperature (°C)	Initial DW used (µg)	Duration (days)	Fixation and measures	Comments (temperature data from paper unless specified otherwise)
van der Meeren and Moksness 2003	E12	Austevoll, Norway	8.8–11.8	41 on day 3	31	Fresh for SL, frozen for DW	Data from bag 1, NC cod, 48% survival
Field studies							
Bolz and Lough 1988	F1	Georges Bank, Northwest Atlantic	4.6–10.2	45 on day 0	90	Corrected for shrinkage	Temperature data from Campana and Hurley (1989), sampling with 61-cm Bongo net and 1- to 10-m MOCNESS and an otter trawl for larger cod
Campana and Hurley 1989	F2	Browns and Georges banks, Northwest Atlantic	5.3–8.4, 5.1–9.9	45 on day 0	120 (90 used)	Not corrected for shrinkage	First age- and temperatue-dependent growth model for field larvae, 3 mm TL at day 0, sampling with 61-cm Bongo net
Meekan and Fortier 1996	F3	Scotian Shelf, Northwest Atlantic	7.6–2.3, 8.0–3.1	45 on day 0	80	Fresh for SL	Temperature data from Department of Fisheries and Oceans, S1 and S2 cohorts, sampling with 2-m^2 trawls
Suthers and Sundby 1996	F4	Browns Bank and northern Norway, Northeast Atlantic	2.5–6.0, 5.9–8.7	45 on day 0	90, 80	Not corrected for shrinkage	Data from both sides of the Atlantic, temperature data for Browns Bank from Department of Fisheries and Oceans and for Northeast Atlantic from Sundby (2000), sampling with 5- and 10-m^2 midwater trawls, respectively
Begg and Marteinsdottir 2000	F5	Northwest Iceland, North Atlantic	7.5–10.6, 3.0–8.2	45 on day 0	93, 84	Modeled fresh TL	Data from 1988, northern and southern area, used 57.5 and 45 mm as reported final TL, sampling with a 324-m^2 pelagic trawl
Anderson and Dalley 2000	F6	Grand Banks, Northwest Atlantic	3.7–7.8, 5.5–8.8	45 on day 0	65, 68	Fresh for TL	Data from cold year (1997) and warm year (1996), authors used 3.5 mm TL on day 0, sampling with 61-cm Bongo net and 73-m^2 IYGPT trawl

Note: L, E, and F denote laboratory, enclosure, and field studies, respectively. NA, northeast Arctic cod; NC, Norwegian coastal cod. Initial weights have been corrected for presence of yolk. SL, standard length; DW, dry weight; WW, wet weight; TL, total length.

[a]L. Buckley, University of Rhode Island/National Oceanic and Atmospheric Administration (URI/NOAA), Cooperative Marine Education and Research Program, Graduate School of Oceanography, Narragansett, RI 02882, USA.

[b]T. Pedersen, Norwegian College of Fisheries Science, University of Tromsø, 9001 Tromsø, Norway.

[c]G. Blom, Department of Biology, University of Bergen, N-5020 Bergen, Norway.

© 2007 NRC Canada

National Research Council Canada | Conseil national de recherches Canada

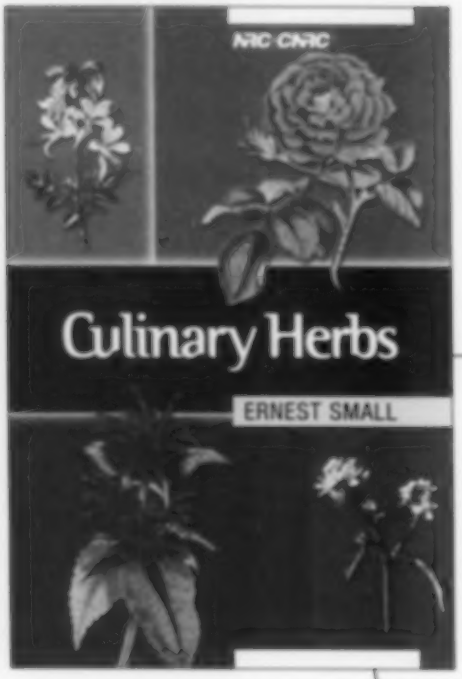

Culinary Herbs

2nd edition

By / Par
Ernest Small

1036 Pages 2006
Hardcover / Édition reliée

ISBN 0-660-19073-7; NRC 44467
ISBN 0-660-19073-7; CNRC 44467

$119.95 CAN; Other countries: $119.95 US
119,95 $CAN; À l'étranger : 119,95 $US

The most comprehensive guide to culinary herbs grown in Canada and the United States. The second edition of Culinary Herbs has been redesigned to incorporate over 400 full-colour illustrations including photographs and historical botanical illustrations. The text of the book features information from up-to-date research and statistics.

L'ouvrage de référence le plus exhaustif sur les herbes culinaires cultivées au Canada et aux États-Unis. La deuxième édition de Culinary Herbs, revue et augmentée, présente plus de 400 illustrations en couleurs, y compris des photographies et des illustrations botaniques classiques. Le texte comprend des renseignements actualisés sur divers aspects, y compris la recherche dans le domaine et les données statistiques.

To order books / Commandez des livres à :

Order Office / Bureau des commandes
NRC Research Press / Presses scientifique du CNRC National Research Council
Conseil national de recherches
Ottawa, ON K1A 0R6, Canada

Telephone / Téléphone : 613-990-2254
Fax / Télécopieur : 613-952-7656
E-mail / Courriel : pubs@nrc-cnrc.gc.ca
Order online / Commandez en ligne :
http://pubs.nrc-cnrc.gc.ca

Shipping and handling extra.
Canadian customers add GST (6%). Prepayment required unless order is accompanied by a purchase order number. Cheques or money orders should be made payable to: "Receiver General for Canada, Credit NRC". For all orders outside Canada, rates are in U.S. dollars. All sales are final.

Frais d'expédition et de manutention en plus.
Clients du Canada, ajoutez la TPS (6 %). Les commandes doivent être payées d'avance à moins qu'elles ne soient accompagnées d'un numéro de bon de commande. Les chèques ou mandats doivent être libellés au « Receveur général du Canada, crédit du CNRC ». Pour les commandes hors-Canada, les tarifs sont en dollars américains. Toutes les ventes sont finales.

NRC·CNRC

Canada

National Research Council Canada
Conseil national de recherches Canada

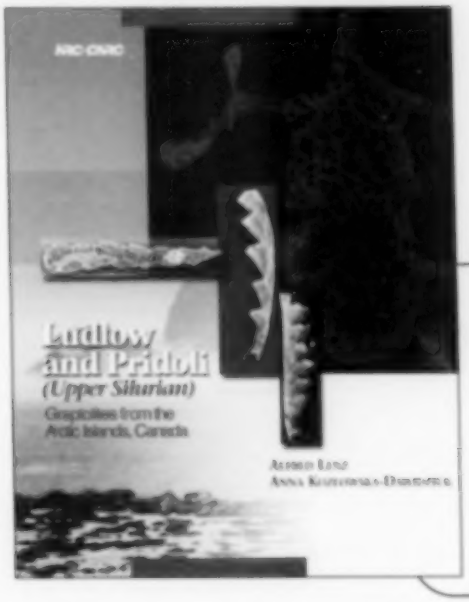

Ludlow and Pridoli (Upper Silurian)

Graptolites from the Arctic Islands, Canada

By / Par
A. Lenz and A. Kozłowska-Dawidziuk

141 Pages 2004
Softcover / Édition brochée

ISBN 0-660-19326-4; NRC 46842
ISBN 0-660-19326-4; CNRC 46842

$54.95 CAN; Other countries: $54.95 US
54,95 $CAN; À l'étranger : 54,95 $US

Graptolites flourished from earliest Ordovician to Early Devonian, a time range of about 90 million years, and were widely distributed as marine benthic and planktonic colonial organisms around the world. They were diverse and rapidly evolving and, as such, make excellent "index fossils" for relative age-dating of their enclosing basinal rocks. Rarely, however, graptolites are beautifully preserved in their original three-dimensional form, and can be extracted from the enclosing rock for detailed study under scanning electron microscopy. Such a unique preservation is pervasive in the latest Ordovician to latest Silurian rocks of the central Arctic Islands of Canada, presenting an opportunity to study their complex morphology and evolution, making the Arctic graptolite sequence unique in the world. The present study examines the isolated, uncompressed as well as flattened forms from the Ludlow and Pridoli (Upper Silurian) graptolites of the Arctic, recognizing 46 species of monograptids and retiolitids of which seven are described as new species or subspecies.

Les graptolites abondaient entre le début de l'Ordovicien inférieur et le Dévonien inférieur, période d'environ 90 millions d'années, et étaient des organismes coloniaux marins benthiques et planctoniques largement répartis dans le monde. Leur diversité et leur rapide évolution en font des marqueurs stratigraphiques exceptionnels. Bien que ceci soit rare, on retrouve des graptolites superbement bien préservés, en trois dimensions, susceptibles d'être extraits de la roche et examinés par microscopie électronique à balayage. La période entre la fin de l'Ordovicien et la fin du Silurien dans l'archipel arctique canadien a été particulièrement favorable à cette extraordinaire préservation. La possibilité d'étudier leur morphologie complexe et leur évolution fait des Graptolites de l'Arctique des spécimens sans égal dans le monde. Dans cette étude, on examine les spécimens isolés et non comprimés de même que les empreintes fossiles de graptolites du Ludlow et du Pridoli (Silurien supérieur) de l'Arctique et on signale 46 espèces de monograptides et de réticolitides, notamment sept constituant de nouvelles espèces ou sous-espèces.

To order books / Commandez des livres à :

Order Office / Bureau des commandes
NRC Research Press / Presses scientifique du CNRC National Research Council
Conseil national de recherches
Ottawa, ON K1A 0R6, Canada

Telephone / Téléphone : 613-990-2254
Fax / Télécopieur : 613-952-7656
E-mail / Courriel : pubs@nrc-cnrc.gc.ca
Order online / Commandez en ligne :
http://pubs.nrc-cnrc.gc.ca

Shipping and handling extra.
Canadian customers add GST (6%). Prepayment required unless order is accompanied by a purchase order number. Cheques or money orders should be made payable to: "Receiver General for Canada, Credit NRC". For all orders outside Canada, rates are in U.S. dollars. All sales are final.

Frais d'expédition et de manutention en plus.
Clients du Canada, ajoutez la TPS (6 %). Les commandes doivent être payées d'avance à moins qu'elles ne soient accompagnées d'un numéro de bon de commande. Les chèques ou mandats doivent être libellés au « Receveur général du Canada, crédit du CNRC ». Pour les commandes hors-Canada, les tarifs sont en dollars américains. Toutes les ventes sont finales.

NRC·CNRC

Canada

National Research Council Canada | Conseil national de recherches Canada

Flower Guide for Holiday Weekends

In Eastern Canada and Northeastern U.S.A.

By / Par
E.W. Larsen and B.I. Roots

149 Pages 2005
Softcover / Édition brochée

ISBN 0-660-19096-6; NRC 46327
ISBN 0-660-19096-6; CNRC 46327

$14.95 CAN; Other countries: $14.95 US
14,95 $CAN; À l'étranger : 14,95 $US

Petite flore pour les longues fins de semaine

dans l'est du Canada et le nord-est des États-Unis

Par / By
E.W. Larsen et B.I. Roots

149 Pages 2005
Édition brochée / Softcover

ISBN 0-660-19096-6; CNRC 46327
ISBN 0-660-19096-6; NRC 46327

14,95 $CAN; À l'étranger : 14,95 $US
$14.95 CAN; Other countries: $14.95 US

To order books / Commandez des livres à :

Order Office / Bureau des commandes
NRC Research Press / Presses scientifique du CNRC National Research Council
Conseil national de recherches
Ottawa, ON K1A 0R6, Canada

Telephone / Téléphone : 613-990-2254
Fax / Télécopieur : 613-952-7656
E-mail / Courriel : pubs@nrc-cnrc.gc.ca
Order online / Commandez en ligne :
http://pubs.nrc-cnrc.gc.ca

Shipping and handling extra.
Canadian customers add GST (6%). Prepayment required unless order is accompanied by a purchase order number. Cheques or money orders should be made payable to: "Receiver General for Canada, Credit NRC". For all orders outside Canada, rates are in U.S. dollars. All sales are final.

Frais d'expédition et de manutention en plus.
Clients du Canada, ajoutez la TPS (6 %). Les commandes doivent être payées d'avance à moins qu'elles ne soient accompagnées d'un numéro de bon de commande. Les chèques ou mandats doivent être libellés au « Receveur général du Canada, crédit du CNRC ». Pour les commandes hors-Canada, les tarifs sont en dollars américains. Toutes les ventes sont finales.

NRC·CNRC

Canada

Daniel Palm, Eva Brännäs, Fabio Lepori, Kjell Nilsson, and Stefan Stridsman	**509–515**	The influence of spawning habitat restoration on juvenile brown trout (*Salmo trutta*) density
Kerri Finlay, Beatrix E. Beisner, Alain Patoine, and Bernadette Pinel-Alloul	**516–529**	Regional ecosystem variability drives the relative importance of bottom-up and top-down factors for zooplankton size spectra
John M. Drake and David M. Lodge	**530–538**	Rate of species introductions in the Great Lakes via ships' ballast water and sediments
Leire Ibaibarriaga, Miguel Bernal, Lorenzo Motos, Andrés Uriarte, David L. Borchers, Mike E. Lonergan, and Simon N. Wood	**539–553**	Characterization of stage-classified biological processes using multinomial models: a case study of anchovy (*Engraulis encrasicolus*) eggs in the Bay of Biscay
Tian Tian, Øyvind Fiksen, and Arild Folkvord	**554–562**	Estimating larval fish growth under size-dependent mortality: a numerical analysis of bias
Sean C. Mitchell and Richard A. Cunjak	**563–573**	Relationship of upstream migrating adult Atlantic salmon (*Salmo salar*) and stream discharge within Catamaran Brook, New Brunswick
T.P. Quinn, D.M. Eggers, J.H. Clark, and H.B. Rich, Jr.	**574–582**	Density, climate, and the processes of prespawning mortality and egg retention in Pacific salmon (*Oncorhynchus* spp.)
	ERRATUM	ERRATUM
A. Folkvord	**583–585**	Erratum: Comparison of size-at-age of larval Atlantic cod (*Gadus morhua*) from different populations based on size- and temperature-dependent growth models

National Research Council Canada
Ottawa, Canada K1A 0R6

Conseil national de recherches Canada
Ottawa, Canada K1A 0R6

Postage paid at Ottawa
Publications mail
Registration No. 40062591

Port payé à Ottawa
Poste-publication
Enregistrement n° 40062591

USPS periodical postage paid at Plattsburgh, NY 12901, USA

Canadian Journal of Fisheries and Aquatic Sciences

Volume 64, Number 3, March 2007

Journal canadien des sciences halieutiques et aquatiques

Volume 64, numéro 3, mars 2007

RAPID COMMUNICATION		COMMUNICATION RAPIDE	
Jon Grant, Gary Bugden, Edward Horne, Marie-Claude Archambault, and Michel Carreau	**387–390**	Remote sensing of particle depletion by coastal suspension-feeders	
ARTICLES		ARTICLES	
Marjorie L. Brooks, Joseph S. Meyer, and Connie J. Boese	**391–401**	Toxicity of copper to larval *Pimephales promelas* in the presence of photodegraded natural dissolved organic matter	
Gregor Thomas and Reiner Eckmann	**402–410**	The influence of eutrophication and population biomass on common whitefish (*Coregonus lavaretus*) growth — the Lake Constance example revisited	
Emmanis Dorval, Cynthia M. Jones, Robyn Hannigan, and Jacques van Montfrans	**411–424**	Relating otolith chemistry to surface water chemistry in a coastal plain estuary	
Willem Goedkoop, Marnie Demandt, and Gunnel Ahlgren	**425–436**	Interactions between food quantity and quality (long-chain polyunsaturated fatty acid concentrations) effects on growth and development of *Chironomus riparius*	
Rex Meade Strange and Carol A. Stepien	**437–448**	Genetic divergence and connectivity among river and reef spawning groups of walleye (*Sander vitreus vitreus*) in Lake Erie	
Thomas P. Hurst	**449–457**	Thermal effects on behavior of juvenile walleye pollock (*Theragra chalcogramma*): implications for energetics and food web models	
Yan Cai, Jay R. Rooker, Gary A. Gill, and Jason P. Turner	**458–469**	Bioaccumulation of mercury in pelagic fishes from the northern Gulf of Mexico	
Thomas E. Helser, Ian J. Stewart, and Han-Lin Lai	**470–485**	A Bayesian hierarchical meta-analysis of growth for the genus *Sebastes* in the eastern Pacific Ocean	
Cindy Breau, Laura K. Weir, and James W.A. Grant	**486–494**	Individual variability in activity patterns of juvenile Atlantic salmon (*Salmo salar*) in Catamaran Brook, New Brunswick	
Brian R. Herwig, David H. Wahl, John M. Dettmers, and Daniel A. Soluk	**495–508**	Spatial and temporal patterns in the food web structure of a large floodplain river assessed using stable isotopes	

Continued on inside back cover / Suite au verso

Front cover: Boko Saito/Toshiyuki Tajima/Dex Image/Getty Images.

Page couverture : Boko Saito/Toshiyuki Tajima/Dex Image/Getty Images.

Canada

Printed in Canada by / Imprimé au Canada par
NRC Reprographic Services / Service de reprographie CNRC
Page production by / Mise en page par
NRC Research Press / Presses scientifiques du CNRC

0706-652X(200703)64:3;1-3